STRUCTURAL ASPECTS OF THE GROWTH AND REPRODUCTION OF SAPROLEGNIA SPP

by

Ian Brent Heath

B.Sc., A.R.C.S.

A thesis presented in part fulfilment

of the requirements for the degree of

Ph.D. of the University of London

July, 1969

Department of Botany and Plant Technology,

Imperial College of Science and Technology,

London. S.W.7.

ABSTRACT

Structural aspects of nuclear division, wall synthesis and spore formation have been studied in Saprolegnia ferax with light and electron microscopy.

Nuclei divide mitotically with an intranuclear spindle which possesses simple kinetochores. Interphase nuclei are accompanied by paired centrioles which, at the end of interphase, form daughters connected at 180° to the proximal end of each parent, thus producing two pairs of adjacent centrioles. Mature paired centrioles are not visibly connected but remain orientated with their long axes at 180°. Each pair of centrioles lie external and adjacent to a differentiated region of the nuclear envelope at the poles of the developing spindle from which the spindle tubules appear to originate. Telophase separation of daughter nuclei is probably aided by an interaction between the nuclear envelope and astral microtubules.

Characteristic vesicles, whose possible origin from the endoplasmic reticulum is discussed, play a part in the formation of the walls of hyphae, sporangia, apical papilla and germ tubes. The outer cyst wall is derived from special structures which are present in the zoospores and which also contain the preformed spines found on the outside of cysts. The inner layer of the cyst wall is probably produced by activity of Golgi vesicles. A new hypothesis is presented for the development of lomasomes.

The cytoplasm of the sporangia is cleaved by enlargement of dense body vesicles. Centrioles develop into kinetosomes which then produce flagella after cytoplasmic cleavage. The structure,

development and mode of attachment of flagella to the spore is described in detail. Flimmer hairs are shown to originate in cisternae of the endoplasmic reticulum. Upon encystment, flagella are withdrawn but the kinetosomes do not revert to centrioles until germtination. Vacuoles of the germinating spore are produced by enlargement of dense body vesicles; an accumulation of vesicles comparable to those involved in wall formation defines the point of emergence.

Comparative observations of Dictyuchus sterile have shown numerous fundamental similarities to S. ferax.

CONTENTS

ABBREVIATIONS

The following abbreviations have been used in the text:-

DNA	deoxyribonucleic acid
E.R.	endoplasmic reticulum
GA	glutaraldehyde
GA/Os	glutaraldehyde fixation, post fixed with osmium tetroxide.
GDP-glucose	guanosine diphosphate glucose
OM	the medium described on page
Os	osmium tetroxide
P	M/15 pH 6.98 phosphate buffer
PAH	periodic acid oxidation followed by silver hexamine staining
PAS	periodic acid oxidation followed by Schiffs' reagent staining
Pb	lead citrate section stain
PTA	phosphotungstic acid
RNA	ribonucleic acid
SITS	4-acetamido;4'-isothiocyanatostilbene-2,2'-disulphonic acid
UAc	uranyl acetate

INTRODUCTION

This work was designed as an ultra-structural study of the fundamental processes of cell wall formation, nuclear division and asexual reproduction in one organism, Saprolegnia ferax (Gruithuisen) Thuret.

In most cellular plants nuclear division, wall synthesis and cell division are structurally and temporally associated. In coenocytes these processes are not structurally associated and thus provide a situation in which they may be investigated separately. Filamentous coenocytes, unlike plasmodia, have a small, well-defined zone of growth which is, in many cases, capable of indefinite, undifferentiated extension. For ultra-structural studies, these organisms possess the additional advantage that most of the cytoplasm is concentrated in a small region adjoining the apex, thus presenting a well-defined zone in which most cellular processes, including nuclear division, occur. Coenocytic algae are demanding in their environment and relatively slow growing but the oomycete fungi will grow rapidly on a wide range of media and, lacking chloroplasts, have a simpler structure. Furthermore, the structural aspects of hyphal growth have not been examined in detail previously.

The hyphal apices of S. ferax are well separated from the region of branch initiation and can easily be induced to change their mode of wall formation to another equally well-defined pattern during zoosporogenesis. Nuclear divisions occur

frequently in the apical region and have been the source of a considerable controversy in the literature where they have usually been described as amitotic but the mechanism of such a processs is unknown.

The easily induced asexual reproductive cycle facilitates the investigation of fundamental processes such as vacuole and membrane formation, cytoplasmic reorganisation, flagellum production and spore germination. The extensive background of light microscopical observations and the ease of preparation of all stages for electron microscopy make S. ferax a very suitable species for such investigations.

This thesis is divided into three sections; wall formation, nuclear division and asexual reproduction. The relevant literature is reviewed at the beginning of each section.

MATERIALS AND METHODS

1) Fungi

Saprolegnia ferax (Gruithuisen) Thuret was obtained fromavegetative subculture originating from a single zoospore isolated by Manton, Clarke & Greenwood (1951).

Saprolegnia furcata Maurizia and *Dictyuchus sterile* Coker (strain 341c) were supplied from the culture collection in the Botany Department at the University of Reading, England, by Dr. M. Dick.

2) Chemicals

All chemicals used were of "Analar" grade obtained from B.D.H. unless otherwise stated. A list of all suppliers is given in the Appendix.

3) Media and Culture Conditions

Fungi were maintained on agar slopes of the following medium (referred to as OM) at 4° C. or 25° C.

Glucose (Hopkins & Williams)	1.0%
Peptone (Oxoid. Bacteriological No.L37)	0.1%
Yeast extract (Oxoid. Powder No.L21)	0.01%
KH_2PO_4	0.1%
$MgSO_4.7H_2O$	0.03%
Agar (Davis Standard)	1.5%

All media were autoclaved at 15 p.s.i. for fifteen minutes.

Routinely, vegetative colonies were grown aseptically either on OM agar or OM liquid in petri dishes at 25° C. for

one or two days in the dark. The inoculum for these cultures was a c 3mm agar tube cut from the edge of a growing colony. Some colonies were also incubated at 10° C., 30° C. and 37° C.

To produce zoosporangia, numerous treatments were employed. The most reproducable results were obtained by growing colonies from an infected hemp seed (Cannabis sativa L. autoclaved or boiled) in liquid OM for 24h at 25° C. The OM was then replaced with sterile tap water which was changed three or four times at hourly intervals. After about 7h at 20° C., zoospores are liberated. Variations on this treatment which have also been used to produce sporangia include the use of agar cubes as inocula, the chick pea medium described by Gay & Greenwood (1966) in place of the OM, and sterile distilled or pond water in place of tap water. The differences in efficiency of these alternatives have not been measured quantitatively but do not appear to be very large. The lengths of incubation are not critical but if the colony is larger than about 25mm diameter when transferred to water, it is often difficult to remove the OM hence sporulation does not occur. These treatments do not produce synchronous sporangium formation; from 7 to 20h after transfer to water, all stages from non-delimited apices to encysted spores are present in the average colony. Motile spores reach a maximum after about 12h.

To obtain encysted zoospores, three or four well-separated colonies of about 25mm diameter were induced to form sporangia as above. After 24h in water, the zoospore suspension was

removed by drawing a fine polythene pipette over the surface of the colonies, which were then washed with fresh sterile water three or four times and the washings collected in the same way. The zoospores were concentrated by centrifugation at 750xg for about 5 minutes. Germinating spores are rare in these populations.

Germinating zoospores were usually produced by suspending encysted spores in OM at 25° C. for 7h, or spreading this suspension over a thin layer of OM agar in a petri dish under similar conditions. Populations obtained by both these techniques ranged from ungerminated spores to sporelings up to about 1 mm long; accurate measurements have not been made. In some experiments, spores were germinated in, or on OM media containing 0.1% (2.5×10^{-3} M) or 0.2% (5.0×10^{-3} M) colchicine.

4) Fixation and Embedding

Material growing on agar was fixed *in situ* by cutting out the entire colony, or portions of it, and immersing these blocks in fixative in covered embryo cups. Liquid grown colonies were transferred to fixative after removal of excess medium with filter paper. After processing in covered embryo cups, the material was transferred to resin in flat polythene dishes (door pulls from any hardware store). Liquid grown hyphae were spread gently with glass needles prior to polymerisation.

Zoospores were usually processed in B.E.E.M. (L.K.B.) capsules; the spores were suspended in each solution and spun

down at about 750 xg for 3 minutes prior to each change. This ensured good penetration of solution without loss of material due to fragmentation of the pellet. The pellet was embedded by spinning down in stage 12 below, removing half the epoxy-propane and adding an equal volume of resin and sealing the capsule for 1 h. The capsule was then left open overnight and placed in the oven without a change of resin.

The main fixation procedure, referred to as GA/Os, is given below using P as an abbreviation for phosphate buffer.

1	Fix	5% Glutaraldehyde in M/15 P pH 6.98	2h
2	Wash	M/15 P pH 6.98	4 x ¼ h
3	Post fix	1% Osmium tetroxide in M/15 P pH 6.98	1h
4	Dehydrate	20% ethanol v/v water	10 min
5	"	40% " " "	" "
6	"	60% " " "	" "
7	"	80% " " "	" "
8	"	100% " " "	2 x 10 min
9	"	100% " " "	overnight(c15h)
10	"	100% " " "	2 x 10 min
11	Infiltrate	50% epoxy-propane in ethanol	1h
12	"	100% epoxy-propane	1h
13	"	50% epon in epoxy-propane	1h
14	Embed	Allow epoxy-propane to evaporate slowly overnight c 15 h	
15	"	Transfer to fresh epon and polymerise at 60° C. 2 days	

All solutions were made up with double distilled water and stored

at 4° C. unless otherwise stated.

Glutaraldehyde (GA) was obtained as a 25% solution from TAAB. Barium carbonate stabilization was not used since tests showed this to be unnecessary. Material was also fixed in GA at the following concentrations, 0.1% in M/30P, 0.5% in M/15P, 1.0% in M/15P and 2.5% in M/15P. The time of fixation in GA does not appear to be critical, no difference has been detected between samples fixed for 2 min, 10 min, 30 min, 1 h, 2 h, or 17 h in 5% GA in M/15 P. This conclusion is based entirely on a subjective examination of a very limited number of electron micrographs; however, observations with the light microscope (see Appendix) show that most changes detectable by this means occurred within 2 min of immersion in GA.

Preliminary trials on hyphae fixed at c 4° C. and c 20° C. did not reveal differences in structure. Since Tilney & Porter (1967) and others show that microtubules disrupt at 4° C., all preparations were made at laboratory temperature (18° - 20° C.).

One sporulating colony was plasmolysed in 2M sucrose for 20 min then fixed in a mixture of 5 parts M/7.5 P, 5 parts 2M sucrose, 2 parts 25% GA, followed by the routine post fixation and embedding.

Buffers Sørensen's sodium potassium phosphate buffer (P) was used routinely at pH 6.98. This was made up as M/7.5 stock solution (Hale, 1965) and diluted as needed to M/15 or M/30. It was thought that the granularity seen in sections

at high magnifications could be a function of the phosphate buffer, consequently a batch of material was fixed by the GA/Os method using a veronyl acetate buffer pH 7.0 (see Osmium tetroxide). As there was no change in granularity, the simpler phosphate buffer was used routinely.

Washing. On one occasion, a single 10 min wash was used instead of the usual 4 x $\frac{1}{4}$ h changes. The results obtained with this are discussed in the Appendix.

Osmium tetroxide (Os) (B.D.H. & TAAB) was used as a 1% solution in P stored at 4° C. in a very clean glass bottle and discarded if it became darker than pink. Some material was fixed in Os alone, omitting steps 1 and 2 above (i.e. no GA or P). Reducing the time in Os below $\frac{1}{2}$ h gives unsatisfactory results; 2 h was the longest time used and was satisfactory. One batch of germinating spores was fixed by the Kellenberger, Ryter & Séchaud (1958) method in an attempt to obtain better preservation of DNA. Spores were suspended for 17 h in 0.5 ml of Kellenberger fixative containing 1 drop tryptone (1% Oxoid L 42 pH 7.0 in 0.5% NaCl). This mixture was then diluted with 4 ml of veronal acetate buffer (pH 6.1), centrifuged at 750 xg for 5 min and resuspended in 0.5% Uranyl acetate in veronal acetate buffer for 2 h. The spores were then dehydrated and embedded as a pellet.

Potassium permanganate was used as a fixative at 2% w/v in P for 1 h followed by the usual steps of dehydration and embedding. This fixation was generally unsatisfactory on

material adhering to agar since residual $KMnO_4$ in the agar prevented polymerisation of the resin.

Dehydration with ethanol solutions apparently gave better preservation than a similar acetone series, thus the latter was little used.

Infiltration was always via 1:2 epoxy-propane. The 50% resin epoxy-propane mix was made by adding an approximately equal volume of resin to the pure epoxy-propane in stage 12. The two components mixed on standing without stirring. At stage 14, slow evaporation of epoxy-propane was achieved by leaving a very small gap in the lid of the embryo cup.

Embedding was in various mixtures of epon 812. All components of the resin were obtained from G.T. Gurr, Ltd. Resins, based on Luft's (1961) formulae, were made as 4A:1B, 3A:1B and all B mixes:-

A mix	Epon 812	46 g
	Dodecenyl succinic anhydride (DDSA)	61.8 g
	Benzyl dimethylamine (BDMA)	2.0 ml
B mix	Epon 812	69 g
	Methyl nadic anhydride (MNA)	57 g
	BDMA	2.0 ml

The 3A:1B mix was satisfactory or preferable for glass knives but the all B mix was the most reliable when used with diamond knives.

5) Sectioning

Hyphae, sporangia or germinating zoospores showing the desired stage of development were selected in the polymerised blocks using a 10 x phase objective and a Vickers 40 x N.A. 0.57 Dyson phase objective with a working distance of 12.8 mm. The selected material was sawn from the block, mounted on a wooden dowel and trimmed under a 90 x stereomicroscope with "Wilkinson Sword" razor blades. Blocks were trimmed to a trapezium topped pyramid containing a single hypha or sporangium at a known stage of development and orientation. Sections were cut on Cambridge "Huxley," Sorvall "MT 1," Reichert "OmU2" or usually L.K.B. "Ultratome 1" ultramicrotomes using glass (L.K.B.) or diamond knives (I.V.I.C. & Ge-Fe-Ri). Most sections collected showed silver or grey interference colours on the water boat indicating a thickness of 50 nm or less (see Section Thickness in Appendix). Ribbons of sections were collected on formvar coated 100 mesh copper or 200 mesh gold grids (Smethurst, Polaron, Mason & Morton). Formvar films were cast on glass slides from a 0.6% solution of formvar (TAAB) in chloroform, floated on a clean water surface and, after addition of grids, collected on nylon mesh and stored in a desiccator.

6) Section Staining

All sections, unless otherwise stated, were stained for 20 min in 2% aqueous uranyl acetate (UAc) at 60° C., rinsed in distilled water and then stained for 7 min in lead citrate

(Pb) at c 20° C. Grids were then washed in distilled water, dried and examined. Staining was carried out by immersing the grids in drops of solution on polythene sheets in petri dishes. Lead citrate was used in a CO_2 reduced atmosphere produced by KOH pellets in the dish; this was designed to prevent precipitation of lead carbonate. Lead citrate was prepared by Reynolds' (1963) method. 1.33 g of fresh $Pb(NO_3)_2$ and 1.76 g $Na_3(C_6H_5O_7).2H_2O$ were added to 30 ml of boiled (CO_2 free) water and shaken vigorously. The solution was then agitated intermittently for ½ h. About 8.0 ml N/1 NaOH (CO_2 free) was added and the solution diluted to 50 ml with more CO_2 free water. The precipitate should just dissolve and the pH was adjusted to pH 12.0± 0.1 with more N/1 NaOH. The solution was stored in full, small, airtight bottles and the clear solution or supernatant was usable until a large white precipitate was formed.

7) Electron Microscopy

Specimens were examined in an A.E.I. E.M.6 or A.E.I. E.M.6.B microscope operating at 75 Kv and 60 Kv respectively. Micrographs were recorded on Ilford N50 plates developed in Kodak D19b developer. All measurements were made on the original plates. Microscopes were calibrated with an A.E.I. diffraction grating replica with 2,160 lines per mm.

8) Electron Microscope Histochemistry

a) Periodic acid, hexamine (PAH)

This reaction was used to identify regions of high

polysaccharide content in an attempt to detect the origin of wall material. There are basically two steps in the reaction. Periodic acid oxidises vic-glycol groups to aldehydes:-

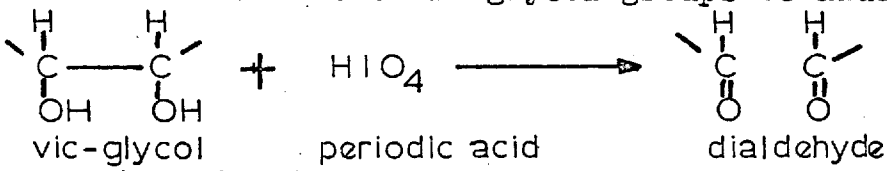

The reaction is stronger with the cis isomer but if the molecules are sufficiently flexible, trans isomers can also be oxidised (Fieser & Fieser, 1961). Many oxidizing agents will also produce the aldehyde but periodic acid is the only one which does not continue the oxidation to acids. Furthermore, as noted by Hotchkiss (1948), the peroxidation is specific for glycol groups and its substituted structures where the hydroxyls are replaced by amino, alkamino groups, or the oxidation product -CHOH-CO- .

The aldehyde groups are detected in the light microscope by their ability to restore the colour to sulphurous acid decolourised fuchsin:-

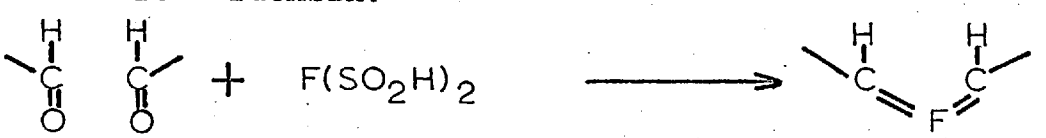

This is the well-known PAS reaction.

For electron microscopy, ammoniacal silver nitrate (Ag oxide) solution is reduced by the aldehydes and allowed to form a deposit of electron dense metallic silver. Hotchkiss (1948) has shown the PAS reaction to be specific for compounds which contain the groupings described above, provided they also a) do not diffuse away in the course of fixation, b) give a

non-diffusable oxidation product and c) are present in sufficient concentration to give a detectable colour. The fixatives used in electron microscopy probably retain more reactive material than those used for light microscopy and the use of silver at the electron microscope level is undoubtedly more sensitive than the detection of a coloured product with the light microscope. Thus, the PAH reaction is likely to produce a more complex picture than PAS. Furthermore, Hotchkiss (1948) and Pearse (1961) list a considerable number of PAS-positive compounds which are not polysaccharide, e.g. phospholipids and unsaturated lipids. Such compounds as ATP and ADP also contain PAH reactive groups and may further confuse the picture if still present in the sections. Clearly, the reaction is not specific for polysaccharide; however, many such molecules, which are often relatively non-diffusable, contain a large number of reactive groups and could lead to a heavier reaction than the rest of the cytoplasm.

Pickett-Heaps (1967b) and others have shown the PAH stain to be useful in detecting the sites of cell wall precursor synthesis, consequently samples of S. ferax have been studied with PAH in the electron microscope and PAS in the light microscope. All PAH work has used gold-silver sections mounted on formvar coated 200 mesh gold grids (copper displaces silver from solution). Grids were immersed in small volumes of solutions on glass or polythene plates in petri dishes. The times quoted are not critical.

The solutions used were those described by Pickett-Heaps (1967a):-

Periodic acid 1% aqueous.

Silver hexamine 0.1% $AgNO_3$ in 1% hexamine in 0.0025 M sodium borate buffer adjusted to pH 9.2 with boric acid crystals and indicator paper.
(Staining was variable but 1 h at 60° C. was found to be acceptable for most sections).

Sodium thiosulphate 1% aqueous was used for ½ h at 20° C. to remove covalently bound silver after all silver incubations.

Sodium bisulphite 2% aqueous was used at 60° C. for 1 h to block aldehyde groups.

Schiffs reagent was made by dissolving 0.5% Basic Fuchsin (CP42500) and 0.5% sodium metabisulphite in 0.15N HCl and shaking until the colour changed from pink to brown. This solution was decolourised by shaking twice with 0.3% charcoal and filtering, kept well at 4° C. in the dark, and was used at 20° C. for 25 min.

Pickett-Heaps (1967a) has demonstrated considerable polysaccharide retention in wheat cells after 2 h $KMnO_4$ fixation without further peroxidation. This method was

applied to germinating, $KMnO_4$ fixed, S. ferax zoospores. As shown in Fig.1, no wall staining occurred but there was a silver deposit specific to all structures containing manganese. This deposit increased with manganese concentration (e.g. in membranes) but was removed by bisulphite prior to staining with silver. Bisulphite not only blocks aldehyde groups but also removes all manganese from the sections (Fig. 2). Since the permanganate clearly did not produce aldehyde groups in the walls (due either to insufficient or excessive oxidation to carboxyl groups), this method was discontinued. Some material was peroxidized (0.5%, 20° C., 2 h) after fixation prior to dehydration, but this also failed to produce wall staining.

If permanganate was removed by bisulphite and the sections peroxidized for $\frac{1}{4}$ h at 20° C. prior to staining, there was still no silver deposited. If, however, this peroxidation was for $\frac{1}{2}$ h at 60° C., an even stain appeared throughout the cytoplasm, was slightly less dense on the mitochondria, and showed no increase over the walls (Fig. 3). This staining was not due to manganese since this was completely removed by the initial bisulphite treatment. It was probably produced by aldehyde groups since a second bisulphite treatment between peroxidation and staining removed all the deposits. The absence of wall stain remains unexplained but may be due to excessive oxidation to carboxyl groups caused by the $KMnO_4$ fixation.

Since cell walls would not stain after $KMnO_4$ fixation, all further work was carried out on the better preserved GA/Os fixed spores and hyphae. As shown by Marinozzi (1961), all osmium must be removed from the sections before silver staining since osmic compounds can reduce the Ag_2O to metallic silver (Fig. 4). Peroxidation removes osmium and produces a bisulphite blockable reaction on the walls and other regions (Fig. 5). All observations described in the results were made on GA/Os fixed material, sections of which were processed according to the following schedule:-

Periodic acid 1%	60° C.	½ h
Water	20° C.	several brief rinses
Silver hexamine	60° C.	1 h
Sodium thiosulphate	20° C.	½ h
Water	20° C.	several rinses

Dry and examine.

Cellular structure could be made clearer by staining in UAc and Pb after the above procedure but this tended to obscure the silver stain. A more satisfactory method is to stain a ribbon of sections with UAc and Pb and examine a few in each ribbon in the microscope. The grids are then processed as above and re-examined. Peroxidation removes Pb and UAc as well as osmium, except in areas irradiated by the electron beam (Fig. 5), so that no metal specific staining is introduced. The silver stain shows up clearly and can be compared with the fine

structure observed previously on adjacent sections.

A few observations on thick epon sections stained for light microscopy with PAS showed colour intensities which visually appeared to correlate with the density of silver in the PAH material.

b) Chromosome stain

Bryan & Brinkley (1964) developed a chromosome or DNA stain for electron microscopy. They used acid hydrolysis to split off bases and open certain pentose rings thus producing aldehydes which they detected with ammoniacal silver solution. These authors hydrolysed the tissue in blocks of methacrylate and stained the sections cut from these blocks. In the present work, all reactions were carried out on GA/Os fixed, epon sections mounted on gold grids. The silver stain was made up according to Bryan & Brinkley's (1964) formula, i.e. 2% $AgNO_3$ titrated with 2% NH_4OH until the precipitate just dissolved. This solution was used fresh at 37° C. for 7 h.

Initially, sections were hydrolysed in N/1 HCl at 60° C. for 35 min followed by silver staining, UAc and Pb. The latter two stains partially obscured the silver which was itself specifically associated with the osmophilic deposits (Fig. 6). In subsequent experiments, osmium was first removed by Marinozzi's (1961) method and the sections stained

according to the following schedule:-

H_2O_2 7.5% in H_2O	20° C.	1 h
Oxalic acid 1%	20° C.	rinse
N/1 HCl	60° C.	20 min
H_2O	20° C.	several rinses until free of Cl
Ag solution	37° C.	7 h
NH_4OH 2%	20° C.	3 x 10 min
H_2O	20° C.	rinse
Dry and examine.		

This procedure removed all osmium but produced no staining although sections contained metaphase nuclei.

The lack of staining is unexplained. There was no reason to doubt the efficiency of the stain and since other aqueous solutions (see Section thickness in Appendix) can penetrate the sections, so also should the HCl. Further tests were not made.

c) Enzyme digestions

i) Nucleic acid

The first method is based on the work of Kislev, Swift & Bogorat (1965). Zoospores germinated for 6 h on thin OM agar were cut out and, together with some undischarged sporangia, were fixed in GA/Os. After Os and before dehydration, they were briefly rinsed in water and incubated in:-

RNAase (0.1% BDH batch No. 215390 in H_2O adjusted to

pH 6.5 with N/1 NaOH and heated to 90° C. for 10 min to remove DNAase)

or

DNAase (0.02% Sigma stock No. DN-C in 0.003 M $MgSO_4$ adjusted to pH 6.5 with N/1 NaOH)

or

$MgSO_4$ (0.003 M at pH 6.5).

All were incubated at 25° C. for 1 h. After incubation, material was rinsed in water, soaked in 5% trichloracetic acid (TCA) at 4° C. for ½ h to remove digested material and then dehydrated as normal.

This technique gave acceptable fixation which was better after DNAase (Fig. 7) than RNAase (Figs. 8 & 9) treatments, possibly due to the Mg ions in the medium, but failed to remove cytoplasmic ribosomes which were used as markers for enzyme activity (Figs. 7, 8 & 9). The absence of activity was thought to be caused by enzyme inactivation due to residual osmium. Consequently, germinating zoospores were prepared in the BEEM capsule process using the enzyme incubations after the buffer washes before osmication. This gave very poor fixation (which was due to the application of TCA prior to osmication since controls without TCA gave good preservation) and no detectable enzyme activity (Fig. 10) relative to the $MgSO_4$ controls.

The above enzyme solutions were also used at 37° C. for 2 h on silver epon sections on gold grids. Once again no

enzyme activity was detected.

A further attempt to show nuclease activity was based on the work of Weintraub & Ragetli (1968) and used fresh enzymes. Hyphae and sporangia were prepared thus:-

Fixed 5% GA in P for 1 h.

Washed 2 x 10 min in P followed by 11 h in P, then 4 x 10 min in P.

Incubated in:- RNAase (0.1% BDH No. 1034200 in H_2O adjusted to pH 6.8 with N/100 NaOH)

or DNAase (0.05% BDH No. 467214/610127 in 0.003 M $MgSO_4$ adjusted to pH 6.8 with N/100 NaOH)

or enzyme free media.

All at 25° C. for 1 h followed by 37° C. for 1 h.

Postfixed, dehydrated and embedded as normal.

Preservation after DNAase was good (Fig. 11). No clear areas appeared in the nucleus but it is difficult to detect enzyme action in the absence of known markers. RNAase control preparations were well preserved (Fig. 12) but became obscure after enzyme treatment (Fig. 13). There is apparently a loss of contrast in the cytoplasmic ribosomes but they are obscured by an increase in the dense background. These results suggest some enzyme activity; further work, possibly using TCA or a protease to remove the background, could be rewarding.

ii) Protease

Sporangia were digested with papain and pepsin using the following procedures based on the work of Weintraub & Ragetli (1968).

Fix 5% GA in P for 1 h.

Wash 2 x 10 min P, followed by 11 h P then 4 x 10 min P.

Incubate in papain (1% BDH No. 2022430 in 0.01 M P, pH 5.5) at 25° C. for 1 h followed by 37° C. for 1 h.

Postfix etc. by the standard procedures

or

Fix 1% GA in P for 1 h.

Wash 10 x 10 min P.

Incubate in pepsin (0.25% BDH powder 1:2500 B.P.C.1959. Product No. 39032 in N/10 HCl) at 37° for ½ h.

Postfix etc. by the standard procedures.

9) Autoradiography

An attempt was made to localise the site of cell wall synthesis using the techniques of pulse labelling and autoradiography at the electron microscope level. The methods were based on Caro & van Tubergen (1962) and Northcote & Pickett-Heaps (1966). The results were of no value in the work on wall synthesis and will not be discussed here. A full description of the methods and problems will be deferred

to the Appendix.

10) Whole Mounts

a) Negative staining

Material was disintegrated with ultrasonics or by crushing with a glass rod. The resulting suspension was mixed with a range of dilutions of negative stain and mounted on formvar coated grids. The drops were dried down to varying degrees with filter paper, air dried and examined. Several stains were used but most observations were made on PTA mounted material. The staining solutions were:-

Potassium phosphotungstate (PTA) 4% aqueous pH 7.01

or Uranyl acetate 2% aqueous pH 5.0

or Uranyl formate 2% aqueous pH 5.0

b) Shadowing

Untreated material or cells degraded with 50% Domestos at 37° C. for 2 h (Parker, Preston & Fogg, 1963) were suspended in distilled water and dried down on formvar coated grids. Shadowing was carried out in a vacuum coating unit (Balzers "Mikro BA3" or A.E.I.) at an angle of 20°- 30° from the horizontal. The shadowing material was a 60% gold palladium alloy (wire, 39 s.w.g. = 0.005" = 0.127 mm diameter. Johnson Matthey) suspended on a V of tungsten wire, or carbon platinum. Carbon platinum was produced by winding about 10 mm of pure platinum wire (0.127 mm diameter from Johnson Matthey)

on a carbon rod (Johnson Matthey Cat. No. JM1B) which was turned to the shape shown:-

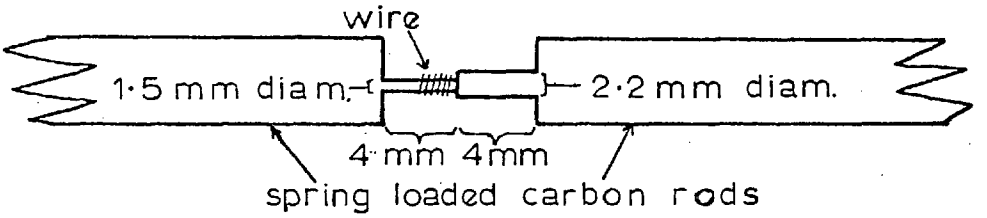

The wire and carbon were evaporated slowly.

c) Scanning reflection electron microscopy

Untreated sporangia in distilled water were dried onto brass foil at 60° C. They were coated with a layer of 60% gold palladium (c 0.02g or 75 mm of 39 s.w.g. with a path length of 150 mm), followed by a layer of carbon. The foil was attached to a specimen planchet with "Durafix" adhesive and examined in a Cambridge "Stereoscan" microscope in the Geology Department of Imperial College by kind permission of Dr. Marjorie Muir. Clearly, the above preparative procedure is unlikely to give good preservation of structure but it proved useful for a rapid survey. A review of more desirable techniques has been given by Echlin (1968).

11) Microdensitometry

Sectioned material frequently contains a granularity which is large relative to the structure under observation. Such granularity obscures the structure and makes objective measurements difficult. Scanning an electron micrograph with a microdensitometer produces a trace showing the "average" distribution of the granules and can be used to obtain objective measurements. The microdensitometer scans an

object with a transmitted beam of light which is focussed onto a slit covering a photocell. The area of the scanning beam is effectively varied by adjusting the size of the slit. Variations in the density of the object are reflected in the current from the photocell which is recorded on a chart recorder. If the beam dimensions are large relative to the granularity, but small compared with the structure scanned, the trace indicates the average density distribution and eliminates the visual confusion of the granules.

The instrument used was a Hilger & Watts recording photoelectric microphotometer in the Applied Optics section of the Physics Department, Imperial College. Electron micrograph plates exposed at instrumental magnifications of 27,390 or 39,190 were scanned with a beam size of 0.1 mm by 0.06 mm (on the plate) at 0.25 mm/min which gave a linear magnification of 202.1 on the recorder chart. Within reason, slit size was uncritical and was chosen arbitrarily to suit the structures measured.

12) Light Microscopy

All observations were made on a Reichert "Zetopan" microscope equipped with phase contrast, anoptoral contrast, interference contrast (Nomarski), polarizing and fluorescence systems. Unless stated otherwise, all micrographs were taken in green light with Koehler illumination, using a time exposure or a Zeiss "Ukatron" flash unit. Images were recorded on Ilford "Pan F" 35 mm film rated at 50 A.S.A. developed in

"Promicrol" (May & Baker) developer diluted 85 ml in 300 ml at 24° C. for 13 min with intermittent agitation. All observations were made on living hyphae mounted in their growth medium unless stated to the contrary.

a) SITS

SITS is the abbreviation used for 4-acetamido-4'-isothiocyanato-stilbene-2,2'-disulphonic acid disodium salt developed by Maddy (1964) as a fluorescent plasmalemma stain.

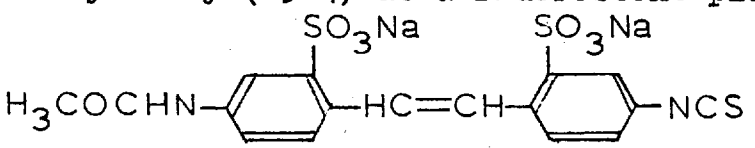

SITS

Fresh material was incubated in 100µM SITS in P for 10 min at 20° C., followed by a brief wash in P, then mounted in P and examined with fluorescence contrast (filters E4 and Sp1) and phase contrast.

b) IKI - H_2SO_4

Fresh hyphae were tested for cellulose distribution by incubating in a 0.2% iodine in 2% potassium iodide solution (IKI) for 15 min at 20° C. They were mounted in IKI and 65% H_2SO_4 was drawn across the coverslip (Jensen, 1962). Cell walls stained blue.

c) Aniline blue

Fresh hyphae were incubated in 0.005% aniline blue in M/15P at pH 8.2 for 10 min then examined in the fluorescence microscope for callose fluorescence (yellow) (Jensen, 1962).

NUCLEAR DIVISION

1) Literature review

Fungal karyology as a whole has been reviewed recently by several authors, e.g. Cutter, 1951; Olive, 1953 & 1965; Robinow & Bakerspigel, 1965. Nuclear division usually involves an intranuclear spindle, chromosomes and a persistent nuclear envelope. There are, however, numerous variations in the fate of the envelope, the form of the spindle and the presence and structure of the centrioles and asters. In a few groups, no features of a normal mitosis have been satisfactorily observed; these divisions are still termed "direct," a descriptive term introduced by Fleming in 1879. The fungi are probably polyphyletic; the variations in their mitotic processes are too numerous and heterogeneous to be usefully described in detail here. This review will centre on the controversy concerning mitosis in the Saprolegniales; a wider comparison with some of the relevant literature will be deferred to the discussion.

In 1895, Hartog described a vegetative mitotic process in Saprolegnia spp involving four chromosomes but no spindle. (The term spindle had been introduced by Fol in 1877 and chromosome by Waldeyer in 1888). In the same year, Trow (1895) disputed this and claimed the absence of any type of mitosis, describing the vegetative divisions as direct, involving a single sponge-like "chromosome" with a persistent nuclear envelope as opposed to the oogonial divisions where

the envelope broke down. In 1923, Smith studied S. dioica hyphae and described an amitotic division with the chromatin remaining attached to the envelope. He suggested that the nucleolus played an active role in division.

However, around 1930 several authors described true mitotic divisions in the oogonia of a variety of Saprolegniales. Oogonial muclei are generally larger than those of the hyphae and, for example, Mäckel, (1928) working on S. thuretii and S. mixta, and Cooper (1929) on Achlya hypogyna figured chromosomes, asters and spindles. Höhnk (1935) described asters, spindles and seven chromosomes in the oogonia of S. ferax but could not detect centrosomes, centrioles or "Zentralkörperchen." In contrast, Raper (1936) showed a dark centrosome at each pole of the spindles in Achlya spp oogonia and Shanor (1937) found similar structures with well marked asters in Thraustotheca sp. None of these authors detected spindles or chromosomes in vegetative nuclei.

Recently Bakerspigel (1960) examined vegetative mitoses in a number of Saprolegniales, including S. ferax. He supported Smith's (1923) work by showing the absence of spindles, chromosomes and metaphase plates. Slifkin (1967) employed a traditional mitotic "poison," colchicine, in work on S. delica. She showed that whilst the oogonial mitoses were blocked, the hyphal divisions were unaffected, once again suggesting a form of amitosis. This work emphasised the earlier findings which suggested that the mechanism of

division is different in the oogonia than in the hyphae. Classically, the protozoans are thought to have different types of division of their macro- and micro- nuclei. Similarly, the large nucleus of Acetabularia is assumed to fragment "directly" to give smaller nuclei which then divide mitotically. However, there is no evidence from recent electron microscopy of any division not involving some form of microtubular spindle. For example, Carasso & Favard (1965) and Jenkins (1967) show microtubules in the spindles of Peritricha and Blepharisma micronuclei. Similarly, the yeasts have for long been said to undergo amitosis, yet Robinow and Marak (1966) and Moor (1966b)have clearly demonstrated a form of mitotic spindle.

Among the few phycomycetes examined with the electron microscope, microtubular intranuclear spindles with polar centrioles have been reported for Albugo, Allomyces, Catenaria and Blastocladiella (Berlin & Bowen, 1964; Robinow & Marak, 1966; Ichida & Fuller, 1968; Lessie & Lovett, 1968). The observation of centrioles in S. ferax by Gay & Greenwood (1966) together with the absence of critical ultrastructural reports of "direct" divisions suggest that a re-examination of the vegetative nuclear divisions in this organism with the electron microscope is necessary.

2) Observations

a) Interphase

When viewed with positive phase contrast, the living

vegetative nucleus is seen as a variously ovoid light region with a diameter of about 3.5 µm. This region is enclosed by a thin, dark envelope which is connected to an irregular 2.5 µm diameter central mass by fine, dark radial strands (Fig. 14). The central mass is usually eccentric and is probably the nucleolus (Bakerspigel, 1960). The nuclei are in fairly constant motion but do not move as fast as the cytoplasmic stream. Their distribution along the hyphae has not been studied in detail but they are rarely observed closer than about 15 µm to the apex. How this distribution and movement is controlled is a complex problem that awaits solution; however Girbart (1968) has shown nuclear motility to be associated with microtubules in Polystictus and there are indications of a specific nuclear envelope-microtubular interaction in S. ferax (see Karyokinesis).

The general shape and size of the nuclei are little changed by the preparative procedures for electron microscopy

. The envelope consists of a pair of membranes separated by a fairly uniformly wide electron pale perinuclear space which is often seen to be continuous with cisternae of the E.R. (Figs. 24 & 45). After GA/Os and permanganate fixations, the envelope has a smooth outline; Os alone (Fig. 15) often produces a very irregular profile which, especially in view of Moor & Mühlethaler's freeze-etch work (1963), is probably an artefact. Since GA/Os gives the best preservation of microtubules and general cell structure, the

following descriptions are based primarily on material fixed in this way.

The nuclear envelope is perforated by numerous nuclear pores of approx. 100 nm diameter which are often plugged by an electron dense material similar to that described in other oomycetes by Bracker (1967) (Figs. 17, 18, 19, 24). Tangential sections of the pores of S. ferax show no radial symmetry as is often found in many other organisms, e.g. De Zoeten (1969). The distribution of the pores in the envelope is not uniform. Clusters can occur with as little as 55 nm between adjacent pores (Fig. 16) or single pores can be widely spaced. Moor & Mühlethaler (1963) have noted similar irregular pore distributions in freeze-etch work on yeast cells; they suggest that the clumping is more common in old cells. There are insufficient observations on S. ferax for further comment.

The nucleoplasm consists of a finely granular low electron opacity matrix containing electron dense particles which resemble cytoplasmic ribosomes in both size and shape. The nucleolus appears to have a more dense matrix and a higher concentration of ribosome-like particles. The radial dark lines seen with the light microscope are not seen in sectioned fixed material.

Colonies growing at 30° C. have a slightly increased growth rate compared with those at 25° C. but are morphologically normal. However, the nuclear ribosomes are absent and

the nucleolar matrix material appears to increase and fragment to produce the irregular dense material shown in Fig.120. This is reminiscent of the stipled nucleoplasm described by Hartog (1895).

In order to determine which of the nuclear components contains the RNA, the effects of different combinations of electron microscope stains were examined. Unstained GA/Os fixed sections (Fig. 17) show the cytoplasmic ribosomes to be more dense than the nuclear ones which have a similar density to the nucleolar matrix. Huxley & Zubay (1961) have shown that uranyl acetate can preferentially stain nucleic acids. When sections of S. ferax were stained in UAc alone, no preferential staining could be detected; there was an equal increase in contrast in all osmophilic structures (Fig. 18). A similar result was obtained with Pb alone (Fig. 19), and the usual combination of UAc followed by Pb further enhances contrast but does not alter the relative density of different structures compared with unstained sections. RNAase digestions also failed to reveal any concentrations of RNA (Figs. 8 & 9). Sections treated with the PAH process gave a heavier reaction over the nucleolus relative to the nucleoplasm (Fig. 20) but this is not due to nucleic acids since Hotchkiss (1948) has shown that both RNA and DNA are PAS negative. This result presumably indicates a higher concentration of compounds containing vic-glycol bonds in the nucleolus. Thus it is not possible, at present, to define

the site of nucleolar RNA in the nuclei of S. ferax.

External to the nuclear envelope there are three structures whose close and constant association with the nucleus warrants a description here. Polyribosome chains are found on the envelope at all stages in the division cycle (Figs. 21, 18). No attempt has been made to determine their relative abundance at different stages in division since there is no clear definition of these stages nor is it possible to identify a polyribosome cluster with accuracy in other than surface sections of the envelope. Tucker (1967) has suggested that the number of polyribosomes on the envelope of Nassula increases at anaphase-telophase, thus implicating them in membrane synthesis (see discussion of Karyokinesis). Their presence at all stages in division in S. ferax may be an indication of continual membrane synthesis; more generally it may be accepted as evidence that the nuclear envelope is active in protein elaboration, thus emphasising that it is functionally as well as structurally a part of the E.R.

In S. ferax, Golgi bodies are usually found associated with the E.R. This has been discussed fully in other sections of this thesis (Wall Formation and Flagellum Formation). It is sufficient to mention here that no more than two bodies have been found associated with one nuclear profile and the association can be found at all stages of division. The envelope under the Golgi bodies can contain nuclear pores and is frequently seen forming vesicles by

evaginations of the outer membrane towards the Golgi (Figs. 22 & 44). This particular association is further evidence of a common function of the E.R. and nuclear envelope throughout interphase and division.

The third structure associated with the nuclear envelope is the centriole. Since these play a major role in nuclear division, their structure and function will now be considered in detail.

b) Centriole structure

A pair of centrioles is associated with each interphase nucleus. Due to their relatively small size they are not seen in many sectioned nuclear profiles, but the presence of paired centrioles with no vestige of a spindle (Figs. 23 & 24) is consistent with their retention throughout interphase. There are reports of centrioles forming in the absence of parent centrioles (Schuster, 1963; Dingle & Fulton, 1966). This implies a cycle of breakdown during interphase and resynthesis at prophase. There is no evidence that this occurs in S. ferax where centrioles always appear to be formed in close association with a pre-existing centriole or kinetosome.

Since the centrioles have the same structure as the proximal end of the basal body or kinetosome in S. ferax, and since all other organisms in which these features have been investigated show a similar homology, they will be considered as one organelle.

Each centriole consists of a cylinder of nine groups, each of three tubules. Following the notation of Gibbons & Grimstone (1960), the tubules in each group will be designated A, B and C from the innermost out (Fig. 33). When viewed from the proximal end (Fig. 36), each group is seen to lie at 45° to the tangent in an anticlockwise direction from A to C, which is the orientation reported for all centrioles and kinetosomes in which this feature has been determined. The overall diameter of the centriole is about 0.2 μm, similar to that reported for other centrioles; the length, 0.2 μm, is comparable to that of most fungi (Berlin & Bowen, 1964; Renaud & Swift, 1964; Lessie & Lovett, 1968; Ichida & Fuller, 1968), but shorter than those of animals which range from 0.4 to 0.6 μm (Pollister & Pollister, 1943; Brinkley, Stubblefield & Hsu, 1967; Robbins & Gonatas, 1964).

The A, B and C tubules have different lengths, A (200 nm) is the longest, B is fractionally shorter and the C tubules are about 20 nm shorter than A (Figs. 23, 24, 30, 34 & 35). These differences are constant at the proximal end, and together with a slight chamfering of the ends of the B and C tubules, give rise to the characteristic proximal wedge shape (Figs. 23 & 24). The distal end may have a similar wedge shape (Figs. 47 & 48) but the length differences of the B and C tubules at this end are variable, perhaps as a function of tubule synthesis (see centriole replication).

The lumen of each tubule has a low electron opacity but

may occasionally contain a little amorphous material. No limiting structure is preserved at the ends of the tubules which thus appear in open contact with the cytoplasm.

The diameter of the tubules measured from sections is approx. 25 nm external and 12 nm internal, similar to that reported for most microtubules. The tubule walls consist of apparently irregularly arranged isodia-metric light and dense subunits in a matrix of medium density. Ringo (1967a) and Ledbetter & Porter (1963) have reported that the walls of the microtubules in Chlamydomonas flagella and Juniperus root cells are composed of ordered light subunits in a uniform dense matrix. Moor (1966b& 1967), using freeze etch surface replicas of fractured yeast tubules, describes a double helical array of dense subunits enclosing 12 clear spaces in the centre of the wall (Fig. 81). Either arrangement may exist in the tubules of S. ferax; the irregular arrangement of subunits described above might be expected in view of the thickness of sections relative to the size of the subunits, but may also be the result of fixation. If the latter is the case, the irregular pattern may represent either the preservation of the light subunits intact and the aggregation of the dense matrix into discrete particles or a simple disorganisation of the subunits on Moor's interpretation. These hypotheses would be more reasonable if the apparently irregular subunits of the wall were to give an "average" wall structure comprising a light centre of fairly uniform width enclosed by two dense

regions. One method of measuring such an "average" structure is to scan a section of the wall with a microdensitometer whose slit is fairly wide in relation to the particles in the wall. Such measurements were made on the walls of flagella tubules, since clear transverse sections of these have been obtained in greater numbers than centriole tubules. It is assumed that the tubules in both situations are homologous since they are continuous with each other and have a similar appearance in section. The results of the microdensitometer scans are shown in Table 1.

Table 1

Measurements taken from densitometer tracings of sectioned microtubules

Distances in nm between:-				
Inner peaks	Troughs	Outer peaks	Peaks of one wall (i.e. wall thickness)	Type of tubule
15.6	17.2	21.6	3.0	Flagellum A
18.4	22.0	24.2	2.9	" "
17.9	22.2	26.4	4.3	" "
12.0	14.1	17.9	3.0	Flagellum B
17.0	19.2	22.6	2.8	Flagellum central pair
15.6	19.4	22.4	3.4	Flagellum central pair
17.9	22.6	24.0	3.2	Spindle tubule
16.2	19.7	23.1	3.5	" "

Distances between peaks of tubules in the E.R (nm)

9.9	9.4	7.6	9.6	7.4
8.5	7.8	7.8	6.9	8.3

A typical trace, e.g. Figs. 38 & 39, shows that the wall is composed of two dense layers enclosing a lighter region with an average width of about 3 nm. Fig. 38 also shows that the wall between two tubules has the same structure as the free walls. A scan along a longitudinally sectioned tubule showed no regular periodicity.

Most reported centrioles have some form of connecting structure, usually a thin lamella, between the A and C tubules of adjacent triplets (e.g. Gibbons & Grimstone, 1960; Gall, 1961; Ichida & Fuller, 1968; Lessie & Lovett, 1968; De Harven, 1968). Similar clear connections have not been found in S. ferax although there are occasional traces of a simple A-C linkage, e.g. Fig. 30.

The proximal region of the centriole contains a structure described by Gibbons & Grimstone, (1960) as a "cartwheel." The cartwheel in S. ferax consists of a 20 nm diameter, 130 nm long tubular hub, apparently without an "axel-pin" as described by Olson & Fuller (1968) (Figs. 30, 34 & 36). The hub is connected to the A tubules by nine straight radial "spokes" composed of thin lamellae with a thickened proximal end. The spokes have the same length as the hub and both end proximally at the same levels as the A tubules. A dense swelling is seen on each spoke at a radius of about 45 nm (Fig. 30). In some sections there is evidence that these swellings, which appear to run the full length of the spoke, are connected to form a ring Figs. 28 & 36). The appearance of a ring is enhanced in some

sections, e.g. Fig. 28, because the triplets are embedded in a dense matrix which terminates at the same radius as the bars, leaving an inner clear area between the spokes. This dense matrix can become more prominent at times, probably coinciding with the formation of cytoplasmic microtubules (Fig. 45). There is no evidence for the presence of "satellites" (De Harven, 1968) or well developed dense halos (Gall, 1961) in S. ferax.

The region defined by the triplets above the cartwheel contains amorphous material from which ribosomes are excluded. There is no preserved structure across the distal end to separate the cytoplasm from the centriole centre.

Centrioles are always found in pairs aligned at about 180° to each other with proximal ends facing (Figs. 23 & 24). The orientation is fairly rigid; members of a pair are rarely more than 20° out of line. Although there is no preserved electron dense material connecting adjacent centrioles (Fig. 29), the gap between them is constant at about 20 nm. The centrioles in S. ferax appear to be identical to those Albugo (Berlin & Bowen, 1964), the only other reported instance of paired centrioles aligned at 180°, in contrast to the otherwise universal orientation of 90°.

Paired centrioles always lie in a well-defined pocket in the nuclear envelope (Fig. 30). This pocket has the form of a 0.5 μm diameter, variously deep invagination of the envelope and is usually free of nuclear pores. The nuclear membranes

forming this pocket have an increased density and a less undulating profile, and are spaced at a very constant distance apart. The constancy of the inter-membrane space may be a function of the bars of material in Fig. 30. The space between the pocket and centrioles has a fairly constant width of about 70 nm, is moderately dense and free of ribosomes. Microtubules are rarely found in this area.

Apart from changes in the dense matrix, the structure, mode of association, and orientation of the centrioles does not alter at any stage in somatic interphase or division except during the process of centriole replication.

A brief examination of S. furcata suggests that this species has similar centrioles to those of S. ferax.

c) Centriole replication

At the end of interphase the centrioles dissociate and move a short distance apart. A daughter centriole then develops on the proximal end of each parent; such development is well advanced at the earliest stage of replication yet detected, (Fig. 43), when the parents are only about 0.3 µm apart. At this stage of replication, although not seen with great clarity, the daughter centrioles appear to have full width cartwheels with hubs and spokes, yet these cartwheels are only about 60 nm long. The arrowed pair (Fig. 43) unequivocally shows an extension of the parent hub connected to that of the daughter and it can also be seen that the proximal edges of the new spokes are as dense as those of the parents.

The short A and B tubules already show the proximal wedge shape, C tubules appear to be absent. The plane of section appears to be exactly parallel to the long axis of all four centrioles, showing that the daughters are orientated very close to the 180° position. One pair (arrowed) shows that the A tubules of parent and daughter are exactly in register. There is no direct connection between parent and daughter tubules, nor is one to be expected since both centrioles have their triplets arranged anticlockwise. Thus triplets of the new centriole lie at an opposed tangential angle to those of its parent as shown in Figs. 25 & 32.

Replication is apparently synchronous (c.f. Gall, 1961; Kalnins, 1968) and is completed at one pole as shown by the four centrioles in Figs. 47 & 48. These daughter centrioles appear to be nearly mature; they have C tubules and each pair has its own nuclear pocket, yet the mid-points of the pairs are still only about 0.37 μm apart. Fig. 46 clearly shows the presence of numerous microtubules radiating out from the region of the centrioles over the surface of the nucleus into the cytoplasm and Figs. 23 and 44 suggest that these are also present during at least part of interphase.

d) Centriole migration

Migration of the paired centrioles to opposite poles begins with centriole replication; they continue to move further apart as the spindle elongates; migration is not complete until two daughter nuclei are formed. Thus Figs. 49

and 50 are early stages in this migration; the figures ascribed to metaphase and telophase are later stages in which centrioles are further apart. The nuclear envelope pocket is associated with the centrioles throughout migration. During migration, the cytoplasmic microtubules which radiate from the one pole at the time of centriole replication become rearranged so that at an early metaphase stage (e.g. Fig. 51) they radiate from both poles. They run along the nucleus towards the opposite pole and also in the opposite direction away from the centrioles into the cytoplasm. Harris (1961) and others have shown that the asters seen with the light microscope in many organisms are composed of microtubules intermingled with vesicles. Microtubules are abundant in the cytoplasm of S. ferax during nuclear divisions but are rare during interphase. This distribution, together with the known association of many of them with centrioles, suggests that they may all be described as astral tubules. This term will be used here to distinguish them from cytoplasmic microtubules of other plants which are in many cases not associated with centrioles (Porter, 1966). There are apparently less than about twenty astral tubules at each pole of vegetative mitoses in S. ferax. This low number and the absence of vesicles is probably the reason for the light microscopists' failure to detect asters in vegetative mitoses of Saprolegnia. Presumably, the prominence of asters in oogonial mitoses indicates that the tubules are more numerous, perhaps more reactive to stains, and

possibly associated with vesicles. The astral tubules in the hyphae appear to have some rigidity since they show only slight undulations and are not deflected sharply around organelles. Further evidence for the rigidity of microtubules is shown in Fig. 56 where flagellum tubules do not bend sharply without breaking as also shown by Gall (1966) and Grimstone & Klug (1966).

There is no evidence to show whether both or only one centriole migrates since there is no known stationary marker on the nuclear envelope. However, as all centrioles are identical, it is likely that the stimulus and mechanism of migration affects them equally, causing both to migrate as suggested by Aist (1969) for Ceratocystis and Fusarium.

e) Spindle formation and structure

In this thesis the term spindle will be restricted to the group of microtubules (otherwise termed spindle fibres in the literature) inside the nuclear envelope as described below. The chromosomes will not be considered as part of the spindle. From the beginning of centriole migration the spindle forms between the separating envelope pockets (Figs. 49 & 50). It is composed of 25 nm diameter microtubules which appear identical to cytoplasmic, flagellum and centriole tubules when examined in section (Fig. 52) or with the microdensitometer (Fig. 39). The spindle tubules terminate at the poles in a region of amorphous osmophilic material adjacent to, and not extending beyond, the inside of the pockets (Fig. 30). This

region is about 30 nm thick with most of the material concentrated around the ends of the tubules, each of which appear splayed out into it. There is an increased quantity of this material and of the osmophilic material around the centrioles in cells in which microtubule formation has been blocked by colchicine (Fig. 55). At the equator of the spindle the tubules are about 80 nm apart, they converge to be about 20 nm apart at the poles where they rarely terminate outside the region of the pockets. As the centrioles migrate, so the spindle elongates and acquires more tubules. The full complement appears to be reached by metaphase when there are about 15 pole-to-pole tubules and a further 20 from each pole to the equator (Fig. 54). These numbers are approximate since insufficient serial sections have been observed; however, they indicate that in all examples seen, about 40 tubules must be inserted at each pole. Since the diameter of the tubules is about 25 nm and they are about 20 nm apart at the poles, an estimate of the area needed for the insertion of forty tubules can be obtained by considering them as circles of diameter 45 nm. The area of the pocket can be approximated to that of a circle of 0.5 um diameter which is about 19 x $10^4 nm^2$. The combined area of 40, 45 nm diameter circles is approximately 6 x $10^4 nm^2$. There is clearly sufficient room for this number of tubules all to terminate within the pocket area as observed.

The absence of detectable chromosomes makes the definition of metaphase difficult; however, in the equatorial region there

are often specialised terminations of some tubules from both poles (Figs. 52, 53, 58, 59 & 63). These terminations are composed of a transverse disc of material about 70 nm diameter by 27 nm thick on the end of the tubule, connected to a similar parallel disc about 27 nm away. The two discs are joined by thin strands of dense material (Fig. 59). The second disc is associated with a slightly dense ill-defined region which is probably a chromosome, thus making the double disc structure a kinetochore or centromere. No more than one tubule has been found on a kinetochore; a finding consistent with the normal absence of grouping of tubules when seen in transverse section. The presence of kinetochores on the equator of the spindle will be used as a criterion of a metaphase condition.

Since the spindle is always contained inside the persistent nuclear envelope (Figs. 61, 63 & 64) and is accompanied by external centrioles, it may be termed "closed-centric" using Jenkins (1967) terminology. Figs. 48 and 57 suggest that centriolar structure, mode of division and migration in D. sterile are identical to those of S. ferax.

f) Chromosomes

In most plant and animal nuclei including the phycomycetes (Ichida & Fuller, 1968) chromosomes stain heavily after GA/Os and UAc/Pb staining. Bryan & Brinkley (1964) devised a preferential stain for chromosomes. Neither treatment has shown clear chromosomes in S. ferax, similarly DNA ase digestions produced no areas of lower density in the nucleus.

Furthermore, Kellenberger, Ryter & Séchaud (1958) developed a fixation procedure for the preservation of DNA in bacteria. This fixation gave very poor results with S. ferax and failed to show chromosomes. The only indication of chromosomes seen in S. ferax is the slightly dense material attached to the kinetochores at metaphase and the similar rather dense regions near the poles in Fig. 65. (See also Fig. 60). The localisation of such areas at the equator of a short spindle, then at the poles of an elongated one is consistent with the general behaviour of chromosomes in mitosis.

Fig. 62 shows one of the rare instances of nuclei which contain regions of highly electron dense granular amorphous material. Such material is divided into irregular regions and, in some cases at least, is arrayed in a ring around the nucleolus with very little included in the spindle. Such examples are rare; it is possible that a temperature fluntuation has produced a fragmentation of the nucleolus as found in 30° C. cultures, but this is unlikely as the material is much darker than that of the nucleolus which is apparently normal. The ringed arrangement is reminiscent of the distribution of chromatin, described by Bakerspigel (1960) for this same organism.

g) Karyokinesis

This section describes all post-metaphase nuclear activity through to interphase. Few favourably sectioned post-metaphase nuclei have been observed; however Figs. 65 & 60 suggest that

the chromosomes become polarized. The latest stage of division detected (Fig. 66) shows that all the pole to pole tubules remain but are considerably elongated. This elongation may be responsible for the separation of the chromosomes as suggested by Ichida & Fuller (1968). It is not possible at present to say if separation is aided by the shortening of the pole to chromosome tubules, nor is their time of breakdown known. At no stage in the division cycle are the centrioles situated at the extremities of the nucleus itself; they are, however, always at the poles of the spindle. The nucleus usually extends beyond the centrioles in the form of more or less pointed projections which are frequently closely associated with the astral microtubules (Figs. 67 & 68). The association of nuclear envelope and astral tubules is apparent from early metaphase (Fig. 51) through anaphase (Figs. 67 & 68) and possibly into interphase (Figs. 69 & 70). The space between the nuclear envelope and an associated microtubule is fairly constant at about 8 nm and is often traversed by thin strands of material not seen in larger clear areas around some microtubules in the cytoplasm. Nuclear pores have not been found in regions of the envelope associated with a microtubule. A similar close association has not been seen between microtubules and other organelles such as mitochondria or cisternae of the E.R., although the former can lie along microtubules.

The nucleolus persists throughout division; it is more or less spherical and eccentric to the spindle at metaphase but

becomes dumb-bell shaped before it is presumably divided at the median constriction to form two more or less equal sized daughter nucleoli (c.f. Smith, 1923; Bakerspigel, 1960).

The opposite ends of the nucleus move further apart until two daughter nuclei are produced. The mechanism of the separation of the daughter nuclei is unknown. Moore (1964) has described a process of division whereby the inner membranes of the nuclear envelope in the isthmus region constrict, then fuse, followed by a similar process in the outer membranes, thus forming two nuclei. Fig. 72 may be an example of this process, but the shape of the nuclei suggests they are not dividing. As this configuration has only been seen in permanganate fixation (Fig. 72 and Moore 1964), it may represent membrane fusions caused by the fixative, but a similar situation probably exists prior to the separation of daughter nuclei.

After the daughter nuclei have separated, the spindle tubules shorten and eventually disappear. At all stages in their breakdown, one end of each tubule is associated with a nuclear pocket. This may mean that the tubules are depolymerised from the non-polar end only. If they are also, or alternatively, only, broken down at their polar ends, there must be some mechanism for moving them towards the pocket to maintain their close association

with it, and the pole-to-pole tubules must become severed before such a process. Robbins & Jentzsch (1969) have recently shown that the spindle tubules in Hela cells break down preferentially at the poles.

Nuclear division has not been observed with the light microscope, thus its time course is not known; however, it is probably similar to the 5-10 min. found by Aist (1969) in Fusarium and Ceratocystis.

A vegetative colony of about 25 mm diameter grown at 25° C. was found to have all the nuclei in eight hyphae selected at random around its edge in similar stages of nuclear division. There was no known stimulus applied to produce this synchrony suggesting that synchronous nuclear division may be a regular occurrence in this organism. Contrary to the findings of Trow (1895) and Smith (1923), apparently normal mitotic figures have been found in sporangia delimited by a complete cross-wall (Fig. 65).

h) Colchicine treatments

Slifkin (1967) has shown that a 2.5×10^{-3} M (0.1%) colchicine solution does not inhibit nuclear division in vegetative hyphae of S. delica yet presents good evidence (Slifkin, 1968) to show that it penetrates the cell walls. However, she also shows that this concentration does inhibit oogonial mitoses. Zoospores pass from a uninucleate to a multinucleate state during germination, thus presenting a source of mitotic figures at various stages within a small population.

Consequently, this material was used to determine the effect of colchicine on the structure of the mitotic spindle of S. ferax. Populations of zoospores germinated in OM with or without colchicine show two types of spore after fixation. Some spores, both before and after germination, have a similar appearance to the vegetative hyphae; such an appearance will be termed normal. However, the most common type appears very dense and structures such as membranes and ribosomes which normally contrast with the pale "background" are less well contrasted, apparently due to an increase in staining of the "background," (Figs. 71 & 73). This increase in background density is probably due to the retention of cytoplasmic material normally lost during fixation. There are, of course, spores which appear to be intermediate between these two "types," but most can readily be identified as "dense" or "normal." Primary and secondary zoospores can be identified by their surface ornamentation (see Encystment). Both can be normal or dense.

Dense sporelings germinated in colchicine contain apparently normal mitotic spindles; the spindle tubules, centrioles and astral tubules are all similar to those of untreated sporelings even after several mitoses (Figs. 71, 73, 74 & 75).

The only microtubules found in the normal sporelings after colchicine treatment are those of the centriolar triplets (Fig. 55). Many nuclear profiles show loose bundles containing numerous 8 nm electron dense solid fibrils (Fig. 80). Such bundles can be up to about 3 um long and are often found

orientated at right angles to each other (Figs. 78 & 79). Bundles frequently push the nuclear envelope out into a tongue-shaped projection (Fig. 77). Smaller bundles of similar fibrils can rarely be found in the cytoplasm (Fig. 76). Results are the same if either 2.5×10^{-3} M (1.0%) or 5×10^{-3} M (2.0%) colchicine is used.

3) Discussion

The above results show that there are many interesting and unusual features of the mitotic process in S. ferax. Some have been discussed briefly already, other more controversial or complex aspects will be discussed below.

a) Centriole structure

The present observations show that S. ferax, S. furcata and D. sterile are typical of the flagellate phycomycetes, and most organisms with a flagellate stage in their life cycles, in possessing a pair of centrioles throughout their nuclear cycle. Ichida & Fuller (1968) and Lessie & Lovett (1968) have shown that the monoflagellate Chytrids and Hyphochytrids also possess two centrioles but one is considerably shorter than the other. Olson & Fuller (1968) show that the small centriole plays no part in flagellum formation and suggest that it is a vestigial organelle indicating a biflagellate ancestor for the monoflagellate phycomycetes. Since Saprolegnia and Albugo (Berlin & Bowen, 1964) possess a pair of identical centrioles, both active in flagellum formation, it is reasonable to believe that their centriolar condition may represent that of the

primitive biflagellate ancestors of the uniflagellate fungi. It should be remembered, of course, that both biflagellates and uniflagellates have probably evolved from a common ancestor whose centriolar characters were those retained by Saprolegnia and Albugo. Perhaps a further ancestral feature retained by the oomycetes is the 180° orientation of the paired centrioles; all other groups of organisms which possess centrioles have the 90° orientation. The significance of this difference in orientation is best seen in connection with centriole replication. The length of the oomycete centrioles may also indicate an ancestral arrangement. In most reported animal cells, for example, (Pollister & Pollister, 1943; Brinkley, Stubblefield & Hsu, 1967), the centrioles are about 0.4 - 0.6 μm long. This is approximately the length of the kinetosomes which the fungi form prior to flagella production. Possibly the process of evolution has favoured a system in which kinetosomes are not built up and broken down at different stages of the life cycle; they are retained full size at all stages, thus eliminating one process of cellular control. However, if the kinetosome tubule subunits are identical to, and interchangeable with, those of the spindle tubules, as they appear to be, then, it could be argued, that to retain full size kinetosomes is a "waste" of subunits; possibly the system in the fungi is more economical in re-using the kinetosome subunits as spindle tubules when flagella are not required.

A further example of the diversity of evolution of centriolar

systems is shown by the fact that not all flagellate organisms studied have been shown to possess paired centrioles. Renaud & Swift (1964) claim that Allomyces (chytrid) only has one centriole per nucleus during interphase, and King & Butler (1968) were unable to find any in Phytophthora (oomycete). Negative evidence is not always convincing; perhaps a re-examination of these species would show them to fit the general pattern of the phycomycetes. There are, however, well documented reports of some other groups which present exceptions to the general pattern of flagellate organisms. Manton & Von Stosch (1966), for example, show only one flagellum without a vestigial kinetosome in Lithodesmium. Macronuclear (Pitelka, 1963) and micronuclear mitoses (Jenkins, 1967; Tucker, 1967) of many protozoa are accomplished in the absence of polar centrioles and several authors (Schuster, 1963; McManus & Roth, 1968; Dingle & Fulton, 1966; Aldrich, 1967, for example,) have been unable to find centrioles in the mitoses and meioses of various myxomycetes. The functional implications of these exceptions will be discussed later; here it is interesting to note that whilst most flagellates have retained or evolved the feature of polar centrioles, some groups have survived successfully without this feature; the evolutionary significance of either arrangement is obscure.

However, whilst there is variation in the presence, size and orientation of centrioles in different organisms, the basic structure is remarkably constant. All centrioles and

kinetosomes examined with the electron microscope are composed of nine groups each of three tubules with a similar organisation. This uniformity of structure has led Sagar (1967) to suggest that centrioles and kinetosomes originated by the pro-karyotic acquisition of a "9 + 2 homologue" symbiont, originally as an aid to motility and later this became involved in nuclear division. There are, however, many anomalies in her general theory.

As mentioned above, the walls of the centrioles are composed of groups of microtubüles. These tubules are continuous with those of the flagellum axoneme and are morphologically similar to spindle and astral microtubules. It will be assumed that all have the same general structure although the centriole tubules appear to be more resistant to colchicine. The structure of the walls of these tubules is the subject of considerable controversy. Ledbetter & Porter (1963) and Ringo (1967a), working with sectioned material, suggest they are composed of about thirteen 4 nm diameter electron translucent subunits in a dense matrix. Grimstone & Klug (1966), Pease (1963), Barton (1967) and others, using the negative stain technique, described the walls as composed of from 10-13 linear fibrils consisting of rows of about 4 nm spherical subunits with a 5-6 nm centre to centre spacing between adjacent fibrils. Moor (1966a& 1967), however, described the spindle tubules of frozen etched yeast cells as having a wall of about 8 nm thickness built up of two concentric

cylinders of 4 nm diameter subunits arranged helically in such a way that they also form linear rows (Fig. 81). Moor's model suggests that the tubules thus have two rows of dense subunits with 10, 12 or 14 spaces between them corresponding to the single row of light subunits proposed by Ledbetter & Porter (1963) and Ringo (1967a). The granular nature of the walls of the tubules in S. ferax and the densitometer tracings suggest that they have a structure similar to that described by Moor; fixation may have disordered the subunits slightly, producing the observed structural and dimentional variations. There is further evidence that the structure proposed by Moor (1966a) is the correct one. Negatively stained tubules frequently show a double wall structure with small, isodiametric, periodic regions of stain between the two layers, e.g. Grimstone & Klug (1966).

Mazia (1967) has shown that spindle tubules dissociate into dimer subunits on isolation and Shelanski & Taylor (1968) report similar dimers in Chlamydomonas flagella. Mazia has shown that these dimers are composed of two subunits of the order of 3 nm in diameter connected by a single sulphydryl bond. He has also shown that the spindle has numerous weaker hydrogen bonds. If the adjacent subunits in the inner and outer layers of Moor's model were linked by the sulphydryl bonds and these units linked to their neighbours by the weaker bonds, it would explain the coherent structure of the wall and its tendency to only break into fibrils in negative stain. Furthermore, Jones & Lewin

(1960) and Shelanski & Taylor (1968) have determined the amino acid composition of the tubule proteins. They show it is very similar to that of elastic fibre fibrils and considerably different from the amorphous material in this tissue (Ross & Barnstein, 1969). Greenlee, Ross & Hartman (1966) show these microfibrils stain strongly with cationic lead and uranyl stains in contrast to the amorphous material which stains only with anionic phosphotungstic acid. Assuming a similar amino acid composition gives a similar staining reaction, one would expect the tubule subunits to appear dense in sectioned material as postulated by Moor (1966), not light as described by Ledbetter & Porter (1963) and Ringo (1966). Moor (1966a) presents good evidence for the helical structure; this is perhaps supported by the diagonal banding shown in some tubules by Grimstone & Klug (1966); furthermore, Tilney & Porter (1967) have suggested the normal microtubules in Actinosphaerium sp are contracted in the cold by re-organisation into a helical pattern possibly indicating a subunit whose structure preferentially links helically.

Whilst there is doubt over the structure of the wall, there can be little doubt that the walls between adjacent tubules in the centrioles are shared. This is clearly shown by the densitometer scans of S. ferax, which are in agreement with the sections shown by Ringo (1967a), and the negatively stained disintegrated centrioles and flagella reported by Wolfe (1968) and Phillips (1966).

The arrangement of the triplet tubules is constant in all organisms studied which suggests there is some common rigid structure responsible for their disposition. There are three structures frequently encountered which could fill this role, namely the cartwheel, the AC links, and the dense material in which the tubules are embedded. Morphologically, the cartwheel appears well suited to this task. The dense bars of material on the spokes are probably the remains of a poorly preserved cylinder as shown by Gall (1961) and others, although the numerous reports of bars as opposed to a cylinder (e.g. Berlin & Bowen, 1964; Lessie & Lovett, 1968; Manton, 1964a) makes this conclusion rather speculative. If the bars are a cylinder in vivo, the cartwheel has both radial and lateral structures which make it suitable for giving form to the centriole. However, Brightman & Palay (1963) have shown apparently normal flagella which lack a cartwheel and Hoffman (personal communication) suggests that the cartwheels degenerate in Oedogonium zoospore flagella. Furthermore, if zoospores of S. ferax are strongly plasmolysed, the flagella become very contorted yet the kinetosomes remain unchanged throughout their entire length although the cartwheels are only present in the lower third. Clearly, the cartwheel is not the sole structure retaining the shape of the centriole, though it probably determines it initially. (See "Centriole replication").

Most organisms show some form of lamellate linkage between adjacent triplets which could easily retain the shape of the

centriole. However, Gibbons & Grimstone (1960) show that at least in some flagellates, these links are part of a complex network system probably responsible for some form of inter-kinetosome coordination. De Harven (1968) has shown the links to be part of a complex extension of the cartwheel system; however, the majority of kinetosomes studied appear to have separate cartwheels and links. The links in most cases extend for the full length of the kinetosome and could shape its entire length. The present work has not clearly demonstrated any A-C or similar links; there are, however, traces and their almost universal occurrence suggests that they probably exist in S. ferax but have not been preserved by the fixatives used. At present it is not possible to decide between a coordinating or a structural function for the A-C links though Gibbons & Grimstone's (1960) conclusions support the former hypothesis.

The triplet tubules are often embedded in a dense matrix which could easily maintain the shape of the centriole; however, this matrix is not always present and there is evidence, discussed later, that it represents disorganised microtubule precursors.

Clearly, no structure so far observed can unequivocally be described as responsible for maintaining the shape of the centriole; the three structures discussed above may all play a role, but it should be remembered that not all structures are either preserved or made electron dense by the processes of fixation and staining.

b) Centriole replication

Correlation of the time of centriole replication in

S. ferax with that reported for other organisms is difficult due to the lack of good, fine structural studies. However, S. ferax centrioles clearly replicate at late interphase before the spindle forms, and their replication is the earliest sign of nuclear division. Robbins & Gonatas (1964), Robbins, Jentzsch & Micali (1968) and Stubblefield & Brinkley (1967) have all shown the centrioles in HeLa and and Hamster cells replicate at late interphase-early prophase before spindle formation, and Johnson & Porter (1968) describe a similar time for Chlamydomonas. Gall (1961) has shown the centrioles of Viviparis produce procentrioles at early prophase; these elongate as mitosis proceeds. Pollister & Pollister (1946) list a large number of animal mitoses, studied with the light microscope, in which the centrioles replicate at metaphase or anaphase, but in view of Gall's work (1961), they were probably detecting elongation, not the earliest stage of replication, although Ichida & Fuller (1968) also place replication between prophase and metaphase in Catenaria. However, most of the available evidence suggests that perhaps the earliest stage in most mitoses is the replication of the centrioles. However, Mazia, Harris & Bibring (1960) using chemical blocking treatments show that at least in sea urchin eggs, the earliest stage in centriole replication is completed in the telophase of the preceding division. This may mean that whilst the procentriole is the earliest stage of replication detectable with electron microscopy, the molecular "trigger" for centriole and

procentriole formation has been pulled in the preceding telophase.

It is firmly established that the centrioles in S. ferax replicate before they become polarized, thus producing four centrioles closely associated with each other. This is in contrast to Ichida & Fuller's work (1968) on Catenaria where they claim replication occurs after the centrioles have migrated to the poles but in agreement with the process in Hamster cells (Brinkley, Stubblefield & Hsu 1967) where centriole replication occurs before polar migration. These findings in S. ferax add weight to Mazia's statement (1961), "We have good reasons to believe that the units which will determine the poles of a given division have completed their reproduction; including both replication and splitting, well before the cell enters prophase, and that the establishment of the actual poles depends on the migration of these units," i.e. the centriole pairs.

Whilst the time of centriole replication is well-defined in S. ferax, its mechanism is not clear. However, by comparison with other organisms, it is perhaps possible to draw up a basic plan of the process. Since almost all centrioles and kinetosomes are formed in close association with a parent centriole, it is probable that the parent is in some way essential for replication. The exceptions to this rule are the apparent de novo synthesis of myxomycete kinetosomes and the blepharoplast system of Marsilia and Zamia (Mitzukami & Gall,

1966). The former are a coherent group which appear to have evolved many unusual systems; the latter organisms form in excess of 100 kinetosomes which clearly needs a rather different replication method from that producing only one or two daughters.

Most organisms produce the daughter centrioles at right angles to the parent in a less closely associated position relative to that found in S. ferax. This suggests that the parent in the latter may be more essentially involved in replication. Perhaps the simplest system would be extension of the proximal end of the parent, followed by constriction to produce the daughter centriole. (The daughters always form the proximal end and the flagella on the distal). Clearly, this does not occur since such a system would produce daughter triplets with a clockwise, not anticlockwise, orientation; furthermore, there is a well-defined space between daughter and parent tubules. At the earliest stages of replication yet detected, the daughters contain a full width cartwheel whose hub is continuous with that of the parent, although no such connection exists in mature centriole pairs. This suggests that the hub plays an important role in centriole replication. A simple hypothesis for S. ferax would be that the parent hub is able to template a daughter hub which enlarges by end synthesis. This hub would have a structure which predetermines the position of the spokes onto which the A tubules are assembled. The molecular configuration of the spokes and the A tubules

would then determine the position of the B and C tubules. Such a system need only form a short proximal length of centriole, the rest could be shaped by direct end synthesis. In order to correctly orientate the daughter, the hub would need to be templated as a mirror image of the parent; it is simpler to visualize this step than the ordering of the complete centriole without a template. The formation of centrioles at right angles to the parent could fit this general pattern if a hub were formed as above and then migrated to one side. De novo synthesis of centrioles would only require hub formation which could then template the rest of the centriole. If such a system existed, one would expect the development of a daughter centriole to show first a hub, then a cartwheel, followed by the addition of 9A, 9B and 9C tubules. These would be short in the early stages and elongate to the normal length later. There are no reports of the detection of bare hubs; however, such structures, if they exist, would be very difficult to detect as they would be short and hubs, even in mature centrioles, are not always well preserved. However, the present work shows short centrioles with only A and possibly B tubules present at an early stage in replication. Similarly, Gall (1961) shows precentrioles in Viviparis containing short cartwheels with the tubules poorly developed or absent. One of the earliest stages of blepharoplast development in Zamia and Marselia shows cartwheels with no tubules (Mitzukami & Gall, 1966) and Johnson & Porter (1968) and Allen (1969) report that developing

kinetosomes in Chlamydomonas and Tetrahymena contain a short (20 nm long) cartwheel with only A tubules; the B and C tubules are added later. Furthermore, Stubblefield & Brinkley (1967) show a short cartwheel in young "procentrioles", although mature Hamster centrioles appear to lack cartwheels. Hoffman (personal communication) shows that the kinetosomes of Oedogonium zoospores contain cartwheels when newly formed but lose them later. Possibly, the lack of cartwheels in some organisms is due to loss after they have functioned in kinetosome or centriole replication. There are reports of kinetosome replication in which cartwheels are not mentioned (Dippell, 1967; Kalnins, 1968). However, both these reports have only appeared as abstracts with no pictures and as Johnson & Porter (1968) have remarked, young centrioles are difficult to detect. However, both Dippell (1967) and Kalnins (1968) do describe the formation of rings of A tubules only followed by the addition of B and C tubules.

Thus, there is considerable evidence for, and little against, the hypothesis that the cartwheel, possibly the hub only, is the first formed part of the centriole or kinetosome and that this determines the arrangement of the tubules. That S. ferax forms its daughter hub in continuous direct connection with the parent is perhaps an ancestral feature. However, since this type of replication can only produce one daughter centriole per parent, organisms which produce more kinetosomes must have a different system, (e.g. Chick, Kalnins, 1968; Viviparis, Gall, 1961;

Zamia and Marsilia, Mitzukami & Gall, 1966). In these cases, and in normal right angled replication, it is not possible to say if the parent produces hubs which migrate before developing further. However, hubs and derived cartwheels can form from non-ordered precursors, as must occur in the myxomycetes. If hubs are produced by the parent, why they should remain in the vicinity of the parent centriole is unknown, but centriole, cytoplasmic and probably spindle tubule precursors also appear to accumulate preferentially around the centrioles. Gall (1961) and Kalnins (1968) describe an osmophilic halo of material around centrioles which are replicating multiple daughters and De Harven (1968) refers to pericentriolar bodies or "massules" (Bessis, Breton-Gorius & Thiéry, 1958) of dense material which appear to give rise to cytoplasmic microtubules (see also P.160 of this thesis) from the centriolar region. This dense hub may be microtubule and therefore centriole precursor in both S. ferax and other organisms. However, whilst there is a build-up of halo during astral tubule formation, no such concentration is found during centriole replication in S. ferax. This might be because very little material is needed relative to multiple replications, for example, in Viviparis (Gall, 1961), although Stubblefield & Brinkley (1967) suggest that microtubules form directly on the parent centrioles.

There are many aspects of centriole replication which need further investigation, however, the result of replication in

S. ferax is the formation of two pairs of centrioles at one "pole" of the nucleus.

c) Centriole migration

In order to obtain a pair of centrioles at each pole of the mitotic figure, the pairs must move apart or migrate. There are three obvious mechanisms for this migration involving, i) membrane elaboration, ii) astral tubules and iii) spindle tubules.

i) Membrane elaboration

As shown in Table 2, there is a considerable increase in nuclear surface area and therefore of nuclear envelope during division.

Table 2

Estimation of amount of nuclear envelope needed during mitosis

Diameter of adult nucleus $\underline{c}$ 3.5 μm

Assuming there is no increase in volume, the surface area of a nucleus is:-

	parent (interphase)	parent (anaphase, assuming shape is equivalent to 10 μm long cylinder)	2 daughter nuclei
Volume (μm^3)	24.4	24.4	2 x 12.2 = 24.4
Surface area (μm^2)	40.7	60.3	2 x 25.7 = 51.4

Recently, Aist (1969) has shown that at least part of this increase occurs during centriole migration in Ceratocystis and Fusrium. If this increase were localised between the centriole

pockets, they could be moved apart. There is, however, little evidence to support this hypothesis and Brinkley, Stubblefield & Hsu (1967) show that in Hamster cells this mechanism is not involved for the following reasons. Normally the centrioles do migrate before envelope breakdown, but since centriole migration in Hamster cells is prevented by treatment with colcimid (which blocks the formation of microtubules, but does not prevent the dispersion of the envelope), it is reasonable to conclude that microtubules are involved in centriole migration. Furthermore, the centrioles do migrate after colcimid is removed, when the microtubules reform but no envelope is present. Whilst it is unwise to compare processes in normal and intra-nuclear mitoses, there is no evidence to show that the envelope does play an active part in centriole migration in S. ferax. However, there is little doubt that as the centrioles migrate, new envelope is formed.

ii) Astral tubules

As shown in the results, astral microtubules radiate from one region during centriole replication and from two regions during migration; clearly there must be reorientation and probably synthesis of microtubules. There is evidence to show that chromosomes are moved by polymerisation and hence extension of pole-to-pole microtubules, possibly aided by shortening of the pole to kinetochore tubules by depolymerisation, e.g. Mazia (1961) and Bajer (1968). Migrating centrioles are at the centre of any astral tubule polymerisation and depolymerisation; it is

possible that the centrioles move along the microtubules which run over the surface of the nuclear envelope, reforming the subunits as reorientated tubules as they go. One may further postulate that the pockets could be pulled along with the centrioles and as they are pulled apart, the spindle could form between them, thus implying that the centrioles orientate the spindle. However, the latter is unlikely since similar spindles to those of S. ferax are found in Fusarium and Ceratocystis (Aist, 1969) and numerous zygomycetes and ascomycetes (Robinow & Marak, 1966, and Robinow, personal communication). These spindles do not possess centrioles, only polar plaques which are similar to the pockets in S. ferax. Clearly, these acentric spindles are not orientated by centrioles; it is probable that the spindle in S. ferax is formed by a similar process.

iii) Spindle tubules

As mentioned above, the spindle in S. ferax probably forms independently of the migrating centrioles; its growth could move the centrioles apart if they were in some way attached to the nuclear pockets, as their constant association with the latter suggests they must be. If this were the case, the rearrangement of the astral tubules would be an effect of centriole migration, not a cause.

In conclusion, it is not possible, at present, to say which set of tubules is responsible for migration, nor can one rule out the possibility that both play an active part. It

does seem, however, unlikely that the nuclear envelope plays a causal part in the migration.

d) Spindle and chromosomes

As the centrioles migrate, so the spindle forms, but to quote De Harven (1968), "The origin of microtubules also remains mysterious." There are, however, numerous diverse examples of microtubules associated with and apparently arising from osmophilic amorphous granular material. Gall (1961) and Kalnins (1968), for example, show regions of dense material around developing centrioles in Viviparis and chick and De Harven (1968) and Jokelainen (1965) show cytoplasmic microtubules radiating from dense pericentriolar satellites in mouse and rat cells. It is usually suggested that the centrioles play a major role in microtubule synthesis; however, there is considerable evidence, both in the present work and the literature which suggests the centrioles are centres around which microtubule precursors aggregate and that these precursors are formed in the E.R. and golgi bodies. In S. ferax, the spindle tubules appear to form from dense material closely associated with the pockets which are specialized regions of the nuclear envelope which, in turn, is part of the E.R. When microtubule synthesis is blocked by colchicine, there is an increase in this dense material both inside the pocket and outside around the centrioles, suggesting a build up of microtubule precursors around their site of synthesis. If the pockets themselves are the site of origin of the precursors,

they could give rise to spindle tubules on one side and centriole and astral tubules on the other side. This would mean the precursors need only pass one way through a nuclear envelope membrane and introduces the possibility of enzyme complexes built into the membrane as the synthetic apparatus in an analogous system to the "islands of synthesis" which produce cellulose fibrils in cell walls (see wall synthesis). Such a system is more probable than two way passage of subunits through the membrane, as suggested by Jenkins (1967). Further evidence for the E.R. as the site of microtubule synthesis is shown by the many intranuclear mitoses which lack centrioles, e.g. Marchella, Conidiobolus, and Mucor (Robinow, personal communication), Saccharomyces (Robinow & Marak, 1966), Myxomycetes (Schuster, 1964, and Aldrich, 1967), Plasmodium (Terzakis, Spinz & Ward, 1967) and Blepharisma (Jenkins, 1967). None of these mitoses have polar centrioles, but all possess a dense region like a pocket or "plaque" at the pole of the spindle. Catenaria (Ichida & Fuller, 1968) and Albugo (Berlin & Bowen, 1964) both have centrioles as well as pockets as in S. ferax, whilst Chlamydomonas (Johnson & Porter, 1968) has centrioles in the cell during mitosis, but these do not lie at the mitotic poles; further evidence against the centrioles forming the spindle microtubules. In Prymesium, Manton (1964b) has shown that when the nuclear envelope breaks down to typical E.R. at metaphase, the fragments often have microtubules attached to them. Furthermore, if regions of the E.R. are

the source of microtubule precursers, this would provide the possibility of multiple sites of synthesis for cytoplasmic tubules and could account for the formation of higher plant spindles which lack centrioles and do not converge to the poles.

In some instances, the Golgi bodies appear to be active in microtubule synthesis. The most direct evidence is that of Bowers & Korn (1968) who show the cytoplasmic microtubules of Acanthameoba originate in dense bars of material associated with Golgi bodies. Gall (1961) shows a high concentration of Golgi bodies around the multiple replicating centrioles in Viviparis and when S. ferax develops flagella, the Golgi bodies concentrate and become active around the basal bodies on the nuclear envelope (see "Flagella formation"). It has been shown by Palade & Caro (1964) that protein often passes from the E.R. to its destination via the Golgi and the present work has shown a close association between the Golgi bodies and the E.R. These examples of Golgi activity in microtubule synthesis are probably a development of the general system of microtubule precurser synthesis in specialized sites of the E.R.

Some workers suggest that the pole to kinetochore tubules are formed from the kinetochores and Lykx (1965b) has shown microtubules in Urechis passing from both sides of a kinetochore to opposite poles at an early stage in mitosis, claiming that one connection is later degraded to produce polarization of the chromosome. No double connections have been seen in S. ferax but at present, the mechanism directing tubules from pole to

pole and pole to kinetochore is unknown.

As shown in Table 3, the spindle of S. ferax is smaller than most reported spindles in terms of numbers of tubules, size of kinetochores and number of tubules per kinetochore; the only nuclei with similar sized spindles are those shown by Robinow (personal communication) in the zygomycetes.

Table 3

Comparison of spindle structures

Organism	No. MTs spindle	No. MTs per kinetochore	Diam. kinetochore (um)	Author
HeLa	500-600	-	-	Krishan & Buck, 1965
Hamster	-	-	0.1 - 0.2	Brinkley & Stubblefield, 1966
Urechis	-	10 - 25	0.2	Lykx, 1965 a
Rat	-	4 - 7	0.2 - 0.25	Jokelainen, 1967
Grasshopper	-	6 - 8	0.25 x 0.35	Brinkley & Nichlas, 1968
Phleum	500+	-	-	Ledbetter & Porter 1965
Haemanthus	5,000-10,000	50-170	0.5-0.6	Bajer, 1968
S. ferax	40	1	0.07	Heath & Greenwood, 1968

Before discussing the significance of the size of spindle, it is necessary to consider the chromosomes which it moves. Trow (1895), Smith (1923) and Bakerspigel (1960) have all doubted that the chromatin in S. ferax becomes organised into chromosomes

although Hartog (1895) and Höhnk (1935) have described four and seven respectively as the haploid number. The numerous reports of chromosomes in the oogonia of the Saprolegniales (Literature Review), together with the present demonstration of a spindle and kinetochores, suggest that the chromatin in vegetative nuclei is also arranged in chromosomes. However, there is little doubt that the chromosomes of S. ferax are not as complex as those of other organisms. Hartog (1895) and Höhnk (1935) show that they are very small; the present work shows a very low osmophilia relative to other organisms and the difficulty in detecting chromosomes experienced by many authors is probably a reflection of their size and lack of dense stainable structure. Furthermore, there are clearly fewer chromosomes in S. ferax than most other organisms (Wilson, 1925), and except in the zygote, the nuclei are haploid. All these observations suggest that the spindle of S. ferax has very little mechanical work to perform relative to other organisms, especially those shown in Table 3. Nicklas (1965) has shown that the size of Melanophus chromosomes has no effect on their speed of movement at anaphase and concludes that "mitotic forces are so organised or regulated that velocity is, within limits, independent of load." In view of the work of Bajer (1968) and Mazia (1961), there is little doubt that "mitotic forces" are produced by microtubules. This would suggest that the lighter the load, the fewer microtubules needed. It is not possible at present to correlate size of

chromosome with number of tubules per kinetochore, due to the shortage of accurate measurements, but the variation in numbers of tubules per kinetochore in any one organism (Table 3) may be a reflection on the sizes of different chromosomes. However, at the opposite ends of the scale, Haemanthus (Bajer, 1968) obviously has far larger chromosomes than S. ferax and far more spindle tubules. Any close correlation between number of tubules and size of chromosomes is unlikely since the force needed to move a chromosome must depend on the medium of the spindle through which it moves, its shape and its surface structure as well as its size.

It should be mentioned that Manton (personal communication) describes an unusual type of mitosis in Lithodesmium where kinetochores appear to be absent; at metaphase, the chromatin is not aggregated into chromosomes but "crawls" along the spindle tubules without the aid of a well-defined structure. Chromosomes only become distinctly separate when they have reached the poles. S. ferax may have a similar mechanism utilizing kinetochores in place of crawling. Smith (1923) noted that an eccentric cap of chromotin was drawn out into narrow trailing processes and arranged itself into two separate portions at the very beginning of mitosis. This could be interpreted as a form of separation like that in Lithodesmium, the chromotin separating on the eccentric spindle before nuclear elongation.

The counts of pole to kinetochore microtubules given in

the present work suggest that there may either be more than one tubule per kinetochore or more than one kinetochore per chromosome, assuming there are seven chromosomes in S. ferax. The former has not been observed, nor have more than fourteen kinetochores been seen in any spindle; usually far fewer. However, if the chromatin were separated by a similar process to that found in Lithodesmium, there may not be a correlation between reported chromosome numbers and kinetochores or microtubules.

The method of chromosome alignment on the spindle, the significance of the chromatin ring reported by Bakerspigel (1960) and the nature of the material in Fig. 62 are all unknown. However, the latter material has a slight similarity to the heterochromatin of Plantago (Hyde, 1967) and also to the extranuclear bodies described by Lafontaine (1968). It possibly represents the ring of chromatin shown by Bakerspigel (1960). Its true nature, function and relation to chromosomes is unknown.

e) Karyokinesis

The absence of clearly stained chromosomes makes a full discussion of their movements difficult; there is, however, no reason to suppose that separation and polarization is effected by means differing from those described by Mazia (1961), Ichida & Fuller (1968) and Bajer (1968). However, the chromatin is not the only part of the nucleus to be moved; the nucleoplasm and nuclear envelope must also be segregated into

two parts. In intranuclear mitoses which contain a large number of tubules in their spindles, the centrioles always appear to be at the leading ends of the separating nuclei, suggesting that the spindle is elongating thus pushing the two ends of the nucleus apart (e.g. Blepharisma, Jenkins, 1967) and Catenaria, Ichida & Fuller, 1965). If such a system alone operates in S. ferax, it is difficult to explain the angular extensions of the nucleus beyond the centrioles. In 1895, Hartog showed similar angular extensions of the nucleus during division and also figures long threads extending from them into the cytoplasm. The present work has shown that these threads are astral tubules with which the nuclear envelope is closely associated. It is possible that the small spindle of S. ferax is only capable of separating the chromosomes and that another mechanism has evolved for moving the nucleoplasm. Grimstone & Klug (1966) and others have clearly shown the microtubules to be fairly rigid; it is possible that the nucleus is moved by the nuclear envelope crawling along the microtubules, thus pulling the nucleus with it. There is evidence in the literature to show that many structures including nuclei can move long microtubules. Holmes & Choppin (1968) show that virus infected Hamster cells form syncitia in which the nuclei migrate into lines which can be isolated intact from broken cells. Such lines are closely associated with bands of microtubules, which are essential to alignment since colchicine treated cells containing no microtubules do

not have aligned nuclei. Porter (1966) has recently reviewed a range of various structures which move along microtubules, for example, food in Tokophrya tentacles (Rudzinska, 1965), melanin granules in melanocyte cells of Fundulus (Bikle, Tilney & Porter, 1966), spermatozoa elongation (Porter, 1966) and axopodia formation in Actinosphaerium (Tilney & Porter, 1967). Furthermore, Kubai & Ris, (1969) have shown that the chromosomes of Gyrodinium are attached to the nuclear envelope and are separated by movement of the envelope along bundles of microtubules which run through channels external to the nuclear envelope.

Clearly, there is abundant evidence for the principle of movement along "tracks" of microtubules; there is good reason to suppose that at least part of the elongation of the nuclei of S. ferax is accomplished by a similar process. The forces and mechanisms involved are unknown as is the structure of that part of the nuclear envelope which is specific to the regions of microtubule attachment.

f) Colchicine

The results obtained with colchicine are difficult to interpret. It is possible that 2.5×10^{-3} M colchicine is a marginally effective concentration, thus some spores receive sufficient to prevent microtubule formation and others do not. This is unlikely since doubling the concentration does not alter the proportion of the population affected, and Slifkin (1967) has shown that 2.5×10^{-3} M is sufficient to block

oogonial mitoses. It is more probable that the dense sporelings possess a wall or membrane structure which is less permeable than that of normal sporelings. This could retain the ground material in the cytoplasm during fixation and also prevent colchicine from entering the cells, thus explaining the retention of microtubules and normal spindles. The hyphae and normal sporelings appear to have a more permeable boundary which allows loss of cytoplasm and entry of colchicine, thus explaining the production of 8 nm fibrils similar to those shown by Robbins & Gonatas (1964) to be produced by colchicine treatment in HeLa cells. Thus, as shown by Slifkin (1967), impermeability is not a factor in the ability of nuclei to divide in the presence of colchicine. The apparently rigid, straight arrangement of the colchicine-produced fibrils in the nucleus suggests that they might still function in the same way as microtubules during nuclear division, though not necessarily with the same efficiency, but it is then difficult to explain the orientation of some groups of fibrils at right angles to others; they could, however, realign for mitosis. The cytoplasmic fibrils appear to be rigid so they could conceivably work as normal astral tubules. However, Freed, Bhisey & Sebowitz (1968) have shown that colchicine treated HeLa cells contain similar fibrils but lose the ability to move on their substrates, which would suggest that the colchicine produced fibrils cannot function as microtubules.

At present, it has not been demonstrated that these fibrils

exist in dividing nuclei. S. ferax appears to need a very high concentration of colchicine to inhibit oogonial mitoses compared with the 10^{-5} or 10^{-6} M needed by HeLa cells (Freed, Bhisey & Sebowitz, 1968; Robbins & Gonatas, 1964). Rosenbaum & Carlson (1969) have shown that Tetrahymena can recover from flagellum inhibition produced by colchicine whilst still in a 10^{-2} M solution. It is possible that S. ferax can overcome the effects of colchicine and produce normal microtubules. Clearly, more work is needed to explain fully the process of nuclear division and the action of colchicine on this process.

WALL FORMATION

1) Literature Review

In 1885, Laurent showed that the sporangiophores of Phycomyces extended only at a very small apical zone and Castle (1937) defined the region of maximum elongation 0.3 mm behind the apex. Reinhardt (1892) was perhaps the first author to show that vegetative hyphae only grow at their tips and, more recently, Smith (J.H. 1923) found that a wide range of fungal hyphae only increase in length in the region above the first septum. Using a fluorescent antibody technique, Marchant & Smith (1968) showed that the addition of wall material was confined to the apex of Fusarium hyphae. In Neurospora, a primary wall is synthesized by incorporation of glucose units into a very small apical region (Rizvi & Robertson, 1965). This primary wall remains plastically extensible for a very brief time in a small sub-apical zone of extension (Robertson, 1958). These observations have led Robertson (1965 & 1968) to develop a general concept that an apically synthesized primary wall is expanded by turgur pressure and then rapidly becomes rigid, or possibly elastically extendable (Rizvi, 1964), thus giving rise to the tube shape of the hypha.

The rigidity of the sub-apical region may be due to sulphydryl bonding of the primary wall since Nickerson, Taber & Falcone (1956) have shown such bonds to be important in the walls of Candida and Geotrichum. Furthermore, Lamport (1965)

has suggested that the walls of higher plants are made rigid by sulphydryl bonding between cellulose fibrils. He suggests that such bonds are associated with specific, hydroxyproline-rich, protein termed "extensin." Hunsley & Burnett (1968) have suggested that sub-apical rigidity is partially due to thickening of the primary wall fibrils in Phytophthora, Neurospora and Schizophyllum. However, the rigidity of hyphal walls is usually attributed to the addition of a secondary wall.

Primary walls consist of randomly orientated fibrils (Aronson & Preston, 1960b) but secondary walls may contain orientated fibrils (Aronson & Preston, 1960a). Roelofsen (1965) has suggested that a similar distribution of fibrils is common to most organisms showing tip growth of tubular cells and further suggests that the orientation of the secondary layer is responsible for the rigidity of the tube.

Marchant (1966) has suggested that in Fusarium, sub-apical rigidity is due to the addition of a layer of inherently rigid chitin. However, layers containing chitin can be expandable since Aronson & Preston (1960a and 1960b) have shown that a random network of chitin fibrils is present at the hyphal apex of Allomyces and Gonapodya. Furthermore, chitin cannot be responsible for the rigidity of oomycete walls since Parker, Preston & Fogg (1963) and Bartnicki-Garcia (1966) have demonstrated its absence from several members of this group including various Saprolegniacae and Phytophthora.

Whilst Parker, Preston & Fogg (1963) showed the presence of 10 - 15% celloluse fibrils in the walls of S. ferax, they did not describe their distribution or orientation. In general terms, the changes in wall structure occurring at the apex of the oomycete hypha are virtually unknown.

Whilst the structure of the oomycete wall is little known, the synthetic mechanisms responsible for its synthesis are even less clear. Pectic substances are absent since Parker, Preston & Fogg, (1963), found no galacturonic acid after hydrolysis of the walls, but these walls are similar to higher plants' in possessing cellulose fibrils embedded in an amorphous matrix. One might, therefore, expect to find comparable structures involved in wall synthesis in both S. ferax and higher plants. There is increasing evidence that cellulose fibrils are produced in a wide range of organisms by enzymic granules which are either attached to the plasmalemma or free in the wall (Preston, 1964; Preston & Goodman, 1968; Mühlethaler, 1967; Staehelin, 1966). The source of the substrates for these enzymes is unknown but cellulose is elaborated from nucleotide sugars, e.g. GDP-glucose (Barker, Elbein & Hassid, 1964), which could conceivably move freely through the cytoplasm and membranes without special transporting structures detectable with the electron microscope.

In oomycetes, cellulose is only a small portion of the wall. The origin of the hemicellulose matrix material in

walls generally is not always clear; however, Mollenhauer, Whaley & Leech (1961), Frey-Wyssling, Lopéz-Sáez & Mühlethaler (1964), Northcote & Pickett-Heaps (1966) and Mühlethaler (1967) suggest that vesicles of Golgi origin play a role in the production and transportation of some of the amorphous wall material and Northcote (1969) suggests that the products elaborated by the Golgi system depend on the stage of development of the cell. However, Porter & Machado (1960) have suggested that primary wall formation in onion involves activity of the E.R. and Villemez, McNab & Albersheim (1968) have presented evidence for the plasmalemma as the site of at least some of the enzymes involved in pectin, cellulose and hemicellulose formation in Phaseolus.

In the fungi, there is more speculation over the synthetic systems involved in wall synthesis. Grove, Bracker & Morré (1967) have suggested, in abstract only, that some parts of the walls in Pythium are produced from the E.R. via the Golgi vesicles. McClure, Park & Robinson (1968) suggest that in several septate fungi, but in no phycomycetes, wall synthesis is associated with "spitzenkörper" composed of numerous vesicles of unknown origin, although clearly not from a Golgi system of standard form since they were unable to detect Golgi bodies in the hyphae they examined. Similarly, Brenner & Carroll (1968) found an apical accumulation of vesicles in Ascodesmus. They considered these vesicles to be involved in wall formation but could not specify their origin.

Several authors have shown a close association between developing fungal walls and cisternae of the E.R. (Bracker & Butler, 1963; Hawker, Gooday & Bracker, 1966; Hawker & Gooday, 1967 and Turian & Oulevey, 1968), and Marchant, Peat & Banbury (1967) have suggested that E.R. derived "multi-vesicular bodies" and vesicles are involved in the synthesis of both chitin fibrils and non-chitinous matrix material.

Perhaps the most controversial structures frequently said to be associated with wall synthesis are lomasomes (Moore & McAlear, 1961). A variety of structures conforming to the definition of a lomasome (a "dome shaped sponge-like intumescence," "contiguous with the wall" containing "granular or vesicular" material interiorly bounded by the plasmalemma. Moore & McAlear, 1961) have been found in most walled cells fixed and examined with the electron microscope. As noted by Bracker (1967),"they have gained much prominence on little information" and, usually with little supporting evidence, have been described as participating in wall formation (Becking, DeBoer & Houwink, 1964; Wilsenach & Kessel, 1965; Barton, 1965; Crawley, 1965; Esau, Cheadle & Gill, 1966; Peat & Banbury, 1967 and Marchant, Peat & Banbury, 1967), excretion (Manocha & Shaw, 1964), glycogen synthesis (Hashimoto & Yoshida, 1966), response to fungal infection (Ehrlich, Schafer & Ehrlich, 1968) and extracellular enzyme production (Calonge, Fielding & Byrde, 1969), although recently Barton (1968) has shown that they are not involved in wall formation

in Chara. The reported distribution and functions of lomasomes have been more extensively reviewed by Bracker (1967) and Marchant & Robards (1968). They bear a superficial similarity to bacterial mesosomes (e.g. Van Iterson, 1964) which are functionally well characterised organelles of the bacteria. This structural similarity has led Hashimoto & Yoshida (1966) to term them fungal mesosomes in Geotrichum but comparable structures have also been termed plasmalemasomes (Becking, De Boer & Houwink, 1964), boundary formations (Esau, Cheadle & Gill, 1966) and paramural bodies (Marchant & Robards, 1968). The structure and function of these formations need further elucidation.

S. ferax is well suited for further work on fungal wall synthesis. The chemical composition of its walls is relatively simple and has been described in detail by Parker, Preston & Fogg (1963). Normal apical growth is rapid and there is no reason to believe that it differs from the fundamental process postulated by Robertson (1958). The normally rigid sub-apical walls can be induced to expand plastically during zoosporangium formation but become rigid, though elastically deformable, before zoospore release (Gay & Greenwood, 1966). During development of the sporangium, a special type of apical growth produces an apical papillum which is broken down, probably enzymatically, at the time of zoospore release (Ward, 1883; Gay & Greenwood, 1966), thus suggesting the presence of a special wall degrading enzyme system. Two

special cases of rapid wall formation occur; the insertion of the delimiting cross wall of the sporangium and the production of a wall which converts the settled zoospores into cysts. Wall development can also be studied in the germination of encysted S. ferax zoospores. Sporangia of D. sterile were also examined since cyst wall synthesis and wall formation at spore germination are both confined to a small, well-defined area amenable to ultrastructural examination.

It was hoped that a comparative study of wall structure and the underlying cytoplasm in these different situations would lead to a better understanding of some of the problems outlined above.

2) Observations

a) Wall structure

The fibrillar component of cell walls is usually considered to be the major source of mechanical rigidity. Since the fibrils of S. ferax walls are obscured by the amorphous matrix material (Fig. 82), their structure and distribution was investigated with "Domestos" cleaned, whole mounts of wall fragments (Parker, Preston & Fogg, 1963). These fibrils form a random network enclosing the apex and appear to show no differentiation in size or orientation along the hyphae (Figs. 85, 86 & 87). A few observations of torn hyphae viewed internally showed a similar network; no trace of orientated fibrils has been seen at any stage.

Dried sporangia are more resistant to collapse than

hyphae (Figs. 83 & 84), and Fig. 89 shows that the sporangium wall is sufficiently rigid to withstand the turgor of the young sporangium growing inside it. This suggests that the sporangium wall is probably more rigid than the hyphae. Sporangium walls (Fig. 90), zoospore cysts (Fig. 88) and spore germ tubes (Fig. 88) all contain a network of fibrils similar in size and orientation to those of the hyphal walls.

The shadowed whole mount technique only shows the surface layer of the wall but the polarizing microscope may give information about both thickness and orientation of underlying fibrils. If old hyphae are viewed with their long axes at 45° to crossed polarizers, the walls at the edges of the hyphae show a white glow which is absent from portions of the wall viewed normally to the light beam (i.e. the upper and lower walls of the hypha) (Figs. 91 & 92). When the hyphae are rotated through 90°, this glow diminishes to extinction but reappears at 180° to the original position (0°). If a first order red compensator is inserted in the light path, the glow appears slightly yellow at the 0° and 180° positions and bluish at 90° and 270°. This suggests that the glow is due to positive birefringence since the interference colours are enhanced (blue) when the long axis to the hypha is parallel to the slow direction of the compensator (Oster, 1955). This means that the maximum refractive index lies along the hypha and the absence of detectable birefringence in the 90° and 270° positions

suggests a negligible component in the extraordinary position. This birefrigence may be produced by reflection at the surface of the hyphae, as can occur at an interface between two media of different refractive indices (e.g. air/water or coverglass/water), but such a system produces light maxima four times per revolution of the specimen, not two as found in walls of S. ferax.

The birefringence is caused by the fibrils since "Domestos" extracted hyphae produced a glow of a similar strength to that of untreated hyphae; they also retain their shape. Since there are two superimposed layers of wall in the regions of the hypha viewed normally, the absence of birefringence could be due to the effects of fibrils orientated in preferred directions exactly cancelling each other but for this to occur, they must lie in a spiral inclined at exactly 45° to the long axis of the hypha. A single layer of fragmented wall also shows no birefringence.

Thus, it is possible that the fibrils exist in a random network throughout the wall. The glow of the "side" walls is probably textural birefringence resulting from the random fibrils viewed as shown in Fig. 96. Assuming the glow is textural birefringence of this nature, an extraordinary component would not be expected since, unless the wall was very thick and the fibrils were woven through the wall as well as along it (which is unlikely), there will be no fibres running at right angles to the long axis of the hypha.

Hyphal apices show very little birefringence; the glow increases gradually along the hypha (Figs. 91 & 92) to a maximum at about 60 µm behind the apex. Zoosporangia side walls, basal cross walls and zoospore cysts (Figs. 93 & 94) show a much stronger birefringence than hyphal walls, but the emerging germ tubes of zoospores have virtually none. In all these cases, birefringence is absent from walls viewed normally. However, in discharged D. sterile sporangia, the walls viewed normally show a detectable birefringence with well marked "holes" corresponding to the point of exit of each zoospore (Fig. 95), (see also Spore Formation). This latter birefringence must be caused by an orientated network of fibrils which are probably in the sporangium wall since it is unlikely that all the cysts would show a similar direction of orientation.

In order to detect changes in the percentage of cellulose along the hyphal walls, a few hyphae were examined with the IKI-H_2SO_4 stain for cellulose. The walls of the hyphae and the apex showed an even blue reaction of insufficient intensity to detect small changes in cellulose content.

It was thought that the rapidly formed sporangium cross walls and the material added to the developing sporangium wall might contain callose. No fluorescence was detected after aniline blue staining suggesting the absence of callose in these and all other walls examined.

Further work on wall formation centred on the use of sectioned material to study the underlying cytoplasm in regions

active in wall synthesis.

b) Vegetative apices

All apices examined with the electron microscope appeared similar when selected in the epon blocks with the light microscope. Some were from liquid grown cultures which had become disordered during preparation so that the position of these apices in the colony was uncertain. However, most were selected from the edges of young, actively growing colonies fixed *in situ* on agar. In one experiment (Table 4) apices adjacent to those fixed were observed to continue growing, suggesting that the fixed apices were also growing normally at the moment of fixation.

Table 4

Growth rate of hyphae in agar

Part of a colony of *S. ferax* on OM agar was removed and fixed. Remaining undisturbed hyphae were examined with the light microscope in the open petri dish at about 18-20° C. Surface hyphae failed to grow further but submerged; randomly sampled hyphae which were originally level with the surface ones continued to grow at the following rates for the next 4 h.

Time (h)	Growth rate (mm/h)
0	0.55
2.0	0.78
2.5	0.73
3.0	0.68
3.5	0.68
4.0	0.66

cf. The average growth rate of a colony (Table 7) which is 0.65 mm/h. at 25°C.

There was considerable variation in structure in apices examined both with the light microscope (Figs. 97 - 100) and with the electron microscope (Figs. 106 - 199); differences between the agar grown and liquid grown apices were not significant relative to the variation within a colony. However, most apices had a similar basic structure and differences were mainly expressed in relative quantities ~~to~~ of the various structures present and the extent of their zonation.

Phase contrast microscopy reveals a highly refractile, non-vacuolate apical region of cytoplasm with little cytoplasmic movement relative to the sub-apical regions. This region may be fairly short (c 10 μm) with a blunt apex (Figs. 97 & 98) or much longer (c 40 μm) and more tapered (Fig. 99), but in both cases, it contains no nuclei or long mitochondria. When viewed with the Nomarski interference contrast system, the strong phase halo is absent and the structure of the apex is more clearly visible (Figs. 102 - 105). These pictures show that the apical 10 - 17 μm contains elongated structures which may be rows of individually unresolved small vesicles, larger elongated vesicles or tubular plasmalemmasomes (see Lomasomes).

Ultrastructural studies reveal a high concentration of vesicles at the apex of both S. ferax and D. sterile. These will be termed wall vesicles for reasons which will become apparent later. After GA/Os, these vesicles contain amorphous material and are bounded by a single membrane (Figs. 107, 108, 112, 113 & 123). They are predominently isodiametric, though

slightly irregular in outline, but can become tubular especially in older regions of the hypha (Fig. 121).

After Os fixation, the wall vesicles have a smoother, more circular outline; stringy contents are less abundant and are frequently replaced by a single dense globule (Figs. 114, 117 & 122). Wall vesicles are not preserved by the permanganate fixation used here (Fig. 106). Table 5 shows a fairly typical distribution of wall vesicles and other organelles.

Table 5

Distribution of organelles in a hyphal apex of S. ferax

An approx. median longitudinal section of a vegetative apex (1839/3) was divided into seven equal arbitrary transverse segments. These segments were covered with a grid of transverse parallel lines spaced 1 cm apart. The length of each organelle transected was expressed as a percentage of the total cytoplasm transected. The author is pleased to acknowledge the 1968-1969 first year botany students of Imperial College who made the actual counts.

	Distance from apex (µm)						
	0-5.5	5.5-11	11-16.5	16.5-22	22-27.5	27.5-33	33-38.5
Wall vesicles	22.5	7.8	5.3	1.7	1.9	5.0	5.4
Mitochondria	1.4	1.8	27.0	35.6	32.6	22.8	20.3
Nuclei	0	0	0	0	2.0	10.5	13.1

In the apex, wall vesicles are numerous throughout the

cytoplasm (Figs. 108 & 114), but sub-apically, they decline in numbers and are more confined to the regions of cytoplasm immediately adjacent to the walls.

When treated with PAH reagents, the wall vesicles fixed in GA/Os give an overall reaction (Figs.126 & 143), which may be heavier than that of the walls (Fig. 150). The Os fixed vesicles give a strong reaction on their membranes but their lumina usually contain little staining, although occasionally a suggestion of staining appears over regions equivalent to the dense globules seen in untreated sections (Figs. 124 & 125). There is evidence that the denser globule may be etched away by the PAH process (Fig. 124) (cf. the etching of starch grains reported by Pickett-Heaps, 1965a).

There are often numerous smaller membrane bound vesicles of up to about 60 μm diameter filled with electron opaque material (Figs. 109, 114 & 117) interspersed among the wall vesicles. They are more closely confined to the apex than the wall vesicles but are not found in all hyphae. The structure of these vesicles is similar to that of RNA containing vesicles described by Dashek & Rosen (1966) in pollen tubes but their nature and function are unknown in S. ferax.

The concentration of wall vesicles is usually sufficient to exclude the larger organelles from the cytoplasm of the extreme apex, but this area does contain numerous ribosomes at comparable densities to other regions of the hyphae. The only other structures which commonly occur in the apical 10 μm are cisternae

of the E.R., profiles of which are usually shorter than in the older regions (Figs. 107, 110, 113 & 114). Mitochondria may occur close to the apex but they are most numerous sub-apically between 10 and 20 µm where they are associated with abundant E.R. (Fig. 106). The profiles of the mitochondria seen in this region are usually short; they become longer in older regions where profiles of 14 µm are seen in sections and considerably longer structures are visible in living material (Fig. 101) (cf. Zalokar, 1959; McClure, Park & Robinson, 1968). This increase in length may be an indication that the mitochondria elongate with ageing; however, there is no evidence concerning their mode of formation in the present work.

Golgi bodies occur throughout hyphae but are most abundant in the mitochondrial zone where 80% of recognisable Golgi bodies are associated with a mitochondrion (Figs. 127 - 133) (Table 6).

Table 6

Specimen	Total recognisable Golgi bodies	Golgi/E.R./ mitochondria association	Nucleus/Golgi association	Unassociated Golgi bodies
1825/6 L.S. 76 µm of apex	23	17	2	4
1839/3 L.S. 42 µm of apex	11	11	0	0
1826A/6 L.S. 62 µm of apex	15	10	2	3
1391/1-11 197 T.S's from a series of about 370 sections equivalent to $\underline{c}$ 19 µm of apex	169*	136	5	28
Total	218	174	9	35
% of total Golgi bodies	-	80	4	16

* High numbers partially due to many Golgi bodies appearing in several serial sections.

Favourable sections (Figs. 127 & 131) clearly show a cisterna of the E.R. between the Golgi body and its associated mitochondrion. A short cisterna is visible in most associations and is frequently seen to be giving rise to vesicles towards the forming face (Mollenhauer & Whaley, 1963) of the Golgi body (Figs. 127, 129, 132 & 133) which itself is producing characteristic vesicles from the margins and outer face of its cisternae (Figs. 127 & 128). Since 4% of the

Golgi bodies are associated with the nuclear envelope, about 84% can be said to have an association with the E.R; some, if not all, of the remaining 16% may well have associated E.R. not intersected by the plane of the section.

Most hyphae, after both GA/Os and Os fixation, contain characteristic structures which will be termed multitubular bodies (Fig. 119). These are usually closely adjacent to the E.R. although no clear connection has been seen between their membranes. The single bounding membrane of the multitubular body encloses dense amorphous material which is permeated by numerous small tubules. They do not occur close to the apex nor are they preferentially located near the walls in the sub-apical regions.

Lomasomes and plasmalemmasomes are frequently found in vegetative apices but are not present in all hyphae. When they are present, they are most abundant at the apex but their morphology and distribution is very variable and will be discussed more fully in the section on Lomasomes.

Most colonies contain regrowing apices, examples of which are shown in Figs. 100, 134 & 214. They are composed of one apex with a normal structure growing inside another apex whose cytoplasm is disorganised and apparently moribund (Fig. 134). The wall of the inner hypha is irregular and numerous lomasomes are trapped between it and the old wall (Fig. 134). The growth of this type of apex has not been observed in life, thus its mode of extension is unknown.

However, the new apex presumably grows up inside the old one and eventually breaks through the old apex, although there is no evidence to support this hypothesis. The origin of such double apices is also obscure. The ring of membranes in Fig. 135 (which is reminiscent of the cortical membrane described by Hawker & McAbbott, 1963, in Rhizopus but has only been encountered once in S. ferax) could represent an early stage in the formation of a regrowing apex; the cytoplasm inside the ring forming the new apex and that outside becoming sequested and moribund with wall forming between the two membranes as described in ascospore formation by Reeves (1967) and Carroll (1967). There is, however, evidence that in older regions of the hyphae, central vacuoles are formed from long profiles of double membranes (Fig. 137), of which Fig. 135 may be an example.

c) Germ tube apices

Short germ tubes are essentially young hyphae which are unlikely to be undergoing changes in apical structure associated with apical dominance shown after branching has commenced. It was thought that these apices might show a similar structure to those of older hyphae but be subject to less variation. Such apices contain numerous wall vesicles, which are more exclusively concentrated at the apex than they are in older hyphae (Figs. 136, 138 & 139); the other organelles have a less well defined zonation. Lomasomes and plasmalemmasomes are usually less abundant but in most respects the variation between

apices is not much less than in older hyphae. A more detailed account of spore germination will be found in the section on spore formation.

D. sterile produces a special type of germ tube when the encysted primary spores produce secondary zoospores (see Spore formation). These germ tubes are formed by addition of material to the primary cyst wall which is pushed through the sporangium wall and is apparently stretched considerably before release of the motile spore (Fig. 155). The apex of these germ tubes is filled with a mixture of wall vesicles, which are less regular and larger than those of the hyphae apex (Fig. 141), and larger vesicles apparently formed by the dense bodies (Fig. 141). The dense body vesicles appear to enlarge preferentially in the region of the germ tube and are probably responsible for the instability of this area during fixation (Fig. 140). Lomasomes and plasmalemmasomes are common in these apices which finally break rather violently, suggesting the release of pressure possibly generated by the enlargement of the dense body vesicles (see Spore formation).

d) Apical papilla

At an early stage in zoosporangium formation, often before cross wall insertion (Hartog, 1895), a small blunt papillum is rapidly produced on the tip of the potential sporangium (Fig. 138 indicates about 10 min for formation). During formation, this papillum contain numerous PAH positive (Fig. 143) wall vesicles, occasionally associated with lomasomes and

plasmalemmasomes (Figs. 142 & 144). The papillum is fully formed before cleavage and at this stage is filled with cytoplasm and organelles similar to those of the rest of the sporangium; wall vesicles and lomasomes are absent (Fig. 145). After cleavage, there is no cytoplasm remaining in the papillum but it often contains a zoospore. The top, but not the side, walls acquire a loose texture (Fig. 147) and appear to be dissolved rather than torn when the spores are released (Fig. 146). Breakdown of the top wall is probably enzymatic (Ward, 1883; Gay & Greenwood, 1966) but may be aided by the beating of the flagella of the uppermost zoospore (Crump & Branton, 1966). The loose texture of the papillum in Fig. 147 may indicate that an enzyme system deposited in the wall before cleavage works slowly but continuously after arrival in the wall until breakdown of the papillum ultimately ensues. If this is not the case, it is difficult to see how the enzymes are "switched on" in the absence of neighbouring cytoplasm after the disengagement of the plasmalemma during cleavage.

A sporangium may form more than one papillum; one apically and the others laterally, the latter show similar development and may also be active in zoospore release.

e) Sporangium walls

One of the earliest events in sporangium formation is the swelling of the hyphal apex to become a club-shaped, or even a more or less spherical, sporangium. This swelling occurs mainly

before cross wall insertion and is presumably caused by softening of the sub-apical walls and their expansion by turgor pressure, the final shape depending on the interaction between these two processes. The final shape of the sporangium is not a function of the volume of the cytoplasm enclosed, since Hartog (1895) has shown that "starved" sporangia may still be large but contain a very large central vacuole. During sporangium development, the walls increase in thickness from about 0.1 μm to 0.3 μm. Before cytoplasmic cleavage, the walls have become rigid and slightly distended elastically since after cleavage and loss of turgor, they decrease in volume by about 10% (Gay & Greenwood, 1966). The addition of wall material continues after cross wall insertion and occurs in the presence of numerous wall vesicles which are located close to the walls (Figs. 148 - 151). These vesicles often appear tubular (Fig. 148), and have a strong PAH reaction (Figs. 149 - 151).

The walls of air dried sporangia examined in the scanning electron microscope showed numerous pits of a similar diameter to lomasomes (Figs. 82 & 84). Since these only occurred on sporangium walls and not on old hyphal walls, they could be caused by collapse of the contained lomasomes on drying.

f) Sporangium cross walls

The expanded sporangium is delimited by the insertion of a cross wall. In S. ferax, this wall is inserted within about 30 sec. (Greenwood, 1966), and in both S. ferax and D. sterile,

it is composed of two or three layers of wall material which enclose portions of sequested cytoplasm (Figs. 11, 152, 154 & 157). This trapped cytoplasm contains membranes, ribosomes and lipid droplets (Fig. 154) but nuclei and mitochondria have not been observed. The mode of formation of this wall is obscure; Fig. 158 may represent a stage in formation in which the cytoplasm contains few organelles due to the accumulation of wall precursors (partially polymerised?) lying free in the cytoplasm. However, at a later stage in formation, the walls usually have an accumulation of typical wall vesicles and a few plasmalemmasomes along both sides (Figs. 11, 153 & 159). These vesicles undoubtedly contribute material to the cross wall after initial insertion and are probably responsible for the additional layer of material tapering from the cross wall back along the hyphal walls and up along the sporangium walls where it becomes the inner layer of the double wall (Fig. 157). Wall vesicles diminish in numbers, and at cleavage, they are absent from both sides of the wall. However, when a new sporangium grows through the old cross wall (Fig. 160), they begin to accumulate on the hyphal side (Fig. 156) and apparently form an extension of the layer of wall added to the original cross wall. This new wall is extended up through the old cross wall which is stretched and broken in the process (Fig. 160).

g) Zoospore encystment and Germination

At the end of their motile life, the primary zoospores of S. ferax withdraw their flagella and produce a cyst (see Spore

formation). When first formed, this cyst wall is thin and easily distorted, contains numerous spines and is moderately electron opaque (Figs. 161 & 162). Untreated shadowed mounts of the cysts show the spines on an underlying textureless surface (Figs. 163 & 164). Wall vesicles occur in the zoospore, although prior to encystment they are difficult to detect due to the poor preservation of the motile spores; however, they do not appear to be numerous (Fig. 278). As the encysted spore ages, a thick inner layer of electron transparent material is added to the walls (Figs. 165, 169, 172 & 232) (cf. Ward, 1883). This inner layer may contain lomasomes and be associated with plasmalemmasomes (Figs. 171, 172 & 233), but these structures are not abundant. The electron translucent layer of the cyst wall gives a strong PAH reaction (Figs. 167 - 172) as does the plasmalemma itself (Fig. 167), but the thin outer layer of the cyst and the spines show only a light reaction (Fig. 167). The synthesis of the inner layer of the cyst wall appears to be accompanied by a small number of vesicles which lack the characteristic contents of the wall vesicles (Fig. 165). Fig. 166 suggests that these vesicles are produced by the Golgi bodies, an observation supported by the increasing PAH reaction across the Golgi cisternae and into the Golgi vesicles (Figs. 168 - 170). Typical wall vesicles appear at the onset of germination when they are localized in the region of extension of the inner cyst layer which breaks out and becomes the wall of the germ tube

(see Spore formation).

The different staining characteristics of the thin outer layer of the cyst and the absence of large numbers of wall vesicles in the spore prior to encystment suggests that it may have a different composition and origin to the inner wall layer. The bars described by Gay & Greenwood (1966) produce the spines of the cyst (see Spore formation) and always occur at the periphery of the spore prior to encystment. Apart from the preformed spines, these bars also contain a thick layer of amorphous material (Figs. 175 & 176) which has a fairly light PAH reaction (Fig. 174) and is presumably released to the exterior of the cell at the same time as the bars. The average encysted spore had a diameter of about 10 μm and a surface area of 314 μm^2. The electron opaque layer of the cyst wall is approximately 0.01 μm thick and must therefore contain about 3.14 μm^3 of material. If a section of a zoospore before encystment is assumed to be approximately 0.04 μm thick (see Appendix), it will intersect parts of all the bars in a section whose thickness is equivalent to 0.04 μm minimum and 0.64 μm plus the length of a bar (0.3 μm) of either side, i.e. 0.64 μm, maximum. Assuming the bars are orientated at random, the average thickness sampled will be 0.04 μm plus half the length of a bar on each side, i.e. 0.34 μm. Assuming the bars are distributed randomly over the surface of the spore, the approximate number contained in a spore can be calculated from the number counted in a section of known diameter (2r) and

calculated thickness (t). This divided into the surface area of the spore will give the total number present. Thus in Fig. 177 there are 15 bars in a section of 7 μm diameter, giving a density of 15 bars in an area of surface equal to $2\ rt\ \mu m^2 = 2\ \ 3.5 \times 0.34 = 7.47\ \mu m^2$. Thus, assuming the spore was of average size, it would contain a total of approximately $\frac{314}{7.47} \times 15 =$ 630 bars before encystment.

The shape of the amorphous material in a bar may be approximated to the following:-

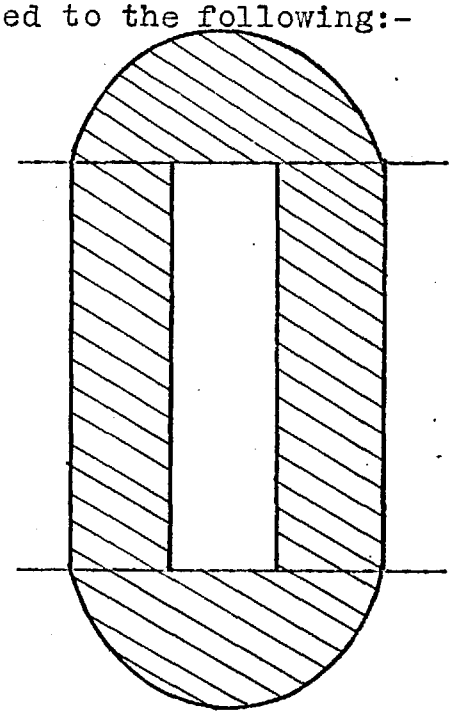

Thus the volume of this material per bar is given by:-

$$r_o^2\ l - r_i^2\ l + 4/3\ r^3 = 0.003779\ \mu m^3$$

Therefore the total volume in a spore before encystment is:-

$$630 \times 0.003779 = 2.385\ \mu m^3$$

compared with that in the average cyst wall of 3.14 μm^3. Assuming that nothing else is added, it means that the amorphous material would have to expand by 24% on release. Clearly, the assumptions made in this calculation preclude the possibility of an exact determination of volume, for example, the replicas and sections of encysted spores show that the distribution of spines, and therefore presumably of bars, is not completely random. However, the figures assumed are representative and give a result consistent with the possibility that the amorphous bar material forms the dense layer of the cyst with a suggestion of some expansion of the material on release.

The primary cysts can germinate to produce a secondary zoospore which also produces a cyst (see Spore formation). Sectioned secondary cysts have a similar inner wall layer to that of the primary ones, but the thin outer layer is absent. It is represented by circular discs (plaques) of dense material around the base of each boathook (Manton, Clarke & Greenwood, 1951) (Figs. 178 & 179). When seen in shadowed whole mounts, these plaques are seen as amorphous material, of a similar texture to the surface of primary cysts, overlying a bare fibrillar network (Figs. 180 & 181). The boathooks are produced by bars which develop in the primary cysts. Since there are few boathooks, and thus

bars, in each spore, sectioned bar profiles are not common but they appear to be spherical (Figs. 182 & 183), (see Spore formation). They have a diameter of about 0.2 µm and are lined with a 0.03 µm thick layer of amorphous material. This would suggest that they contained a volume of 0.002764 μm^3 of amorphous material per bar.

The plaque surrounding each hook on the cyst has a radius of about 0.59 um, a thickness of about 0.0125 µm, and thus a volume of 0.01365 μm^3. This suggests that the amorphous material of the bar must swell by about five times to produce the plaque around the hooks. However, observations of the secondary bars are few and the volume of their enclosed amorphous material is not known as accurately as that of the primary bars. Furthermore, the thickness of the plaques is difficult to determine since the few sections of them suggest that they have a thin inner dense layer which becomes more diffuse towards the outside of the spore (Figs. 178 & 179). However, the correlation between the appearance of the amorphous lining of both the primary and the secondary bars and the similar staining characteristics of the dense outer primary cyst wall layer and the plaques on the secondary cyst all suggest that the dense cyst material is produced from the bars.

D. sterile produces primary zoospores which encyst within the sporangium (Fig. 184) (see Spore formation). These spores

contain spines which are also surrounded by dense amorphous material (Figs. 188 & 189) but which are not released to the surface of the primary cysts. The primary cyst wall has no dense outer layer (Figs. 185 & 186) and is formed in association with numerous wall vesicles (Figs. 152 & 184). During formation of this cyst wall, there is a considerable formation of excess plasmalemma (Fig. 185) and plasmalemmasomes and lomasomes are common (Fig. 186).

The primary spores of D. sterile produce secondary zoospores. These secondary spores encyst and release spines to the surface where they are attached to a thin, dense outer layer of material, comparable to that on the primary cysts of S. ferax (Fig. 187). Due to insufficient observations, it is not possible to make calculations similar to those above.

h) Lomasomes and Plasmalemmasomes

The morphology and functions reported for structures lying between the plasmalemma and the wall has led to a confusing terminology which, however, Marchant & Robards (1968) have recently attempted to clarify by proposing a system based on the origin of the structures. Since the origin and mode of formation of these structures is rarely clear, this system is difficult and often impossible to apply. In the present work, the term lomasome will be used to refer to vesicular material embedded within the wall, external to the line of the plasmalemma, and plasmalemmasome for the various membranous configurations external to the plasmalemma, often projecting

into the cytoplasm and which, though often incorporating wall material, are less obviously embedded in the wall. Such terms are used for convenience only, since there appears to be a continuous spectrum between two obvious extreme, in one of which there is no involvement with deposits of wall material, and in the other, a complete sequestration of the membranous complex within the layers of the wall.

i) Lomasomes

After permanganate fixation, the apical walls contain regions of granular or poorly defined vesicular material (Fig.192). Following GA/Os or Os fixations (Figs. 107, 110, 111, 114 & 117), corresponding regions appear as aggregations of various sized vesicles, more or less deeply embedded in the walls. These lomasomes only occur at the apices of vegetative hyphae where they are completely sequested in wall material. Their absence from older hyphae suggests that they are easily removed, perhaps by sloughing off as indicated in Figs. 190 & 191. A similar process of loss must also occur in the apical papilla of sporangia, since they occur here during development but are absent from the mature papillum. However, in the walls of the zoosporangium, they remain as a permanent feature, still present after discharge of the spores.

The lomasomes of the hyphal apex and apical papillum of the sporangium contain only membranous material; however, those of the sporangium wall may include cytoplasm and ribosomes (Fig. 194). The sequested material in the cross walls contains

a considerable quantity of cytoplasm and, apart from the irregular nature of the membranes, it resembles the lomasomes of the lateral walls (Figs. 154, 157 & 159). These lomasomes which contain cytoplasm are not lost from the walls, but those containing membranes only are apparently quickly removed. The size and number of lomasomes in all situations varies from specimen to specimen; the only place in which they are invariably present is the cross wall of the zoosporangium which always contains sequested material.

ii) Plasmalemmasomes.

Whilst the structure of lomasomes is variable, the configuration of plasmalemmasomes is even more variable and, unlike the lomasomes, can apparently be altered to a certain extent by the fixation procedure. The distribution of plasmalemmasomes is closely correlated with that of lomasomes but whilst the latter are frequently persistent, the plasmalemmasomes appear to be transitory, depending on the activity of the cytoplasm.

Plasmalemmasomes can be preserved by permanganate fixation after which they appear as granular or vesicular material contained in a pocket of the plasmalemma (Fig. 196). Their size and distribution has not been studied in detail with this fixative. After GA/Os fixation, plasmalemmasomes range in structure from well defined 1 μm deep depressions of the plasmalemma closely packed with various sized vesicles (Figs. 190, 193, 197 & 198) to long shallow depressions more loosely

packed with tubular membranes (Figs. 111, 199, 200 & 203). Connections between the vesicles and tubules and the plasmalemma can occur but are rarely found (Figs. 201 & 203). The tubular type of structure appears to be aligned along the long axis of the hypha and is similar in appearance to membranous material found in vacuoles (Thomas & Isaac, 1968) and dense body vesicles (see Spore formation). These tubular plasmalemmasomes are not very obviously involved with wall materials (Fig. 200); however, there is perhaps a morphological sequence from tubules to vesicles (Figs. 190, 195 & 201). These vesicular plasmalemmasomes are apparently embedded in wall material (Figs. 171, 193 & 195) and have a high PAH reaction (Fig. 171), this suggesting that they can ultimately become sequested to form lomasomes (Figs. 190 & 193).

Vesicular and tubular plasmalemmasomes can also occur after Os fixation (Figs. 117 & 199). However, some Os fixed apices contain irregular aggregations of membrane around their periphery (Figs. 204 - 207). These areas are composed mainly of irregular elaborations of the plasmalemma (Fig. 206) but include distorted wall vesicles. Tubular or vesicular plasmalemmasomes are absent from these areas which are, however, confined to regions of the hyphae in which lomasome normally occur. They have not been seen in material fixed in GA/Os or permanganate.

iii) SITS

The range and variation found in plasmalemmasomes and the

known labile nature of membranes during fixation suggested that at least some of the plasmalemmasome configurations may be caused by the action of the fixative. The proximity of such structures to the highly refractile cell walls of the hyphae does not favour their detection with the phase contrast microscope, but Maddy (1964) has developed a fluorescent stain (SITS) said to specifically stain the plasmalemma. The stain is supposed to bind with specific sites in the plasmalemma, but its specificity for this membrane appears to be caused primarily by its inability to penetrate the permeability barrier (Maddy, 1964). Since plasmalemmasomes and lomasomes are composed of membranous material external to the plasmalemma, they may be expected to bind the stain and, as they are frequently larger than the limit of resolution of the light microscope, they should be visually detectable when stained.

Incubation in SITS caused almost instantaneous cessation of cytoplasmic movement, but material fixed in GA/Os after incubation showed a normal structure, including plasmalemmasomes, apart from the appearance of fibrils in the nucleus (Figs. 208 & 209). These are similar to those produced in colchicine treated nuclei but their occurrence has not been studied in detail. If they are always formed as a response to SITS, it suggests that at least part of the molecule must penetrate the cells, as witnessed by the cessation of cytoplasmic streaming. Maddy (1964) has suggested that SITS can bind to SH groups and Mazia (1961) has discussed the importance of sulphydryl bonding

in the structure of spindle tubules. The SITS produced fibrils may be the result of a disruption of spindle tubules by the interaction of SITS with their sulphydryl bonds, but clearly further work is needed on this interesting topic.

No structure examined showed autofluorescence, but after incubation in SITS, a strong pale blue fluorescence is detected in all hyphae. It is usually most intense at the apex and decreases gradually sub-apically (Figs. 210 - 216). "Regrowing" apices usually show strong fluorescence in the young apex, but a variable amount in the old one (Fig. 215). The distribution of fluorescence is usually even, but in a few hyphae (e.g. Figs. 215, 218 & 222) and discharged sporangia (Fig. 225), there are regions of concentrated fluorescence in or near the walls. Some of these are almost certainly caused by lomasomes (Figs. 215 & 225) which are often abundant in the regions shown, whereas plasmalemmasomes are absent from discharge sporangia. However, the more diffuse patches are probably caused by plasmalemmasomes (Figs. 218 & 222).

Both the plasmalemma (Figs. 220 & 224) and the walls (Figs. 224 & 227) bind the stain and if both are present, there is a corresponding increase in fluorescence (Fig. 227). That SITS is not specific for membranes is clearly shown by its strong reaction with elder pith and pea tissue (especially the spiral thickening of the xylem), although it does not become absorbed on all surfaces, e.g. polystyrene.

In order to detect any changes in distribution of

plasmalemmasomes caused by fixation, some hyphae were stained with SITS and observed during the addition of GA or Os to the preparation. No changes were detected in the distribution of the stain (Figs. 230 & 231), but there was a gradual loss of fluorescence. Hyphae fixed in GA for 1.5 h, 5 min and 15 sec followed by incubation in SITS all showed fluorescence in the old hyphae but virtually none in the apices (Fig. 229).

iv) Fixation time

If the configuration of the plasmalemmasomes is produced by the interaction of the fixative with the membranes, it was thought that very short fixation times may reveal different structures. Typical plasmalemmasomes are found after 2 min in 5% GA (Fig. 111). These experiments will be discussed more fully in the appendix.

v) Plasmolysis

If extensions of the plasmalemma can become embedded in wall material in life, as some fixed plasmalemmasomes appear to be, it might be expected that the plasmalemma and cytoplasm would be difficult to separate from the wall. Hyphae were plasmolysed in 2M sucrose and 4M calcium chloride (Figs. 232 - 236). The sub-apical cytoplasm becomes strongly contracted and breaks into a string of small spheres in both solutions, but the apical cytoplasm is never seen to leave the walls. This would appear to indicate a very close association between the walls and the plasmalemma, possibly due, in part, to the attachment of the cellulose wall fibrils to the enzyme granules

which are producing them (see discussion). If no special adhesion existed between these structures, it would seem likely that the apical cytoplasm would have been withdrawn into a spherical mass as occurred in the older vacuolate region of the cytoplasm.

vi) Growth temperature

The structure and distribution of the plasmalemmasomes suggests that they may be the result of the formation of excessive plasmalemma relative to that needed to line the cell wall. If this hypothesis is correct, it is possible that variations in growth temperature may differentially alter the relative rates of wall formation and plasmalemma production, thus varying the abundance of plasmalemmasomes and lomasomes. Colonies grown on agar at 10° C., 25° C., 30° C. and 37° C. had radial growth rates shown in Table 7. The figure given for the 10° C. colonies is lower than the actual growth rate of individual hyphae since most of them grew with a fairly constant left-hand curve producing a "catherine wheel" pattern of colony.

Table 7

Effect of temperature on growth rate

Colonies grown on OM agar for 47 h from similar inocula cut from adjacent regions of the parent colony. At least two colonies per temperature were measured across several diameters.

	Temperature (° C.)			
	10	25	30	37
Average diameter (mm)	12	61	68	0
Average growth rate (mm/h)	0.13	0.65	0.73	dead

There were essentially no differences between apices grown at 10° C. (Figs. 113 & 114) and 25° C. (Figs. 108, 109 & 110); all observed variations were within the range occurring in a colony. However, four of the five apices examined from the 30° C. colonies had a very characteristic organisation which has only been seen in one of the numerous 25° C. apices examined (Figs. 118 & 119). The cytoplasm in these 30° C. apices contains a high density of ribosomes (Fig. 115), the nucleolei enlarge and fragment (Figs. 119 & 120) and the nuclear envelope is often swollen and appears to have more connections with the E.R. The latter is itself seen as longer, continuous profiles (Fig. 119). Golgi bodies are absent and mitochondria are larger and more spherical with narrower tubular cristae and a dense matrix (Fig. 120). Typical wall vesicles and accompanying dense vesicles have only been seen in two hyphae (Figs. 116 & 117); however, all contain large vesicles between the plasmalemma and the wall (Figs. 119 & 120). These vesicles contain a few ribosomes, are apparently not connected with the cytoplasm, and occupy a region extending back from the apex to at least 70 µm. In this region, the vesicles may resemble tubular plasmalemmasomes (Fig. 119) and are accompanied by a convoluted plasmalemma which may project deeply into the cytoplasm as simple parallel sheets (Fig. 116). Lomasomes have not been observed in the walls of the 30° C. hyphae.

3) Discussion

a) Wall structure and synthesis

The fibrils revealed in the walls of S. ferax after "Domestos" treatment are probably cellulosic since Parker, Preston & Fogg (1963) have shown that approximately half of the alkali insoluble fraction of the walls is soluble in cupram and a similar percentage of this fraction also remains after "Domestos" extraction. Furthermore, Foster (1962) has shown that only cellulose fibrils remain after "Domestos" extraction of radish root tips. Whilst the amorphous matrix material (c 90% of the walls) undoubtedly contributes some rigidity to the walls, the retention of hyphal shape after "Domestos" extraction suggests that the cellulose fibrils are probably the major mechanical component. However, the solidification of the sub-apical walls cannot be due simply to the addition of a cellulose network of inherent rigidity since the apex is completely enclosed by the network which must, therefore, expand and be reorganised to allow hyphae to elongate.

The sub-apical increase in birefrigence of the hyphal side walls may indicate an increase in thickness of the fibrillar layer; these results, however, should be treated with caution since the changes are small and variations in intensity of birefringence can be caused by changes in the curvature of the wall giving rise to a deeper layer of suitably orientated fibrils. This effect is undoubtedly partially responsible for the stronger birefringence of the sporangia walls (Fig. 94)

in which the intensity of the rotated light is approximately proportional to the diameter of the sporangium. However, apart from the extreme apex, the diameter of any one hypha is constant, thus sub-apical increases in birefringence of vegetative hyphae probably do indicate an increase in fibril content.

There is no evidence for the presence of orientated fibrils in sub-apical walls and, although detailed measurements have not been made, the fibrils do not appear to show an increase in diameter comparable to that shown in the sub-apical walls of Phytophthora, Neurospora and Schizophyllum by Hunsley & Burnett (1968). It is most likely that the increase in birefringence is to be accounted for by an increase in the numbers of randomly arranged fibrils laid down in the apical 60 µm. However, the solidification of the walls responsible for the tube shape of the hypha must occur on the shoulders of the apex (i.e. within about 10 µm of the apex), thus the increase in fibrillar material occurring in the sub-apical 60 µm is unlikely to be a major factor in this rigidity.

The rigidity of the sub-apical wall is probably produced by chemical bonding between the cellulose fibrils. In higher plants, Lamport (1965) has suggested that wall rigidity is due to sulphydryl bonding between fibrils caused by a hydroxyproline-rich protein and Nickerson, Taber & Falcone (1956) have suggested that sulphydryl bonds are important in the wall structure of Candida and Geotrichum. Furthermore, Zalokar

(1959) has found a high concentration of sulphydryl groups in the apical 50 µm of Neurospora hyphae. Since Maddy (1964) has shown that SITS will bind to sulphydryl groups, part of the apical fluorescence seen after this treatment would be consistent with the presence of free SH groups in the apical wall prior to the formation of disulphide bridges. Clearly, more cytochemical work is needed to establish the solidification factor in the wall of S. ferax.

Though it must be borne in mind that part of their higher birefringence is due to their larger diameter, the intensity of birefringence in the more rigid walls of the sporangia suggests that these contain a relatively higher percentage of fibrils than those of the vegetative hyphae. Since the primary cysts have a similar diameter to that of the hyphae, the stronger birefringence in their walls indicates a larger fibrillar content, no doubt partially due to the greater thickness of the walls, though primarily caused by changes in the percentage of fibrils present. The presence of unmasked fibrils on the surface of the secondary cysts suggest that their walls have a virtual absence of hemicelluloses or other matrix materials. It cannot be assumed that these fibrils are identical with those of the hyphae; they may be of a different crystalline polymer such as the gluco-mannans and mannans found in Hydrodictyon, ivory nuts and dates by Kreger (1960) and Meier (1958). However, they appear similar in thickness and shape to those in the other walls of S. ferax. The variations in

fibrillar content of these different types of wall suggest that the synthetic mechanisms involved in their production may also differ; the spores containing a system forming predominantly fibrils, the hyphal apices one forming mainly matrix materials, and the sporangia forming an equal amount of both types.

With the exception of the zoospores of S. ferax, wall synthesis is always accompanied by wall vesicles which are most abundant in vegetative apices, sporangial apical papilla and the primary zoospores of D. sterile. Comparable vesicles, also specifically associated with wall synthesis, have been described in many fungi (Grove, Bracker & Morré, 1967; Brenner & Carroll, 1968; McClure, Park & Robinson, 1968; Hemmes & Hohl, 1969), and also in pollen tubes (reviewed by Rosen, 1968, and also Sassen, 1964), root hairs (Sievers, 1968), root tip cells (Mollenhauer, Whaley & Leech, 1961; Frey-Wyssling, López-Sáez & Mühlethaler, 1964) and algal cells (Drauert & Mix, 1961/62). Mühlethaler (1967) and Northcote (1969) have put forward evidence that in most plants these vesicles contribute pectic substances and hemicelluloses to the walls. Since Parker, Preston & Fogg (1963) were unable to detect galacturonic acid on hydrolysis of the walls, and the present author found no ruthenium red positive substances, it is reasonable to conclude that the vesicles are not contributing pectic material to the walls of S. ferax.

The strong PAH reaction of the GA/Os fixed vesicles

suggests that they contain a polysaccharide, and since these vesicles can have a more dense reaction than the walls, the polysaccharide may be in a condensed form which expands on release to the walls. The lack of reaction over the lumen after Os fixation (which retains a reaction in the walls) possibly indicates the presence of a more soluble precursor or low polymer which is lost during fixation. The dense PAH reactive globule in the Os fixed vesicles may be the condensed remains of the polysaccharide, but is more probably the condensed electron opaque material which is seen dispersed in the vesicles after GA/Os. The staining properties (Pb/UAc) of this material are consistent with that of a protein. If this can be confirmed, it will be important to establish if it is a hydroxyproline-rich protein comparable to "extensin" which Lamport (1965) has suggested is responsible for the rigidity of higher plant walls. That the material in the wall vesicles is a sulphydryl rich protein is supported by Zalokar's (1959) demonstration of a high concentration of SH groups at the apex of Neurospora which has been shown to contain a vesicular apical spitzenkörper by McClure, Park & Robinson (1968).

The wall vesicles may also contain enzymes; for example, Hawker & Gooday (1969) have suggested that similar vesicles, which occur abundantly around dissolving walls in Rhizopus gametangia, contain wall degrading enzymes. In hyphal apices of S. ferax, the wall vesicles are unlikely to contain enzymes

leading to wall degradation, although in the apical papillum of the sporangia, they could contain the enzymes which effect its subsequent disintegration. However, it is quite possible that they contain the enzymes responsible for the polymerization of the wall material. The structure of the wall vesicles resembles that of microbodies, a general term which Frederick, Newcomb, Vigil & Wergin (1968) propose should be adopted for membrane bound, enzyme containing, organelles including lysosomes and peroxysomes. The enzymes most frequently reported in microbodies are peroxidase, catalase, and enzymes associated with photorespiration (Tolbert, Oeser, Kisaki, Hageman & Yamazaki, 1968). Although Zalokar (1959) has shown an apical concentration of peroxidase in Neurospora, there is little reason to believe that the wall vesicles of S. ferax contain enzymes other than those directly involved in wall formation. Thus, if these vesicles are considered as microbodies, it is probable that the range of enzymes found in these organelles will have to be extended. In the absence of detailed information on the contents of wall vesicles, it is probably more useful to retain the term wall vesicle whilst noting their possible relationship with the incompletely defined microbodies.

The origin of wall vesicles is not clear. Grove, Bracker & Morré (1967) and Hemmes & Hohl (1969) suggest that similar vesicles in Pythium and Phytophthora are produced by the Golgi bodies, although the former authors suggest that the material

in the vesicles originates from the E.R. and is elaborated during transit across the Golgi body. Similarly, it is usually assumed that the vesicles producing hemicelluloses in such plants as have been examined, originate from the Golgi bodies (reviewed by Mühlethaler, 1967). However, McClure, Park & Robinson (1968) concluded that the spitzenkörper vesicles were not of Golgi origin since they were unable to detect Golgi bodies in the fungi they examined. Golgi bodies are common in S. ferax, but intensive efforts in the present work have failed to detect any evidence for a Golgi origin of the wall vesicles with the exception of the primary cysts. In the hyphae, wall vesicles are not found associated with Golgi bodies, no PAH reaction has been observed on either Golgi bodies or E.R., and Golgi bodies are absent from the extreme apex where wall vesicles are most numerous. The occurrence of Golgi bodies throughout the hyphae suggests that they have functions apart from wall synthesis. However, it is possible that the wall vesicles are produced from a modified Golgi system. Whaley, Kephart & Mollenhauer (1959) have shown that when Golgi bodies are highly active, they tend to fragment into large vesicles. However, these vesicles are still recognisable as Golgi bodies in their material (Maize); there is no evidence for such a hypertrophied system in S. ferax.

De novo formation of membrane bound vesicles may occur, but there are few reliable precedents for such a process in the literature. The most obvious origin of the wall vesicles is

the E.R., cisternae of which are abundant near the apex. Again, there are no vesicles or swollen regions of the E.R. morphologically intermediate between E.R. cisternae and wall vesicles; however, the latter may appear tubular, especially in the sporangia. The findings of Hawker, Gooday & Bracker (1966), Hawker & Gooday (1967), Marchant, Peat & Banbury (1967) and Turian & Oulevey (1968) all suggest a direct involvement of the E.R. as such, rather than via the Golgi, in wall formation in fungi, including oomycetes, and Porter & Machado (1960), Pickett-Heaps (1967) and Clowes & Juniper (1968) present good evidence for a similar involvement in other plants. The dissimilarity between the contents and PAH reaction of the E.R. and wall vesicles suggests that the elaboration of polysaccharide, and possible protein, from the "invisible" to the detectable state, occurs only in the vesicles after they are separated from the E.R. Grove, Bracker & Morré (1967) suggested that the material released to the wall via the Golgi vesicles first originated in the E.R. of Pythium. The postulated system in S. ferax is, therefore, essentially similar, and if such a process occurs widely in the fungi, it could explain the origin of the vesicles in the fungi examined by McClure, Park & Robinson (1968) and Brenner & Carroll (1968).

The activities in which Golgi bodies are involved in vegetative hyphae of S. ferax remain obscure. However, their constant association with the E.R. and a mitochondrion would suggest an energy dependent elaboration of an E.R. product,

possibly a protein (Palade & Caro, 1964). The characteristic association between the Golgi, E.R. and a mitochondrion has only previously been reported in another coenocyte, Vaucheria, by Greenwood (1959), although reports of an association between the Golgi and E.R. are common in both plants and animals (e.g. Novikoff, Quintana, Villaverde & Forshirm, 1964; Brown & Bold, 1964; Grove, Morré & Bracker, 1966; Holtzman, Novikoff, Villaverde & Claude, 1968; Hemmes & Hohl, 1969). The addition of a mitochondrion as an energy source in this association could have functional significance in a coenocyte where cytoplasmic streaming is vigorous and mitochondria and Golgi bodies might otherwise become separated by considerable distances; other coenocytes, e.g. myxomycetes, however, are able to function without such an association (observations not reported in this thesis).

Whilst the apical and sporangial walls appear to be formed without the participation of Golgi bodies, there is evidence that Golgi vesicles contribute to the inner layer of the zoospore cysts. These walls probably have a high cellulose fibril content and correspondingly little matrix material. Since their primary function is to resist adverse conditions, they may also contain a chemically different, more impermeable matrix material, the synthesis of which might demand activity of Golgi bodies. The Golgi bodies may also produce a more concentrated form of wall material, a hypothesis consistent with their known functions as concentrating structures and which may also account

for their absence in the hyphal wall synthetic system. Furthermore, if the Golgi bodies are producing a more concentrated wall component than the E.R., the relative sparsity of vesicles and plasmalemmasomes in the zoospores would be accounted for. When the zoospores germinate to form germ tubes, the wall of these is continuous with, and indistinguishable from, the inner cyst wall, yet is formed in association with typical wall vesicles (see Spore formation), possibly suggesting a dual origin for a single product, although similarity of appearance in sectioned wall material is no proof of a chemical similarity.

In conclusion, the collective evidence points to the production of the matrix material in the walls of the hyphae, sporangia and D. sterile primary zoospores by E.R. derived vesicles and in the primary systs of S. ferax by Golgi vesicles. This does not account for the origin of the fibrillar system.

In Chaetomorpha, Cladophora, Chlamydomonas (Frei & Preston, 1961; Preston & Goodman, 1968), yeast (Moor & Mühlethaler, 1963), Chlorella (Staehelin, 1966; Mühlethaler, 1967) and pea (Northcote & Lewis, 1968; Northcote, 1969) there is evidence that the fibrillar component of the walls is produced by enzymatic particles attached to the plasmalemma, or free in the wall (Staehelin 1966). Such particles are not preserved by conventional fixation techniques (Mühlethaler, 1967) but are only seen after freeze-etching; thus the present work is unlikely to reveal them if present. However, there is evidence

of plasmalemma activity in wall synthesis, shown most strongly by the PAH reaction of the zoospore plasmalemma during synthesis of the highly fibrillar inner cyst wall. Furthermore, Staehelin (1966) and Mühlethaler (1967) suggest that in Chlorella, the enzymic granules can be found on the inner side of the membranes of the Golgi vesicles which are transporting matrix material to the wall. The strong PAH reaction of the Os fixed wall vesicle membranes and the zoospore plasmalemma may be due to the presence of cellulose synthesizing enzyme granules which have fibrillar ends (Preston & Goodman, 1968) or short polymers of cellulose attached to them. More information about the structure of the membranes and attached granules and their relation to fibril synthesis will only be obtained by freeze-etch investigations.

The final steps in the formation of the dense outer layer of the primary cysts of S. ferax differ considerably from the other types of wall formation in this organism. The similarity of staining properties, the approximate volumetric correlations and the necessity to account for the fate of the amorphous material in the bars when the spines or boathooks are passed to the exterior of the encysting zoospore, all indicate that this amorphous bar material becomes the outer layer of the primary cyst and the plaques on the secondary cysts.

The origin of the bars themselves is obscure and will be discussed in the section dealing with spore formation.

Since the plaques surrounding the boathooks on the secondary spores do not form a complete layer, the process of encystment is not dependent on the formation of this outer layer. The unmasked fibrils of the secondary spores suggest that initial encystment is achieved by the almost exclusive production of fibrils which are presumably cross linked to form a coherent wall. The amorphous bar material probably functions as an adhesive for attachment of hooks or spines to the cyst.

The primary cysts of D. sterile possess neither spines nor a dense outer layer. The formation of these cysts appears to involve the production of more matrix material than in S. ferax since there are more wall vesicles involved. The sporangia of D. sterile also differ from those of S. ferax since they appear to contain fibrils orientated in the plane of the wall in such a way as to enable them to rotate a beam of polarized light when viewed normally. This difference may be correlated with the greater rigidity of the hyphae in this organism but a detailed study has not been made.

The mechanism of formation of the cross wall at the base of the sporangium has not been elucidated in either S. ferax or D. sterile. Only one of the many hyphae examined in the appropriate region before cross wall formation showed any differentiation and this was only a clearing of the cytoplasm with the exclusion of nuclei and mitochondria. The reduced

concentration of ribosomes would be consistent with the occupation of the cytoplasm by an accumulation of wall precursors prior to the insertion of the wall. Rothert (1888) has observed the release of cytoplasm (as witnessed by bacterial swarming) at the time of cross wall insertion, thus suggesting that the plasmalemmas on either side of the wall form independently with a gap between them. However, further details are unknown. Once formed, the initial wall is apparently added to by wall vesicles, and, since it is strongly birefringent, by fibrils also.

This account suggests that there are three basic mechanisms involved in wall synthesis; vesicles, probably derived from the E.R., plasmalemma-bound enzyme particles and bars. This work was initially conceived partially to clarify the role of lomasomes in wall synthesis. Lomasomes have not been discussed among possible wall synthetic mechanisms since the results have led to the conclusion that they are not the specific sites of wall synthesis; their nature will be discussed below.

b) Lomasomes and plasmalemmasomes

Bodies, referred to as lomasomes and plasmalemmasomes, although reported first in fungi, occur widely in walled cells throughout the plant kingdom (see Literature review). Marchant & Robards (1968) have suggested that some lomasomes are produced from multivesicular bodies which have migrated from the E.R. through the plasmalemma. They further hypothesize that other

lomasomes (their plasmalemmasomes) arise as elaborations of the plasmalemma. In S. ferax, it is improbable that any lomasomes are derived from multivesicular bodies since structures comparable to those described by Marchant, Peat & Banbury (1967) and Marchant & Robards (1968) have not been observed in any of the stages examined in the present work. The multitubular bodies reported here have a considerably different structure and no evidence has been found to suggest that they are involved in lomasome formation; their function is unknown. However, contrary to the statement of Marchant & Robards (1968) founded apparently only on a misreading of another text in which these bodies are not mentioned, lomasomes are abundant in S. ferax. This would suggest another origin for such structures and, since the walls of S. ferax contain no chitin, these lomasomes cannot be involved in chitin production as postulated by Marchant & Robards (1968).

The one common factor in most reports of lomasomes is their preferential occurrence in regions of an organism active in wall formation. From the results presented here, it is possible to hypothesize that all lomasomes in S. ferax and D. sterile are produced by the sequestration of plasmalemmasomes in the developing cell wall. Thus, both plasmalemmasomes and lomasomes would be produced when the balance between turgur pressure, wall elasticity (and thus cell expansion) and membrane synthesis is disturbed. Under conditions where wall formation and hyphal extension are in balance with membrane formation,

there will be no production of plasmalemmasomes or lomasomes. Alterations in this balance resulting in excess plasmalemma formation could produce plasmalemmasomes, their size and number depending on the extent of imbalance, thus partially explaining the observed variation between similar regions of the colony.

An important factor affecting the balance would be the presence of a mechanism capable of removing subunits from the plasmalemma, thus causing a reduction in its surface area. Such a system probably exists in the zoospores of S. ferax since there are vesicles which, in fusing with the plasmalemma, contribute additional membrane to it. As the cyst does not expand, the plasmalemma must in some way be maintained at a constant area, otherwise plasmalemmasomes would be more common than observed, even allowing for the relatively smaller vesicular activity in the synthesis of these walls compared with the hyphal apices. Similarly, the primary zoospores of D. sterile produce a cyst within the sporangium; thus they cannot expand. These cyst walls are produced by copious wall vesicles which give rise to a considerable excess of plasmalemma, yet the abundance of lomasomes in mature spores is less than would be formed if all the excess plasmalemma observed in the early stages of wall production became sequested in the wall.

When plasmalemmasomes are found on developing septa in ascomycetes, e.g. Wilsenach & Kessel (1965), the balance is

probably not affected by turgur pressure but a comparable imbalance could still exist between membrane production and increase in wall area. Similarly, Hawker & Gooday (1969) report extensive plasmalemmasomes (as defined here) along walls which are not expanding. However, these walls are being degraded; apparently by the contents of vesicles which coalesce with the plasmalemma. The authors report a considerable variation in the extent of the plasmalemmasomes, thus suggesting a variation in the effectiveness of mechanisms which remove excess plasmalemma. A further factor affecting the balance in both Rhizopus gametangia (Hawker & Gooday, 1969) and in the present work could be the degree to which contents of the vesicles are in a condensed form. Conceivably, a balance normally operates between the volume of vesicular contents, the area of membrane enclosing this volume and the rate at which any excess membrane can be removed from the plasmalemma; if less condensed vesicular contents were produced, the plasmalemma contraction system could become temporarily inadequate.

In S. ferax, the balance between formation and removal of plasmalemma is apparently considerably affected by the incubation temperature; thus colonies grown at 30° C. consistently appear to contain more plasmalemma elaborations, although the nature of the large vesicles along the wall in these hyphae is not fully understood. However, since plasmalemmasomes can occur at 10° C., it is probable that

small temporary fluctuations of lower temperatures may also produce excess plasmalemma. Such small fluctuations undoubtedly occur during the interval between removing the colony from the incubator and immersing the hyphae in fixative, thus offering a further potential cause for the variation observed in the hyphae. Furthermore, as mentioned in Table 4, surface hyphae of agar colonies failed to grow after being disturbed whilst the submerged hyphae grew on apparently unaffected. This suggests that surface hyphae are more susceptible to shock than submerged ones and since examined hyphae were both submerged and on the surface, this could further account for the variations observed.

All causes of variation need not be considered abnormal. Hyphal apices must undergo changes in their growth rates which allow branch apices to "catch up" with the edge of the colony and then remain level with the apices already present. This control is both normal and probably endogenous and could result in the production of a temporary imbalance producing plasmalemmasomes.

The principle of plasmalemmasome formation as a consequence of excess plasmalemma production is relatively simple but the configurations assumed by the excess membrane are probably as variable as the mechanism of their production, and they can also apparently be varied by the fixative used. However, the sequested membranes of the lomasomes embedded in wall material are apparently unaltered by the fixations,

and it is, therefore, probable that their configuration closely represents that of the plasmalemmasomes at the time of sequestration. This hypothesis is supported by the presence of vesicular, or possibly irregular highly anastomosing tubular, plasmalemmasomes which are lightly enclosed in wall material. These structures are apparently intermediate between a plasmalemmasome and a lomasome. The tubular plasmalemmasomes probably undergo progressive reduction into vesicles prior to sequestration.

The status of the irregular plasmalemma elaborations seen in Os fixed material is uncertain. The SITS treatment gave localised areas of staining which could be ascribed to plasmalemmasomes, but the technique was not able to distinguish between the Os configurations and an aggregation of tubular structures. There are, however, reports of membranous lamellae which are preserved after GA/Os but disrupted by Os alone (Tormey, 1964; Franzini-Armstrong & Porter, 1964). These observations suggest that Os fixation could disrupt an initially tubular form into the irregular configurations seen in Figs. 204 - 207. However, the observation that tubular membranous elaborations occur in the cytoplasm associated with some dense bodies after GA fixation but not after Os (see Spore formation) suggests that in S. ferax the tubular plasmalemmasomes might also be produced by GA fixation. However, tubular plasmalemmasomes can be found in GA/Os fixed material after only 2 min in GA and Os fixation also preserves them.

An unequivocal description of the configuration of the plasmalemmasomes in life is clearly not possible based on observations of chemically fixed material. Freeze-etch studies could solve this structural problem; however, the present observations do indicate that excess plasmalemma becomes vesicular before sequestration. The sparsity of factual information on the molecular architecture of the plasmalemma renders comments on the mechanisms of its configurations purely speculative; thus the reasons why excess membrane becomes localized in tubules attached to small regions rather than by accommodation in a more general irregular folding remains unknown. However, on the hypothesis presented above, the plasmalemma is in essence a labile structure which may be expected to exhibit a considerable turnover of its constituents rather than a steady or intermittent accretion of permanent material. The loss of portions of this membrane as lomasomes is probably accidental contrary to the removal of membrane units during normal cell turnover.

The membranous inclusions of the sporangial cross walls may be considered as lomasomes if such are defined as membranous material sequested in the wall. However, the different configurations of these trapped membranes suggests that their formation is the result of a process rather different from that producing lomasomes in other walls of S. ferax. The high rate at which the cross wall forms may not allow sufficient time for a rounding off process to take place. The presence

of considerable quantities of cytoplasm with the membranes suggests that they may have originated, at least in part, from cytoplasmic membranes rather than from the plasmalemma alone. However, their position within a developed wall would suggest that they be classed as lomasomes, though of special origin. Similarly, some of the lomasomes apparently trapped between the young apex and the old wall in "regrowing" apices are probably formed by the sequestration of cell membranes as well as plasmalemma; again a different origin but still definable as lomasomes.

The hypothesis presented here for the formation of lomasomes from excess plasmalemma becoming sequested in the developing wall fits the observed facts for S. ferax and D. sterile. More generally, it also appears adequate to account for most reported lomasomes. For example, the abundant lomasomes of Phytophthora sporangia (Chapman & Vujičić, 1965; Hemmes & Hohl, 1969) could be a consequence of the synthesis of the inner wall layer from vesicles; the old wall prevents expansion of the new wall and local accumulation of extra plasmalemma could become trapped in the developing wall. The literature contains more reports of lomasomes (as defined here) than plasmalemmasomes (see the review of Marchant & Robards, 1968, and Bracker, 1967). This is probably due to the transitory nature of plasmalemmasomes compared with lomasomes which persist and can be detected long after their formation. The only known report directly contrary to the present hypothesis is that of Barton (1965) where it is

suggested that some flecks (analagous to flattened lomasomes) do arise from the sequestration of plasmalemmasomes (or "charasomes") but others do not. There are numerous reports (e.g. Marchant, Peat & Banbury, 1967; Marchant & Robards, 1968; Robards & Kidwai, 1969) of different origins of the initial excess plasmalemma; these are not always convincing but the origin of the membrane does not affect the general concept of sequestration of the excess postulated here. Furthermore, the present hypothesis suggests that plasmalemmasomes are only coincidentally involved in wall synthesis, if at all. They are apparently concentrations of plasmalemma which, whilst they may arise from the addition of membranes of vesicles carrying wall materials, precursors or enzymes, they, and their derived lomasomes, are not structures normally adapted to a specific function. In this, they contrast with the bacterial mesosomes which appear to have the role of major organelles. This concept alleviates the problem encountered by most authors in ascribing a function to such a variable structure which is not consistently found specifically associated with any process.

The present work suggests that plasmalemmasomes and lomasomes are to be attributed to basic similarities of organisation in walled eukaryotic cells rather than a specific fungal structure as suggested by the authors (Moore & McAlear, (1961), who first defined them.

SPORE FORMATION

1) Literature review

The asexual cycle of the Saprolegniales was accurately described at the light microscope level by such early workers as Büsgen (1882), Ward (1883), Rothert (1888) and Hartog (1895), and their results, summarized in Figs. 237 & 238, have provided a framework for this section. Hyphal apices, which are destined to become sporangia, swell to a varying degree (Ward, 1883) and fill with protoplasm with streams from the sub-apical regions (Fig. 237, 2-3). The sporangium initial is then isolated from the hypha by a cross wall (Fig. 237, 3), inserted either shortly before or after the formation of an apical papillum (Rothert, 1888). The cytoplasm cleaves into uninucleate spore initials (Fig. 237, 5-6), each of which develops a contractile vacuole and produces two flagella (Fig. 237, 6-7). The apical papillum then opens to release the pyriform zoospores which swim for a few minutes (Fig. 237, 8), then lose their flagella, round off and become spherical cysts (Fig. 237, 9). After a few hours a cyst may germinate, via a germ tube, into a new colony (Fig. 237, 10), or it may release a secondary zoospore which is reniform, biflagellate and usually swims for up to several hours before it too encysts. Secondary cysts usually produce a germ tube but repeat emergence of secondary type zoospores is not unknown for Saprolegnia (Höhnk, 1933).

Spore delimitation is accomplished by development of the central vacuole which eventually fuses with the plasmalemma,

thus allowing contraction of the sporangium and leading to the "homogeneous" phase of sporangium development (Fig. 238, 5-6) (Rothert, 1888, and Hartog, 1895). Gay & Greenwood (1966) have shown that vesicles which contain "dense bodies," possibly composed of phospholipids, enlarge, fuse with each other in the cleavage planes and with the central vacuole and finally, just prior to the homogeneous phase, fuse also with the plasmalemma, thus delimiting the zoospores. However, in Phytophthora, Hohl & Hamamoto (1967) suggest a Golgi origin for the cleavage vesicles and Ho, Zachariah & Hickman (1968) postulate the origin of "dense bodies" from accumulated waste material.

Mäckel (1928), Shanor (1937) and Schrader (1938) suggested that asters guided the cleavage planes in oogonia and zoosporangia of Thraustotheca and Saprolegnia, but Höhnk (1935) held the opposite view for S. ferax oogonia. Slifkin (1967) described irregular cleavage of S. delica zoosporangia in the presence of colchicine, thus supporting the hypothesis that astral tubules are involved in cleavage orientation, but asters have not been reported in electron microscopical investigations of zoosporangia.

Fischer (1894) described two types of flagella, "Flimmergeissel" which bore lateral hairs or "Flimmer", and "Peitschengeissel", which lacked hairs. Although the biflagellate nature of Saprolegnia zoospores had long been established (e.g. Ward, 1883), Vlk (1939) was the first to demonstrate the heterokont nature of the primary and secondary zoospores of Saprolegnia and the secondary spores of Dictyuchus.

Couch, (1941), noted that both flagella are active in spore propulsion, the tinsel one being borne anteriorly and the whiplash posteriorly; he also discussed the significance of the flagellum types in the phylogeny of the fungi.

The increased resolution of the electron microscope enabled Manton, Clarke & Greenwood (1951), and Manton, Clarke, Greenwood & Flint (1952) to demonstrate the presence of nine double and two single fibres in both flagella of S. ferax and other flagellates. They described the flimmer as composed of a thick proximal rod, probably attached to the fibres, terminating in a long hair point and also found fine threads on the whiplash flagellum. Vujičić, Chapman & Colhoun (1965) also noted hairs on the whiplash flagellum of Phytophthora, but Kole (1965) did not mention such hairs in a review of fungal flagella. Sparrow (1958) and Alexopoulos (1962) have used the type of flagellation of zoospores as a major taxonomic criterion.

Cotner (1930) described the development of a variety of Phycomycete flagella from a basal granule associated with the nucleus, noting also that uniflagellate species develop flagella earlier in spore formation than biflagellate types. Following the development of ultrathin sectioning, the structure of numerous flagella has been elucidated (reviewed by Manton, 1964c & 1965, Satir, 1965 and Ringo, 1967b), and that of several uniflagellate fungi has been examined in detail (Fuller & Reichle, 1965 & 1968; Fuller, 1966; Reichle & Fuller, 1967; Olson & Fuller, 1968, and Lessie & Lovett, 1968). Renaud &

Swift (1964) and Lessie & Lovett (1968) described the development of the flagellum in Allomyces and Blastocladiella and showed it to occur before cleavage. The biflagellate fungi have been relatively neglected (Colhoun, 1966). Chapman & Vujičić (1965) suggested that the flagella of Phytophthora erythroseptica develop after cleavage, whilst King & Butler (1968) state that in P. infestans they are formed before cleavage. In various biflagellates including S. ferax, Hartog (1895), Cotner (1930) and others placed flagellum formation after cleavage and possibly after spore release (Ward, 1883), but Crump & Branton (1966) and Gay & Greenwood (1966) have shown flagellate spores prior to their release from the sporangium. However, the development and structure of S. ferax flagella remains obscure.

Whilst Crump & Branton (1966) found that the primary spores of Saprolegnia withdraw their flagella immediately prior to encystment and the secondary shed them, they were unable to detect withdrawn flagella in sectioned primary cysts, although Fuller & Reichle (1965) found naked axonemes in Rhizidiomyces cysts. Meier & Webster (1954) showed that the flimmer remains on the exterior of the primary cyst of S. ferax but the breakdown process of the axoneme is unknown.

Manton, Clarke & Greenwood (1951) described "boathooks" on the surface of S. ferax cysts. They suggested that these hooks may be an aid to spore dispersal and that they occurred on primary cysts, whereas Meier & Webster (1954) claimed that the

boathooks were only present on secondary cysts and the primary cysts were adorned with fine hairs. Nagai & Takahashi (1962), however, suggested that similar boathooks occurred on both primary and secondary cysts of S. diclina. Although Gay & Greenwood (1966) suggested that these cyst ornamentations may be produced from structure which they termed "bars", the origin and distribution of these hooks and spines clearly need further elucidation.

Whilst there have been numerous ultrastructural studies on the germination of higher fungal spores, there are no reported ultrastructural studies on secondary spore release or germ tube production in the oomycetes.

The extensive background of knowledge about S. ferax and the ease of induction of sporulation makes this organism very suitable for a comprehensive investigation of the fine structure in relation to some of the controversial aspects of asexual reproduction in biflagellate phycomycetes.

2) Observations

The various aspects of spore formation which have been examined will be considered individually.

a) Dense bodies

Dense bodies were first described in S. ferax by Gay & Greenwood (1966). Although their structure is variable after GA/Os fixation, they are characteristically single membrane bounded vesicles which contain a more or less spherical electron opaque structure which frequently appears to fragment around

its periphery into various amorphous, granular or myelin-like configurations shown in Figs. 142, 144, 145, 184, 185 & 240. The appearance of the dense bodies is partially dependent on their intrinsic constitution, since various configurations can be found in a single specimen, but is also affected by the fixative. GA/Os favours myelin-like configurations, whereas Os alone tends to disrupt the membranes, and the fragmented parts of the dense globule form small dense granules which are slightly larger than ribosomes (Figs. 154, 158 & 244), although myelin-like configurations can occur in Os fixed material (Figs. 140 & 244) and the dense granules in GA/Os prepared specimens (Fig. 243). Permanganate fixation usually preserves the dense bodies as lighter structures with dense peripheries (Fig. 246) which completely fill the vesicles. A myelin-like configuration has only been seen once after permanganate fixation (Fig. 247). The PTA stained contents of disrupted sporangia contain numerous spherical bodies which are not penetrated by the stain and often have characteristic extensions (Fig. 245). Since these bodies have a diameter similar to that of the dense bodies, they are assumed to be homologous. Frequently, in GA/Os fixed specimens, the dense body vesicles are enlarged and often protrude into a neighbouring vacuole (Figs. 242 & 243), and occasionally the dense body vesicle appears to be associated with an aggregation of tubular membranes reminiscent of tubular plasmalemmasomes (Fig. 241).

Dense bodies do not occur in hyphae growing on OM but

appear when these hyphae are transferred to water to induce sporulation; they become abundant before sporangia are clearly recognisable. Hyphae growing on a hemp seed in any medium contain dense bodies, but these hyphae will not produce sporangia in OM. The role of the dense bodies during cytoplasmic cleavage has already been described by Gay & Greenwood (1966). This aspect of spore formation will not be described in the present work.

Whilst some of the dense bodies are used up during cleavage, most are incorporated into the zoospores where they remain, apparently unaltered in numbers and structure, throughout motility and encystment. When cysts are placed in OM, they produce a germ tube. The vacuole of the sporeling is produced by the expansion and coalescence of the dense body vesicles (Figs. 136, 248 & 249). In some spores, the dense bodies retain their shape and decrease in size (Fig. 248), in others they fragment and form an irregular, dense lining around the expanding vacuole (Fig. 249).

Dense bodies also occur in D. sterile (Figs. 184 - 186), but their role in cleavage has not been investigated. When the primary spores of this species develop germ tubes (or dehiscence papillae), some dense bodies appear to enlarge (see Wall formation), and those remaining in the secondary cysts produce the vacuoles of the germinating spore (Fig. 250).

b) Golgi and E.R.

The association of Golgi bodies with cisternae of the

E.R. and mitochondria (see Wall formation) is still found during the early development of sporangia, but becomes difficult to detect as the cytoplasm approaches cleavage. At this time, up to four Golgi bodies flank the apex of each pyriform nucleus (Figs. 253 & 254). Their forming faces are usually parallel and closely associated with the nuclear envelope which can produce vesicles towards the Golgi bodies (Fig. 254). At this time, the Golgi bodies produce numerous vesicles, many of which are characteristically "hairy," "alveolar" or "bristle coated," (Fig. 253) (Manton, 1966). Golgi bodies remain active and adjacent to the nucleus in the motile and newly encysted spores (Figs. 255, 263 & 278) at which times there are apparently no Golgi bodies unassociated with the nucleus. However, as the cyst ages, the Golgi bodies become less active and lose their nuclear association so that at the onset of germination (Figs. 239 & 248) they are again associated each with a mitochondrion and an E.R. cisternum. In D. sterile, the Golgi bodies behave similarly but retain their activity and nuclear association in the primary cysts.

During zoospore formation, prior to cleavage, the E.R. becomes predominantly, though not exclusively, aligned as "rough" parallel sheets around the base of the nuclei (Figs. 252 & 271); a configuration which is retained during swimming (Fig. 278) and in encysted spores (Figs. 240 & 255). At the onset of germination, the E.R. resumes its vegetative configuration.

During vegetative stages of the life cycle, the E.R.

cisternae are typically flattened and of more or less constant width with traces of amorphous contents. Shortly after cross wall insertion, sporangia contain bundles of tubules enclosed in vesicles. The membranes of these vesicles may have attached ribosomes and can be continuous with flattened cisternae of the E.R. and the nuclear envelope (Figs. 239, 256-262). There are examples of ribosome coated E.R. cisternae which are swollen and contain a few tubules and a large amount of amorphous material (Figs. 260 & 266).

In cross section, these tubules have a thin wall composed of dense subunits (Figs. 257 & 266), surrounded by a variable amount of amorphous material, occasionally extended as connections between adjacent tubules (Fig. 261). Densitometer scans (Figs. 40 & 42) suggest that the walls are composed of a single row of dense subunits. The walls of some negatively stained tubules show a single row of isodiametric 5 nm diameter subunits (Figs. 264 & 265). Markham rotation experiments on transverse sections of these tubules (Markham, Frey & Hills, 1963) frequently showed no image reinforcements; only $n = 5$ and $n = 6$ produced reinforcement of dense subunits (Fig. 266). The data for tubule diameters is collected together in Table 8.

Table 8

Diameter of E.R. enclosed tubules

Diameters (nm) were measured with a magnifying scale directly from electron micrographs exposed in a recently calibrated microscope at an instrumental magnification of 96.3×10^3 (excluding PTA measurements). The lumens of tubules observed in section were too small and poorly defined for accurate measurement of the internal diameter.

	Number of measurements	Average diameter	Range
Longitudinal sections	69	15.0	12.0-18.7
Transverse sections	81	17.2	14.5-21.8
PTA whole mounts	many on 4 tubules	12.5 5.9*	12.2-12.8
Microdensitometer tracings of T.S. (Table 1)	10	8.3'	6.9-9.9

* denotes internal diameter.

' denotes peak to peak measurements.

Tubules occur in bundles of up to about 60; they may show hexagonal packing, and each tube is separated from its neighbours by at least 10 nm. When sectioned longitudinally, tubules are usually straight and parallel to each other with all tubes in a bundle often terminating at the same level at both ends (Figs. 256 & 258). The length of the tubules with well defined ends is about 1.5 μm; shorter lengths,

often cut obliquely, are common, but the longest tubules recorded were 1.6 µm. The space between the ends of the 1.5 µm apparently "mature" tubules and the square ended vesicle enclosing them has a fairly constant length of about 0.3 µm and is filled with ill defined, possibly tapering, rods (Figs. 256 & 258).

These tubules show an essentially similar appearance after GA/Os and Os only fixation and were unaltered after plasmolysis (Fig. 275), DNAase, RNAase (Fig. 13), papain digestion and incubation in colchicine (both 0.1 and 0.2%) (Fig. 240). They have not been observed after permanganate fixation or pepsin treatment, although the effect of the latter has not been examined intensively. The vesicle containing the tubules has a conspicuously light PAH reaction but the tubules give a moderate silver deposit (Fig. 170).

Tubules have not been seen in the E.R. of vegetative material; they appear in the sporangium at about the time of cross wall insertion and are abundant in motile, primary spores (Figs. 278 & 279), primary (Figs. 86 & 87) and secondary cysts and in germinating primary cysts with germ tubes up to 18 µm long. Although studied in less detail, D. sterile contains similar tubules at the same stages in the life cycle (Fig. 188).

c) Flagella

i) Kinetosomes

Kinetosomes develop from centrioles. Since no stages

intermediate between normal interphase centrioles and fully developed kinetosomes have been found, the changes must occur rapidly and simultaneously. Kinetosomes and their associated root system assume the configurations described below shortly after cross wall insertion; apart from flagellum formation, the system undergoes no obvious changes through cleavage and motility until encystment.

Probably throughout vegetative interphase (see Nuclear division), the two centrioles of each nucleus are orientated at 180° to each other and associated with a pocket of the nuclear envelope; this is presumably the state of the nuclei which migrate into the sporangium before cross wall insertion. After a cross wall has developed, nuclei can still divide (Fig. 65) and some may degenerate (Figs. 142 & 274). However, the nuclei of the spore initials become pyriform with the nucleolus in the basal region and two kinetosomes, still associated with the nuclear pocket, at the apex (Figs. 252, 254, 271 & 272). Nuclei are orientated radially with the kinetosomes closely adjacent to the wall (Figs. 252, 271 & 272).

The A and B tubules of both centrioles (see Centriole structure) elongate to about 0.78 μm and the C tubule to 0.6 μm; the proximal ends of the centrioles retain their chamfered appearance (Figs. 263 - 267). The distal C tubule terminations have not shown free ends comparable to those described by Olson & Fuller (1968) and Ringo (1967b) (Figs. 269 & 270). Approximately 60 nm above the C tubule terminations, a

transverse electron opaque plate is inserted (Figs. 267 - 273). This basal plate is about 20 nm thick at its centre, tapers to 5 - 10 nm where the A and B tubules pass through it unchanged (Figs. 267 - 273) and widens to 20 nm again at its rim, which is about 40 nm outside the doublets. Attached proximally to the centre of the basal plate is a 60 nm diameter, 80 nm long, slightly electron opaque cylinder (Figs. 268, 272, 273 & 275) which appears to be connected with the doublets (Figs. 268, 273 & 275). This cylinder is extended for about 40 nm distal to the plate and has thin radiating arms, or a cylindrical lamella, radiating from its distal end. These arms enclose a conspicuously clear space c 40 nm deep (Fig. 268), distinct from the amorphous background density of the surrounding cytoplasm. There is a suggestion of a dense amorphous cap on some kinetosomes at this stage (Figs. 272 & 273), but a capping vesicle has not been seen. Ribosomes are excluded from the area defined by the doublets.

Proximally the kinetosome contains a cartwheel unchanged from that of the centrioles (Fig. 276). The region enclosed by the tubules between the cartwheel and the basal plate contains amorphous material and a few dense granules (Figs. 272 & 273), similar to those seen in Stigeoclonium by Manton (1964a), who suggested they may be ribosomes. The granules in S. ferax differ in size and electron opacity from the cytoplasmic ribosomes, but their nature is unknown.

Fig. 275 shows that the kinetosome has greater structural

rigidity than the flagellum. This suggests that some stabilizing factor is present along its full length, but absent in the flagellum. Such a stabilizing factor may be the A-C links which are rarely preserved but can be seen in Fig. 276 (see Centriole structure).

Centrioles realign during conversion so that kinetosomes are always found as pairs with the long axes in a V configuration with an included angle of about 130° (Figs. 267 - 270). The kinetosomes are rarely coplanar, their bases are out of line by about half their diameter (c.f. Ringo, 1967b).

During the cleavage of the sporangium, numerous membrane bounded vesicles accumulate around the kinetosomes. Each vesicle is about 0.5 μm in diameter and up to 1 μm long, and contains concentrically arranged fibrous material (Figs. 252 - 254 & 271) which is strongly PAH positive (Fig. 149). These structures, which will be termed fibrous bodies, are not found in hyphae or sporangia until kinetosomes are formed; they persist during cleavage and flagellum production, but have not been observed in encysted spores or D. sterile. In the latter organism, numerous crystal containing vesicles (crystalline bodies) (Fig. 184 & 185) have been observed, mainly around the nucleus, in primary cysts but not vegetative hyphae of secondary cysts.

ii) Flagellum formation and structure

Kinetosomes do not elongate further than shown in Fig. 268

until the protoplast has cleaved. The A and B tubules then elongate and adopt a smaller tangential angle to become the doublets of the flagellum axoneme (Figs. 280 & 292). Arms (Afzelius, 1959) have not been observed on these doublets; their wall structure has been discussed under centriole structure. A diagrammatic reconstruction of the kinetosome and transition region of the flagellum is shown in Fig. 277. All flagella examined, including those on which the diagram is based, were on spores within the sporangium prior to dehiscence; since most of these spores lacked flimmer, it is assumed that they were not mature and were still elongating their flagella. There is no evidence to show that the kinetosome and transition regions of the flagella alter during later stages in its development.

The basal plate comes to lie at the surface of the spore (Fig. 279). Its rim is attached to the membrane which surrounds the spore and is extended to form the sheaths of the flagella (Figs. 280 & 28). This membrane is strongly PAH positive (Fig. 174). The transition region of the flagellum undergoes several changes from its precleavage state. The dense cylinders and basal plate remain virtually unchanged, but above the plate a densely staining thick walled collar develops (Figs. 277 E, 281, 288 & 295). After cleavage, the zoospores proved difficult to fix; in 5% GA they appear condensed and plasmolysed (Fig 278); in 1% GA and lower they are "blown up" (Figs. 177 & 296). In both fixations, the dense collar appears

concertina-like (Figs. 281 & 296). The dense collar has radial strands in its wall (Fig. 295) and encloses a clear space, possibly traversed by thin strands connecting the dome on the basal plate to the collar. There are suggestions of connections between this collar and the doublets (Fig. 287) and also the amorphous material at the base of the central pair (Fig. 289) but they are not well defined. The distal end of the thick collar is continuous with a straight cylinder or thin collar which surrounds the proximal c 60 nm of the central pair, although not connected to them (Figs. 290 & 291). Nine double radial lamellae, or struts, connect the thin collar to the doublets of the flagellum (Figs. 290 & 291). The central pair of the flagellum axoneme terminates in a small quantity of amorphous material level with the junction between the thick and thin collars (Figs. 289 & 290).

Manton, Clarke & Greenwood (1951) have shown that the central pair extends beyond the outer doublets at the tip of both flagella of S. ferax, thus, since the doublets are of a similar length to the central pair, Figs. 300 - 303 are probably from the tip of a growing flagellum and suggest even synthesis of all the tubules with concurrent synthesis of sheath material. Rosenbaum & Child (1967) and Rosenbaum, Moulder & Ringo (1969) have demonstrated tip growth of Ochromonas and Chlamydomonas flagella; there is no reason to believe that S. ferax differs in its mechanism of flagellum extension. Since flagella of at least 5 μm (compared with the

mature length of about 15 - 30 μm) have been observed on zoospores which bore no flimmer on either flagellum, it is reasonable to conclude that the flimmer hairs are added when the flagellum is more or less fully grown. However, Figs. 298 & 299 and the flimmer on cysts which were found inside the sporangium (Fig. 165) show that flimmer is added to the flagellum before the spores are released.

In shadowed preparations, a flimmer hair has a shaft of about 1.6 μm long terminating in a finer, less rigid, hair point about 1.1 μm long. Sectioned flimmer hairs (Figs. 165 & 307) are tubular with an external diameter of about 14 nm, and Figs. 298 & 299 suggest that they are attached to the sheath rather than the axoneme (contrary to Manton, Clarke & Greenwood, 1951). The tubular structure is perhaps replaced by an ill defined tapering structure at the point of attachment (Figs. 298 & 299). This tapering end is also evident on flimmer hairs after they have been shed (Fig. 304), but more observations of sectioned flimmer are needed to confirm these observations. The flagella of D. sterile have not been examined.

iii) Flagellum attachment

From an early stage in cleavage (Figs. 252 & 270), through motility (Figs. 280 - 283) and into encystment (Fig. 162), the two kinetosomes of a pair are connected by a striated fibre composed of numerous, loosely woven, parallel longitudinal fibrils with two or three dense transverse bands (Figs. 282 &

296). From serial sections (it has not been observed in transverse section), it appears to be about 90 nm square in cross section, and is connected to the tubules of the kinetosome about halfway along them; frequently an extension of the main fibre appears to curve round at least one of the kinetosomes (Fig. 270).

The bases of the kinetosomes are often embedded in electron opaque material from which numerous microtubules radiate (Figs. 267, 272 & 273). Some of the tubules pass close along the nuclear envelope, others run into the cytoplasm (Figs. 252 & 271). These tubular "roots" do not occur in pairs or other multiples; there are apparently about seventy tubules close to the nucleus at its apex and an unknown number running into the cytoplasm. The absence of tubules at the base of the nucleus shows that they are either fairly short, or more probably, they continue in straight lines from the apex into the cytoplasm. The tubular roots are formed early in cleavage (Fig. 252); persist through the motile phase of the life cycle (Figs. 280 - 283) and are found in recently encysted spores (Figs. 162, 306 & 307). The roots disappear as the cyst ages and are absent at germination, although analogous astral tubules occur during nuclear division. Figs. 184 and 251 suggest that the root system of D. sterile is similar to that of S. ferax, although the few observations of the former species failed to detect a striated fibre.

d) Encystment

i) Flagellum withdrawal

The withdrawal of the flagella as the primary zoospore encysts has been described by Crump & Branton (1966). In the present work, a sporangium was observed to slowly discharge some of its zoospores. At the time of fixation, this sporangium (Specimen number 1642) contained a number of spores which had just encysted, a zone of those which were encysting and a few which were still flagellate. The spores which were encysting (Figs. 161 & 305) were surrounded by a thin, dense wall (see Wall formation) and contained axonemes which showed no evidence of coiling around the spore. These axonemes are apparently depolymerised rapidly, Fig. 308 suggesting that the doublets become free prior to depolymerization. The axonemes break down to leave a pair of kinetosomes similar to those in the sporangium during cleavage (Figs. 306 & 307). The kinetosomes remain unchanged so that at germination, a spore which had undergone one nuclear division still contained a recognisable kinetosome (Fig. 309). However, in a similar spore (Fig. 311) which had also undergone one division, the kinetosome is apparently reverting to a normal centriole. Crump & Branton (1966) reported that some flagella form beads prior to withdrawal and Ho, Zachariah & Hickman (1967) have shown a coiled axoneme in similar beads on Phytophthora flagella. Fig. 255 is probably an example of such a bead in S. ferax. As shown by Meier & Webster (1954) and Fuller (1966),

the flimmer remains outside the spore and a tuft of it becomes attached to the cyst wall (Fig. 165).

ii) Bars

At an early stage in sporangium formation, the cytoplasm contains numerous randomly distributed structurestermed bars by Gay and Greenwood (1966) (Figs. 175 & 176). These primary bars are membrane bounded and contain an amorphous layer of material surrounding about 5 - 17 tubular structures, each about 0.24 µm in length and 9 nm in diameter. After cleavage, the bars move to the periphery of the spores (Figs. 177, 278 & 279). They are absent from encysted spores. Primary cysts bear numerous spines on their surface (Figs. 163, 164 & 173) (c.f. Meier & Webster, 1954). These spines are often clustered and have a diameter of about 10 nm and vary in length from about 0.2 µm to 0.4 µm.

Older primary cysts contain a few structures which will be termed secondary bars (Figs. 182 & 183). These are also confined to the periphery of the spores. The few profiles examined have shown variable structures, all of which could be accounted for if the bars were 0.2 µm diameter spheres composed of a bounding membrane enclosing a 0.03 µm thick peripheral layer of amorphous material inside which was a smaller sphere composed of amorphous material with a dense lining and a hollow centre (Fig. 183). Bars of this type have not been seen in secondary cysts which can be identified by the absence of both spines and a continuous dense outer wall layer. Attached to

the surface of secondary cysts are a few boathooks, each surrounded by a basal plaque of dense material (Figs. 178 - 181) (see Wall formation). The shaft of these hooks is about 15 nm diameter (Fig. 179).

The primary spores of D. sterile encyst within the sporangium. These cysts liberate secondary zoospores, which also encyst. Secondary cysts may produce a germ tube (Fig. 250), but repeated emergence of motile spores is common (Meier & Webster, 1954). Primary cysts of D. sterile contain "bars" which are membrane bounded and lined with amorphous material, each enclosing one c 2.4 µm long dense spine (Figs. 188 & 189) which is similar to the spines on the secondary cysts (Figs. 187 & 250). Germinating secondary spores may also contain similar spines (Fig. 250).

e) Germination

i) Secondary zoospore release

This process has only been observed on one occasion in S. ferax (Fig. 310). The secondary spore emerges through a small hole in the primary cyst wall. It contains dense bodies, neutral lipid and secondary bars, but no specialised structures which could be related to the process of escape. The emergence of the secondary spores of D. sterile has been described in Wall formation.

ii) Germ tube formation

As the cyst ages, the electron translucent inner wall increases in thickness (see Wall formation). The first sign

of germination after transfer to a nutrient medium is an accumulation of wall vesicles at the point near the inner wall (Fig. 249). Additional inner wall is then synthesized and pushed out through the broken outer dense wall (Figs. 249 & 248). Fig. 312 shows the accumulation of wall vesicles, some of which are tubular, at the point of germination. The germ tube then continues to grow with an apical concentration of wall vesicles (Figs. 136, 138, 139 & 249).

3) Discussion

a) Dense bodies

Gay & Greenwood (1966) have postulated that the cleavage vacuoles in the zoosporangia of S. ferax are derived from dense body vesicles. Since the sporangia do not swell significantly during cleavage although the vacuole enlarges considerably, the cytoplasm must become reduced in volume; presumably by passage of water from the cytoplasm into the cleavage vacuoles. Nir, Klein & Poljakoff-Mayber (1969) have shown that in maize cells which were dehydrated by growth under water stress, the E.R. becomes aligned in parallel arrays similar to those observed in developing spores of S. ferax. The enlargement of cleavage vesicles necessitates a considerable formation of new membrane. The presence of tubular aggregations of membranes associated with some of the vesicles after GA/Os fixation and the ability of the dense bodies to cause a considerable increase in the membrane of vacuoles into which they sometimes enlarge is an indication of their involvement in membrane formation. The strong osmophilia of the dense bodies and their tendency to form myelin-like figures suggests that they may contain phospholipids. Furthermore, Gay (personal communication, and Gay, Greenwood & Heath, in preparation) has shown that shortly after transfer from OM to water, a process which induces dense body formation, there is an increase in the lecithin content of hyphae; an observation suggesting that lecithin, known to be a component of many membranes, is a

constituent of the dense bodies. The present observations, therefore, provide evidence for the ability of dense bodies to form membranes. They also extend the general role of dense body vesicles in vacuole formation to germinating spores where vacuolation occurs by enlargement and fusion of the dense body vesicles.

The hydrolytic breakdown of high molecular weight lipids, such as those probably contained in the dense bodies, could produce smaller molecules which would raise the osmotic pressure of the fluid in the dense body vesicles and thus cause them to draw water from the cytoplasm and swell. The formation of myelin-like figures may be a stage in this cleavage process. Only a few dense bodies in the sporangium swell during cleavage, but they all enlarge when the cysts germinate; this evidence for a specific control of their functional behaviour invites further investigation. The production of tubular membranous aggregations, apparently from the dense body vesicles, during treatment with GA but not with other fixatives, is probably an artifact, but further study may help interpret the more general problems of membrane structure and the process of fixation.

b) Flagella

The formation of the kinetosomes and the development of their microtubular roots takes place at an early stage in spore development and may play a significant part in the cleavage process. The disposition of the roots, together with their known stabilizing effect on the cytoplasm (see Porter, 1966, and also Nuclear

division), would fit them to forming lines of weakness along which the cleavage vacuoles might travel, thus delimiting uninucleate masses of protoplasm. This hypothesis is supported by Slifkin's (1967) observations that spore cleavage is irregular in the presence of high concentrations of colchicine, and agrees with the views of Mäckel (1928), Shanor (1937) and Schrader (1938). The forces responsible for the orientation of the kinetosomes against the sporangium wall is unknown.

After cleavage, the roots are strongly attached to the kinetosomes, since they remain together after spores are disrupted (e.g. Manton, Clarke, Greenwood & Flint, 1952; Manton, Clarke & Greenwood, 1955, and present observations not illustrated). This firm connection suggests that they attach the flagella to the spore. The association of the roots with the nucleus is mechanically advantageous because the nucleus appears to be the largest and most solid component of the zoospore; it is thus well suited to act as a firm base for flagellum movement and probably helps to absorb the reaction to the beating of the flagella. The association of these tubular roots with the nuclear envelope probably involves similar forces to those acting when the nuclei apparently crawl along microtubules at anaphase-telophase (see Nuclear division).

The microtubular roots are probably also responsible for the shape of the spores. Their cytoskeletal function has already been mentioned and their observed disposition in the

spore would be likely to produce a pyriform shape. When the zoospores encyst, the microtubules of the flagella are depolymerized. If the depolymerization process is a generalised one and the root tubules were also broken down, this would allow the now unsupported spore to assume its characteristic shape of minimum surface area, i.e. a sphere, before acquiring a wall. However, the observations of roots around the kinetosomes of recently encysted spores show that their depolymerization need not be complete to allow loss of shape. They are probably shortened, a hypothesis which is difficult to verify, and "reeled in" to the base of the kinetosome (c.f. spindle tubules in Nuclear division).

The reniform shape of the secondary spores may be a result of the formation of the roots in a differently shaped enclosure from that of the primary spores. However, Reichle (1969) has demonstrated a "backbone" and "ribs" type of microtubule root system in the reniform spores of Phytophthora. Since Phytophthora spores and the secondary spores of S. ferax have a similar shape and are also both more competent and durable swimmers than the primary spores of S. ferax, they may have a similar root system.

The motile algae and uniflagellate fungi which have been examined with the electron microscope have been shown, in most cases, to possess a complex root system, usually involving some type of striate rhizoplast and often multitubular roots, e.g. Manton (1964a, 1965 & 1968), Ringo (1967b), Fuller & Reichle

(1968) and Lessie & Lovett (1968). The root system of the primary spore of S. ferax is less complex than those referred to above and this difference may be associated with the lesser duration and competence of the swimming phase, although, as noted by Manton (1965), details of the root systems probably also have phylogenetic significance.

The striated fibre connecting kinetosomes has been reported in a wide range of algae, e.g. Polystoma (Lang, 1963), Oedogonium (Hoffman & Manton, 1963), Mesostigma (Manton & Ettl, 1965) and Chlamydomonas (Ringo, 1967b). The present work gives the first report of this structure in biflagellate fungi. A common function of this structure may be the maintenance of the arrangement of the basal bodies and resistance to the action of the flagella. In S. ferax, the attachment of the basal plate of the kinetosome to the spore membrane is probably also a part of the anchorage system, comparable to, but simpler than, the props in Phlyctochytrium described by Olson & Fuller (1968).

The source of the precursors or subunits for the synthesis of the microtubules in the root system and the flagella is uncertain. Evidence for the pocket in the nuclear envelope as the site of microtubule subunit synthesis has already been reviewed (see Nuclear division). The dense material surrounding the base of the kinetosome from which the tubular roots radiate could be an accumulation of subunits produced in the persistent pocket during spore formation. However, the proximity of apparently highly active Golgi bodies around the kinetosomes

suggests that they have a role in some aspect of flagellum production, possibly microtubule synthesis, as discussed in Nuclear division (see page 77). The continued activity of Golgi bodies around the nucleus shortly after encystment, however, may point to an additional or different function such as cyst wall production (see Wall formation), but could also be due to a continuation of microtubule subunit production. The appearance of the fibrous bodies in the spores prior to cleavage and their absence after flagellum production suggests that they may have a specific role in the production of the flagellum. The high PAH reaction of the fibrous bodies relative to the low reaction on the flagella tubules may indicate the presence of a high concentration of microtubule precursors in the former. However, they may contain membrane components because as the flagella grow, there is also a considerable extension of the PAH positive sheath membrane. The appearance and disappearance of the crystal containing bodies in D. sterile at similar stages in spore development as the fibrous bodies in S. ferax may indicate the homology of these two structures; the origin of both is unknown.

The structure of the kinetosomes is the same in both flagella (c.f. King & Butler, 1968), and is comparable in essentials to that reported in most plant cells. However, the transition zone shows considerable differences from the already wide array of described structures. The stellate structure reported in many algae by Manton (1964c) and Ringo (1967b) is

replaced by the dense concertina collar which has only been noted previously in the Chrysophyte, Sphaleromantis tetragona (Manton & Harris, 1966). The thinner collar and surrounding struts have not been reported previously. The wide variation in the details of the transition zone structures in the limited number of organisms so far reported makes speculation on the function and phylogeny of these structures unprofitable at present. The preservation of the flagellum itself has not been sufficiently good in S. ferax to show the presence of arms on the doublets (Afzelius, 1959) or an eliptical membrane and radial spokes surrounding the central pair (King & Butler, 1968).

The development of the flagella after cleavage in S. ferax is comparable to that reported in Phytophthora erythroseptica by Chapman & Vujicic (1965) and contrasts with the precleavage development reported for Allomyces (Renaud & Swift, 1964), Blastocladiella (Lessie & Lovett, 1968) and P. infestans (King & Butler, 1968). The present work supports the early observations of Cotner (1930) who noted post-cleavage flagellum development in the biflagellate fungi and pre-cleavage formation in the uniflagellates. The mechanism of flagellum growth is uncertain; presumably tubule subunits are added at some point above the basal plate. The basal plate is attached to the spore membrane around its entire periphery and gives the appearance of being a dense barrier penetrated only by the A and B tubules of the kinetosome. The lumens of these tubules could form direct channels for the transport of subunits accumulated at the base

of the kinetosome up to the site of assembly which may be at the tip of the flagellum (c.f. Rosenbaum & Child, 1967), although incorporation at its base or at intermediate positions cannot be excluded.

The nature of the 15 nm tubules in cisternae of the E.R. has been uncertain. Similar tubules in the E.R. of developing Coleus cells were thought to be involved in wall formation (Hepler & Newcombe, 1964), a view also expressed by Fuller (1966). However, apart from Coleus, similar tubules have only been reported in the E.R. of organisms which produce flimmer flagella, e.g. Ochromonas (Gibbs, 1962a and 1962b), Vacuolaria (Koch & Schnepf, 1967), Rhizidiomyces (Fuller, 1966), Saprolegnia (Crump, 1966), Phytophthora (King, Colhoun & Butler, 1968, and Reichle, 1969) and Synura (Greenwood, 1966b). Bouch (1969) has suggested that similar E.R. enclosed tubules in Fucus and Ascophyllum become the flimmer on the flagella of the antherozoids; a suggestion supported by the observations of Leadbeater (1968) on Olisthodiscus and Massalski (1969) on Bumilleria and Tribonema. In the present work, the constant mature length, the close correlation in diameter and the characteristically "disorganised" tapering ends of both the tubules in the E.R. and the thick portion of the flimmer hairs suggests that the latter develop in cisternae of the E.R. which have ribosomes attached to their membranes. However, the tubules in the E.R. lack hair points; the origin of these and the hairs on the whiplash flagella are unknown. The wall of the E.R.

enclosed tubules is apparently composed of five or six dense, 5 nm diameter subunits arranged in a single row in a less dense matrix. The size of these subunits is comparable to that of the flagellum tubule subunits (see Nuclear division), but the resistance of the E.R. tubules to colchicine suggests that their subunits have either a different composition or a difference in their manner of binding. The variable peak to peak measurements of the microdensitometer scans across these tubules indicate an irregular arrangement of the subunits probably caused by the fixation procedures. Although they are produced in stages of the life cycle related to the development of flagella, the abundance of tubules in the E.R. of encysted and germinating spores shows that the amount of tubules produced is not closely correlated with the amount of flimmer required.

c) Encystment

The present observation of flagella axonemes inside recently encysted spores of S. ferax confirms the withdrawal of the primary spore flagella described by Rothert (1894) and Crump & Branton (1966). As noted by Meier & Webster (1954) and Fuller (1966), the flimmer hairs remain outside the cyst and are often attached to it. Thus, whilst the spores have found it evolutionarily advantageous to conserve the flagellum subunits, it is apparently preferable to shed the flimmer and produce more for the secondary spore. Such differences in fact may be correlated with the apparently rigidly constructed

flimmer relative to the more easily disrupted tubules of the flagella.

The development of cyst walls has been noted under Wall synthesis. The position in the stages of the life cycle, the association with the surface of the motile spores, the clumping of the spines on the surface of the cyst and the dimensions of the spines are all consistent with the origin of the spines on the primary cysts of S. ferax from the bars in the motile spores. Similarly, the spines on the secondary cysts of D. sterile are preformed in bars found in the primary cysts. The boathooks on the secondary cysts of S. ferax are probably produced from the secondary bars in the primary cysts; however, in this case, the boathook does not appear to be fully developed in the bar before release. Further observations are needed to reveal details of the changes which occur when the boathooks are released. The origin of all these bars is uncertain since only mature bars have been recognised. However, the fibrous bodies referred to in connection with flagellum formation occasionally contain suggestions of enclosed spines. It is possible that these bodies either fragment or condense to produce the bars. However, bodies with a structure intermediate between fibrous bodies and bars are rare, especially at an early stage in spore production before cleavage when there are only a few large fibrous bodies but many mature bars. The origin of both the fibrous bodies and the bars remains obscure.

d) Germination

The present observations suggest that the formation of a

germ tube is the product of an interaction between increased pressure in the spore due to the swelling of the dense body vesicles and the localized activity of the wall vesicles in producing a break in the dense cyst wall with an accompanying increase in the inner wall layer. The development of an inner wall layer at germination is a common occurrence in higher fungi (Bracker, 1967).

The reorganisation of the cytoplasm and organelles, including the association between the E.R., mitochondria and Golgi bodies, into their vegetative configurations is probably symptomatic of the resumption of normal vegetative metabolism after the specialized processes associated with spore production.

Whilst the work reported in this thesis may have given a clearer picture of some of the ultrastructural aspects of the life of S. ferax, it is clearly incomplete in many respects. It is hoped that it has shown the most profitable directions along which further research should proceed.

EXPLANATION OF PLATES

All figures are of S. ferax grown at 25°C, fixed in GA/Os and stained on the sections with UAc and Pb unless stated as otherwise. All dimension lines are equivalent to 1 µm unless otherwise indicated. The following abbreviations have been used on the plates and in the legends:-

A	apical papillum
a	astral tubule
B	bar
Bp	basal plate of kinetosome
C	centriole
cb	crystalline body
Cf	fibrils produced in the presence of colchicine
ch	chromosome
cl	thick concertina-like collar
Cp	Centriole position observed in serial sections
cw	cyst wall
D	dense body
E R	endoplasmic reticulum
F	flagellum
f	E.R. enclosed tubules
Fb	fibrous body
fl	flimmer hairs
G	Golgi body
GT	germ tube
H	hypha
I	area of section irradiated by the electron beam

K	kinetosome
L	lomasome
l	neutral lipid
L.S.	longitudinal section
M	mitochondrion
mtb	multitubular body
N	nucleus
Ne	nuclear envelope
Np	nuclear pore
Nu	nucleolus
P	pocket of the nuclear envelope
Pl	plasmalemmasome
r	microtubular roots of the flagella
S	sporangium
s	spindle tubules
sf	striate fibre
Sw	sporangium wall
T.S.	transverse section
V	vacuole
W	hyphal wall
Wv	wall vesicles

Figures in legends refer to specimen and negative numbers respectively.

Fig. 1. Encysted zoospore showing manganese specific silver deposits after silver hexamine staining of untreated section. $KMnO_4$. unstained. 1778B/5. 10677.

Fig. 2. Encysted zoospore after removal of manganese from the section with sodium bisuphite followed by silver hexamine stain. $KMnO_4$. unstained. 1778B/9. 7437.

Fig. 3. Encysted zoospore. Manganese was removed from the section with sodium bisulphite and aldehyde groups were introduced by peroxidation at 60°C for 30 min. These were detected by the silver hexamine stain. $KMnO_4$ unstained. 1778B/11. 10720.

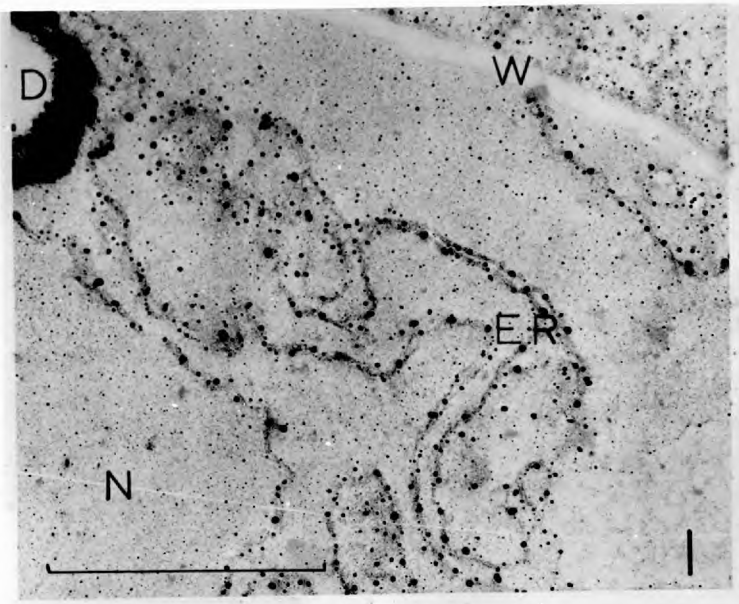
D
W
ER
N
1


W
N
2

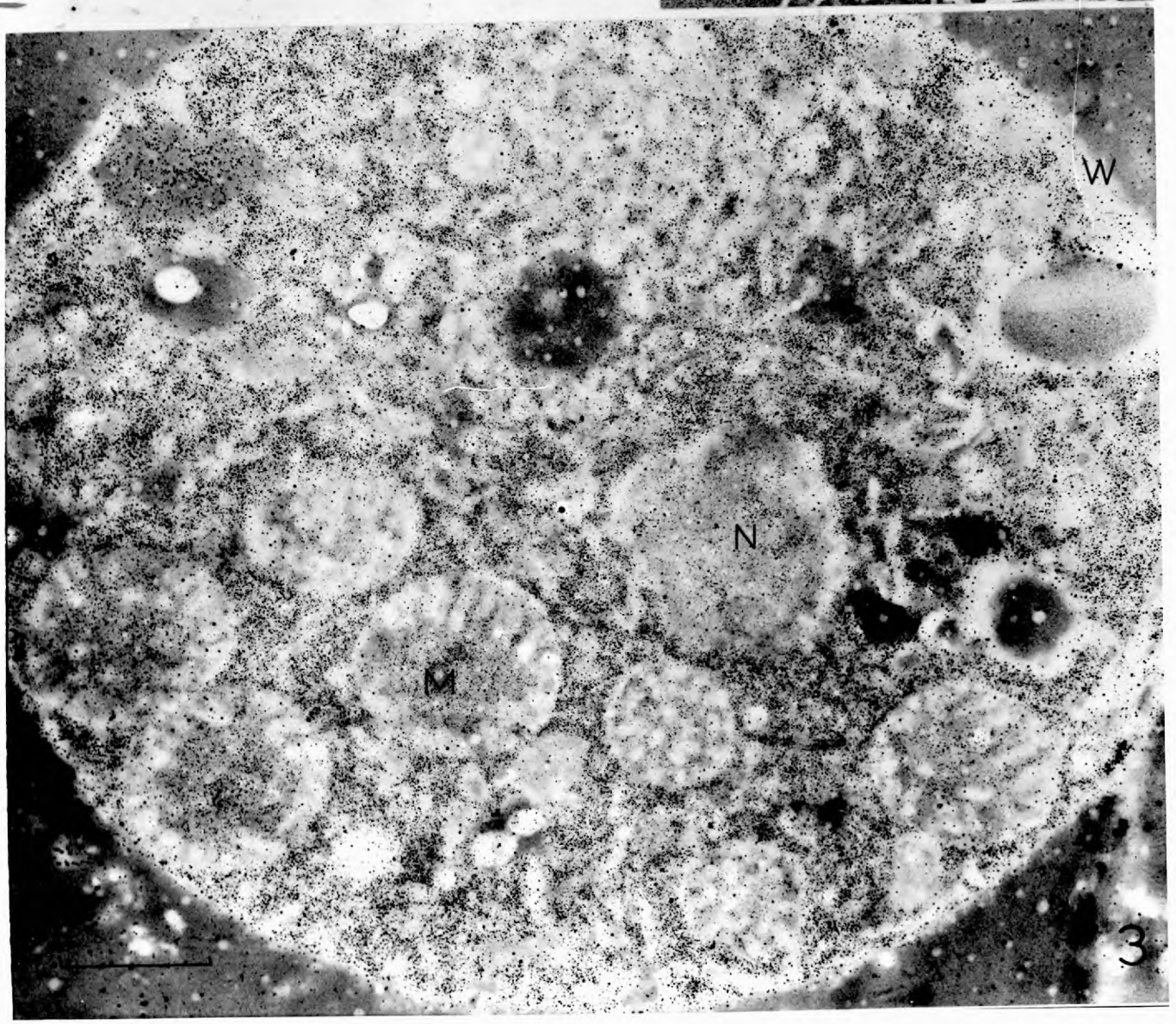
W
N
M
3

Fig. 4. Sporangium after section staining with silver hexamine alone showing strong osmium specific silver deposit. Unstained. 1776/9. 10672.

Fig. 5. Hypha after peroxidation and silver hexamine stain showing retention of osmium and consequent silver deposit in area irradiated with the electron beam (I) before peroxidation and loss of osmium in non-irradiated area. Note wall stain introduced in non-irradiated area (w) absent in irradiated region. The heavy stain at the edge of the irradiated zone is characteristic of irradiation. 1835/3. 10955.

Fig. 6. Hypha containing dividing nuclei hydrolysed and stained to show chromosomes. Note strong osmium specific silver deposits. 1547H/1. 8947.

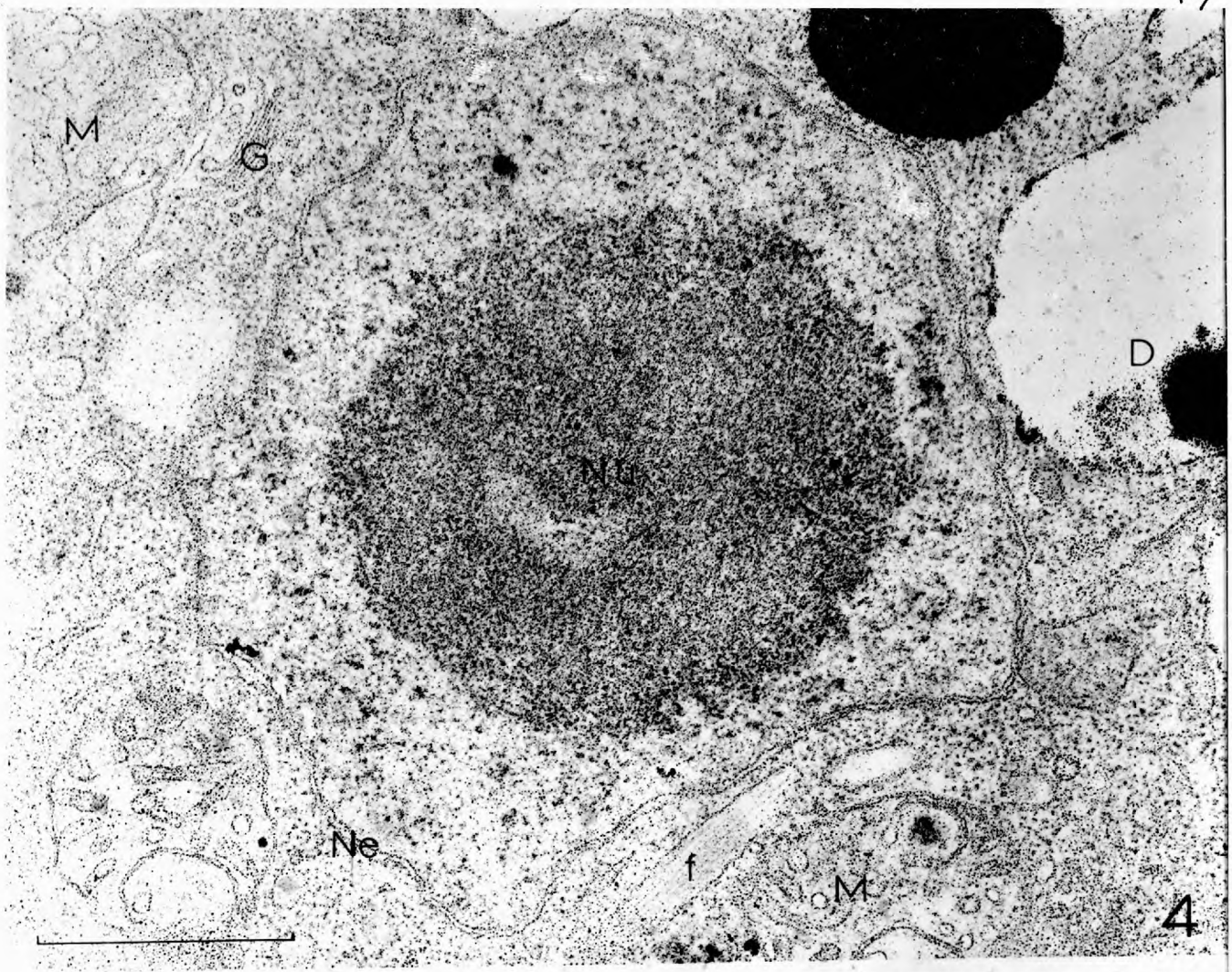
M
G
D
Nu
Ne
f
M
4

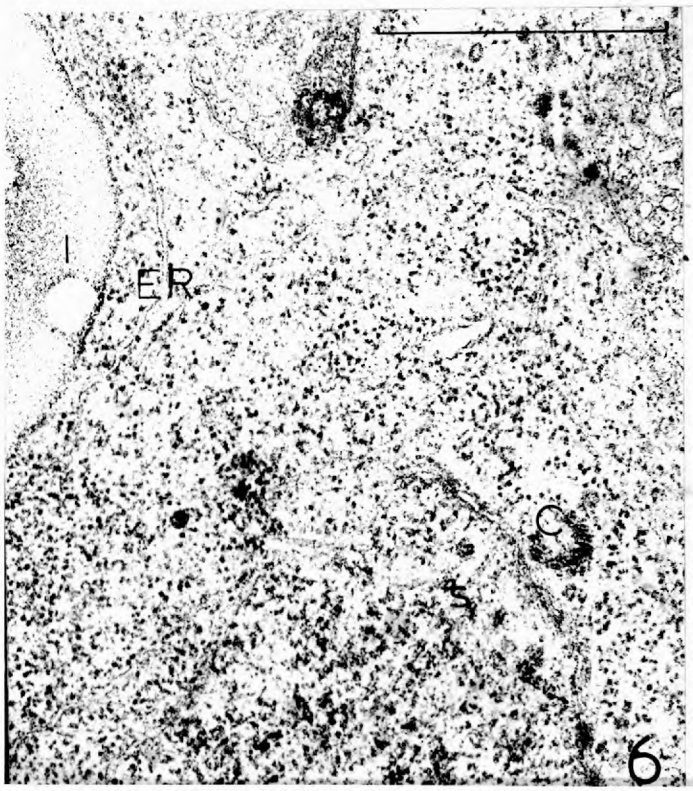
I
ER
C
6


W
I
5

Fig. 7. Hypha incubated in DNAase after osmication showing good preservation. Enzyme activity was not detected in this treatment. 1726A/1. 10103.

Fig. 8. Hypha incubated in RNAase after osmication. Note abundant ribosomes and dense nucleolus but poorer fixation than Fig.7. 1725A/1. 10099.

Fig. 9. Hypha treated as Fig. 8. showing apparently normal centrioles and ribosomes. 1725A/1. 10098.

Fig.10. Zoospore incubated in RNAase before osmication showing poor fixation and insignificant enzyme activity in the nucleolus and ribosomes. 1740/1. 10171.

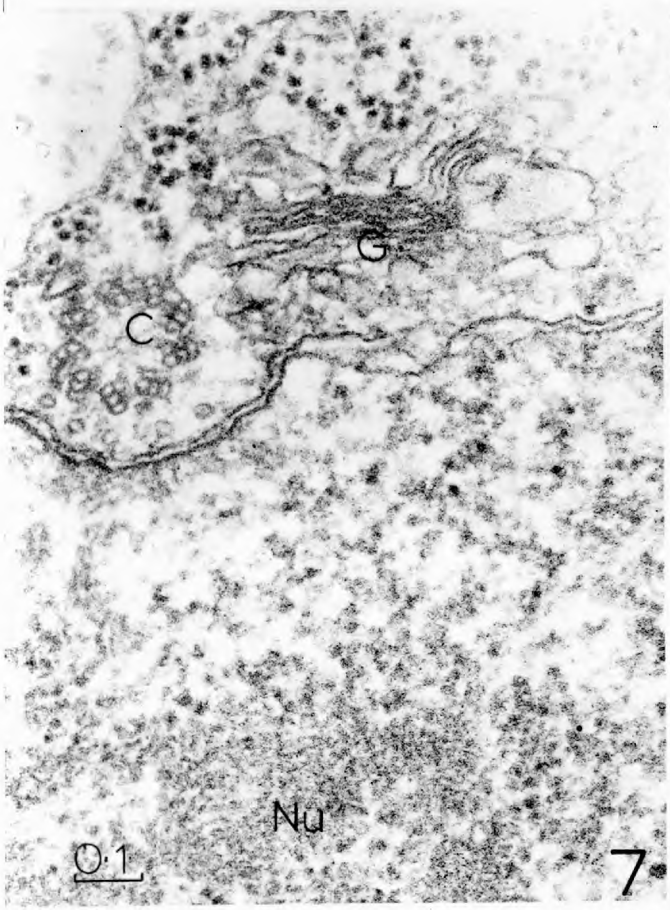
G
C
Nu
0·1
7

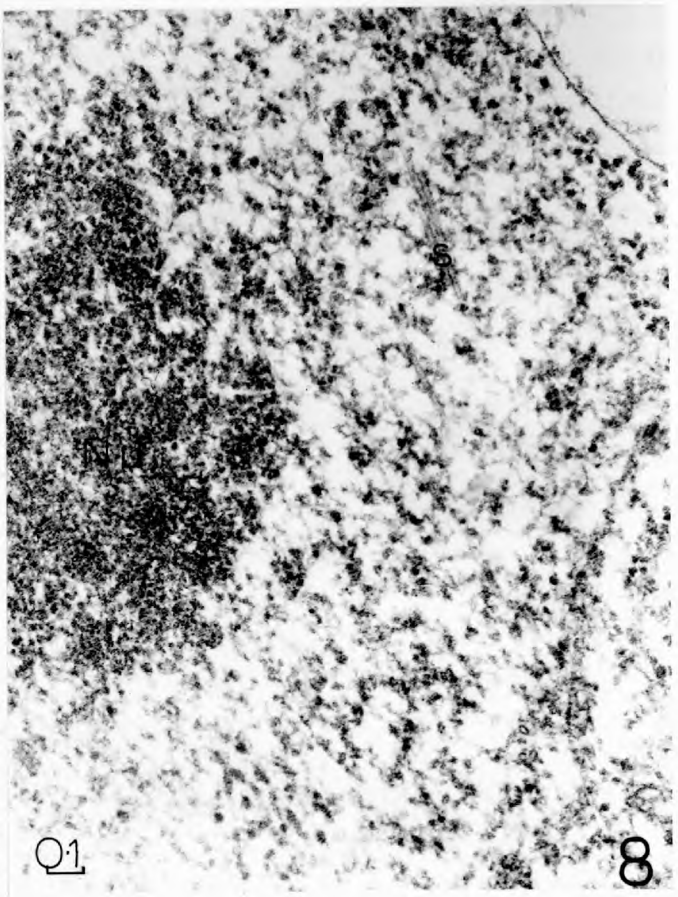
Nu
0·1
8


G
S
0·1
9

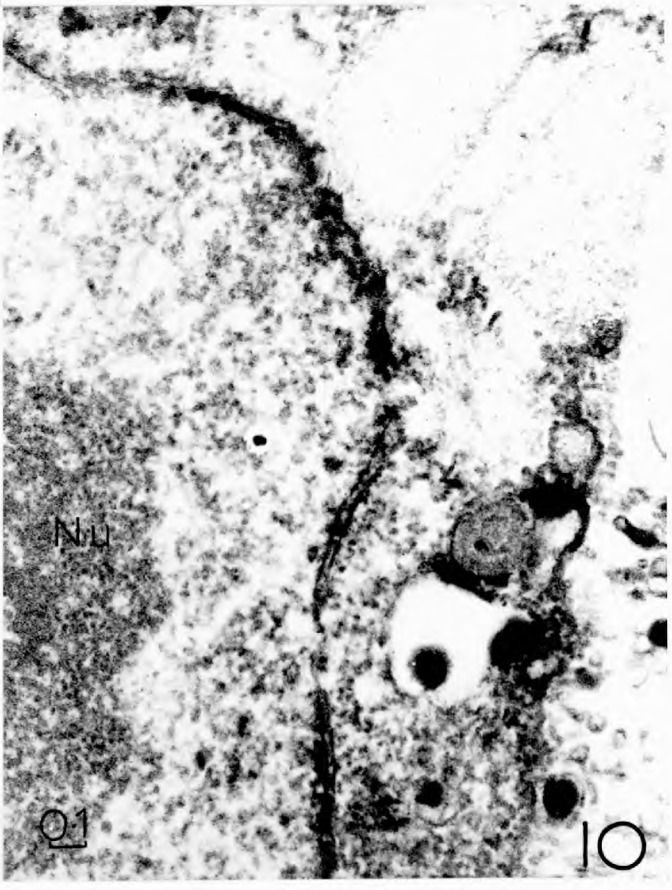
Nu
0·1
10

Fig.11. Zoosporangium cross wall prior to cleavage incubated in DNAase after prolonged washing in P before osmication. Note good preservation, curvature of the wall and the concentrations of wall vesicles (wv). 1891/3. 12390.

Fig.12. Zoospore showing ribosomes and tubules in the E.R. This is the control material for Fig.13 and was incubated in the RNAase medium free of enzyme. 1890/3. 12359.

Fig.13. Zoospore incubated as Fig.11 but in RNAase. Note possible loss of contrast in ribosomes obscured by dense background material. The tubules in the E.R. appear to be unaffected. 1889/3. 12365.

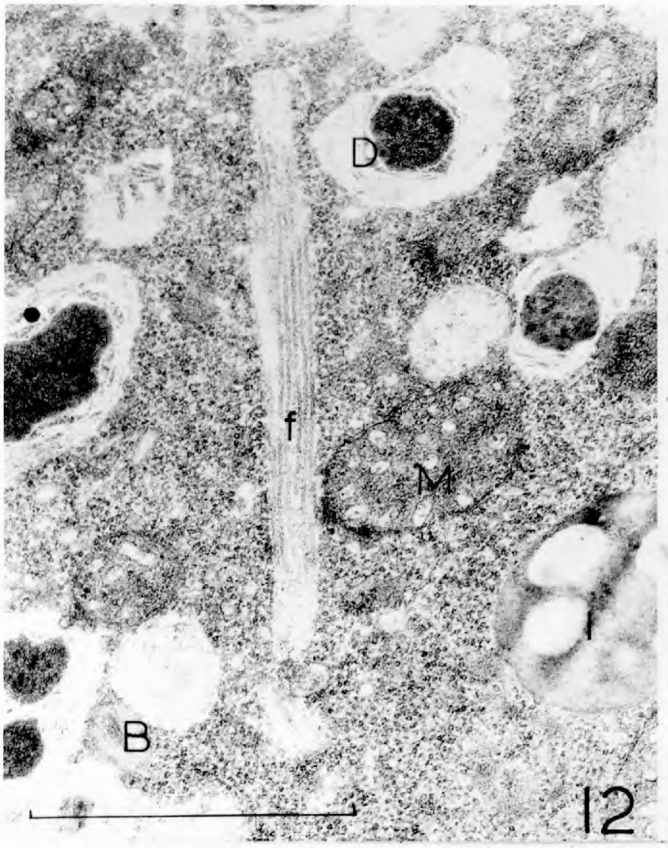

12

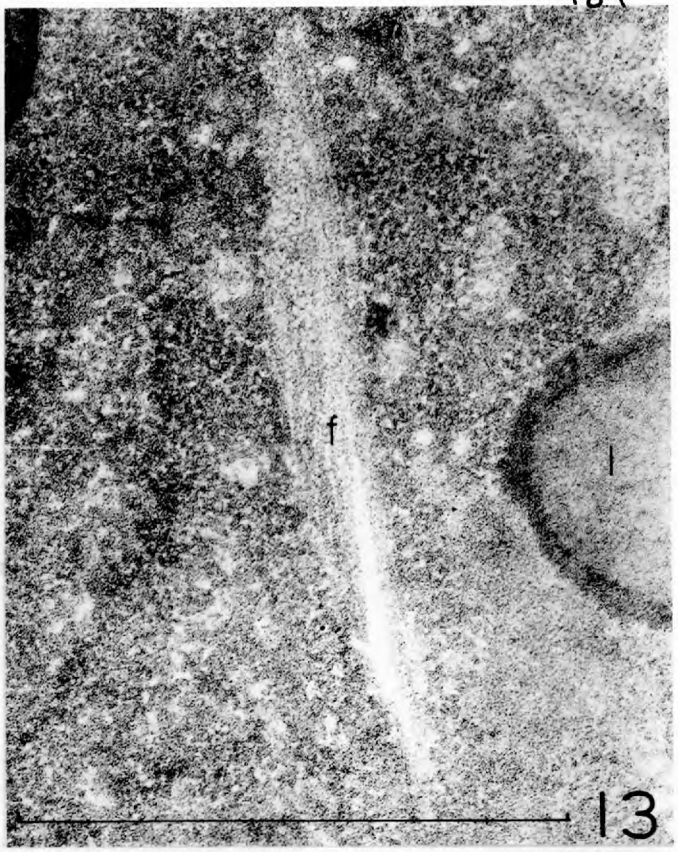

13

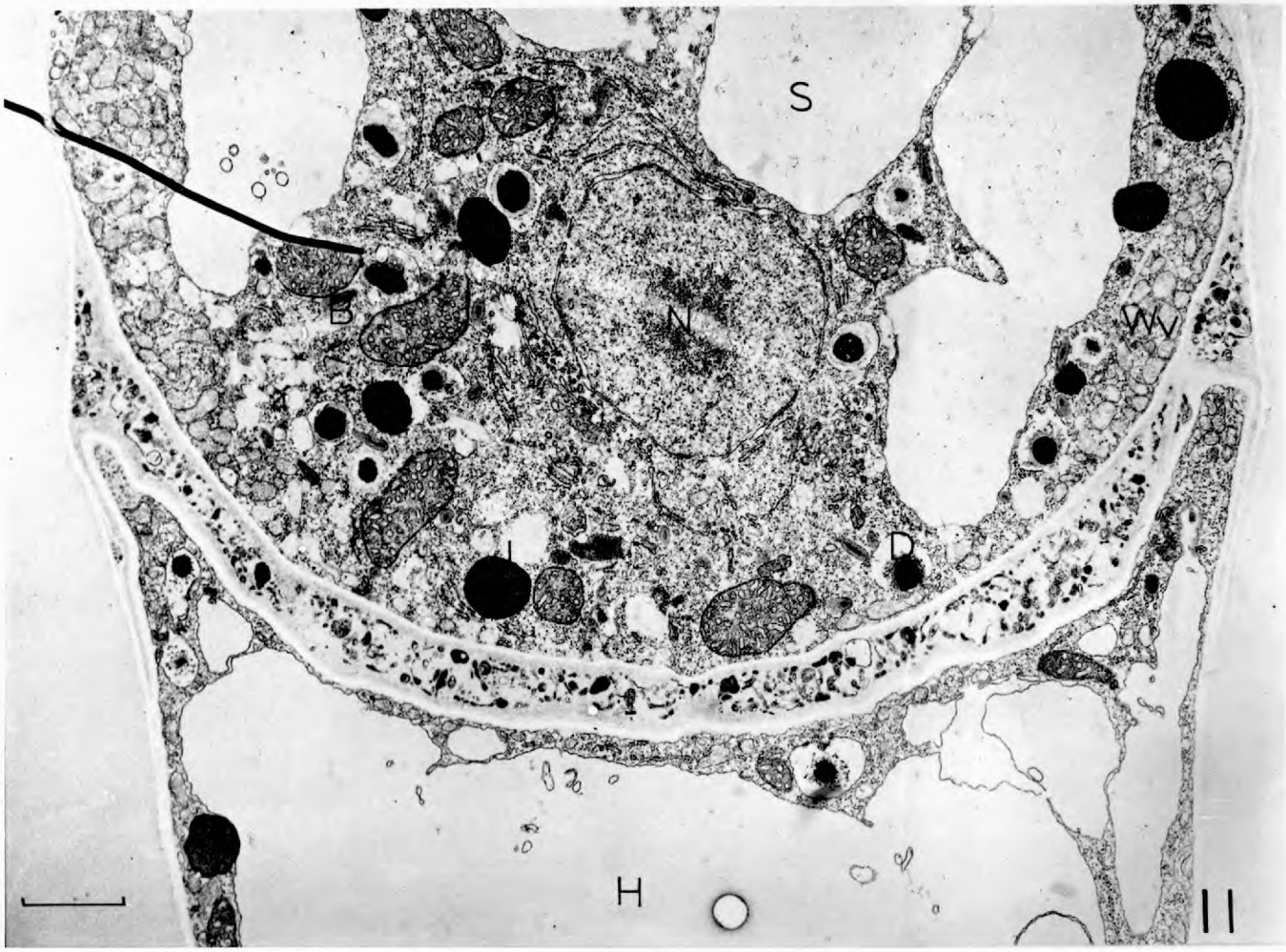

11

Fig.14. Phase contrast micrograph of living hypha and branch base with clear nuclei and fine strands (Arrowed) connecting the nucleolus to the periphery of the nucleus. 207.

Fig.15. Hypha with 2 nuclei having irregular membrane after Os fixation. Note poorly preserved centriole in a pocket of the envelope. Os. 1826A/6. 10784.

Fig.16. Nuclear envelope with 3 nuclear pores(arrowed) very close together. 1692D/3. 10005.

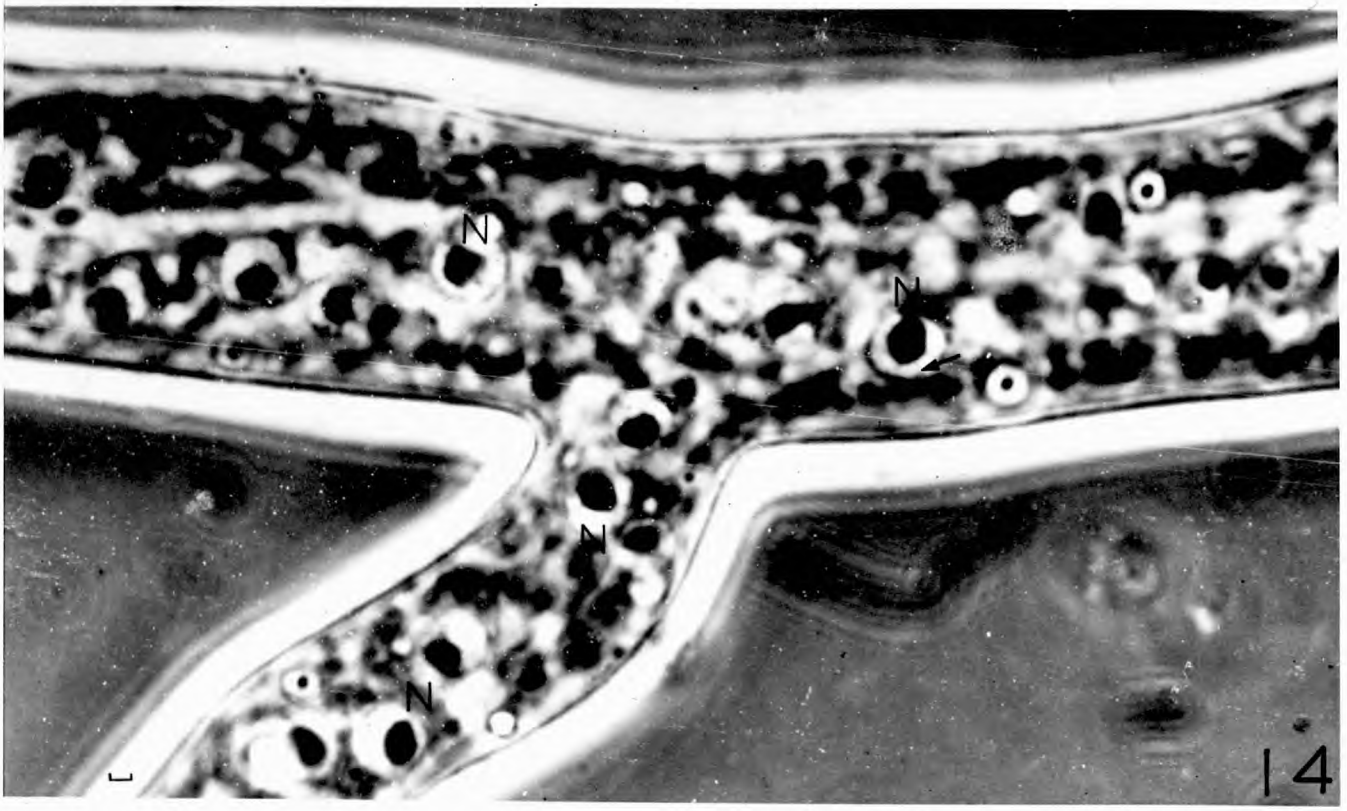
N
N
N
N
14

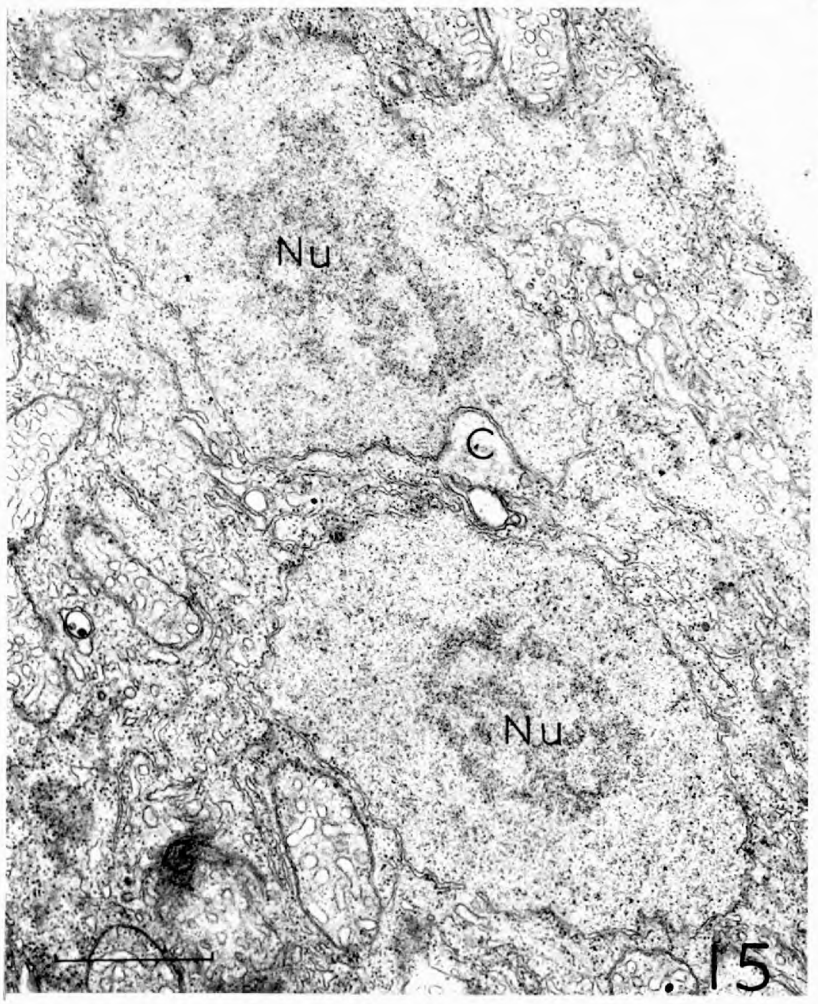
Nu
C
Nu
15

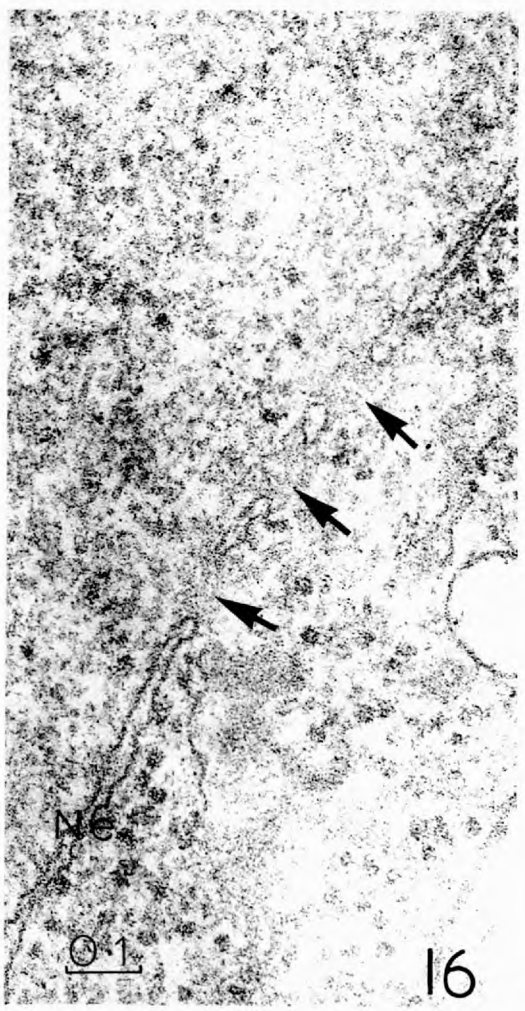
NE
0·1
16

Fig.17. Nucleus and cytoplasm. Contrast is due to osmium alone since the section was not stained. Unstained. 1836C/1. 14346.

Fig.18. Nucleus and cytoplasm with contrast due to osmium and UAc section stain. Note dense material in nuclear pore. UAc only. 1836C/1. 14347.

Fig.19. Nucleus and cytoplasm with contrast due to osmium and Pb section stain. Pb only. 1547H/8. 7318.

Fig.20. Sporangial nucleus after treatment with the PAH technique. Note heavy deposit on nucleolus, the fibrous bodies(Fb) and the tubules in the E.R.(f). PAH. 1848/4. 10965.

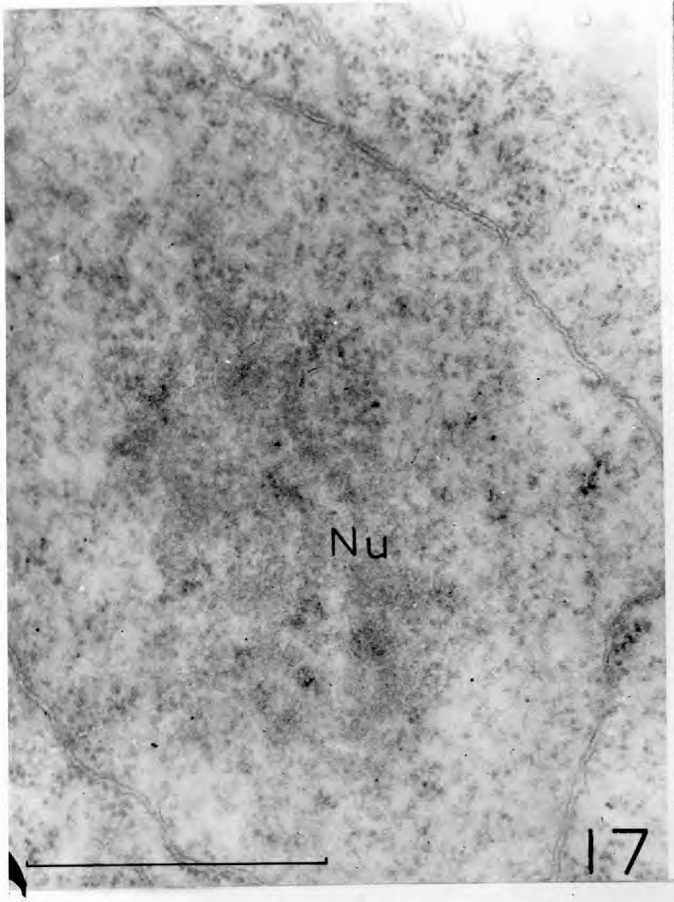
Nu
17

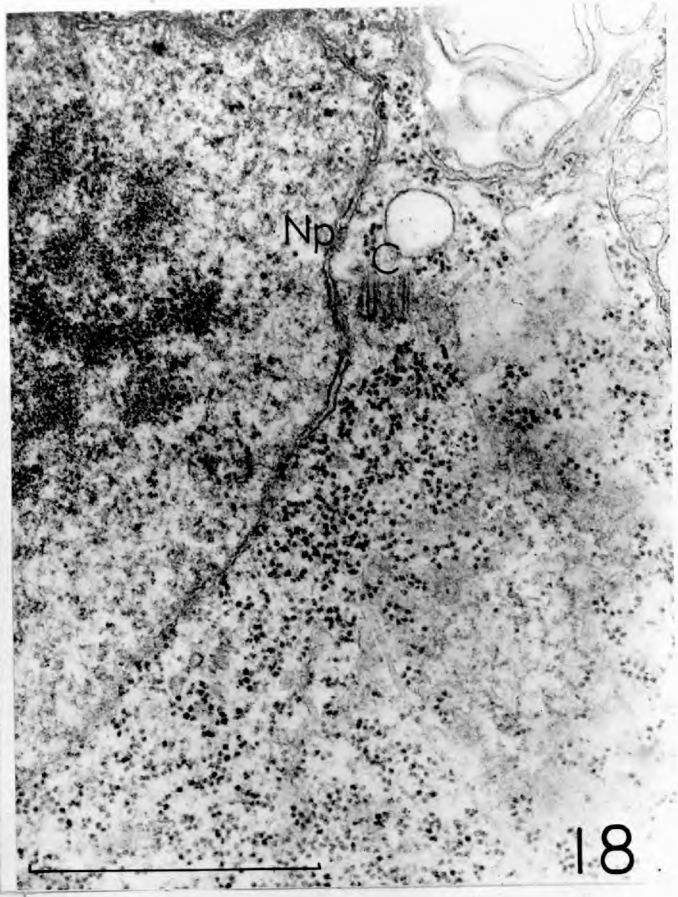
Np
C
18

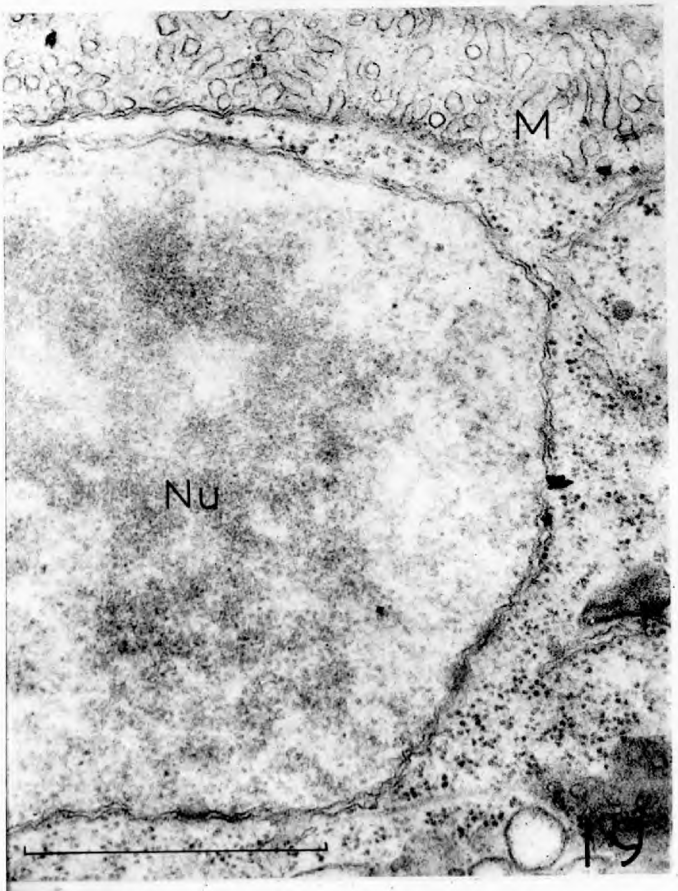
M
Nu
19

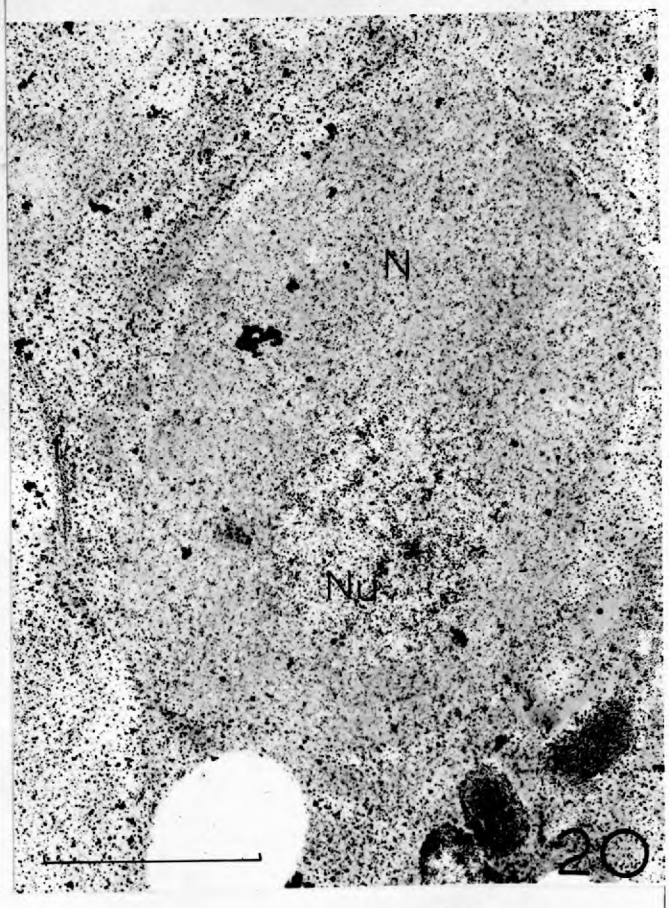
N
Nu
20

Fig.21. Oblique section of nuclear envelope showing polyribosome chains on the outer surface and the astral tubules(a) running along the surface of the envelope. 1836C/2. 14354.

Fig.22. Nuclear envelope containing nuclear pores(Np) producing dark surfaced vesicles(o) towards a Golgi body. Note dense material in the nuclear pores. 1388A/25d. 6136.

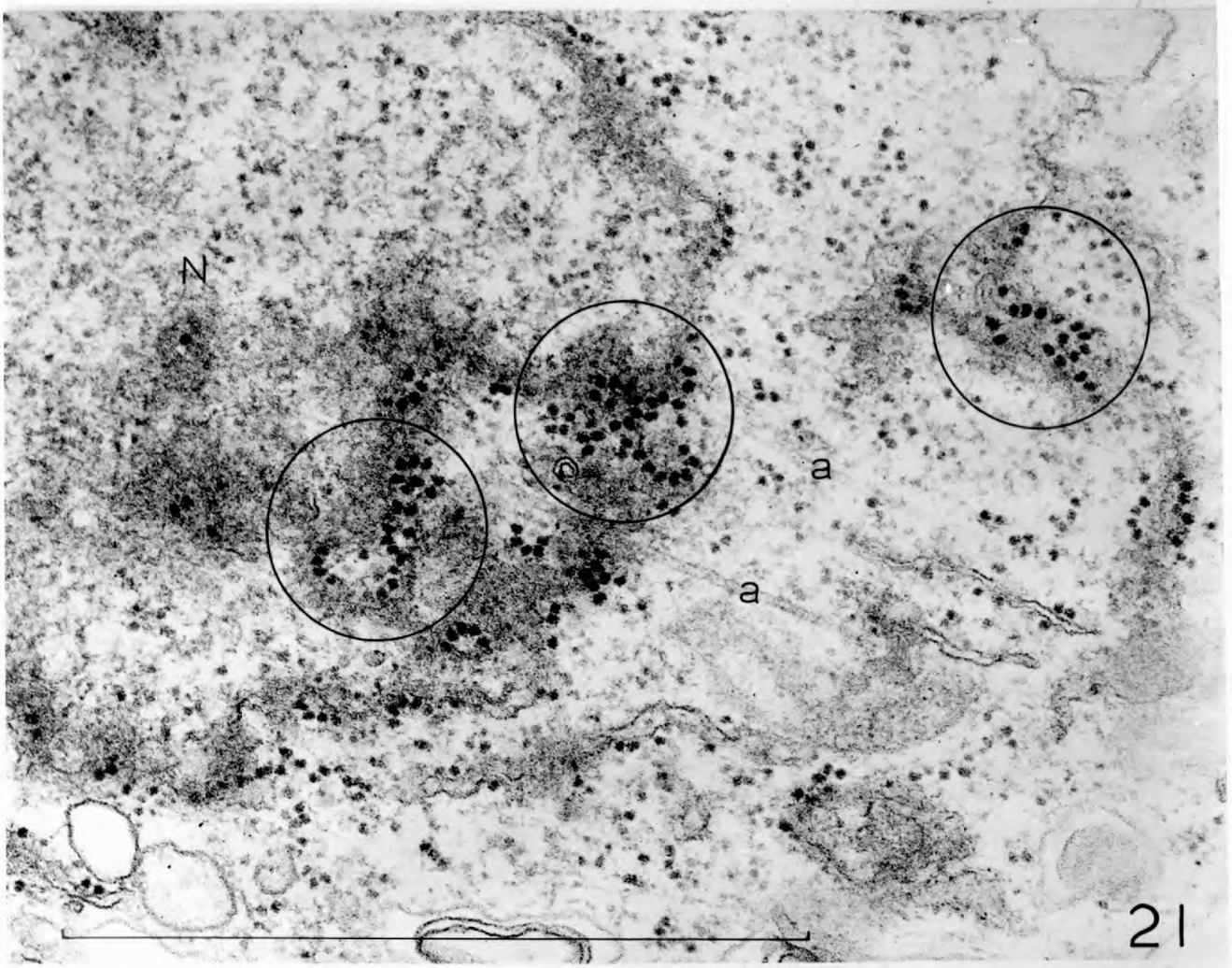
N
a
a
21

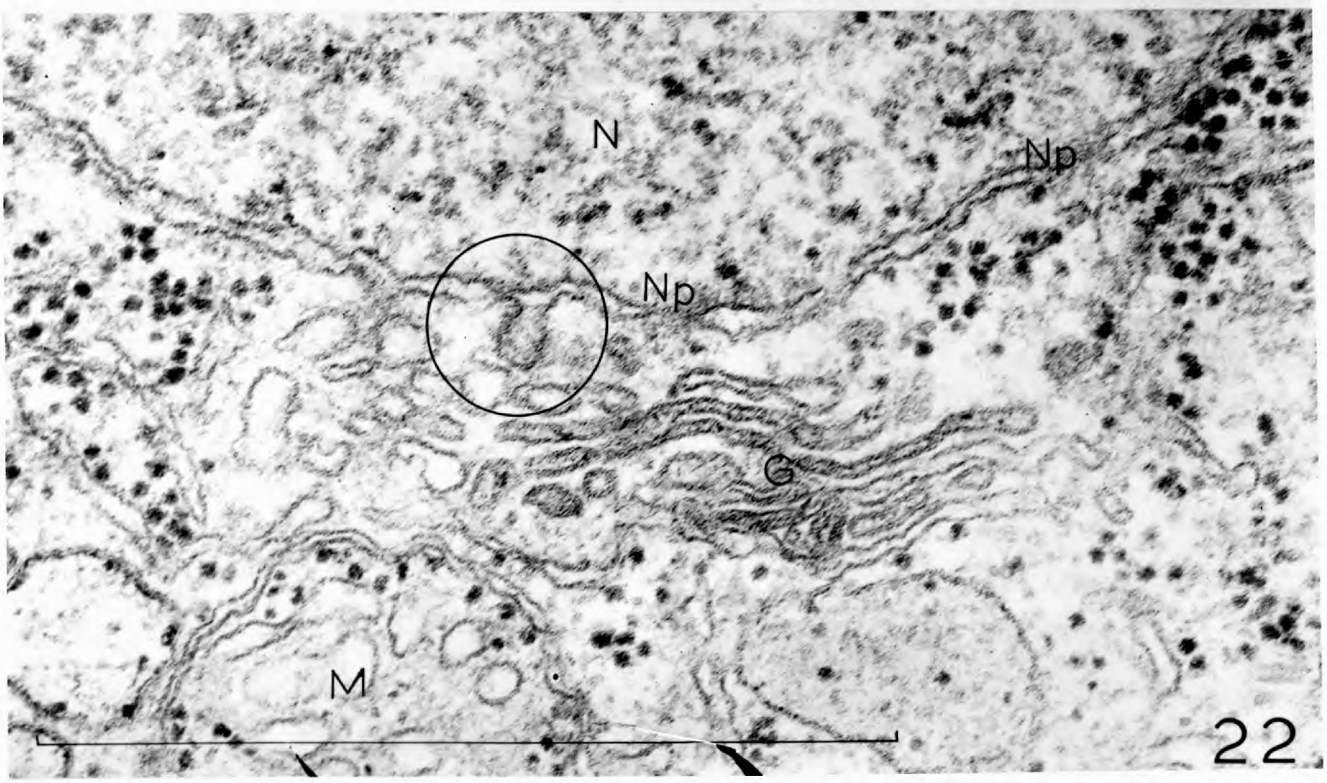
N
Np
Np
G
M
22

Fig.23. A pair of centrioles in a nuclear pocket. This probably represents an interphase condition but it is possible that a spindle exists out of the plane of section. Note astral tubule(a). 1547G/4. 8597.

Fig.24. A pair of centrioles probably associated with an interphase nucleus(See Fig.23). Note connections between nuclear envleope and the rough E.R. 1645G/9. 12490.

Figs.25-32. 12 serial transverse sections through a pair of centrioles at a pole of a metaphase spindle showing the absence of C tubules at the distal end of each one(Fig.25 & 32) and at the proximal end(Fig.30). Note reversed orientation of triplets between the 2 centrioles(Fig.28 & 30), absence of cartwheel in the distal ends(Figs.25,26,27,32) and the absence of a detectable strucutre between the pair(Fig.29). Note also the dense bars of material within the nuclear envelope of the pocket region(Fig.30) and the dense material adjoining the pocket from which the spindle tubules(s) appear to originate (Figs.28,29,30). Numbers in rings refer to the position in the series, sections 4,6,9 and 11 were obscured. 1645G/3. 10379, 10378, 10377, 12500, 10375, 12498, 12497, 12496.

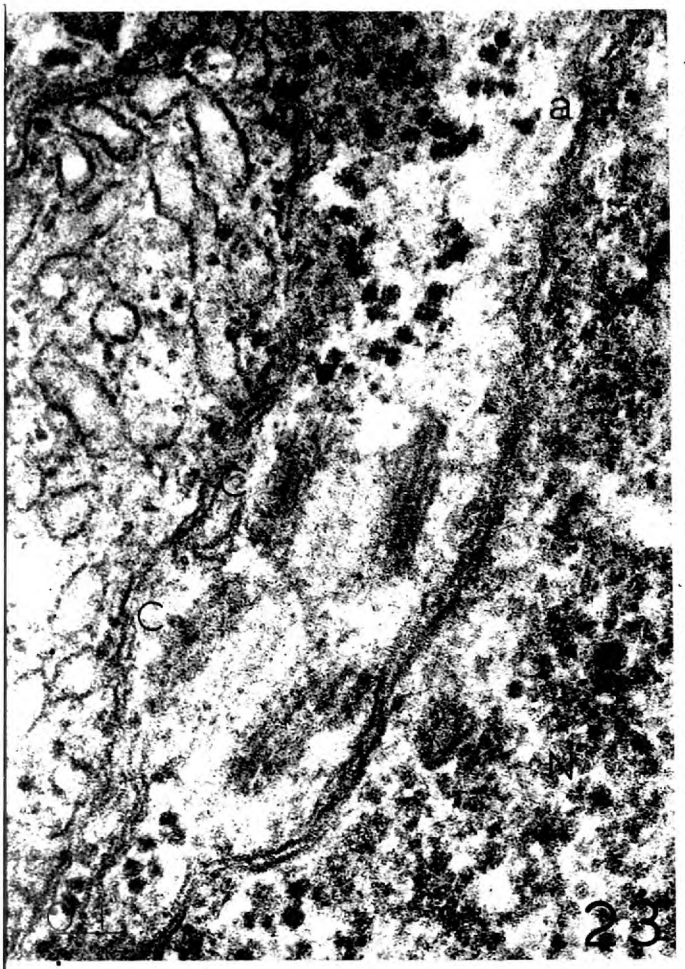
a
C
C
N
0.1
23

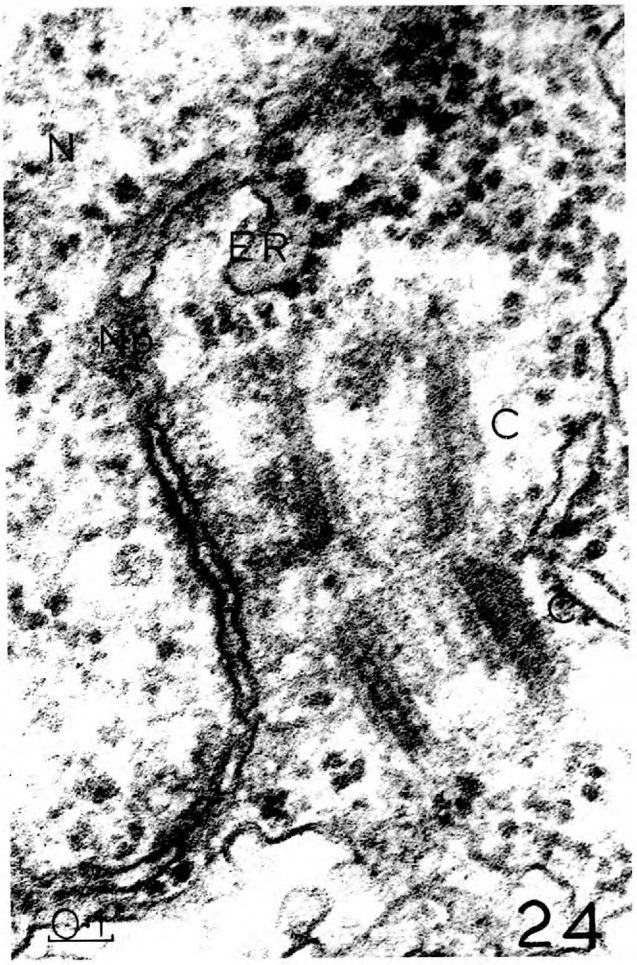
N
ER
NB
C
C
0.1
24


1
0.1
25


2
0.1
26

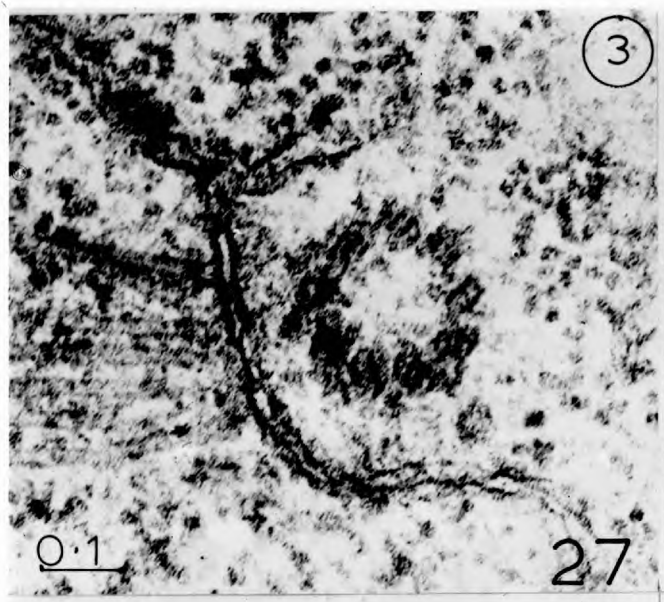
3
0·1
27

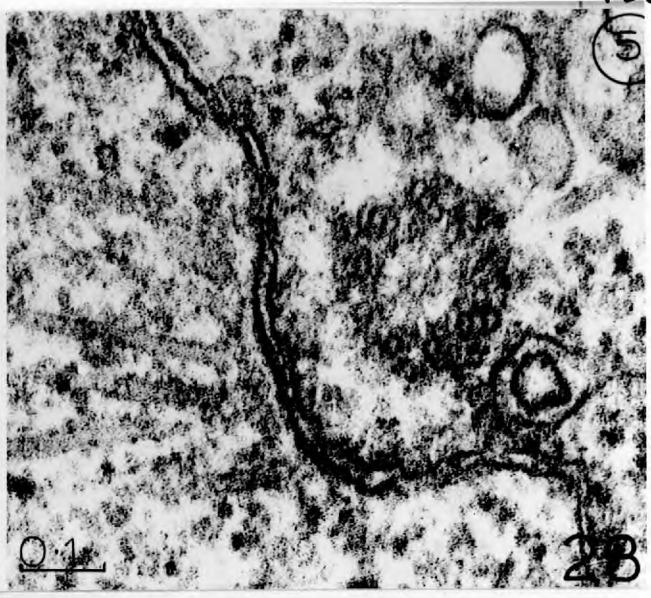
5
0·1
28

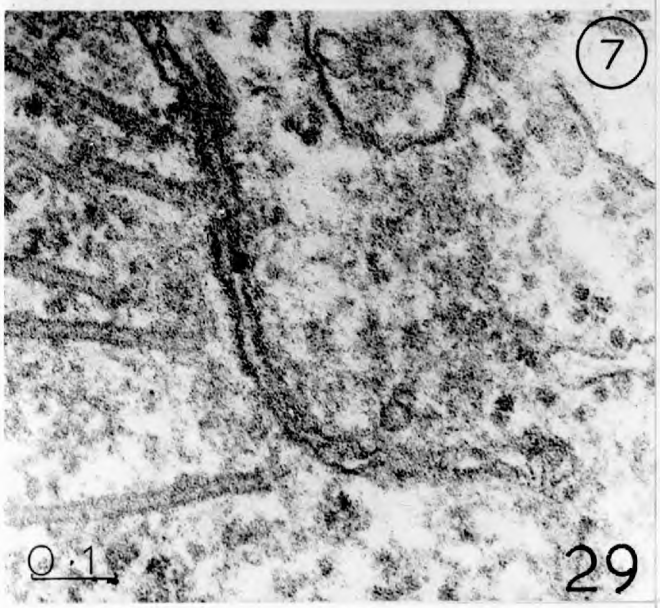
7
0·1
29

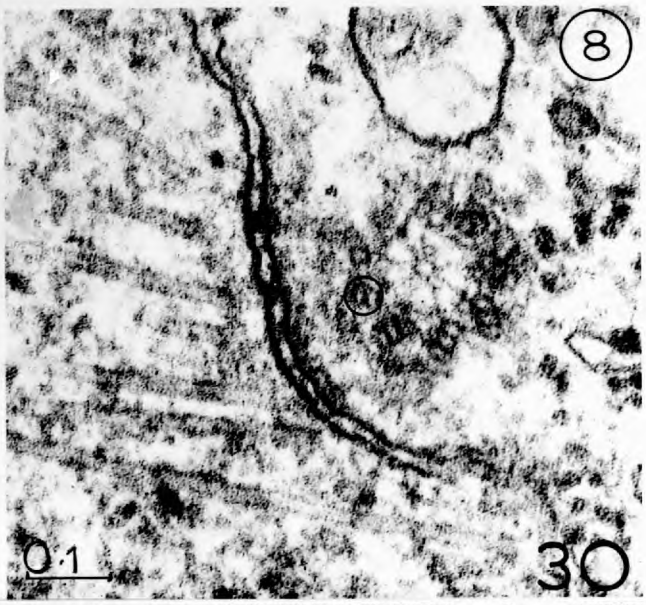
8
0·1
30

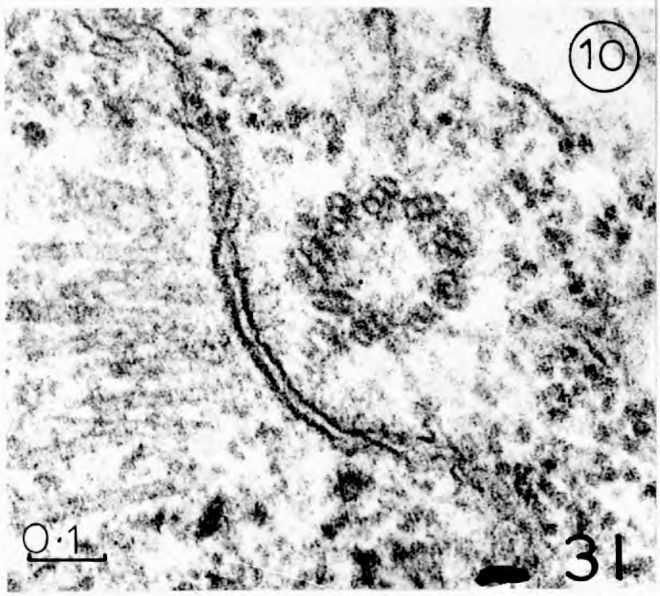
10
0·1
31

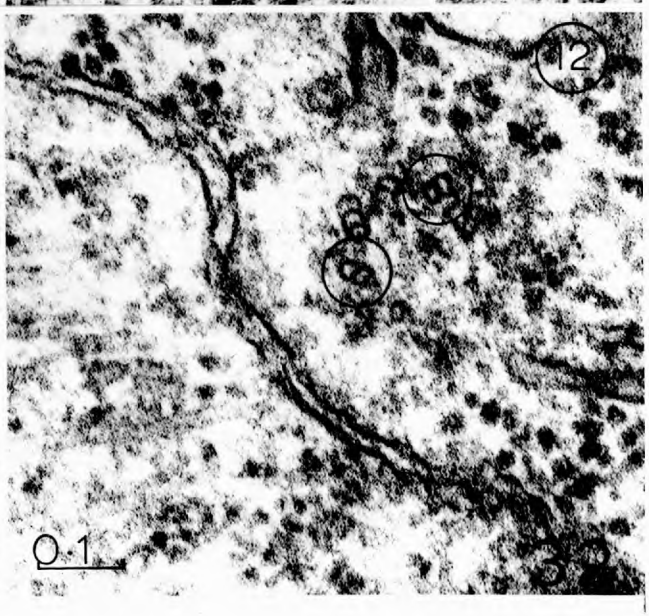
12
0·1

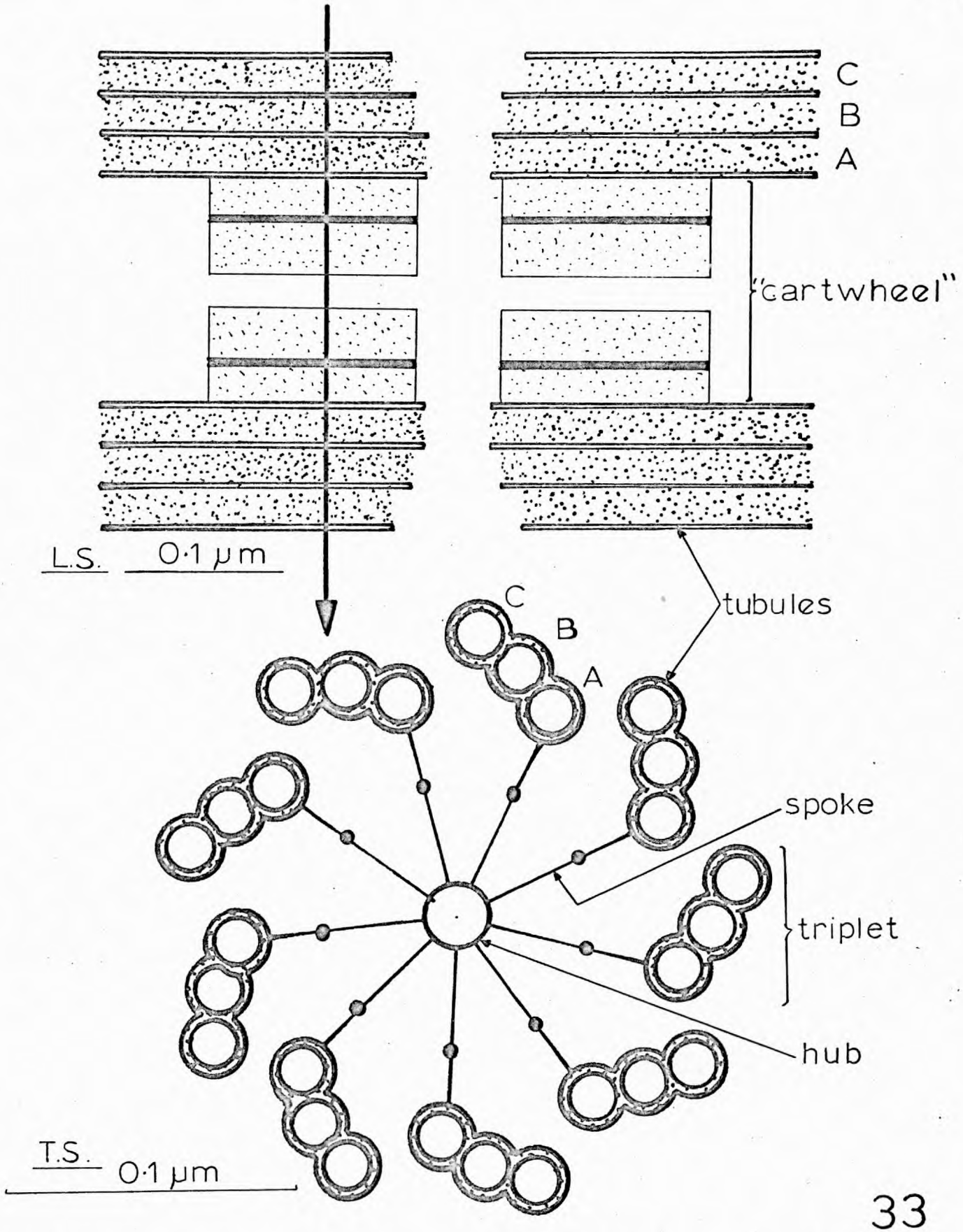

33

Scale diagram of S.ferax centrioles. (pair seen in L.S.)

Fig.34. Transverse section of proximal end of centriole showing cartwheel (hub arrowed) and absence of C tubules in 8 of the 9 triplets. 1693/1. 8862.

Fig.35. Transverse section of distal end of centriole in which the C tubules have terminated before the A & B tubules. The cartwheel is absent at this end. 1547E/1. 8589.

Fig.36. Transverse section of proximal region of centriole with apparently continuous ring on cartwheel and 9 triplet tubules. 1693A/1. 8892.

Fig.37. A pair of centrioles at the pole of a nuclear spindle also showing an astral tubule(a) along the nuclear envelope. 1825/1. 10807.

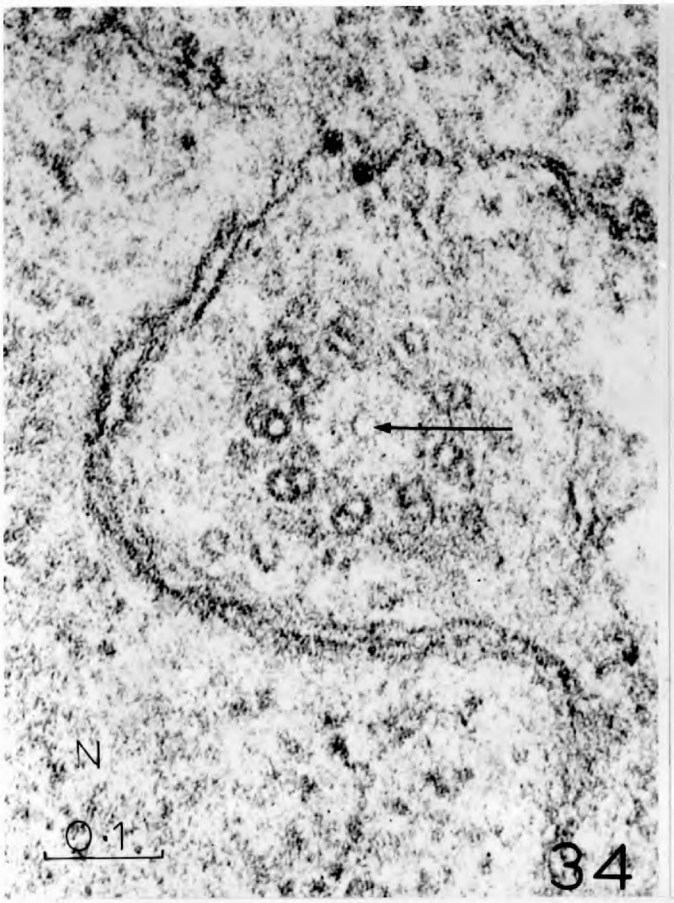

34

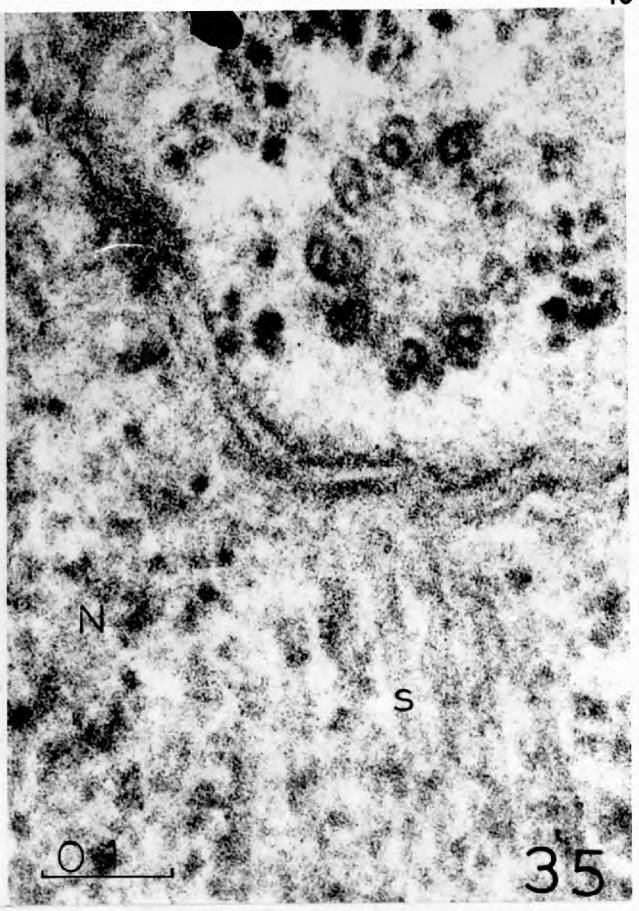

35

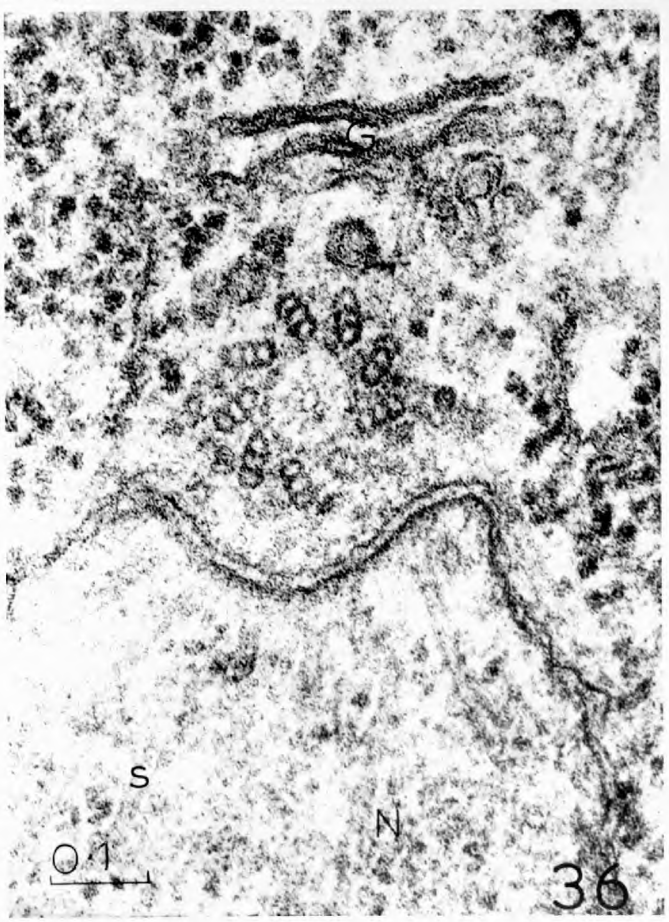

36

37

Fig.38. Reproduction of a microdensitometer trace from a scan across a transverse section of a flagellum microtubule doublet showing the double structure of the outer walls and a similar double peak of the shared central wall. Peaks indicate high transmission on the negative i.e. increased electron density in the print. Slit size 0.1 x 0.06mm. 1849A/2..Scan..no. 18. 10893.

Fig.39a) Microdensitometer scan of a transverse section of a spindle fibre. Slit size 0.1 x 0.08mm. 1547B/1_n. 8588. Scan.no.6.

Fig.39b) Microdensitometer scan of a transverse section of one of the central pair of tubules in a flagellum. Slit size 0.1 x 0.06mm. 1887/4. 12722. Scan no. 21.

Fig.40. Microdensitometer scan of one of the tubules in the E.R. showing single peak nature of the walls. Slit size 0.05 x 0.06mm. 1739/1. 10179. Scan no.8/1.

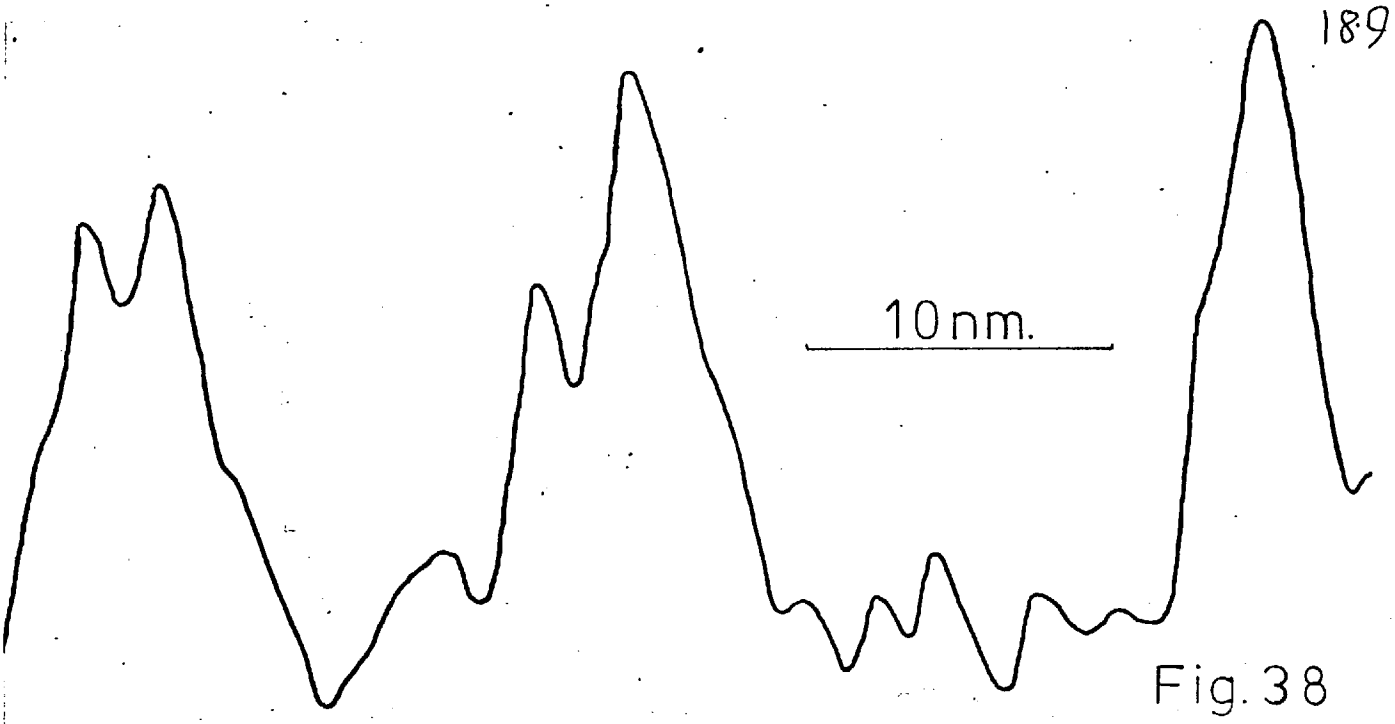

Fig. 38

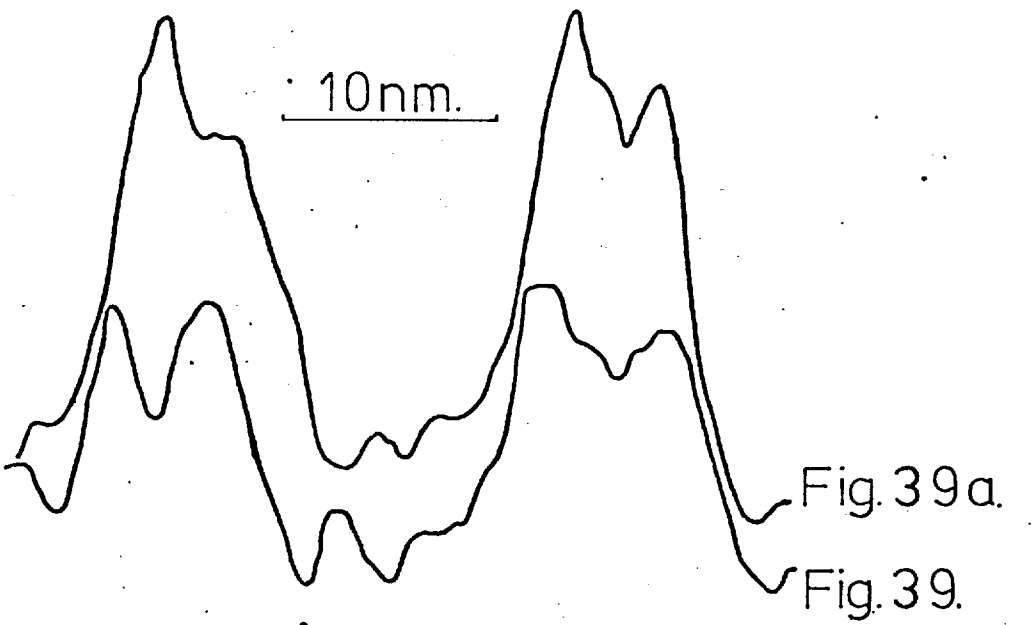

Fig. 39a.

Fig. 39.

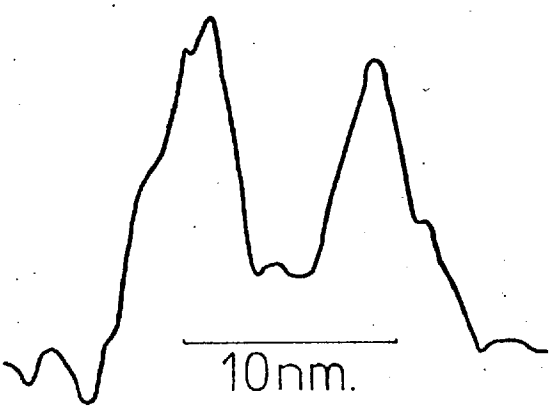

Fig. 40

Fig.41. An average trace constructed from 10 traces of flagellum central pair tubules by centering each trace on the inner left peak(line) and measuring the height of the trace above an arbitrary base line at $\frac{1}{2}$cm intervals along the x axis. This graph is plotted from the total heights of each point. Scan nos. 20,21,22,23,24,25,26,33,34a,34b.

Fig.42. Average trace of the tubules in the E.R. constructed in a similar way to Fig.41 from 11 traces. Scan nos.8/1,8/2,9/1, 9/2,9/3, 10/1,10/2,10/3,11,12/1,12/2.

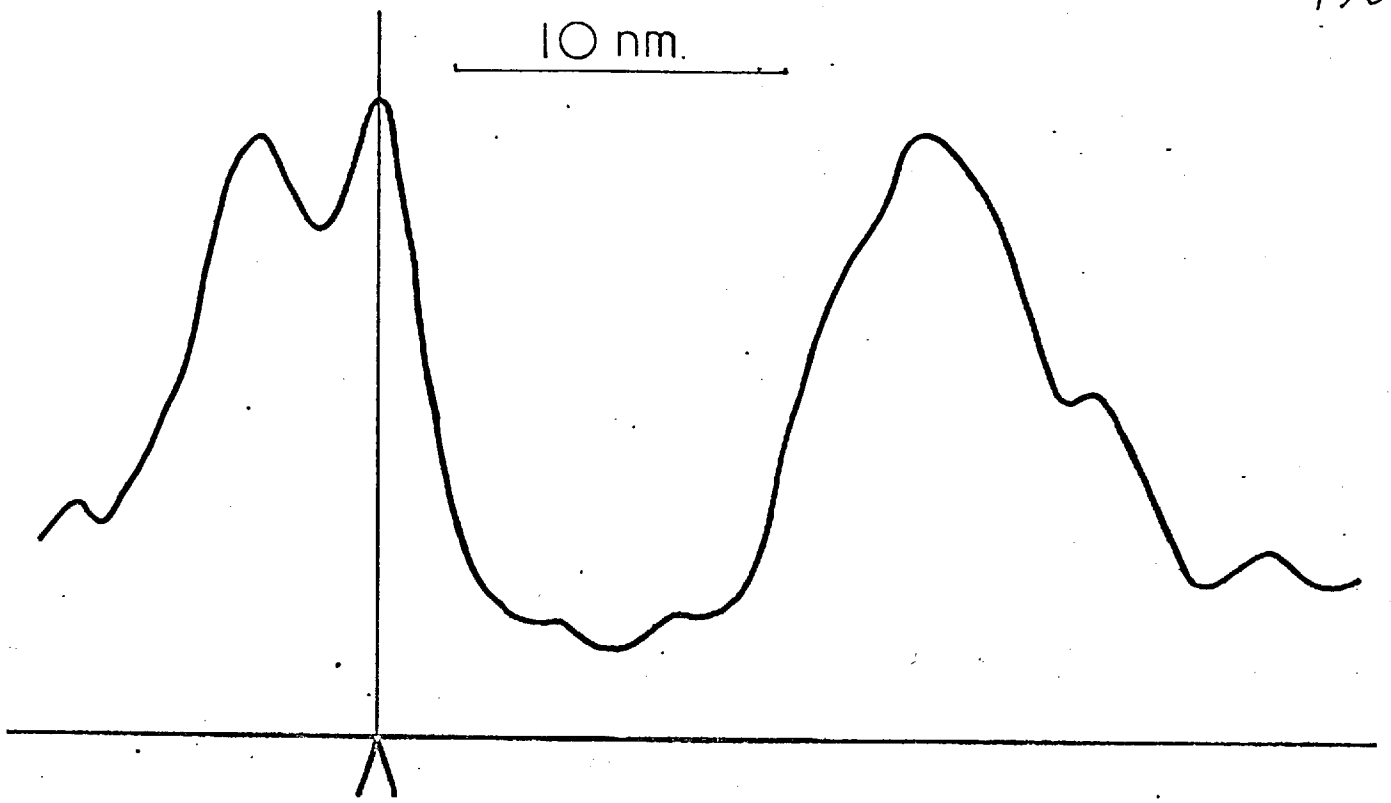

Fig. 41

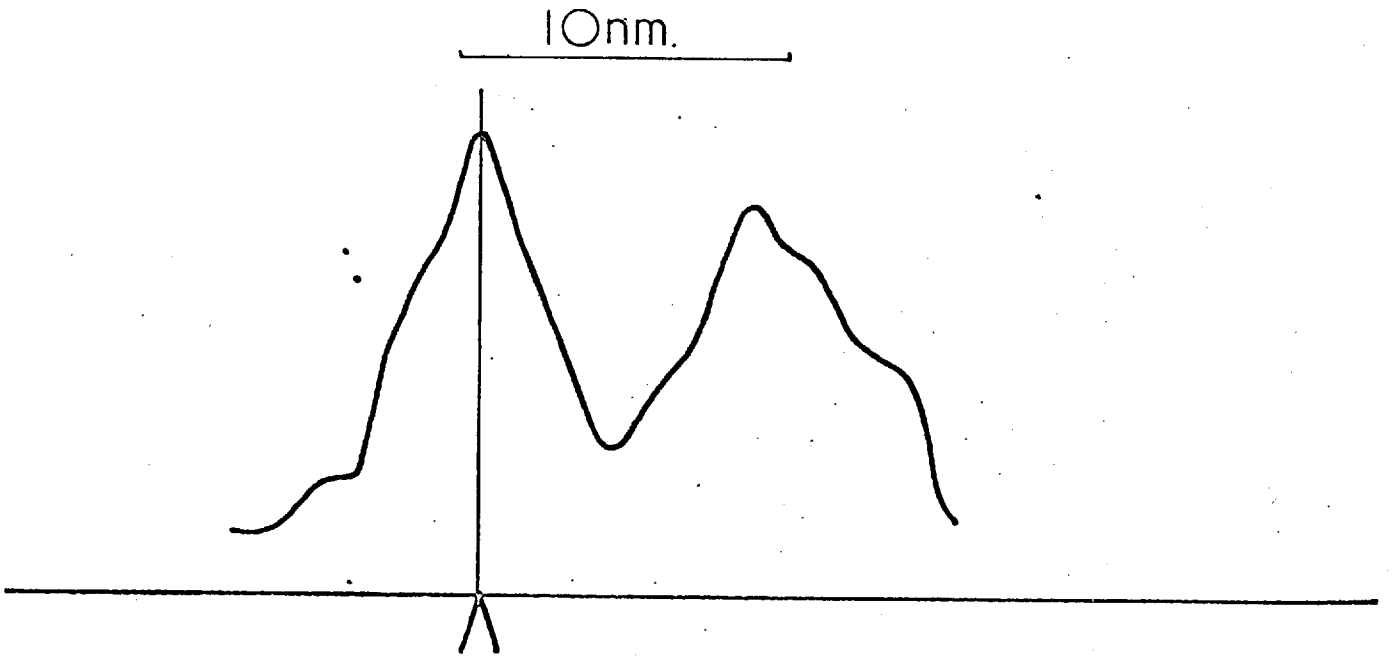

Fig. 42

Fig.43. An early stage in centriole replication showing 2 parent centrioles (C_1) and 2 daughters whose A tubules appear to be exactly in register with the parent. The daughters appear to only posses A and possibly B tubules and contain short cartwheels, the hub of one of which is clearly connected to the parent(arrowed). Note also the proximal thickening of the parent and daughter spokes in the arrowed pairsand the presence of astral tubules. This section was separated by one section from Fig.46. 1547/9e. 8538.

Fig.44. An astral tubule originating from the region of a pair of centrioles. The nuclear envelope adjacent to the pocket appears to be active in the production of vesicles towards the Golgi body. 1645G/9. 12491.

Fig.45. Astral tubule terminating in dense material around the centriole; note also the continuity between the nuclear envelope and the E.R. 1645g/9. 12492.

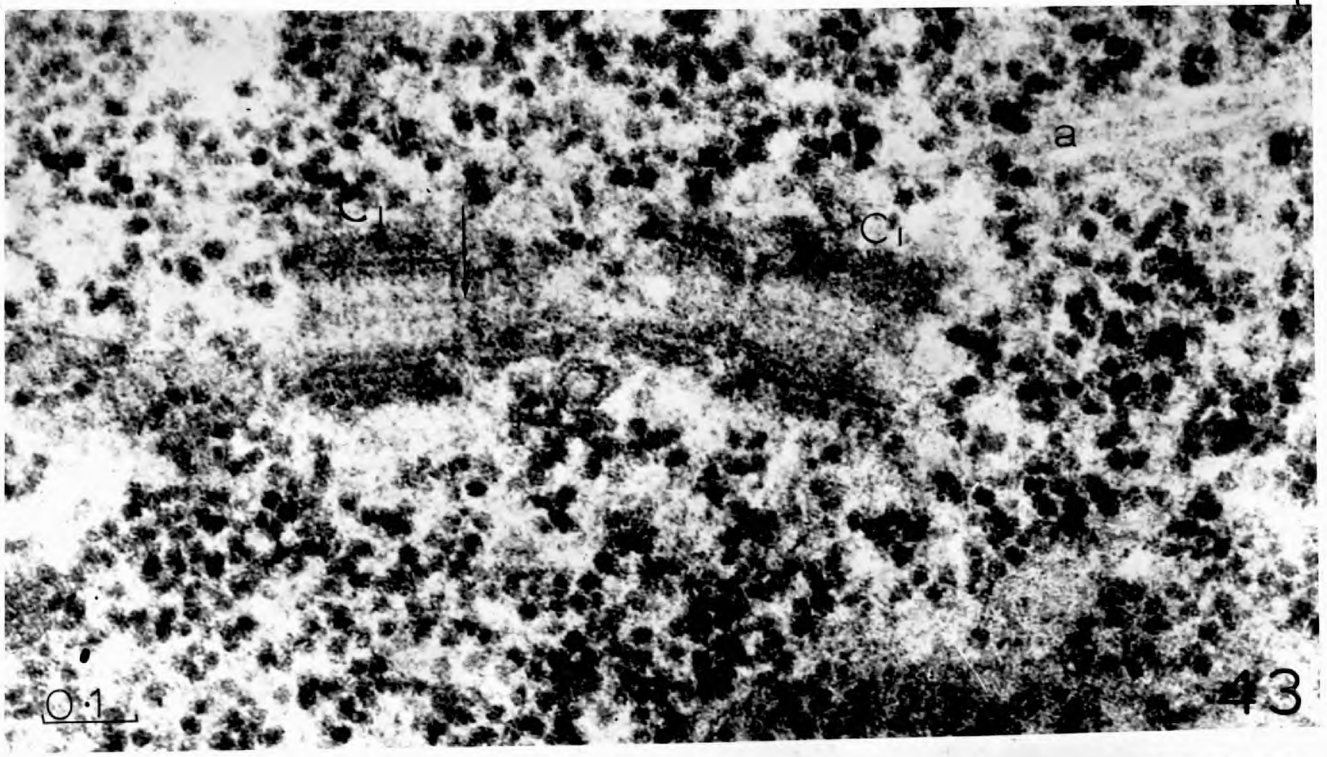
a
Ci
Ci
0·1
43


G
D
a
N
0·1
44

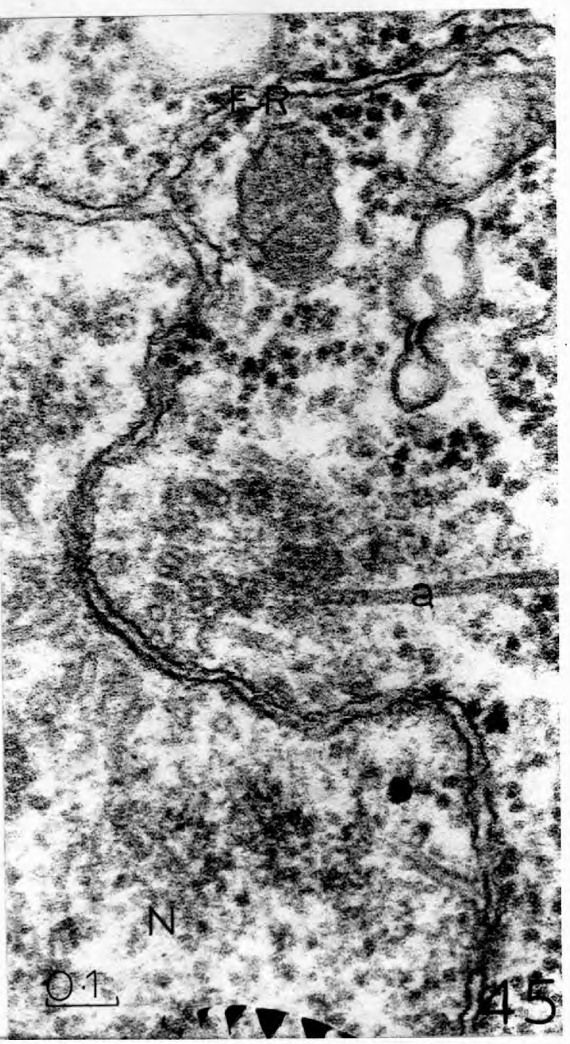
E.R
a
N
0·1
45

Fig.46. Surface section of the nucleus below the replicating centrioles in Fig.43 showing numerous astral tubules radiating over the surface of the nucleus into the cytoplasm. 1547/9c, 8537.

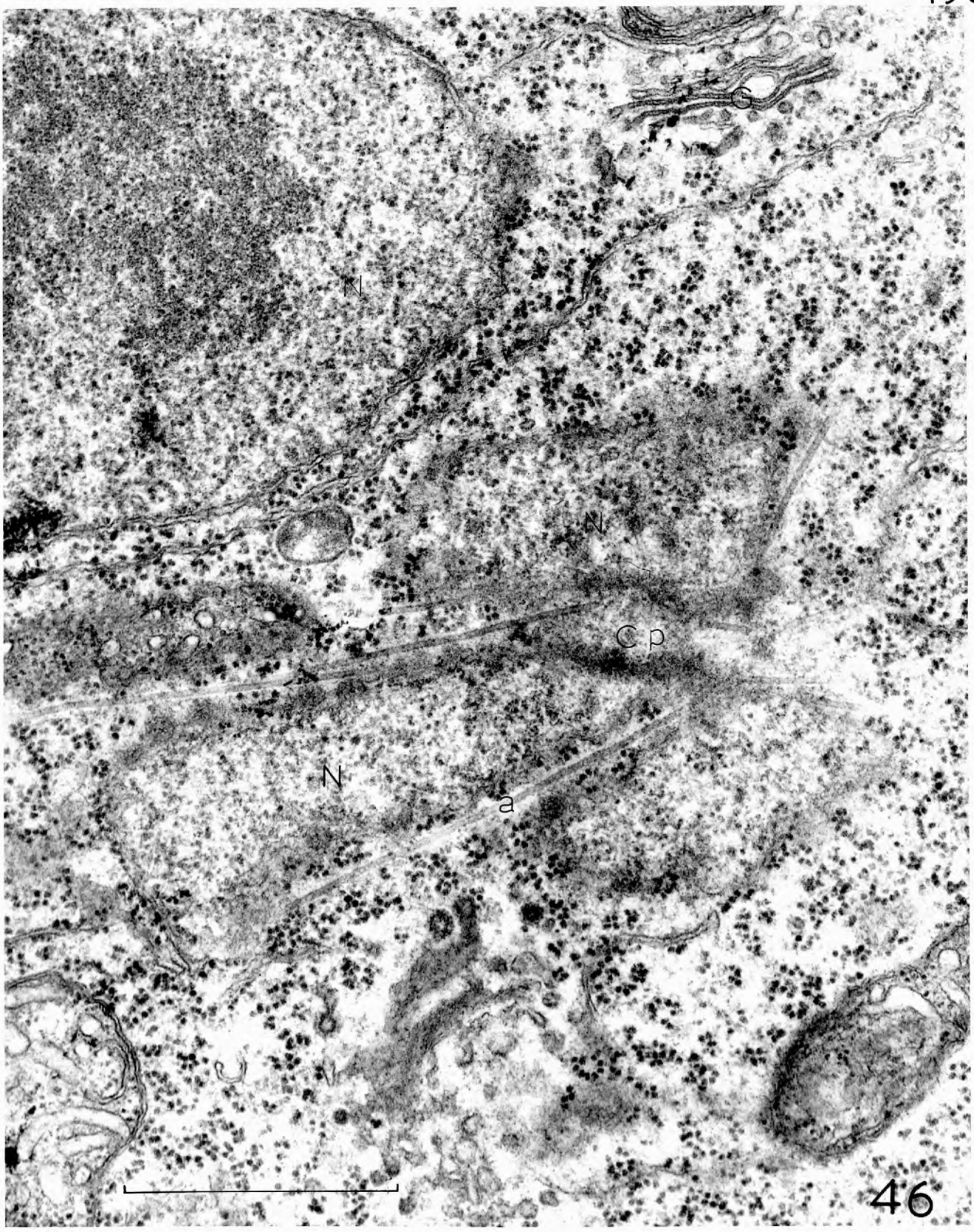

46

Fig.47. 4 centrioles at one "pole" of a nucleus before migration. Each pair has an associated nuclear pocket. 1547A/3. 8552.

Fig.48. D. sterile. 4 centrioles at a "pole" of a nucleus before migration. Note the spindle tubules beginning to form and the trace of a connection remaining between the parent and daughter hubs(arrowed). 1853A/2. 12192.

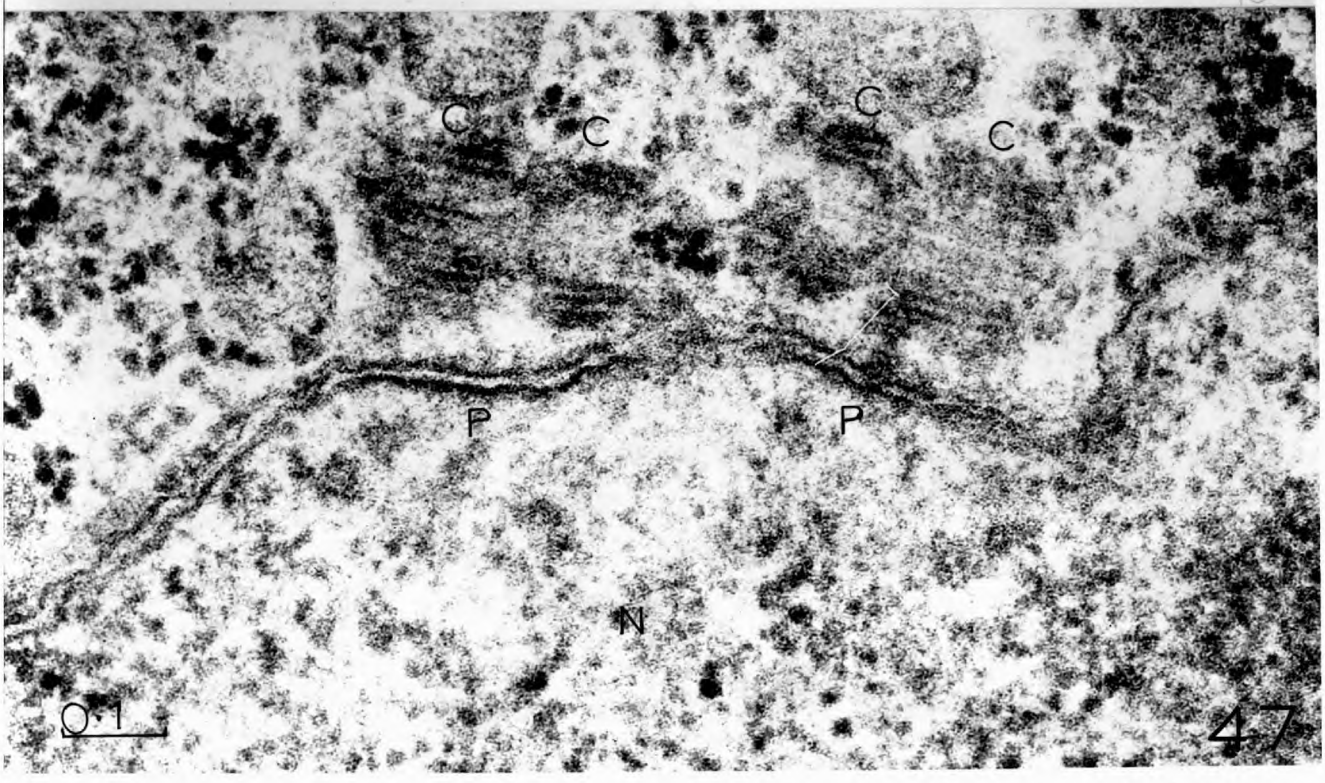
C
C
C
C
P
P
N
0·1
47

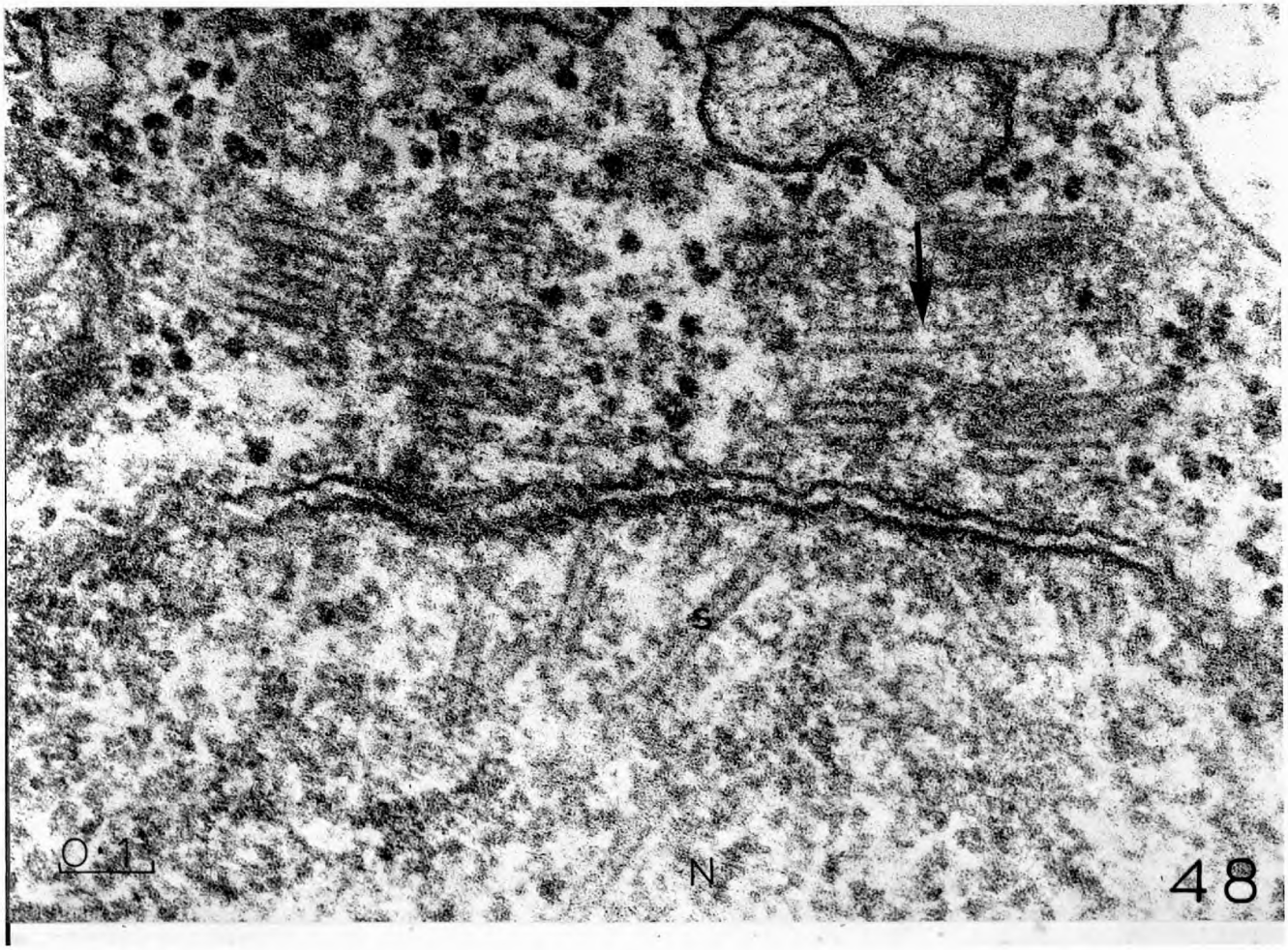
S
N
0·1
48

Fig.49. Oblique section of 2 pairs of centrioles at the beginning of migration in a walled off sporangium. The spindle tubules are forming between the pockets. 1645G/2. 10373.

Fig.50. 4 migrating centrioles in a young non-delimited sporangium. Note spindle tubules and astral tubules. 1848B/2. 10933.

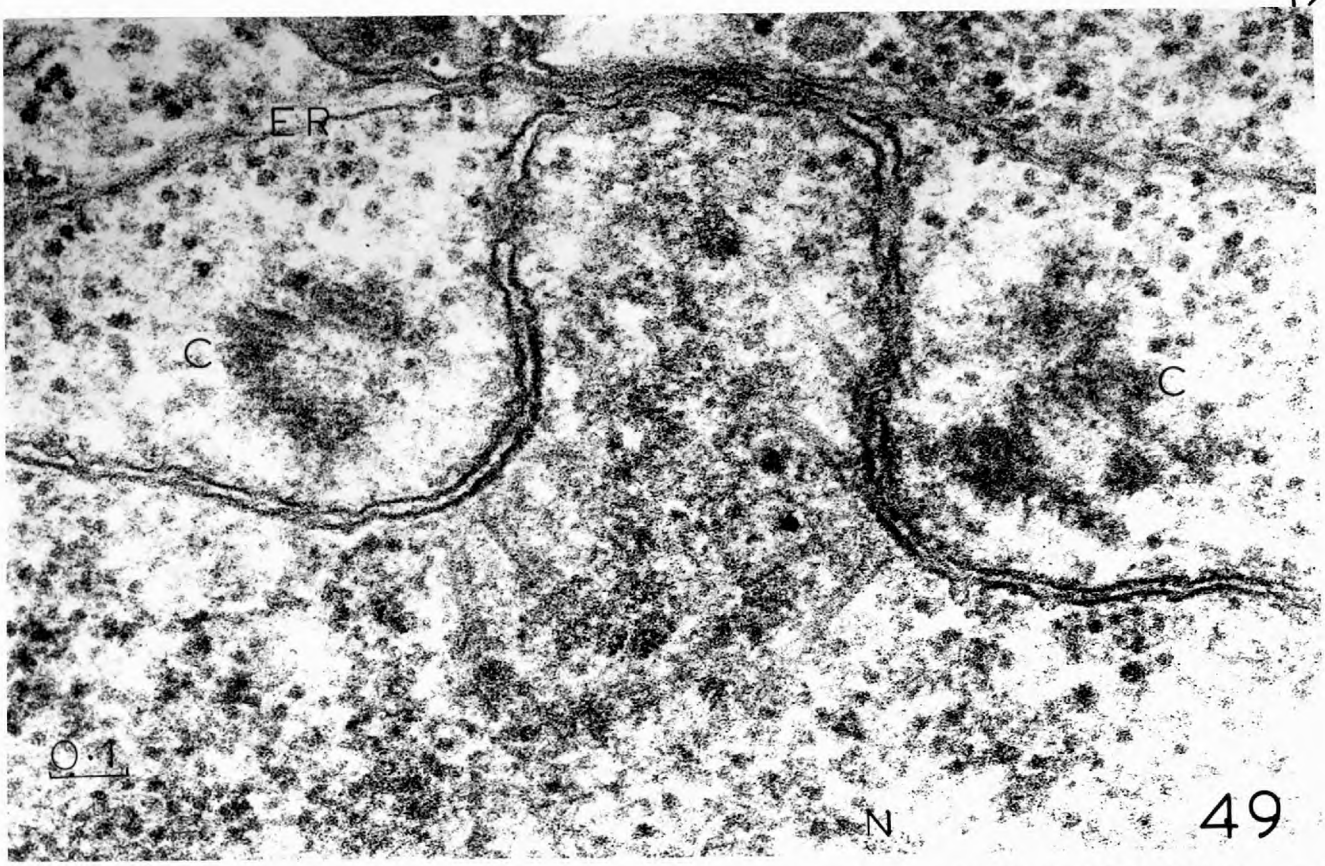

49

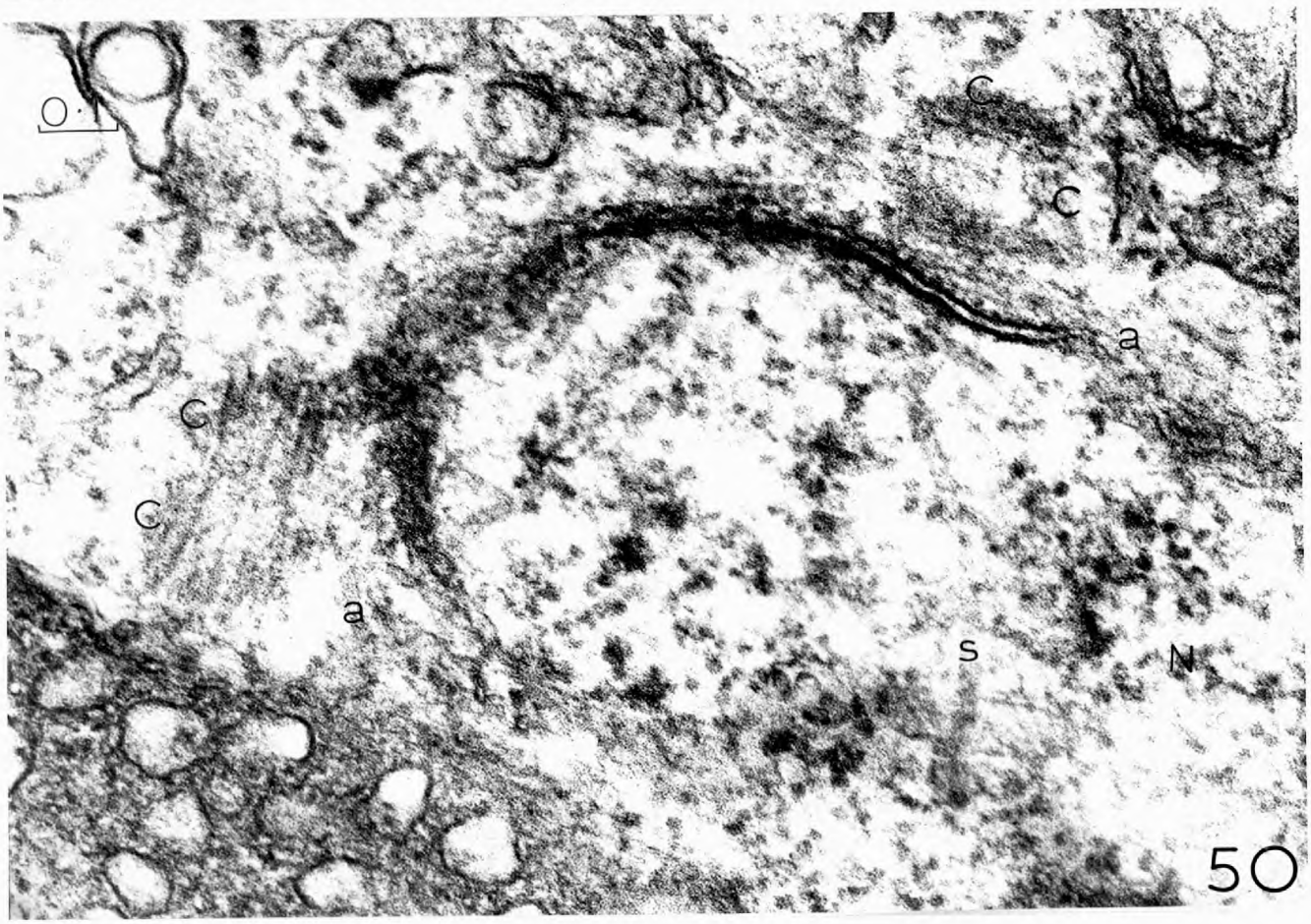

50

Fig.51. Early metaphase nucleus showing equatorial kinetochores, one polar centriole and a portion of the nuclear envelope apparently crawling along an astral tubule. Note eccentric position of the spindle relative to the large nucleolus and polyribosomes on the nuclear envelope. 1547/5. 8531.

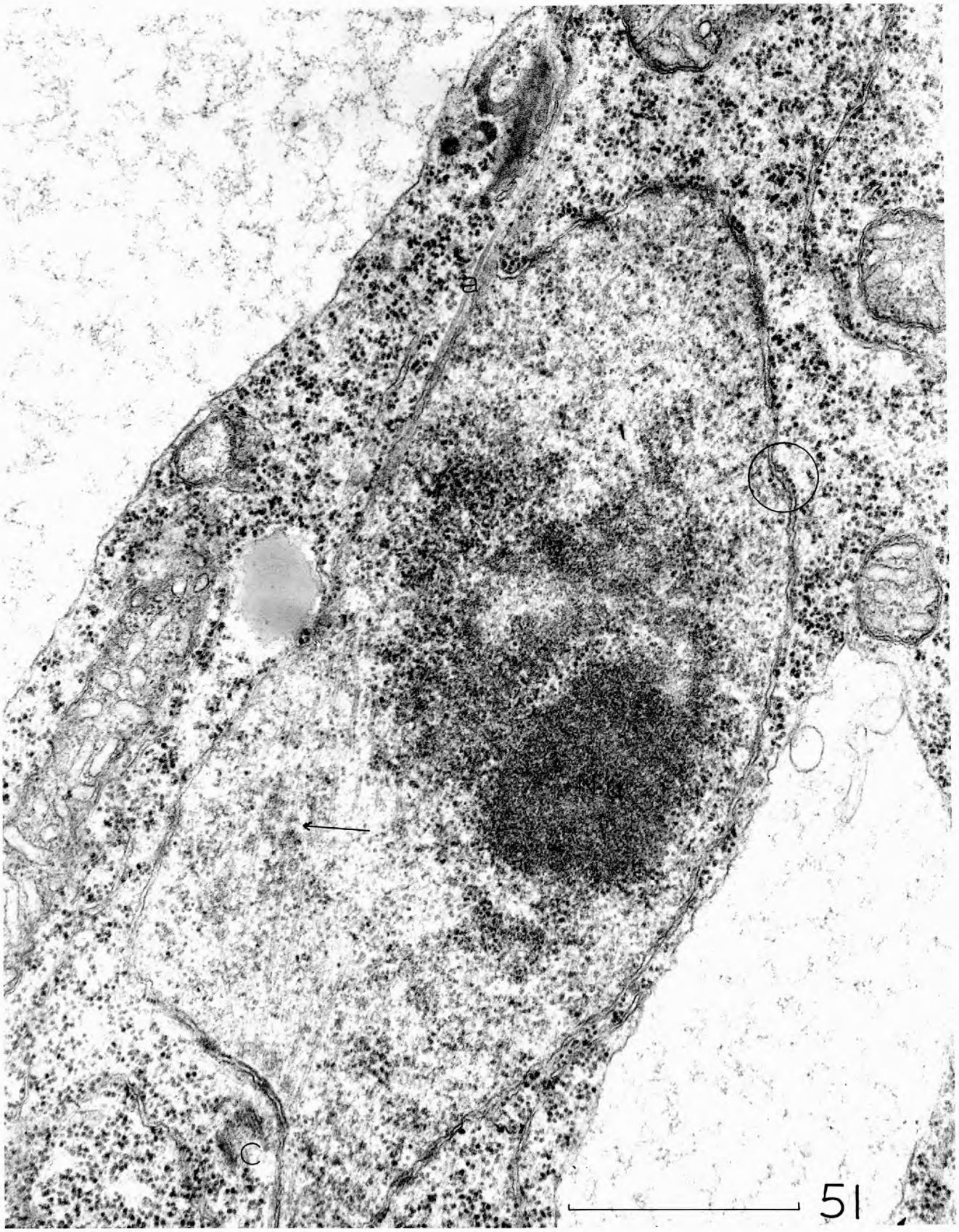
a
c
51

Fig.52 & 53. Adjacent transverse sections of the equatorial region of a metaphase spindle showing the termination of the arrowed tubule in a kinetochore. Note the absence of structure in a similar position on the adjacent section. The other structures ringed are probably also tubules terminating in Fig.52. These two sections are n and m in Fig.54. 1547D/1. 8588, 8587.

Fig.54. Diagram of the distribution of microtubules in a series of 14 transverse sections through the equator of the spindle. 15 tubules were present in all sections probably corresponding to the pole to pole tubules. Others were not present in all sections. 19 tubules present in n do not occur in a and 9 in a are absent from n. These may be equivalent to pole to kinetochore tubules. Where possible, tubules absent from part of a series are placed in the same line as other tubules present in a similar position in other members of the series. The numbers of spindle tubules quoted in the text are based largely on this series. Sections marked x were obscured. 1547D/1. 8577-8588.

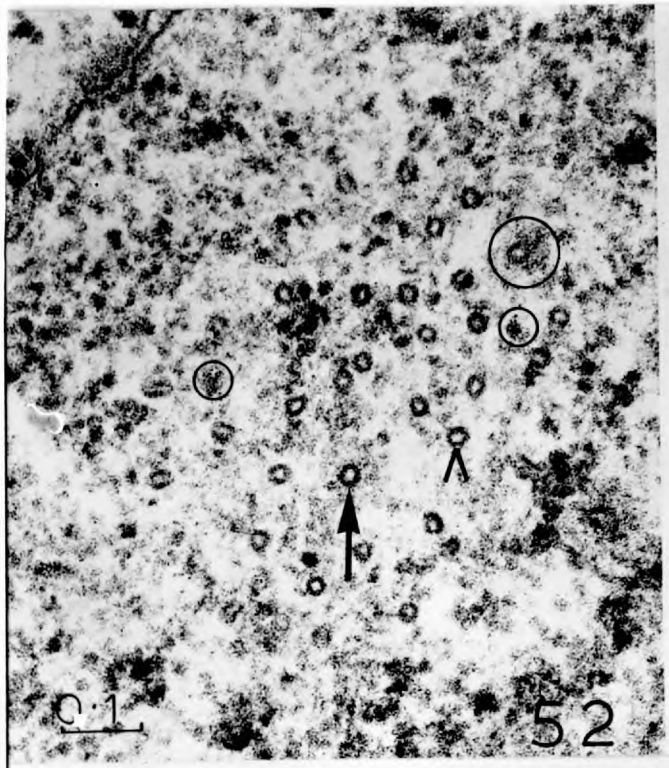

52

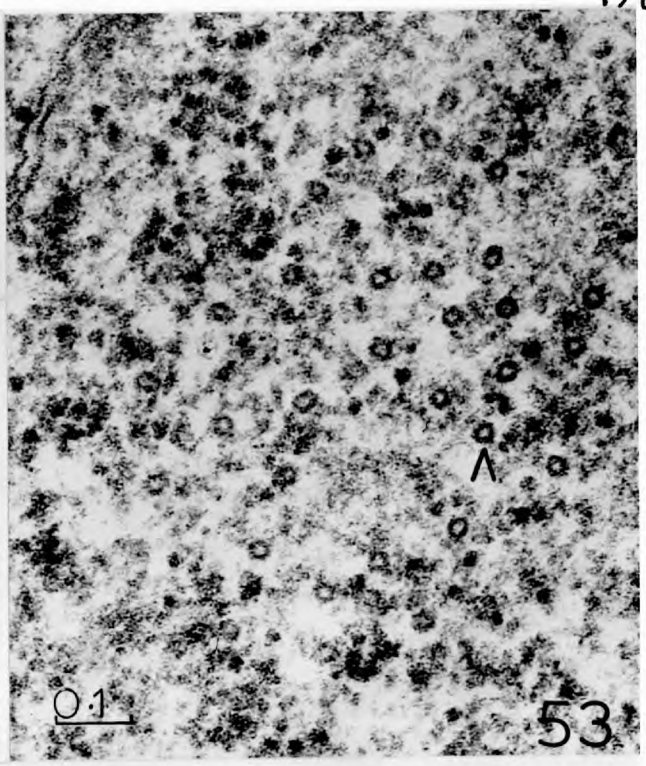

53

54

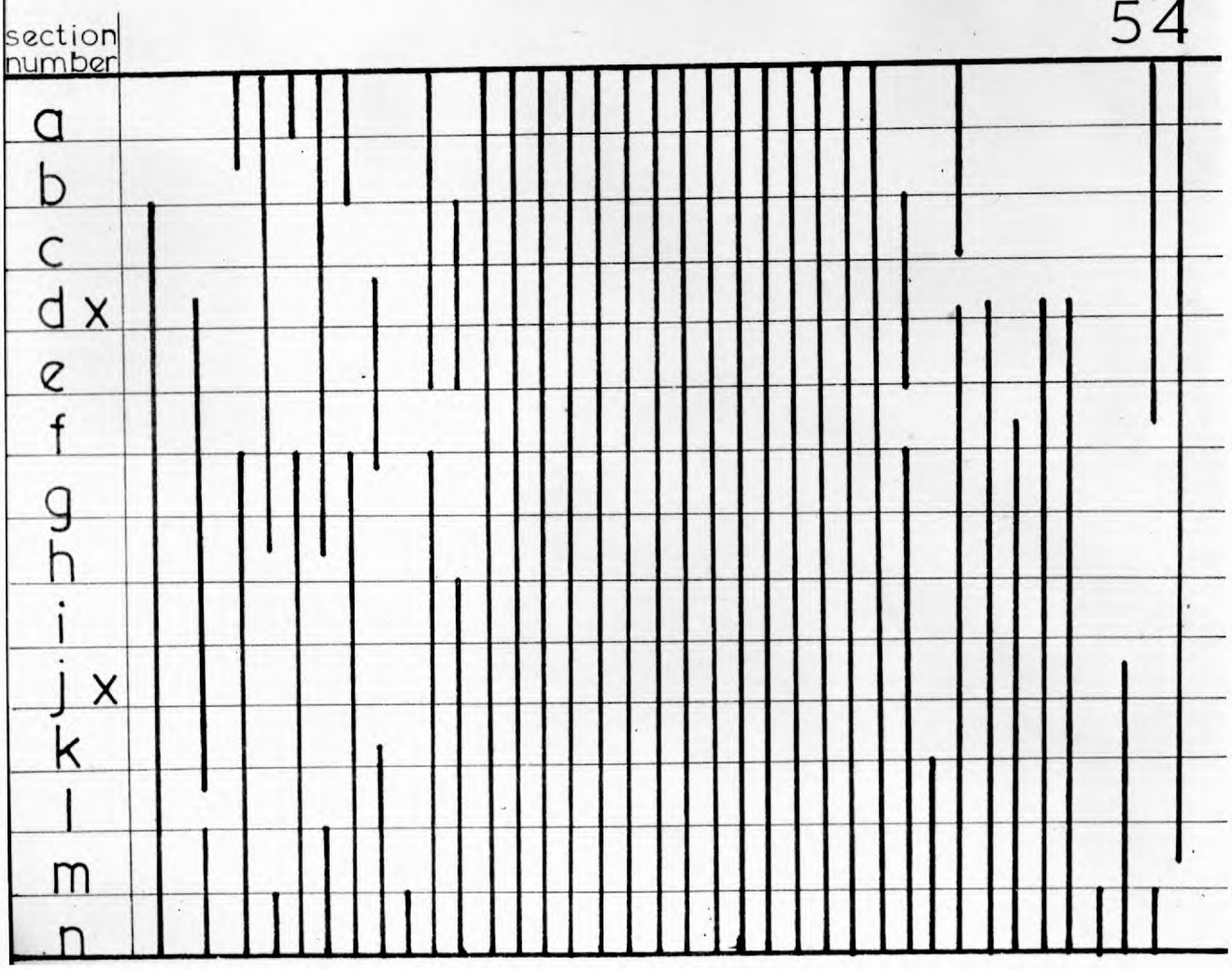

Fig.55. Nucleus and centriole in a germinating zoospore incubated in 0.1% colchicine. Fibrils(cf) which appear to replace microtubules in "normal" colchicine treated spores suggest that microtubule synthesis has been blocked. The centriole structure is unaffected but a build up of dense material around the centriole and its associated pocket may be tubule precursors. 1779/4. 14061.

Fig.56. Damaged flagellum suggesting rigidity of the microtubules which break rather than bend sharply. 1887B/1. 12753.

Fig.57. D. sterile. L.S. interphase centrioles. 1853A/2. 12190.

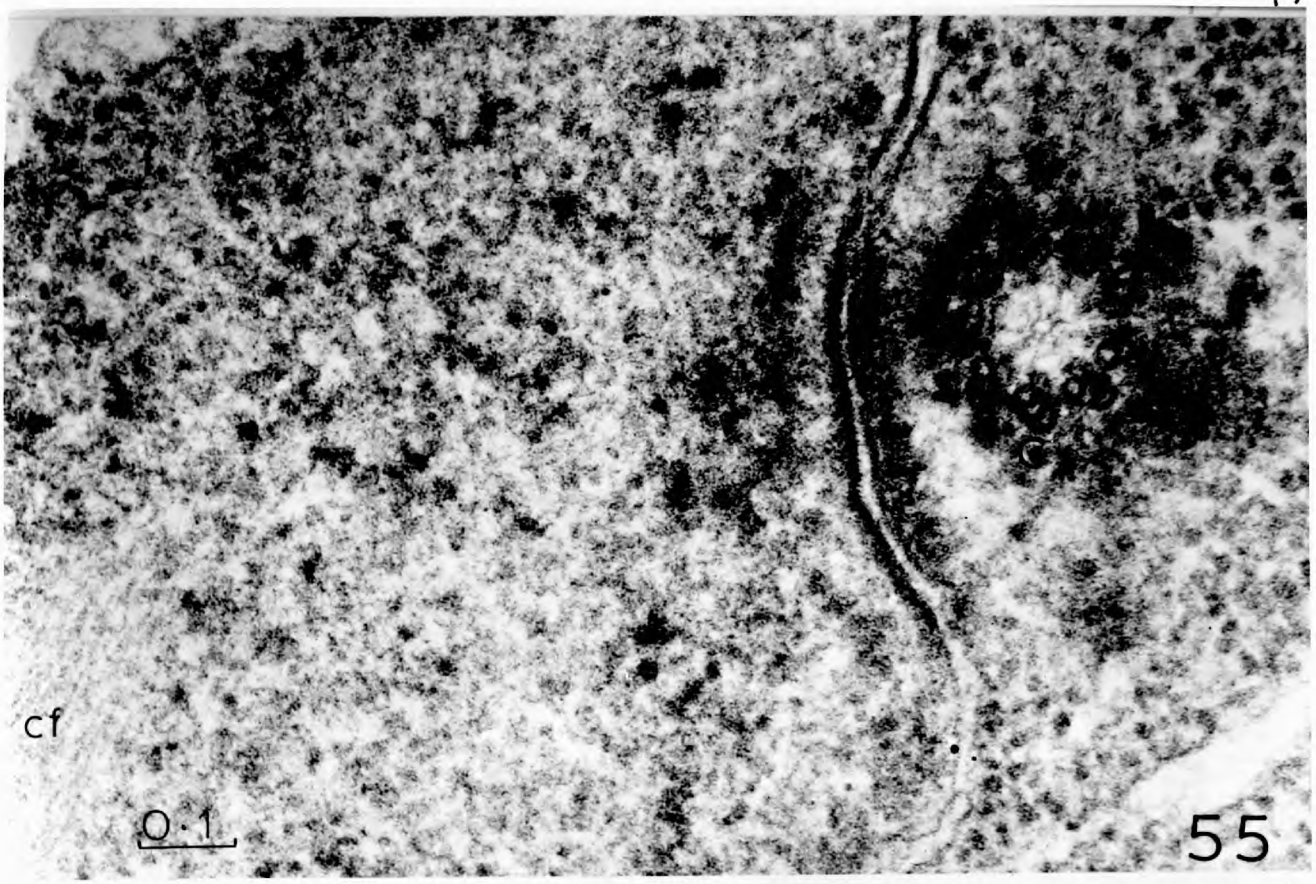
cf
0·1
55

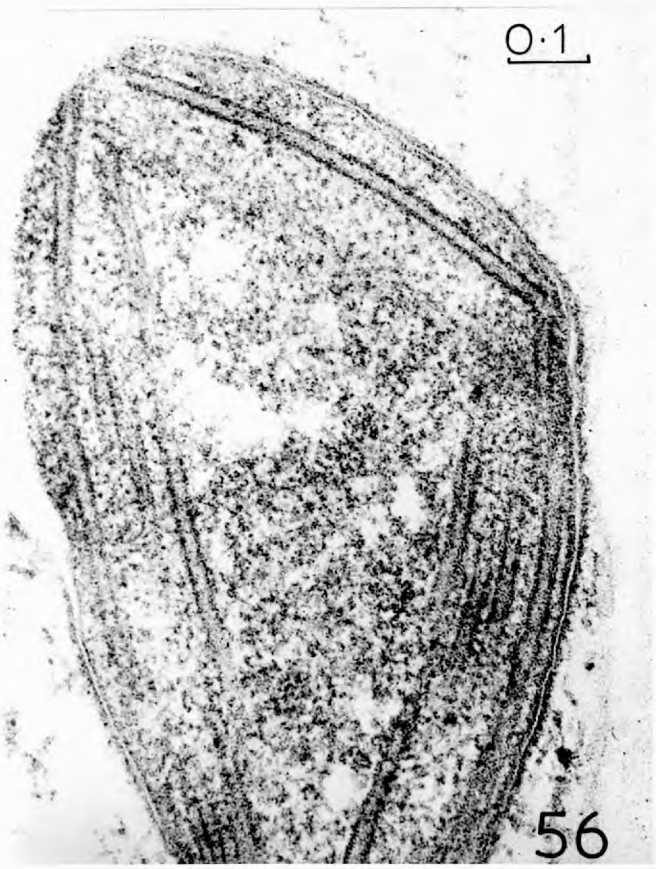
0·1
56

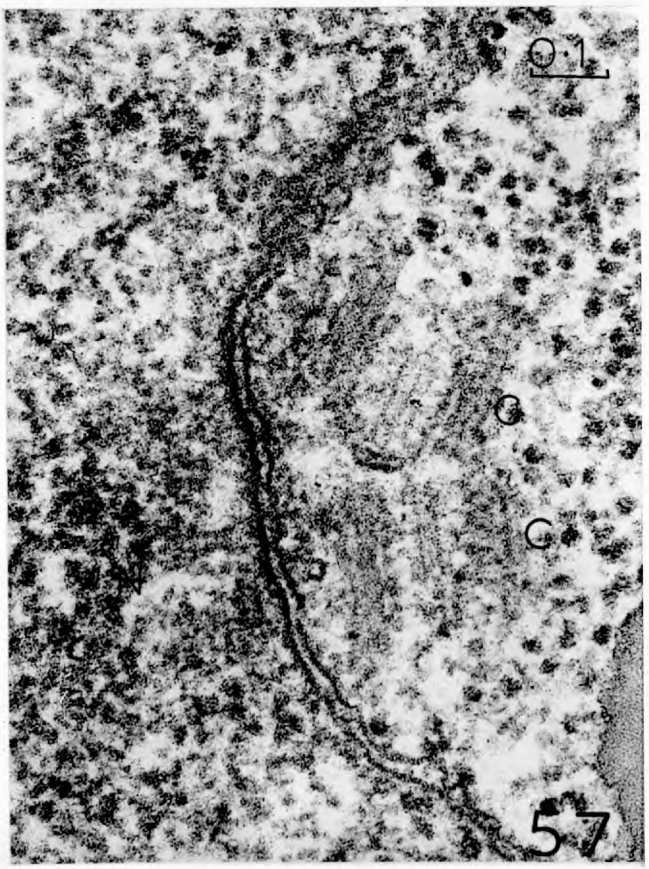
0·1
57

Fig.58. L.S. equatorial region of metaphase spindle shown in Fig.61 with kinetochores on tubules from both poles. Note dense strands between the 2 parts of the kinetochore at arrow and dense region of chromosome (ch). 1547/1b. 8517.

Fig.59. Adjacent section to Fig.58 showing another kinetochore from the opposite pole to that arrowed in Fig.58. 1547/1a. 8516.

Fig.60. Pole of late telophase nucleus showing long pole to pole tubules(more clear in low power serial sections) and a short tubule believed to terminate at a kinetochore(ringed)suggesting polarization of the chromosome. 1825/3e. 10811.

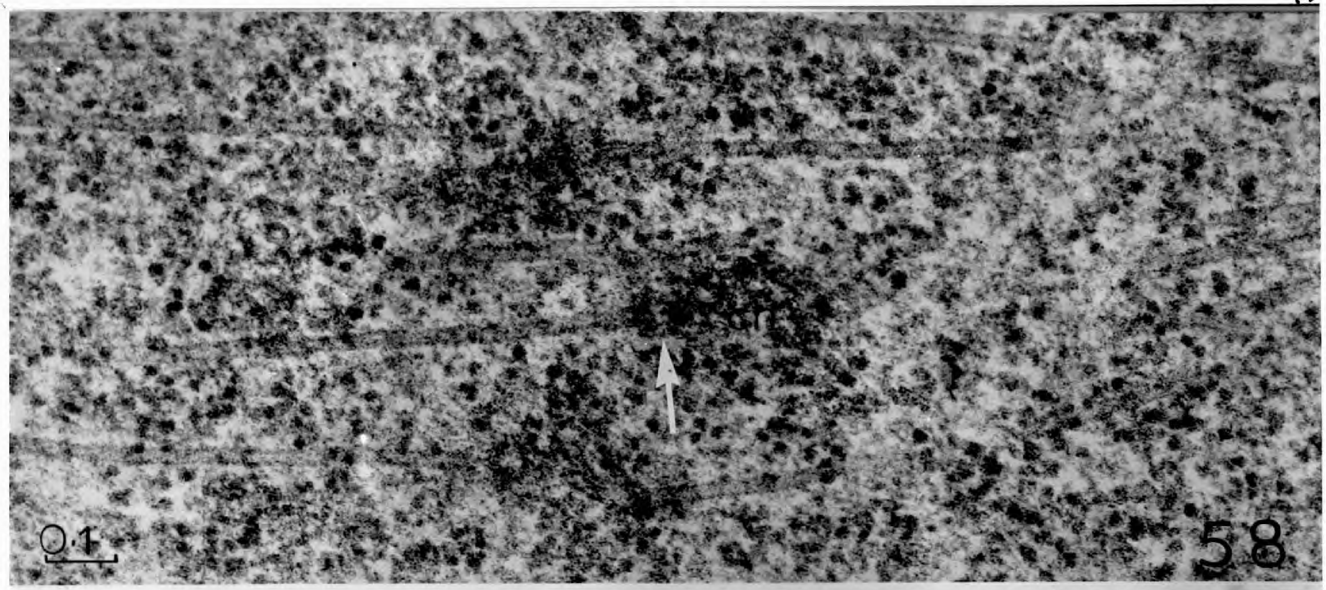
0·1
58

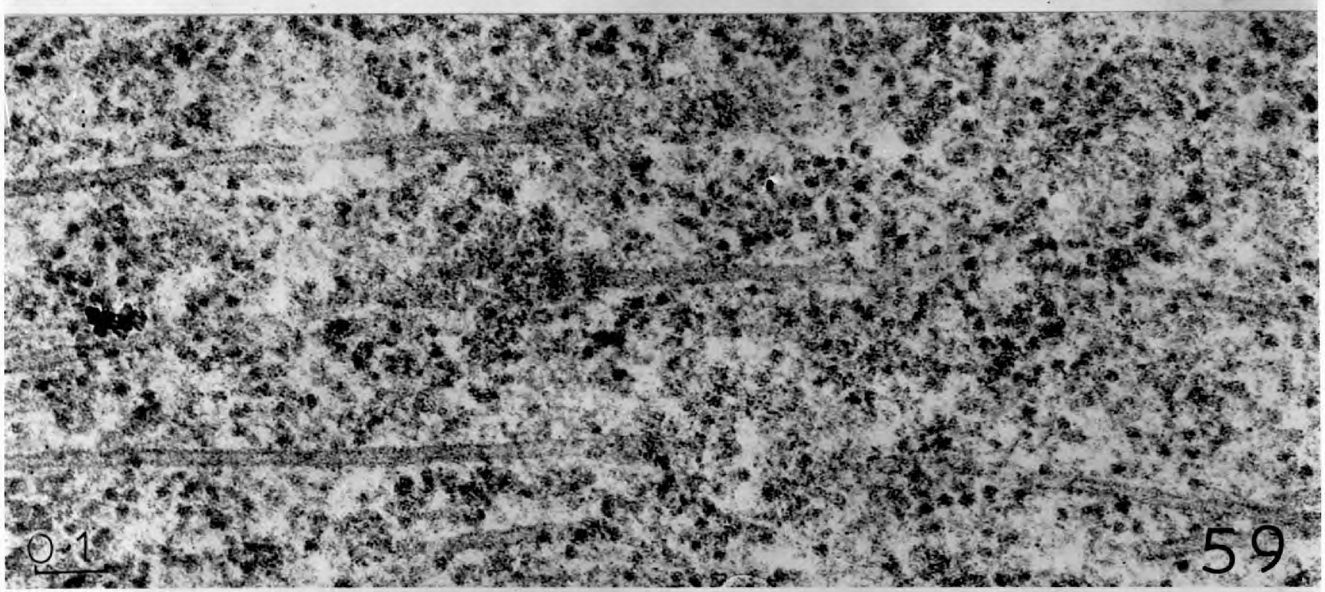
0·1
59

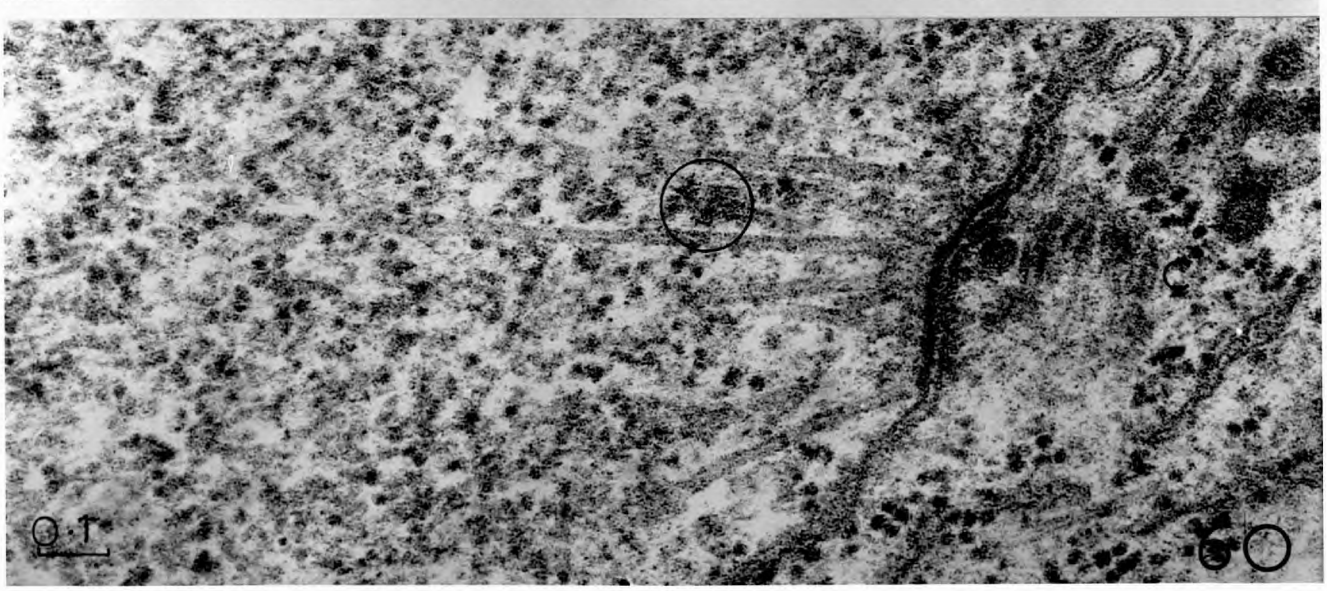
0·1
60

Fig.61. Metaphase nucleus of S. ferax. 1547/1d. 8518.

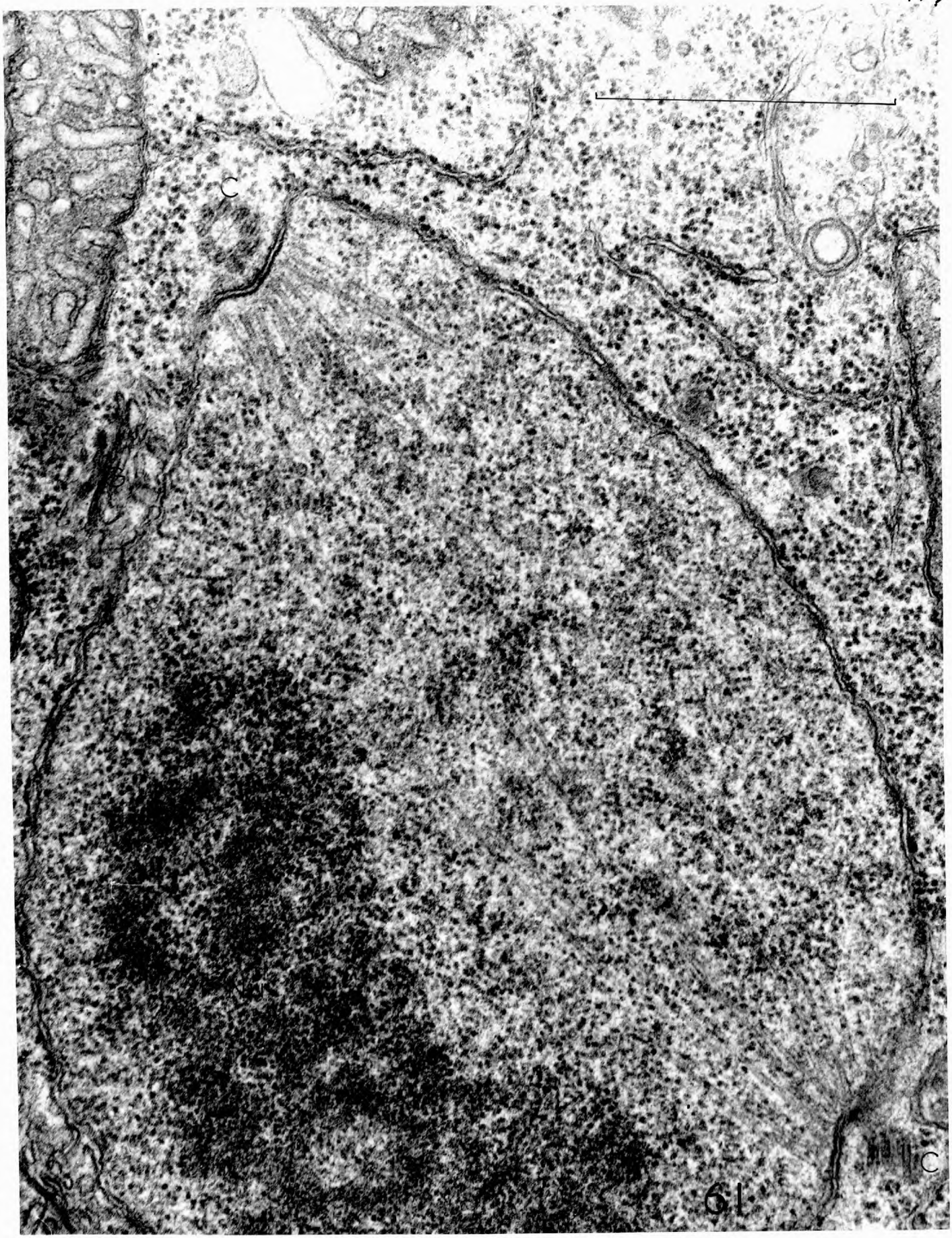
C
C
61

Fig.62. Dense material of unknown nature in metaphase nucleus. .
1693B/1. 14370.

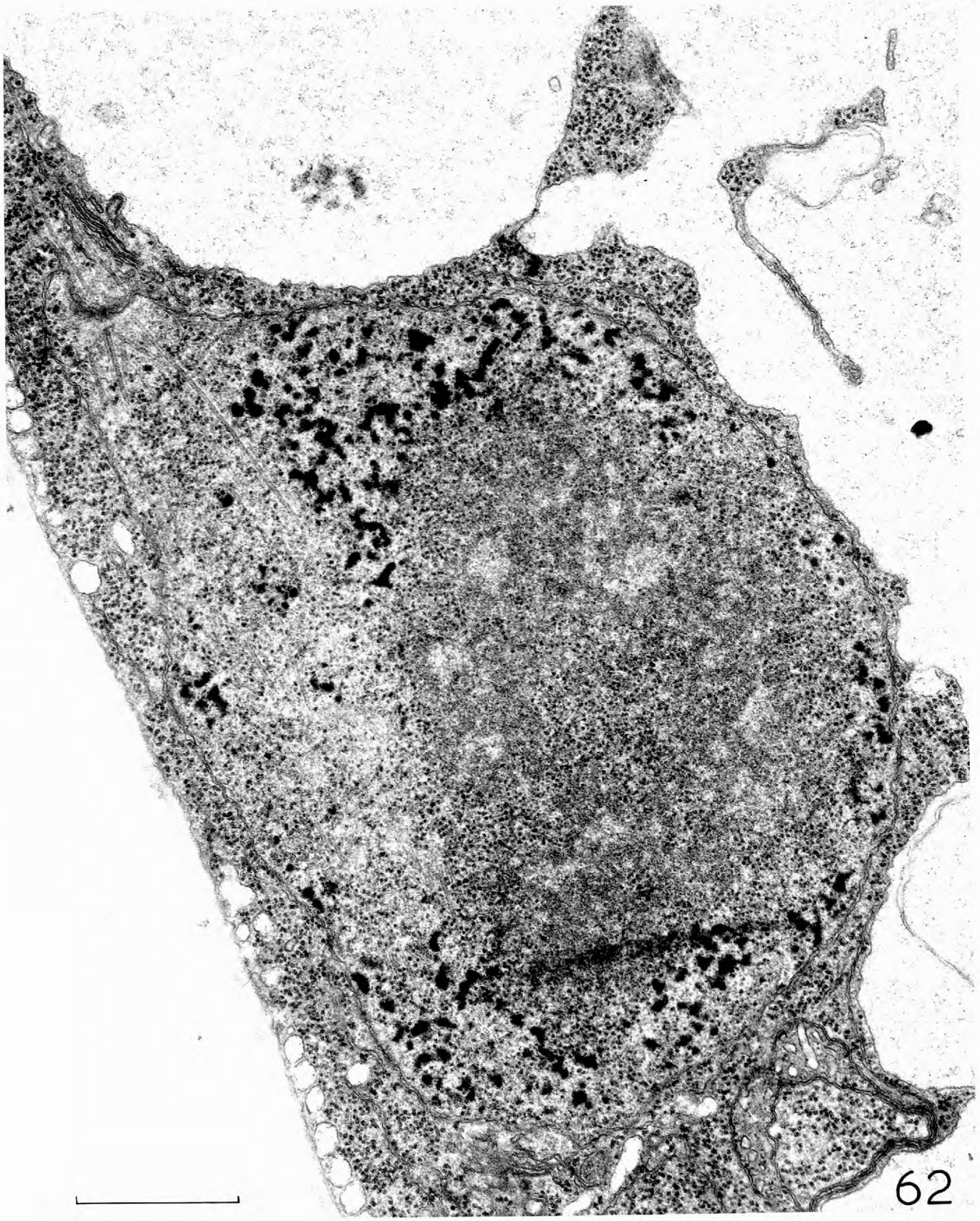

62

Fig.63. Metaphase nucleus with equatorial chromatin? and Golgi body associated with the nuclear envelope. Note the absence of C tubules in the distal ends of both centrioles. 1547B/3a. 8554.

Fig.64. Early metaphase spindle with clear pole to pole tubule(s) and kinetochore(ringed). 1643G/6. 10382.

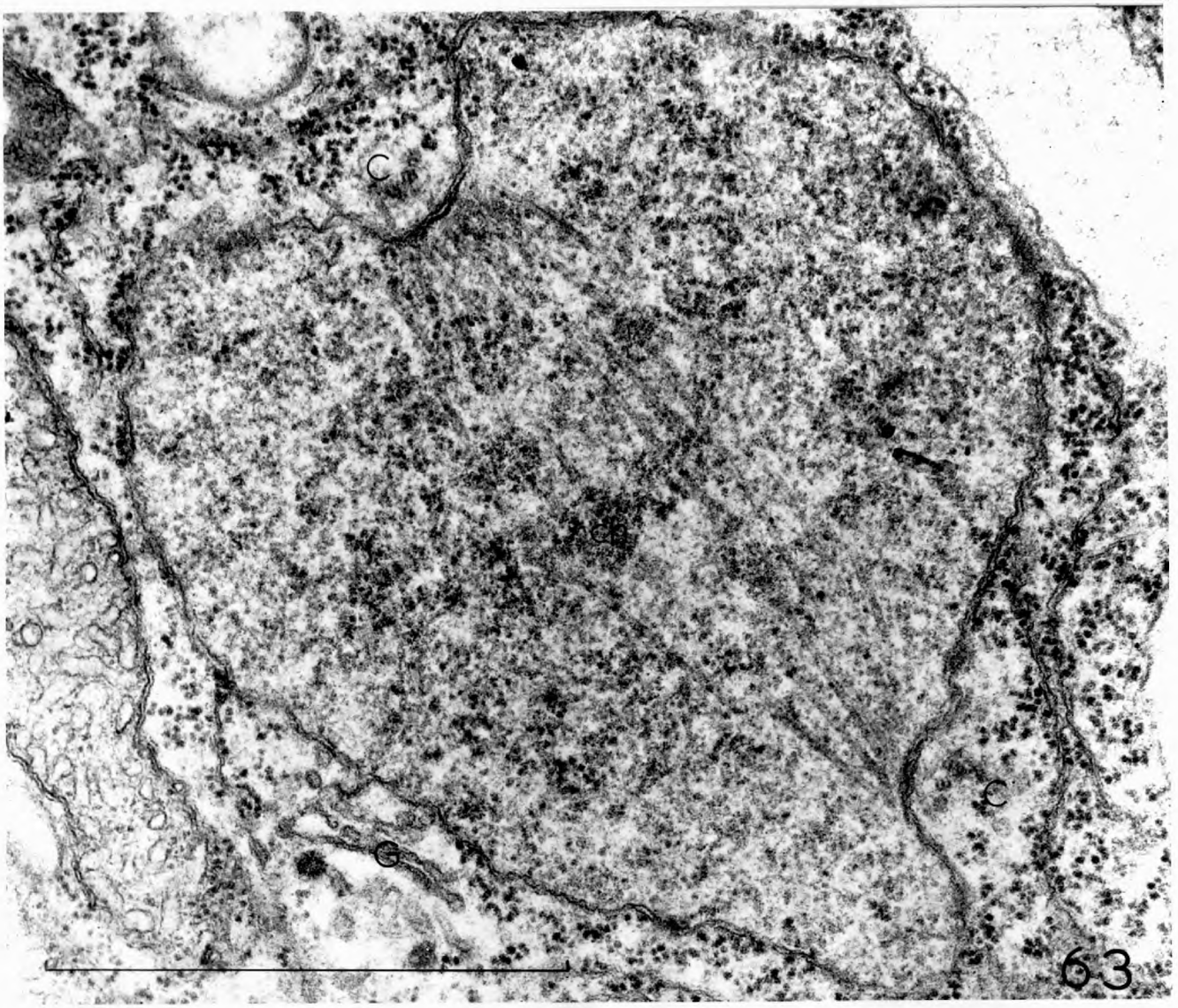
C
C
63

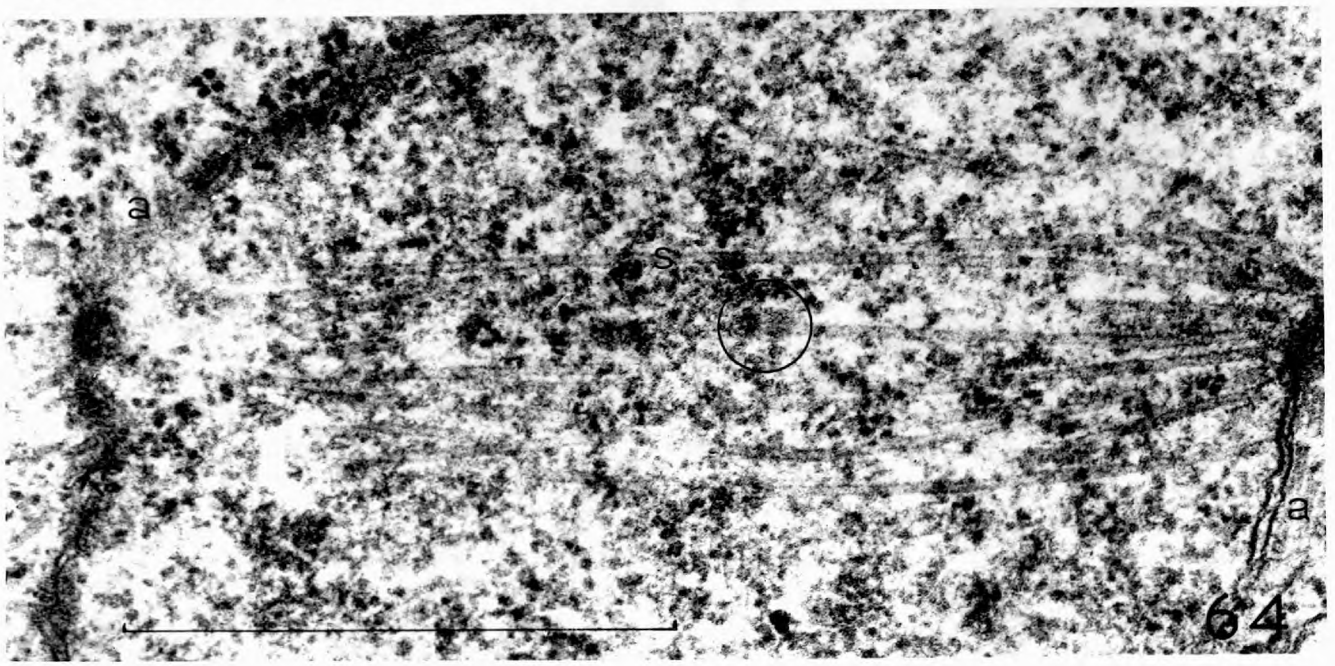
a
S
a
64

Fig.65. Late anaphase nucleus inside a sporangium delimited by a cross wall. Note dense masses which are probably chromatin, polar centrioles, astral rays and pole to pole spindle tubules. 1848B/2. 10932.

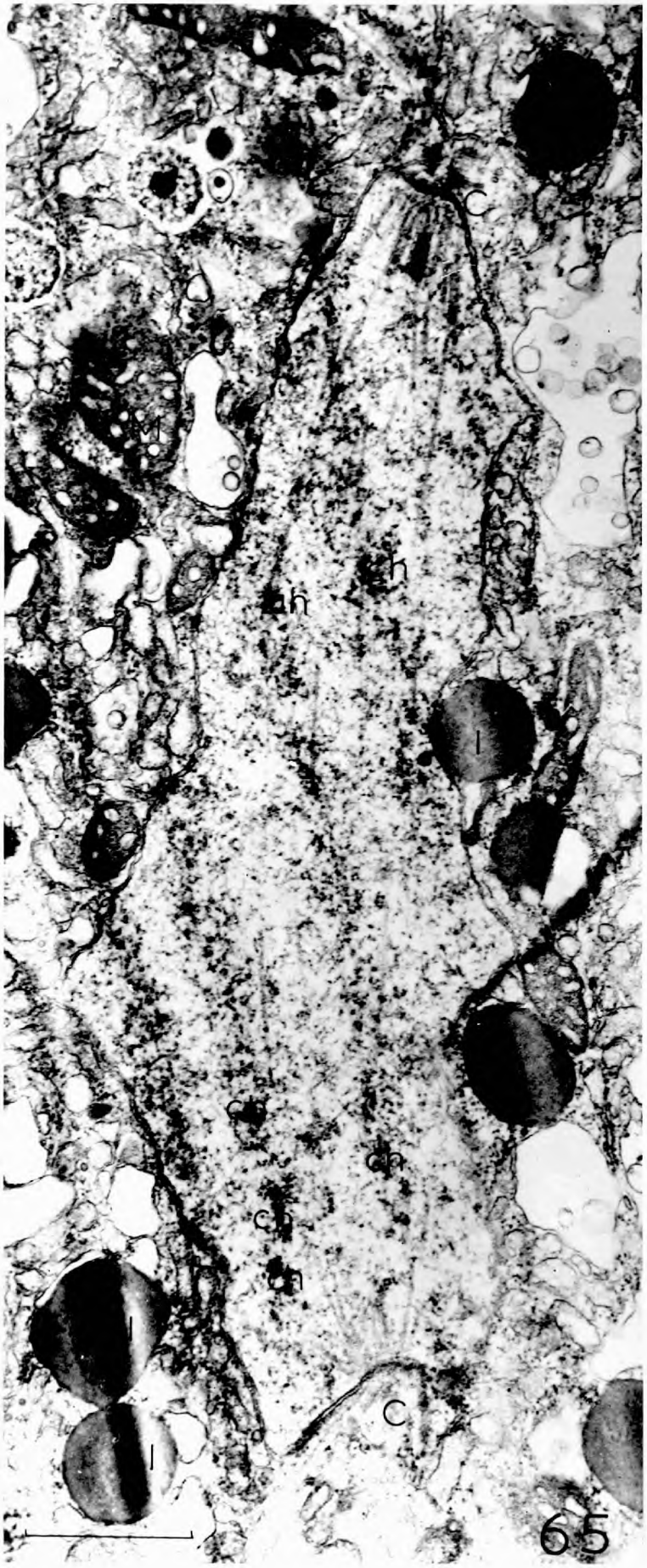
C
M
O
h
h
h
I
ch
ch
ch
I
I
C
65

Fig.66. Late anaphase nucleus showing elongated nucleolus and pole to pole spindle tubules(↕). Serial sections showed the centriole located under the positions marked Cp. 1547G/3. 8772.

66

Fig.67. End of nucleus in Fig.66 showing extension of nucleus associated with astral tubules beyond centriole position(Cp). 1547G/3. 8595.

Fig.68. Opposite end of Fig.66 showing similar structure to Fig.67. 1547G/3. 8590.

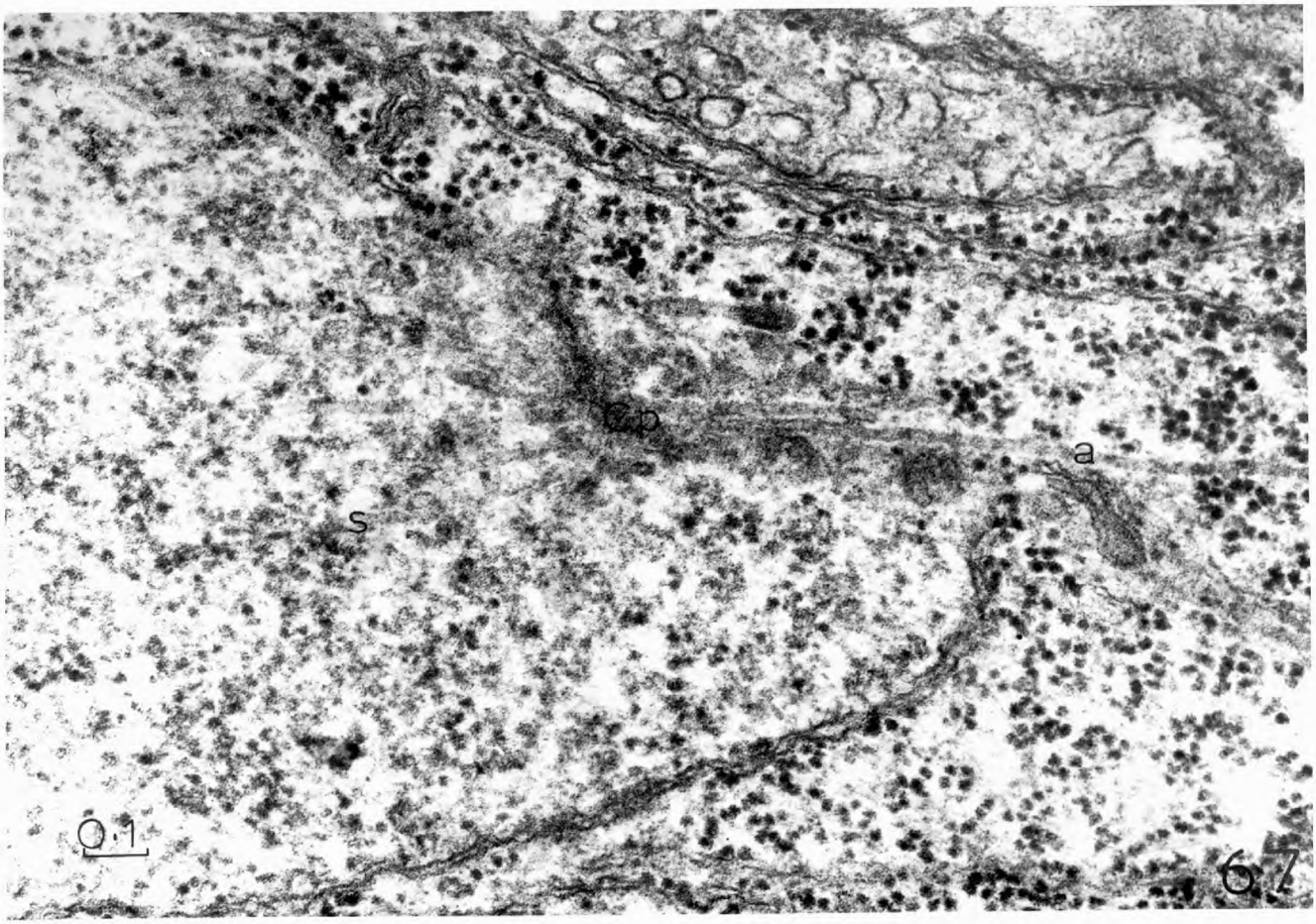
Cp
a
s
0·1
67

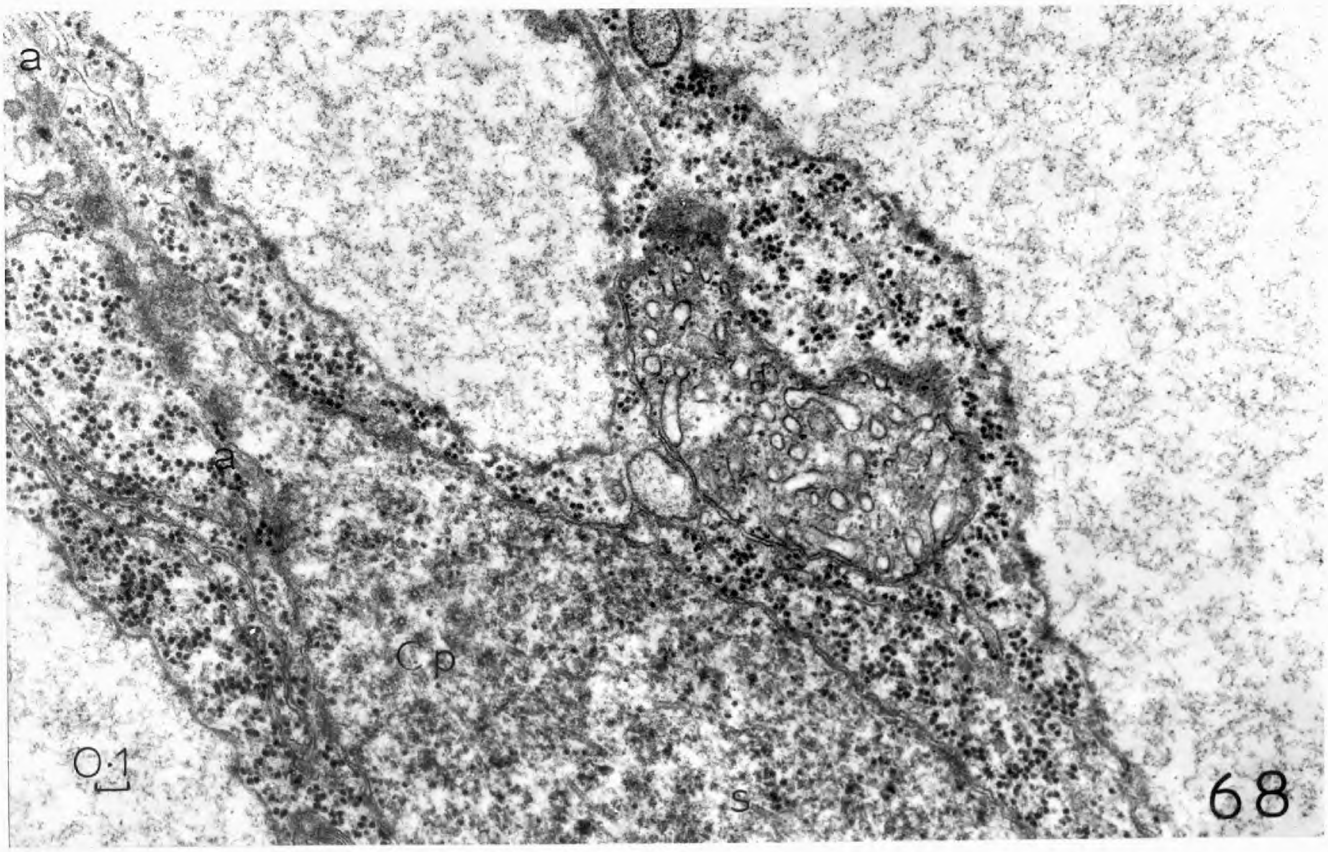
a
a
Cp
0·1
s
68

Fig.69. Association between nuclear envelope and astral tubule. 1547/6. 12874.

Fig.70. Association between nuclear envelope and astral tubule. 1547/8. 12876.

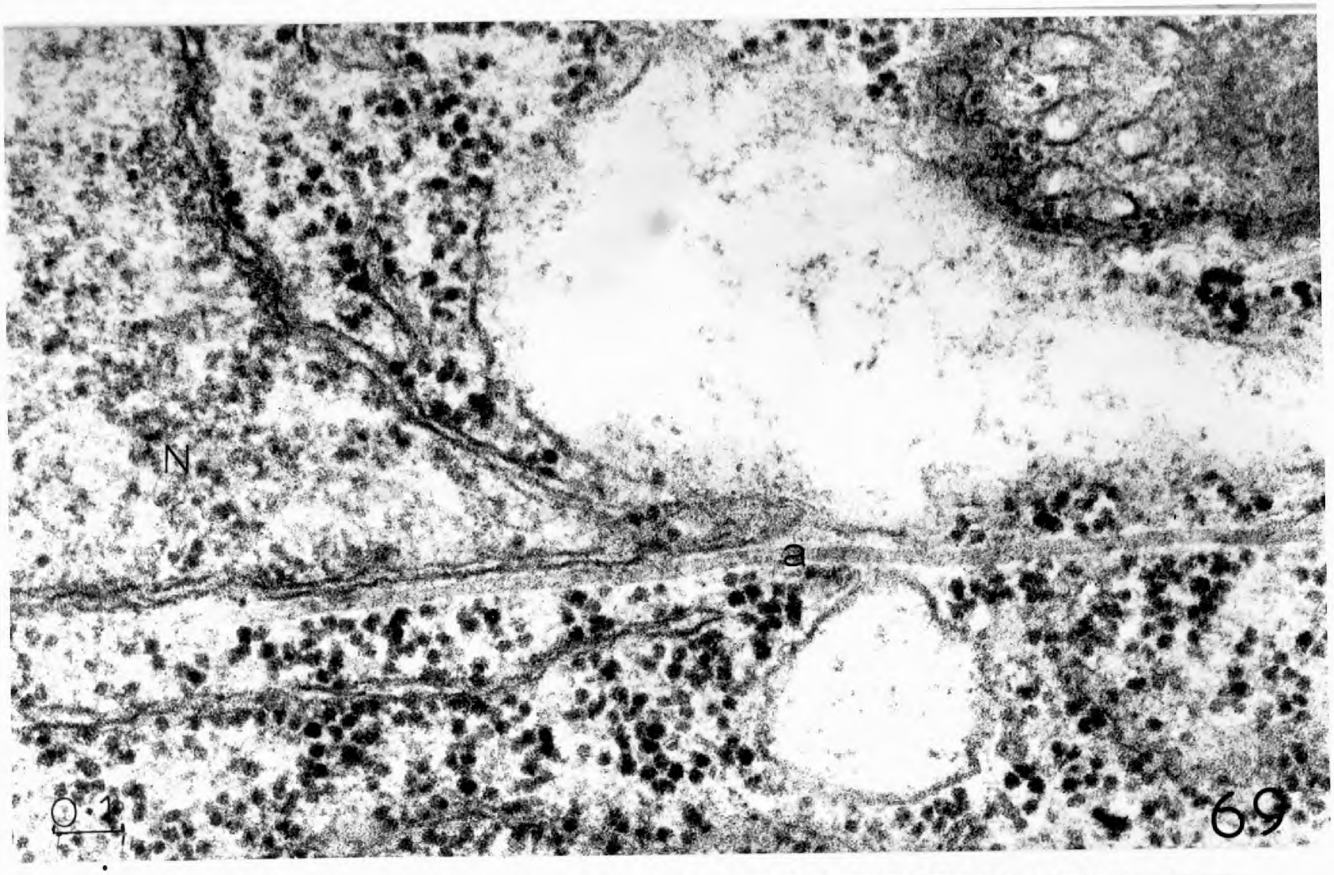
N
a
0·1
69

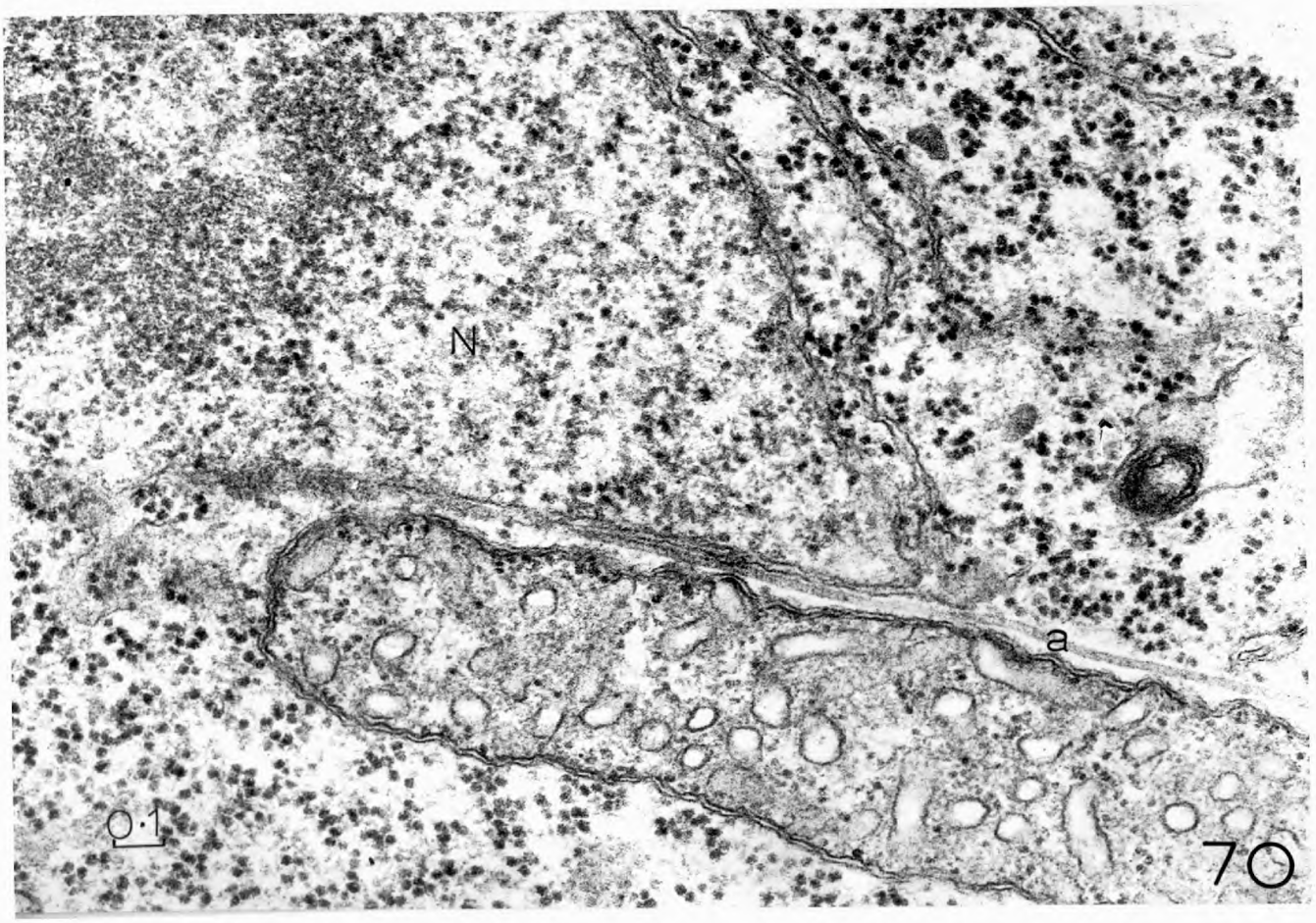
N
a
0·1
70

Fig.71. Germinating zoospore after two nuclear divisions in 0.1% colchicine showing three apparently normal spindles for the 3rd series of division. 1779/1. 10492.

Fig.72. Nuclei in hypha fixed with $KMnO_4$. The connection between the two may be a final stage in karyocherosis or may be due to membrane fusion caused by the fixation. Note extensions of the envelope forming E.R. Permanganate. Unstained. 1780B/2. 10501.

Fig.73. "Dense" zoospore germinated in 0.1% colchicine. After several nuclear divisions an apparently normal spindle is still formed. 1772/1. 10277.

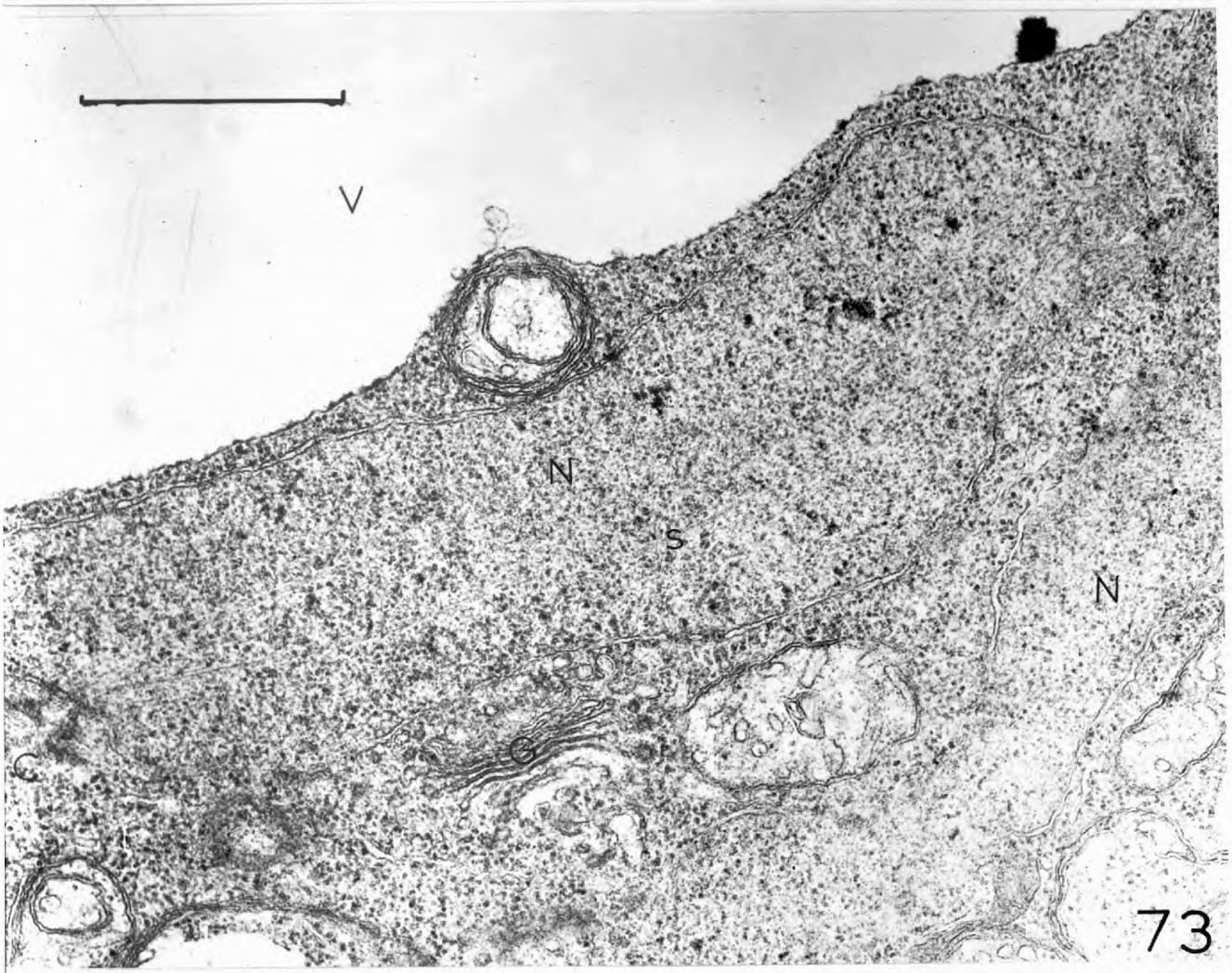
V
N
S
N
G
73

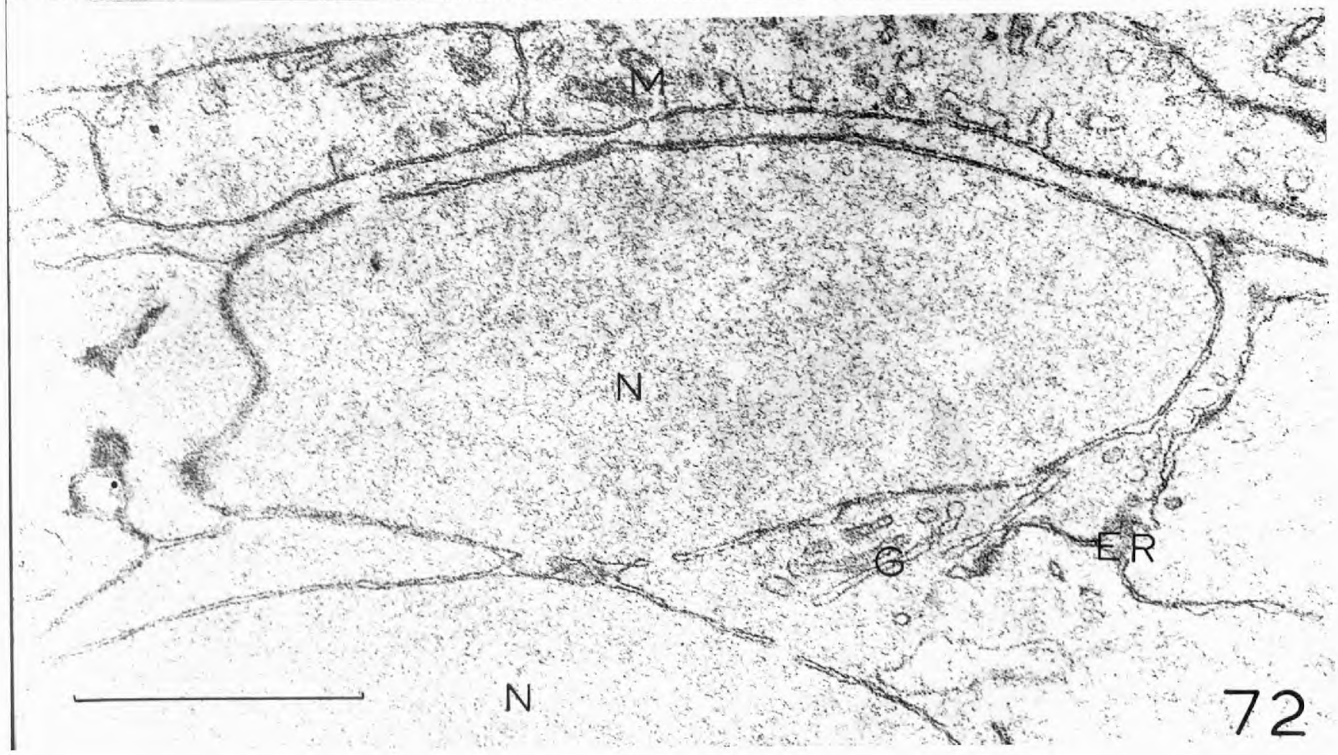
M
N
G
ER
N
72

Fig.74. An apparently normal spindle and centriole (oblique) in a "dense" spore germinated in 0.2% colchicine. 2110/2. 14310.

Fig.75. Centriole and astral tubules in a spore germinated in 0.1% colchicine. 1779/2. 14129.

Fig.76. A "normal" spore germinated in 0.1% colchicine with 8nm diameter fibrils in the cytoplasm. 1779/1. 14103.

Fig.77. Germinating spore in 0.1% colchicine showing "tongue" of 8nm diameter fibrils in the nucleus and unaffected tubules in the E.R.(f). 1778/4. 12999.


0·1
C
N
74

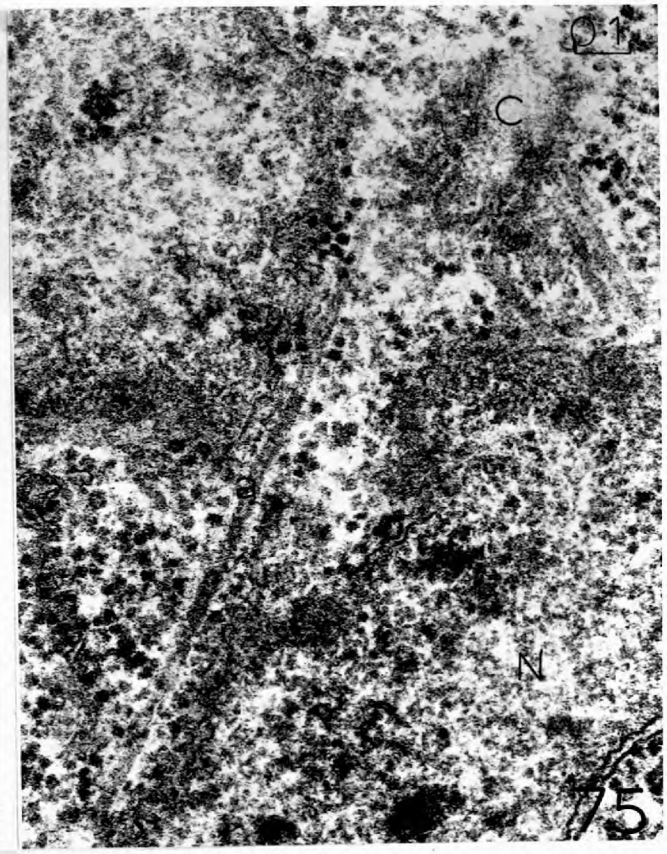
0·1
C
N
75

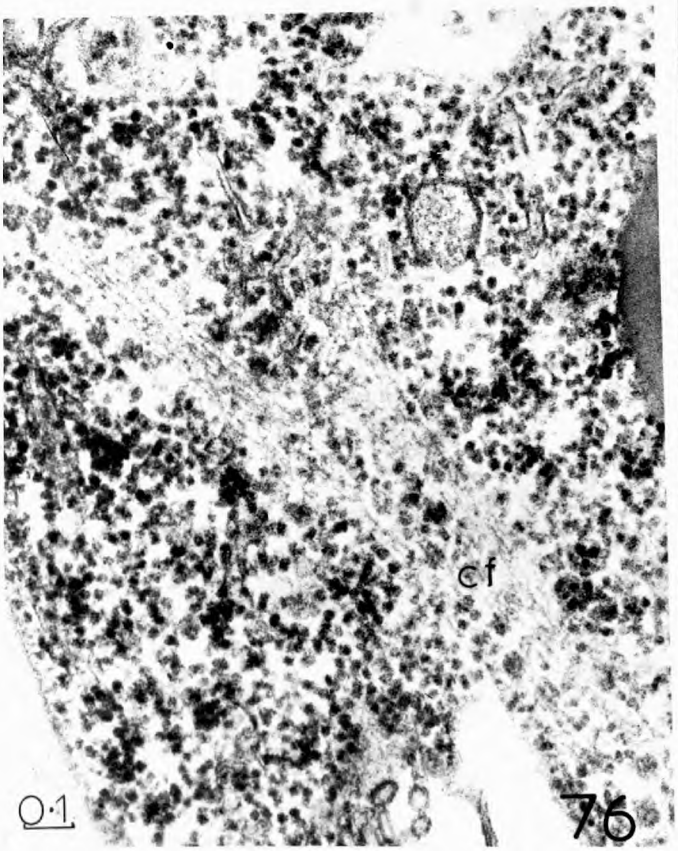
cf
0·1
76

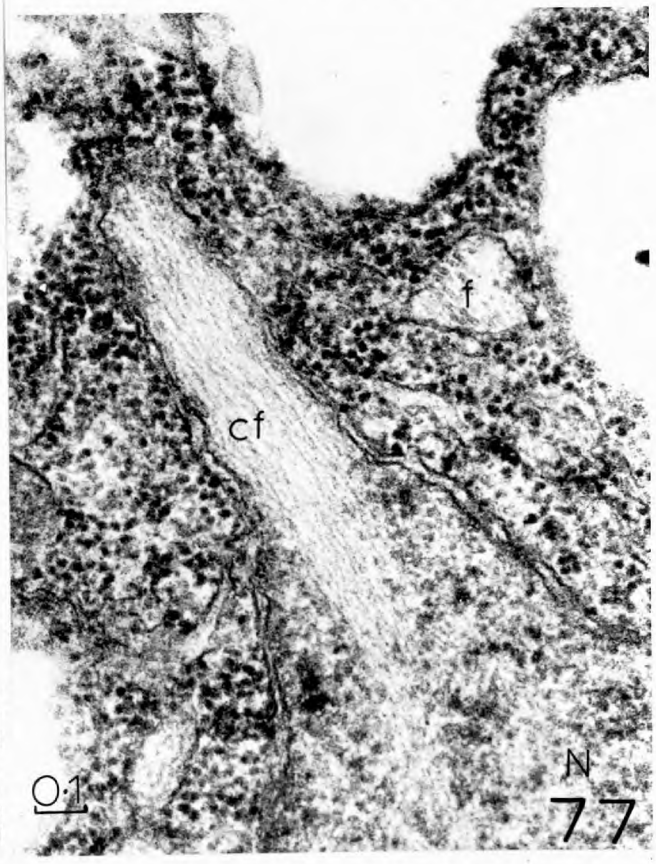
f
cf
0·1
N
77

Fig.78. Zoospore germinated in 0.1% colchicine showing band of fibrous material in nucleus. 1779/1. 10490.

Fig.79. Nucleus containing bundles of colchicine produced fibrils at right angles to each other. Note also apparently normal tubules in the E.R. 1779/2. 14020.

Fig.80. Detail of 8nm diameter colchicine produced fibrils within the nucleus. 1779/2. 14019.

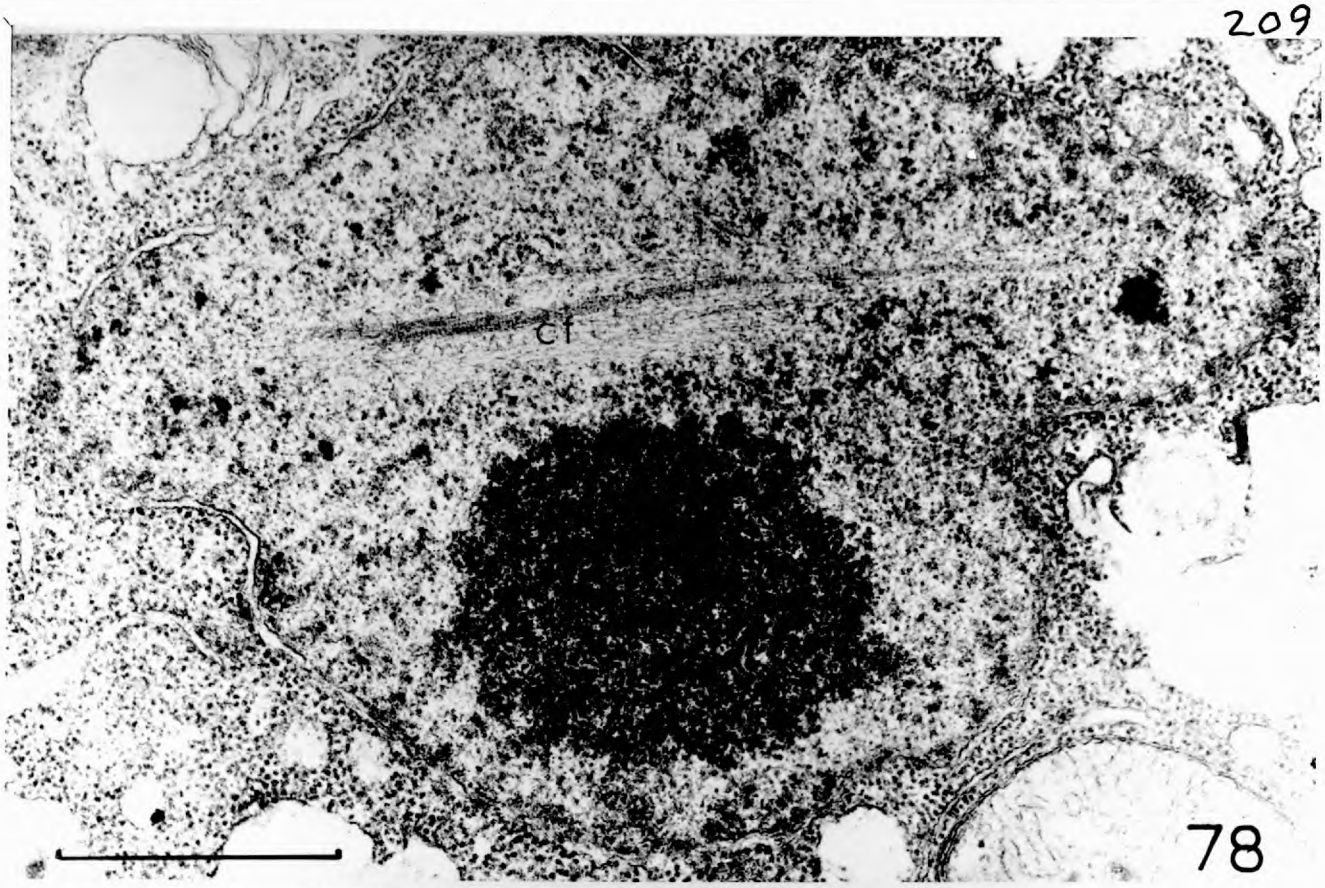

78

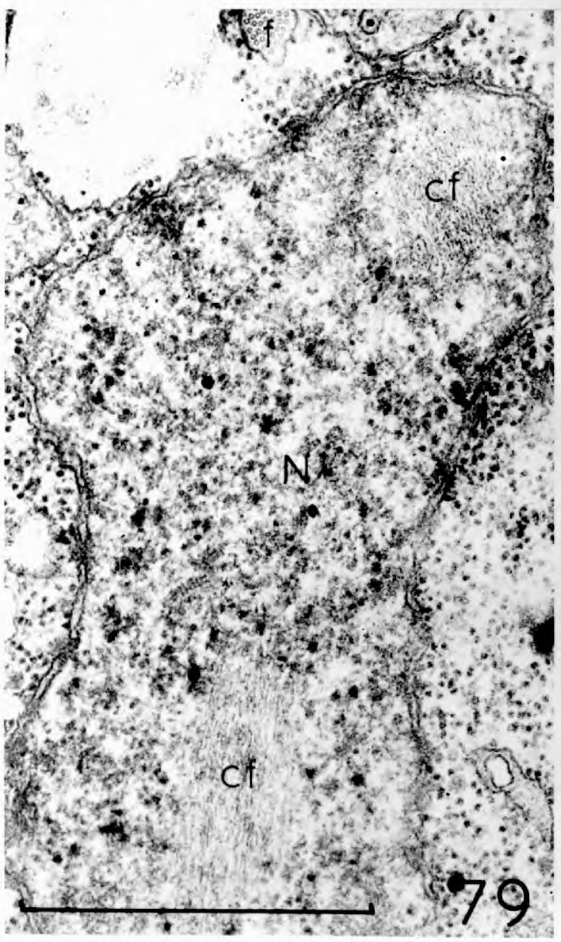

79

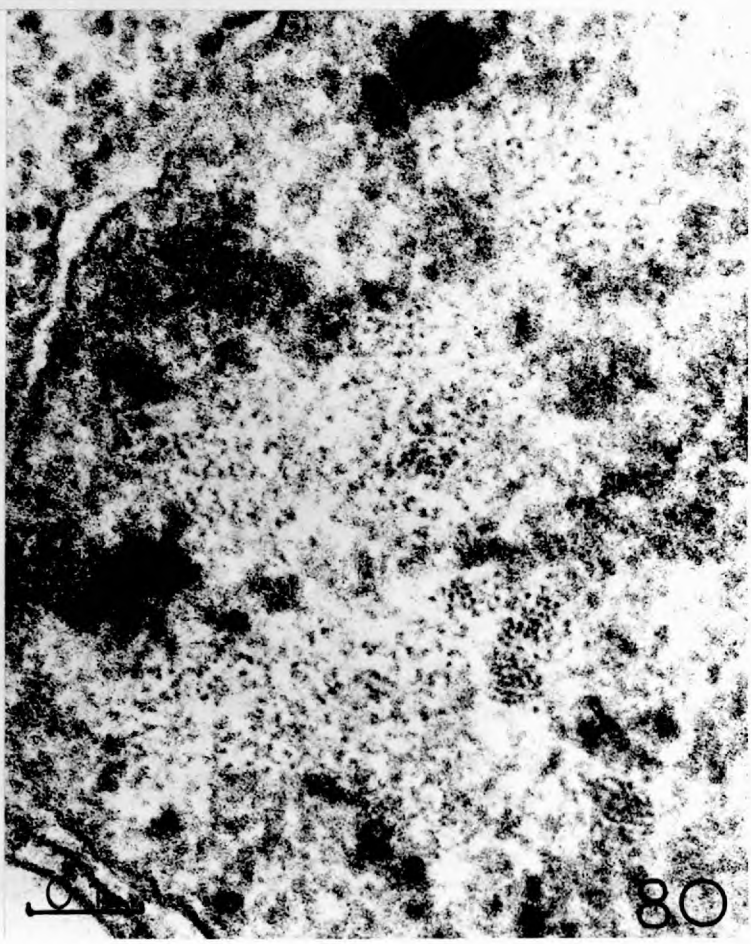

80

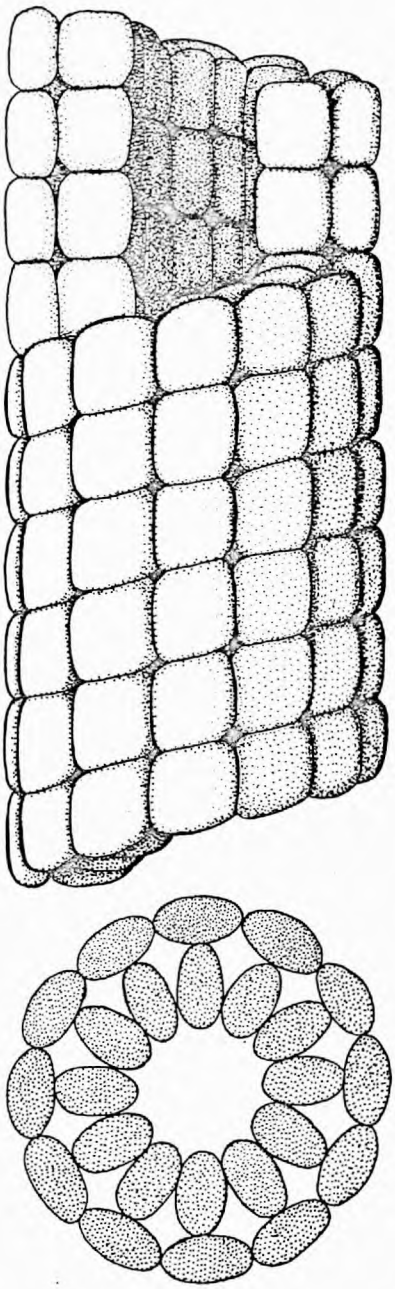

Fig. 81 Model of the fine structure of a spindel-tubule, constructed on the basis of the 40 Å-subunits and containing 12 particles per turn of the screw. A cross-section of the model (below) shows 12 gaps between the subunits of the tubular wall. From Moor 1966a

Fig.82. Sporangium wall with sunken area possibly corresponding to a collapsed lomasome. Note smooth texture of wall. Stereoscan S_1.

Fig.83. Sporangium cross wall with apparently rigid sporangium and more collapsed hypha. Stereoscan S_4.

Fig.84. Little collapsed sporangium apex. Apical papillum appears to have collapsed. Note numerous pits, probably sunken lomasomes. Stereoscan S_2.


L
82

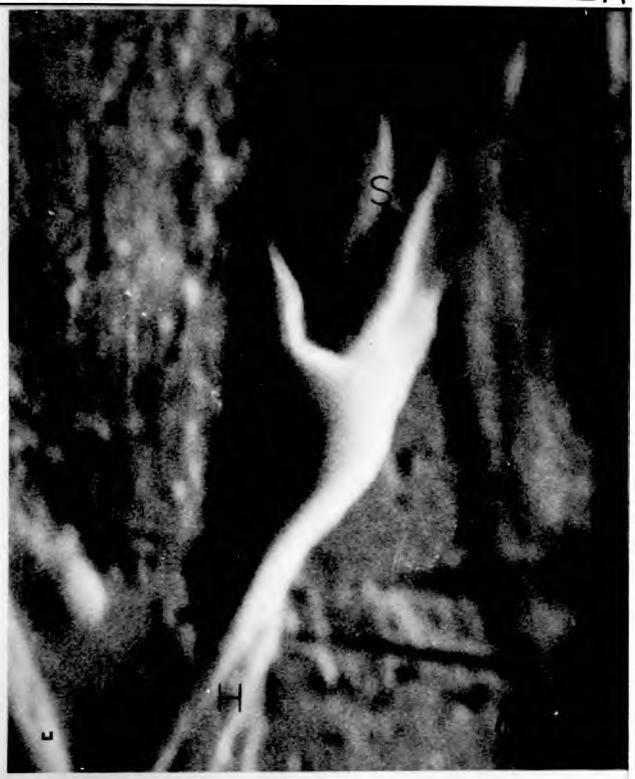
S
H


84

Fig.85. Shadowed whole mount of "Domestos" extracted hyphal apex with random network of fibrils enclosing apex. 2211/10. 14524-25.


8 5

Fig.86. Detail of Fig.85 showing fibrillar structure at apex. 2211/10. 14530.

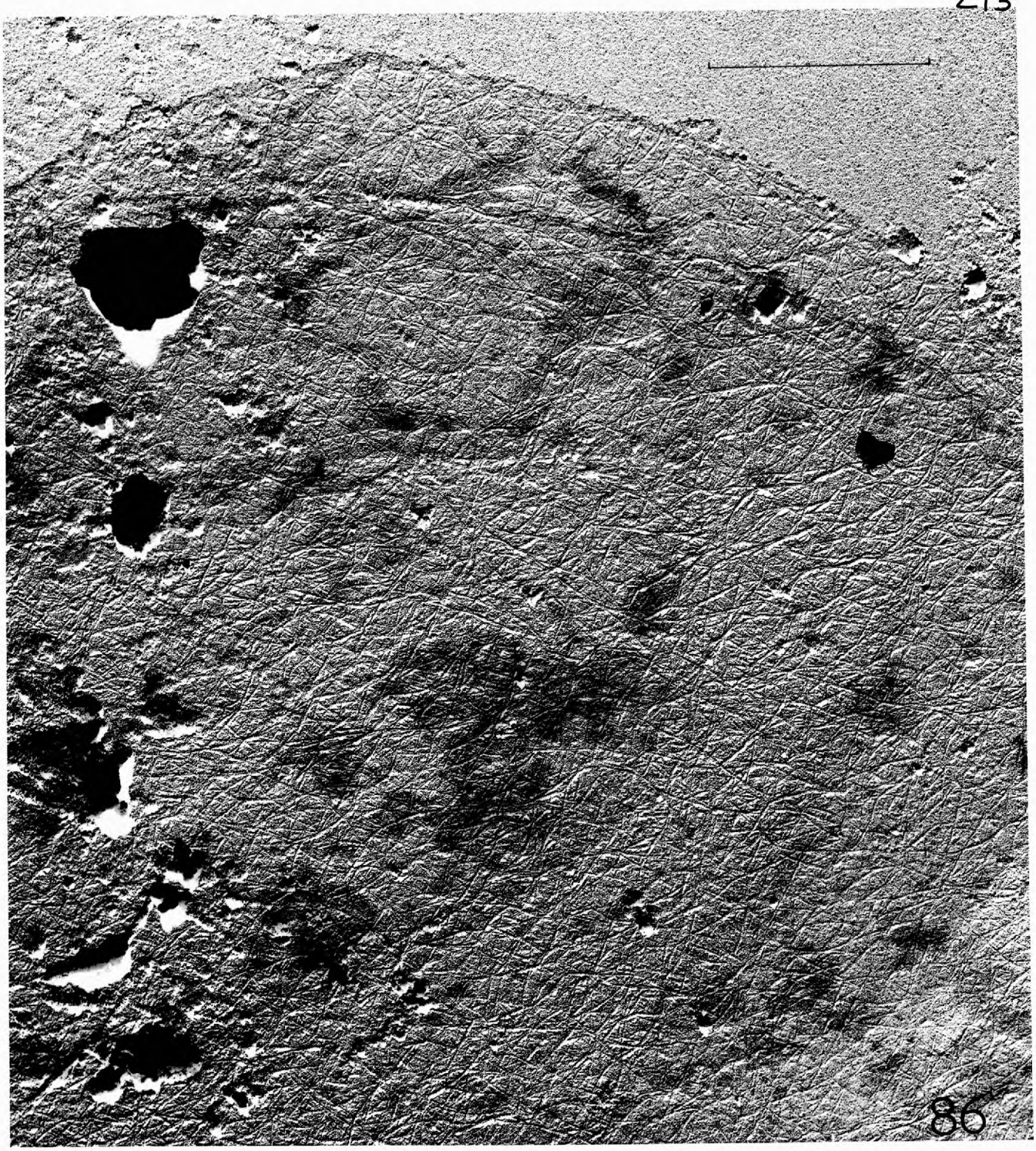

Fig.87. "Domestos" extracted hypha with fibrillar network covering apex. 2211/10. 14532.

Fig.88. "Domestos" extracted wall of germinating cyst showing similar fibrils in the germ tube and cyst wall. 1844/3. 10853.

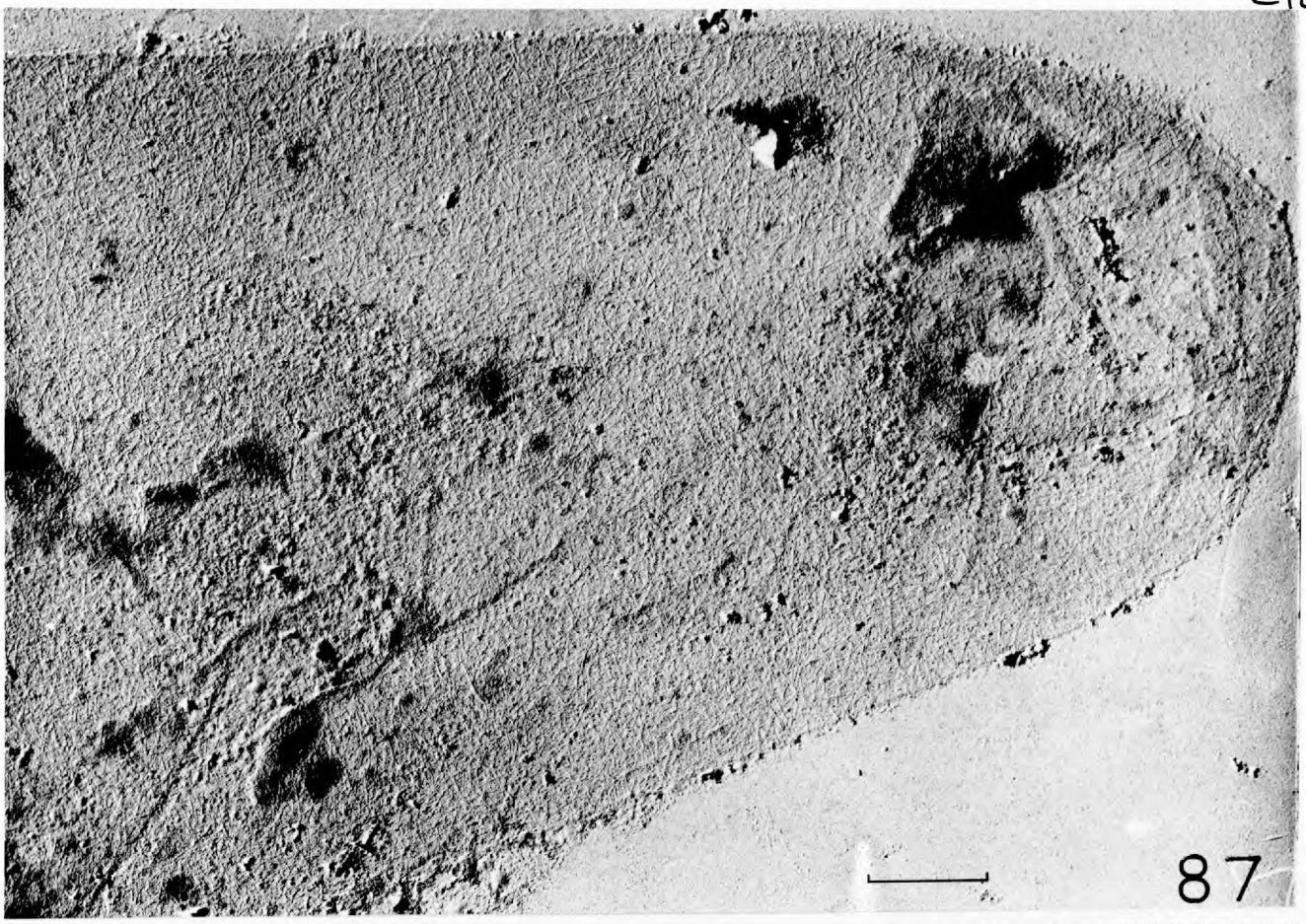

87

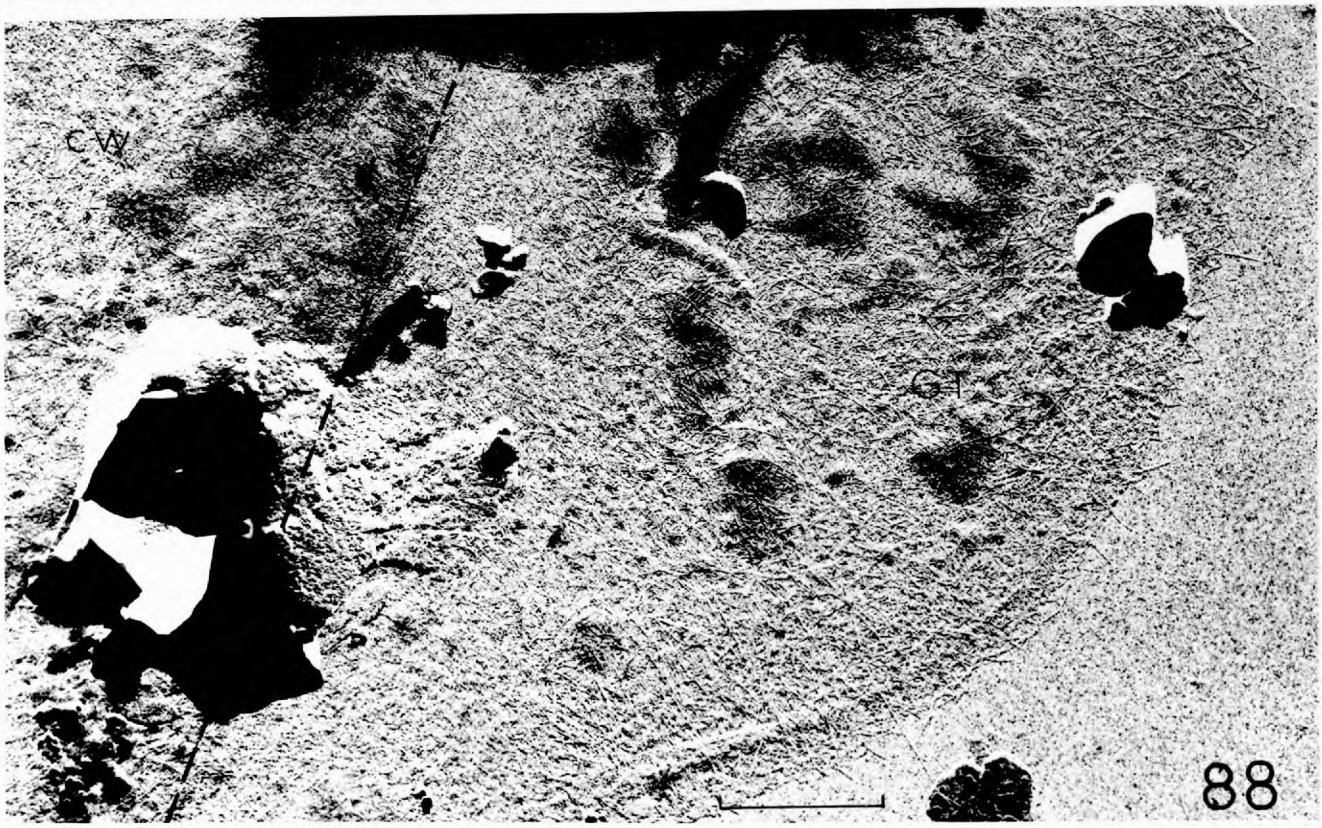

88

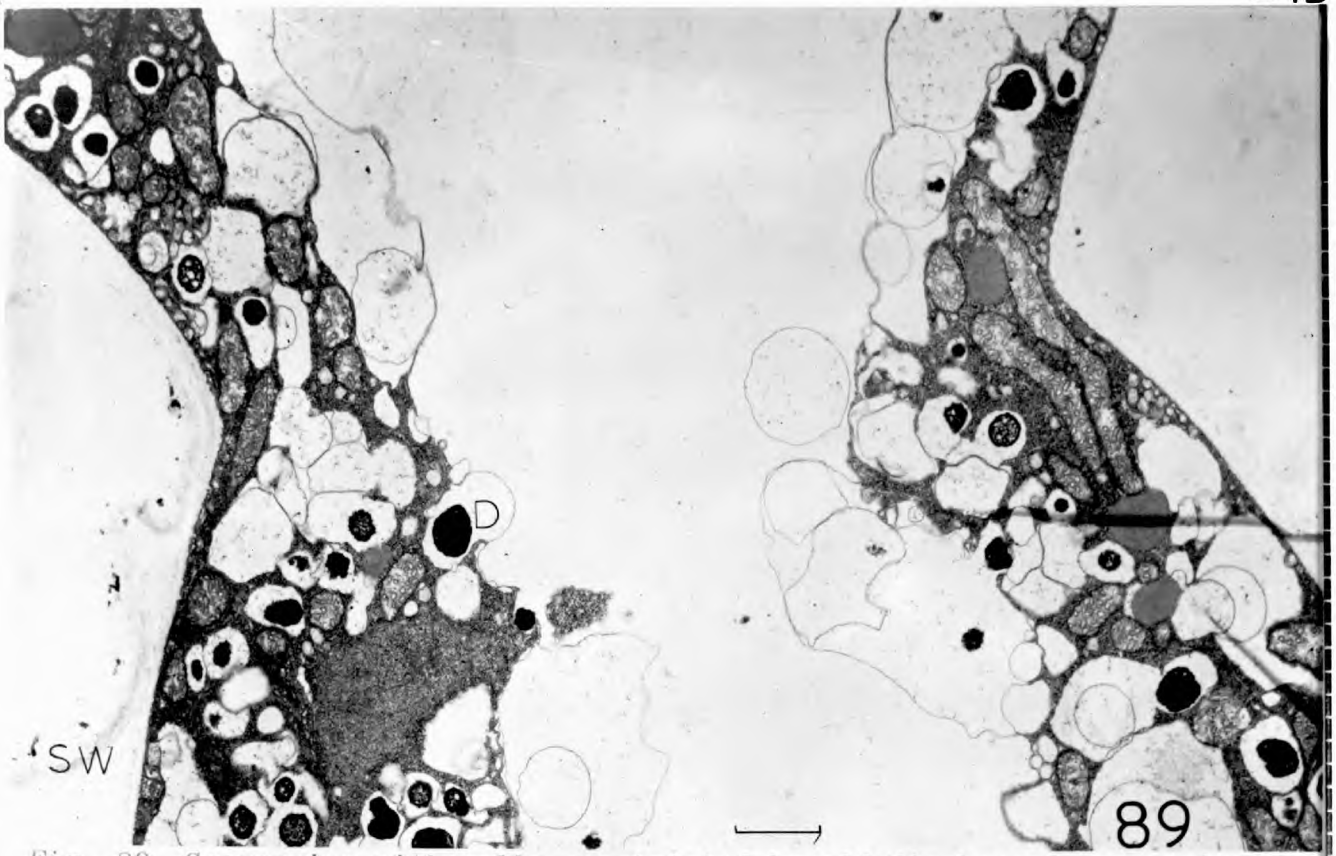

Fig. 89. Sporangium with walls constricted by old discharged sporangium through which it is growing. 1848D/5. 12015.

Fig. 90. Domestos extracted wall fibrils of a sporangium. 1844/1. 10849.

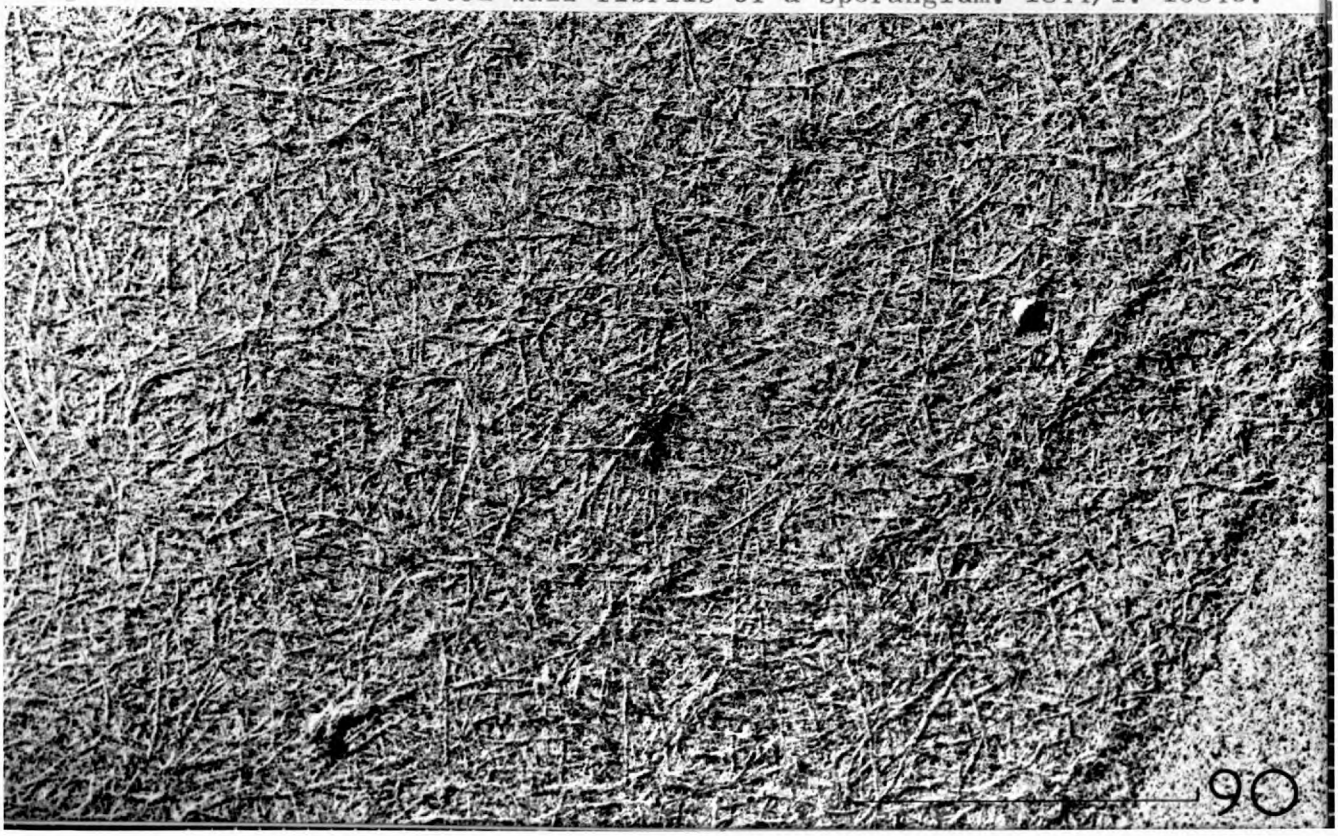

Fig.91. Hyphae viewed through crossed polarizers showing low apical birefringence and stronger birefringence in "side walls" of older hypha. Part of a photomontage in which sub-apical increase of wall birefringence was more readily detected. 593.

Fig.92. Polarized light micrograph of hyphal apex with increased sub-apical wall birefringence. 654.

Fig.93. Primary cysts germinating within sporangium. Birefringence is strong on the cyst and sporangium walls but absent in the germ tube. 565.

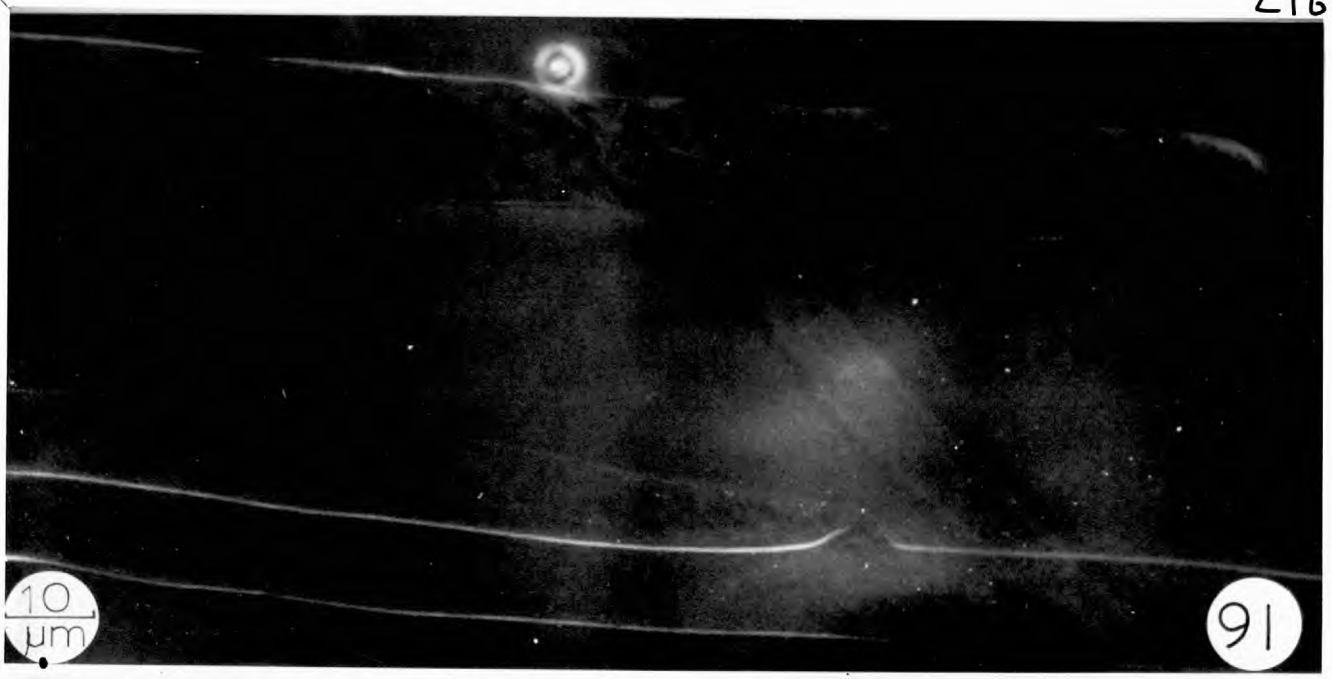
10
μm
91

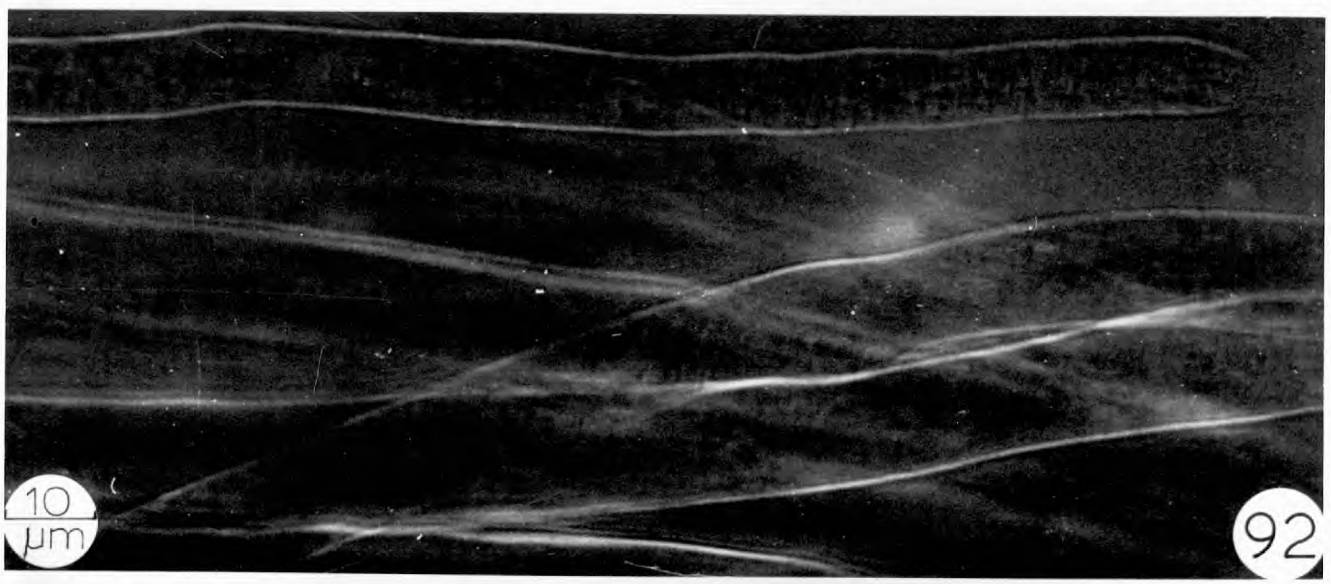
10
μm
92

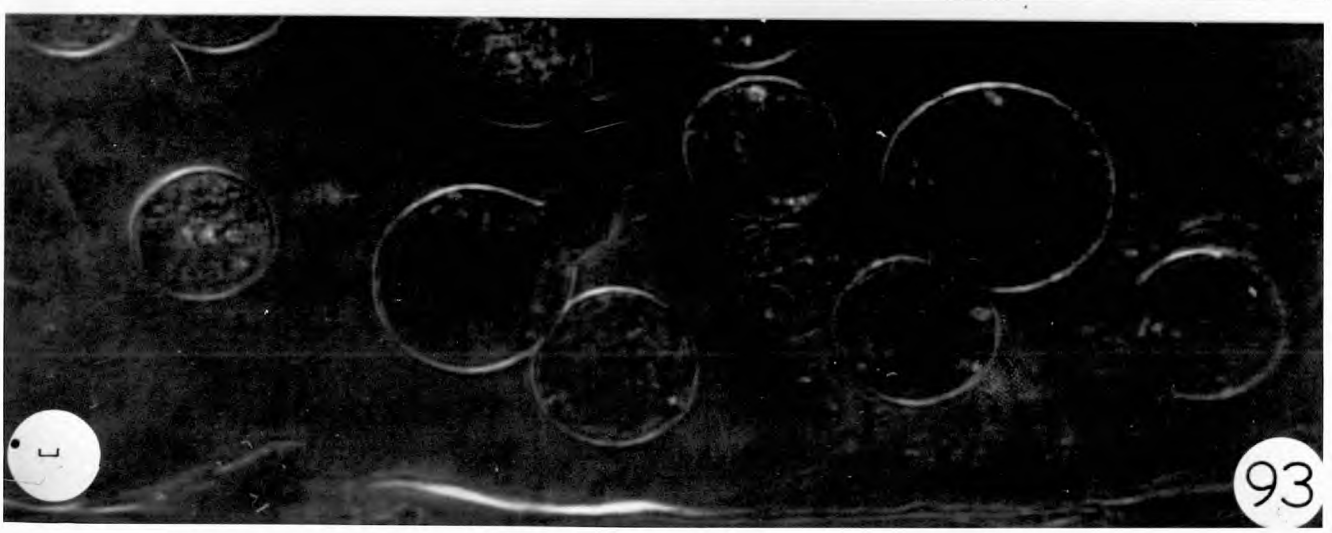
93

Fig.94. Strong birefringence in the walls of discharged sporangia. 447.

Fig.95. D. sterile. Sporangium containing primary cysts which have liberated secondary spores. Birefringence is strong in the "side walls" but detectable in the walls viewed normally. Note dark circular area in each primary cyst wall corresponding to the germ tube or exit papillum. 648.

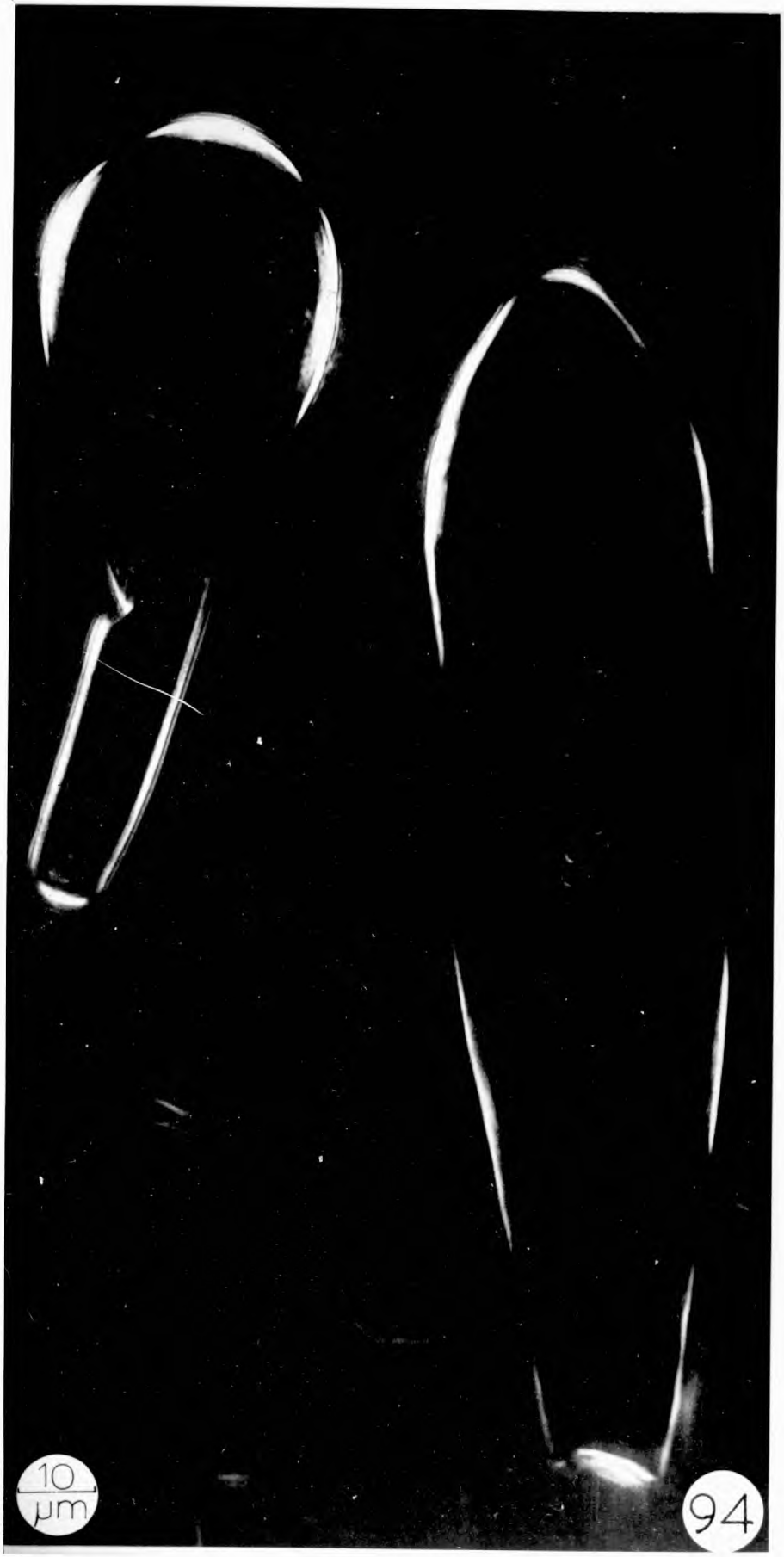

94

95

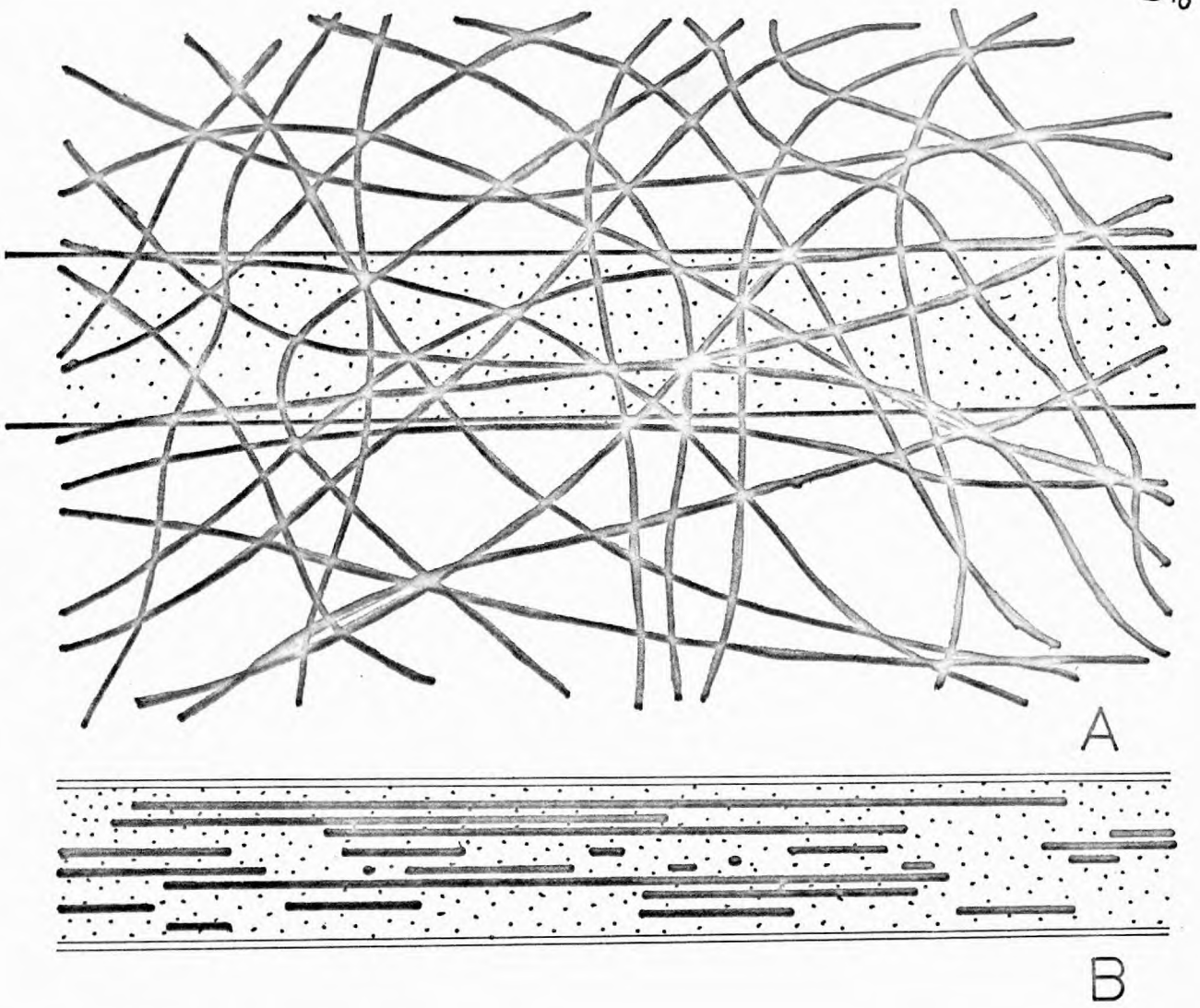

Fig. 96.

Diagram of a random network of wall fibres (A) showing the way in which textural birefringence is produced in the side walls (B). Walls viewed tangentially (B) contain fibrils which are orientated along the long axis of the hypha thus producing birefringence.

Figs.97-99. Typical vegetative apices showing varying extent of organelle-free apical cytoplasm. Phase contrast.229,222, 722.

Fig.100. Regrowing apex. A healthy blunt apex is apparently growing inside a degenerate apex. 210.

Fig.101. Old region of hypha with long dark filamentous mitochondria. 201.

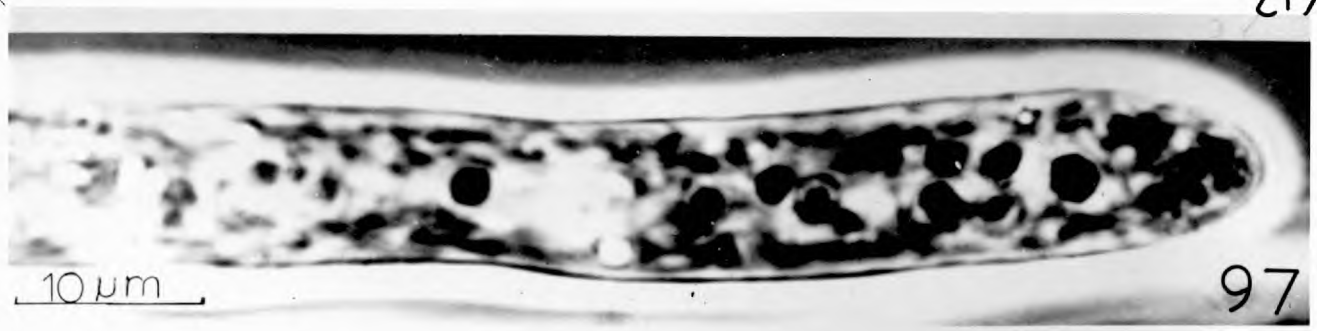
10 µm
97


10 µm
98

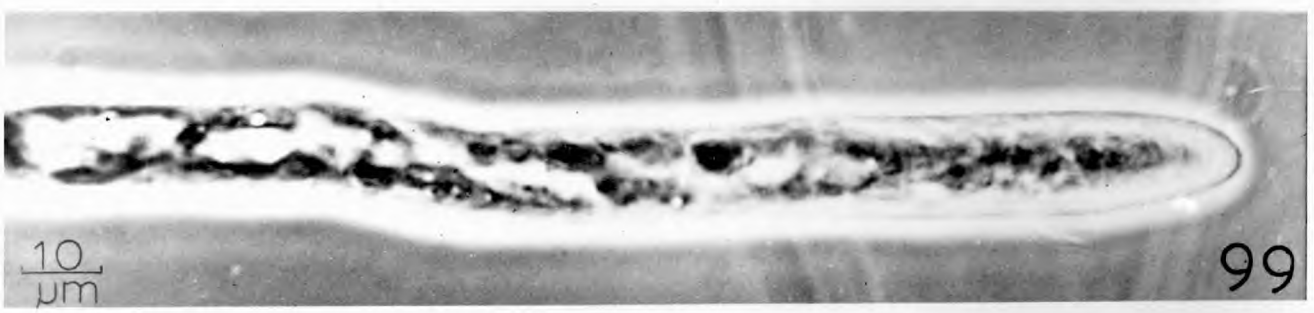
10
µm
99


10 µm
100

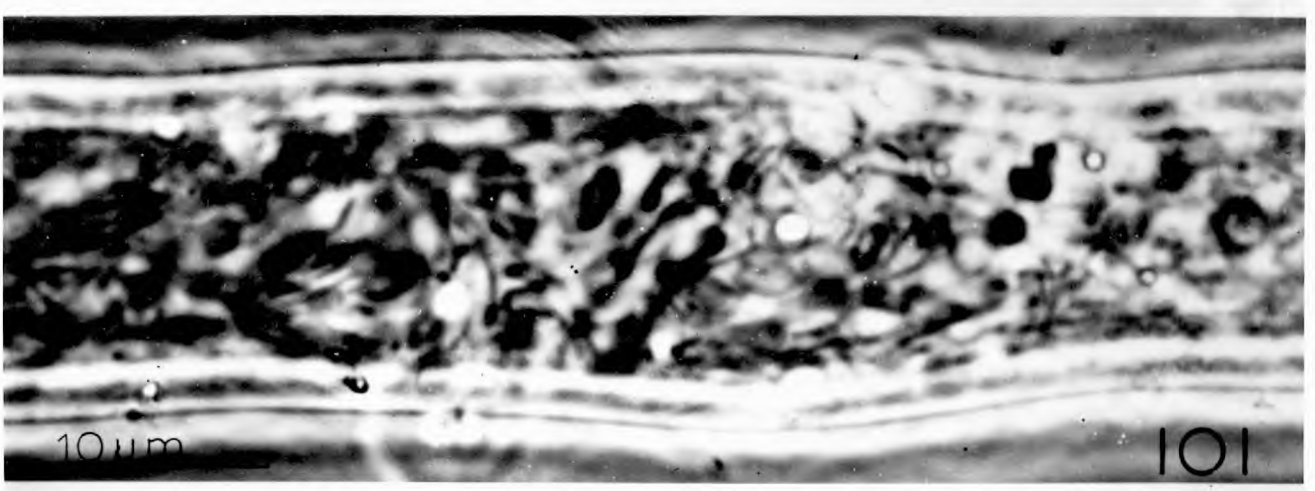
10 µm
101

Figs.102-105. Nomarski interference micrographs of a hyphal apex after 0,5,12 and 19 min. Note slightly elongated structures in the organelle-free apical region. 650-653.

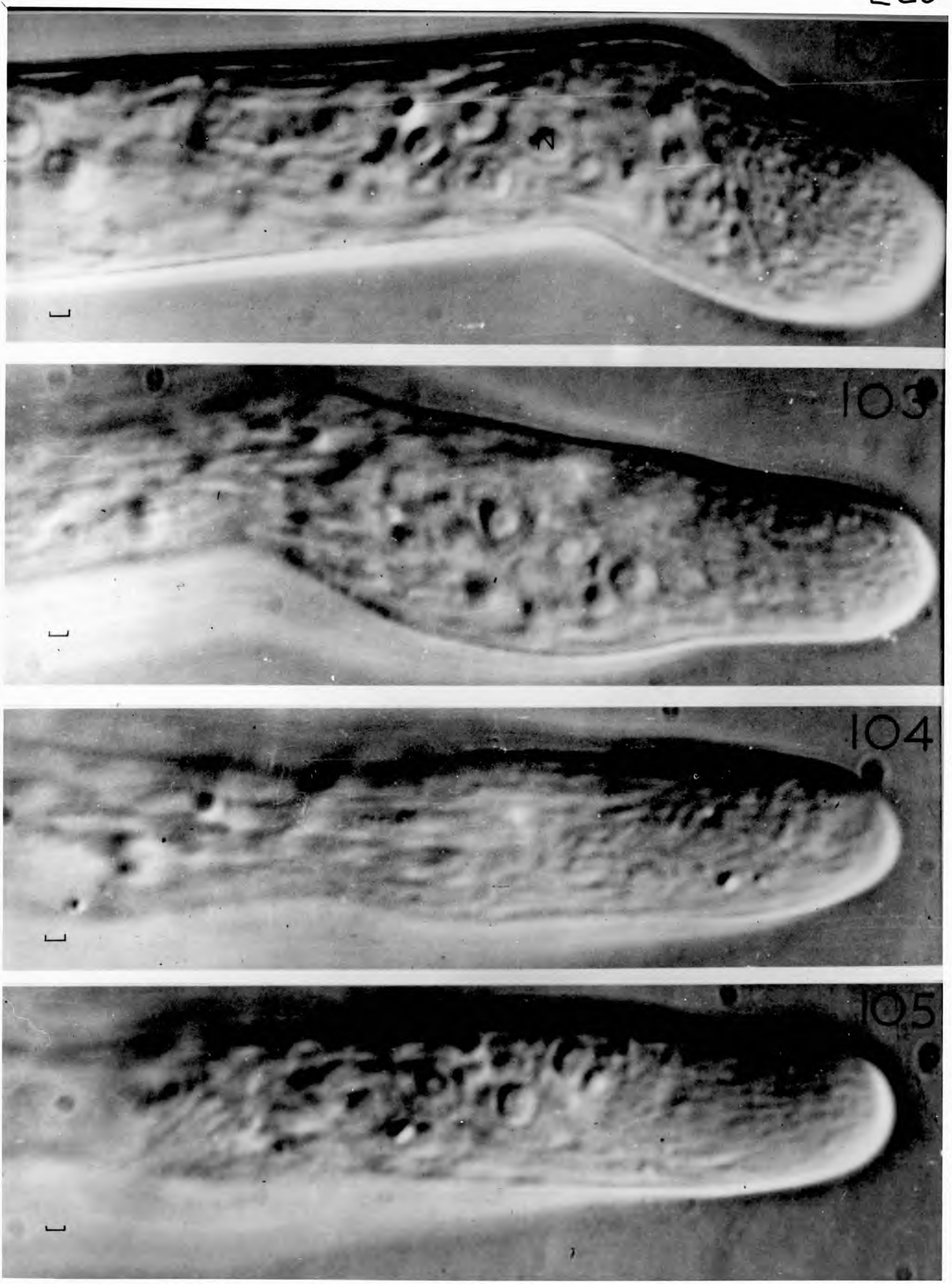
103
104
105

Fig.106. Median L.S. of a permanganate fixed vegetative apex. Note absence of wall vesicles, and Golgi bodies associated with the nucleus and with mitochondria. 1780B/5. 10502.

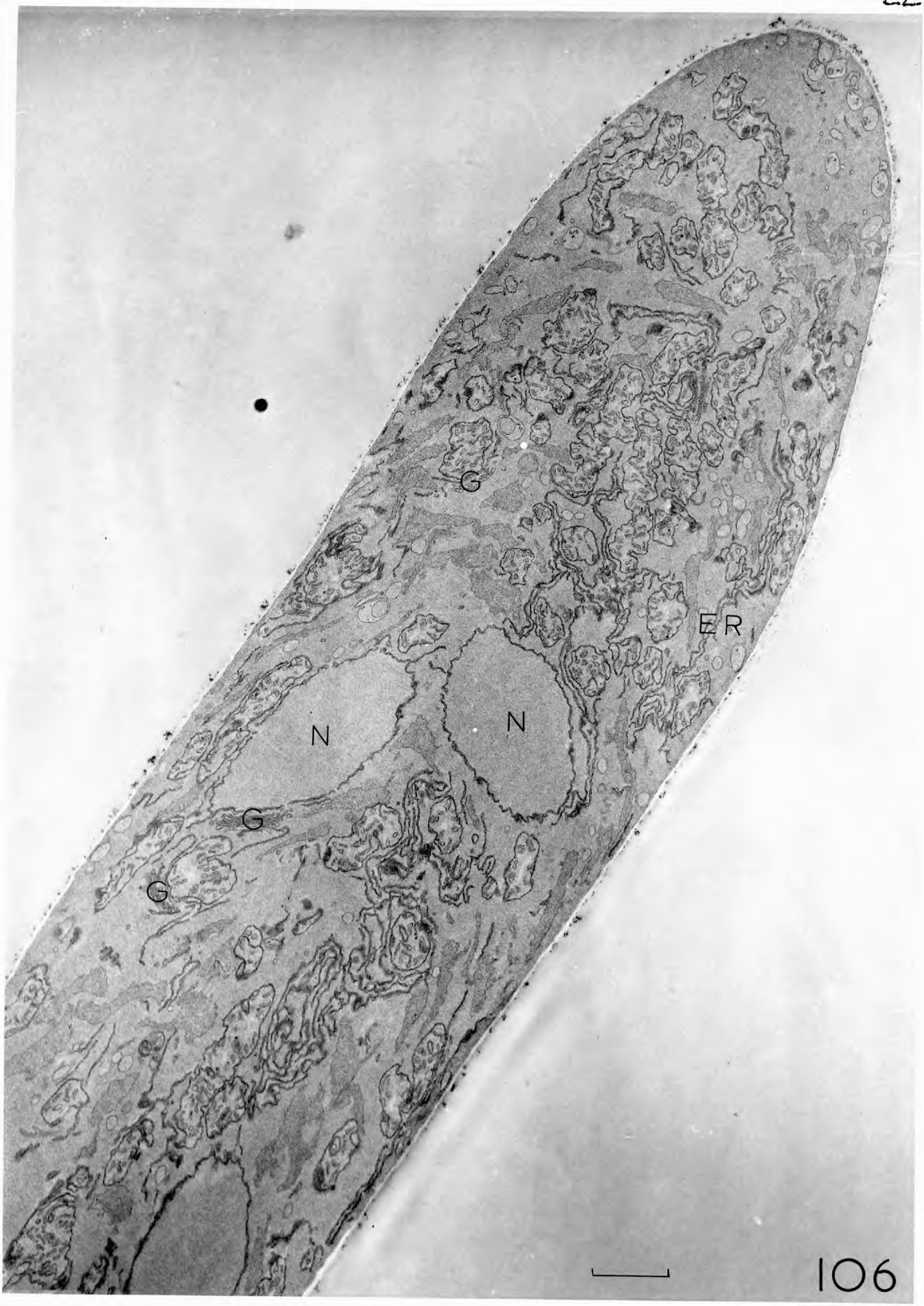

106

Fig. 107. Median L.S. hyphal apex with lomasomes, wall vesicles and E.R. The dense membranous structure in the vacuole occurs abundantly in some hyphae but only after GA/Os fixation. 1837/7. 12044.

Fig.108. Median L.S. vegetative apex from same colony as Fig.107. Lomasomes, plasmalemmasomes, wall vesicles and E.R. are abundant but mitochondria are small and sparce. 1837B/1. 12199.

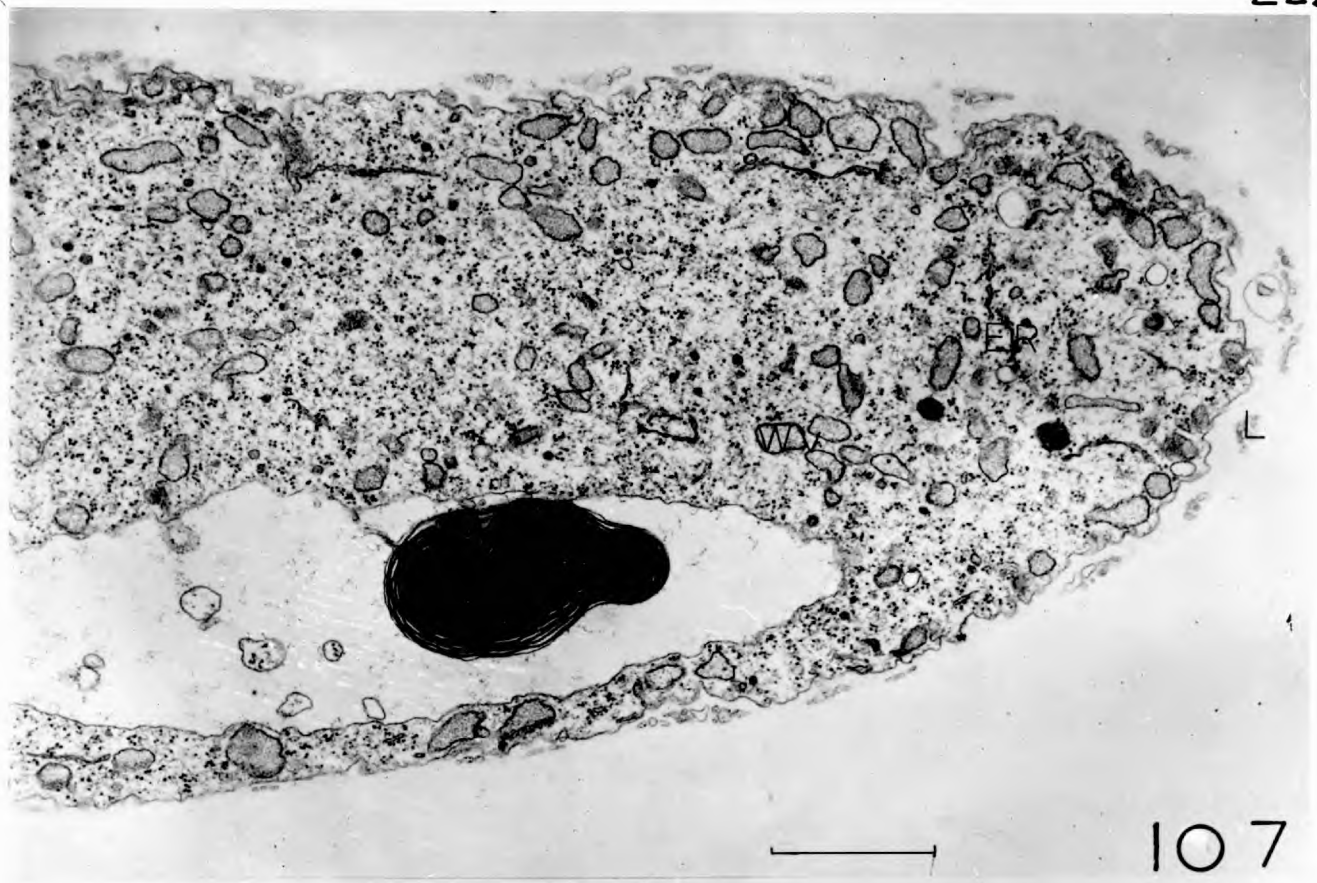

107

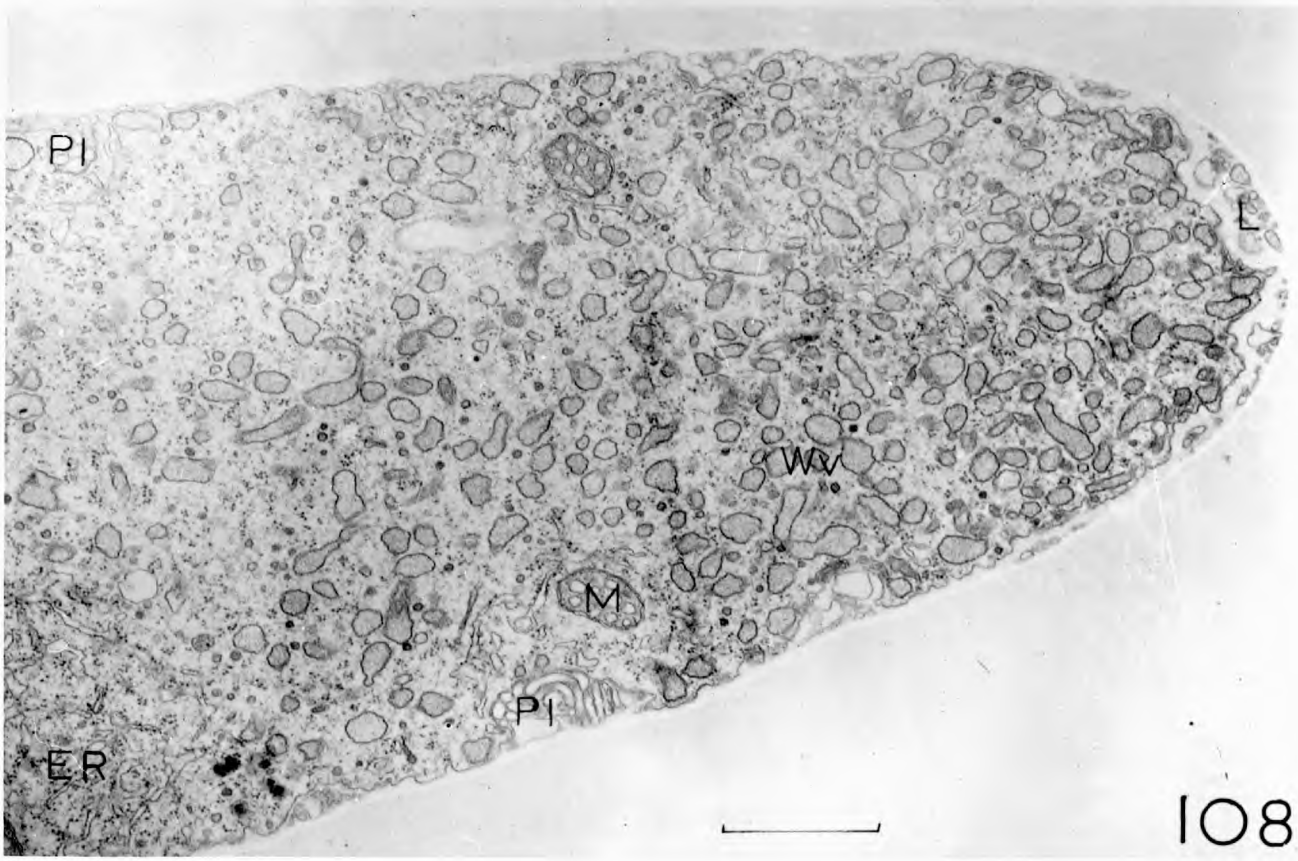

108

Fig.109. L.S. hyphal apex from edge of colony. Apical zone well defined but wall vesicles distorted and few in number. Note abundance of small dense vesicles at apex and increase in density of mitochondria and Golgi below the apex. Portion of a 62µm long montage. Os only. 1826A/6. 10781-10783.

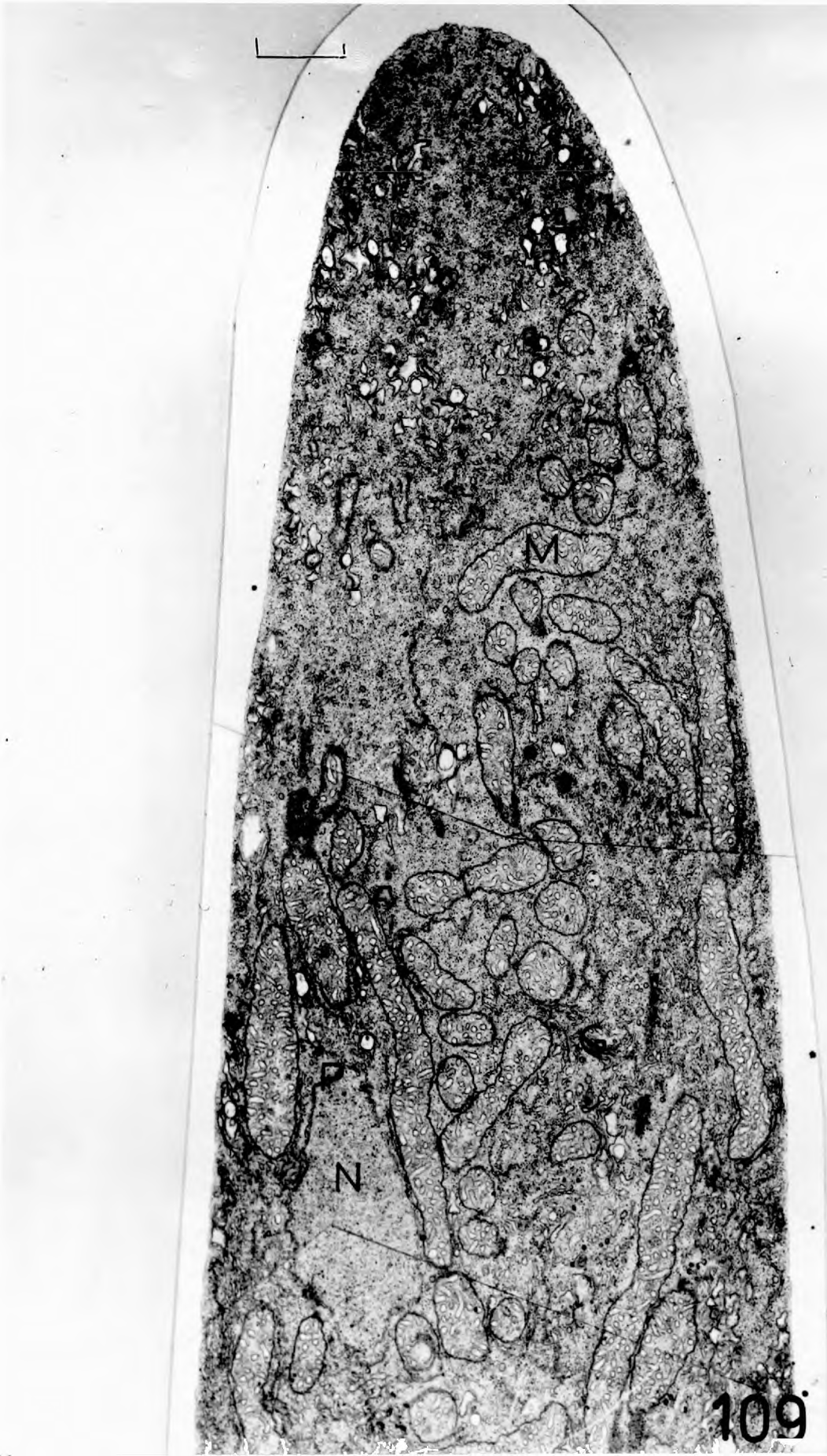
M
P
N

Fig.110. Median L.S. hyphal apex showing typical distribution of E.R., wall vesicles, lomasomes and mitochondria. 1825A/2. 10803.

110

Fig.111. T.S. hyphal apex fixed for only 2 min in 5% GA. Note plasmalemmasomes, lomasomes, wall vesicles and thick, obliquely sectioned apical wall. 1655/4. 8469.

Fig.112. T.S. hyphal apex with high density of wall vesicles, some of which are tubular, and staining "dirt" frequently encountered specifically on walls. 1548/7. 8472.

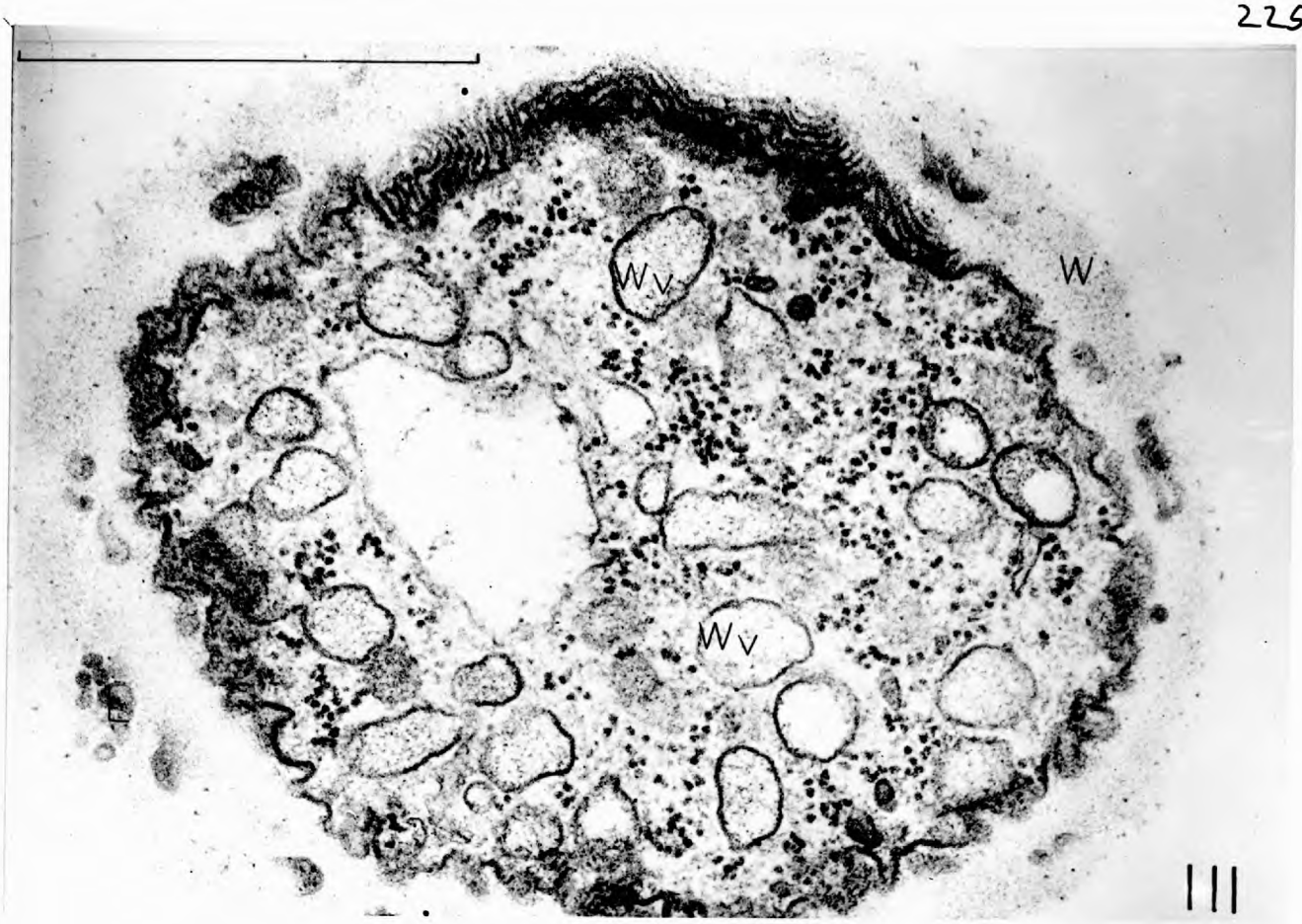

111

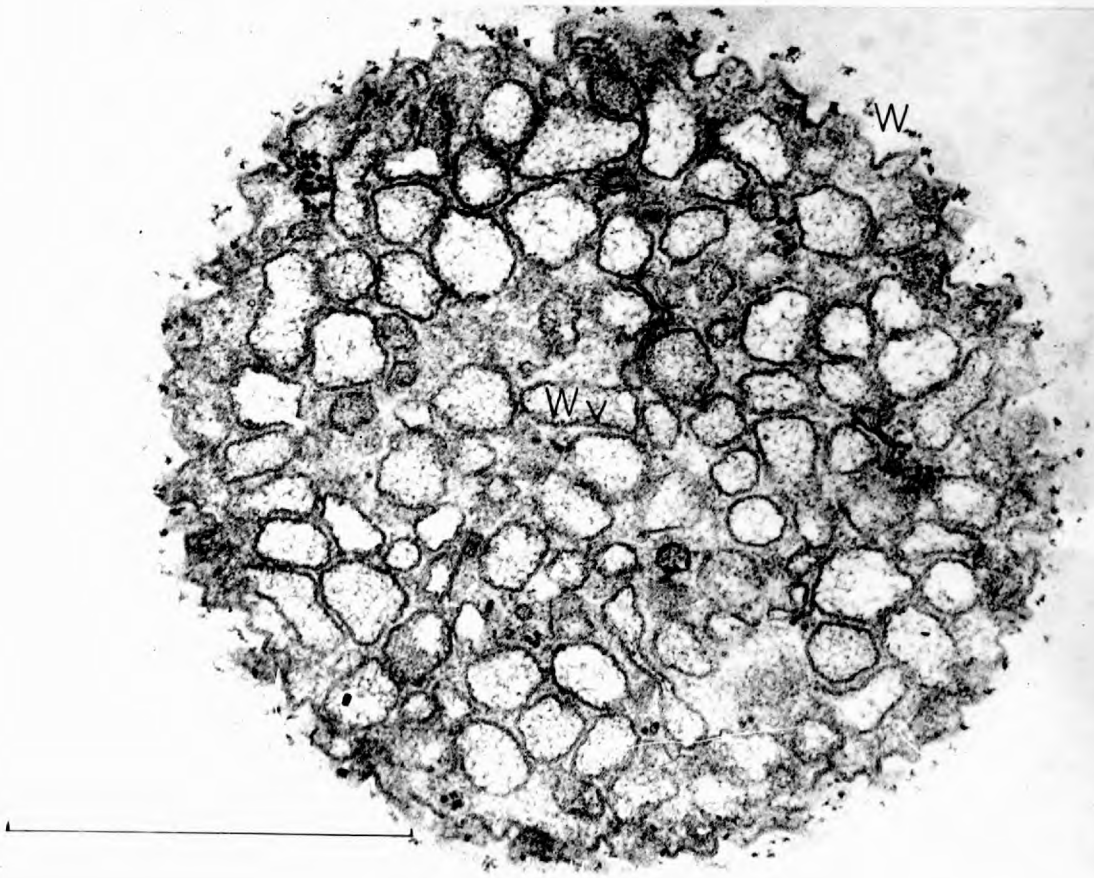

112

Fig.113. L.S. vegetative apex grown at 10°C. Wall vesicles, E.R. and plasmalemmasomes are comparable to those of hyphae grown at 25°C. 1840A/1. 12018.


Pl
Pl
ER
Wv
Pl
113

Fig.114. L.S. hyphal apex grown at 10°C fixed in Os only. Wall vesicle and E.R. zonations and lomasomes similar to hyphae grown at 25°C. Note appareance of wall vesicles after Os fixation. Part of a 40µm montage. 1839/3. 10908.

Fig.115. L.S. hyphal apex grown at 30°C. Note absence of wall vesicles, high density of ribosomes and vesicular material exterior to the plasmalemma. Portion of a 50µm montage. 1836/1. 10914.

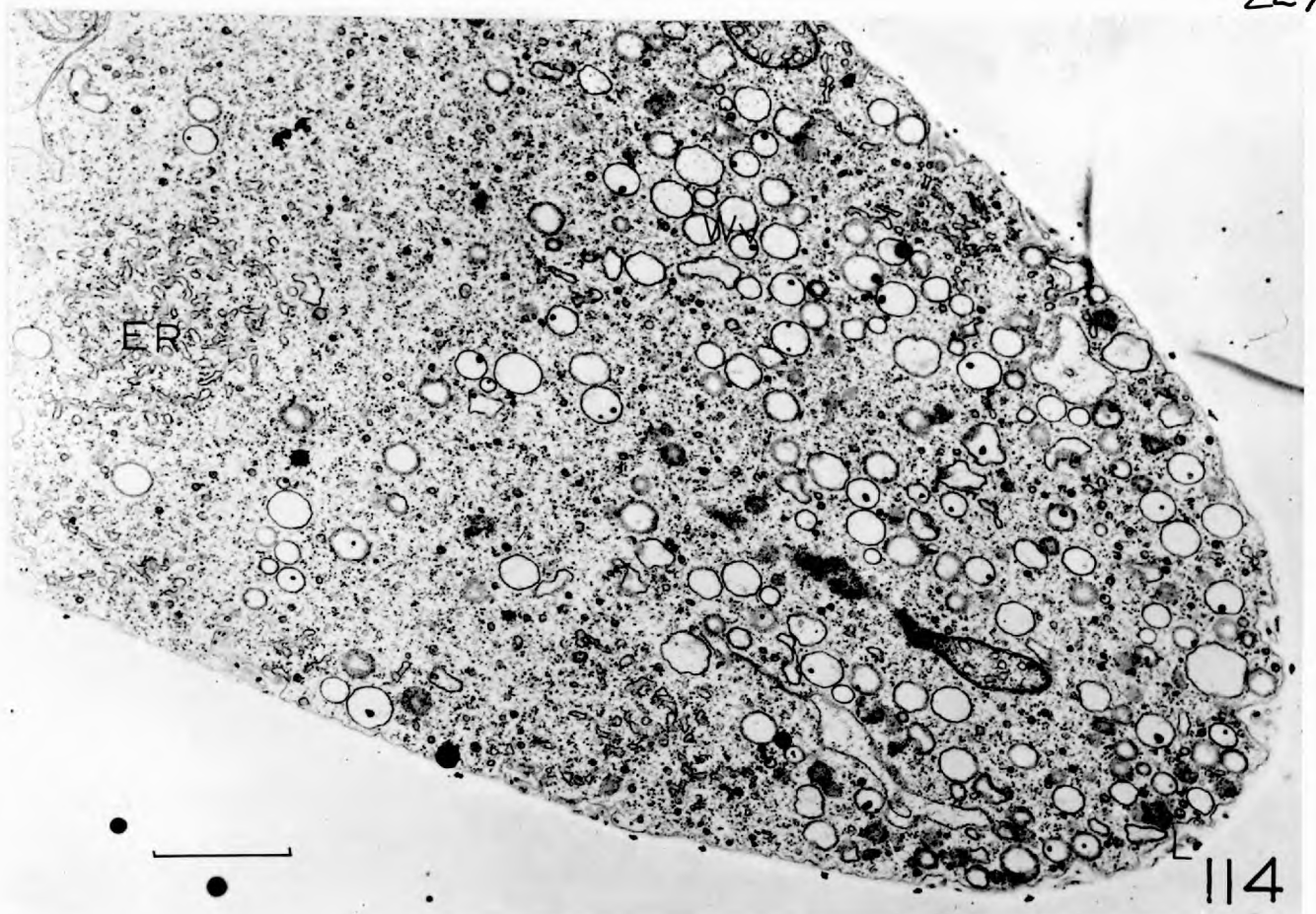

114

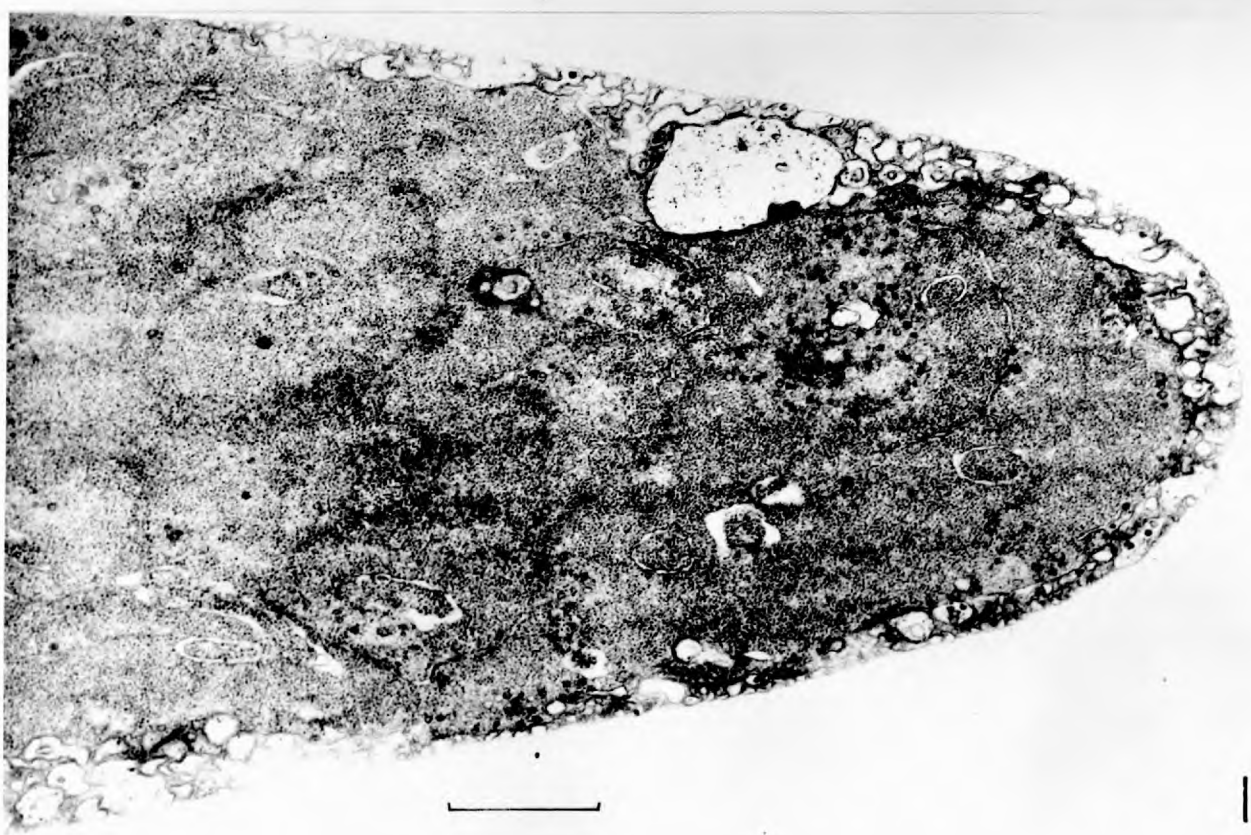

115

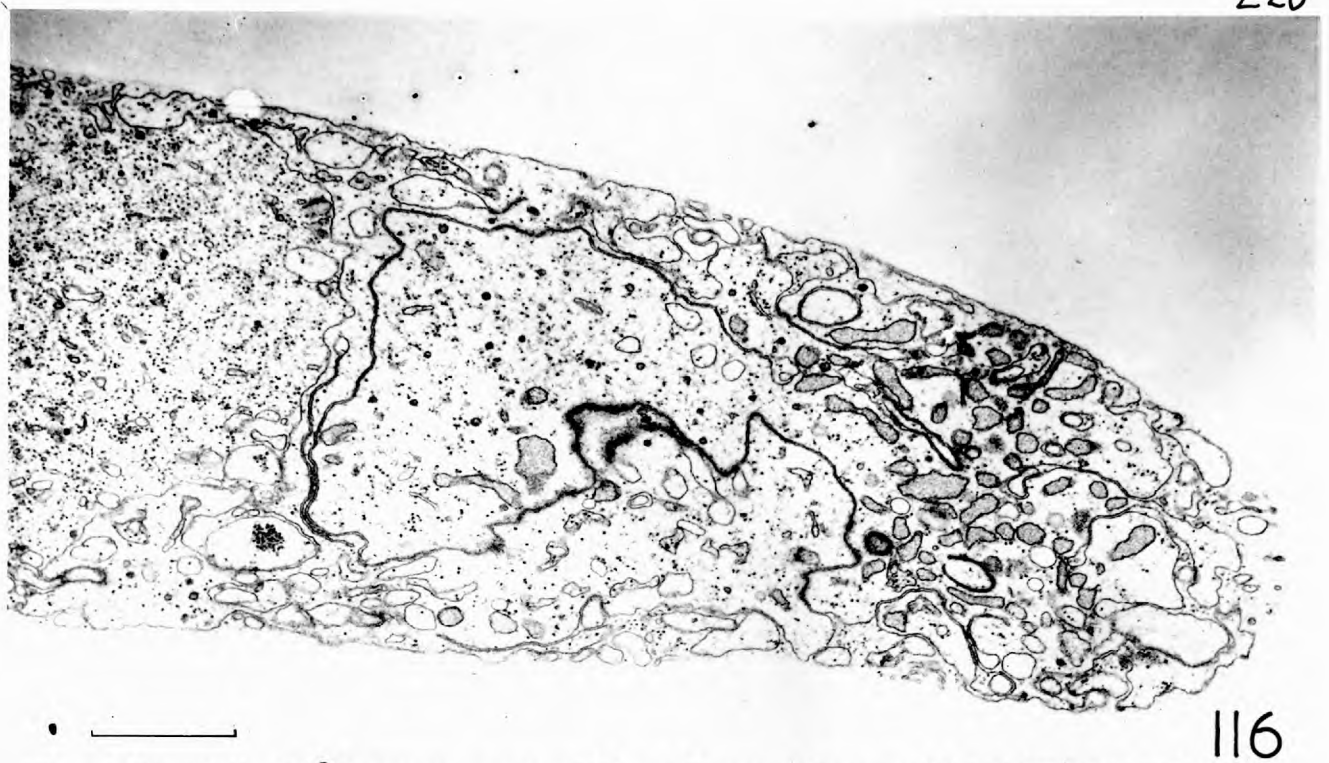

116

Fig. 116. L.S. 30°C grown apex with wall vesicles and highly irregular plasmalemma. 1836B/11. 12203.

Fig. 117. L.S. 30°C grown, Os fixed apex with normal wall vesicles, E.R., and plasmalemmasomes. 1835A/2. 12032.

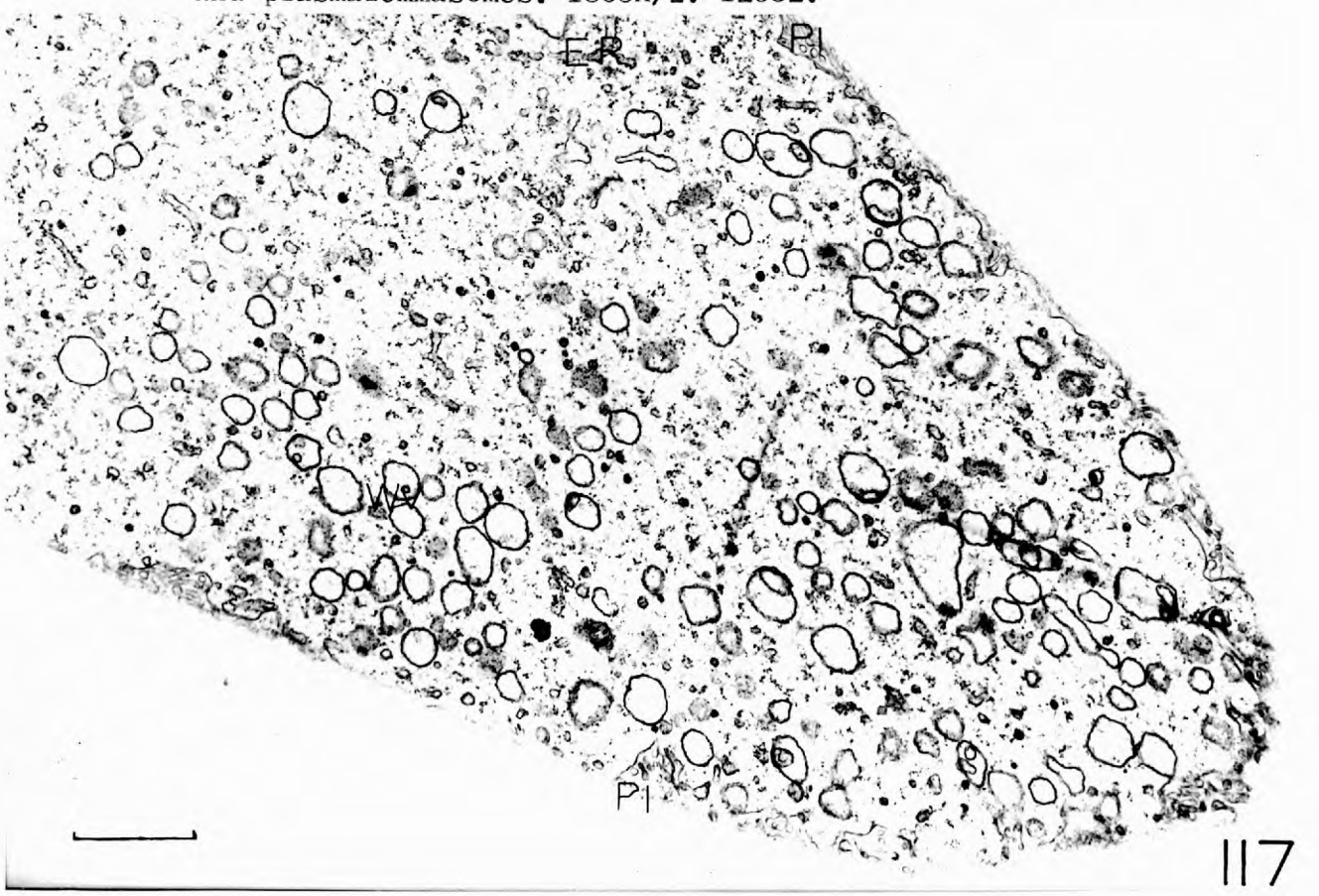

117

Fig.118. L.S. apex from a 25°C grown hypha. This hypha appears similar to those grown at 30°C. Note vesicular material external to the plasmalemma, distorted mitochondria and E.R. Os only. 1838/4. 12046.

Fig.119. Sub-apical part of 62μm montage behind apex in Fig.118. Note characteristic E.R., fragmented nuclei and tubular cristae in swollen mitochondria. Also two multitubular bodies. Os. only. 1838/4. 12051.

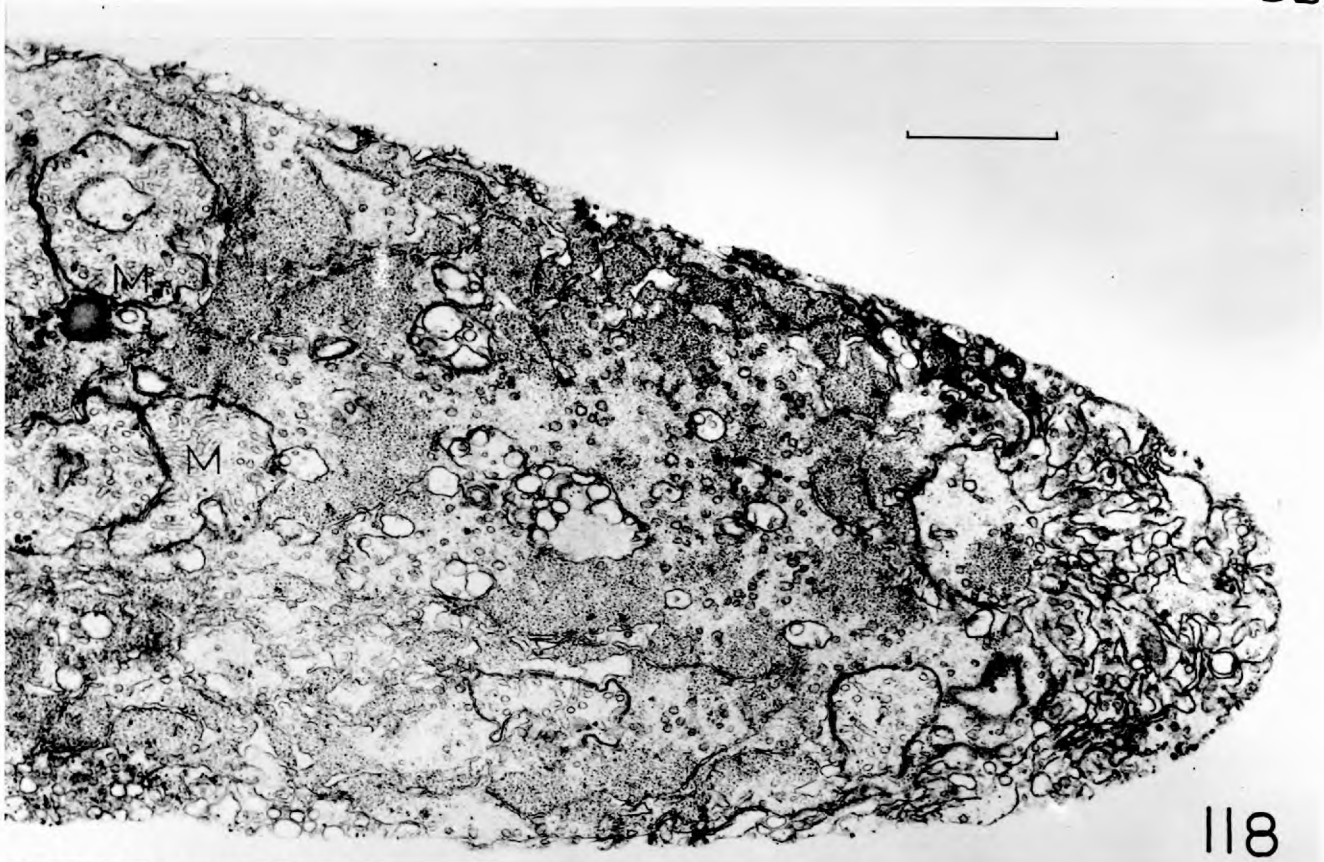

118

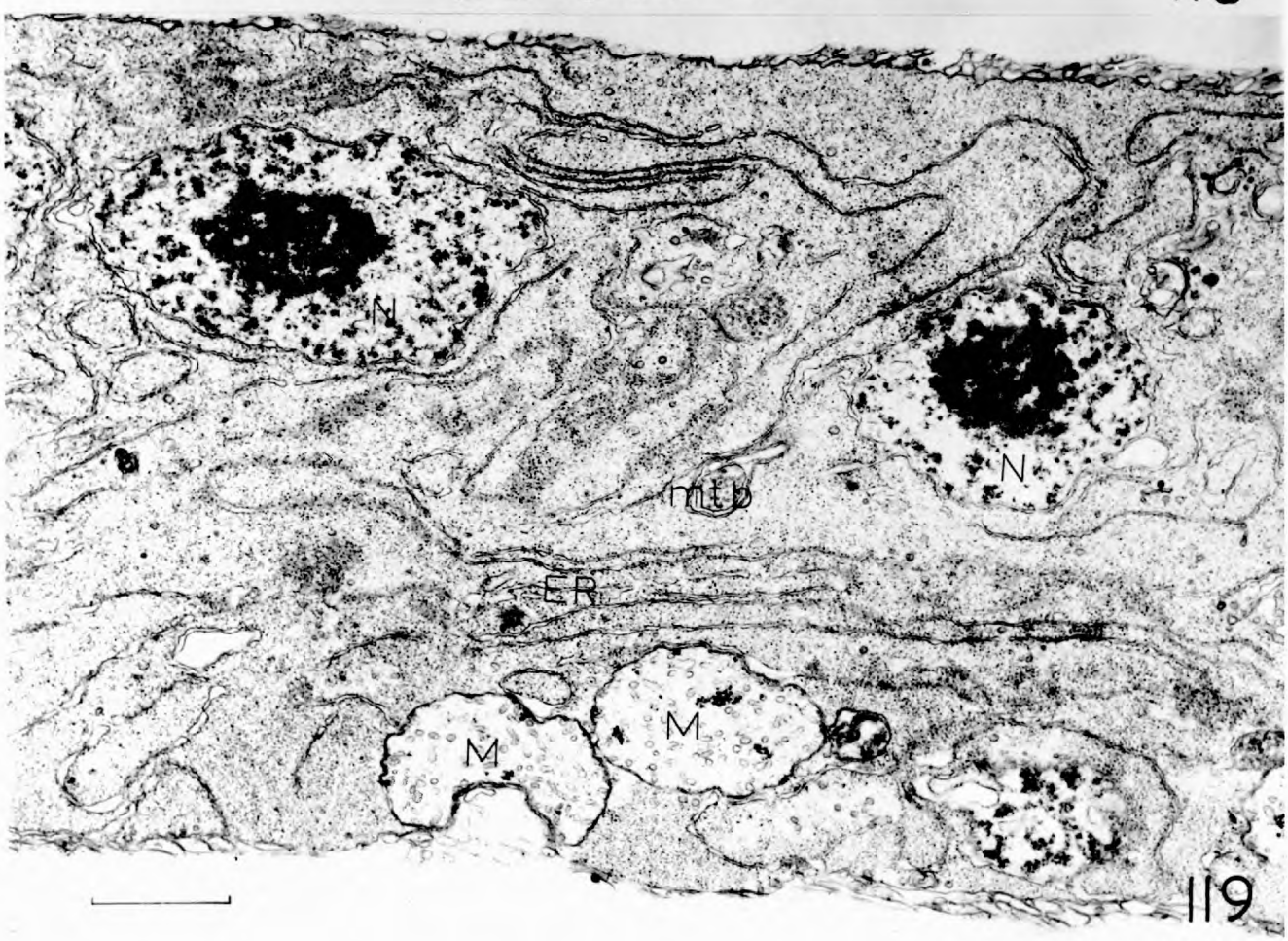

119

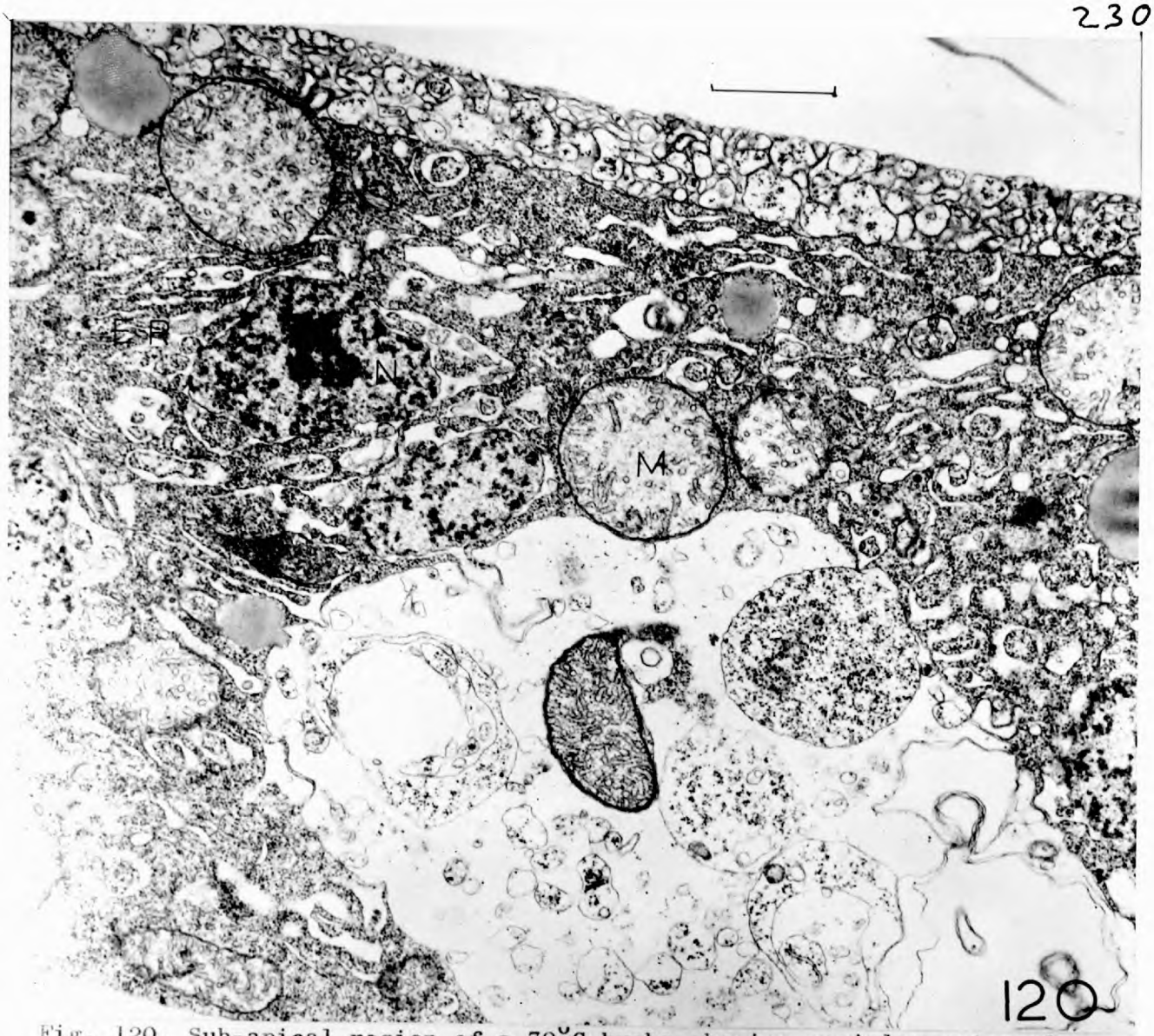

Fig. 120. Sub-apical region of a 30°C hypha showing vesicles external to the plasmalemma and swollen E.R. c.f. Fig. 119.1836A/1. 12025.

Fig. 121. Plasmalemmasome becoming sequested and tubular wall vesicles. 1837/7. 12043.

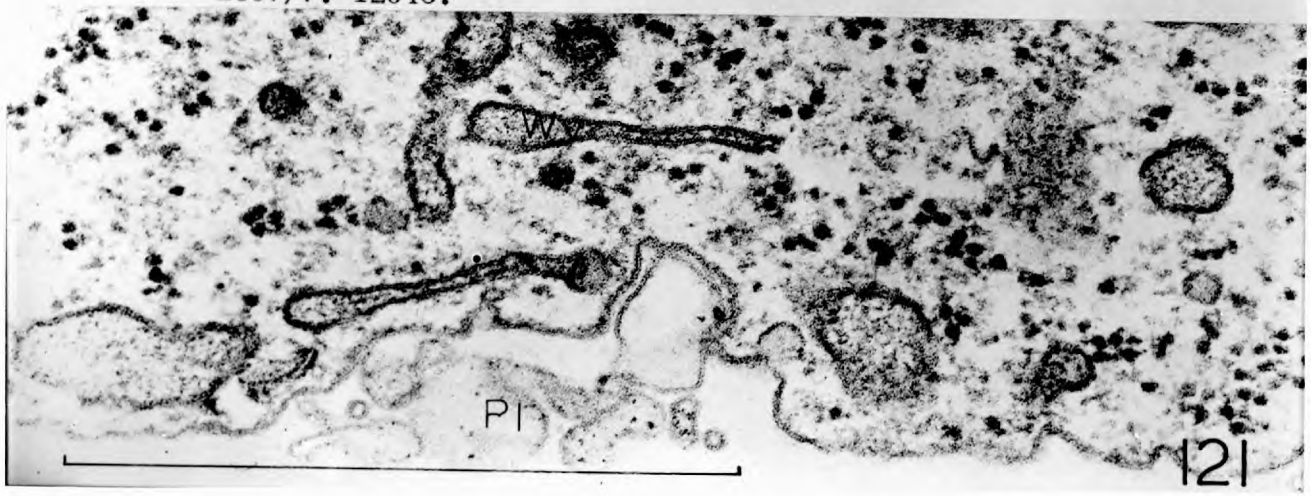

Fig.122. D. sterile. Vegetative apex with distorted wall vesicles fixed in Os only. 1855/2. 12160.

Fig.123. D. sterile. Wall vesicles at hyphal apex after GA/Os fixation showing granular contents. 1854/1. 12158.

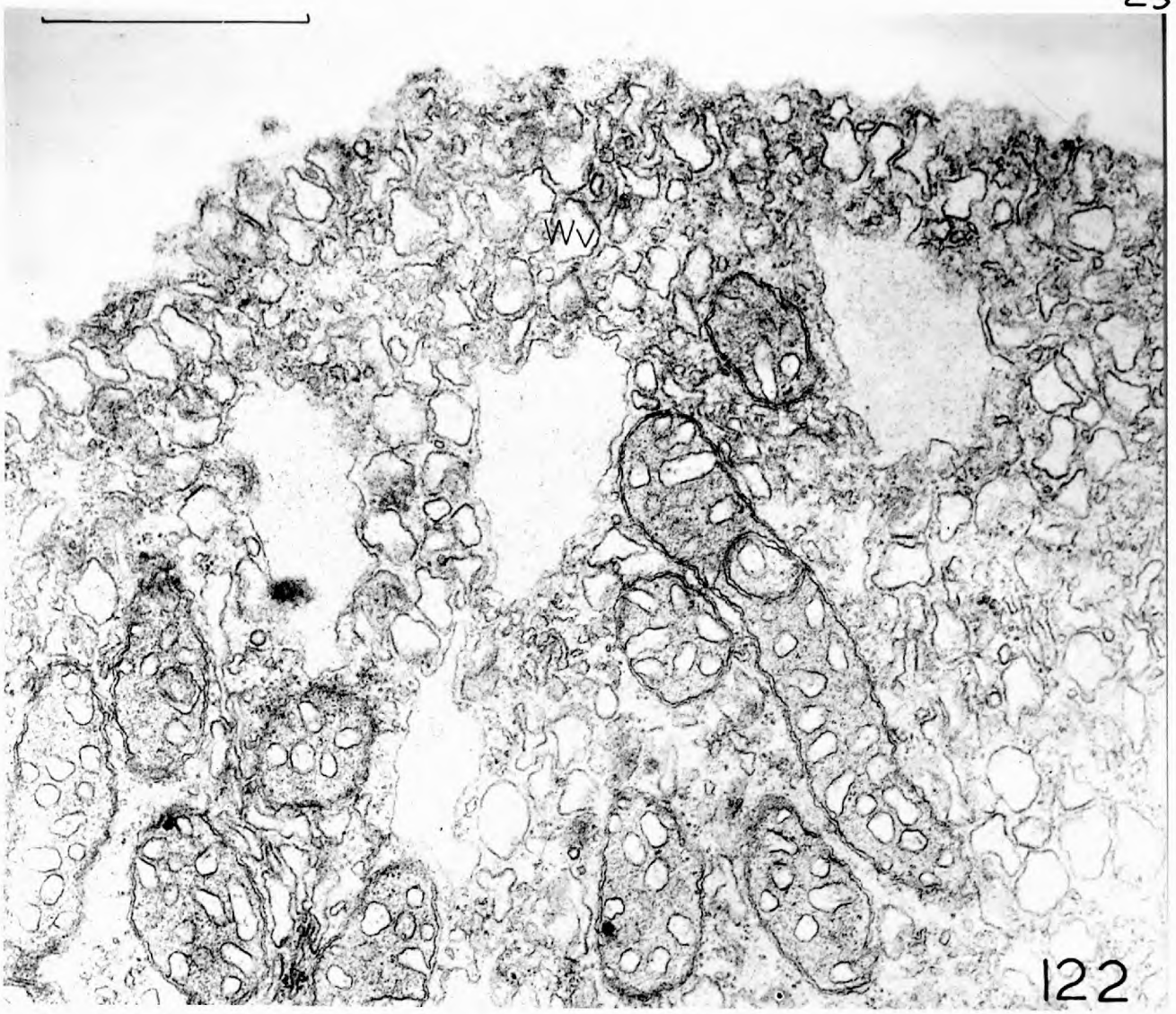
Wv
122

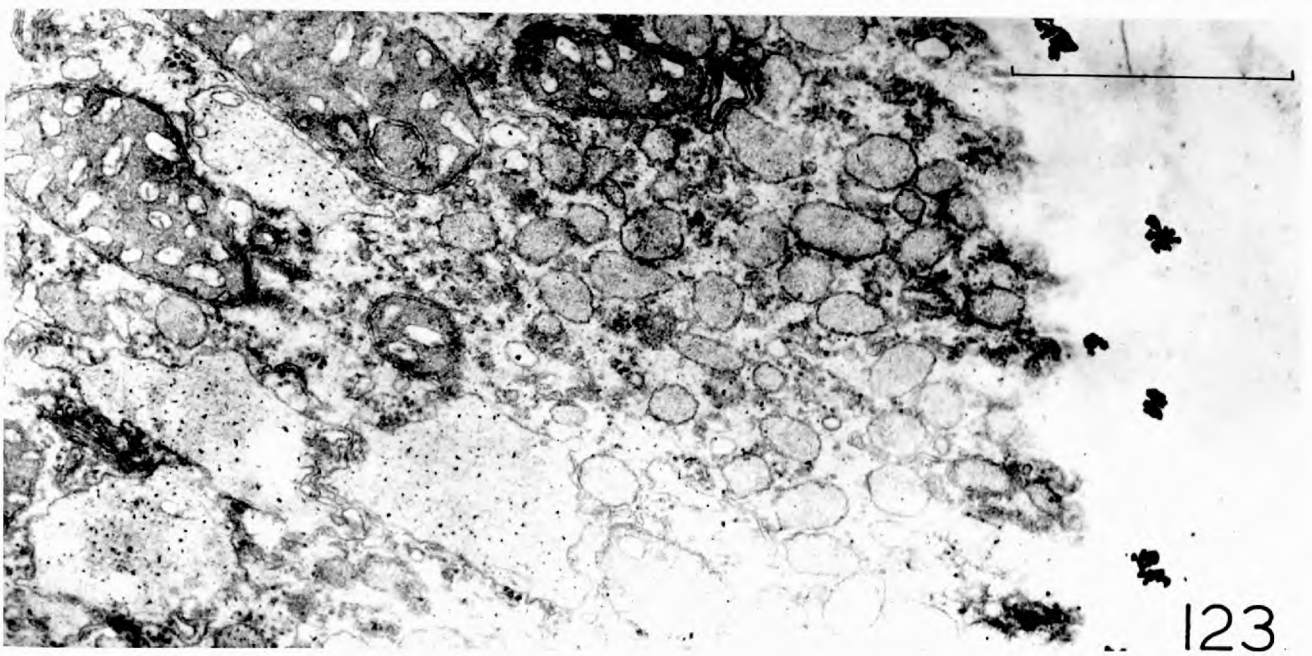
123

Fig.124. Os fixed hyphal apex treated with PAH reagent. Wall vesicle membranes and walls stain. Note clear holes in some wall vesicles (↑) c.f.Fig.114. 1839/5. 10962.

Fig.125. Detail of PAH reaction on Os fixed wall vesicles(c.f Fig.114) 1839/3. 10961.

Fig.126. Detail of PAH reaction over GA/Os fixed wall vesicles (arrowed). 1825/5. 10866.

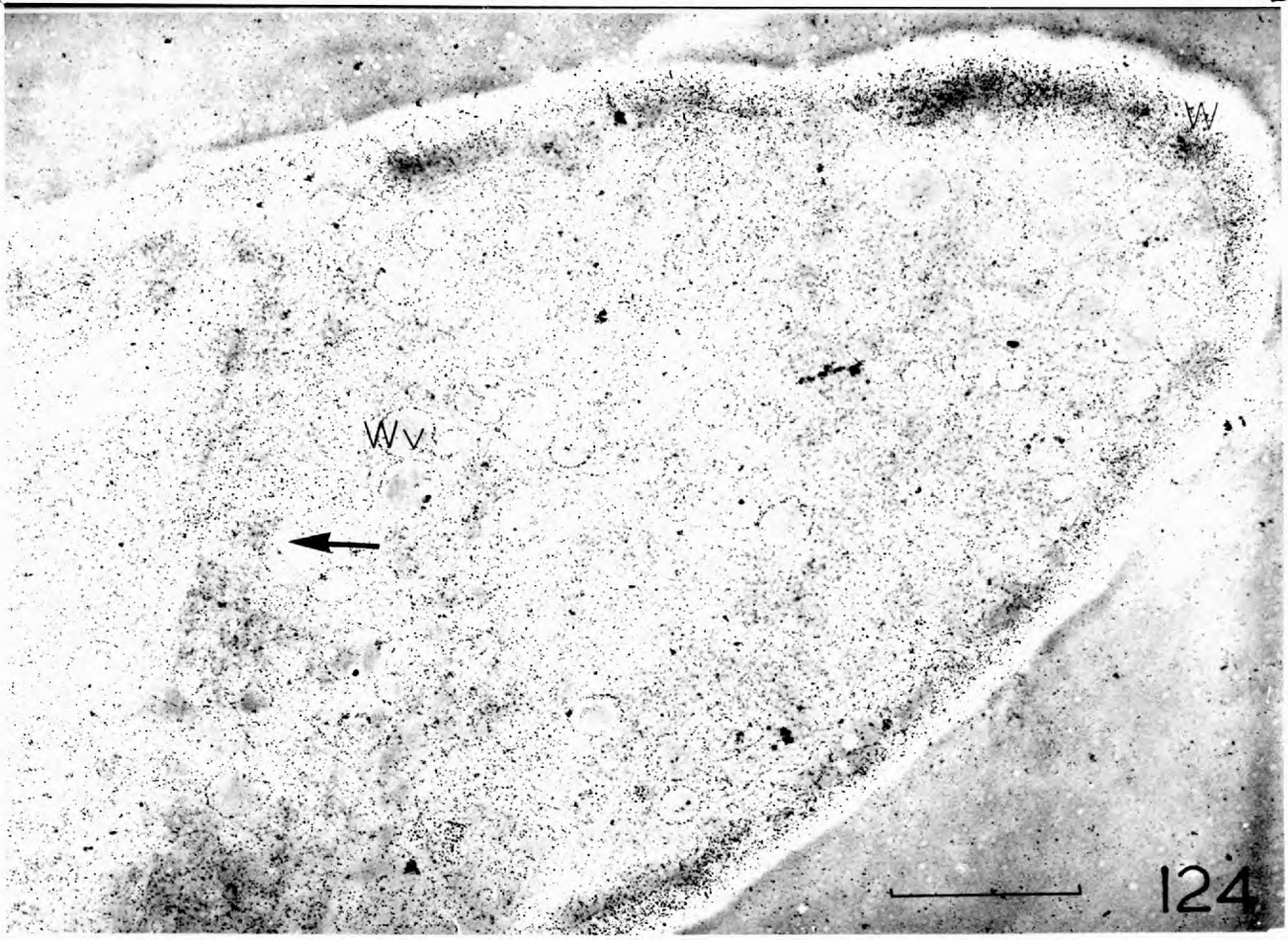
Wv
Wv
124

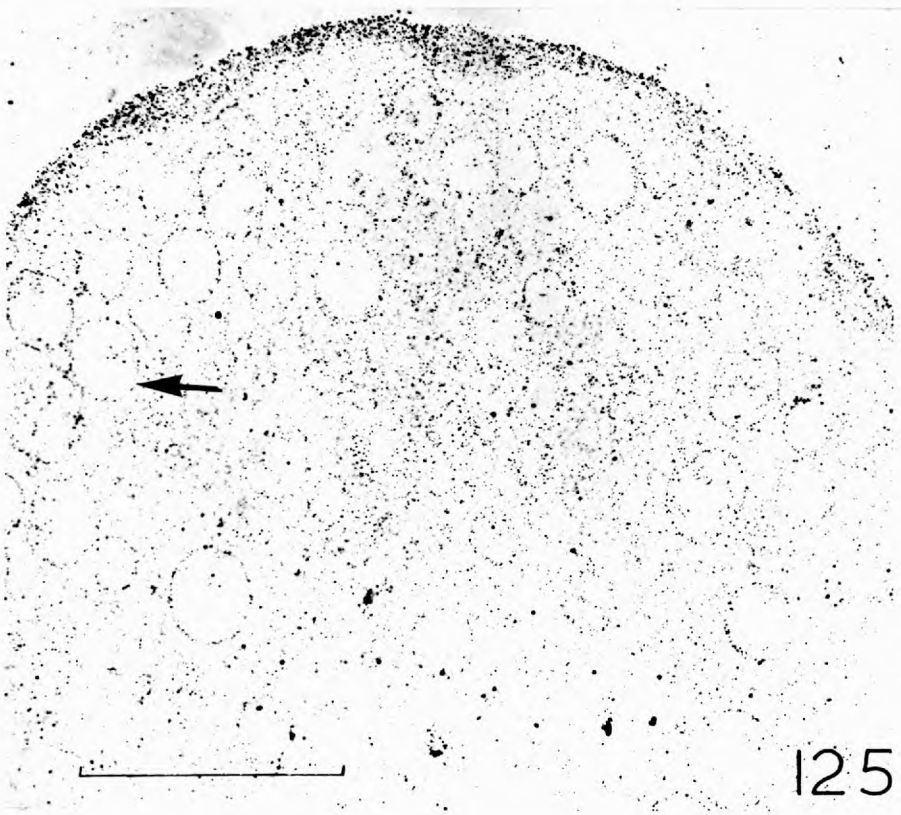
125

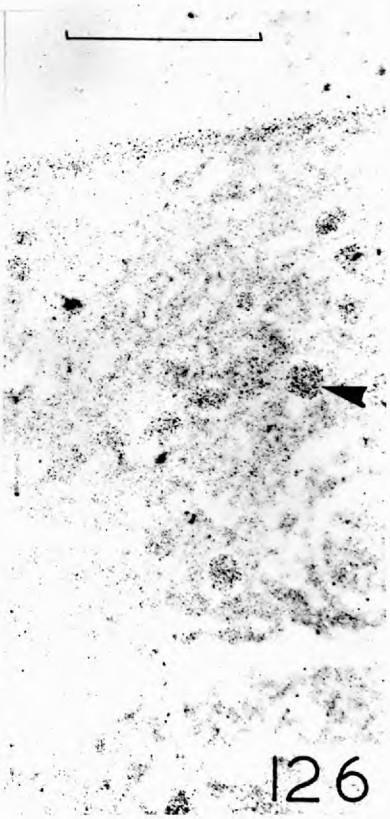
126

Fig.127. Two Golgi bodies associated with a cisternum of the E.R. and mitochondria. Note possible DNA strands in mitochondria. 1696A/2. 8897.

Fig.128. Golgi, E.R., mitochondria associations. Permanganate fixation. 1493/1. 6418.

Fig.129. E.R. forming a bud towards an associated Golgi body. Note rough texture of bud membrane. 1241I/5. 7025. Os only

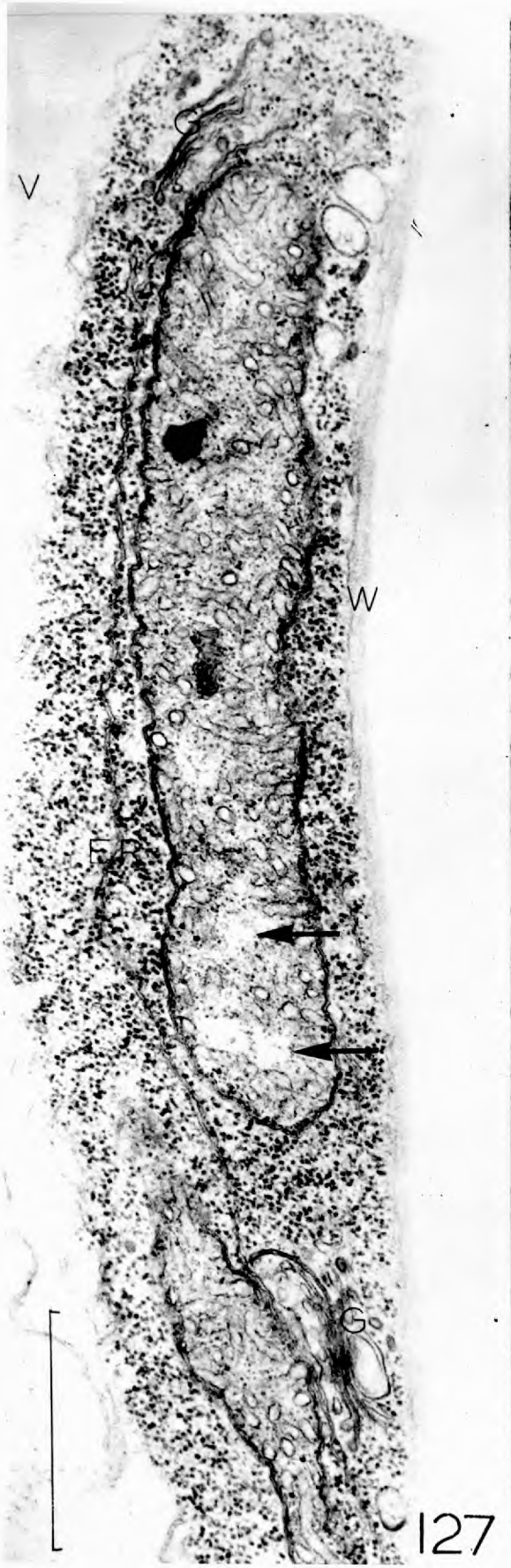

127

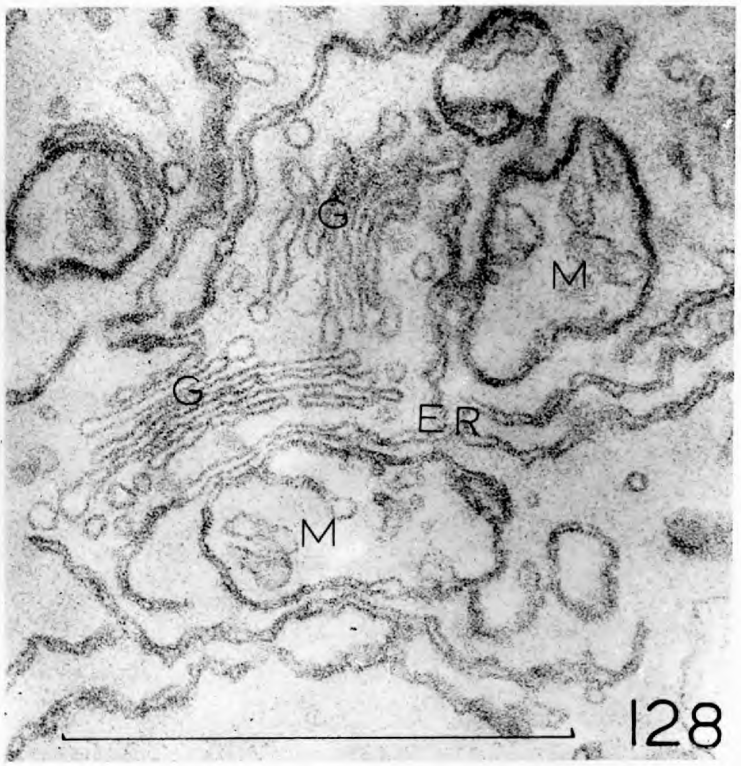

128

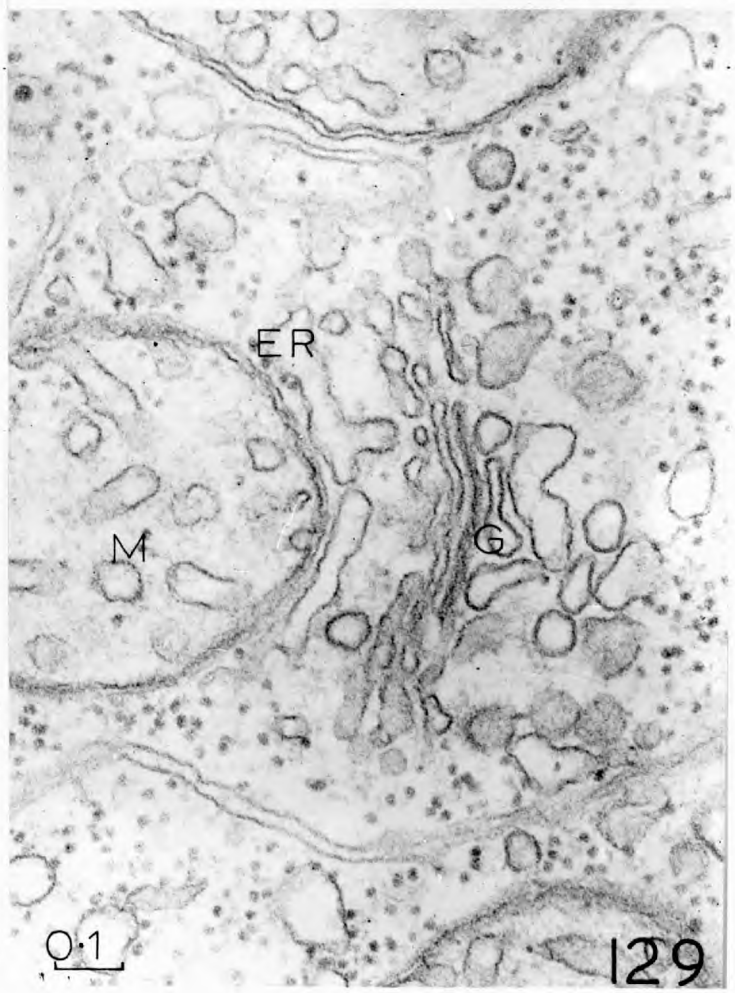

0·1

129

Fig.131. Golgi body and mitochondrion adjacent to a cisternum of the E.R. showing clear connections to longer ribosome studded cisternae. 1547/6. 12875.

Fig.132. Dense surfaced vesicles attached to cisternae of the E.R. and Golgi and also lying free in the space between these organelles. 1645G/9. 10506.

Fig.133. An E.R. cisternum adjacent to a mitochondrion and forming dense surfaced vesicles towards the associated Golgi body. 1836C/2. 14353.

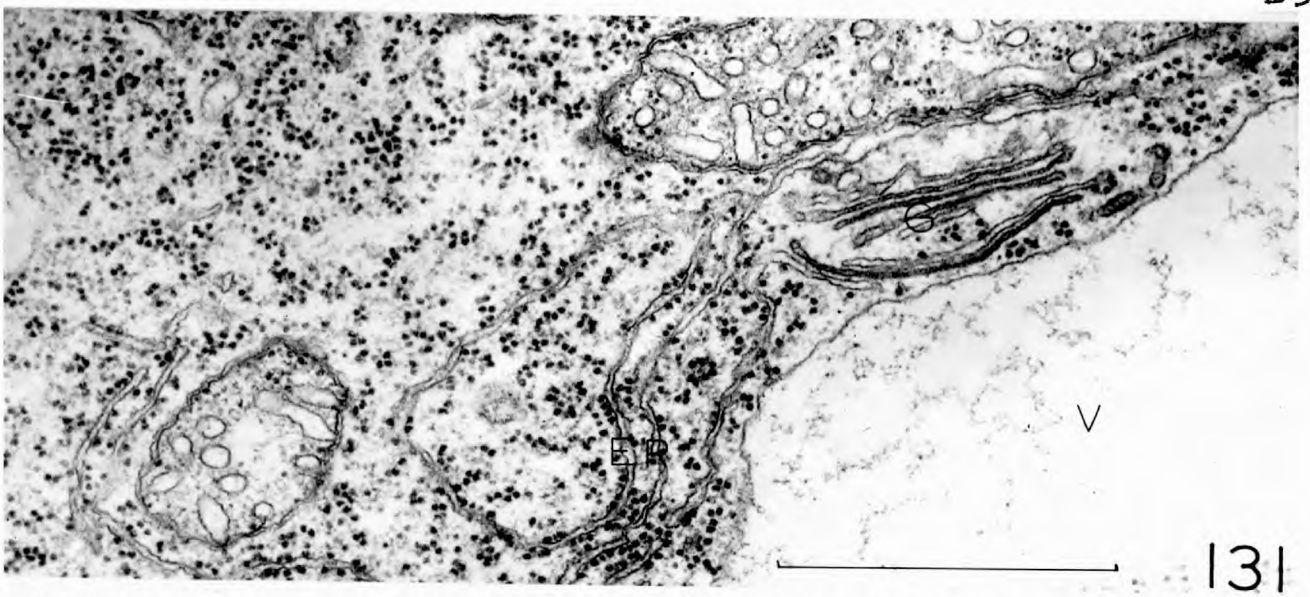

131

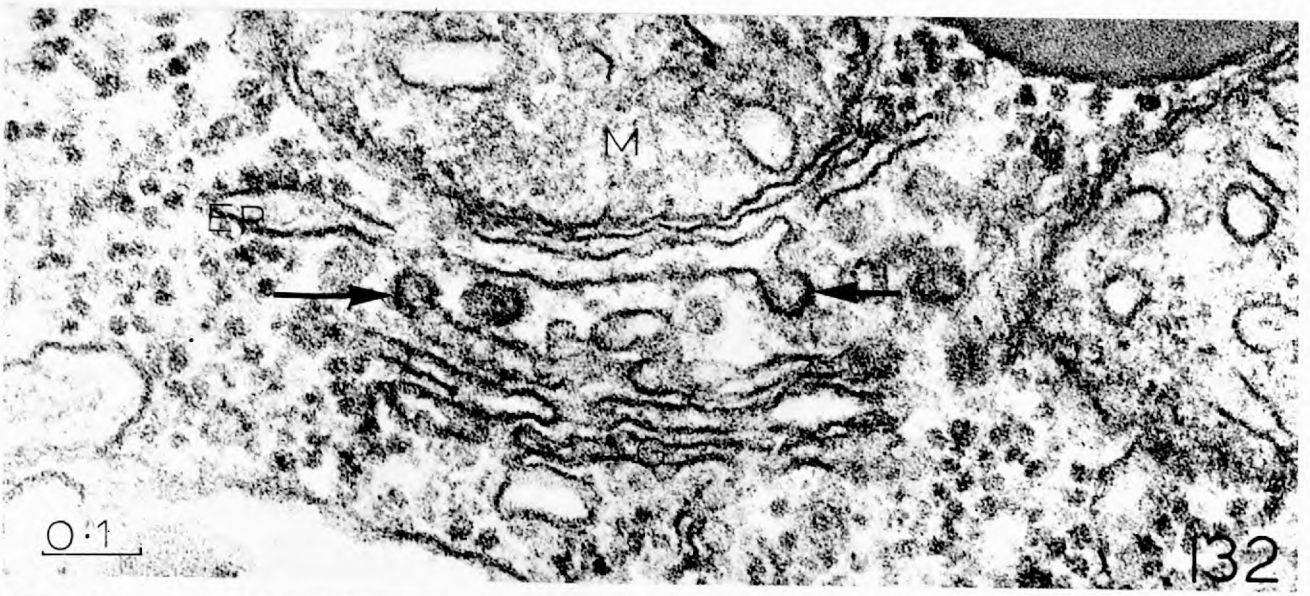

132

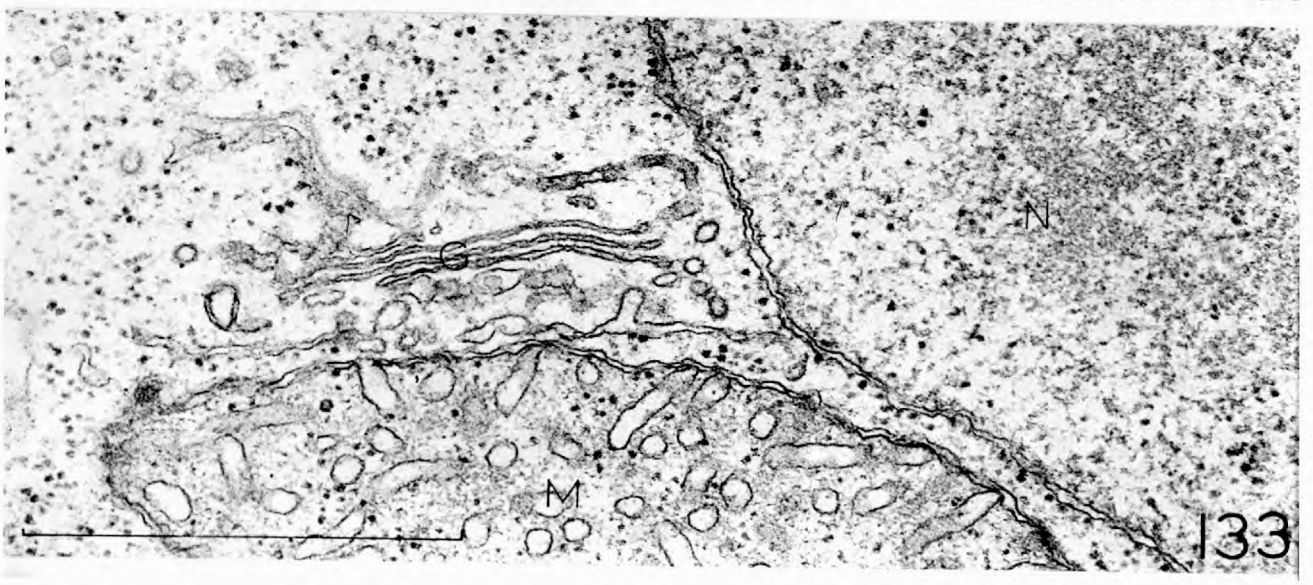

133

Fig.134. Regrowing apex. Note young healthy apex inside a hypha with an apparently disordered protoplast. Lomasomes containing ribosomes can be seen between the young and old walls. 1388A/17. 6112.

Fig.135. Hyphal apex with a continuous ring of double membrane apparently dividing the cytoplasm into two regions. 1548/5h. 8436.

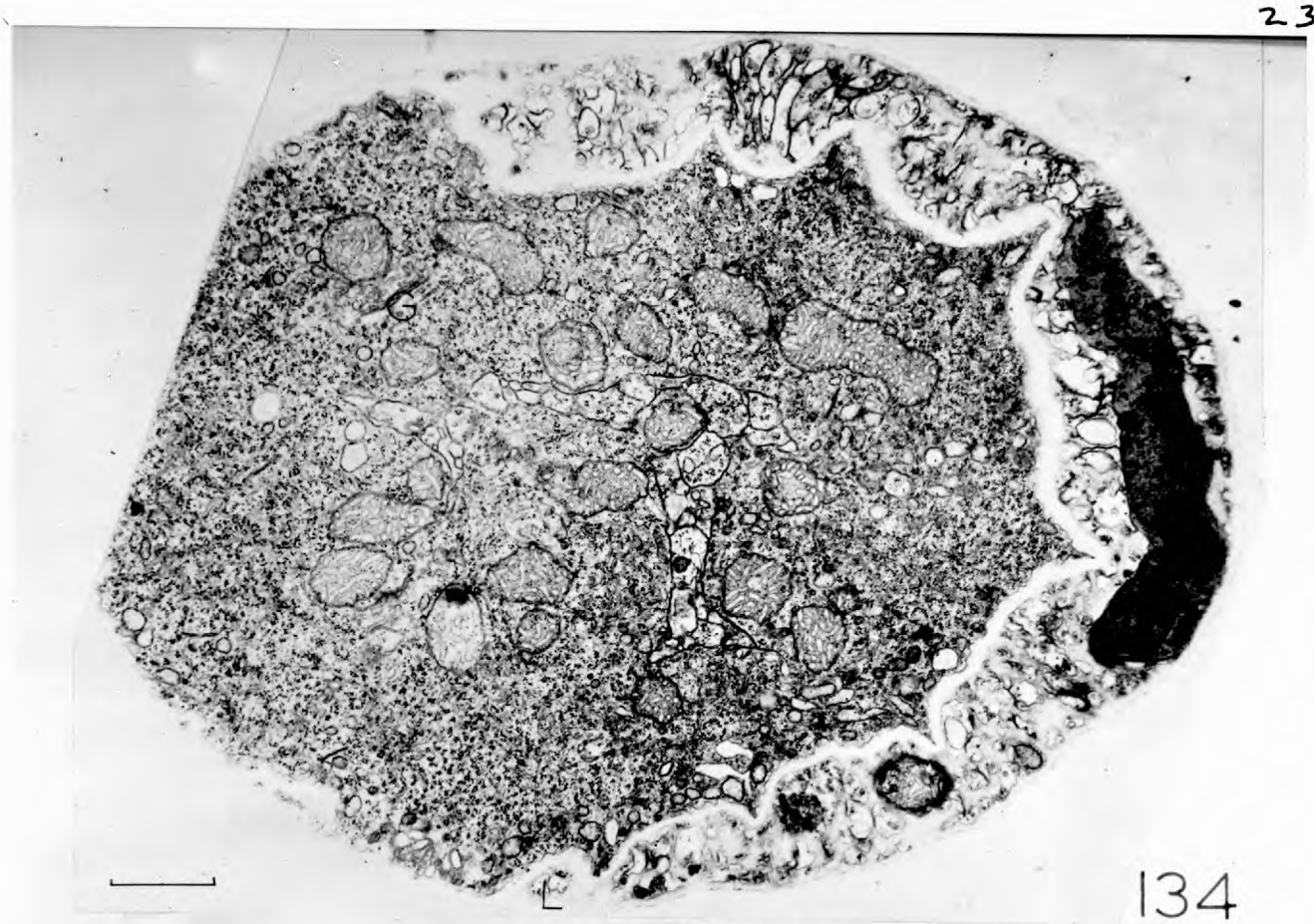

134

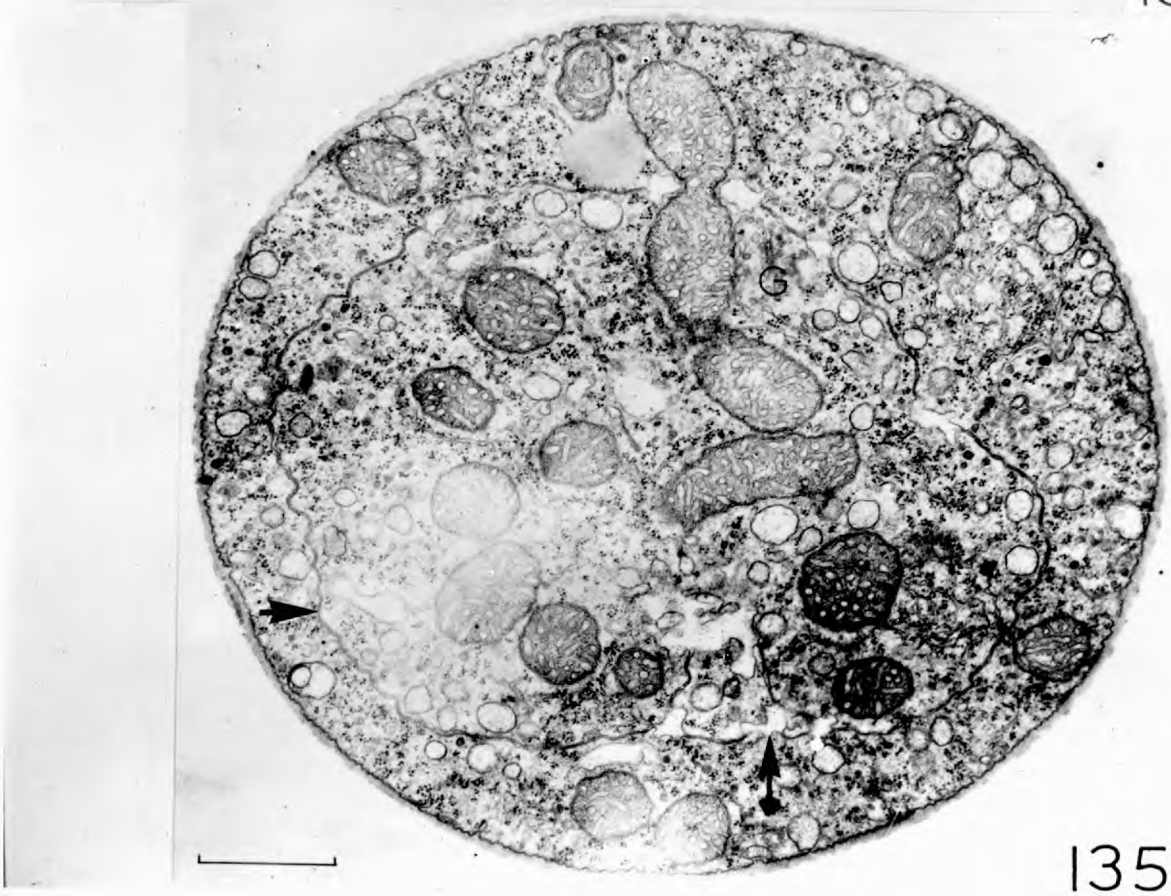

135

Fig.136. Germinating primary cysts with enlarging dense body vesicles, an apical concentration of wall vesicles, fibrils in the E.R. (f) and irregularly shaped nuclei commonly found in these spores. 1692C/1. 8945.

Fig.137. Vacuoles connected to lengths of double parellel membranes which are free of attached ribosomes. 1547H/3. 8942.

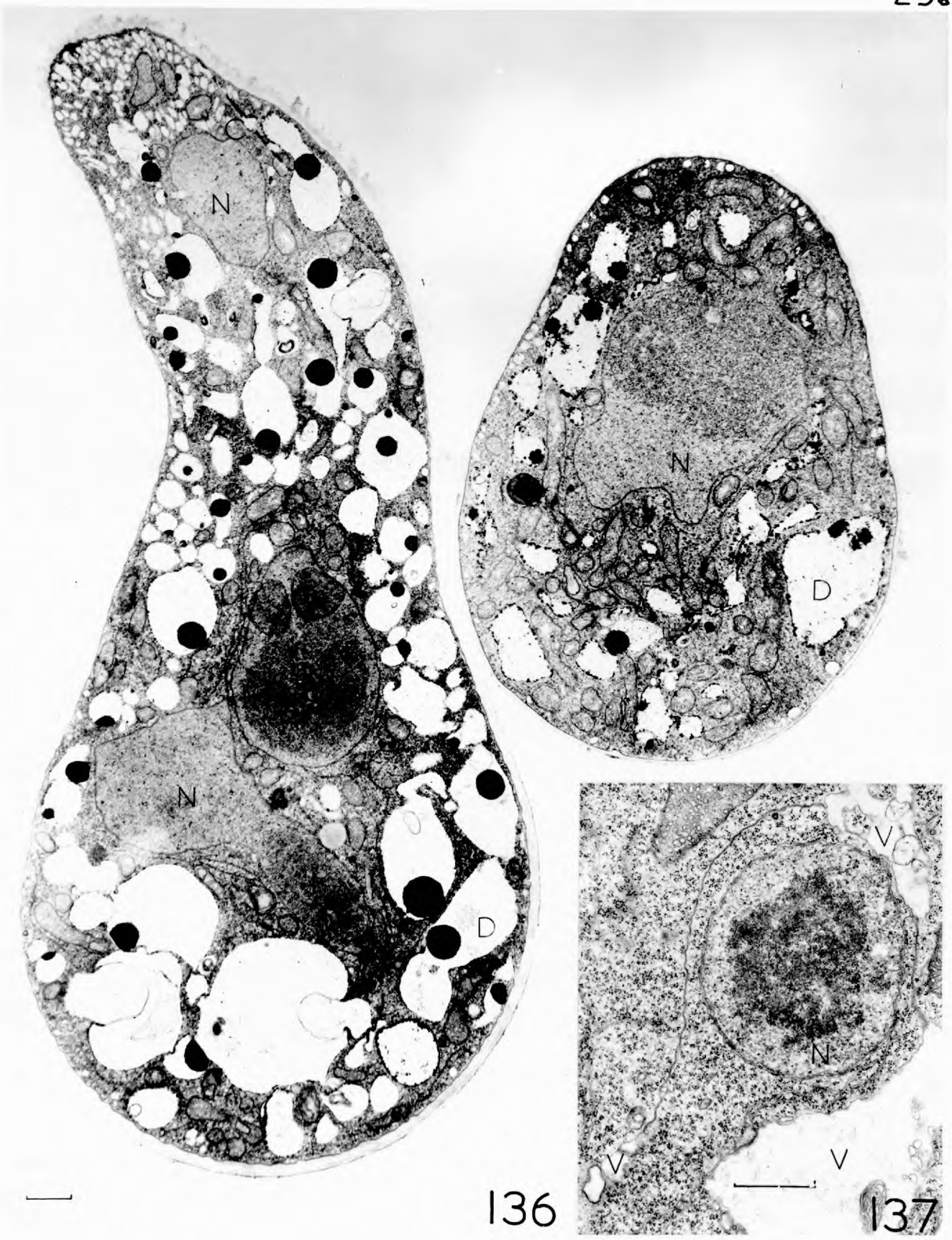

136

137

Fig.138. Apex of a c 10-20 µm germ tube with high apical concentration of wall vesicles. 1691/2. 8937.

Fig.139. Apex of a 40 µm germ tube. Note wall vesicles. 1693B/5. 8886.

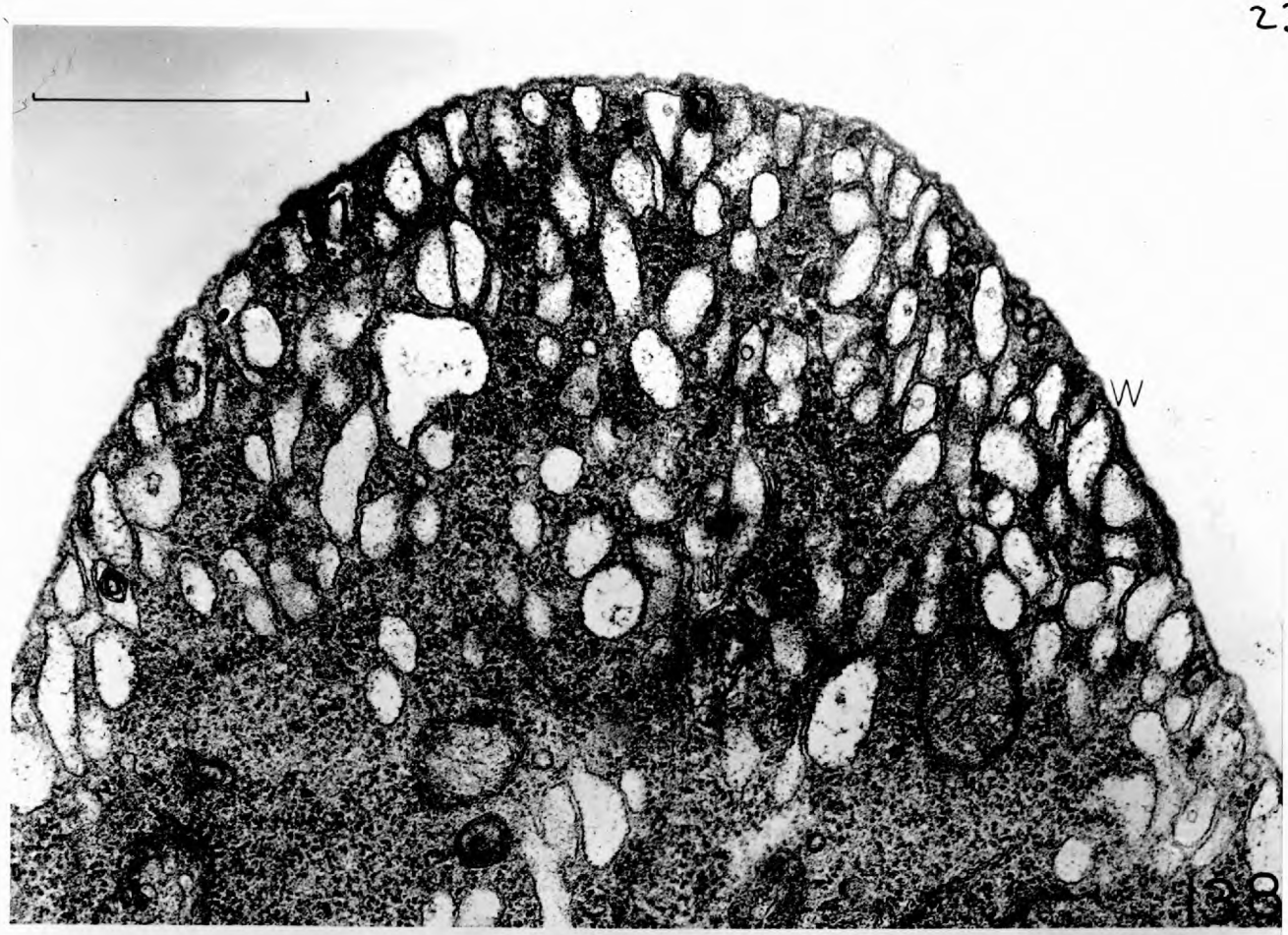

138

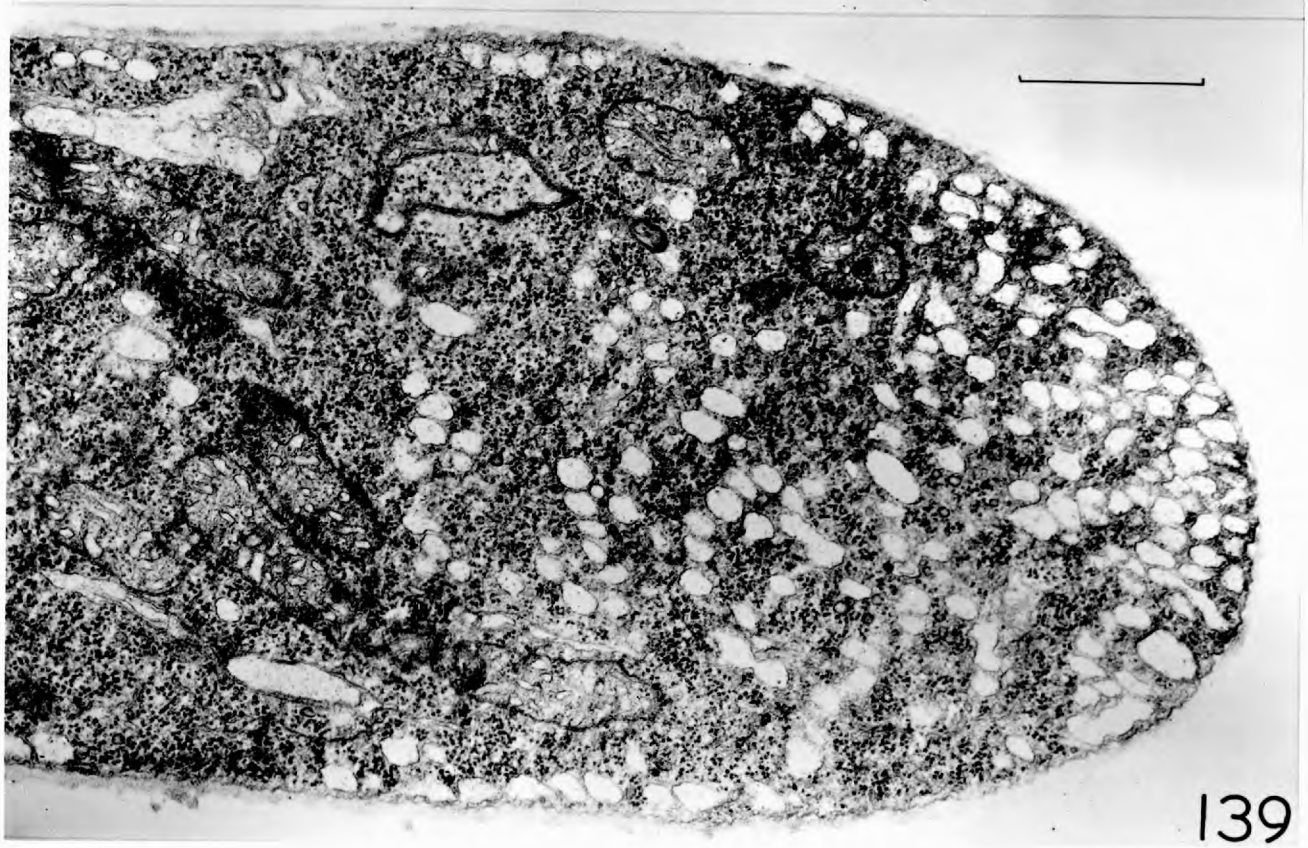

139

Fig.140. D. sterile. Germ tube emerging from primary cyst. The cyst wall is expanded and pushed through the sporangium wall. Note instability of dense bodies and distorted wall vesicles. The Golgi activity is probably concerned with flagellum formation (see Spore formation). Os only. 1852/3. 12184.

Fig.141. D. sterile. Germ tube of primary cyst containing numerous lomasomes, wall vesicles and expanded dense body. Note dense body material in apical plasmalemmasomes. 1853/3. 12149.

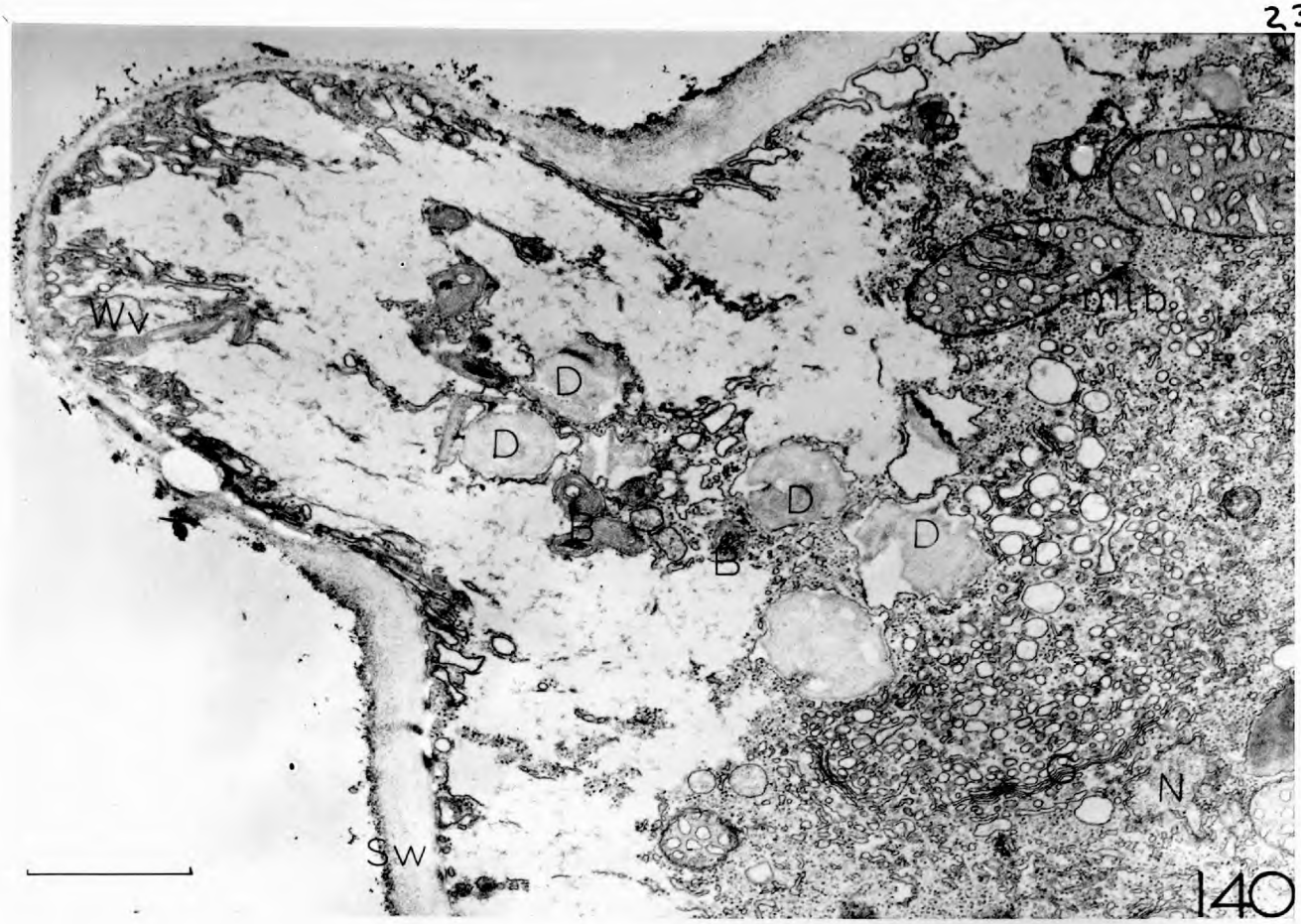

140

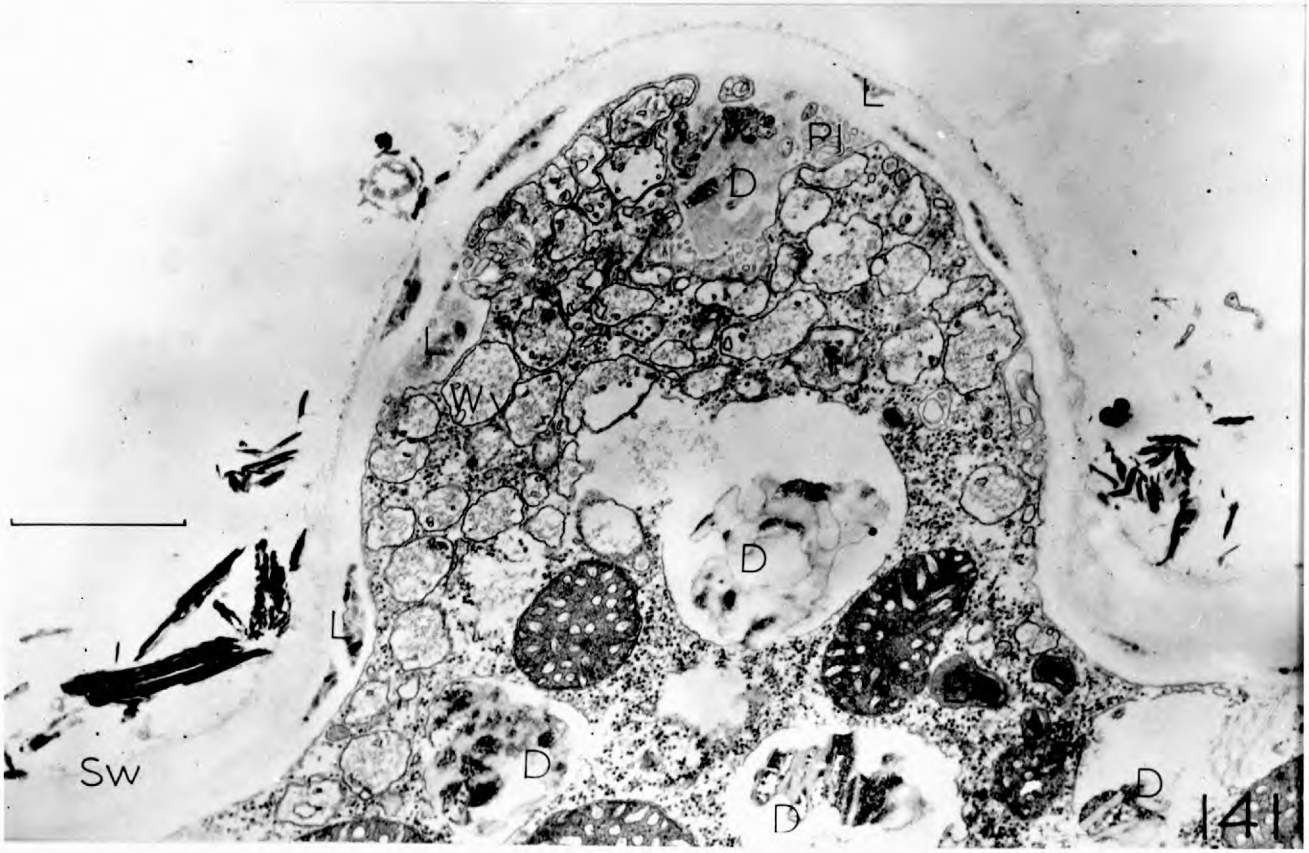

141

Fig.142. Developing apical papillum containing numerous wall vesicles, a plasmalemmasome, lomasomes, bars and a very wide spectrum of dense body types. The labelled nucleus may be degenerating c.f. Fig.267. 1647F/1. 10304.

Fig.143. Apical papillum after PAH treatment. Note heavy reaction over wall vesicles. 1827A/4. 10856.

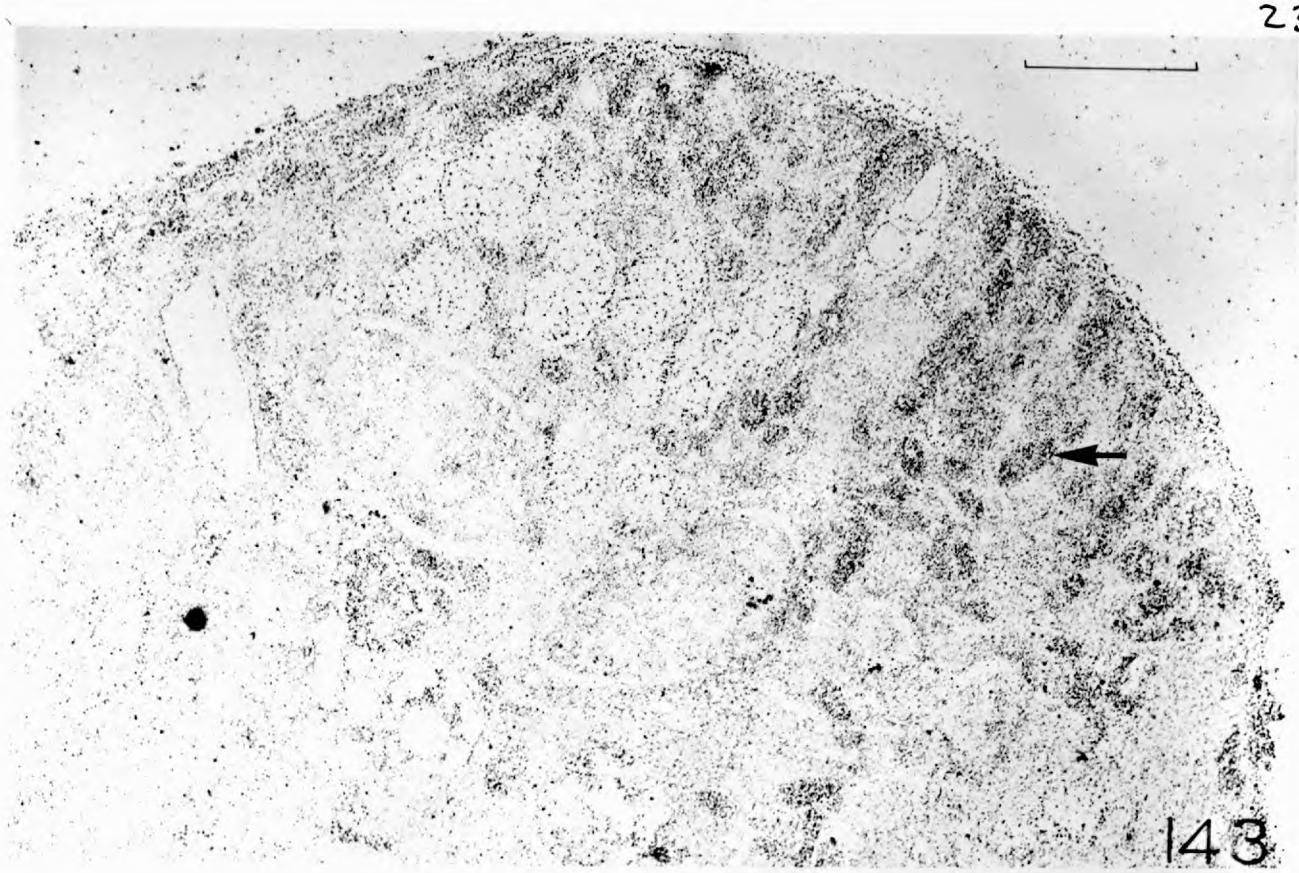

143

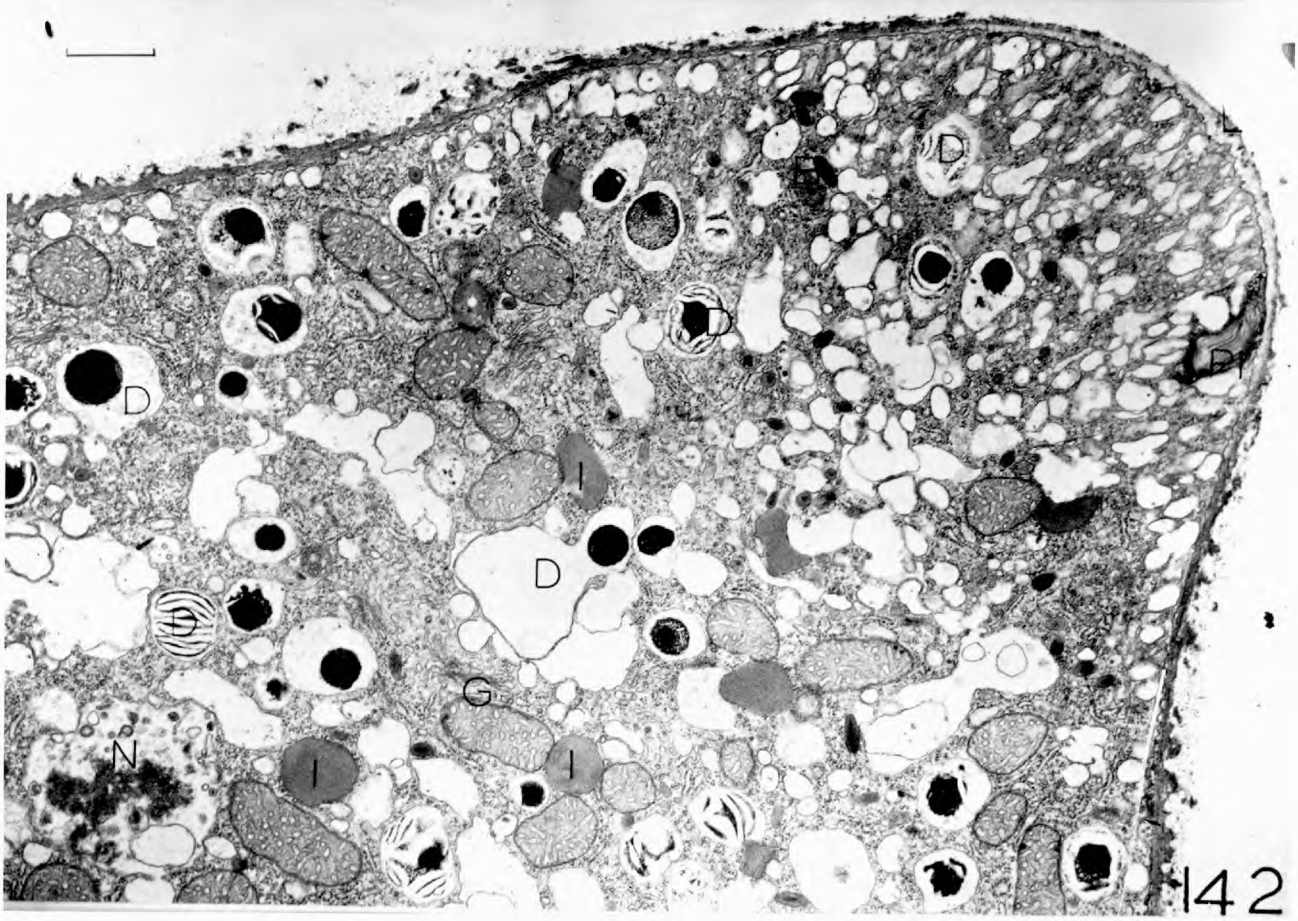

142

Fig.144. Late stage in apical papillum development. Note reduced number of wall vesicles and also a plasmalemmasome. 1645H/1. 10030.

Fig.145. Nearly mature apical papillum with few wall vesicles and no lomasomes. 1848C/2. 10996.

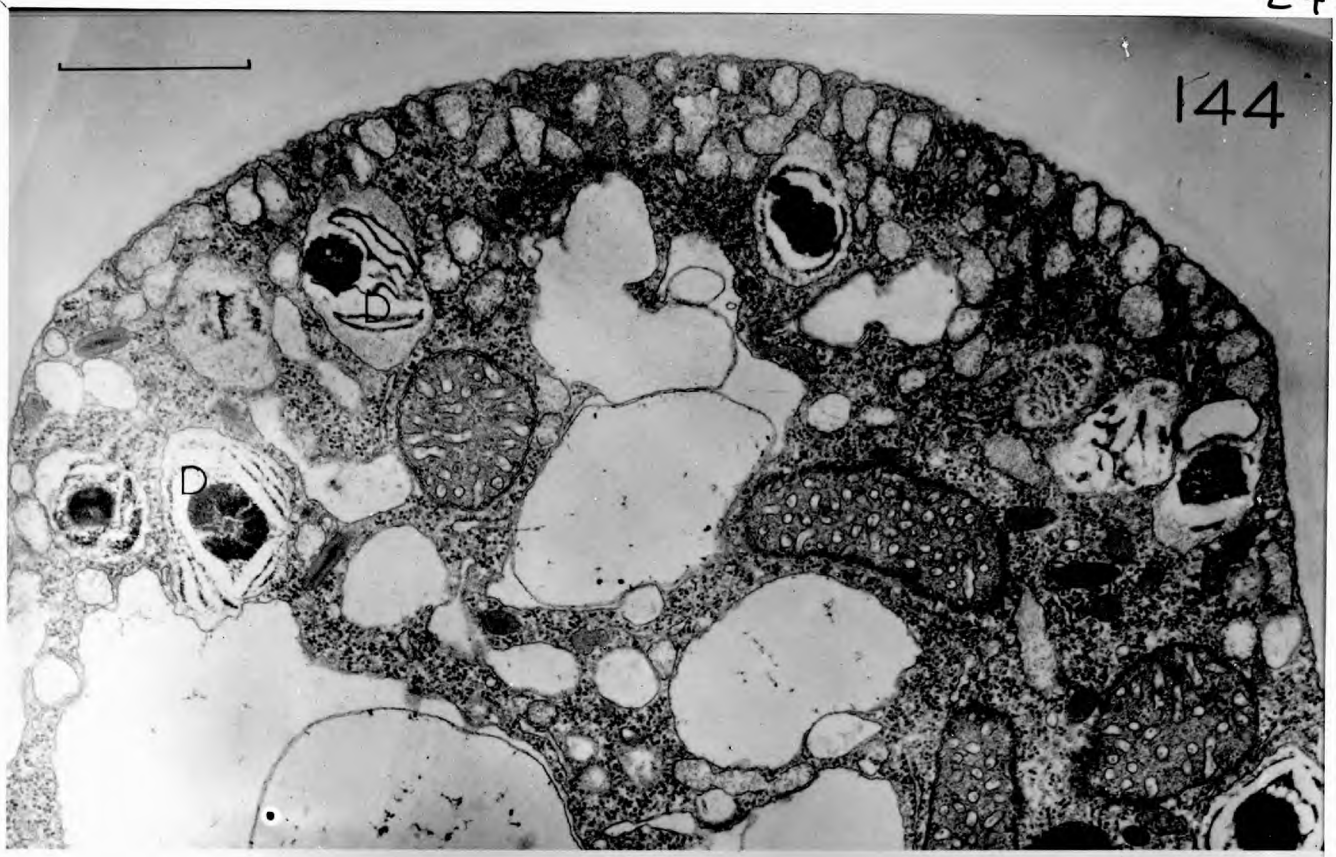
144
D
D

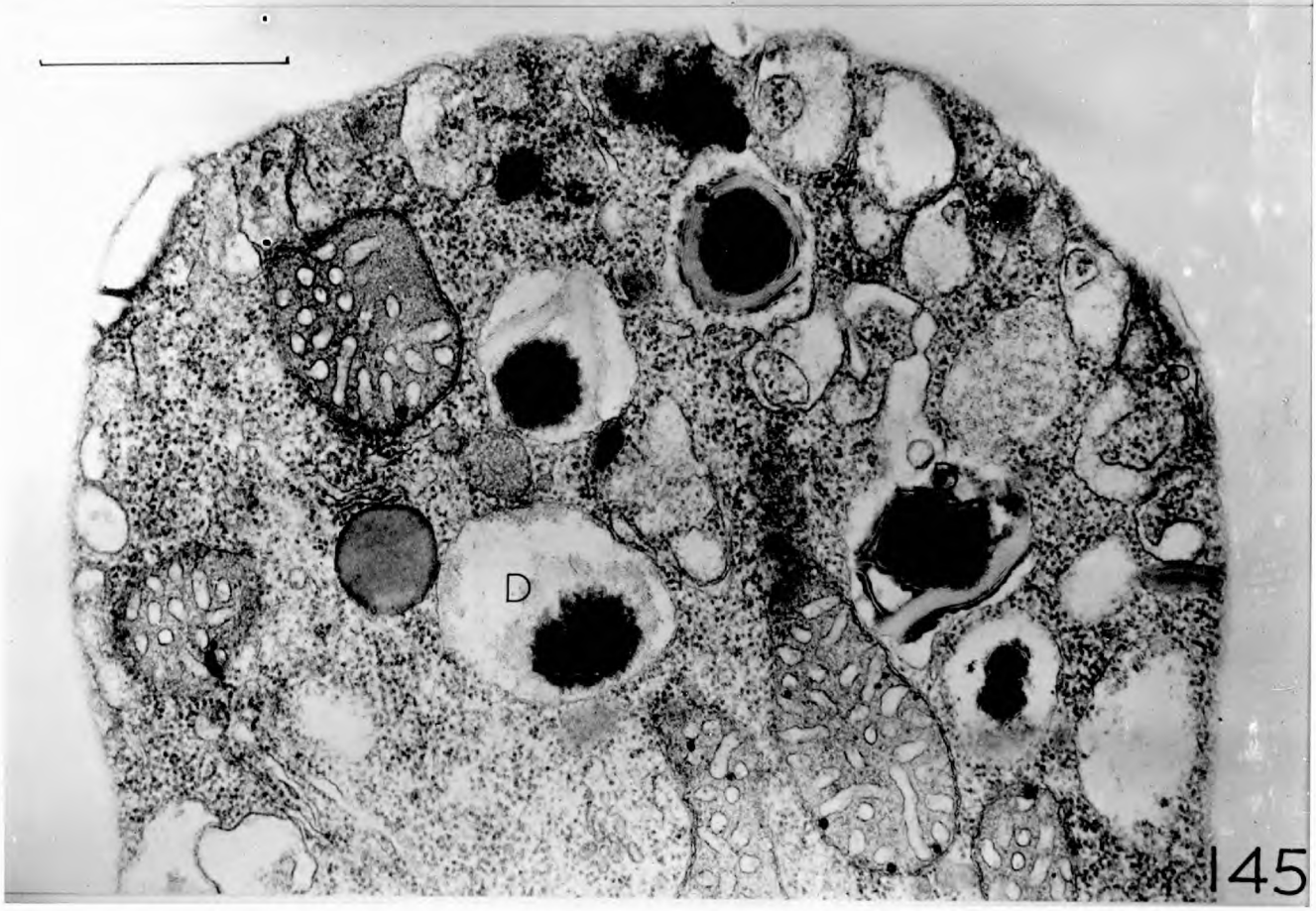
D
145

Fig.146. Zoospore passing through open apical papillum. Note sharp well defined edges to papillum walls. 1847A/3. 10941.

Fig.147. Apical papillum after cleavage prior to spore release. The top wall of the papillum has a more loose texture than the side walls. 1848E/1. 12012.

Fig.148. Sporangium wall with adjacent wall vesicles, some of which are tubular, and an aggregation of membranous tubules in a vesicle which contains material similar to that found in dense body vesicles. 1848C/2. 12000.

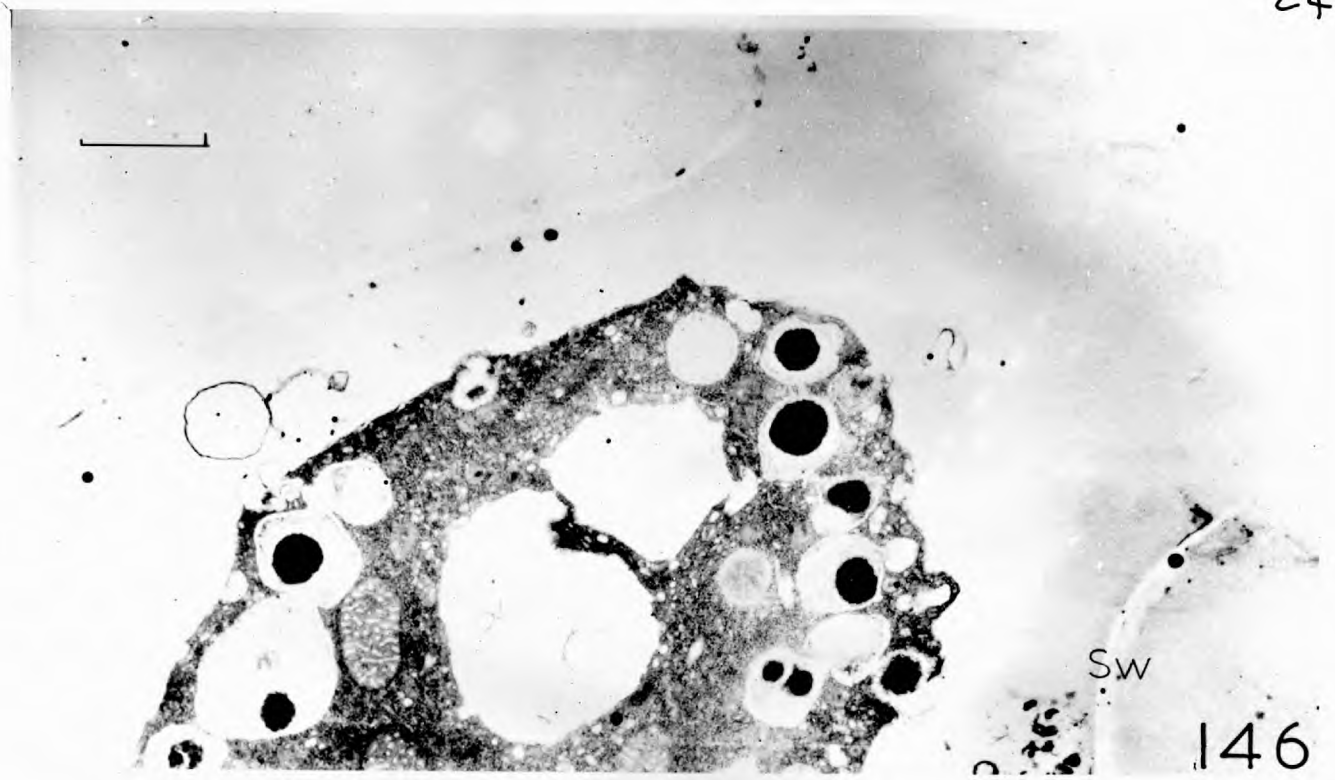
Sw
146


0·1

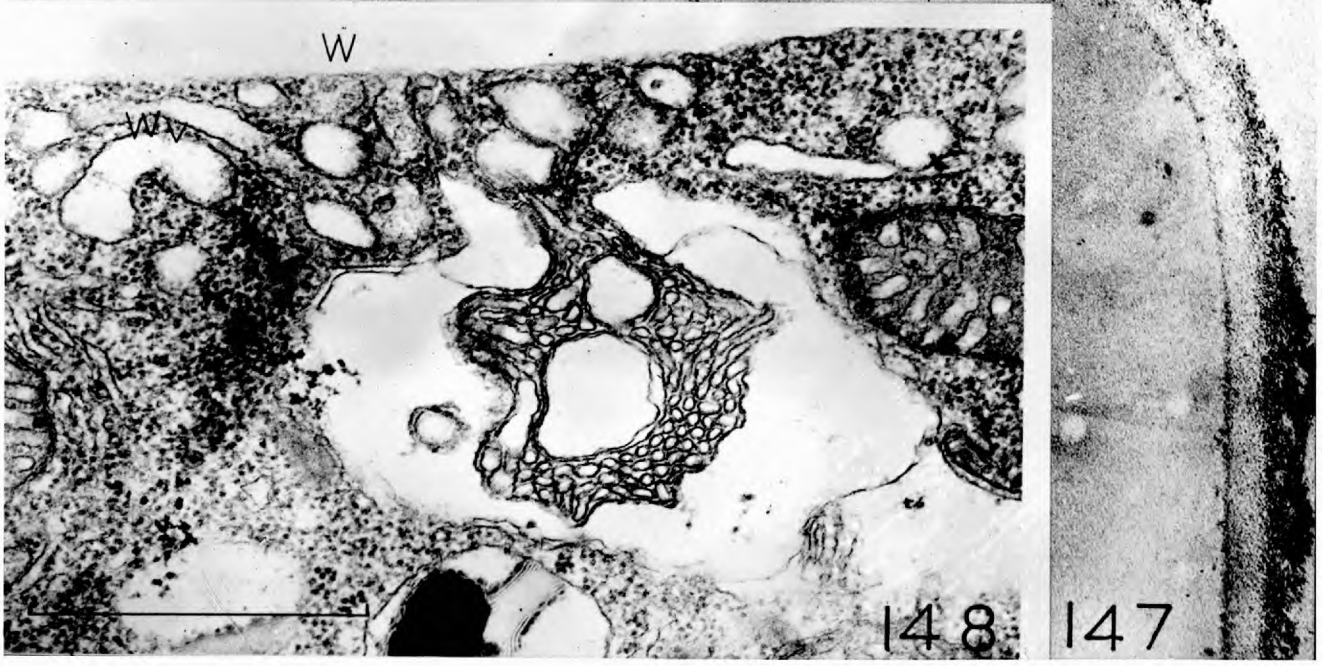
W
WV
148
147

Fig.149. Pre-cleavage sporangium after PAH treatment showing dense reaction on fibrous bodies, wall vesicles and wall. The upper kinetosome is sectioned along its surface and shows a slightly heavier deposit than the cytoplasm. 1848/4. 10969.

Fig.150. Pre-cleavage sporangium showing slightly heavier silver deposit over the tubular wall vesicles relative to the wall. 1848/4. 10966.

Fig.151. Pre-cleavage sporangium showing typical PAH silver distribution. Holes are probably etched away dense bodies which frequently stain heavily. 1848/4. 10964.

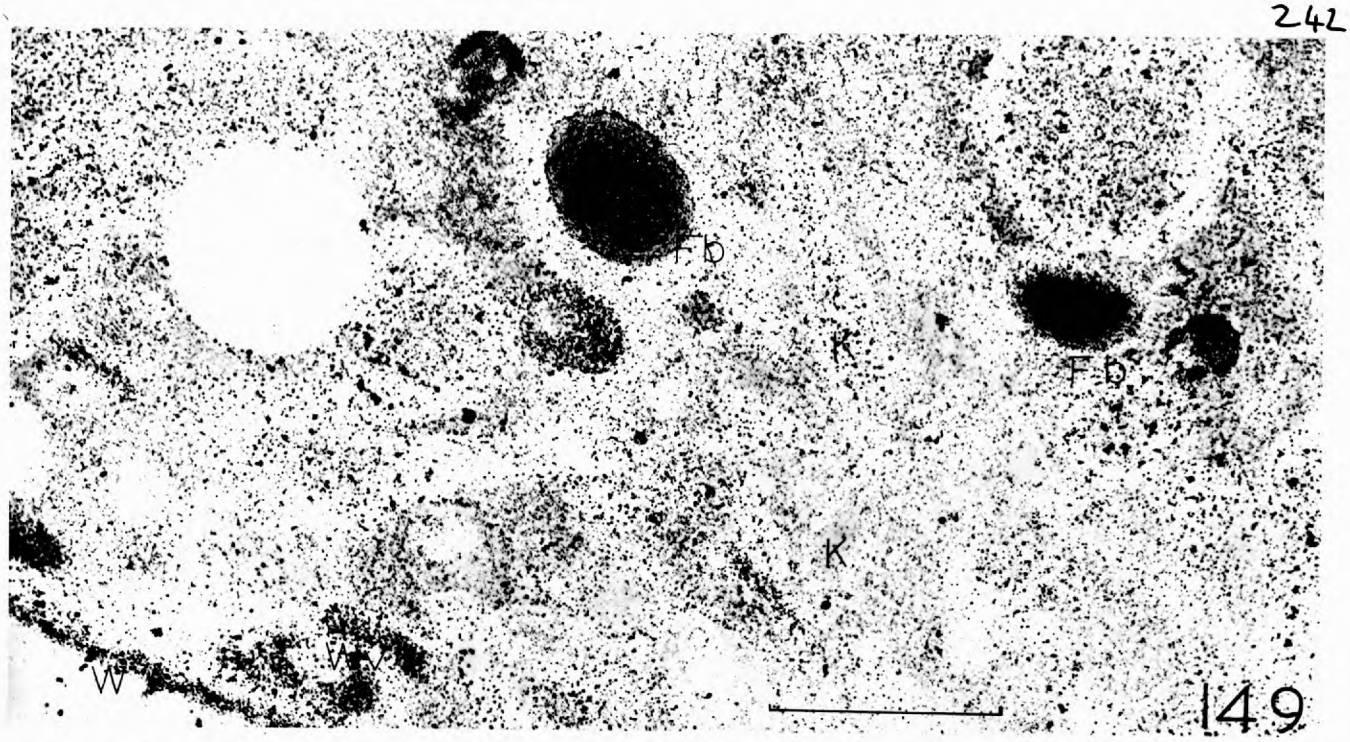

149

150

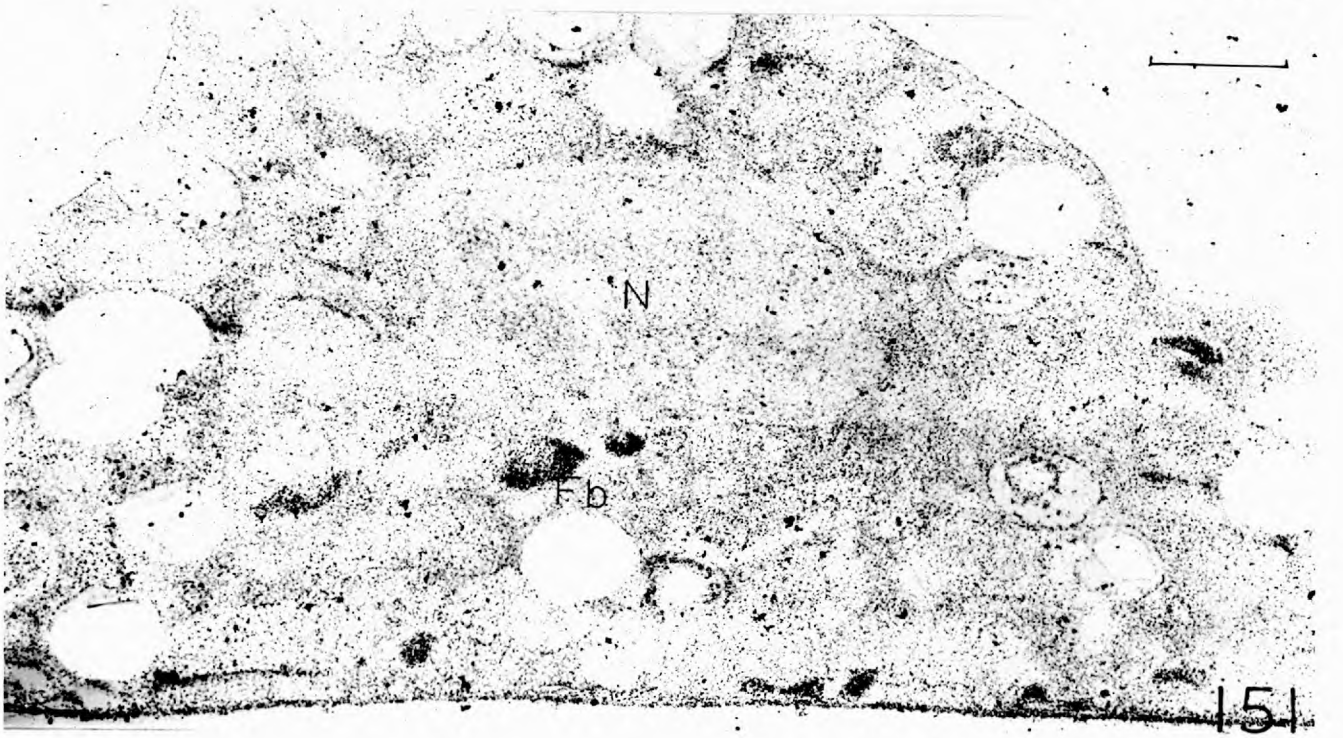

151

Fig.152. D. sterile. Sporangium cross wall and encysting primary spores. Note wall vesicles along spore peripheries and below the cross wall. 1853B/1. 12168.

Fig.153. D. sterile. Detail of Fig.152. 1853B/1. 12170.

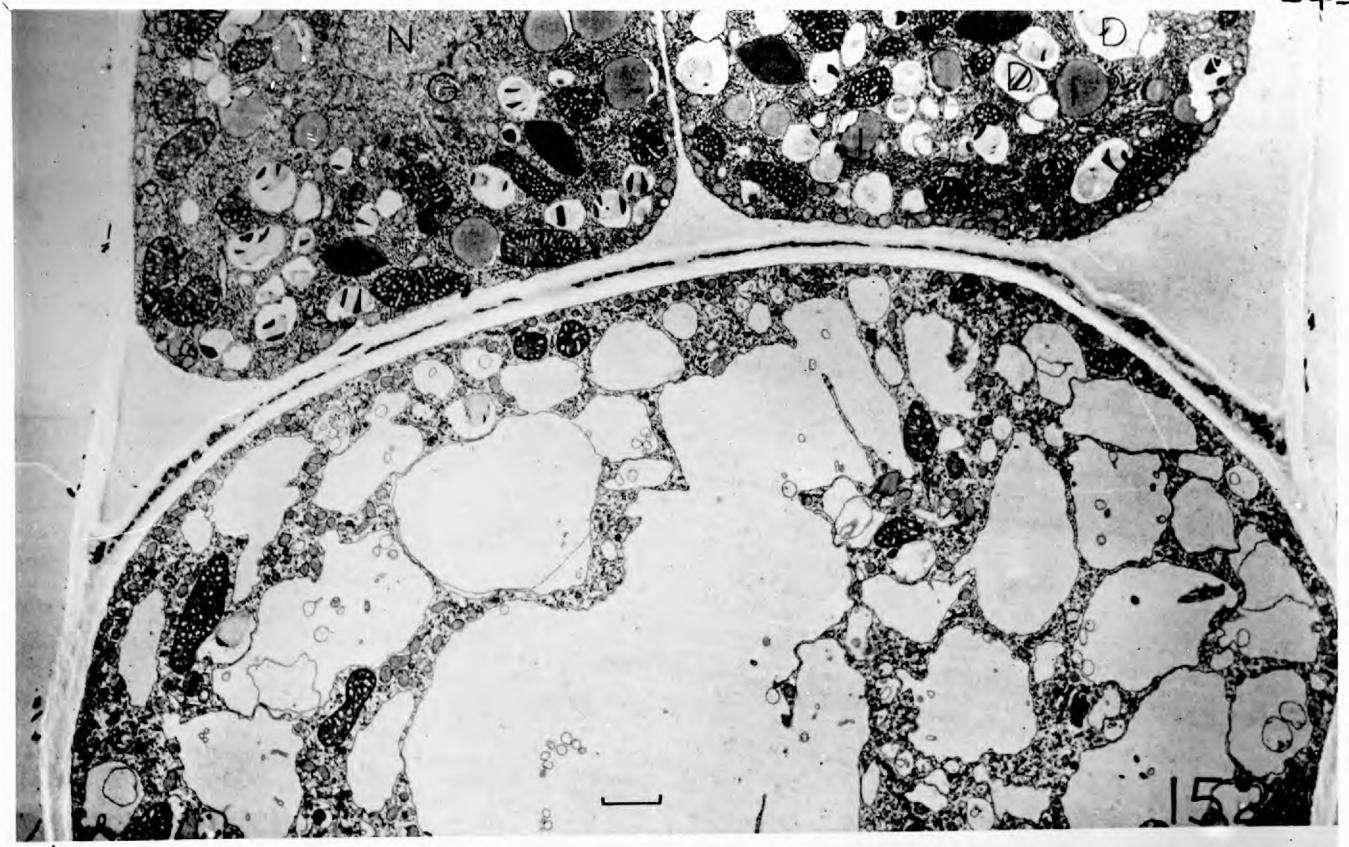
N
G
D
D
152


cb
ER
f
I
D
M
Wv
L
Wv
153

Fig.154. Three layered sporangium cross wall containing layers of trapped cytoplasm including lipid droplets and ribosomes. Note disruption of dense body vesicles and their contained characteristic dense globules after Os fixation. 1241C/3. 8276.

Fig.155. D. sterile. Empty primary germ tube after discharge of secondary zoospore. Germ tube wall is clearly an extension of the cyst wall and has the appearance of being stretched. 1853/1. 12146.

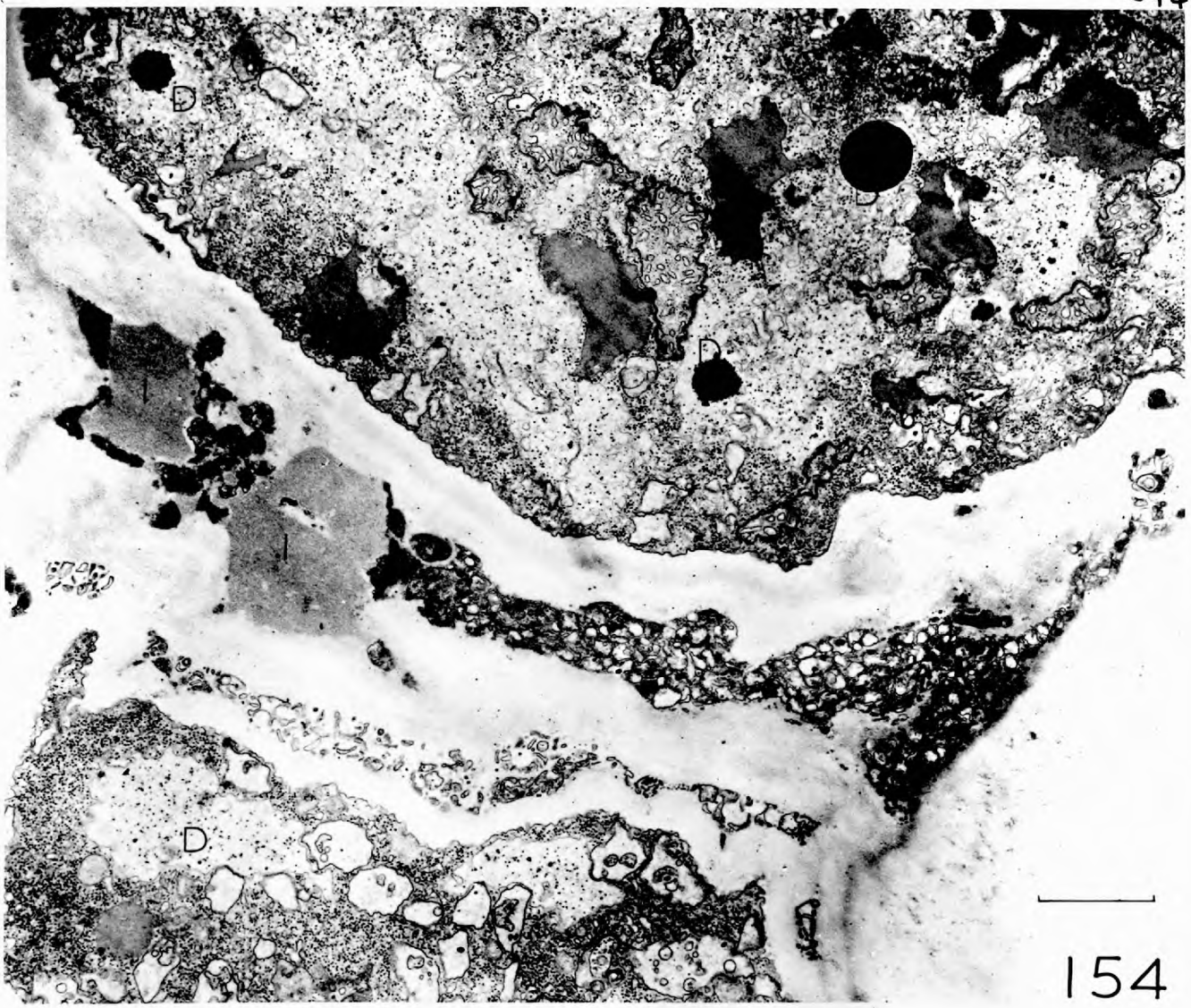

154

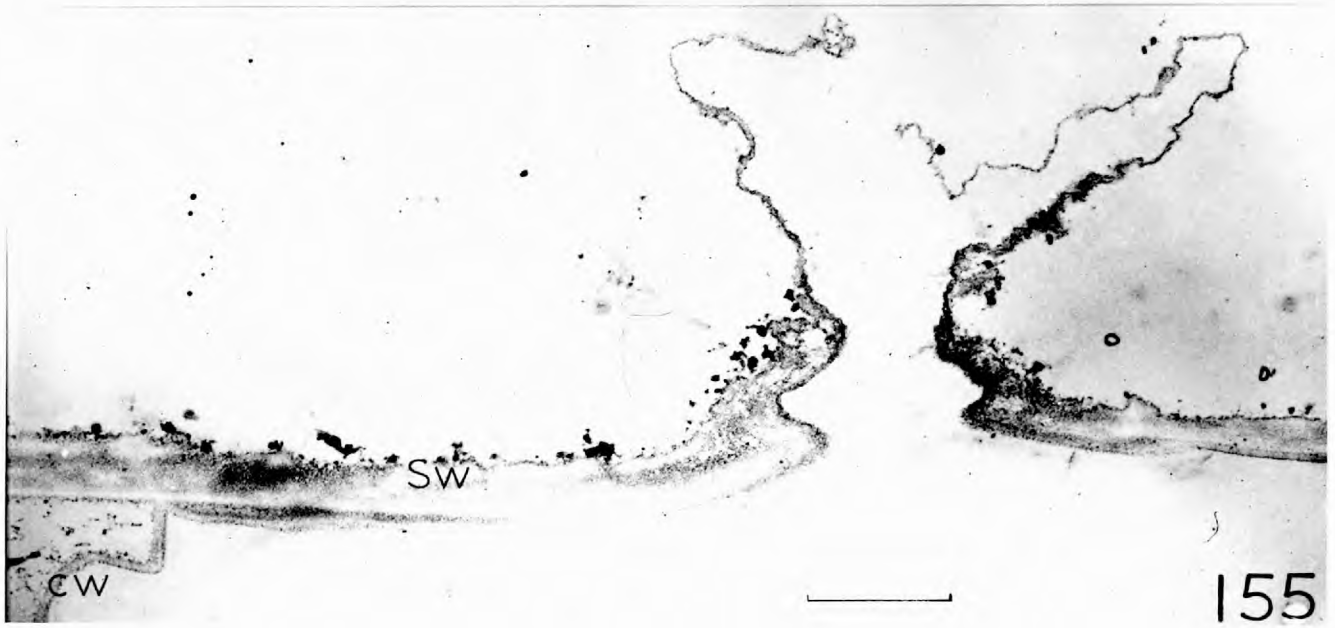

155

Fig.156. Point at which hypha is growing up through cross wall of a discharged sporangium. Note concentration of wall vesicles and plasmalemmasomes. 1644/3. 10366.

Fig.157. Base of a sporangium plasmolysed in 2M sucrose before fixation. Note undisturbed trapped cytoplasm in the croo wall and the manner in which the cross wall tapers off as a second wall layer inside the hyphal and sporangial walls. 1849/1. 10887.

Fig.157a. Detail of the end of a cross wall showing the continuous outer wall and the inner layers of the cross wall. 1830/1. 10814.

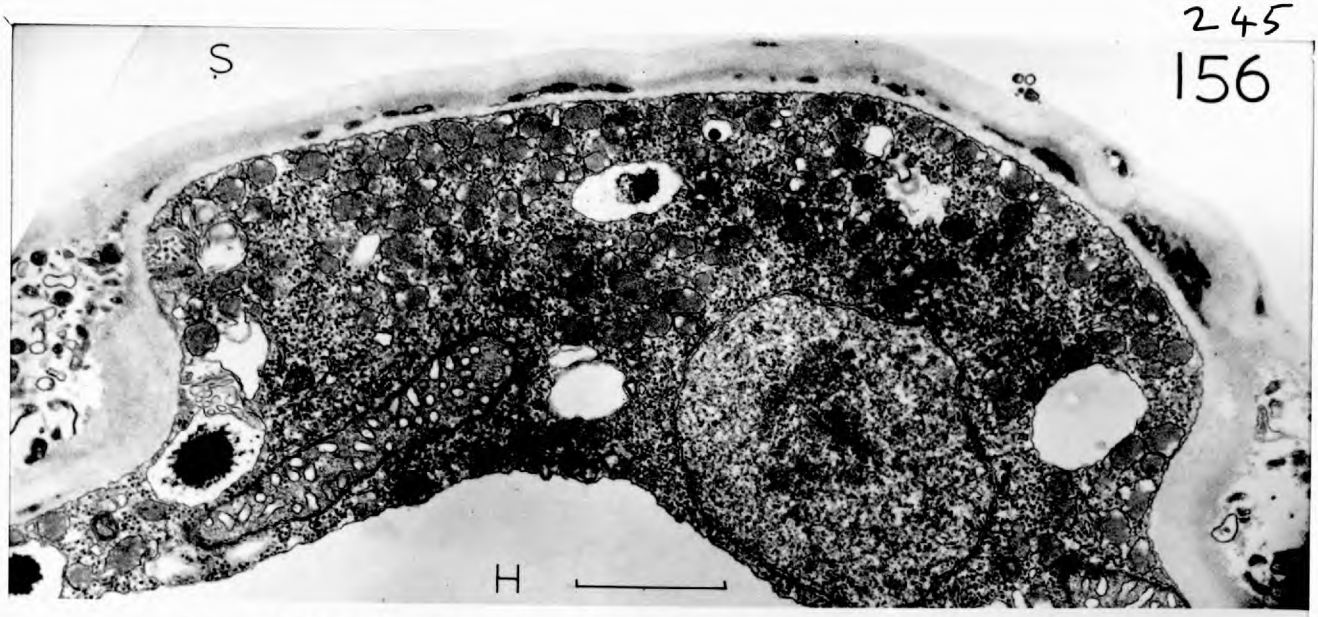

156

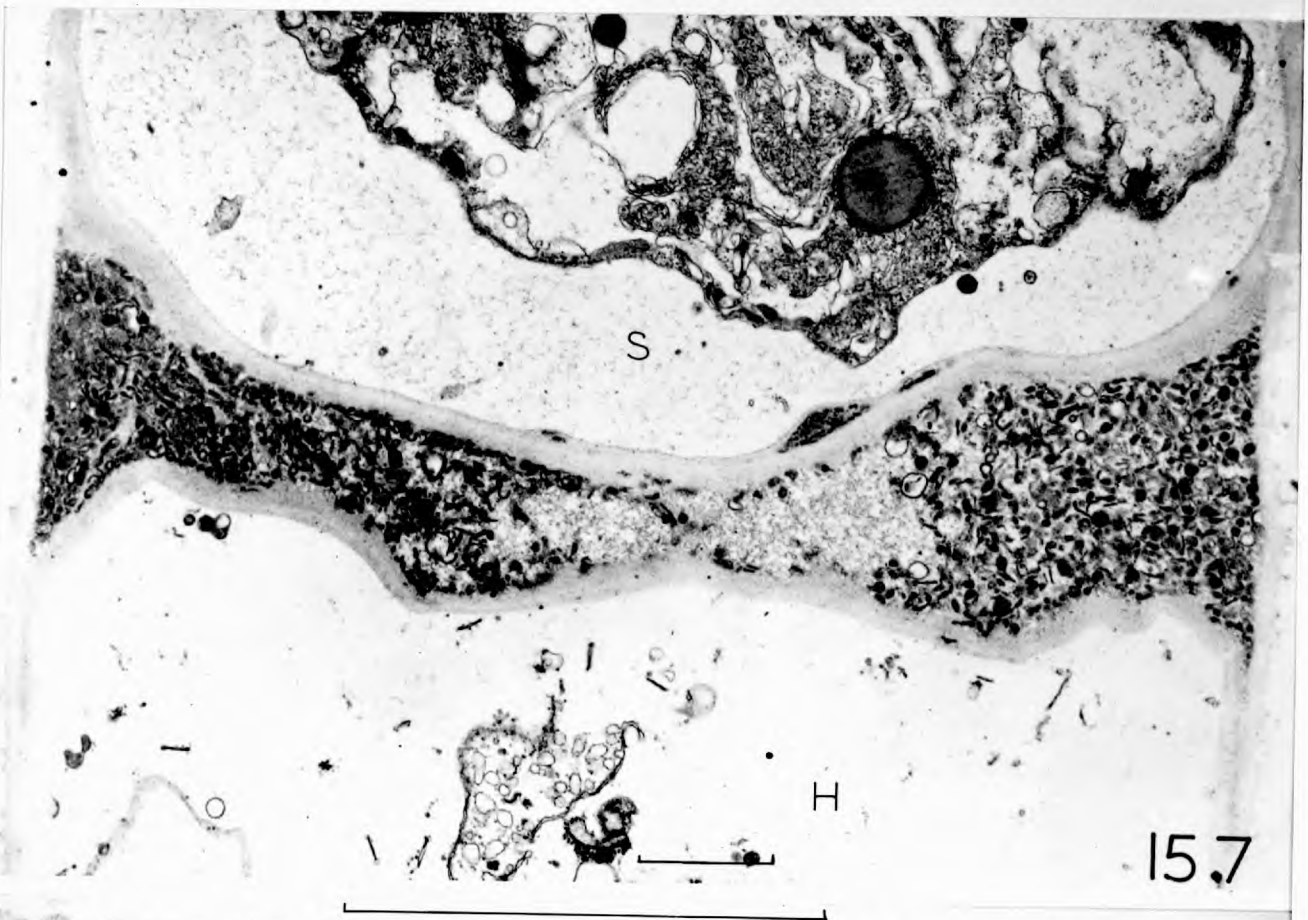

15.7

157a

Fig.158. Swollen hypha in the region where the cross wall should appear. Note low density of organelles and unusual circular structures. Os only. 1241D/2. 8270.

Fig.159. Developing cross wall with numerous wall vesicles on each side. 1645/2. 10020.

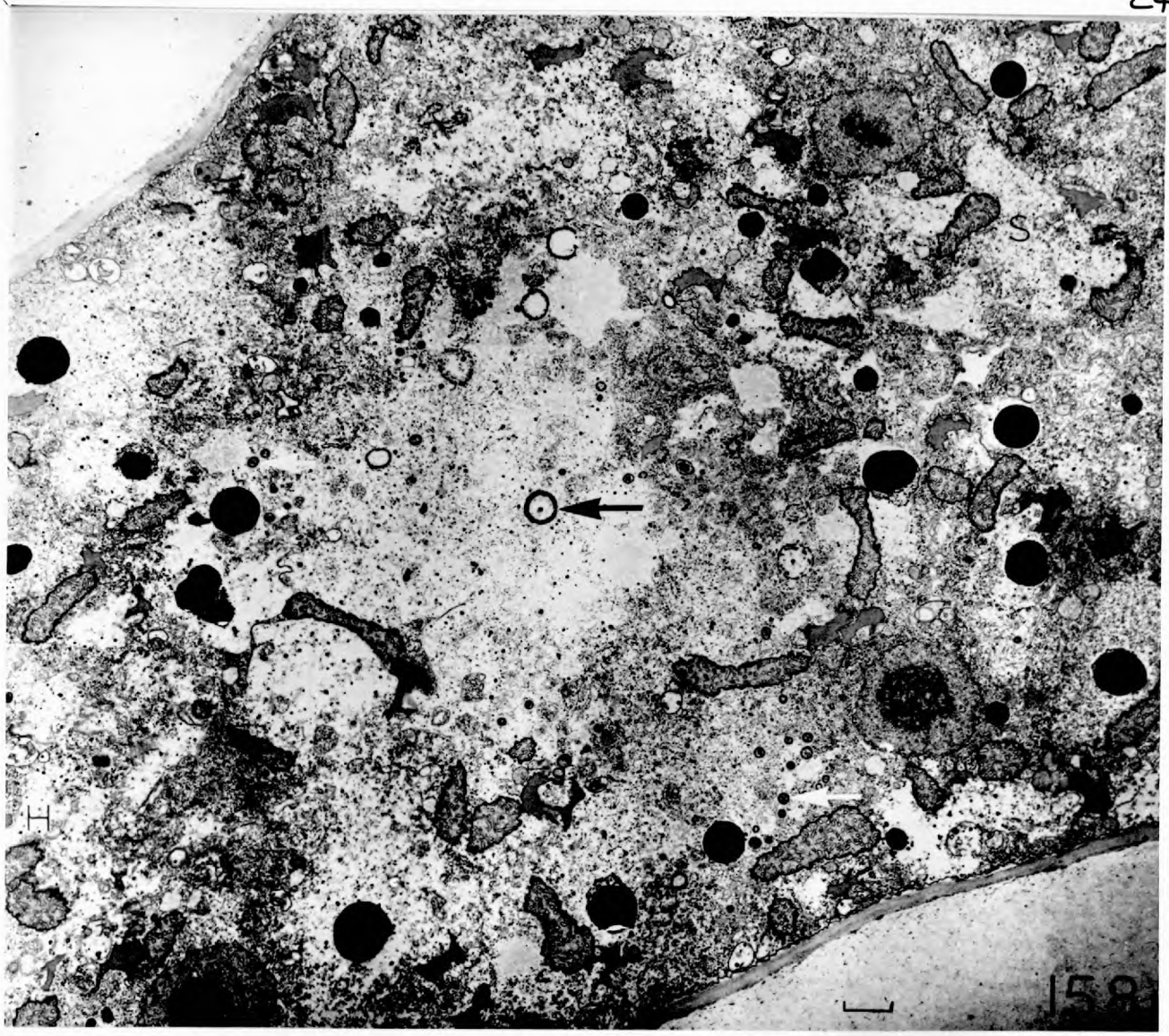
S
H
158


Wv
S
Wv
H
159

Fig.160. Pre-cleavage sporangium which has developed a cross wall after growing through the cross wall of a discharged sporangium whose wall can be seen outside the present sporangium. 1848D/5. 12013.


S
S
H
160

Fig.161 Spore observed to be encysting with the light microscope before fixation. Note thin distorted cyst wall which is probably not fully formed since the spore has a plasmolysed appearance similar to that of motile spores(c.f.Fig.146) and still contains one or two bars. The flagellum axoneme is still visible. 1642/4. 12063.

Fig.162. An older encysted spore in the same sporangium as Fig.161. Flagella have depolymerized to the kinetosomes, the flagella roots are present and the Golgi is still active. Note thin dense cyst wall with spines and flagellum and flimmer probably belonging to one of the unencysted spores which were present. 1642/4. 12069.

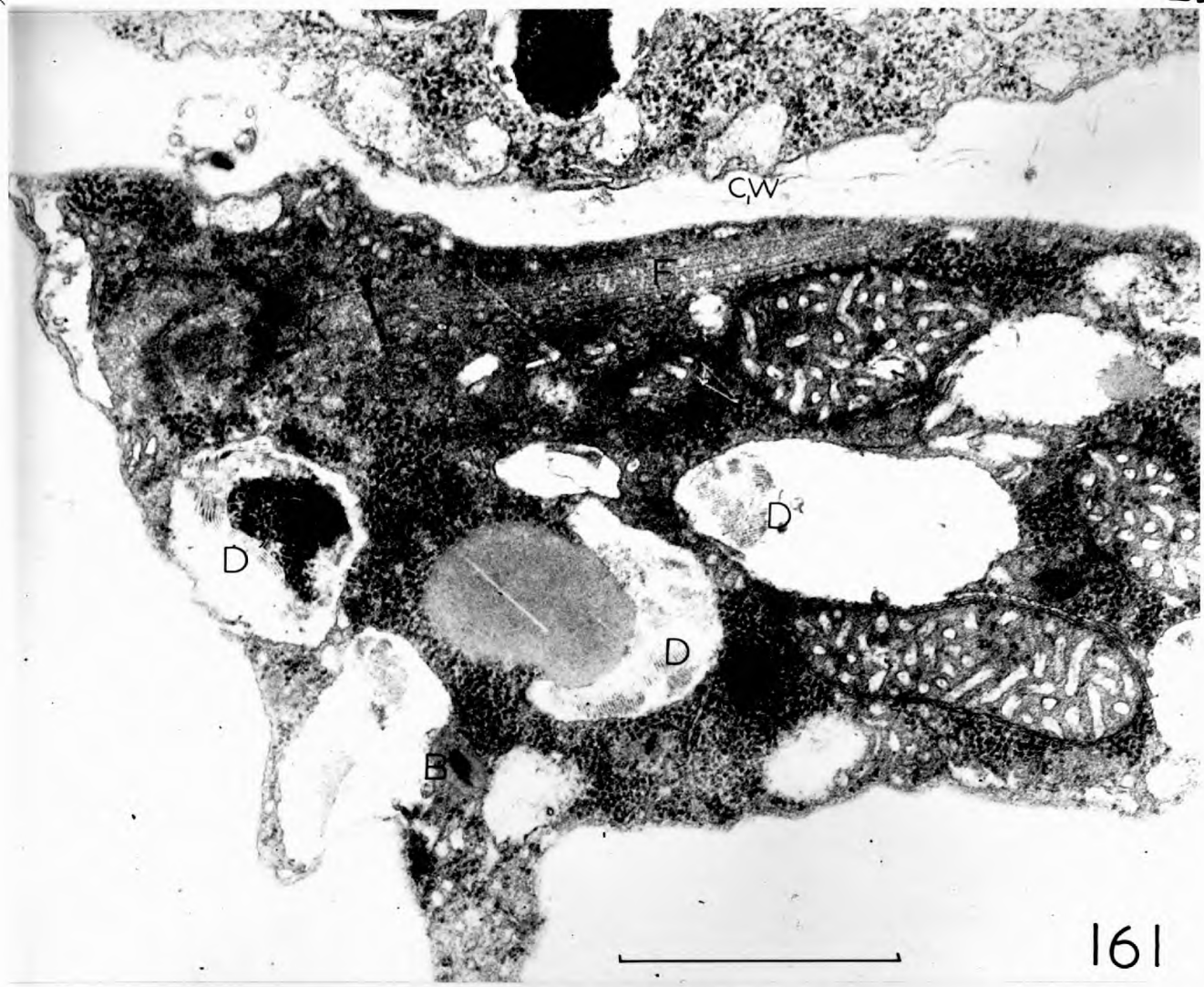

161

162

Fig.163. Shadowed untreated mount of a primary cyst showing amorphous surface layer with short spines, often attached in groups. 2102/1. 14053.

Fig.164. Detail of untreated, shadowed primary cyst. 2102/2. 14063.

163

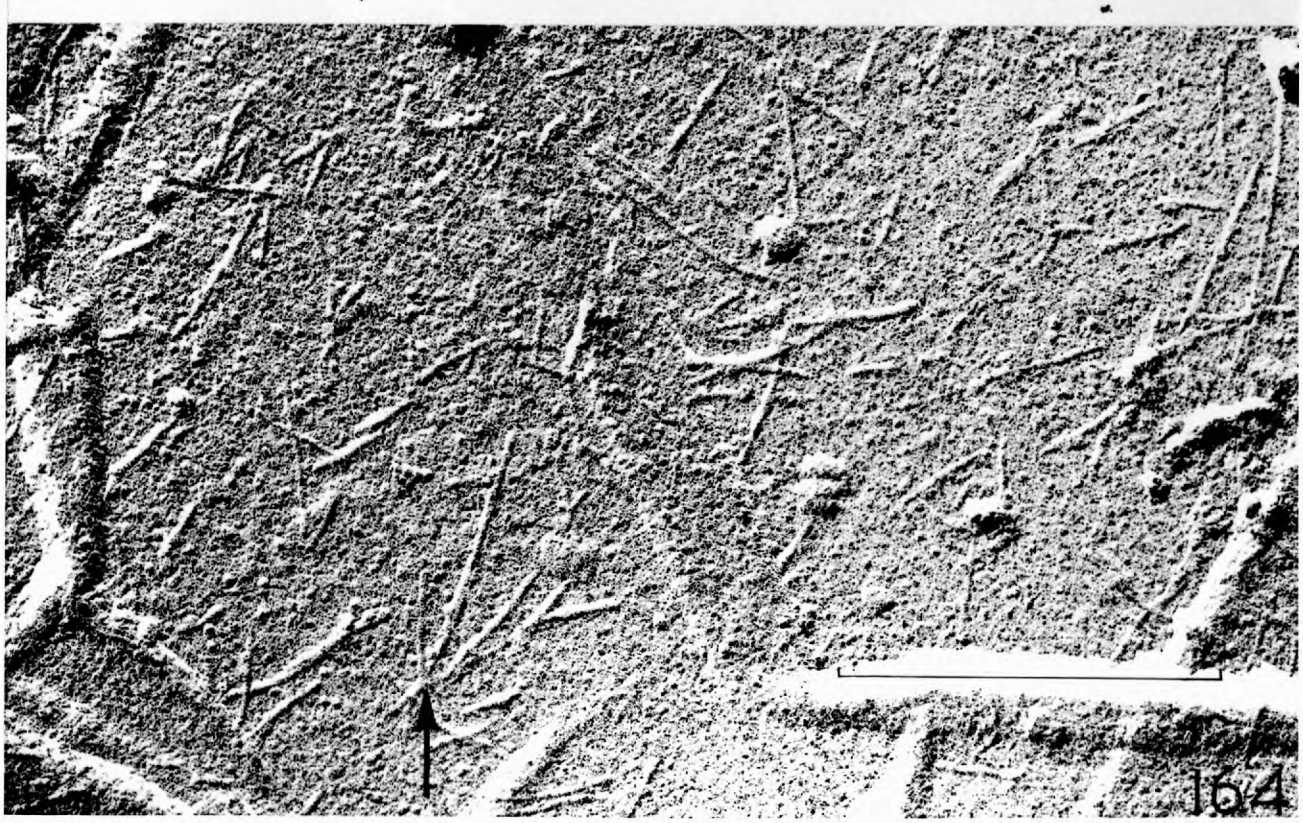

164

Fig.165. Primary cysts within a sporangium showing 2 layered cyst wall and distorted, tubular flimmer attached. Note fibrils in the E.R. 2099/3. 14307.

Fig.166. Primary cyst showing a possible Golgi origin for the vesicles which apparently contribute material to the cyst wall. Note fibrils in the E.R. 1776/1. 10484.

165

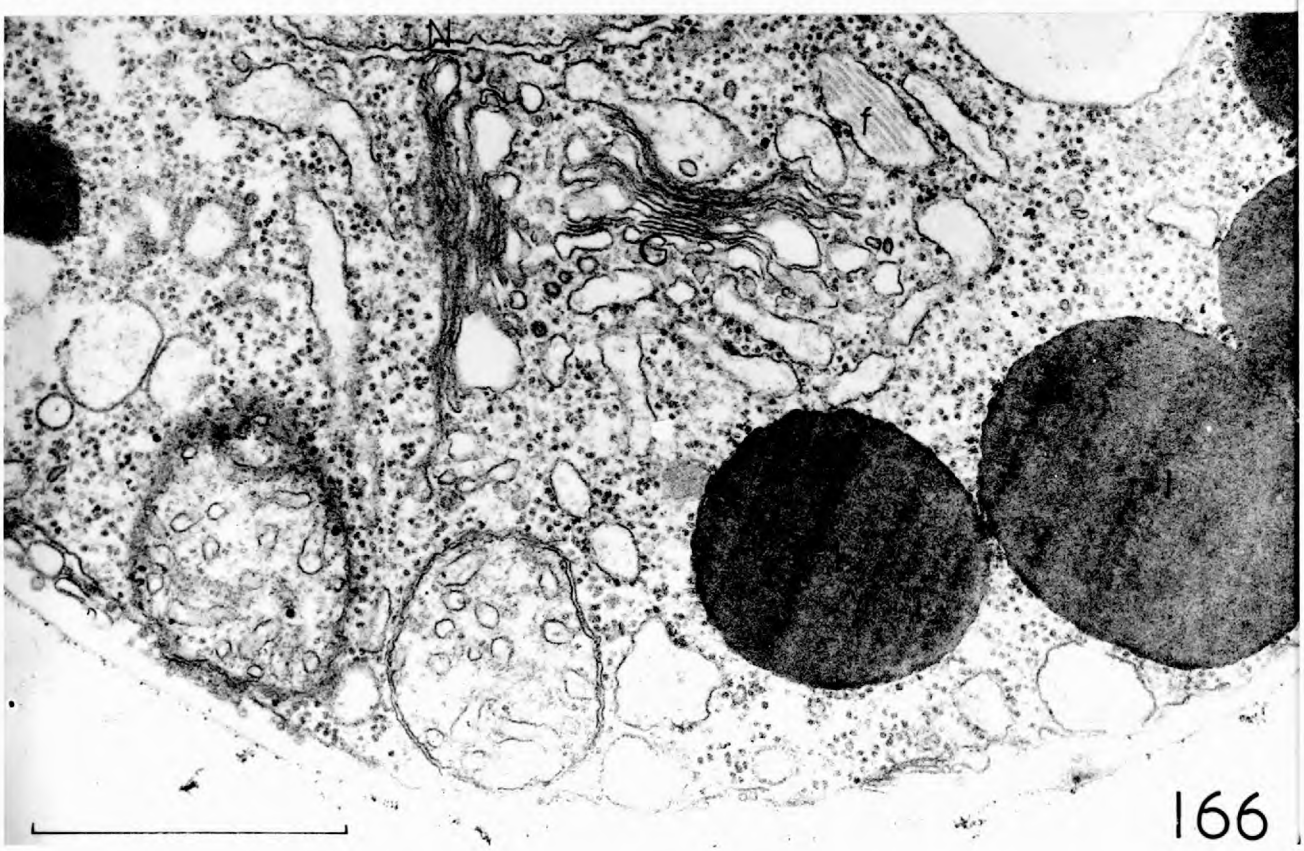

166

Fig.167. Damaged primary cyst with heavy PAH reaction on the plasmalemma and inner wall layer but low deposit on the outer wall and spines. 1776/13. 10868.

Fig.168. Increased PAH reaction in Golgi cieternae away from the nucleus and into the Golgi derived vesicles. Note characteristic primary cyst wall reaction. 1776/13. 10874.

Fig.169. Increased PAH reaction of Golgi cisternae away from the mitochondria and into Golgi vesicles. 1776/13. 10878.

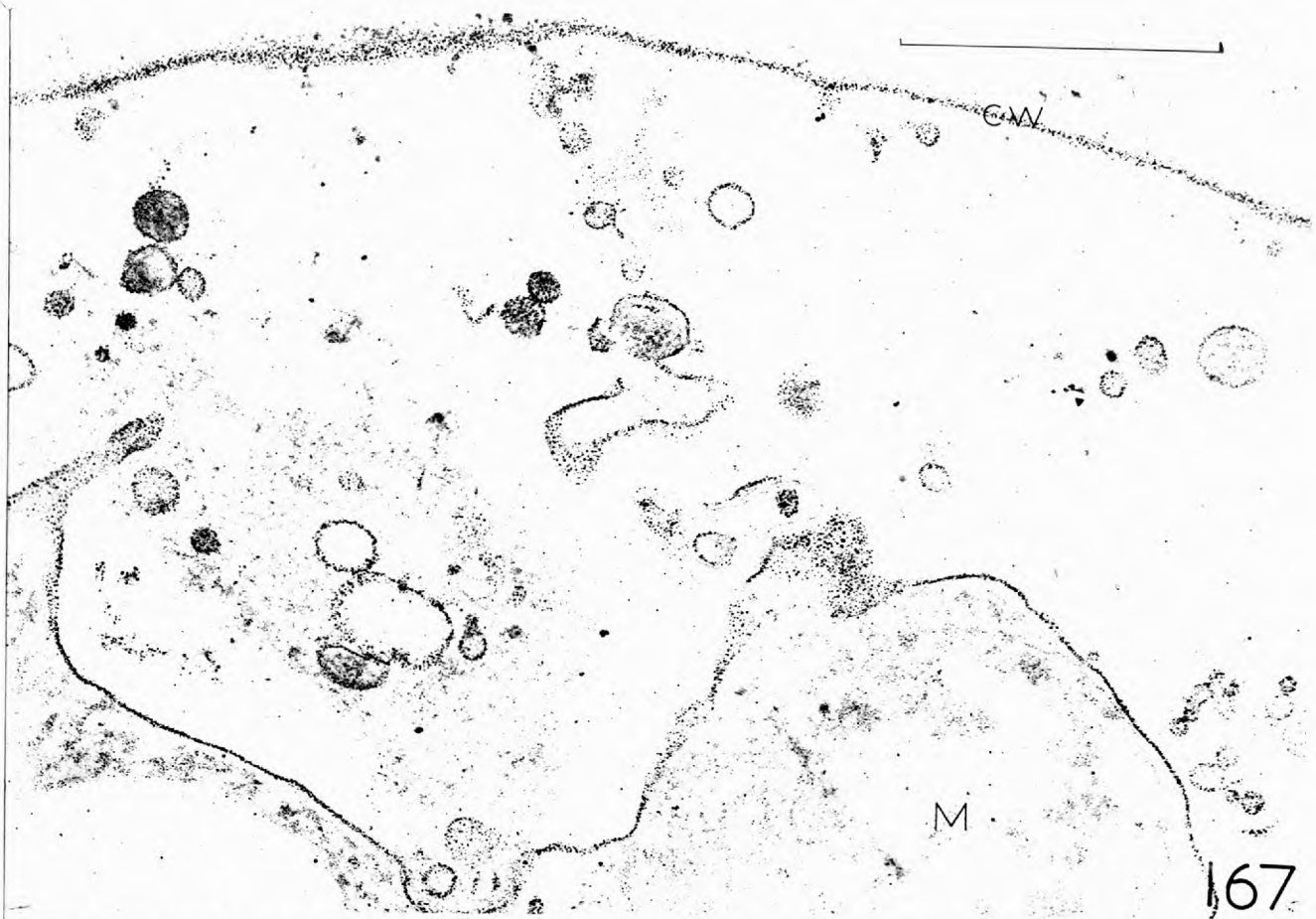

167

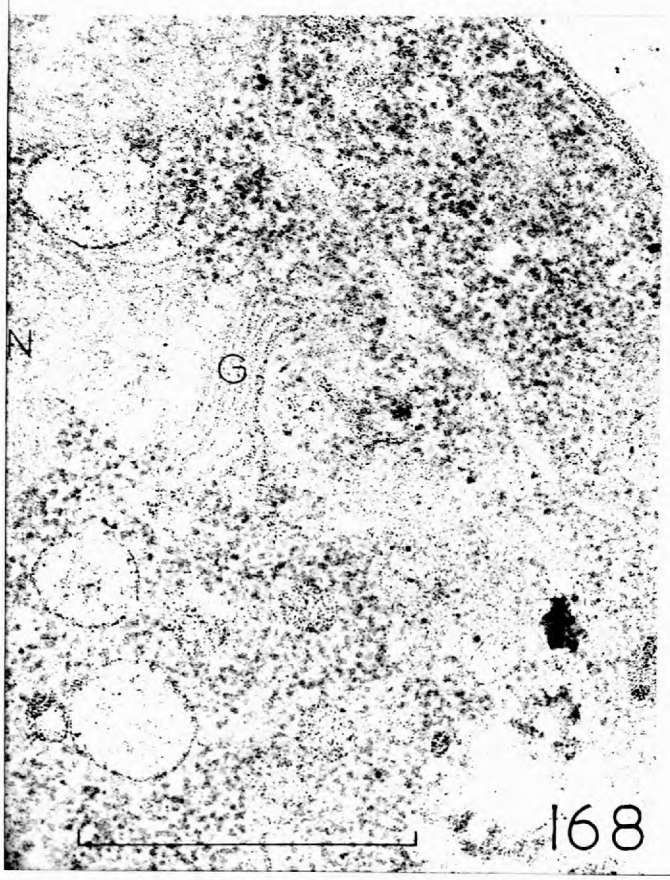

168

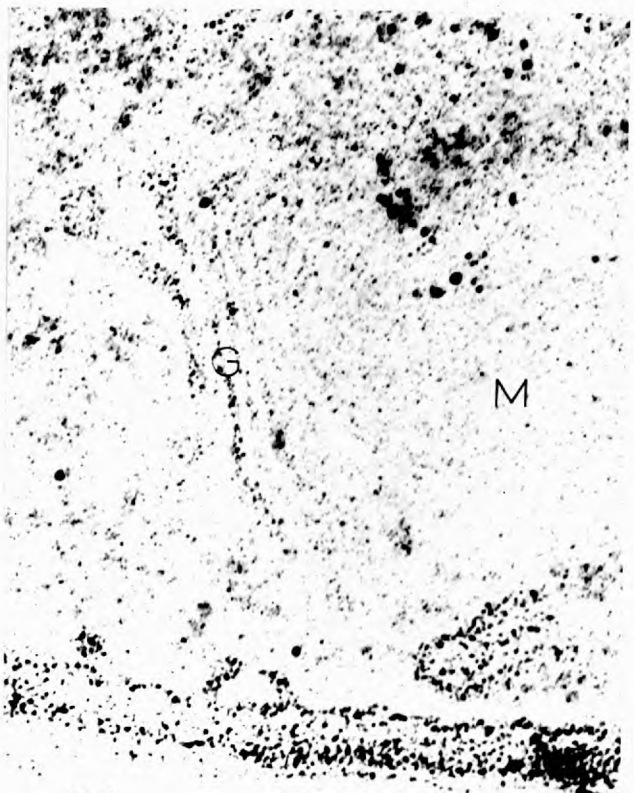

0·1

169

Fig.170. Primary cyst showing PAH reaction of E.R. contained fibrils and increasing reaction of Golgi cisternae away from the mitochondrion. 1776/13. 10877.

Fig.171. Primary cyst with strongly PAH posative plasmalemmasome. 1776/15. 10880.

Fig.172. Primary cyst with PAH posative inner wall layer and lomasome but light reaction on outer wall layer and spine. 1776/13. 10876.

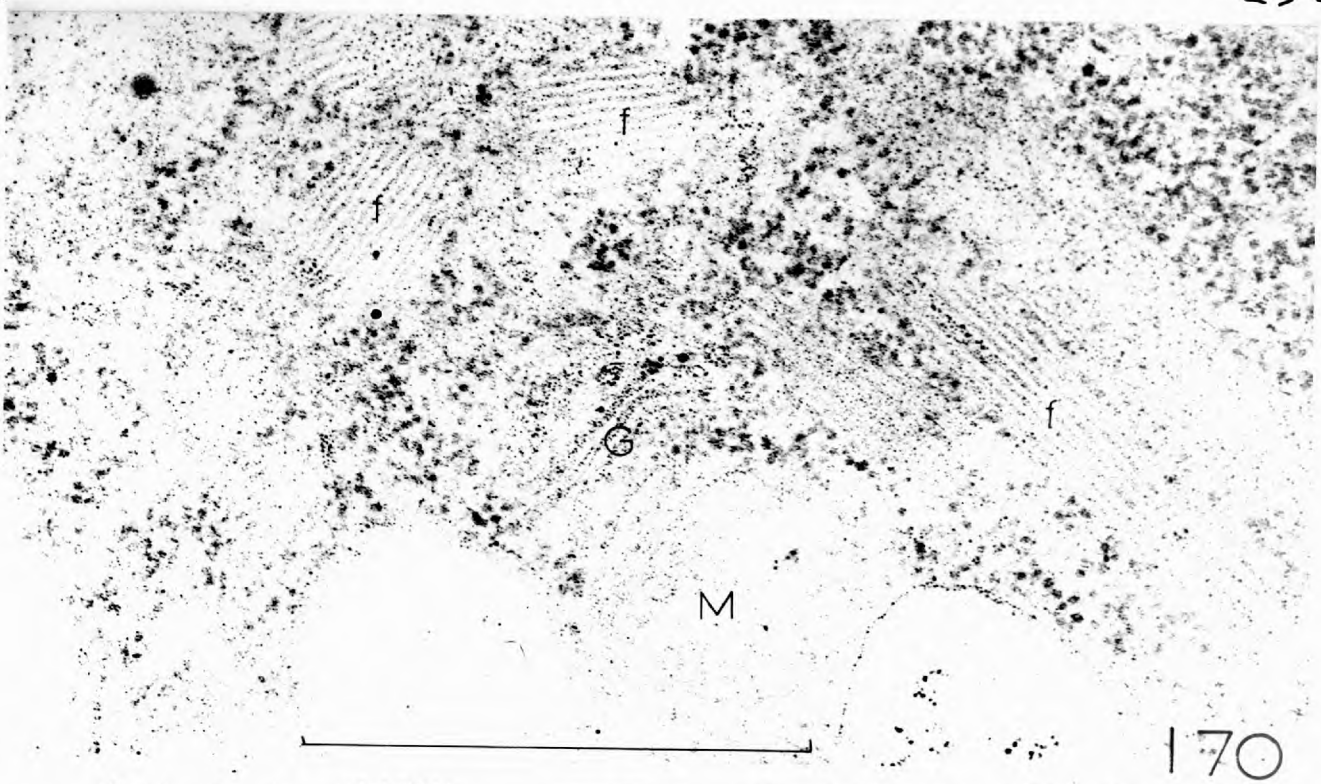

170

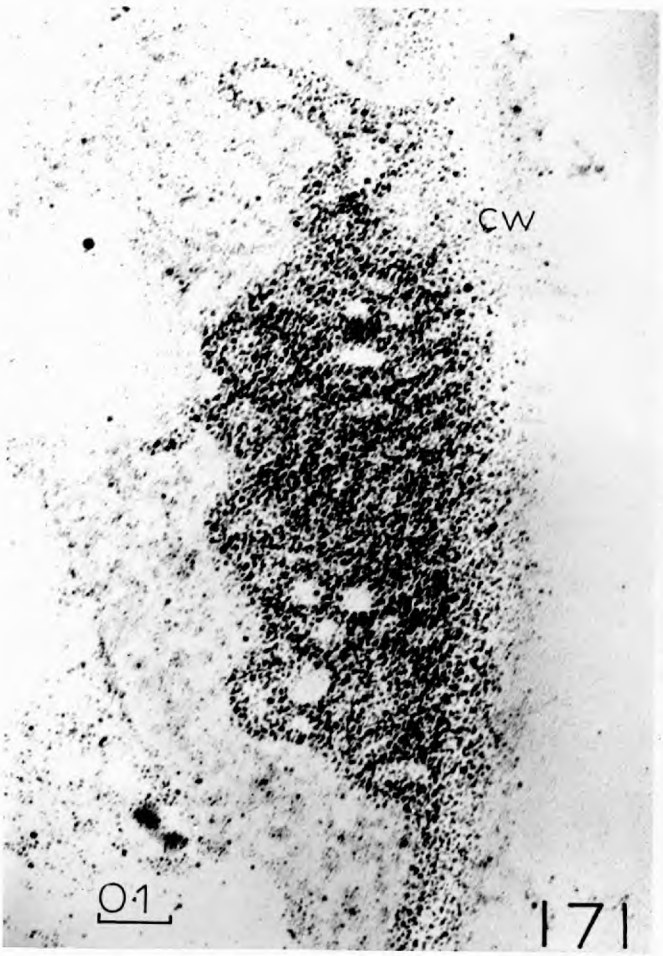

171

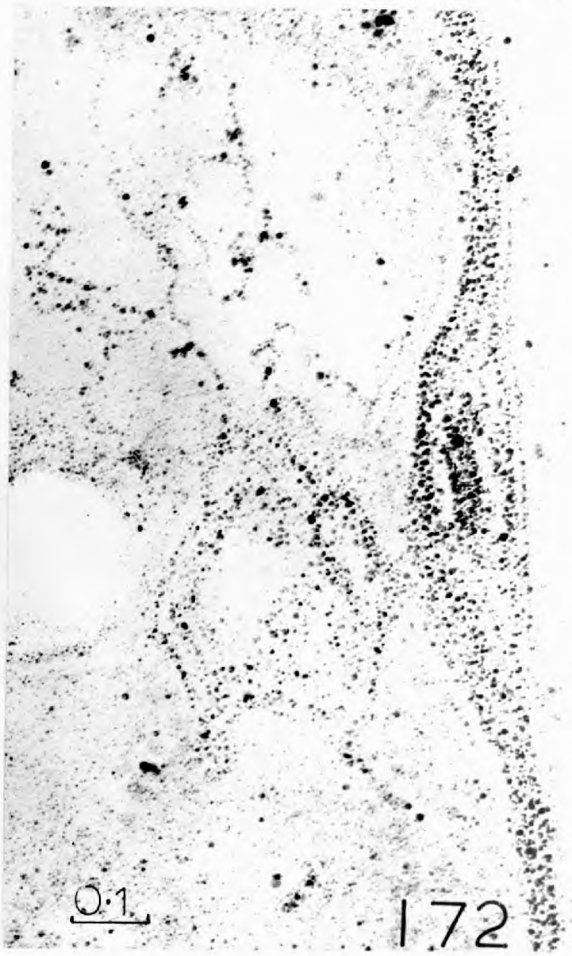

172

Fig.173. Primary cyst showing clusters of spines. 2061/2. 12966.

Fig.174. Primary zoospore with strong PAH reaction on the plasmalemma and lighter reaction on the primary bars. 1887/6. 12721.

Fig.175. Primary bars in zoospore. Note amorphous material lining bar and the enclosed tubules. 1887/4. 12709.

Fig.176. Primary bars. The zoospore plasmalemma was damaged during fixation. 1887/4. 12710.

173

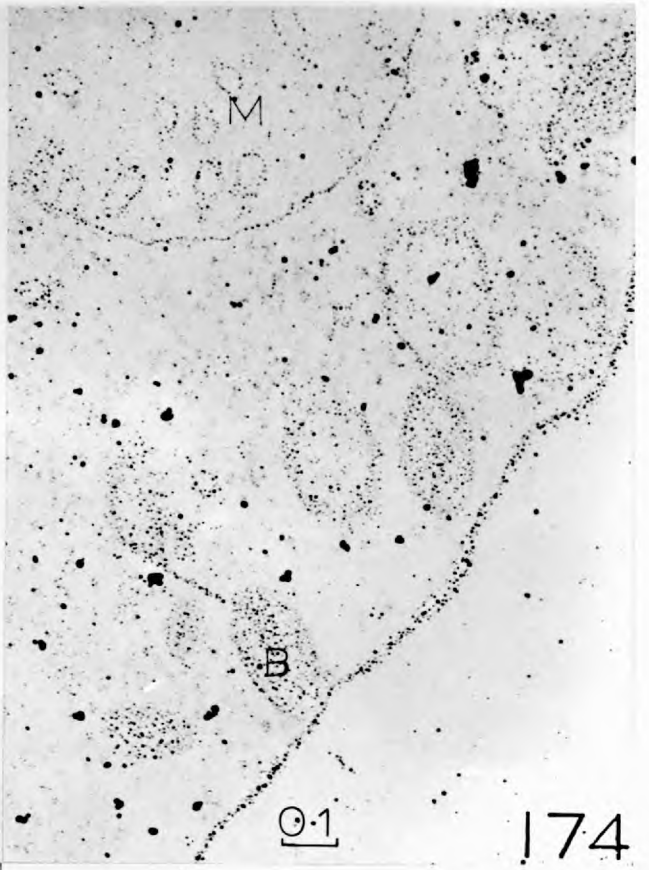

174

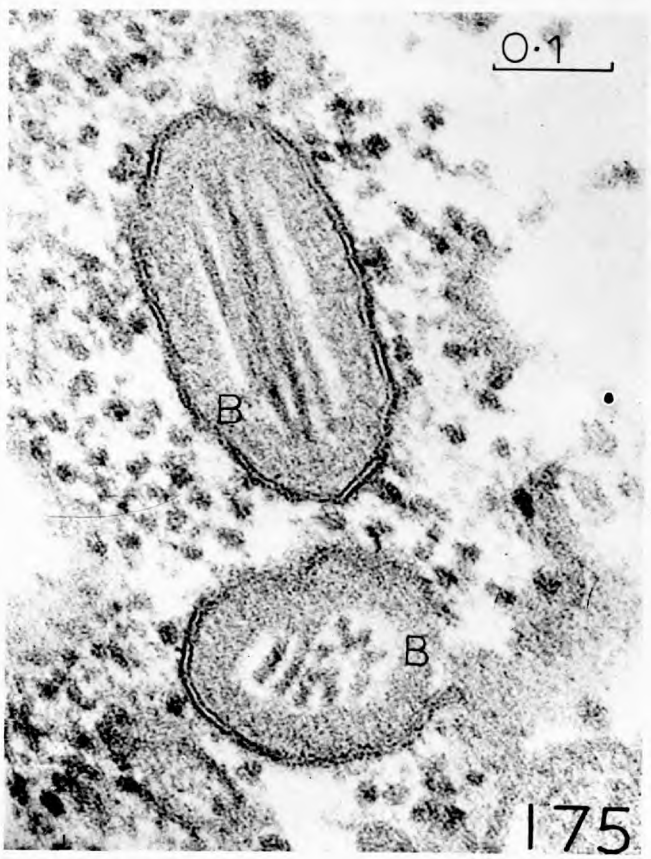

175

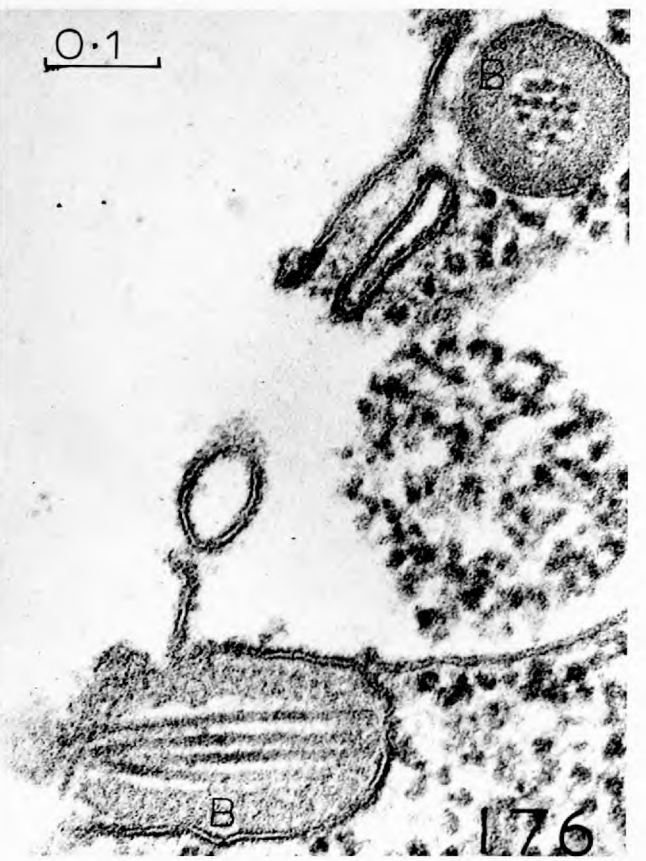

176

Fig.177. Section of primary zoospore(before encystment) showing number and distribution of bars. 0.1% GA. 1887/4. 12708.

Fig.178. Secondary cyst with boathook adjacent to an empty primary cyst with spines. 1779/1. 14102.

Fig.179. Secondary cyst showing boathook and plaque(arrowed) on less dense wall. 1779/1. 14097.

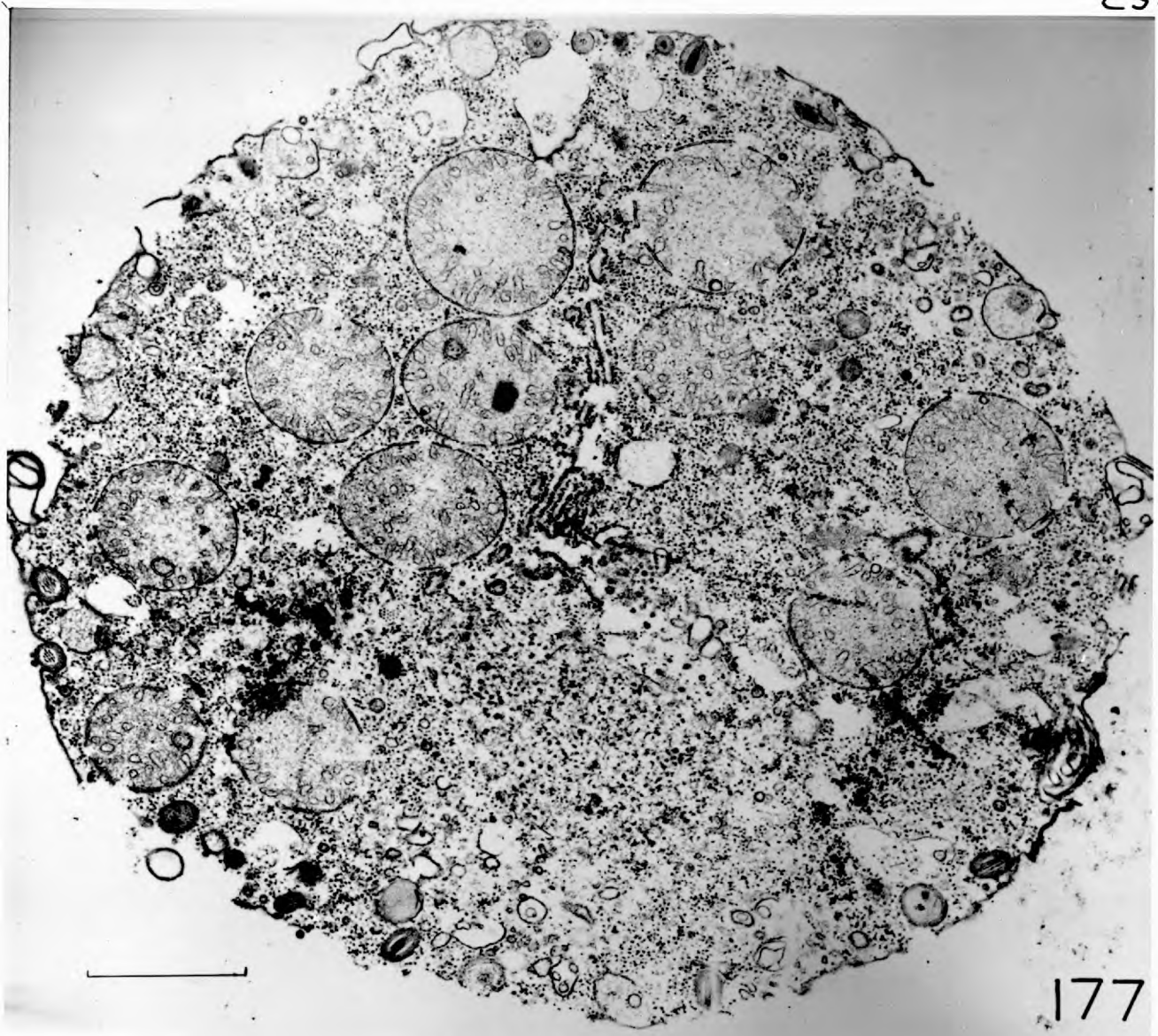

177

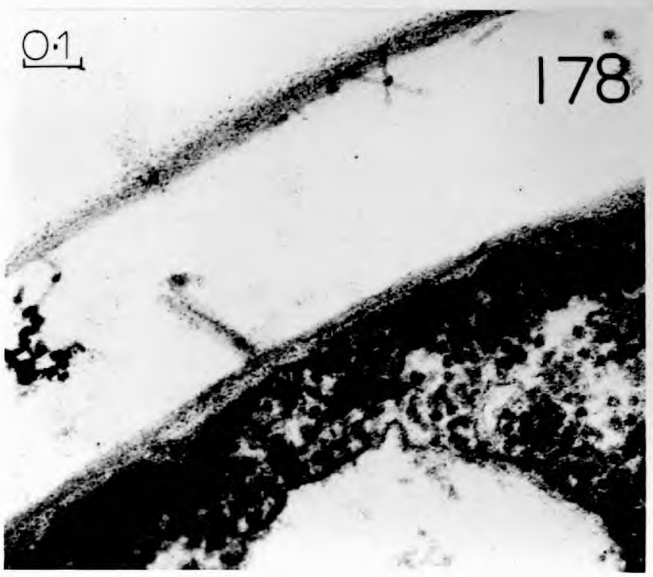

178

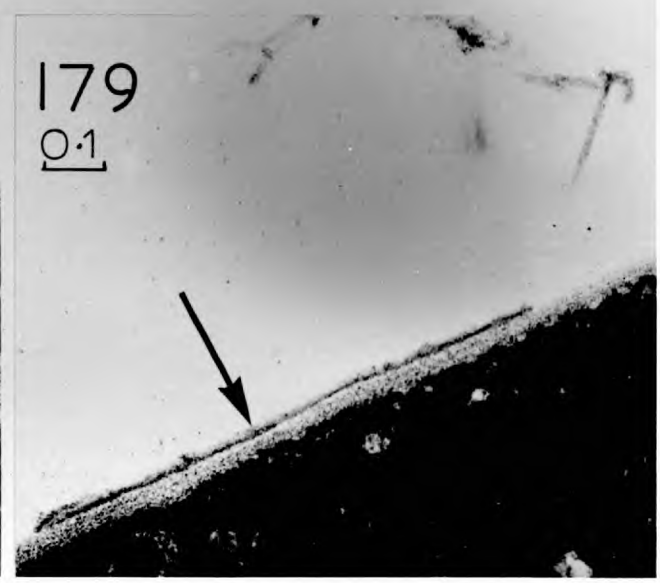

179

Fig.180. Untreated shadowed secondary cyst showing fibrillar nature of the wall and boathooks whose bases are surrounded by amorphous plaques overlying the fibrils. 2102/2. 14064.

Fig.181. Detail of similar secondary cyst to Fig.180. 2102/1. 14052.


180

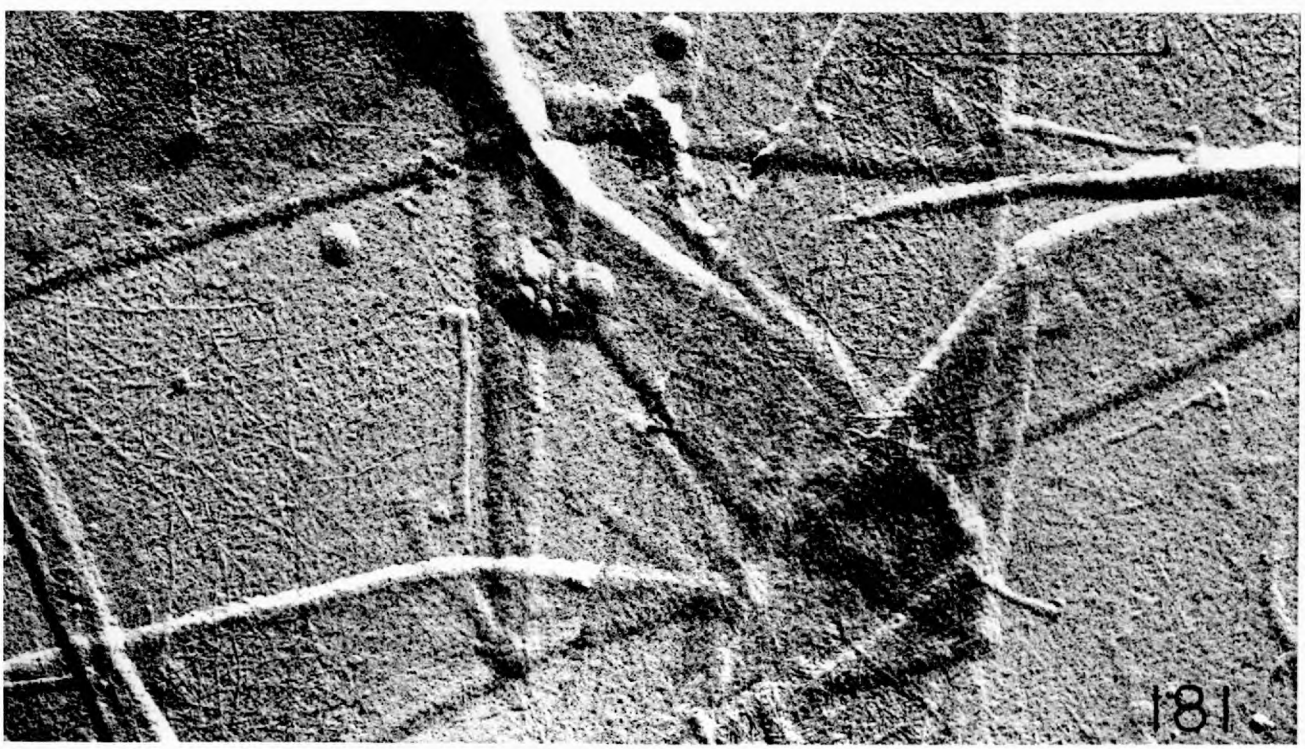
181

Fig.182 & 183. Typical views of secondary bars in primary cysts. Fig.182 is probably accentric whilst Fig.183 is equatorial. 1779/2. 14112 & 1779/2. 14109.

Fig.184. Encysting primary spore of D. sterile. Note kinetosomes, flagella roots, active Golgi and numerous wall vesicles and excess plasmalemma around the developing cyst wall which looks an electron opaque outer layer. 1853B/1. 12163.

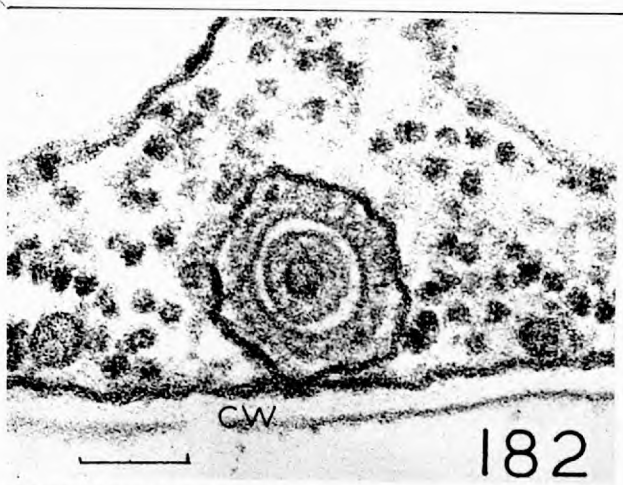
CW
182

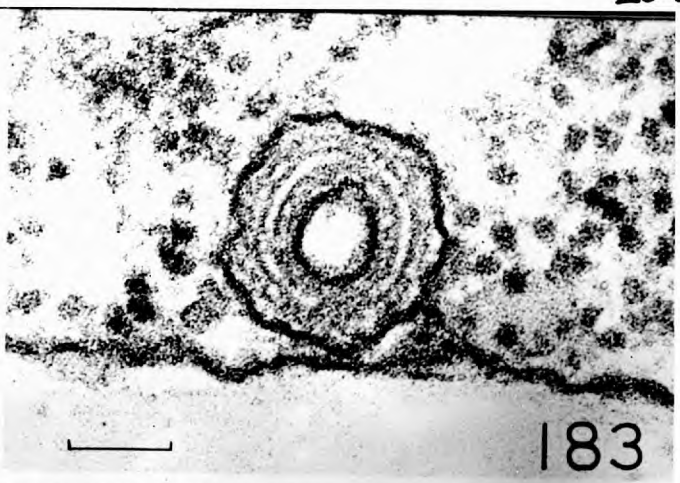
183

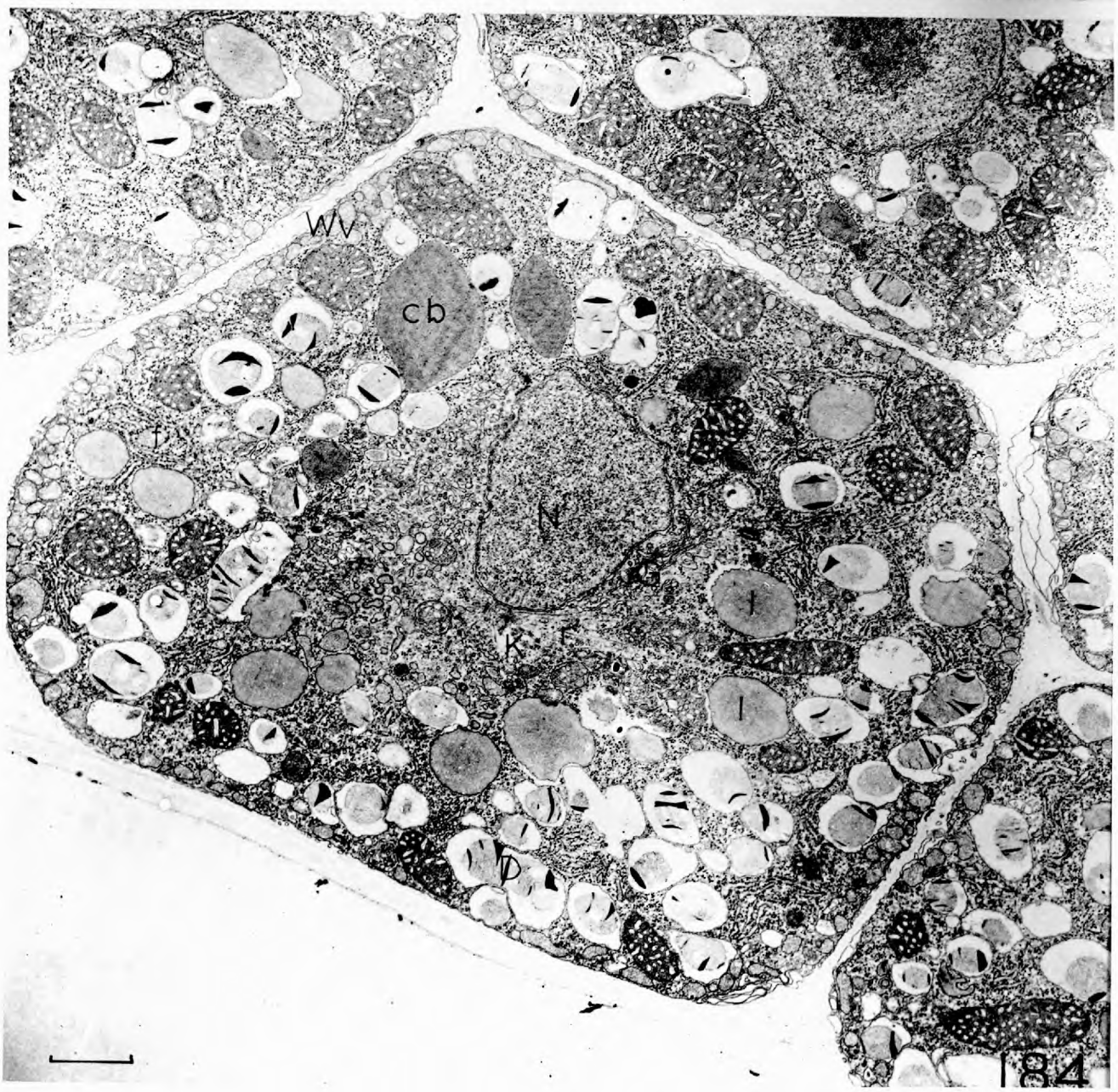
WV
cb
f
N
K
184

Fig.185. D. sterile. Detail of spore in same sporangium ~~and~~ as Fig.184. Note crystalline bodies and excess plasmalemma on developing cyst wall. 1853B/1. 12166.

Fig.186. D. sterile. Later stage in cyst wall formation. Note lomasomes and plasmalemmasomes. 1853/1. 12154.

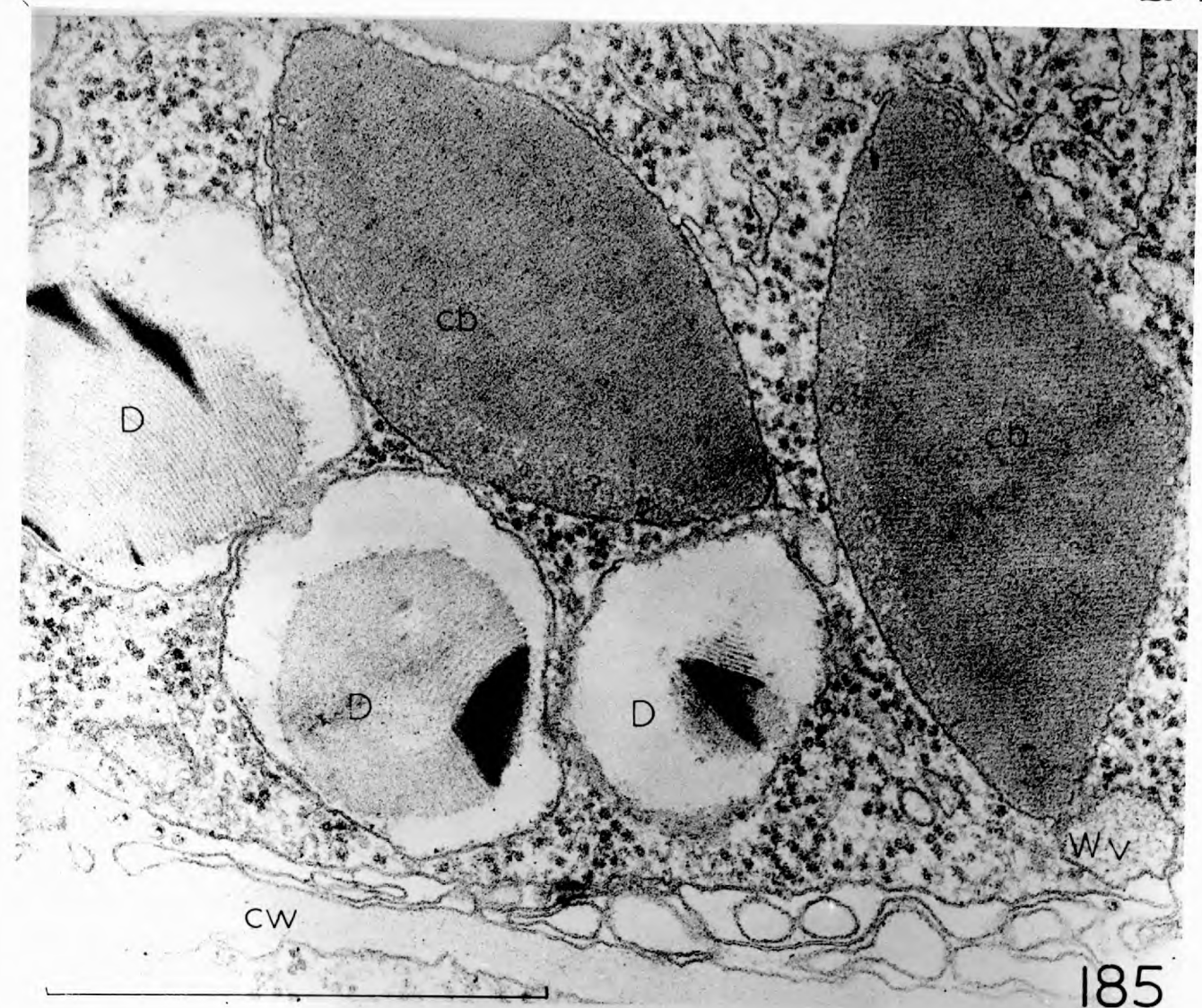
cb
D
cb
D
D
Wv
cw
185

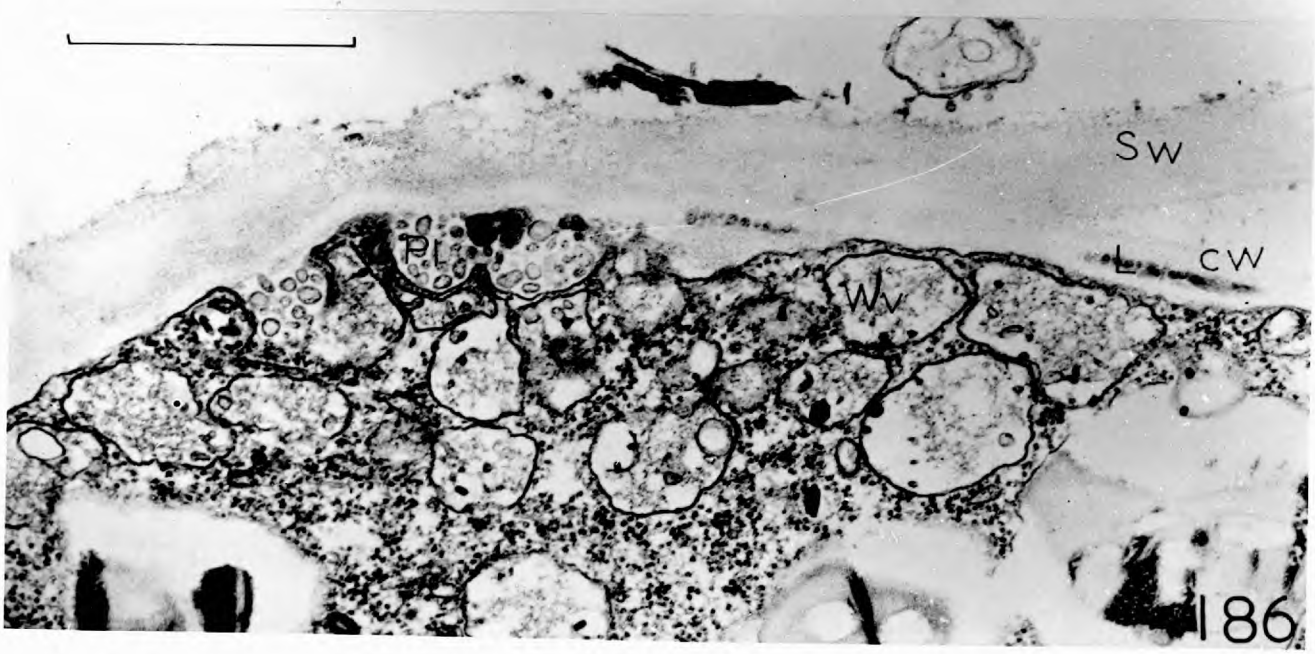
Sw
Pl
cw
Wv
186

Fig.187. D. sterile. Secondary cyst with a typical spine. Note two layered wall structure. 1853A/2. 12187.

Fig.188. D. sterile. Primary cyst in sporangium showing a spine surrounded by amorphous material which constitutes a bar and apparently mature fibrils in a vesicle. 1853/1. 12197.

Fig.189. D. sterile. Detail of a bar in a primary cyst. Os only 1852/2. 12178.

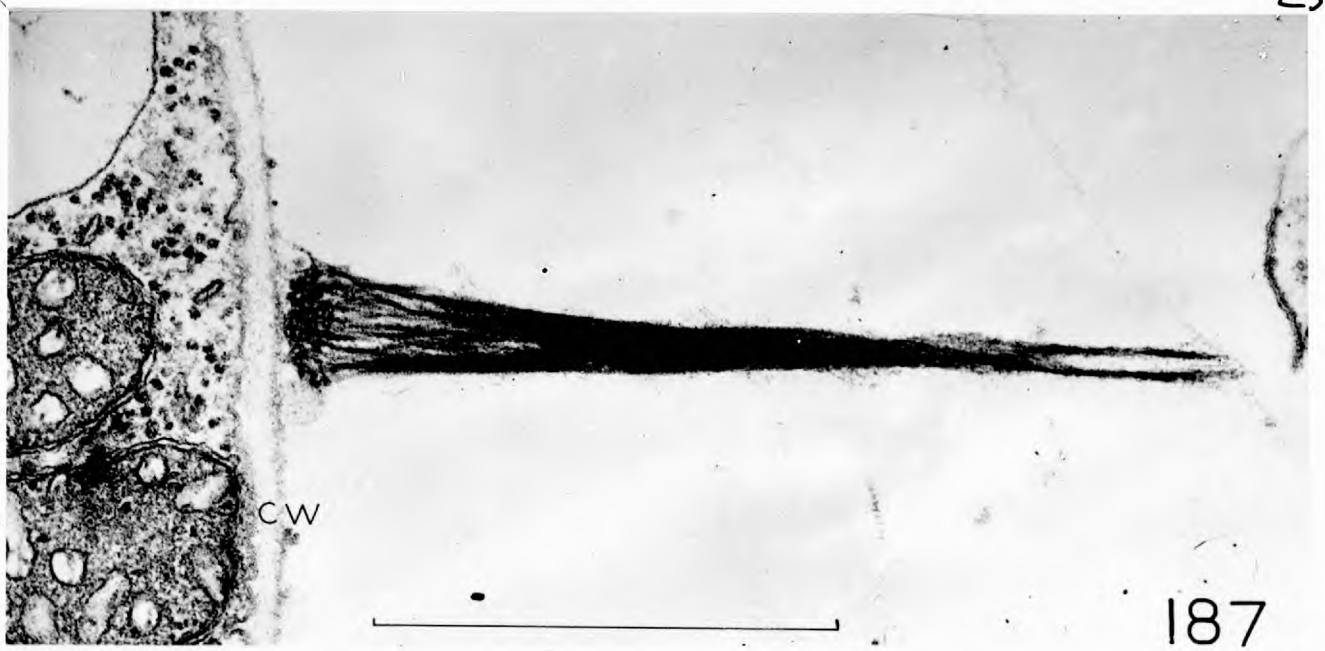
CW
187

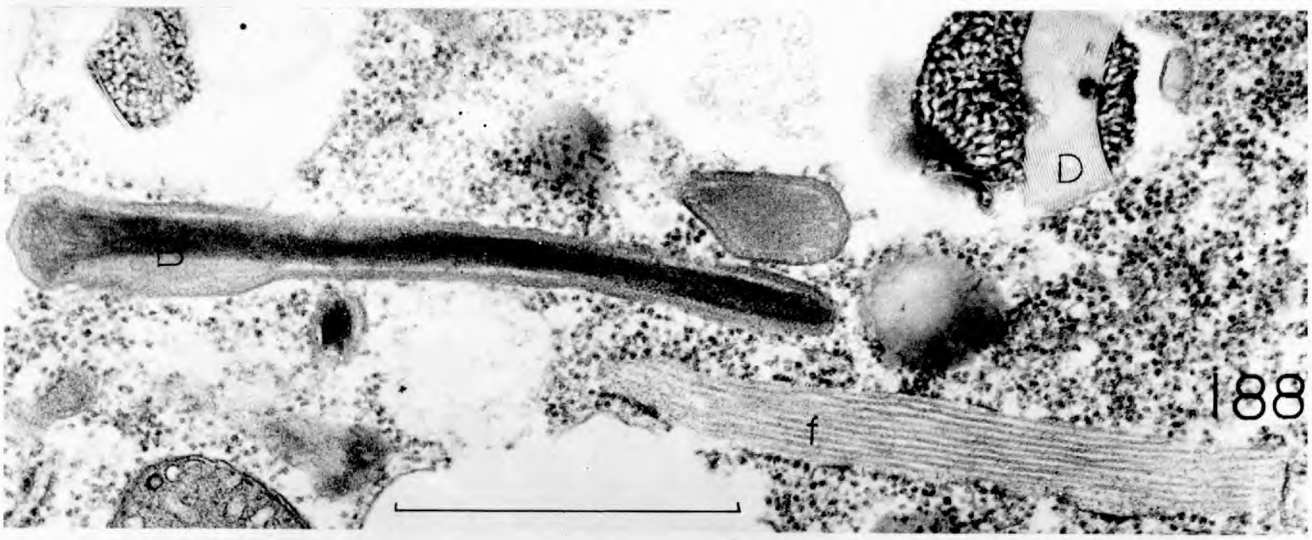
D
D
f
188

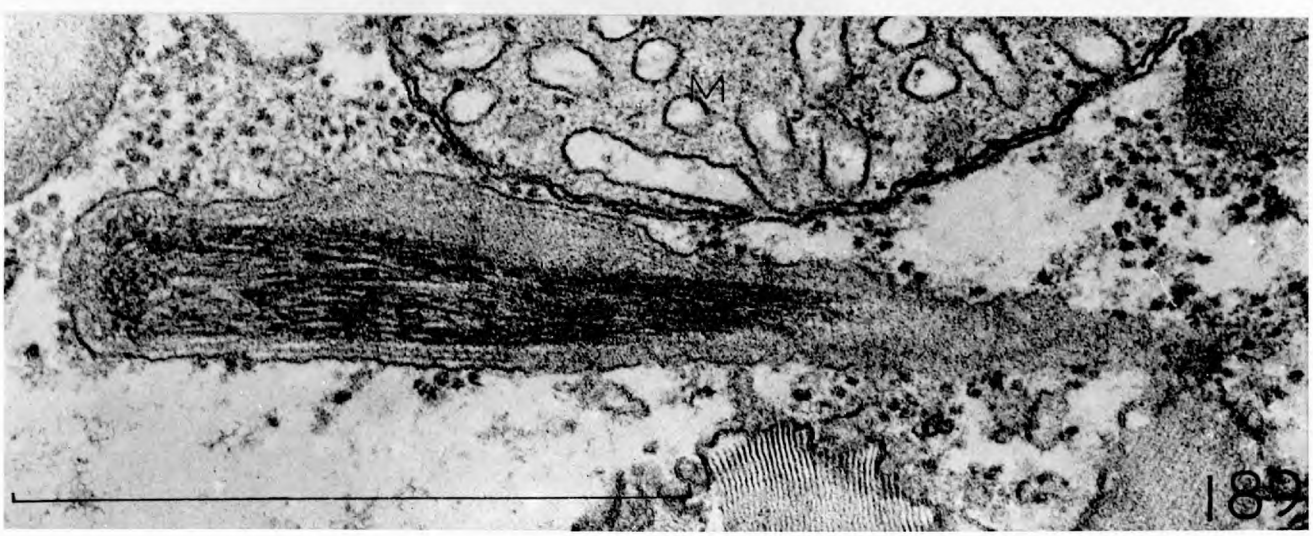
M
189

Fig.190. Probable development of a lomasome showing plasmalemmasomes, embedded lomasome and a smaller lomasome becoming lost as the wall ages. 1644/3. 10369.

Fig.191. The probable pattern of passage of a lomasome through a wall. This is in fact an old discharged sporangium wall with degenerating outer layers. 1647/1. 10359.

Fig.192. Permanganate fixed lomasome. 1387B/3. 8250.

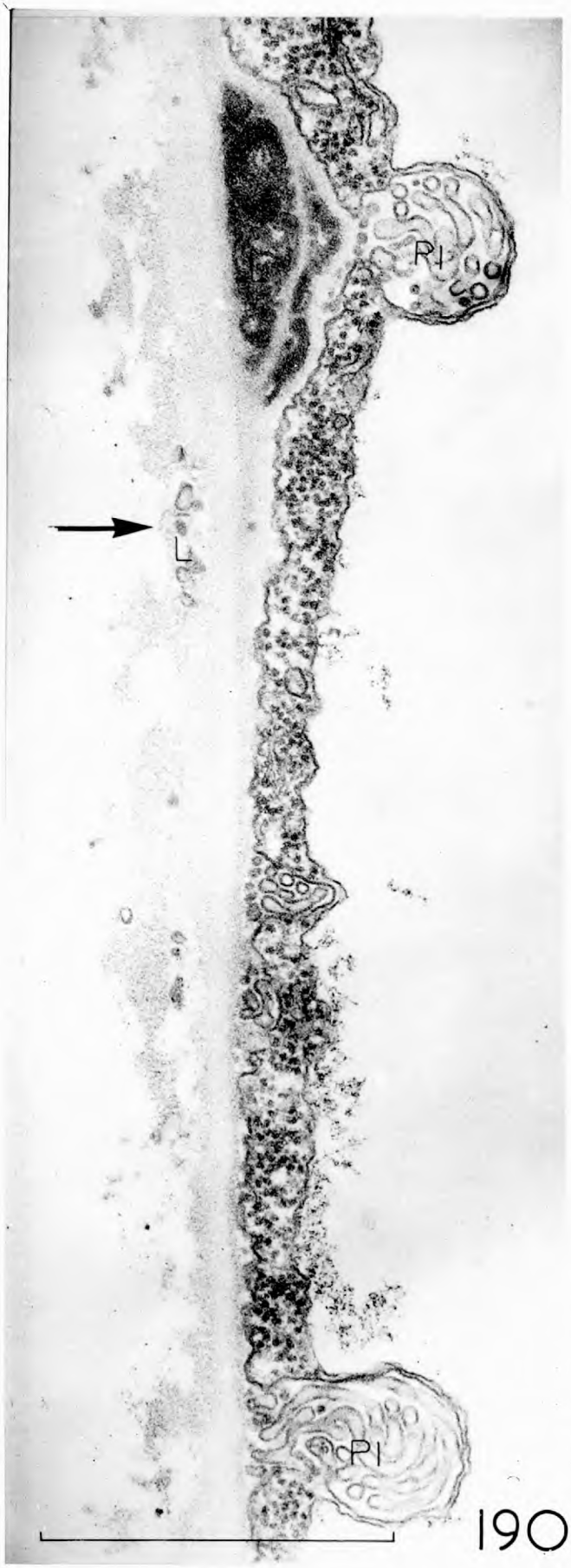

190

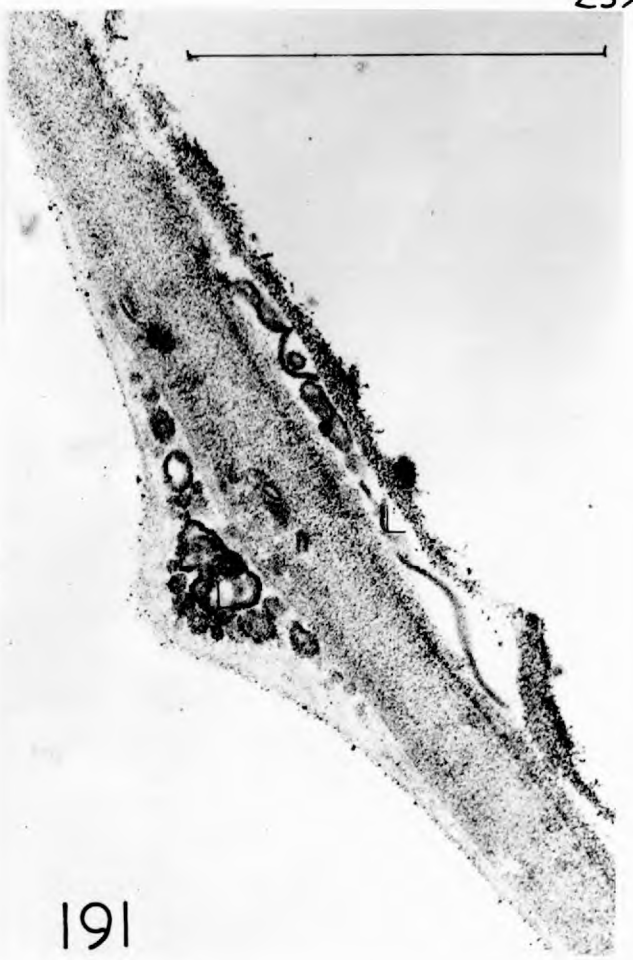

191

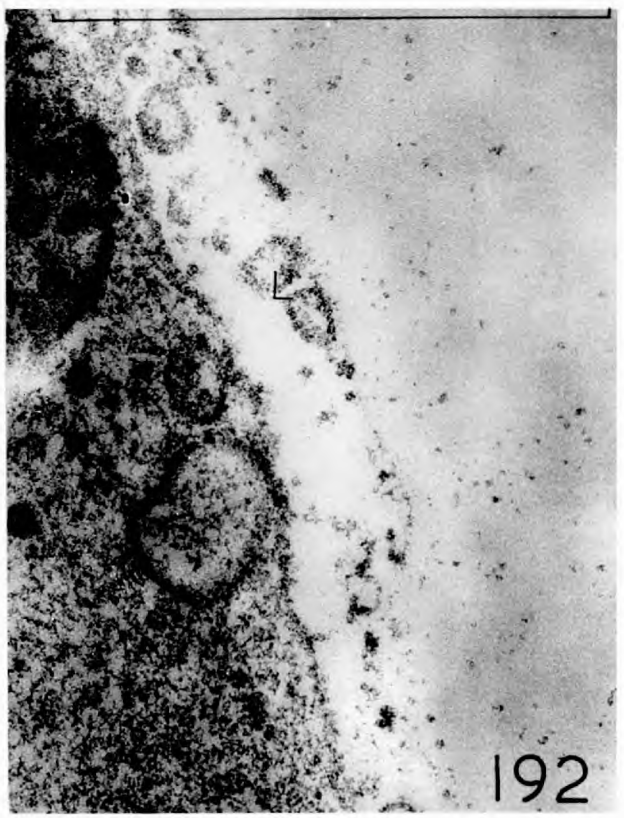

192

Fig.193. Plasmalemmasome adjacent to a lomasome. 1388/18. 6084.

Fig.194. Lomasomes in a sporangium wall. Note ribosomes included in lomasome. Os only. 1241B/2. 8274.

Fig.195. Plasmalemmasome showing wall specific staining deposit. Os fixed, acetone dehydrated. 1651/2. 8476.


Pl
V
W
0·1
193

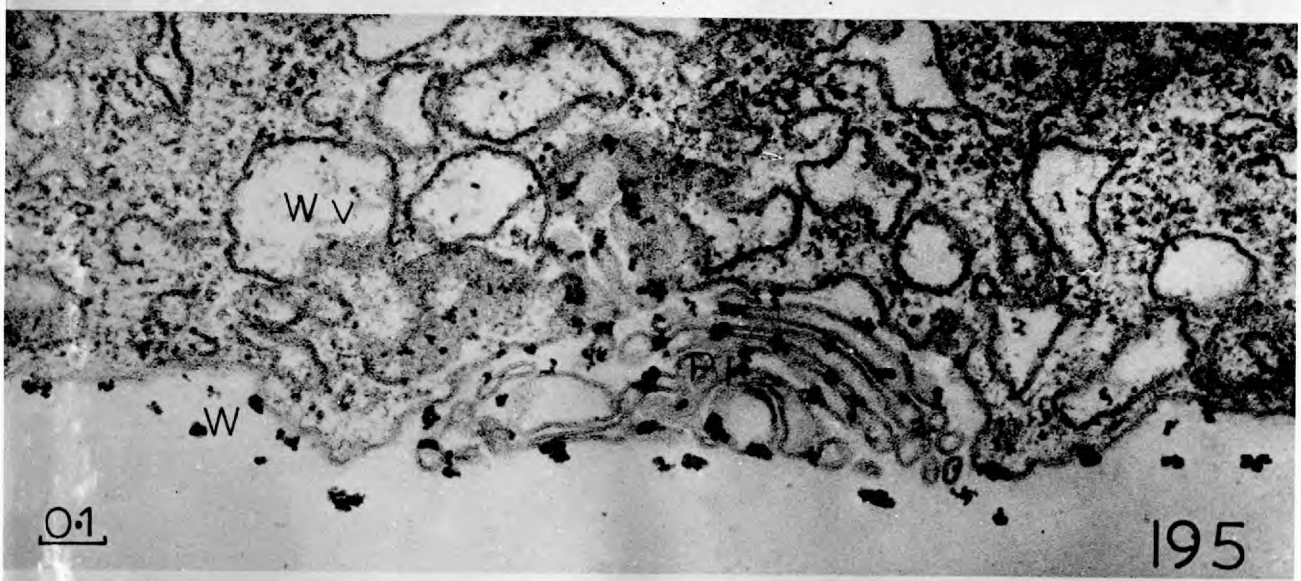
W
V
Pl
W
0·1
195

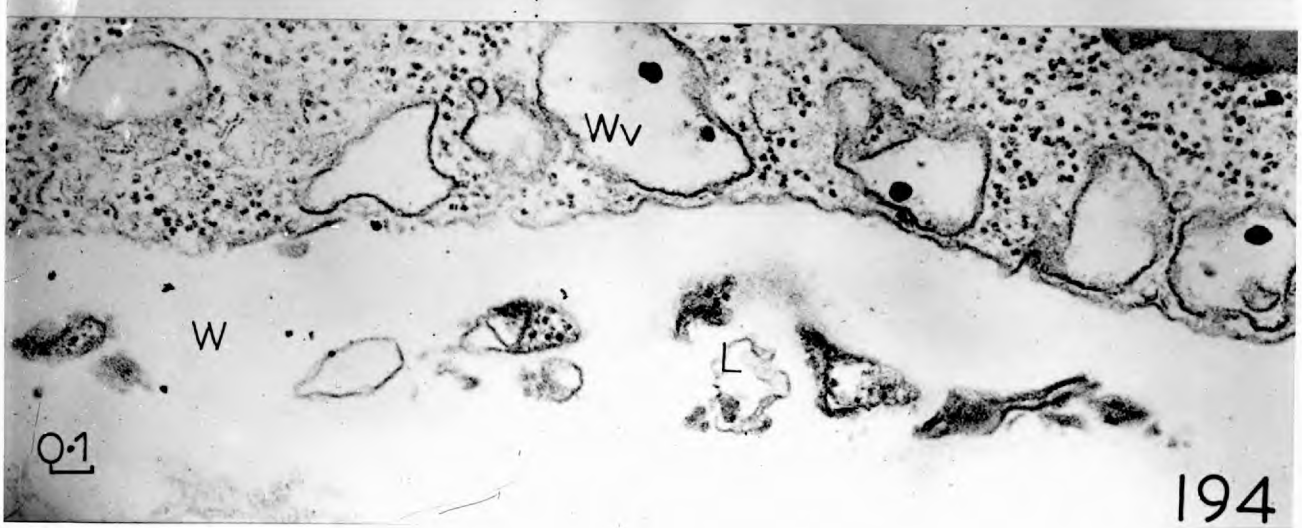
Wv
W
L
0·1
194

Fig.196. Plasmalemmasome and Golgi, E.R., mitochondrion association after permanganate fixation. 1493/1. 6419.

Fig.197. Tubular-vesicular plasmalemmasome. 1388/14. 6089.

Fig.198. Plasmalemmasome with a possible connection between the plasmalemma and a vesicle. 1301/8. 6016.

Fig.199. Tubular plasmalemmasome after Os fixation. 1652A/5. 8515.

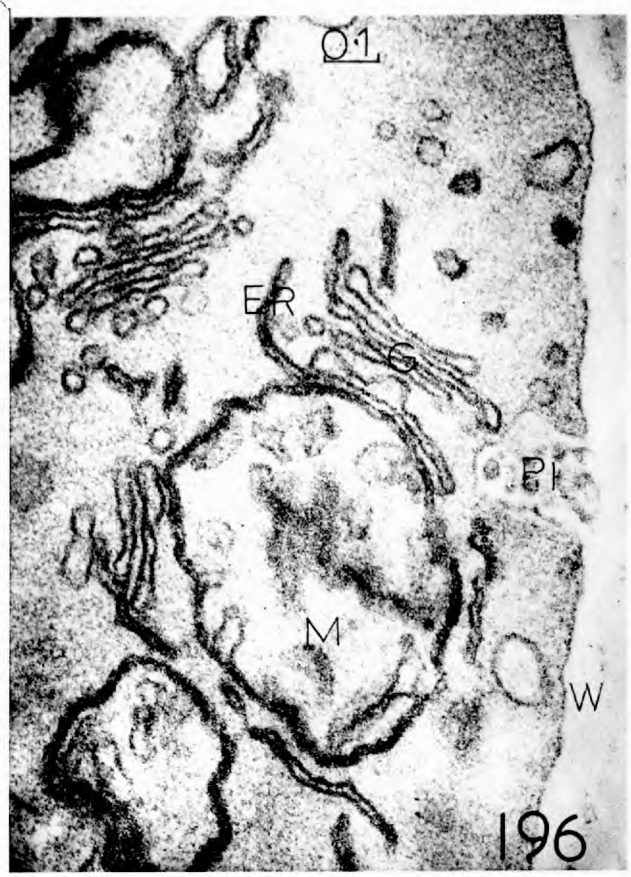
0·1
ER
G
Pl
M
W
196

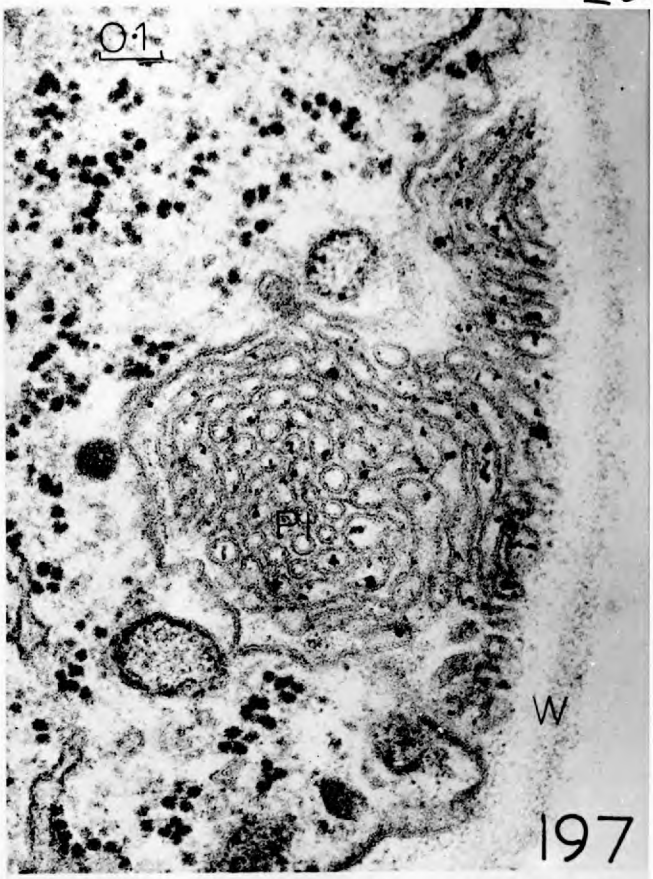
0·1
Pl
W
197

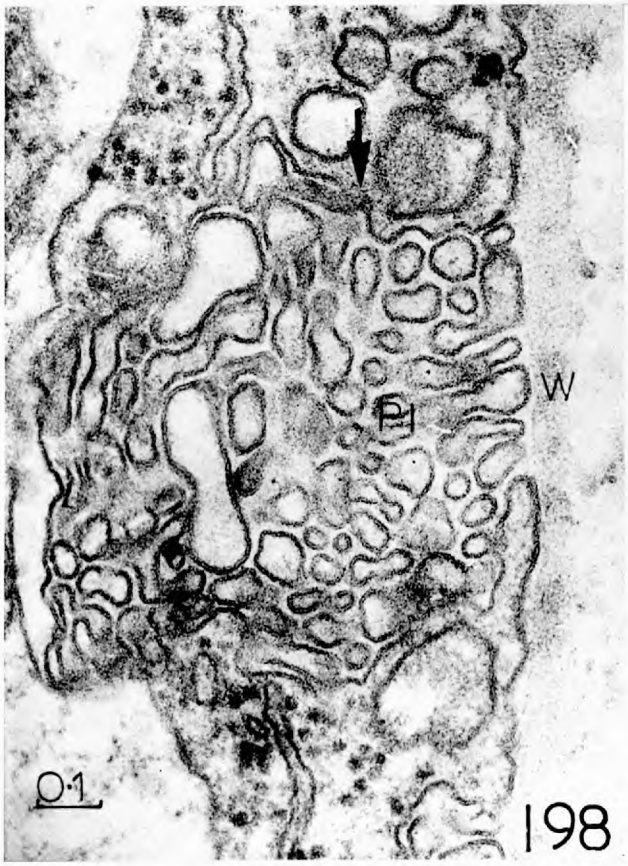
W
Pl
0·1
198


W
0·1
199

Fig.200. Tubular plasmalemmasomes and a multitubular body. 1302/4. 5706.

Fig.201. Plasmalemmasome with connections between tubule and plasmalemma. 1509A/1. 8227.

Fig.202. Plasmalemmasome with wall vesicle expanded into it. 1509A/1. 8228.

Fig.203. Tubular plasmalemmasome with clear extensions of plasmalemma as a tubule.1302/4. 5707.

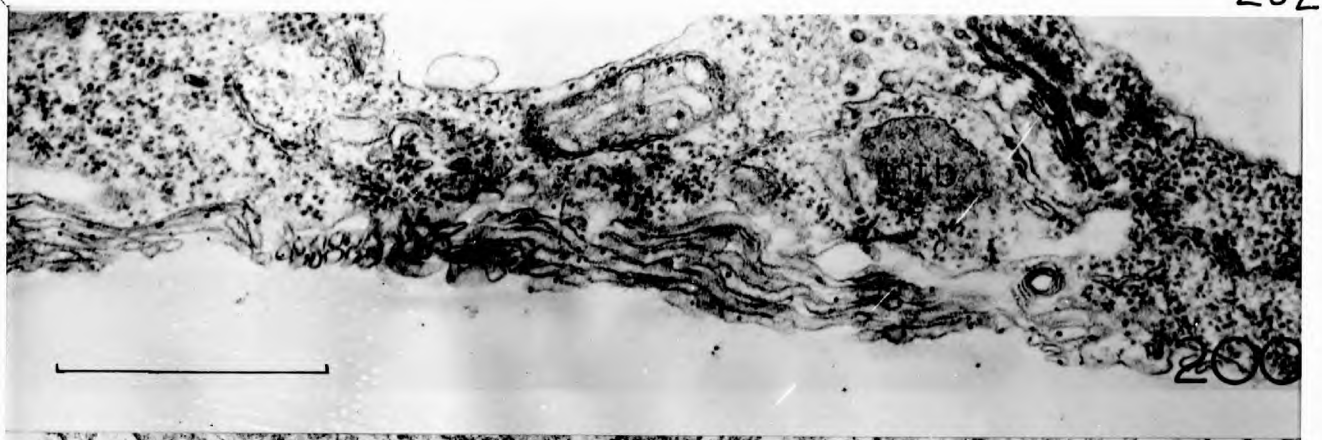

200

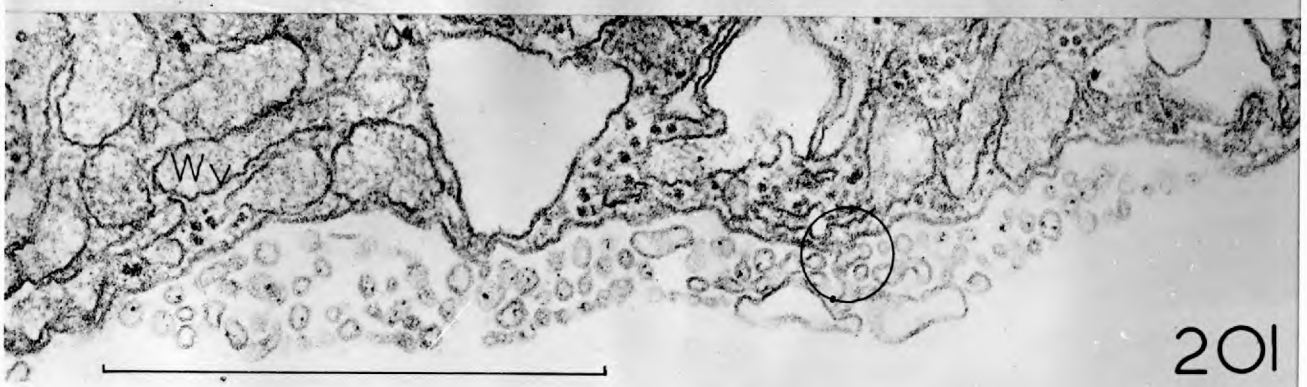

201

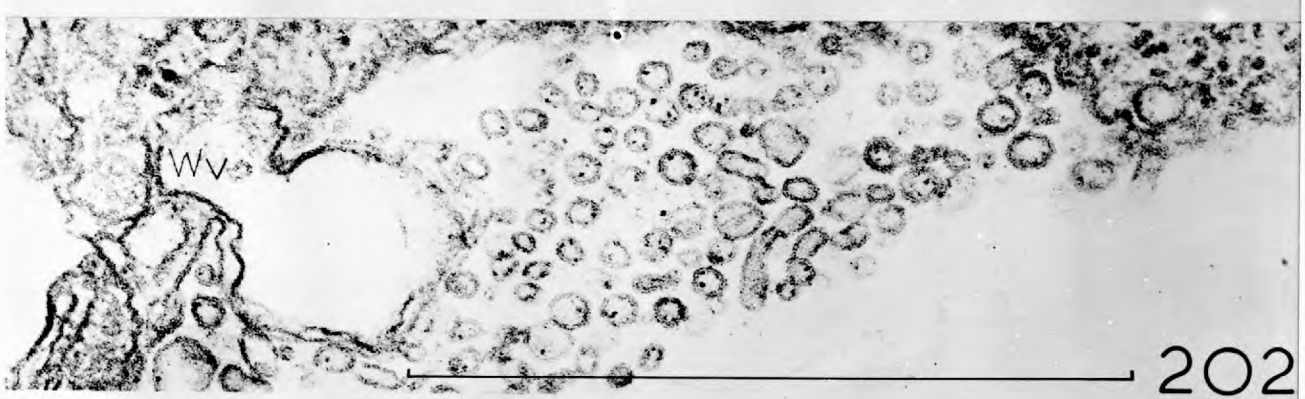

202

203

Fig.204. T.S. extreme apex showing irregular membranes found exclusively after Os only fixation. 1652/3. 8418.

Fig.205. L.S. similar apex to Fig.204. Os only. 1694/1. 8851.

Figs.206 & 207. Apical region showing irregular membranes. Os only. 1220/1. 8257 & 1220/1. 8259.

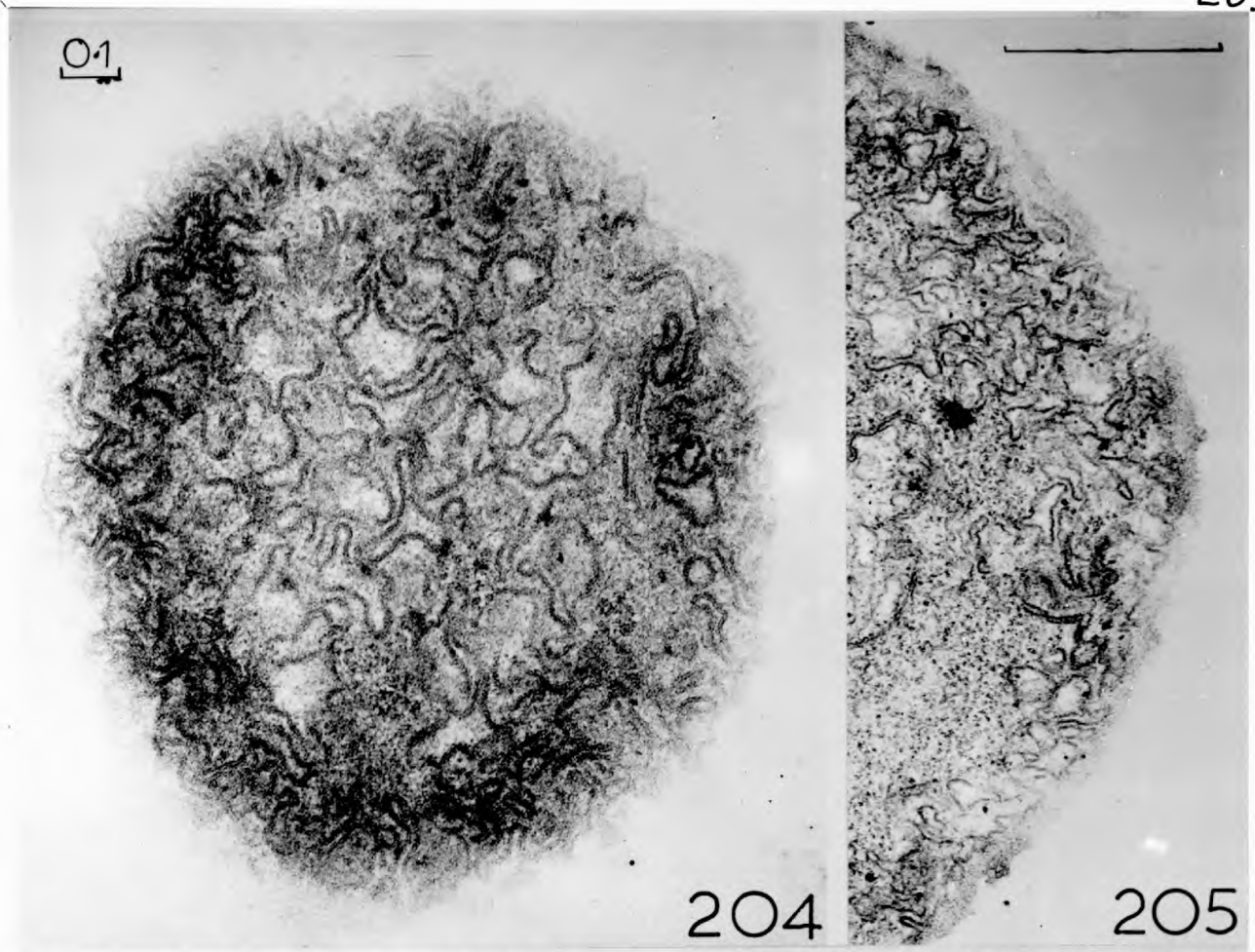
0·1
204
205

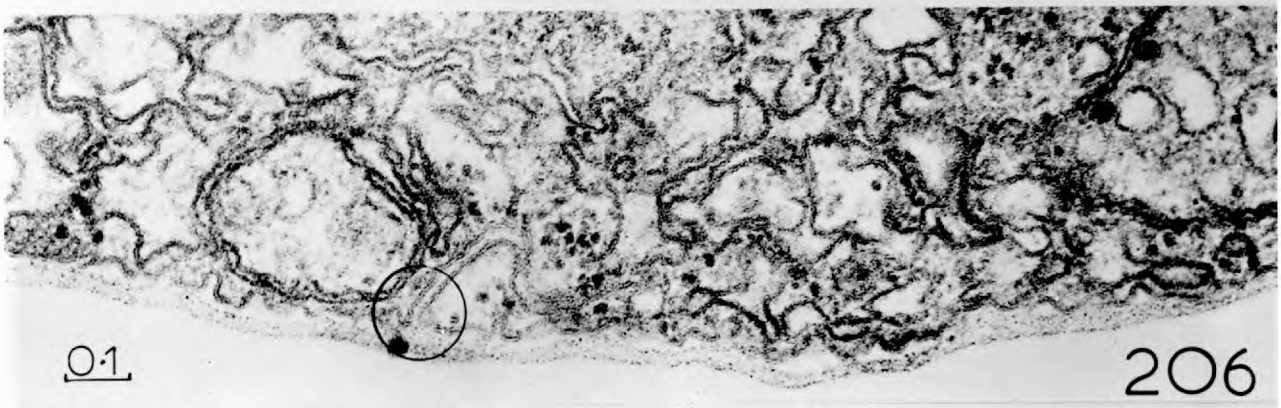
0·1
206

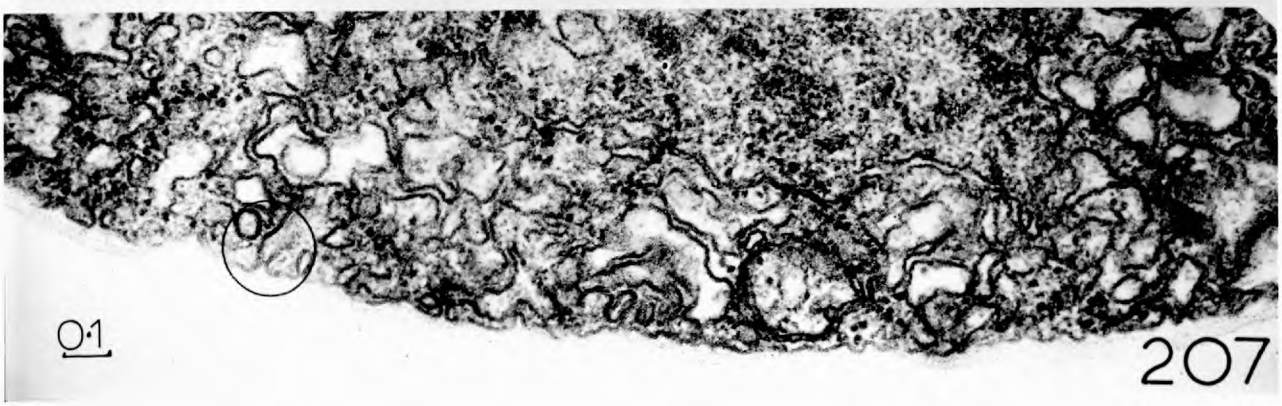
0·1
207

Fig.208. Fibrils comparable to those produced by colchicine. Hypha incubated in SITS prior to fixation. Note normal astral tubules. 1737/1. 10093.

Fig.209. Hypha incubated in SITS prior to fixation. Note "normal" plasmalemmasome. 1737/1. 10095.

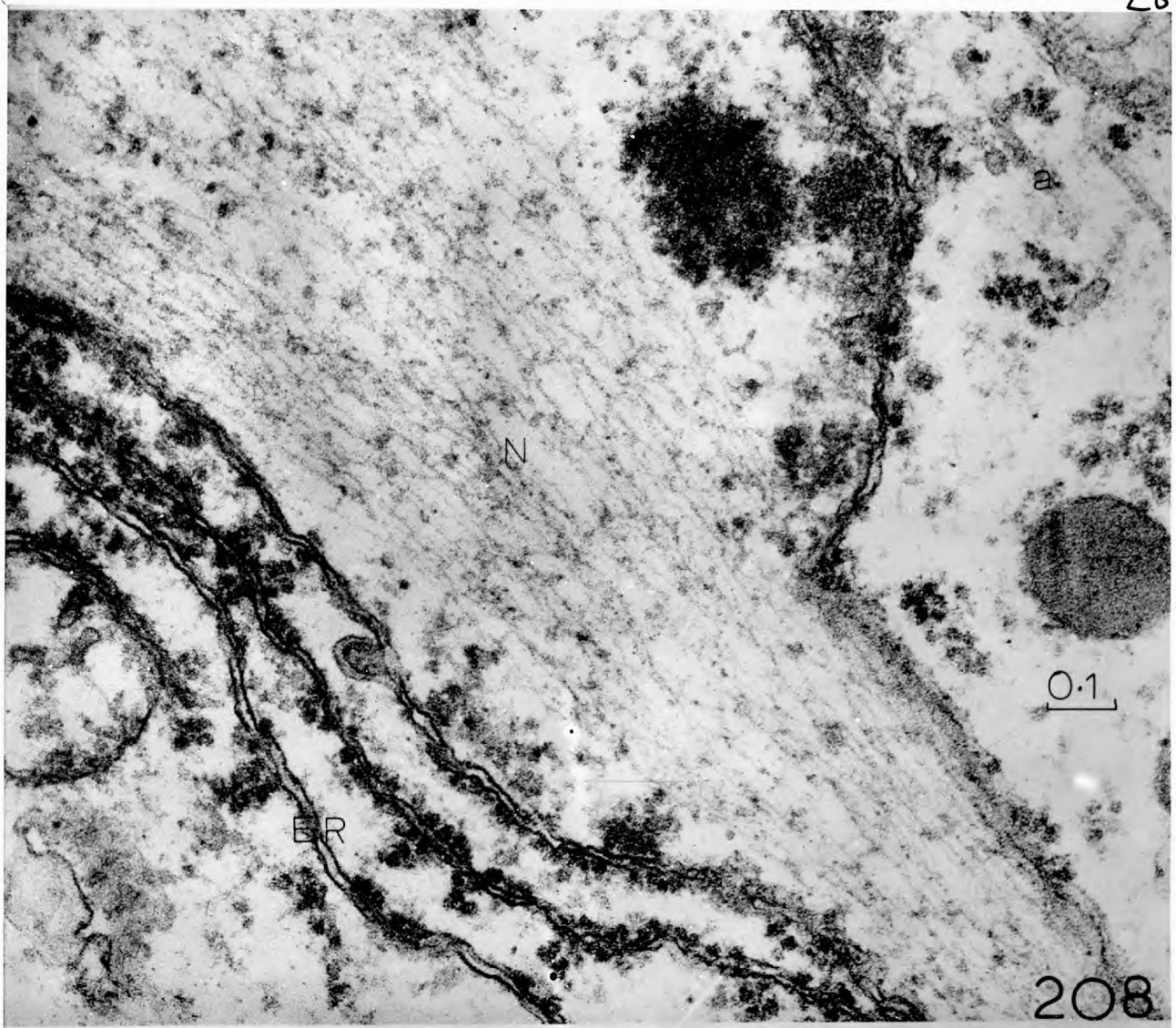

208

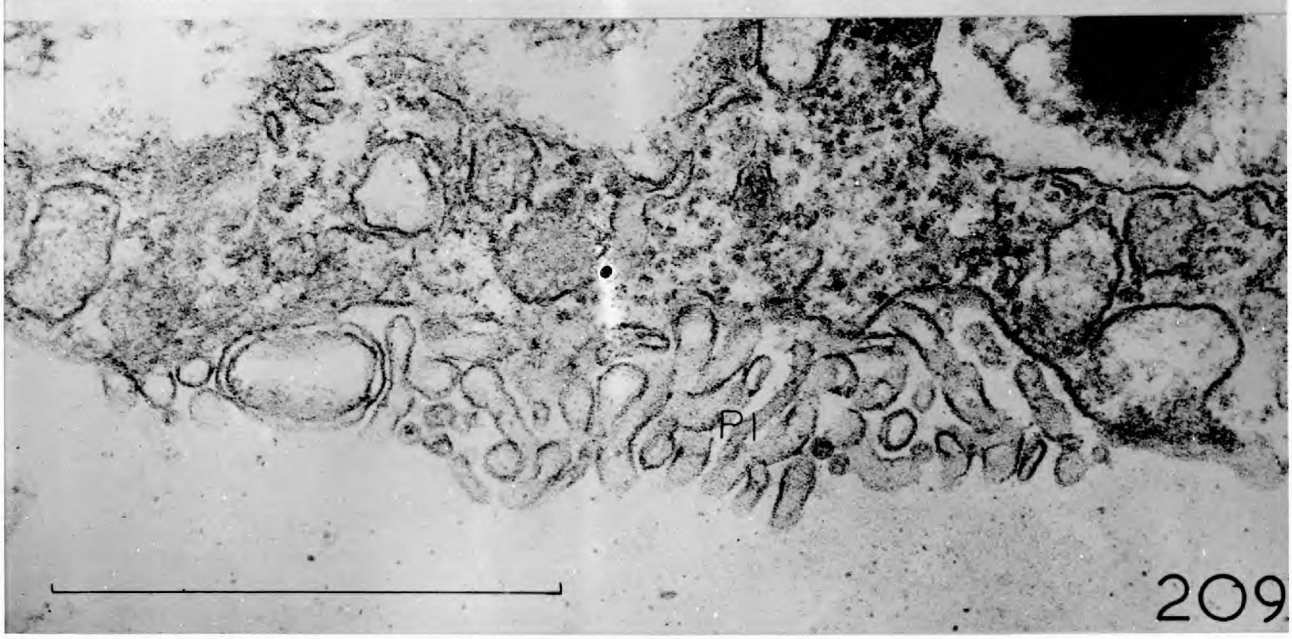

209

Figs.210-215. Paired phase contrast and U.V. micrographs of SITS stained hyphae.

Fig.210-211. Uniform apical fluorescence. 362 & 363.

Fig.212-213. Regrowing hypha with uniform fluorescence in young apex but no glow detectable in old apex. 369 & 368.

Fig.214-215. Regrowing hypha with fluorescence in old apex and localized regions of fluorescence, probably corresponding to lomasomes, in young apex. 289 & 285.

Fig.216. Fluorescence in SITS stained apex and branch. 277.

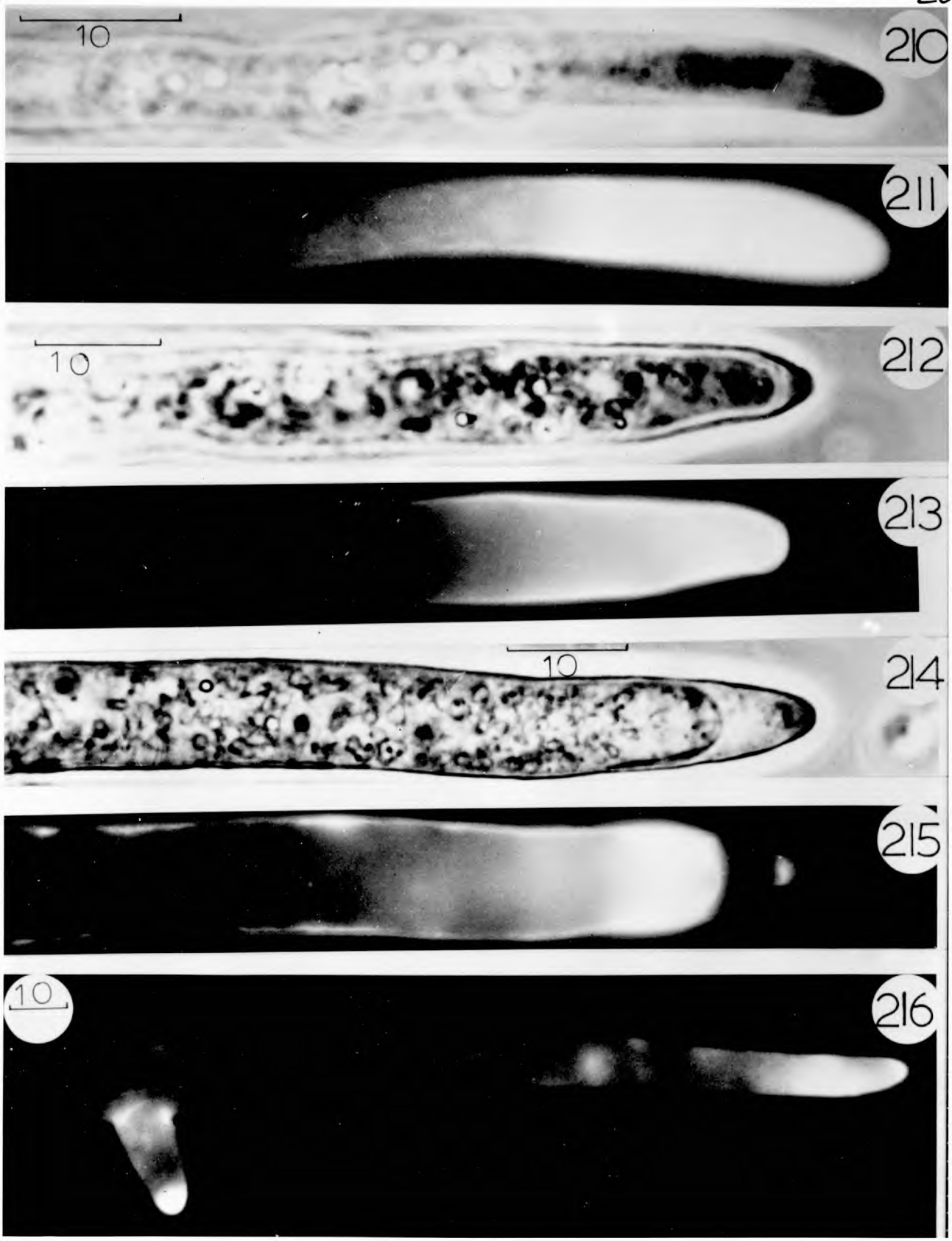
10
210
211
10
212
213
10
214
215
10
216

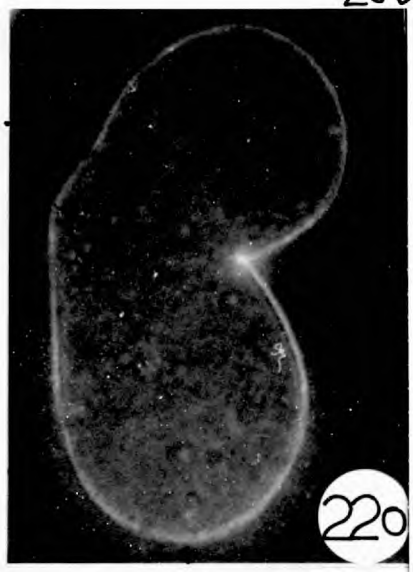

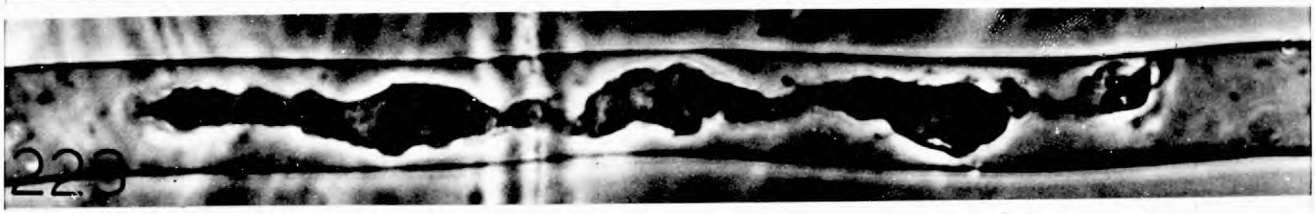

Figs. 217-218. Hyphal apex showing uneven distribution of SITS stain due to plasmalemmasomes. (Mag.x2,975.) 372 & 373.

Figs. 219-220. Naked protoplast showing SITS staining on plasmalemma. (Mag. x 780) 310 & 311.

Figs. 221-222. SITS stain on a "normal" hyphal apex. (Mag. x 2,700) 261&266

Figs. 223-224. SITS staining of walls and protoplast of a plasmolysed hypha. (Mag. x 1,205). 591 & 592.

Fig.225. SITS stained discharged sporangium. Localized brightly fluorescing areas are probably lomasomes.(Mag.x 688) 566.

Figs.226-227. Young sporangium developing below a discharged one. Although SITS stains empty walls there is stronger fluorescence when a protoplast is present.(Mag.x 840). 309 & 308.

Figs. 228-229. Vegetative apex fixed in 5% GA for 1.5h then incubated in SITS. Old walls stain as strongly as unfixed ones but the usual strong apical glow is absent. (Mag.x 840). 294 & 295.

Fig. 230. Apices showing strong fluorescence after SITS staining. (Mag.x 1113). 291.

Fig.231. Same apices as Fig.230 after 6 min in 5% GA. Note reduced intensity of fluorescence. (Mag.x 1113). 293.

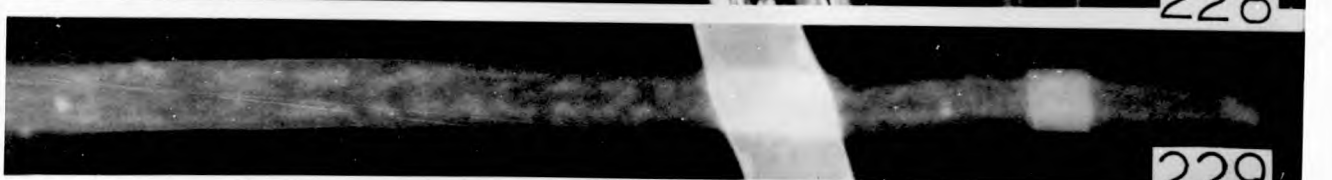

SITS

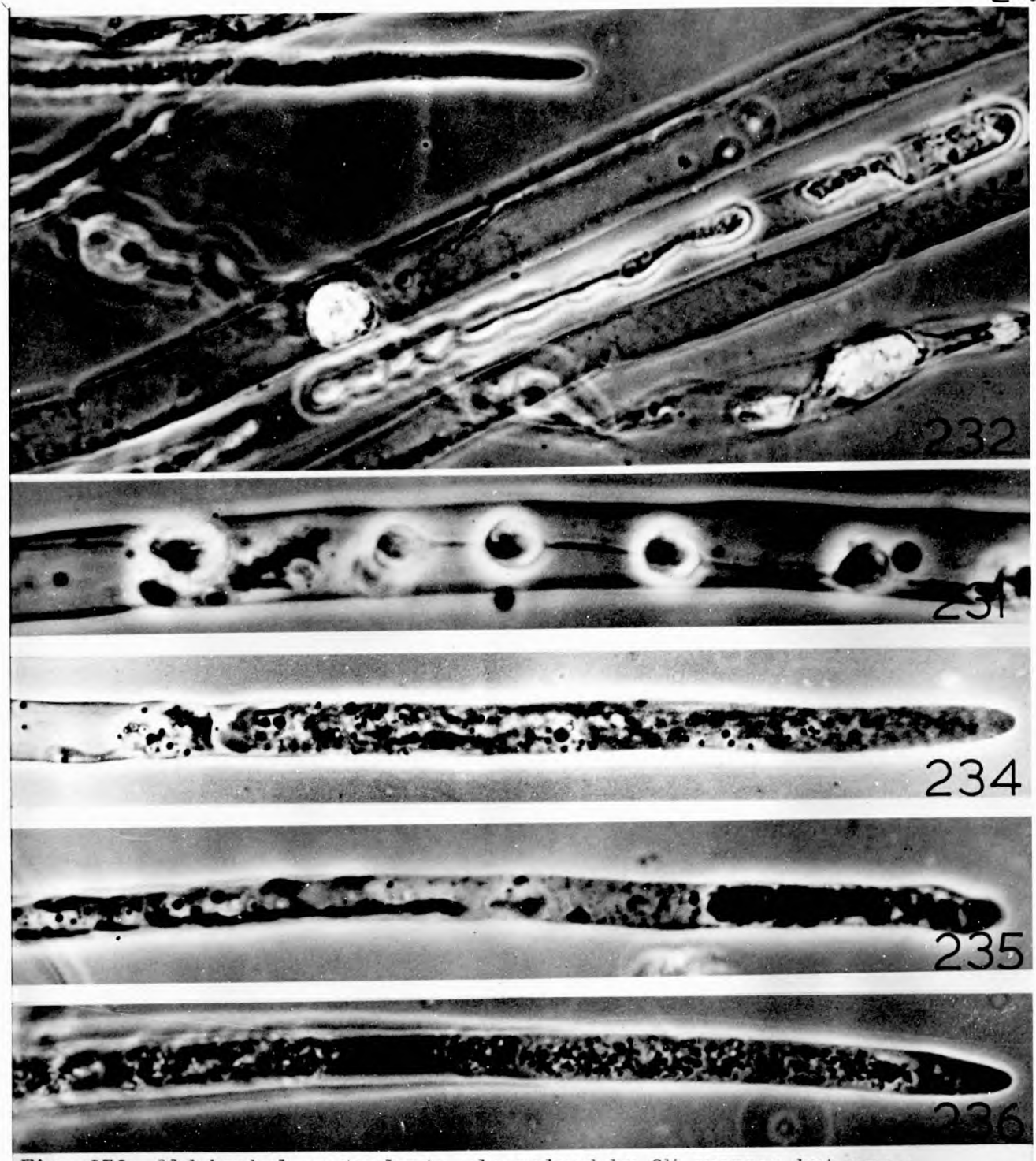

Fig. 232. Old hyphal protoplasts plasmolyed by 2M sucrose but apex apparently unaffected. (Mag. x 735). 581.

Fig. 231. Typical "beading" of subapical protoplast in 2M sucrose. (Mag. x 1,255). 586.

Figs. 234-236. Typical plasmolysed hyphae in which the sub-apical cytoplasm has contracted from the walls but the apices are not plasmolysed. (Mag. x 834). 573, 589 & 580.

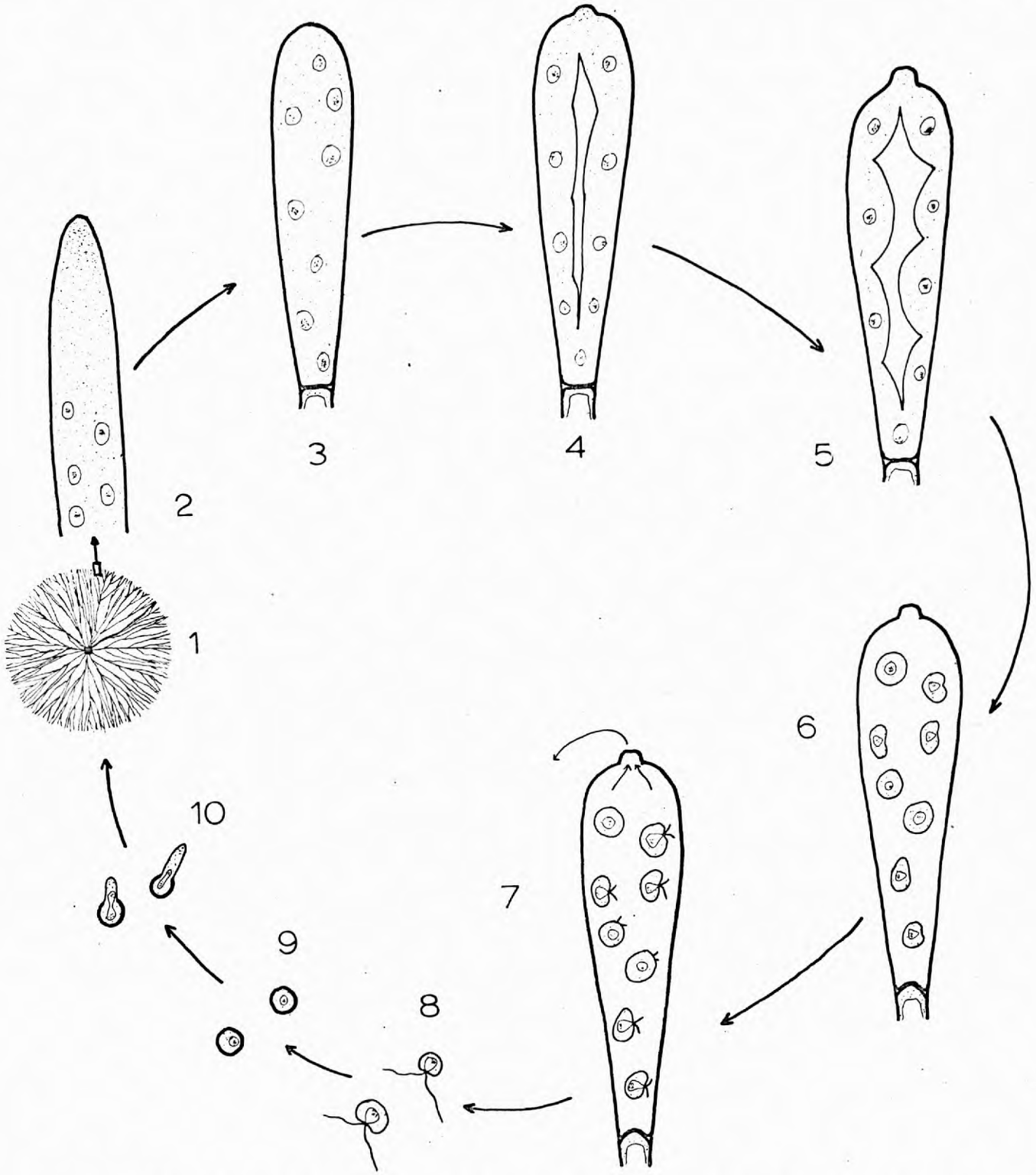

Fig 237. Diagram of the Asexual Life-cycle of S.ferax. 1-2) vegetative hyphae. 3) cross-wall insertion. 4-5) cytoplasmic cleavage. 6-7) flagellum development and release. 8) zoospores. 9) encystment. 10) germination.

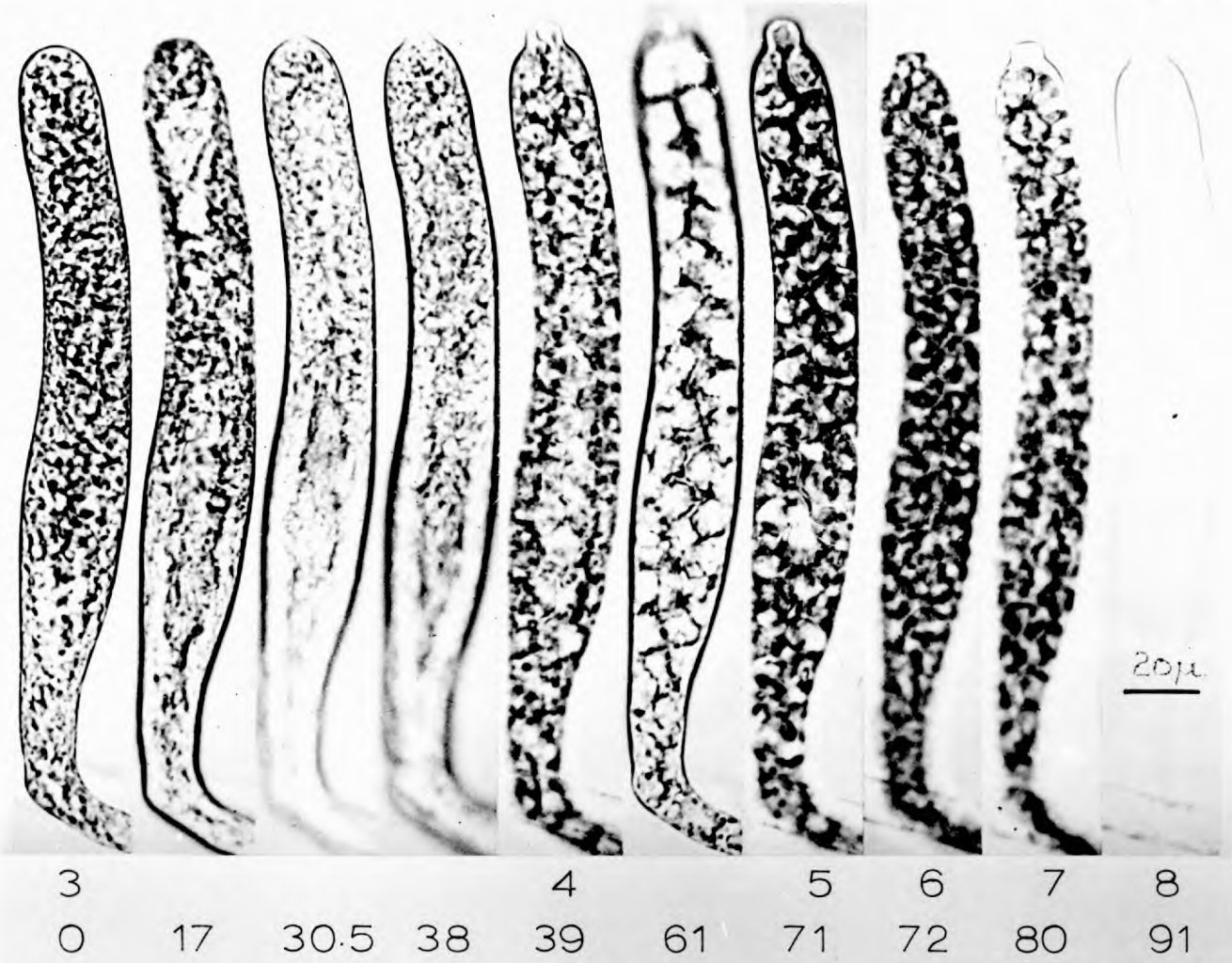

Fig.238. Light micrograph of a developing zoosporangium from cross wall insertion(3) through papillum development (4) and cytoplasm cleavage(5) to the homogeneous stage(6 . Note shrinkage of sporangium when the cleavage vesicles fuse with the plasmalemma) and finally the empty sporangium (8). These micrographs were taken from a cine film made by A.D. Greenwood in the University of Leeds 1951 . The author is very grateful for permission to reproduce them here.

Fig.239. Primary cyst prior to germination. Note thick inner wall, Golgi-E.R.-mitochondrion associations, T.S. and L.S. of fibrils in the E.R., extension of the nuclear envelope, spindle tubules and dense bodies beginning to enlarge. 1691B/5. 10014.

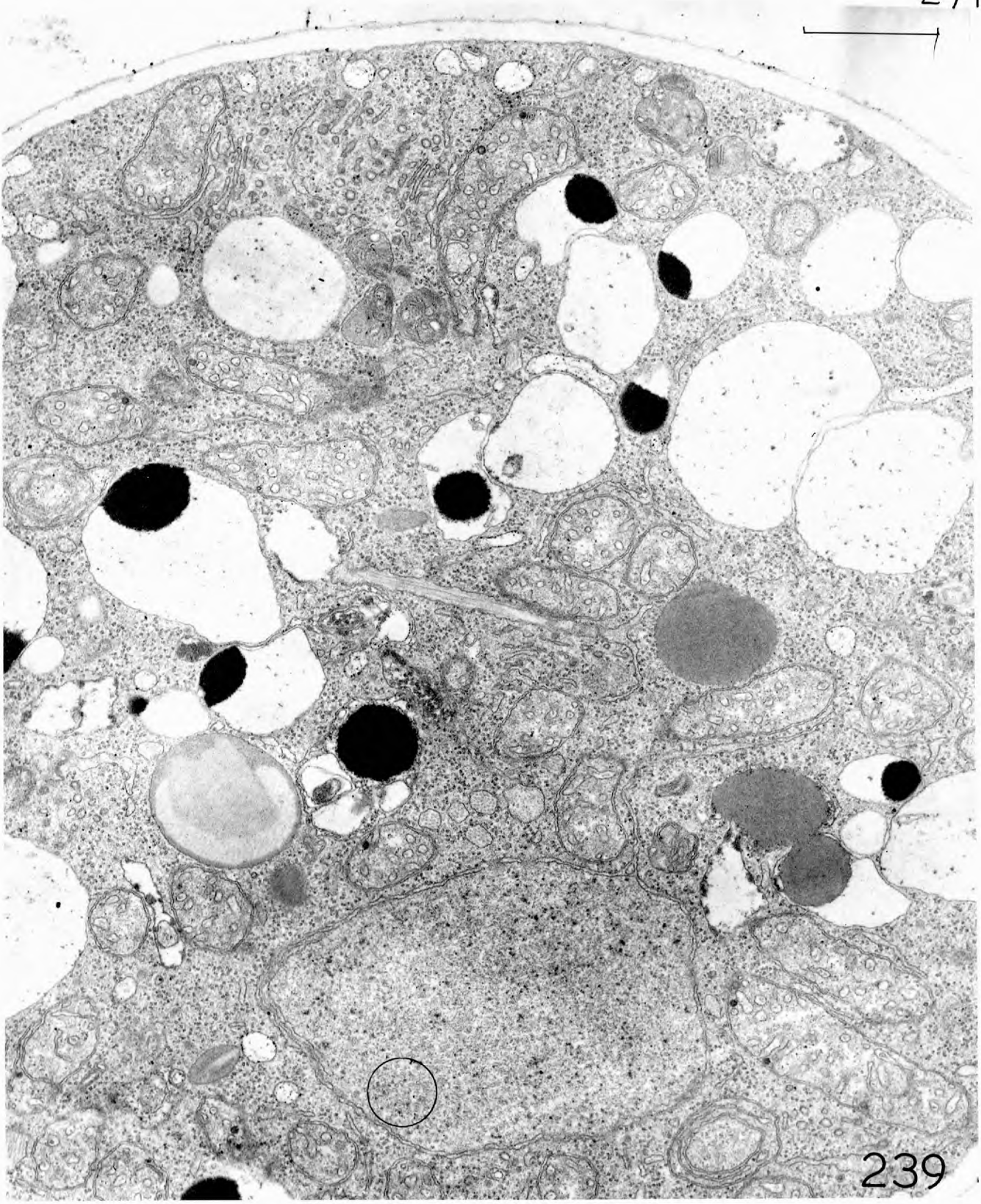

239

Fig.240. Encysted primary zoospore suspended in 0.1% colchicine for $6\frac{1}{2}$h prior to fixation. Note colchicine fibrils in the nucleus, well developed fibrils in the E.R much of which is in a parellel array, plasmalemmasomes and dense bodies. 1779/2. 14012.

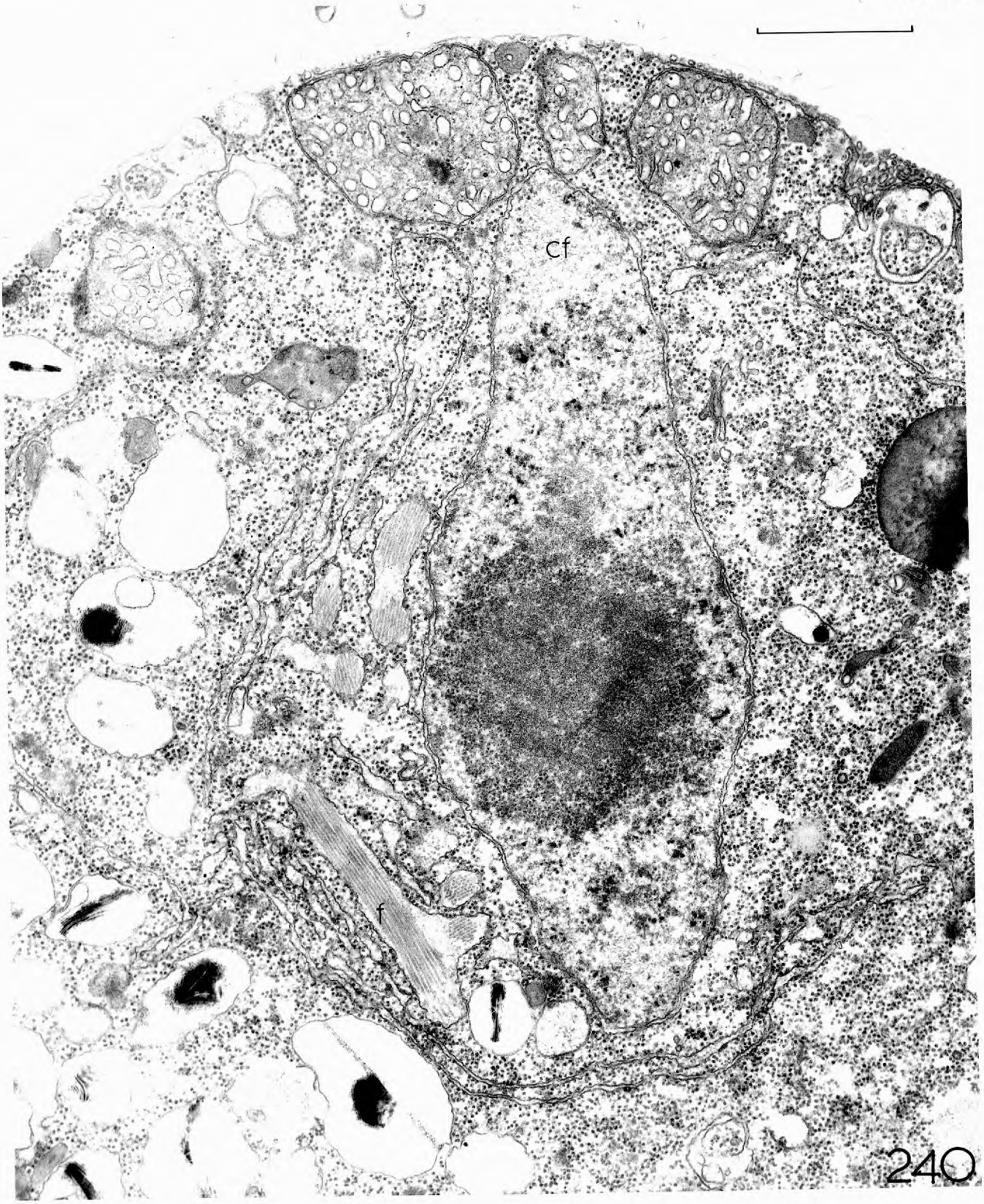
Cf
f
240

Fig.241. Tubular membranous material apparently connected with a dense body vesicle. 1848C/2. 10997.

Fig.242. Expanded dense bodies which have broken their own membranes but extended the vacuole membrane. 1644/3. 10368.

241

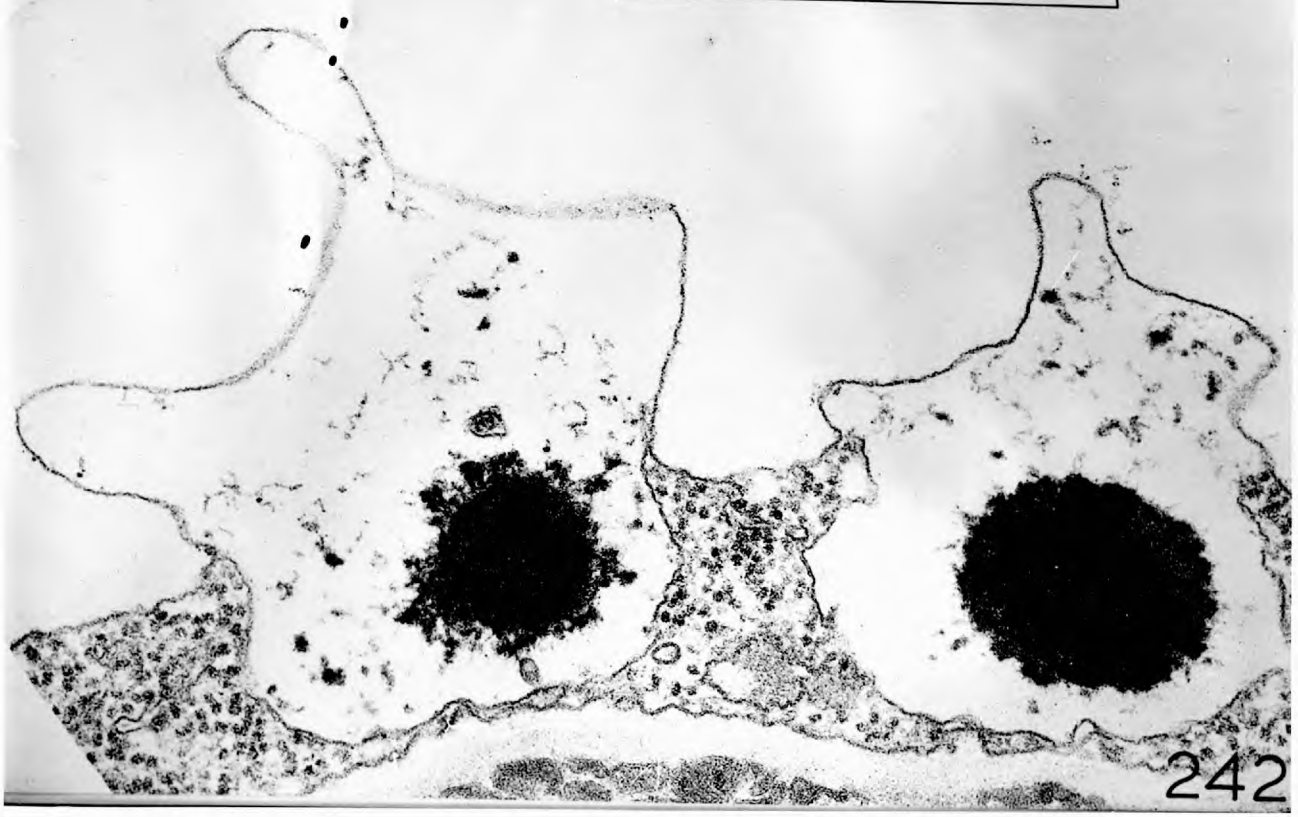

242

Fig.243. Vesicle containing granules, characteristically found in dense bodies, apparently produced by an expansion of the dense body vesicle into a vacuole. The membrane (arrowed) is that of the vacuole. 1848C/2. 12004.

Fig.244. Typical dense bodies after Os fixation. Note dense granules and trances of myelin-like patterns. 1241I/4. 8386.

Fig.245. Negatively stained dense body in PTA. 1884/3. 12319.

Fig.246. Typical permanganate fixed dense body. 1778B/3. 10500.

Fig.247. Permanganate fixed dense body showing myelin-like pattern. 1778B/3. 10500.

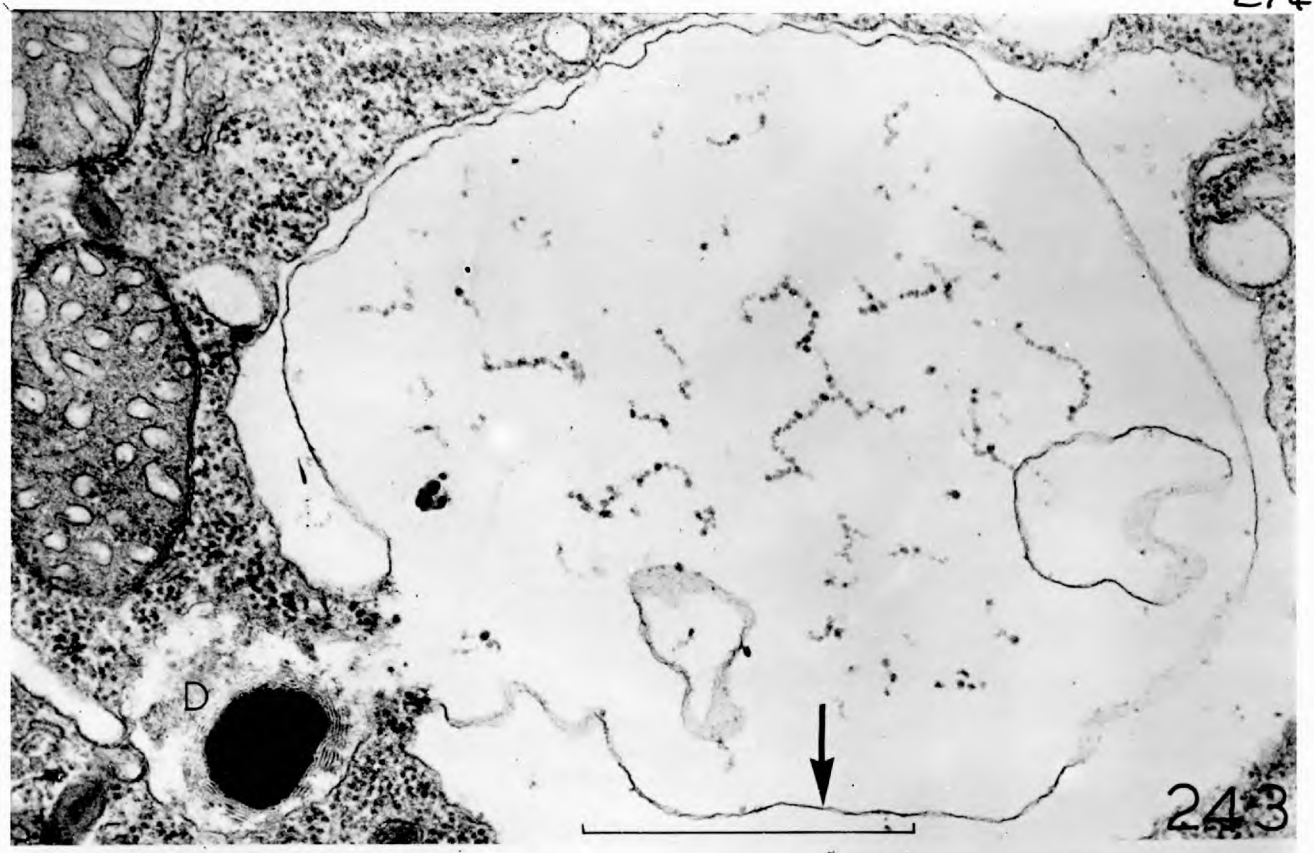
D
243

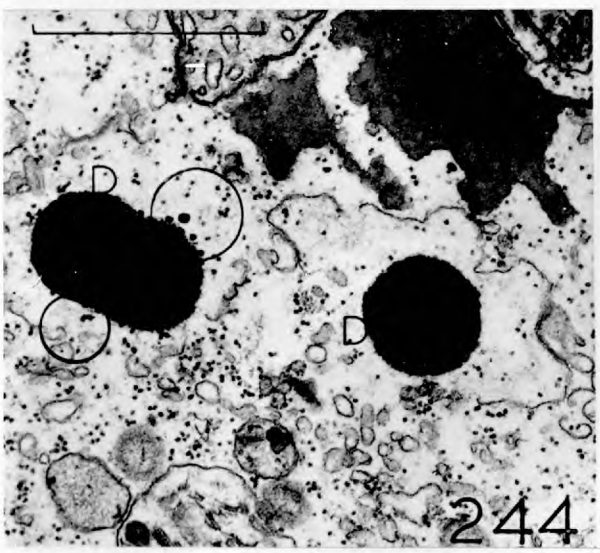
D
D
244

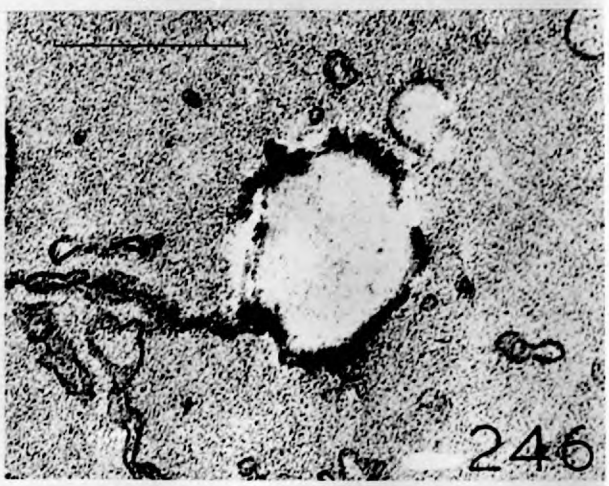
246

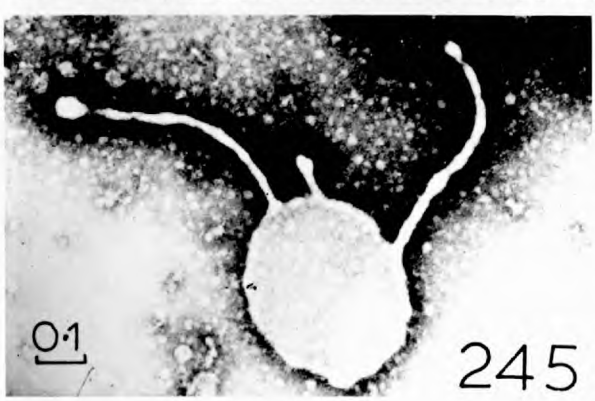
0·1
245

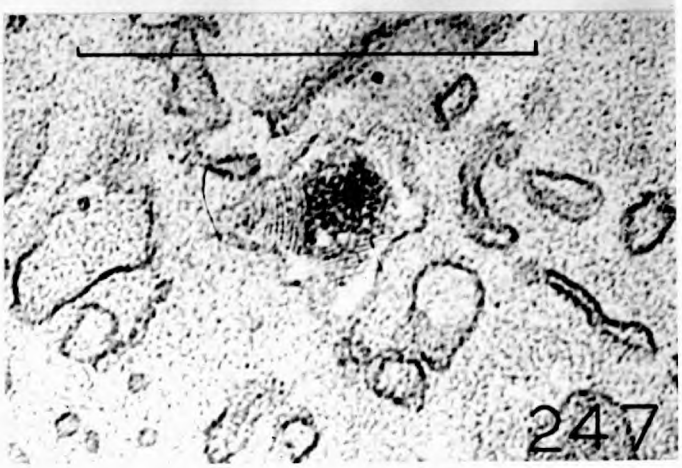
247

Fig.248. Germinating primary cyst. Note coalesced dense body vesicles, Golgi, E.R., mitochondrion associations, apical wall vesicles, split dense layer of cyst wall and fibrils in the E.R.(o). 1692B/2. 8956.

248

Fig.249. Germinating primary cysts. Dense bodies have become dispersed around the peripheries of the expanding vesicles. Note accumulation of wall vesicles at point of emergence of spore on the right. 1691D/3. 10010.

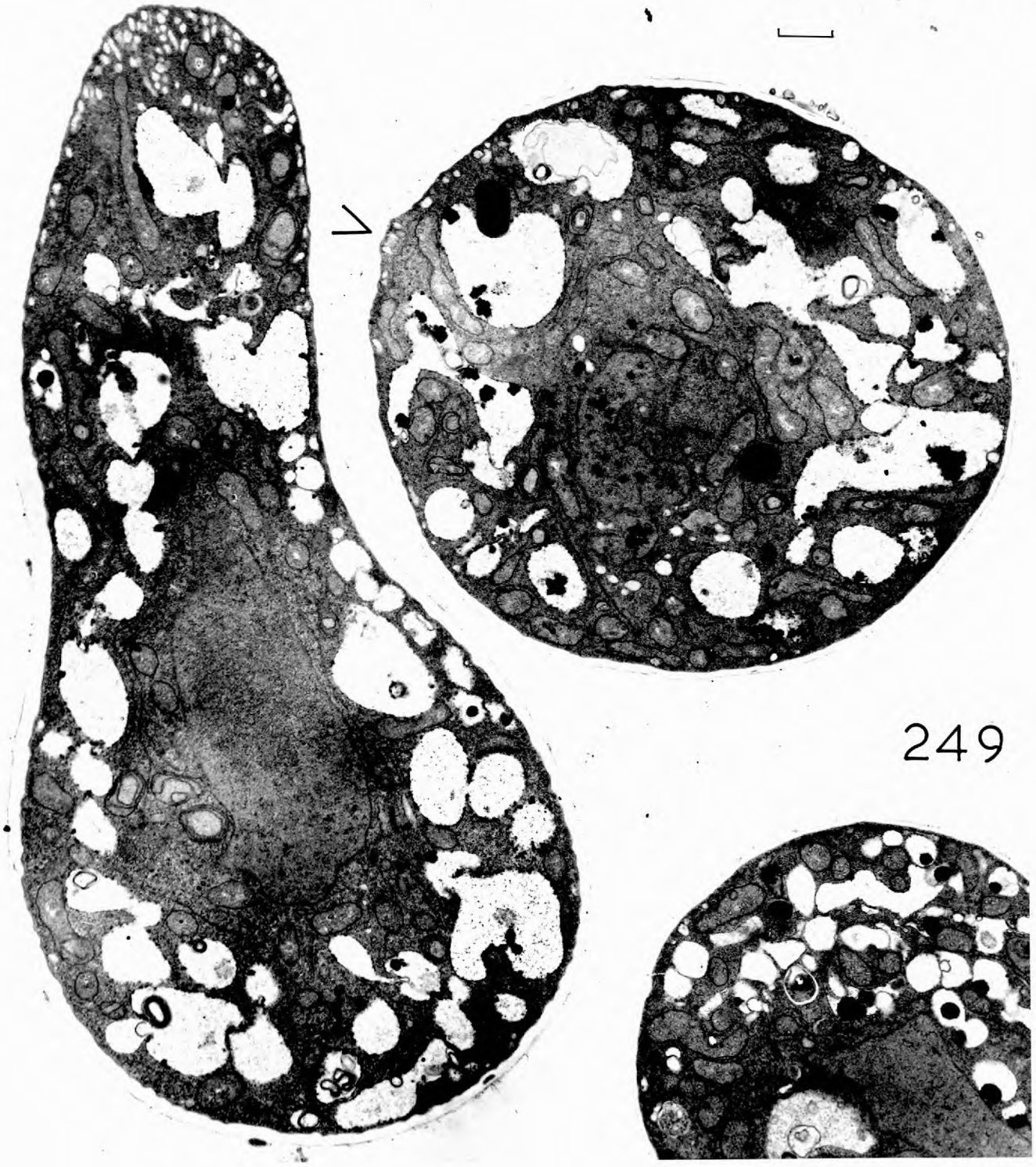

249

Fig.250. Germinating secondary cyst of D. sterile. Note spines on the cyst wall and similar spines in the bar. 1853A/2. 12189.

Fig.251. Kinetosome and roots in a primary cyst of D. sterile. 1853B/1. 12167.

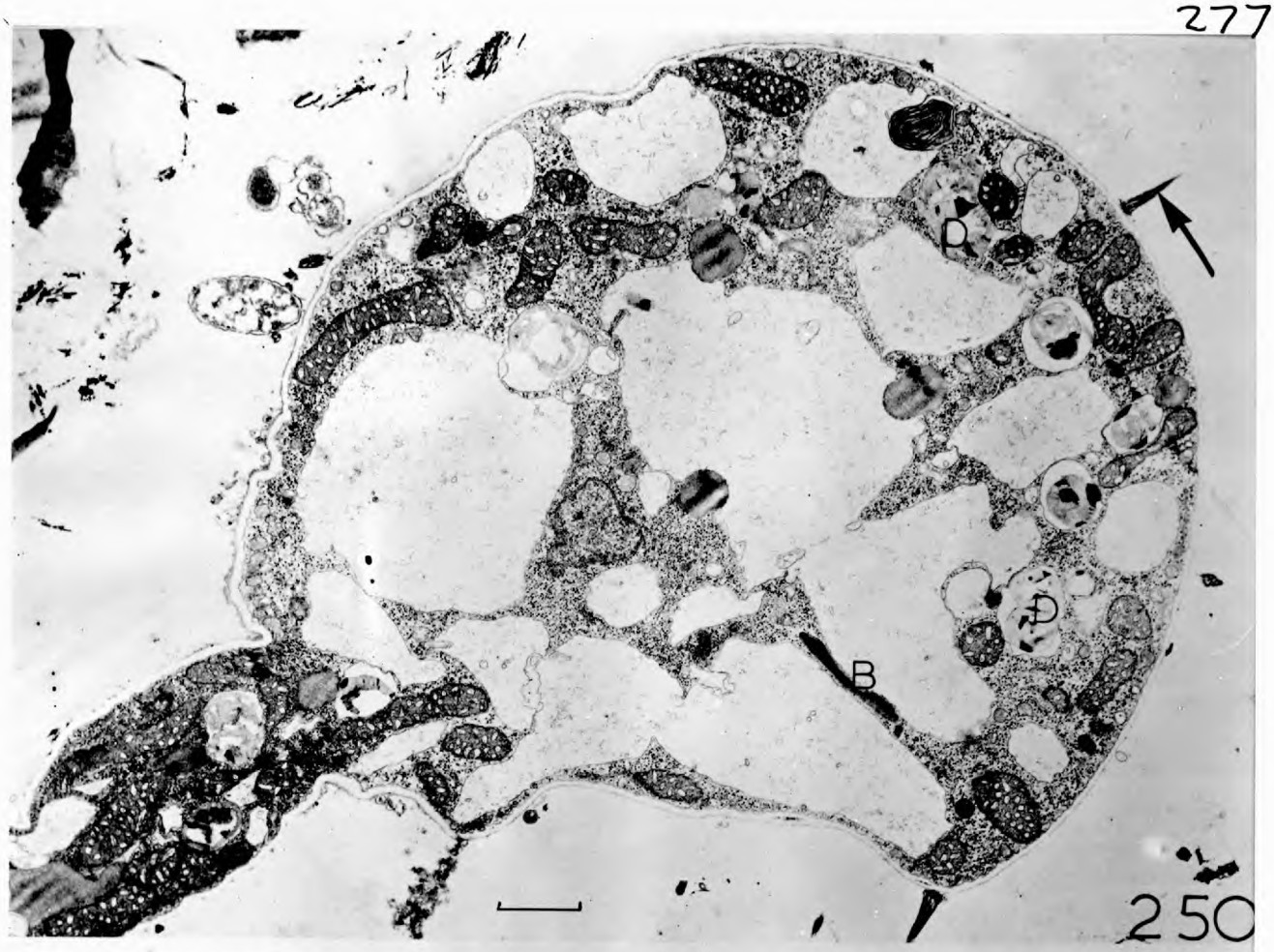
P
D
B
250


K
25

Fig.252. Pyriform nucleus in pre-cleavage sporangium. Note tubular roots, kinetosome, striate fibre, parallel array of "rough" E.R. and tubules wich are frequently found inside the nucleus at this time. 1847/2. 10937.

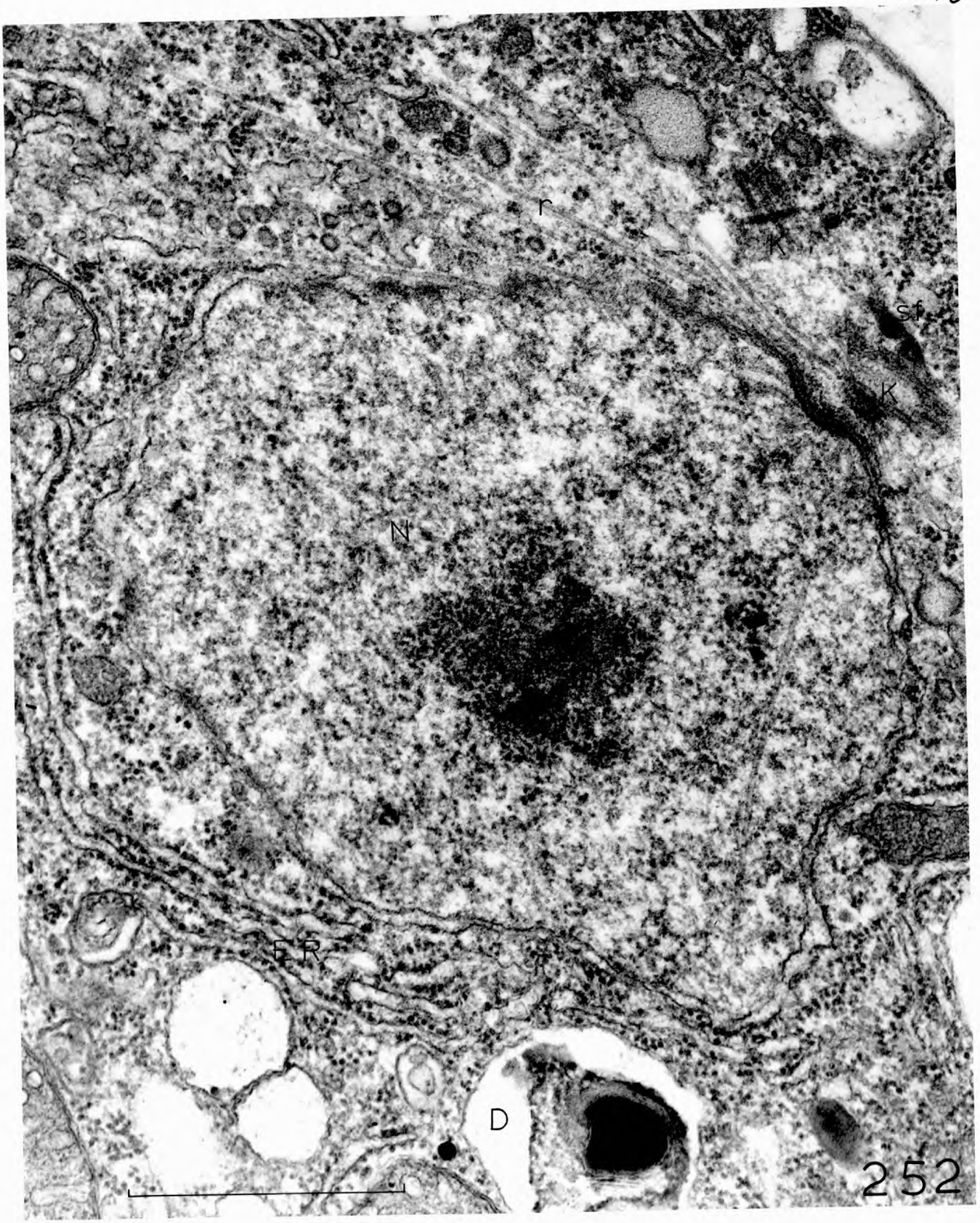
r
K
Sf
K
N
ER
D
252

Fig.253. Transverse section of the apex of a pre-cleavage pyriform nucleus. Note the tubular roots close to the nuclear envelope and the Golgi bodies which are very active in producing vesicles, some of which are "hairy". 1645H/1. 10031.

Fig.254. Pre-cleavage nucleus with buds on nuclear envelope adjacent to the active Golgi bodies. Note kinetosome with striate fibre and fibrous body. 1848C/1. 10989.

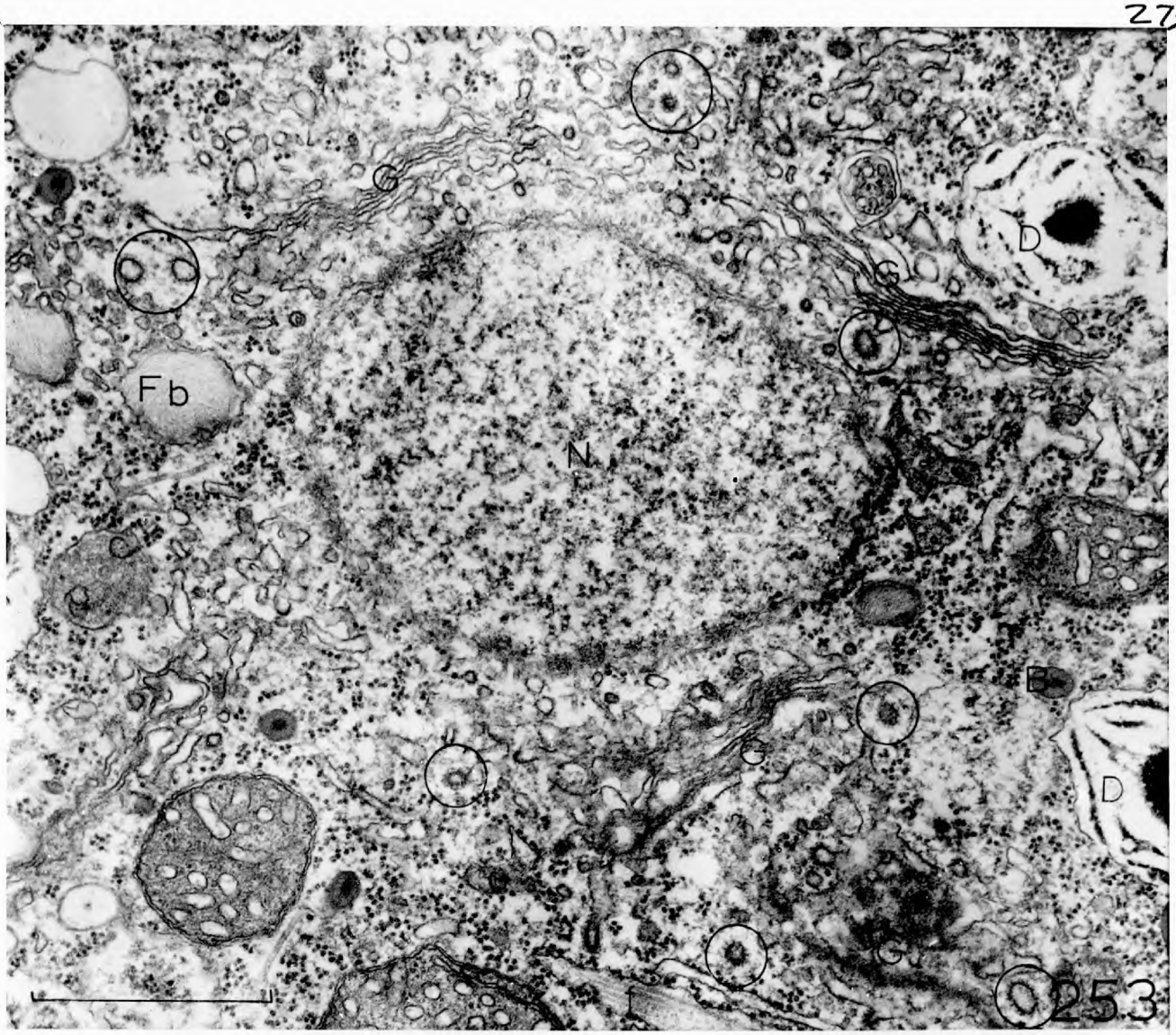
G
D
G
Fb
N
B
D
G
253

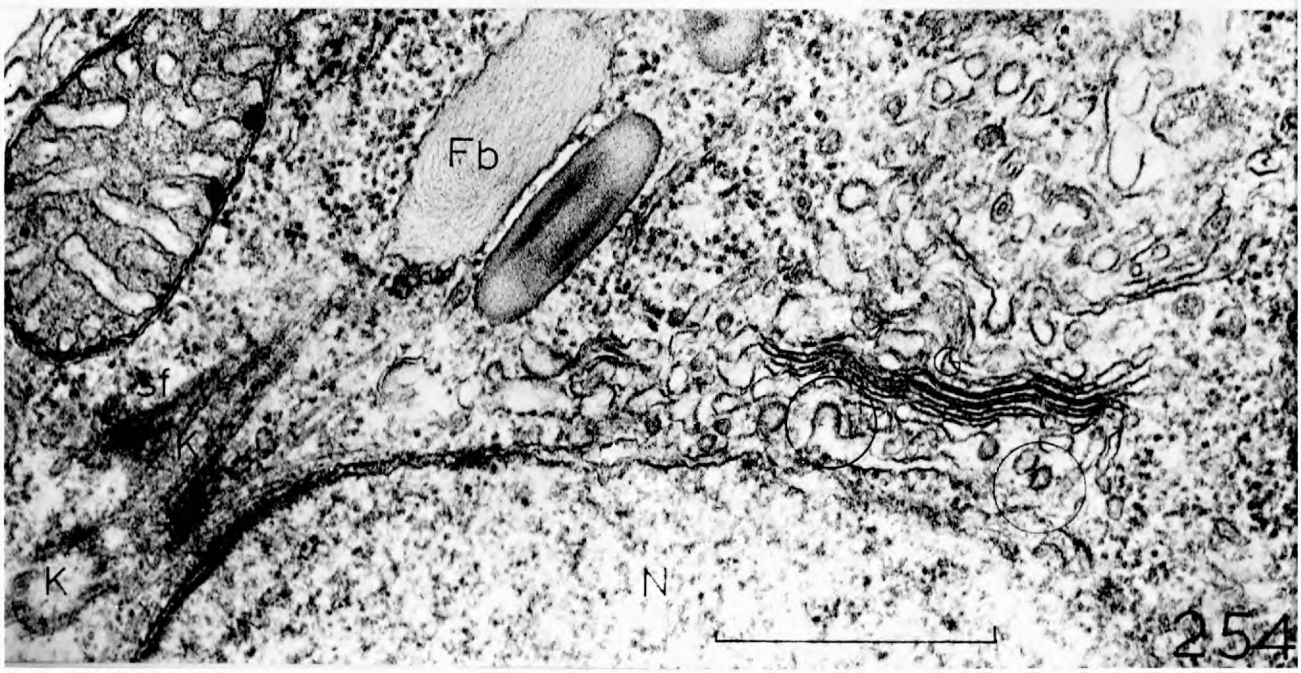
Fb
Sf
K
K
N
254

Fig.255. Young primary cyst with active Golgi and aligned E.R. Note spines on dense layer of cyst wall and flagellum bead containing distorted axomenes. Os only. 1830A/1. 12195.

Fig.256. Tubules in a square-ended, ribosome studded vesicle. Note ill defined tapering ends of the tubules. 2061/1. 12965..

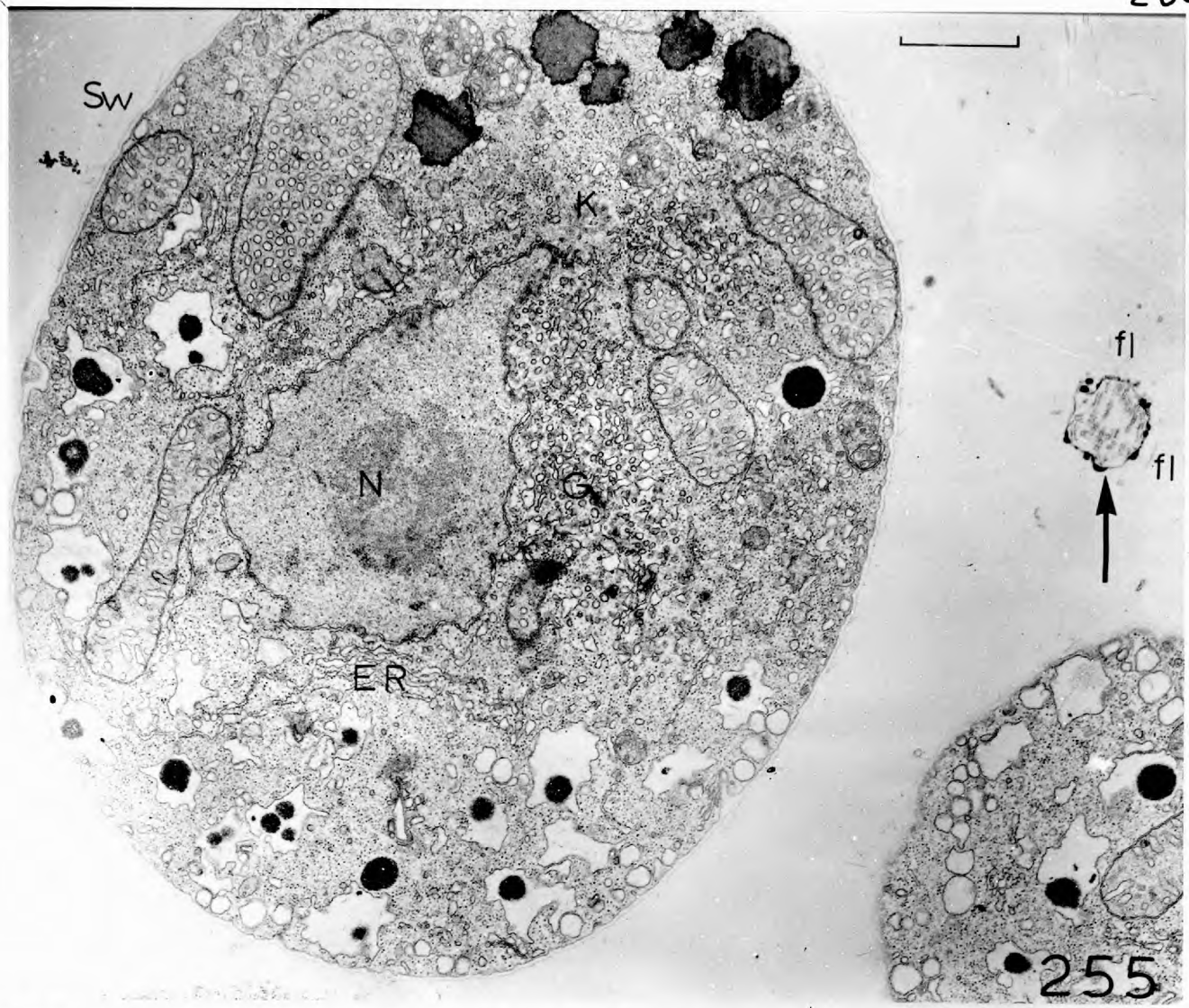
Sw
K
N
G
ER
fl
fl
255

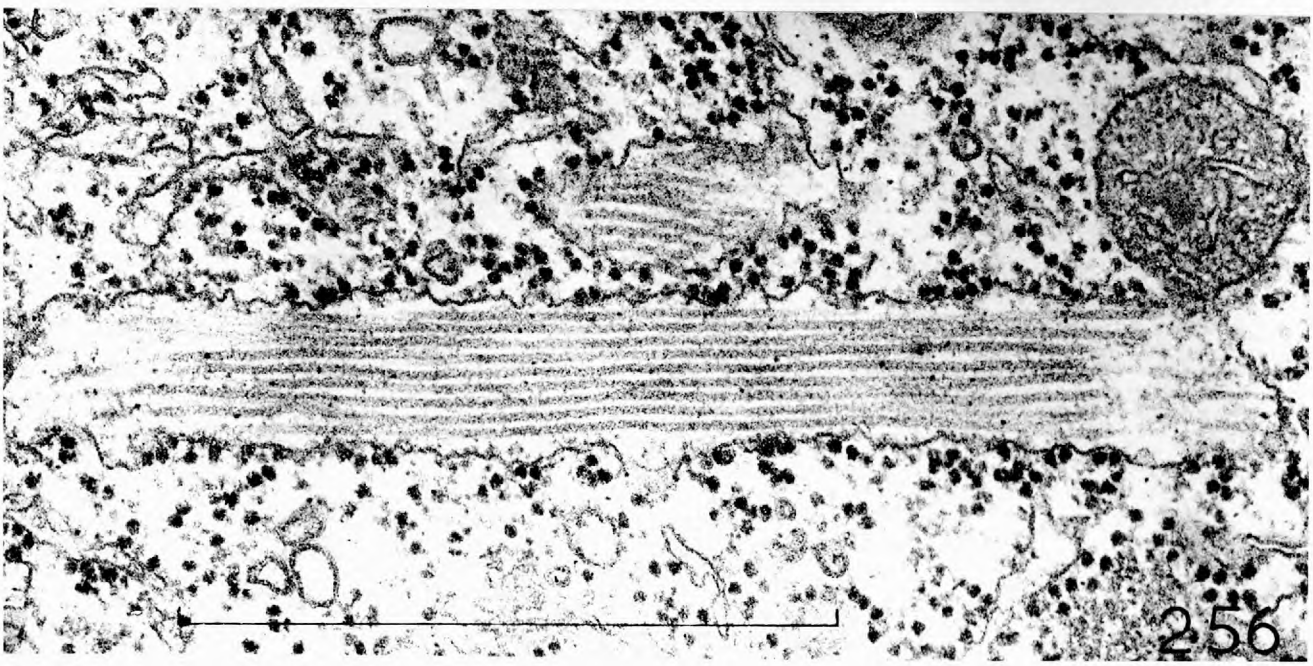
256

Fig.257. Tubules in the E.R. and perinuclear cavity of a primary cyst. 1739/1. 10179.

Fig.258. Tubules in ribosome coated vesicle of a primary cyst. Note constant length of tubules and characterisitic terminations at both ends of the lower bundle suggesting an anti-parallel arrangement. 1778/2. 14007.

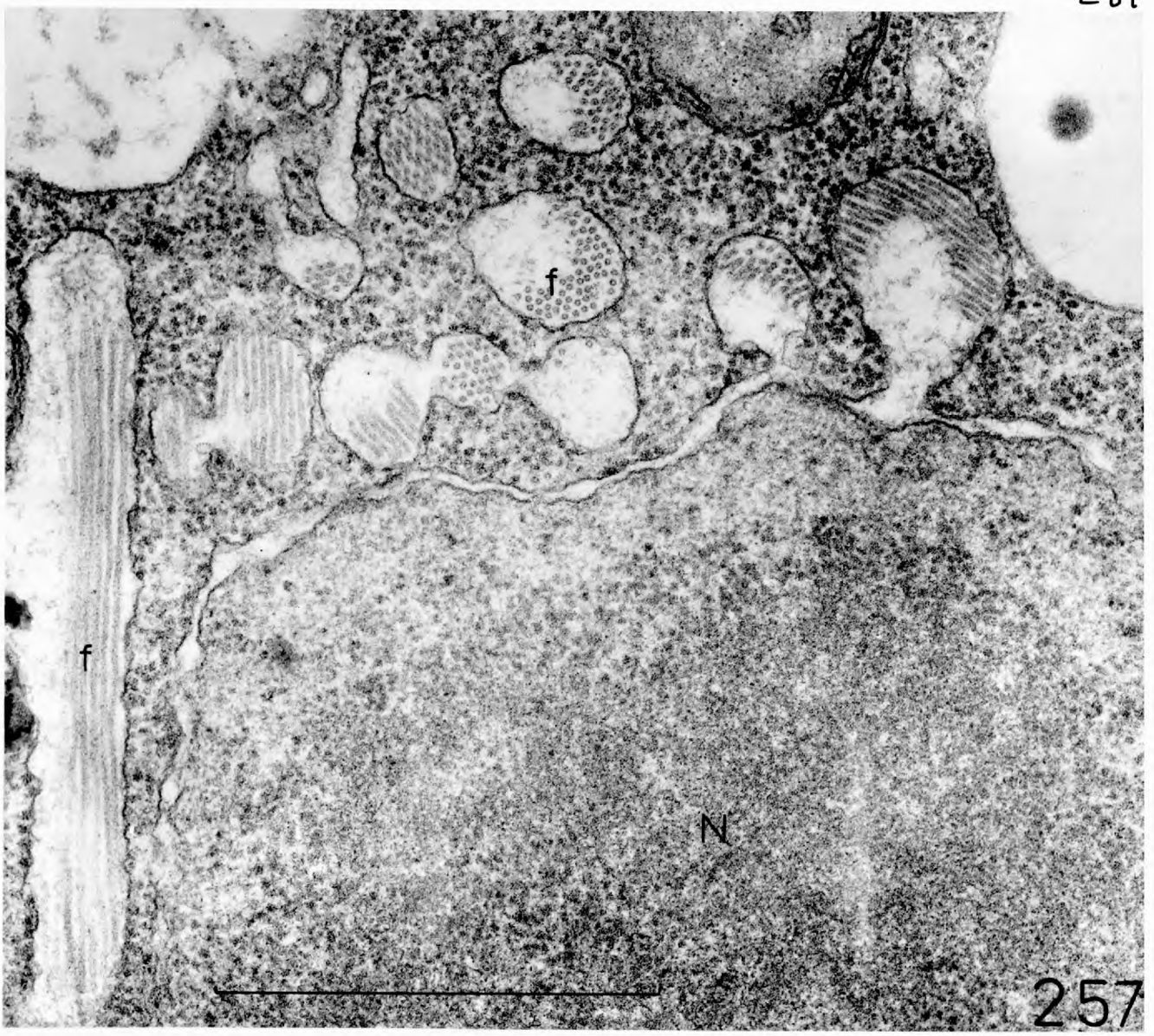
f
f
N
257

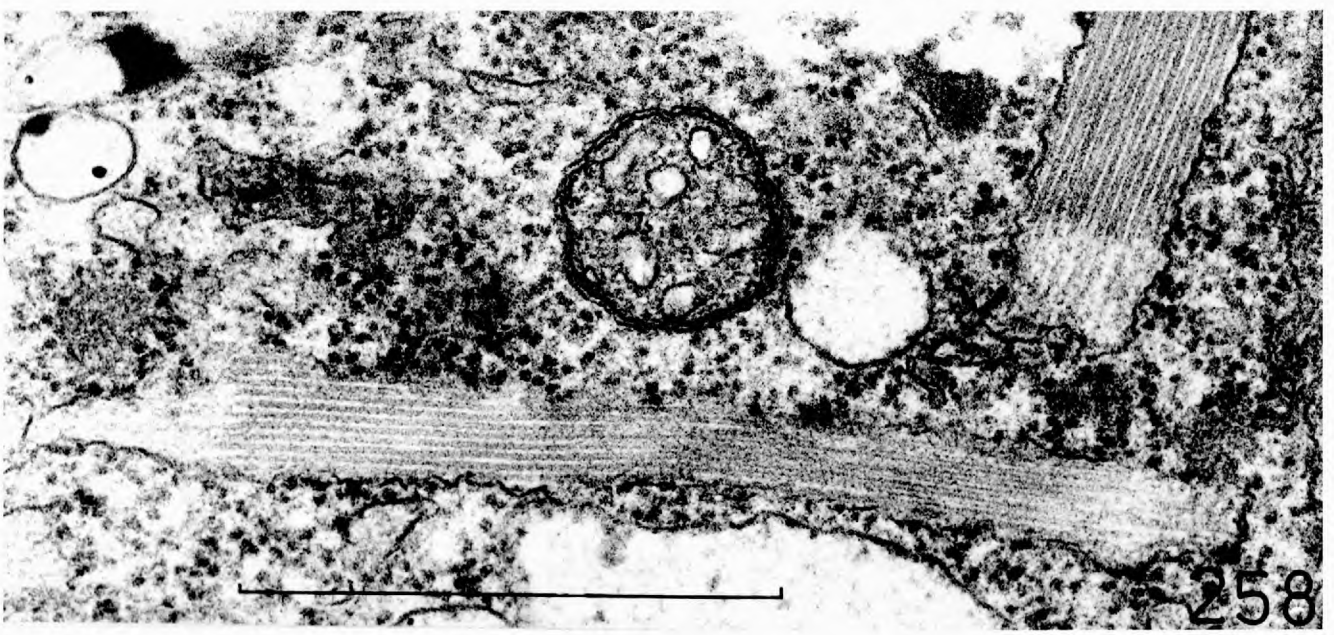
258

Fig.259. Tubules in a cisternum of the E.R. which is associated with a Golgi body and a mitochondrion. 1739/1. 12297.

Fig.260. A swollen E.R. cisternum containing amorphous material and a few tubules. 1779/2. 14113.

Fig.261. Tubules in ribosome studded vesicles. Note thin connections between adjacent tubules. 1645II/4. 10043.

Fig.262. Tubules in an E.R. cisternum filled with amorphous material. 1848C/1. 10994.

259

260

261

262

Fig.263. Recently encysted primary spore. Note active Golgi around nucleus and easily distorted dense cyst wall. The absence of an inner cyst wall layer and the presence of a bar in the spore suggests that encystment may not be complete. 1642/2. 8805.

Fig.264. Negatively stained tubule from a disrupted sporulating colony which contained very few motile spores. The size of the tubule suggests that it is one of those from the E.R. or a flimmer hair. Note apparent "subunits" in walls. 1914/3. 12340. (Mag.x 260,000.)

Fig.265. Similar tubule to Fig.264 but wall is not broken into "subunits". 1914/3. 12338. (Mag.x 260,000)

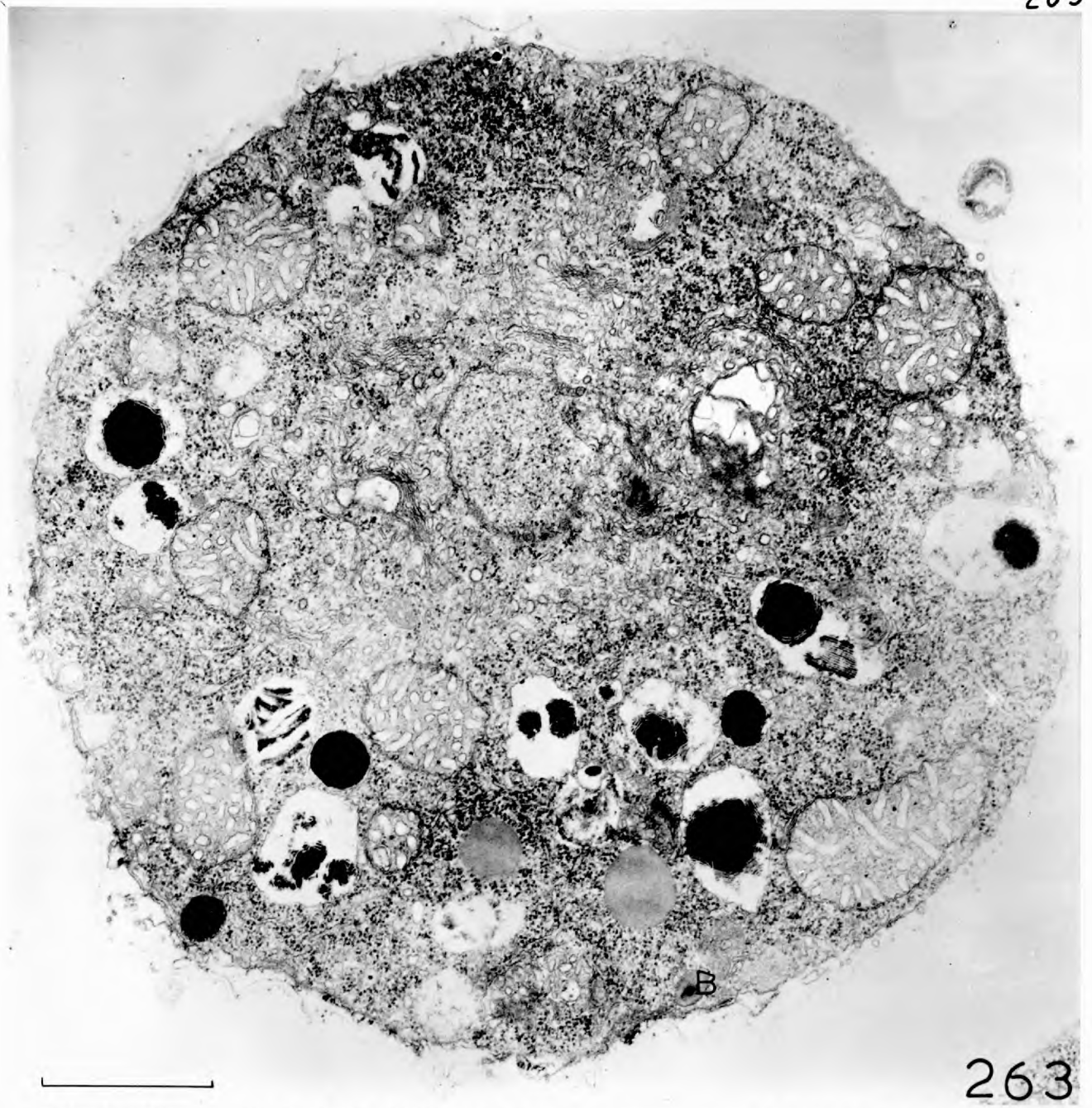

263

264

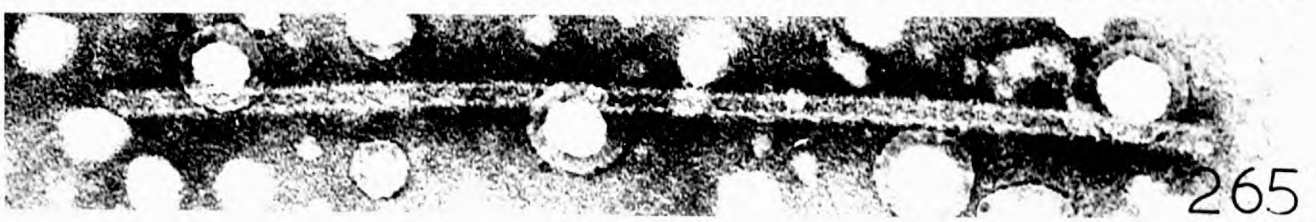

265

Fig.266. Five tubules from the E.R. of Fig.257 subjected to analysis by the Markham rotation technique. A suggests the presence of 4 dense subunits, B. and C. show 5 subunits and D. and E. indicate 6. Many other tubules showed no reinforcement of dense subunits. 1739/1. 10179.

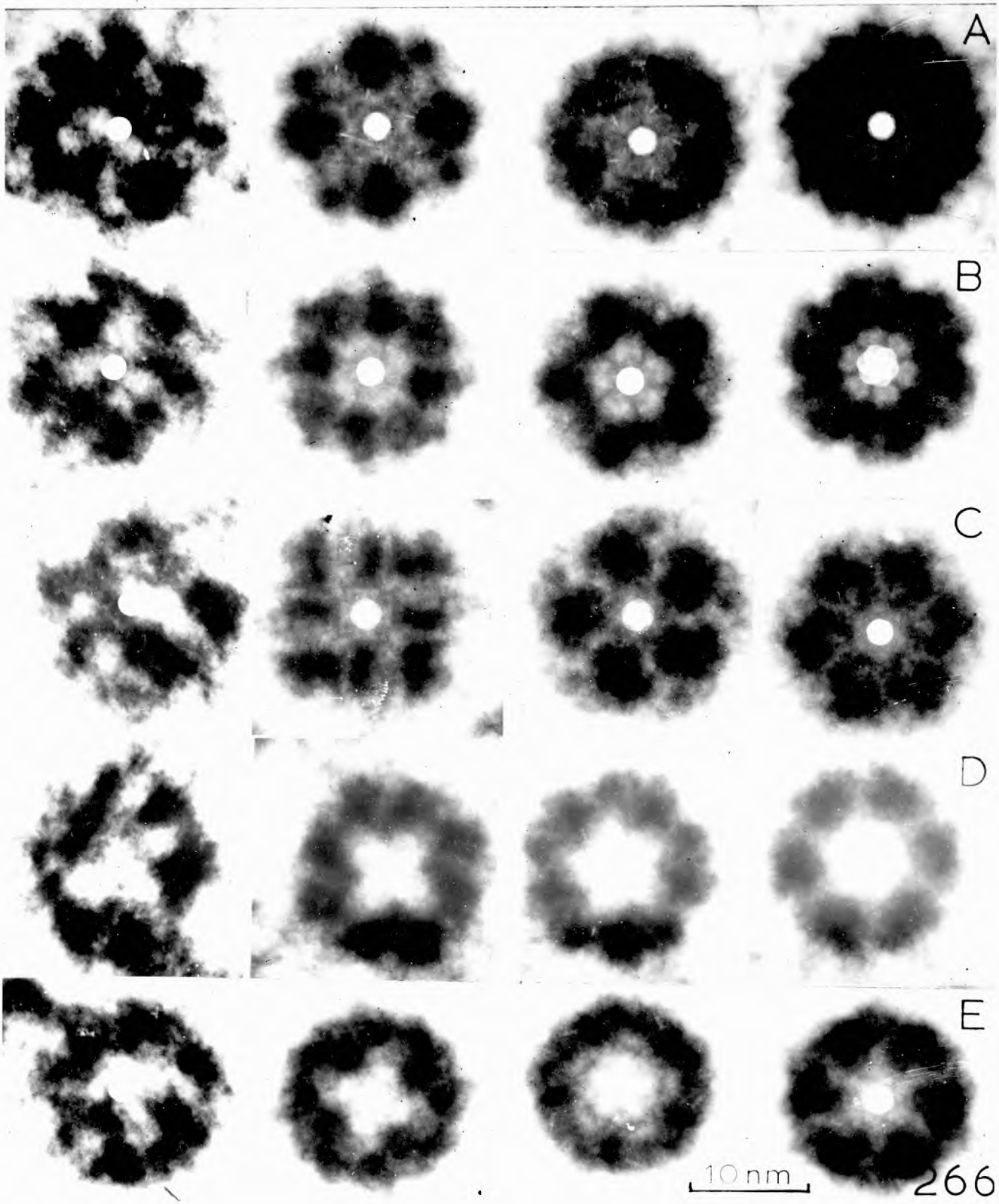
N= O
4
5
6
A
B
C
D
E
10 nm
266

Figs.267-270. Serial sections through a pair of pre-cleavage kinetosomes. Note dense cylinder, with arms, on a basal plate(Fig.268), C tubule terminations(Figs.269 & 270), striate fibre(Fig.270) and tubular roots terminating in dense material at the base of the kinetosomes(Fig.267). 1645H/1. 10032,10035,10036,& 10037.


267

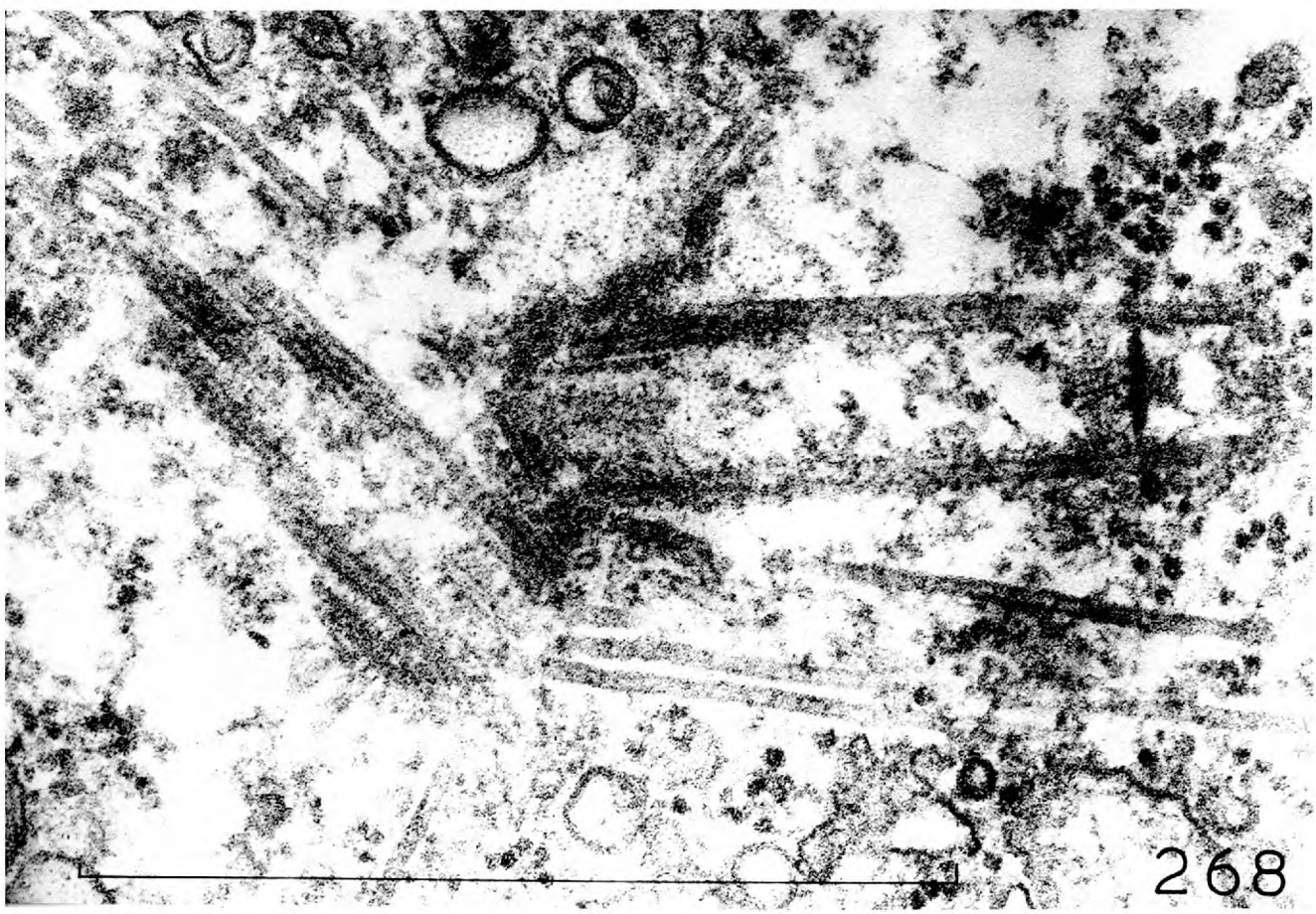
268

269

270

Fig.271. Pre-cleavage nucleus with kinetosomes, parallel E.R, nuclear pocket, active Golgi and tubular roots along the apex of the nuclues. 1848/1. 10929.

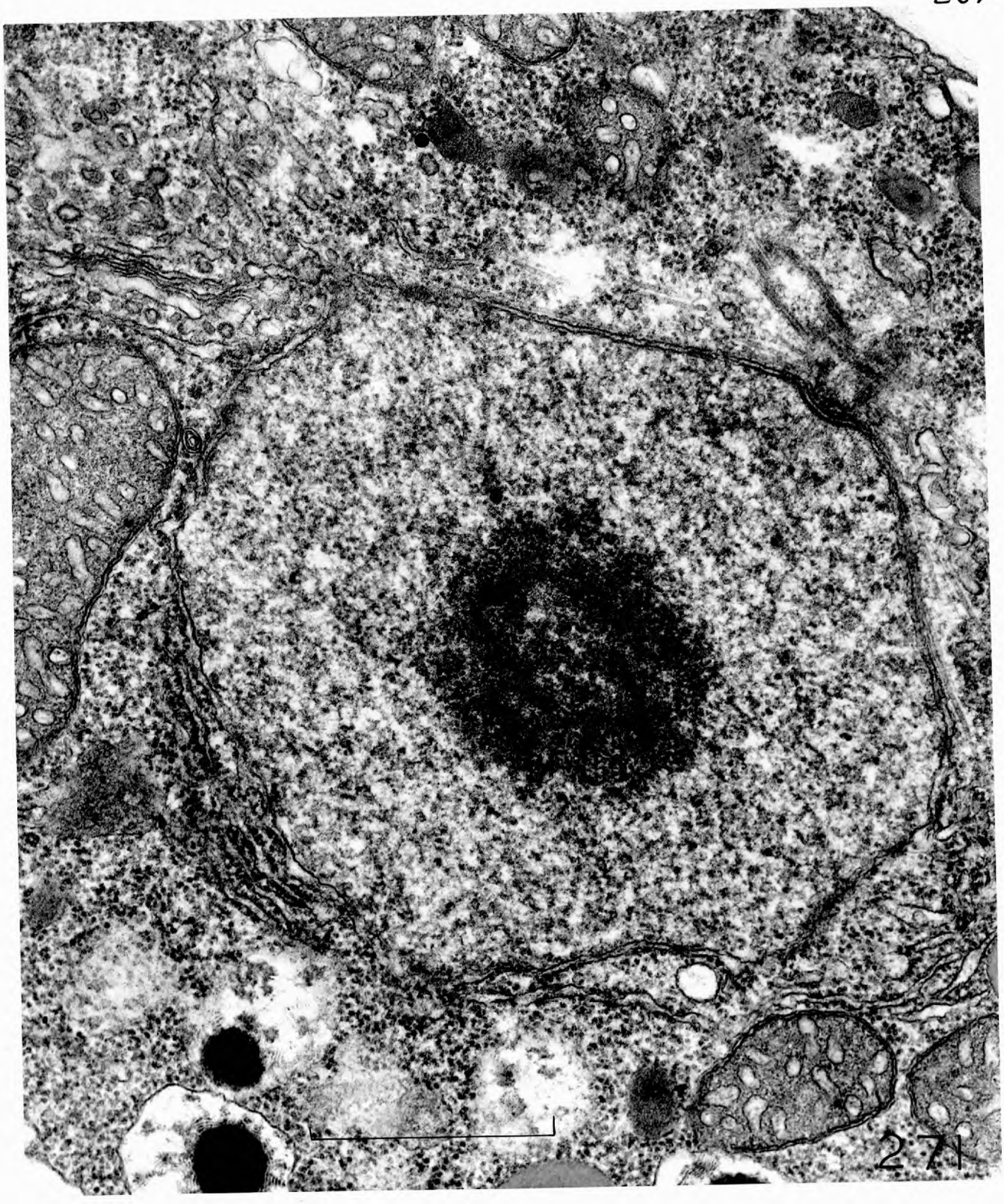
271

Fig.272. Pre-cleavage kinetosomes showing slightly dense terminal cap and cylinder on basal plate. Note tubular roots radiating from dense material, and nuclear pocket. 1827A/2. 10827.

Fig.273. Pre-cleavage kinetosome with dense cap and tubular roots. 1848/1. 10931.

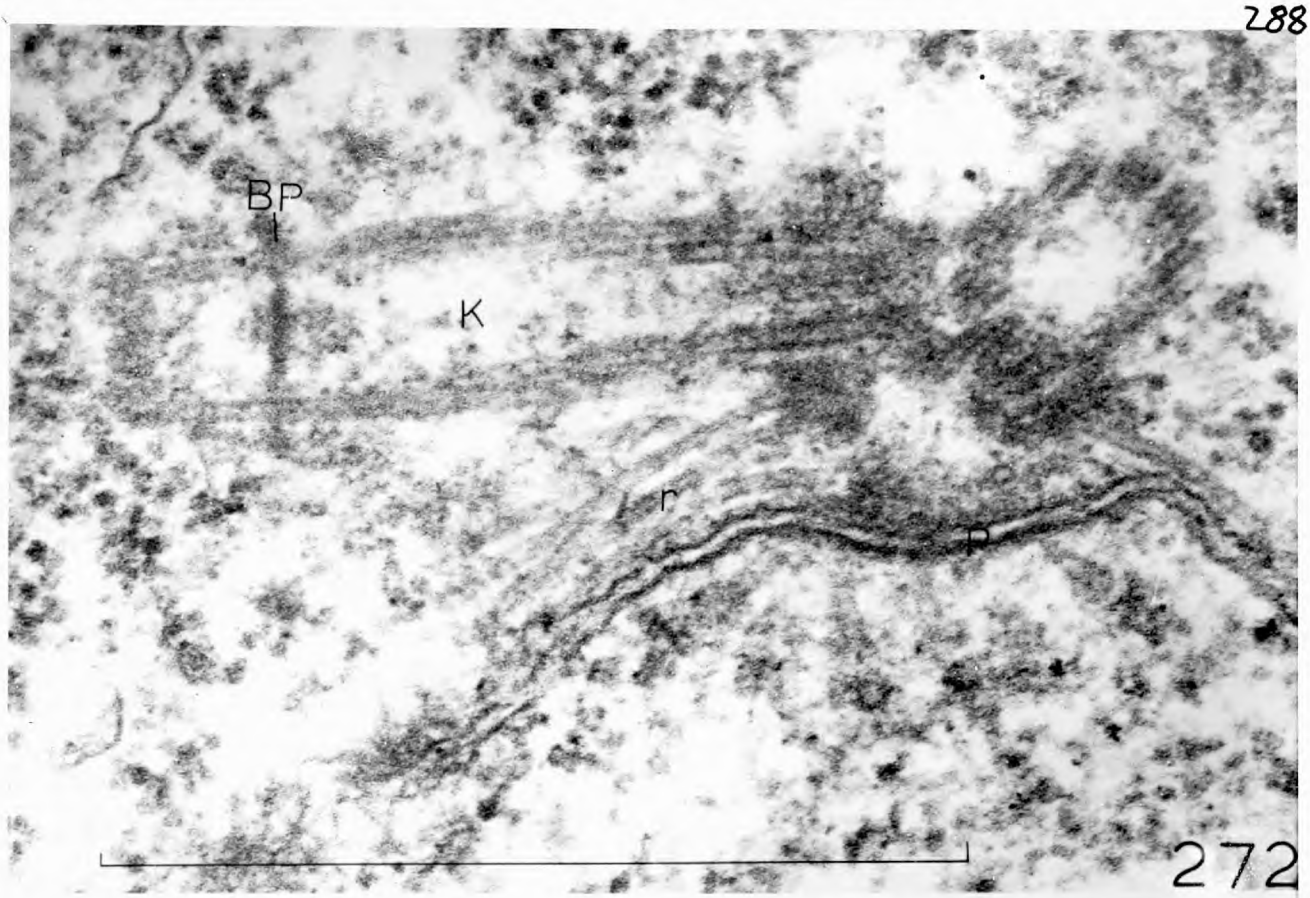
BP
K
r
P
272

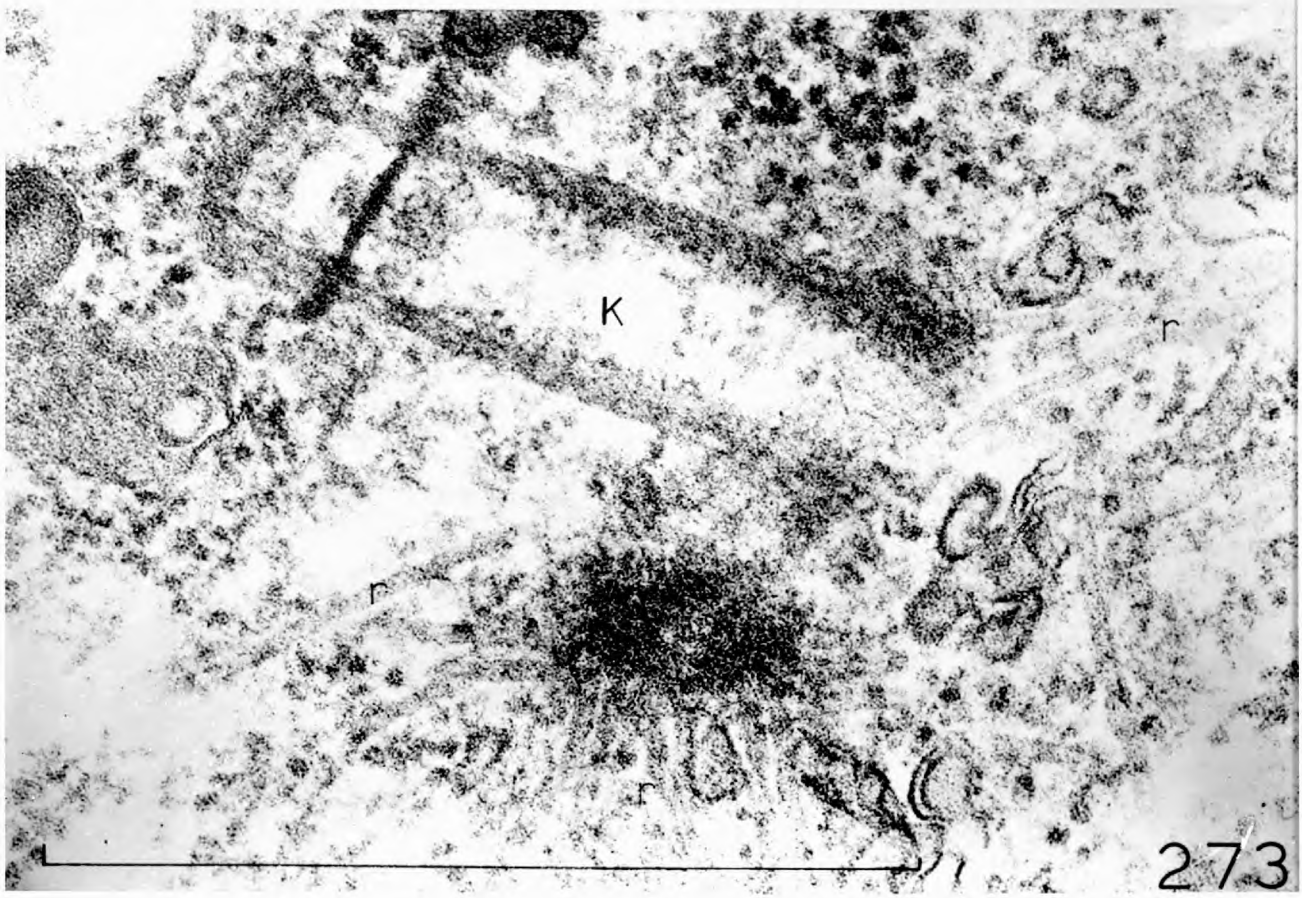
K
r
r
r
273

Fig.274. Degenerating nucleus and centriole in a healthy uncleaved sporangium. 1827A/3. 10831.

Fig.275. Damaged zoospore showing structural integrity of the kinetosome and E.R. ~~anchored~~ enclosed tubules but distorted flagellum axoneme. 1642/6. 12068.

Fig.276. Pre-cleavage kinetosomes showing an A-C link between the triplets in the cartwheel region. 1647F/1. 10307.

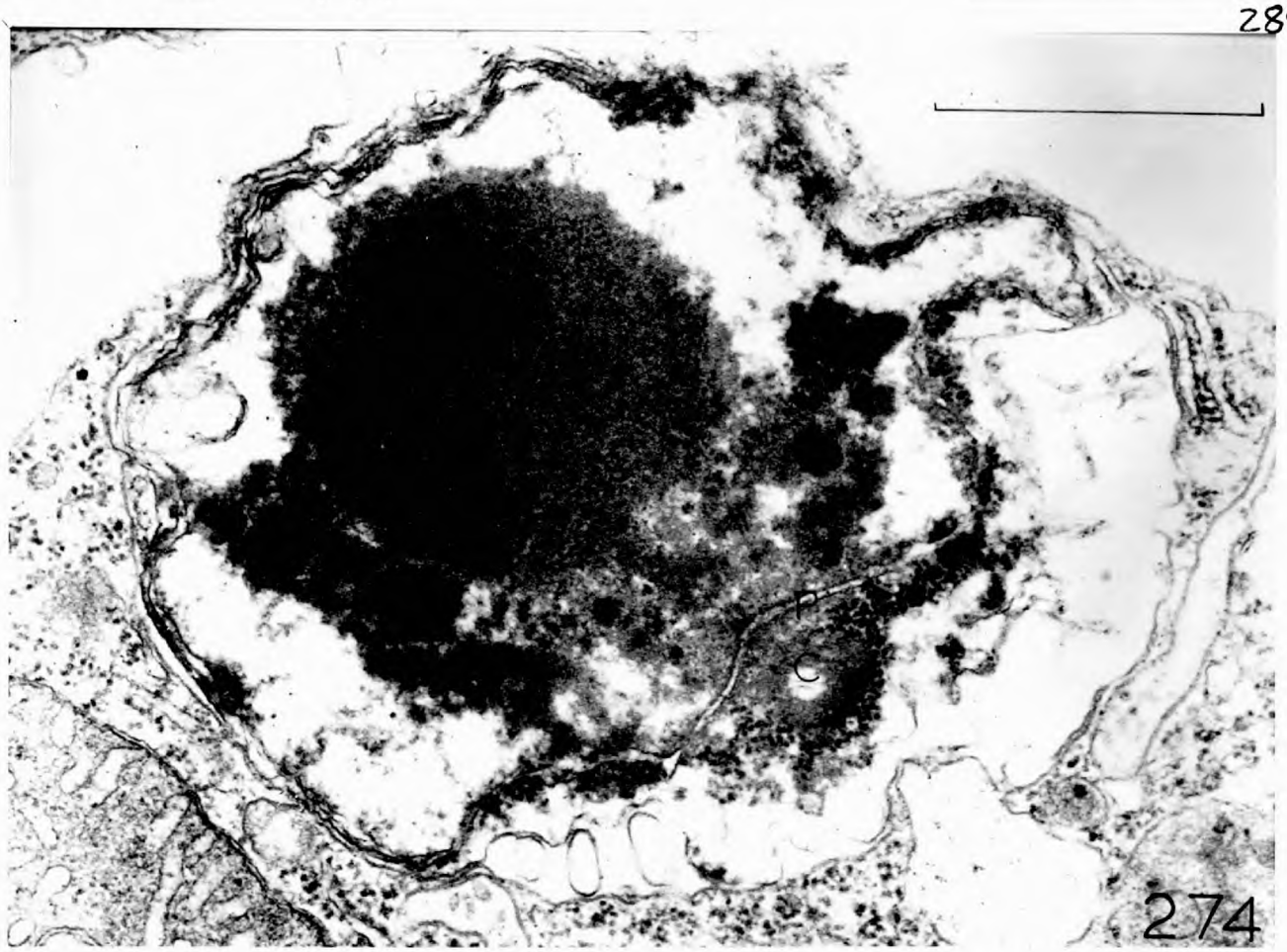
C
274


F
RP
K
f
0·1
275


K
N
Sw
0·1
276

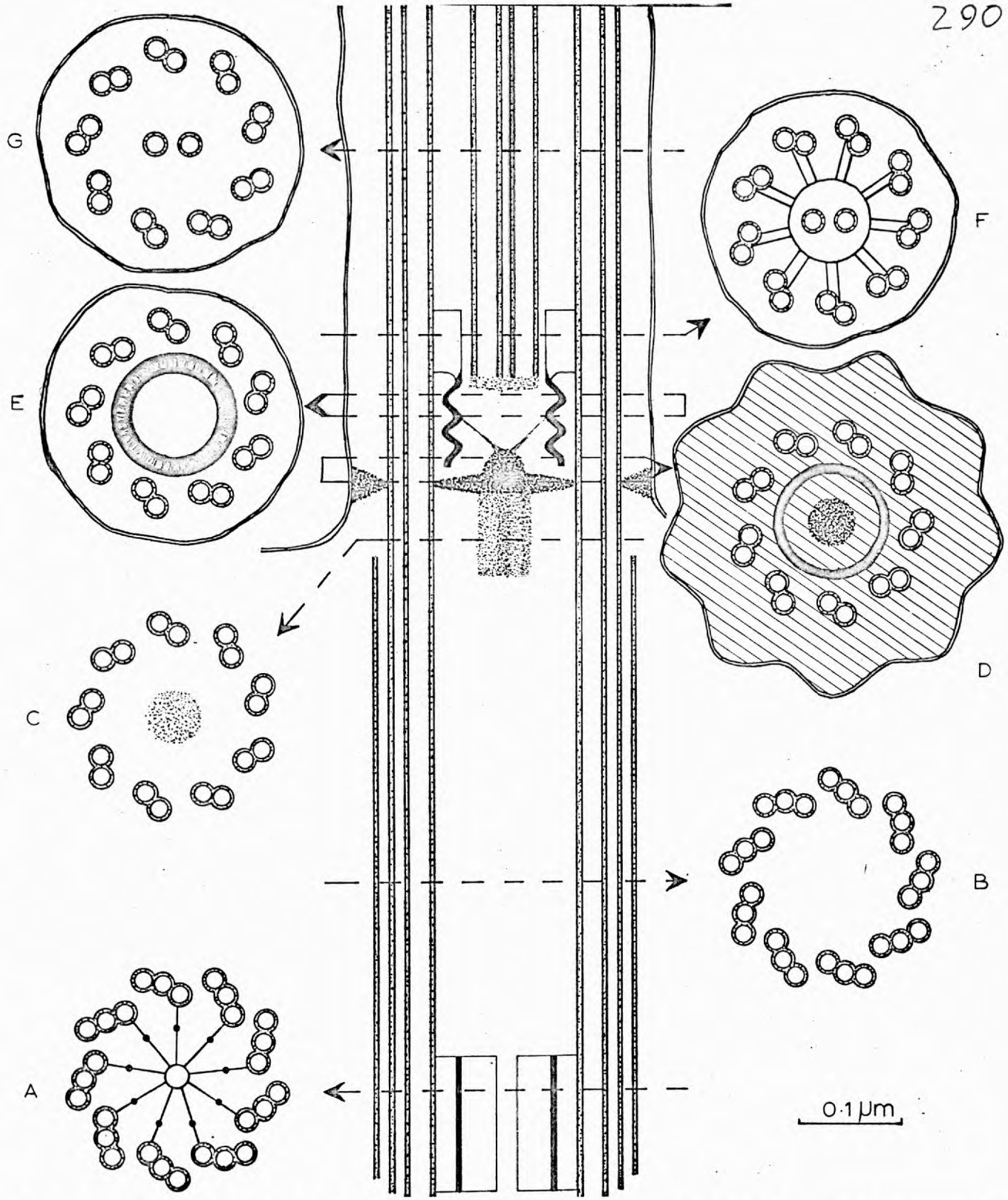

Fig. 277. Diagramatic reconstruction of a median longitudinal section of a kinetosome and proximal end of the flagellum of S. ferax. A) cartwheel. B) triple tubules. C) doublets above C terminations. D) basal plate with lower end of collar. E) thick collar. F) struts between thin collar and doublets. G) typical transverse section of flagellum.

Fig.278. Typical primary zoospore fixed in 5% GA. Note Golgi bodies, kinetosomes on a prominence in a groove, pyriform nucleus. with "rough" parellel E.R. about its base, dense bodies, tubules in the E.R. and bars concentrated around the periphery of the spore. 1848A/1. 10936.

Fig.279. Typical primary zoospore after 5%GA fixation followed by papain digestion. The structure is essentially similar to undigested spores but much of the background density has been removed revealing the structure more clearly. Note bars primarily, though not exclusively, arranged around the periphery of the spore. 1893/1. 12485.

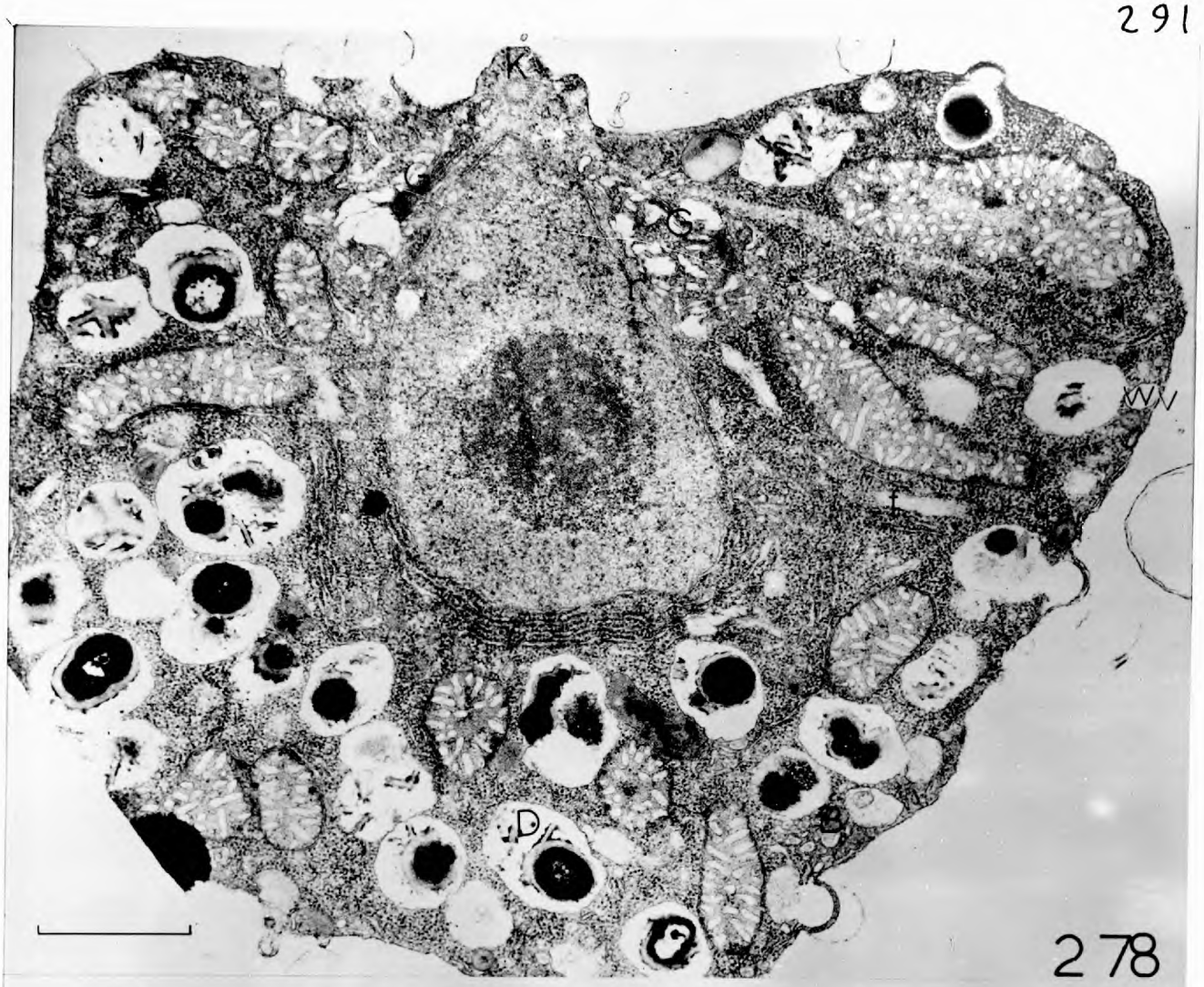

278

279

Fig.280-283. Serial sections (one missing between 281 and 282) of the kinetosomes in Fig.279. Note concertina-like thick collar, basal plate attached to the membrane of the spore and striate fibre. 1893/1. 12484a, 12485a, 12486, 12487.

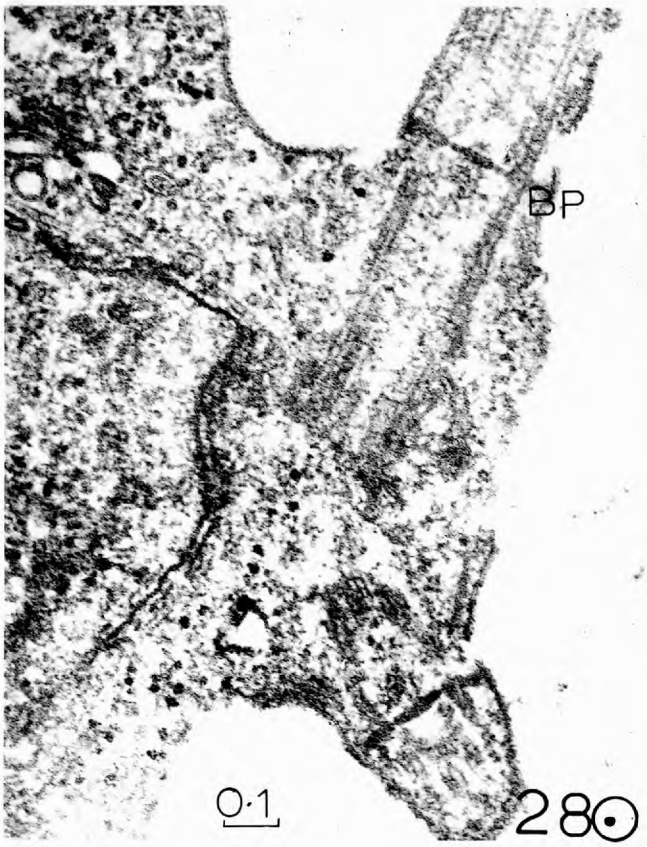

280

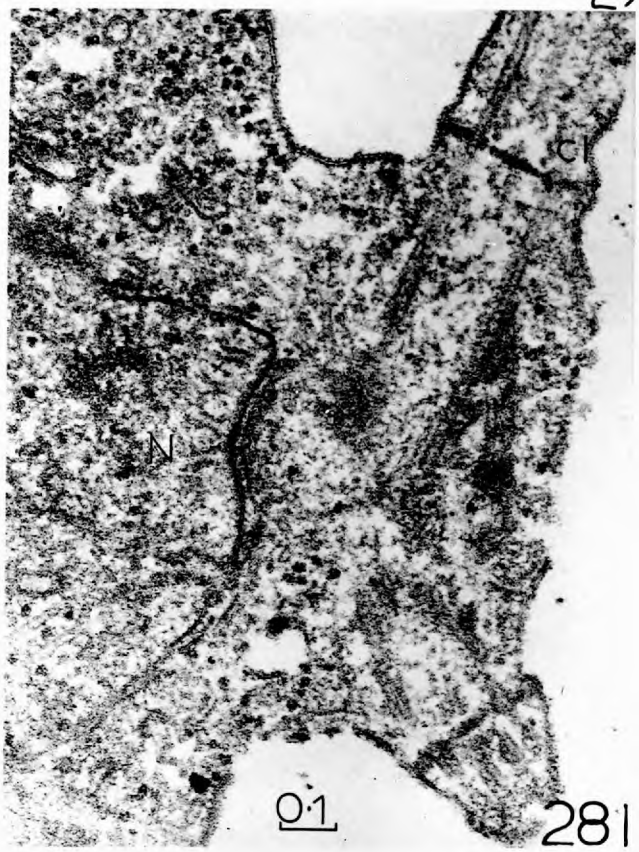

281

282

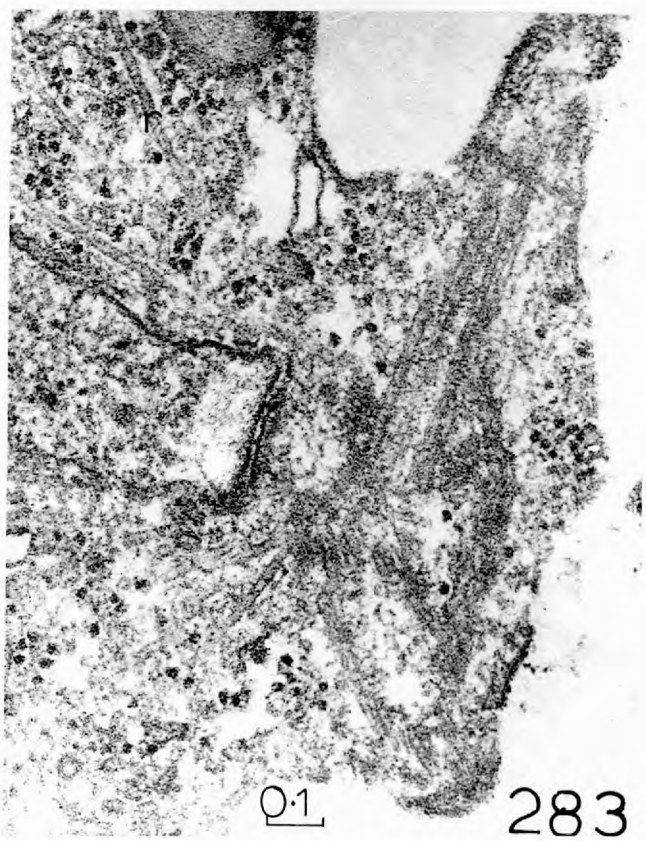

283

Fig.284-293. Part of a series of 18 serial sections through the transition region of a kinetosome and flagellum.(Letters denote section numbers starting proximally at a). Note C tubule terminations at Fig.284, dense cylinder below basal plate(Fig.285), oblique section of part of basal plate(Fig.287), thick collar (Fig.288), transition between thick collar and thin collar with dense material at the base of the central pair (Fig.289), thin collar with struts and one of the central tubules (Fig.290), thin collar and struts with central pair (Fig.291), top of thin collar (Fig.292) and typical section of the remainder of the flagellum(with the exception of the tip)(Fig.293). This material was digested with papain between GA and Os. The structure of the rest of the spore was not significantly altered. 1893/2. 12374-12382 & 12384. (All Mag.x 142,000.

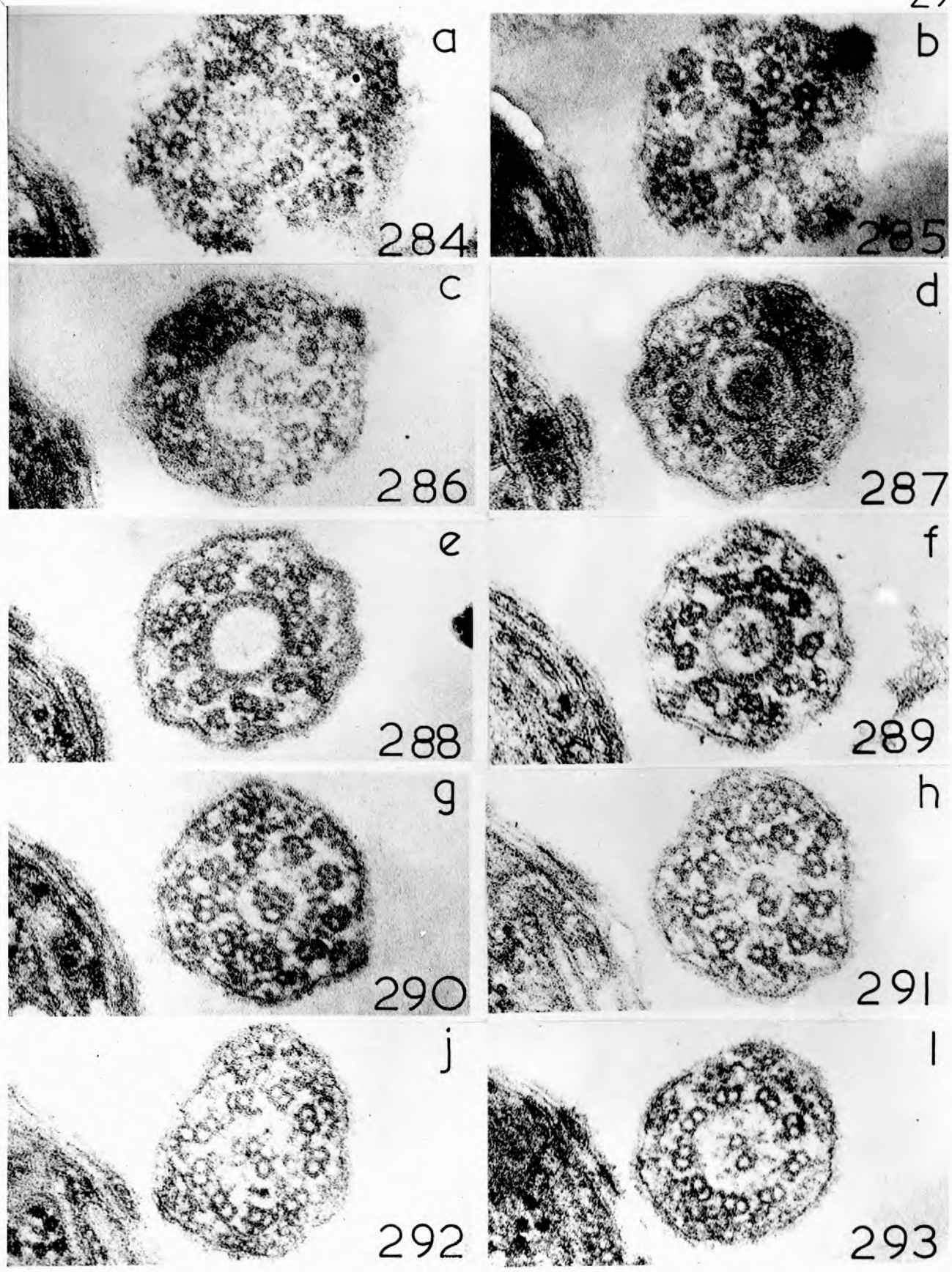
a
284
b
285
c
286
d
287
e
288
f
289
g
290
h
291
j
292
l
293

Figs.294-295. Adjacent oblique sections through the transition region of a kinetosome and either the axoneme of the other flagellum or the other axoneme of the flagellum shown in Fig.299. Note radial strands in the wall of the thick collar and possible connections between this collar and the cylinder on the basal plate(Fig.295). 0.1% GA in M/30P. 1887/4. 12727 & 12726.

Fig.296. Kinetosomes of a primary zoospore. Note collar, striate fibre and tubular roots. One of a series of sections. 0·1% GA 1887A/1. 12755.

Fig.297. Glancing section of thick collar showing concertina structure. One of 6 serials. 1893/1. 12476.

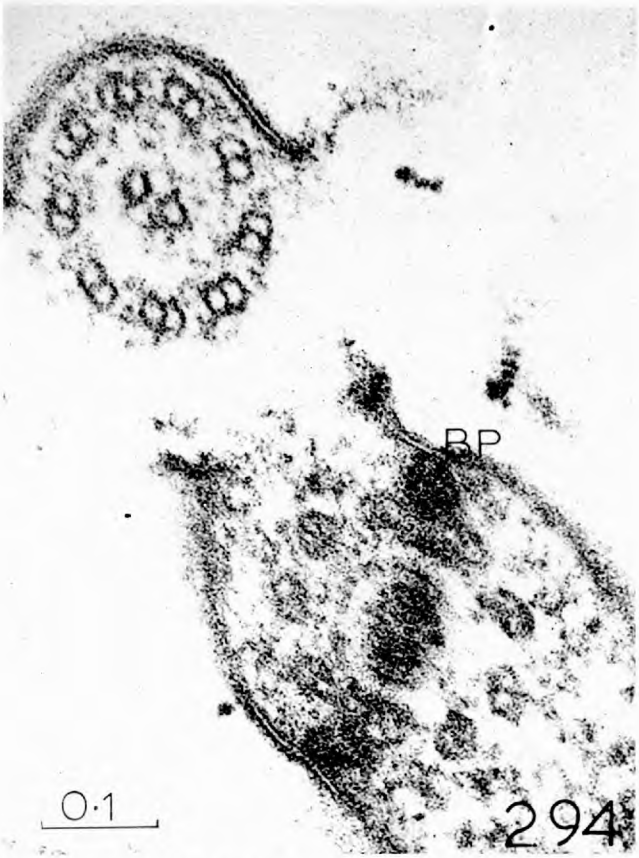
BP
0·1
294

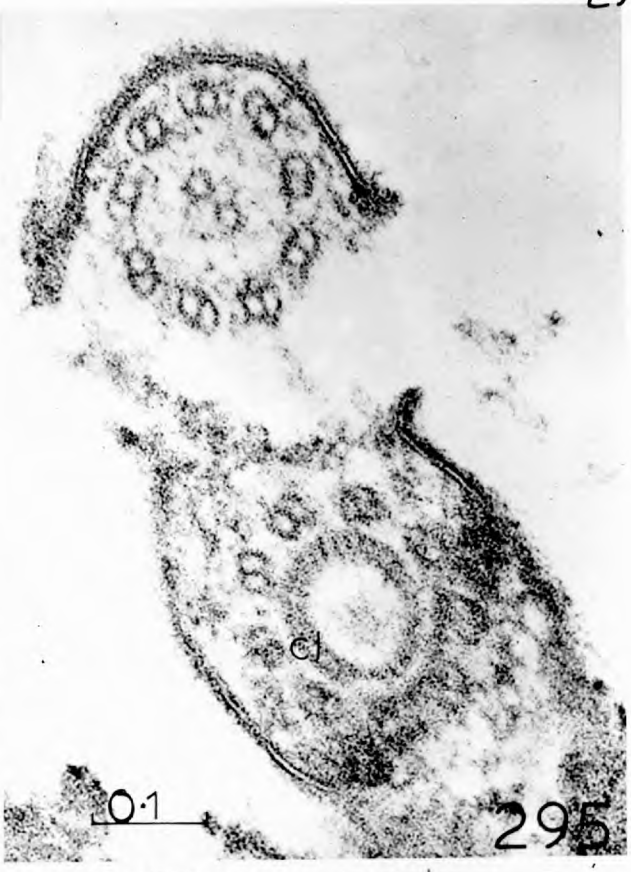
cl
0·1
295


0·1
sf
BP
cl
296

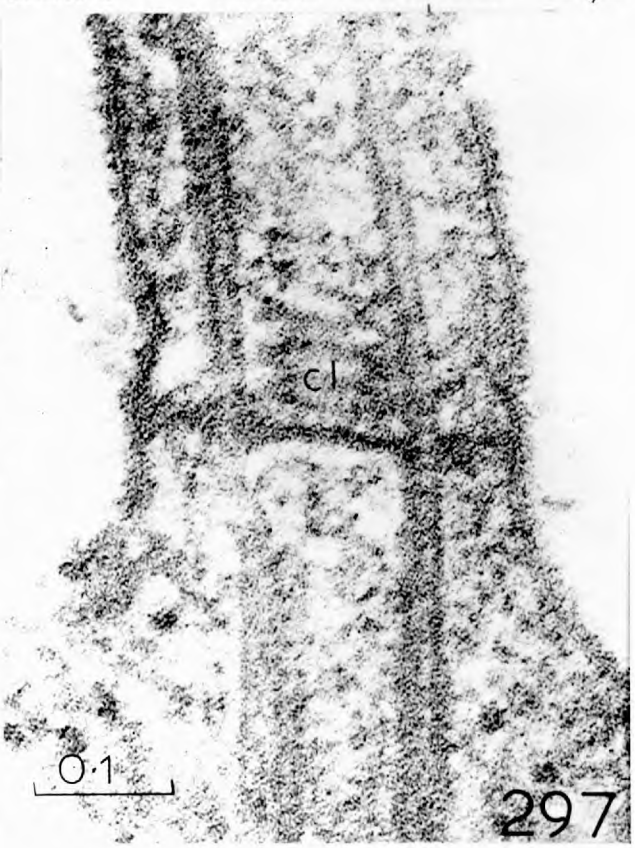
cl
0·1
297

Fig.298. Flimmer hairs attached to sheath of flagellum by tapering granular material. 1848E/1. 12010.

Fig.299. A flagellum with two axonemes and probably tapering flimmer hair bases. Flimmer was visible around this flagellum. 1887/4. 12731.

Figs.300-303. Serial sections of the tip of a growing flagellum. 1893/1. 12481-12484. (All Mag.x 115,000.

Fig.304. Shed flimmer hairs in a sporangium in which all the spores had encysted. Note tapering granular points. 1647E/6. 8883.

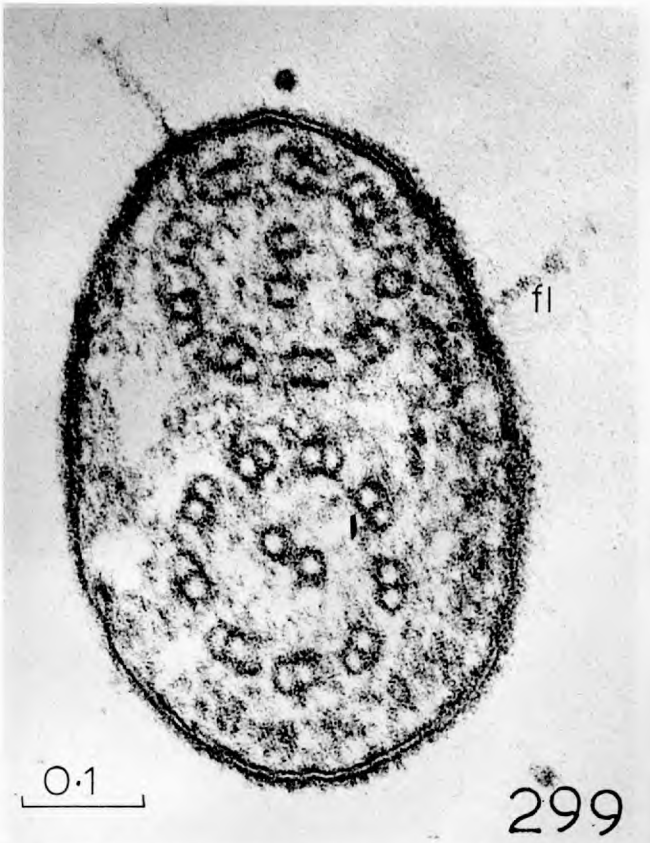

299

298

300

301

302

303

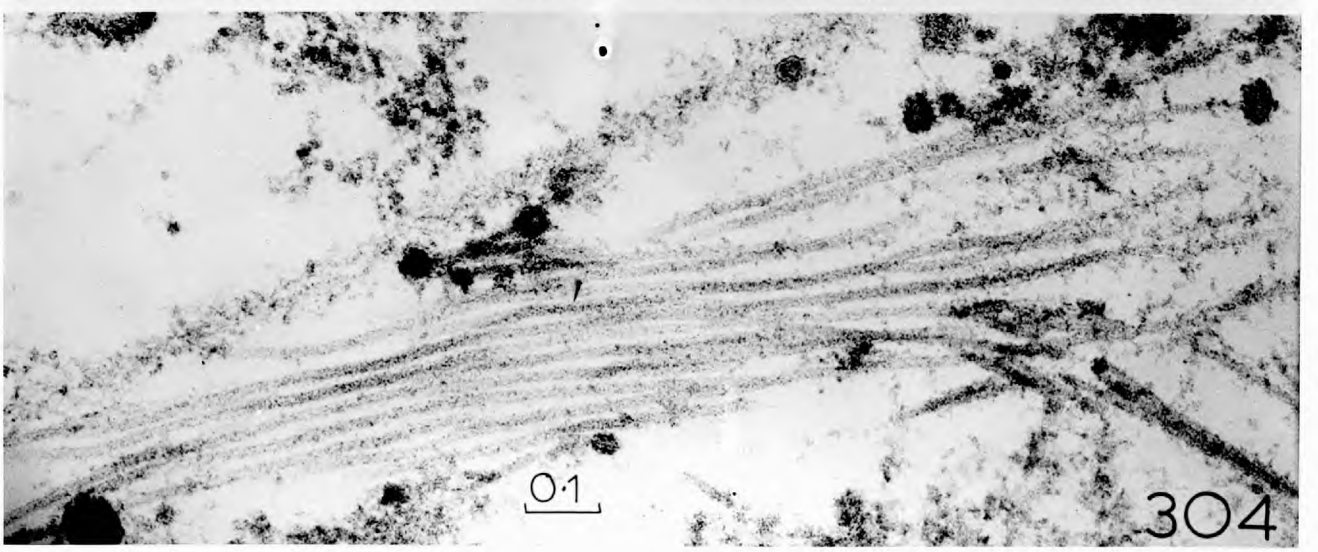

304

Fig.305. Recently encysted zoospore with naked withdrawn flagellum axoneme. 1642/8. 12071.

Fig.306. Kinetosome in a primary cyst. Note basal plate with attached cylinders and tubular roots. 1739/1. 10175.

Fig.307. Kinetosome in a primary cyst. 1739/1. 10177.

Fig.308. Recently encysted primary spore showing two free axoneme doublets. 1642/8. 8803.

Fig.309. Germinating primary cyst which had undergone one nuclear division. Note kinetosome and centriole or kinetosome at 90° to it. 1776/1. 10486.


F
K
N
305

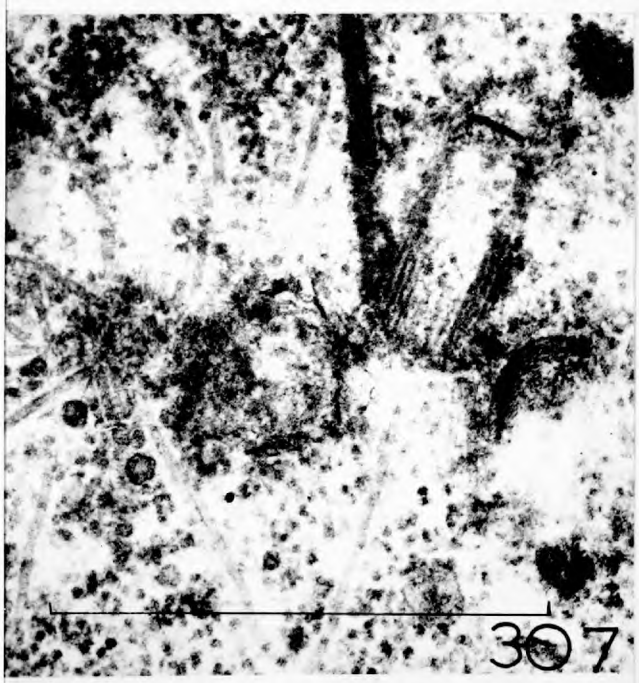
307

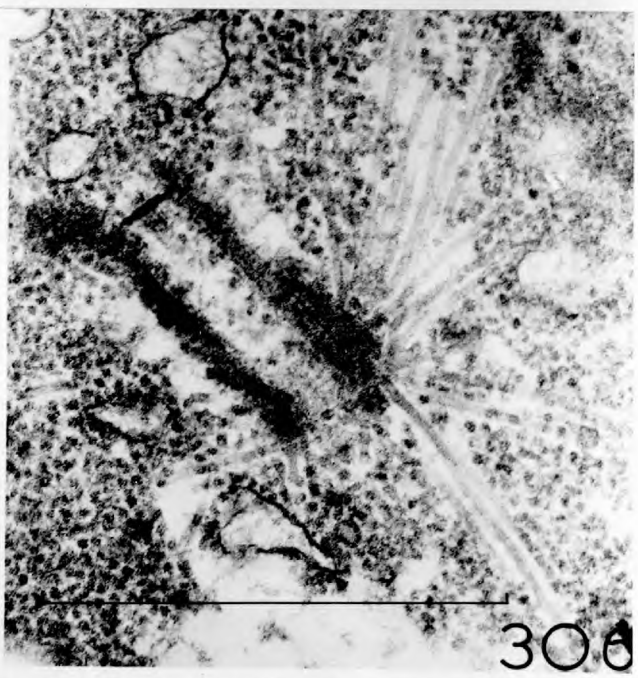
306

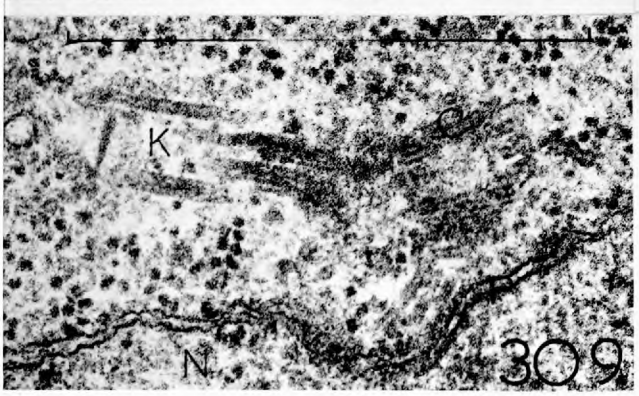
K
N
309

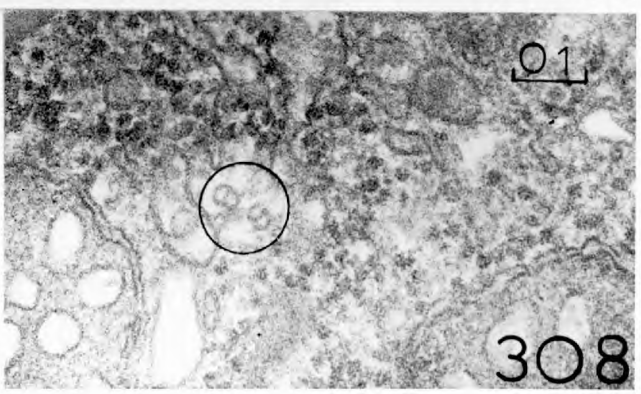
01
308

Fig.310. Primary cyst liberating a secondary zoospore. Note secondary bars. 1779/1. 14098.

Fig.311. Primary germinating cyst which has undergone one nuclear division. The kinetosome has lost its basal plate and is at 180° to a centriole. 1692D/3. 10006.

Fig.312. Glancing section of the point of emergence of a primary germinating cyst. Wall vesicles are tubular. 1691C/4. 10017.

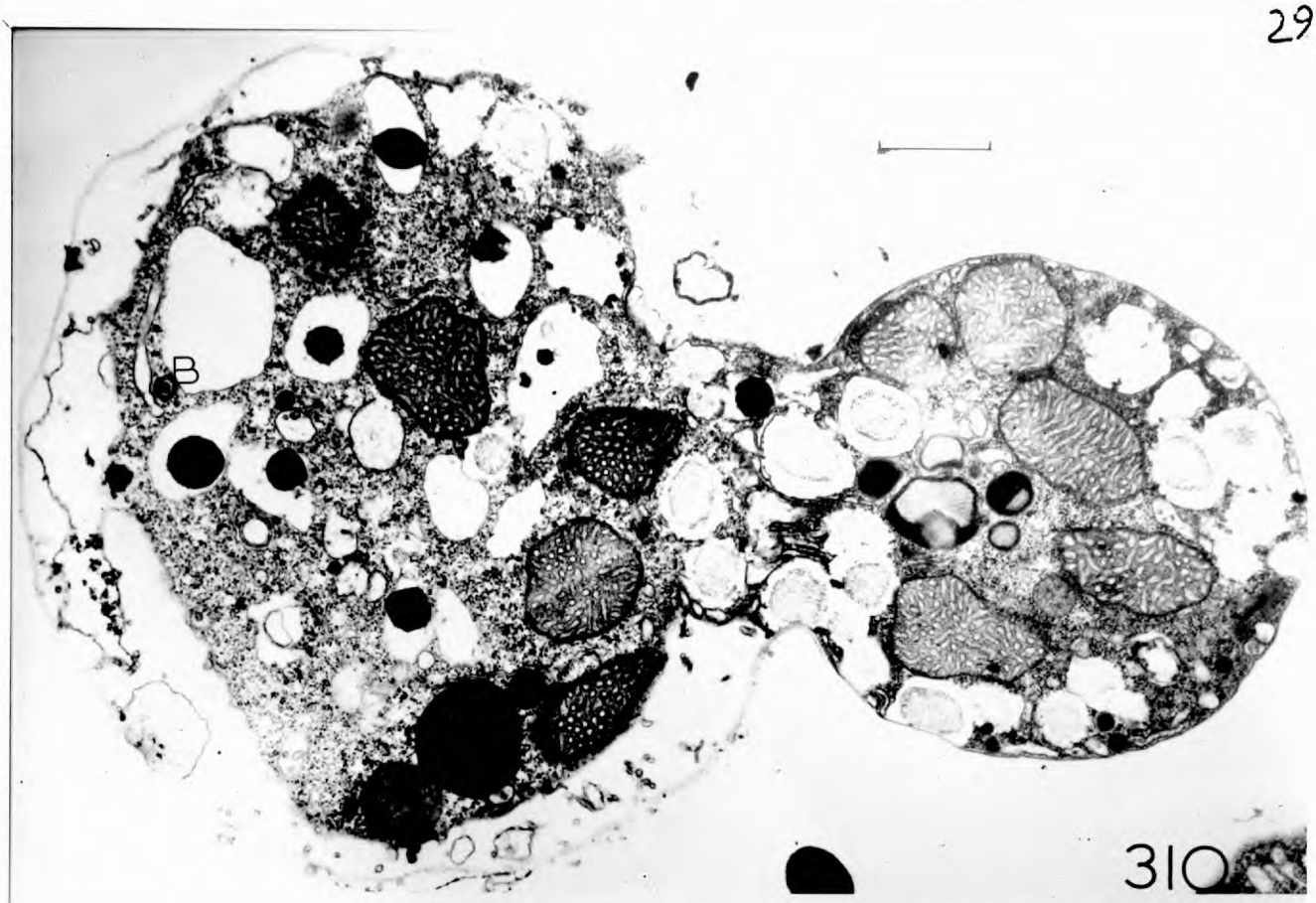

310

312

311

APPENDIX

1) Fixation

The structural changes which occur during the preparation of material for electron microscopy are not well documented, although their importance to ultrastructure interpretation is obvious. The relatively small hyphae of S. ferax are more amenable to light microscopical observations during the course of fixation than are most tissues.

Growing hyphae of S. ferax were mounted in OM under a coverslip and examined with phase contrast microscopy. The effects of the various solutions used for electron microscopical preparations were examined by drawing the solutions across the preparation with filter paper whilst observing the hyphae through the coverslip. Such observations were only possible with a x40 objective; excessive specimen movement precluded the use of the preferable oil immersion objectives.

Initially, a hypha was examined through all the fixation and dehydration processed to the addition of resin. All detectable changes occurred in the initial fixation with 5% GA in M/15 P, consequently subsequent observations were restricted to this stage of preparation. In both 1% Os in M/15 P and 5% GA in M/15 P, cytoplasmic streaming ceased almost instantly when the fixative reached the hypha (time = 0). Hyphae varied in their response to the fixative and, although few observations were made in Os fixative, it appeared to

cause similar changes to those described below for 5% GA fixation. Generally organelles such as nuclei became less distinct within about 2 min. The cytoplasm tended to become darker and the phase halo brighter, both changes occurring within one or two min. although possibly becoming more pronounced over about 20 min. In some hyphae, e.g. Figs. 317 - 320, there were apparently no definable structural changes, although this is difficult to prove as the apparent structure varies with the focal level of the micrographs. However, in other hyphae, there were very marked changes, e.g. Figs. 313 - 316. Generally, the vacuole enlarged considerably and the cytoplasm became pressed against the walls of the hyphae. Cytoplasmic strands across the vacuoles usually broke and there was an ill defined, slight clearing of the peripheral apical cytoplasm. All these changes occurred within about 0.5 min., further changes rarely were observed after this time, although on one occasion, the apical cytoplasm appeared to become increasingly vacuolate up to about 40 min.

These observations suggest that most gross morphological changes occur during the first 0.5 to 1 min. after adding the fixative, a finding in agreement with the observed similarity between sectioned material fixed for 2 min. and 2 h. in GA. However, the increase in vacuolation and refractive index of the cytoplasm after longer times in GA in some hyphae may indicate that the process of stabilization of cell contents takes considerably longer, although Flitney (1966) has shown

that both 6% and 0.6% GA completely fix albumen in a gelatin gel in about 1 min. Thus, when penetration is not a problem, a fixation time of as little as 0.5 min. is likely to give similar morphological results to longer fixation time.

2) Section thickness

a) Introduction

An accurate knowledge of section thickness is essential for quantitative autoradiography and serial reconstructions, and also aids the interpretation of any sectioned material. The interference colours shown by thin sections on the water bath provide a guide to their thickness (Peachy, 1958, and Cosslett, 1967), but such a guide is extremely subjective, and the range of thickness corresponding to any given colour is large. Sjöstrand (1953) and Porter & Blum (1953) have shadowed sections at a known angle and measured the shadow length at the edge of the sections, but this gives no indication of the variation in intrasection thickness and is subject to considerable error if the section is not perfectly flat on a smooth surface, a condition not easily achieved. Zelander & Ekholm (1960) and others have used optical methods of measuring section thickness, but such methods involve the use of specialized equipment. Similarly, Williams & Meek (1966) have investigated section thickness of araldite sections with an interference microscope and an autoradiographic technique. However, all these techniques are either unreliable, complex, or require special apparatus and specially prepared sections.

It was thought that the resection technique, used originally by Phillips & Shortt (1964) for metals, would provide a simple means of investigating the thickness of routine sections, both before and after examination in the microscope. It could also provide information on the penetration of stains into the sections.

b) Techniques

Initially, sections of a recorded subjectively estimated colour were collected without any form of expansion on normal unfilmed 200 mesh grids and coated on both sides with gold/ palladium alloy in a vacuum shadow caster. These grids with their sections were then embedded in epon resin and polymerized. The metal coated sections were clearly visible in the polymerized blocks so that the block could be trimmed to produce a face containing a portion of a section orientated at right angles. This face was then sectioned in the normal way and the resections examined in the microscope without further treatment. The thickness of these sections was difficult to measure because the metal coating tended to be granular and obscured the boundaries of the sections (Fig. 321). Subsequently, sections of non-vacuolated, undifferentiated pea leaf tissue were collected on filmed Maxtaform H6 labelled grids. The sections were stained with various combinations of UAc and Pb (see below), then located on the grid with the light microscope, or, in the case of the irradiated specimens, in the electron microscope. These sections were then embedded and

resectioned as above, using the grid labelling system to locate the now invisible sections. The orientation of the resectioned sections was easily controllable to $\pm$ 10°, which gives a maximum error of about 1.6%, i.e. 0.7 nm in 45 nm. The boundaries of these resectioned sections were sharply defined in the electron microscope by their stained cellular structures (Figs. 323 & 324). Sections which were to be examined for the effect of the electron beam were irradiated by slowly scanning a chosen grid window with a focussed electron beam until the whole window had been covered. Each area of the section thus treated would have been irradiated for about 15 sec.

c) Observations

i) Section thickness

The boundaries of the resectioned metal coated sections were obscured by the metal so that accurate measurements were not possible. Uncoated resections had well defined edges but were all found to be considerably undulated, apparently in all planes (i.e. dimpled, not furrowed). Since the sections were flat before embedding, they must have expanded during this process and thus become thinner to produce the undulated appearance. Thus, the resections were not only thinner than untreated sections, they were also frequently obliquely resectioned, thus adding further inaccuracy to the method. However, by measuring the width of straight, apparently normally resectioned regions of the section, the measurements shown in Table 9 were obtained.

Table 9

Thickness of resectioned section

Colour on water boat	Number of sections	Average thickness (nm)	Range
Grey	4	58.7	45.8 - 81.6
Silver	9	99.5	61.2 -135.0
Pale gold	3	111.8	104.5 -119.8

Due to the undulation of the sections and the obvious thinning which must have occurred, these results are only a guide to the actual thickness of the sections. They are, however, in close agreement with those obtained by Williams & Meek (1966) and do illustrate the range of thickness found within a subjectively estimated colour range. The thickness recorded for the grey sections is undoubtedly an over estimate of that achieved in more recent work with more experience and an improved knife; for example, the gap between two centrioles in Figs. 43 & 48 is only about 20 nm. Since neither centriole appears in Fig. 29, this section must be 20 nm or less in thickness, yet it did not appear to be as thin as others used in recent work. Zelander & Ekholm (1960) have also noted sections of less than 20 nm.

More sophisticated methods may overcome the problem of section undulation in embedding, but these would be too technically laborious for use as a routine method for investigating section thickness.

ii) Electron beam evaporation

Sections which had not been placed in a vacuum or irradiated showed an even thickness. Sections which were metal coated (i.e. vacuum treated) showed some signs of differential thinning, but the thinning described below may be attributed mainly to the effects of the electron beam rather than the high vacuum. Areas of irradiated sections containing high concentrations of osmophilic structures were not appreciably thinned by the beam (e.g. membranes, ribosomes and lipid droplets, Fig. 323). The degree of thinning is approximately proportional to the percentage of epon in the section except that cell walls appear to be thinned more than pure epon (Fig. 322). This differential thinning or removal of epon is undoubtedly responsible for the increased contrast observed in a normal section after a short period of examination. The removal of material evenly from both sides of the specimen suggests that loss is by simple evaporation from the heated resin, no doubt partially explaining the contamination found in all microscopes.

iii) Stain penetration

In order to investigate the rate of penetration of UAc and Pb into epon sections, thick (200 - 300 nm) sections were floated on drops of stain. This meant that the stain would only penetrate from one side. The use of thick sections was designed to give the stain a longer path to travel, thus providing a better opportunity of detecting the penetrating

"front" of stain as an asymmetric increase in electron opacity of the cytoplasmic structures in the section. Sections were examined after various staining treatments which independently varied the times of UAc only from 10 to 40 min., Pb only from 1 to 8 min., Pb after UAc from 1 to 8 min. and the length of the water washes between UAc and Pb and after Pb from 1 to 16 min. The optimum treatment for normal viewing of this material was 20 min. UAc, 1 min. H_2O, 5 min. Pb and 1 min. H_2O. In some instances, an asymmetry of staining appeared (Fig. 325), but the results were not conclusive or consistent (Fig. 324). They did, however, suggest that UAc usually traversed the thickness of the average silver or grey section within 10 min. and that Pb could cover the same distance in 1 min. The washes did not appear to remove any stain, even after 16 min. Thus, it would appear that time dependent increase in staining is due to a build up of concentration rather than an effect of penetration.

3) Autoradiography

a) Introduction

Several workers (e.g. Caro & Palade, 1964, and Northcote & Pickett-Heaps, 1966) have detected the organelles responsible to the synthesis of a particular end product by feeding tissue with a short pulse of radioactive precursors, followed by unlabelled precursor and tracing the passage of the radioactivity by sampling the tissue at timed intervals by means of electron microscope autoradiography. It was hoped

that since one of the major activities of hyphal apices is the production of wall material, the organelles responsible for its production could be detected in a similar manner using radioactive glucose. Although glucose is not a specific precursor of wall material, it was hoped that since a large amount of wall material is formed, most of the glucose would pass into the wall.

b) Techniques

The techniques used were based on the work of Caro & van Tubergen (1962) and Northcote & Pickett-Heaps (1966). Living hyphae which were growing rapidly on OM were given a short pulse of radioactive glucose (see below) on cubes of agar removed from the colony. These hyphae were then fixed and embedded as described in Materials and Methods. Gold/silver sections of hyphal apices were collected onto formvar coated 100 mesh copper grids and stained with UAc and Pb. They were then coated with a thin layer of carbon and covered with a layer of silver halide emulsion. This was applied by melting 10 g of Ilford L4 emulsion in 20 ml of distilled water at 45° C. for 15 min. (in indirect light from an Ilford 904F safelight). The emulsion was then cooled in iced water for 5 min. and allowed to gel at c 25° C. for 30 min. When the viscosity of the gel was correct, a 4 cm. diameter loop of thin copper wire was dipped into the emulsion, withdrawn slowly and the thin, even film of emulsion allowed to gel completely. The film was broken over one or several grids, supported on corks. The

grids were stored in a vacuum desiccator in the dark at 4° C. or 20° C. until test grids indicated sufficient exposure. The emulsion was developed in Kodak D19b at 23° C. for 2 min. followed by 1 min. in water and fixed for 2 min. in non-acid hypo, followed by a further water wash, and allowed to dry. It was necessary to stain the grids with Pb again, since the earlier section stain had been removed during processing.

c) Observations

Initially, hyphae were given a 10 min. pulse in 1 ml of uniformly labelled C^{14} glucose containing 10 mc (Radiochemical Centre, specific activity 10 mc/mM). This pulse was followed by direct fixation or a chase of OM for 5, 10, 30 or 60 min. The autoradiographs were developed after four months' exposure, test grids having shown little increase in grain numbers since one month. On these grids, the background was generally low, but there were only 3 or 4 grains per section which were arranged over the periphery of the cell or on mitochondria. However, their low number in all preparations rendered counts meaningless (Fig. 327).

Consequently, further small, but rapidly growing, colonies were labelled similarly with 5, 15 and 60 min. pulses of D-glucose 6-T (Radiochemical Centre, Specific activity 1.34c/mM) at the rate of 0.05 ml per colony, equivalent to 0.25mc/colony. These pulses were followed by chasers of OM for 0, 5, 15, 30 and 60 min., or 0, 15, 30 and 60 min., or 0 and 60 min. Sections from these blocks were exposed for two months, after

which extremely variable results were found. The background grain count was generally low, though often there was an accumulation of grains around the grid bars. This is probably caused by the higher electrode potential of copper relative to silver which enables copper to displace metallic silver from the silver halide in the emulsion. Other results followed no detectable pattern, apart from a generally high grain count around the periphery of the hyphae and a lower internal count (Fig. 328). The high peripheral counts occurred after both 5 min. pulse with no chaser and 60 min. pulse, followed by a 60 min. chase. They probably illustrate an effect of surface absorption, rather than incorporation.

The results will not be described in further detail. However, they did illustrate numerous limitations to the technique as applied to fungal hyphae.

The major limitation is the size of the grain relative to the size of the organelles under investigation. In S. ferax, the organelles at the hyphal apex are closely packed together; the large grains shown in Fig. 326 and the 0.1 μm resolution shown to be the best obtainable by Caro (1962) make it almost impossible to determine which structure is associated with a particular grain. Furthermore, the size and high concentration of grains in Fig. 328, for example, obscure the underlying structures. The use of another developer can give smaller grains (Ray, 1967), but the resolution is still poor and such developers are often found to be unpredictable. However, a

statistical analysis of a large number of hyphae showing an optimum concentration of grains of the smallest size may be capable of indicating an association between the grains and a type of organelle. Thus, to obtain meaningful results, in the order of a hundred apices would need to be examined. The technical difficulties involved in the production of this number of apices are formidable; clearly, a more homogeneous population of small cells is more amenable to autoradiographic studies.

Figs.313-316. Hyphal apex in OM(Fig.313) showing changes occurring after the addition of 5% GA in P for 0.5min(Fig.314), 3min(Fig.315) and 22min(Fig.316). Note increased vacuolation, "disappearance" of nucleus and darker cytoplasm. (Mag.x 1,872). 722,724,726,& 728.

Figs.317-320. Hyphal apex in OM (Fig.317) showing relatively few changes, other than a darkening of the cytoplasm, after 2min(Fig.318),7min (Fig.319) and 80 min(Fig.320) in 5% GA in P. (Mag.x 1,872). 691,693,695, & 697.

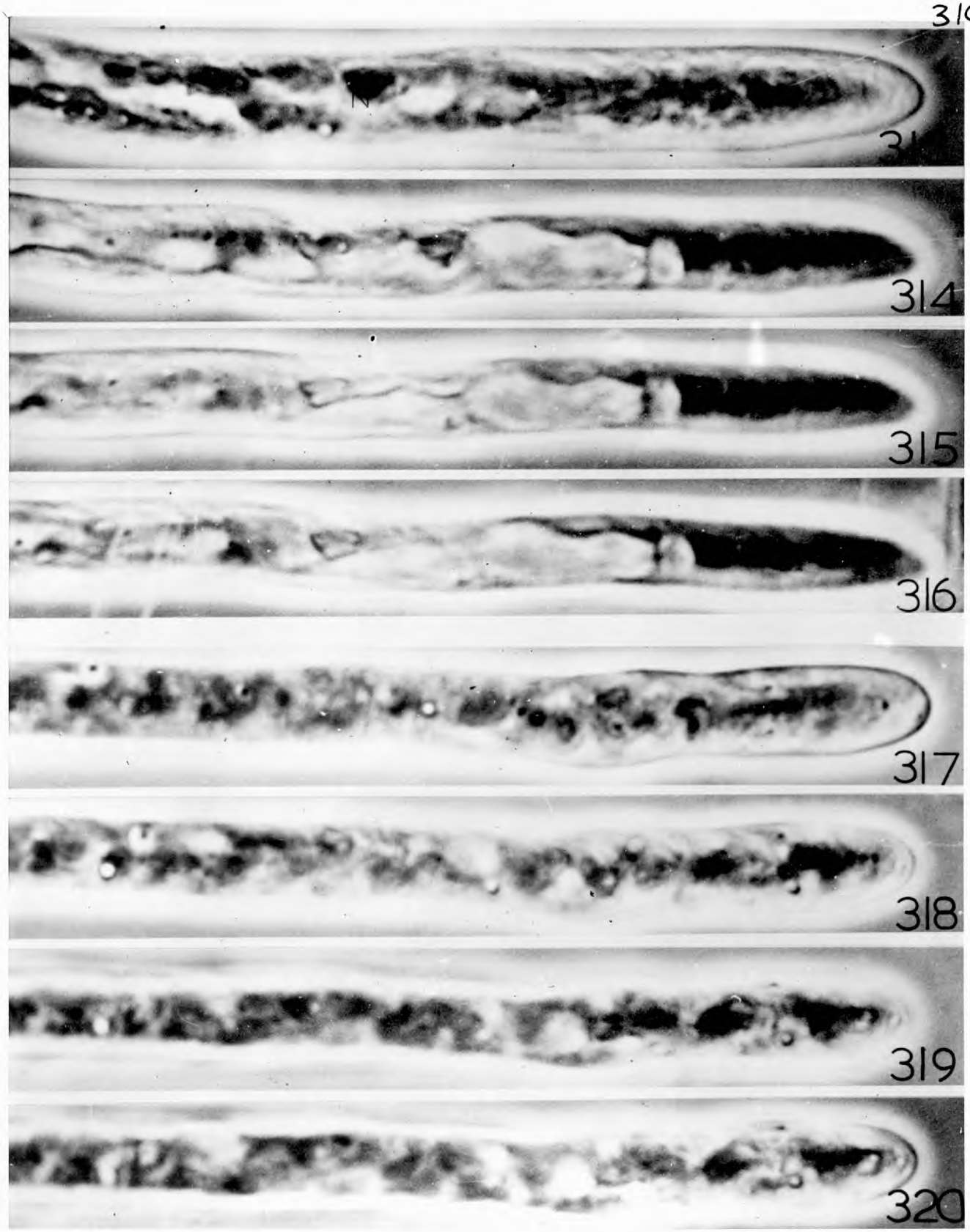
313
314
315
316
317
318
319
320

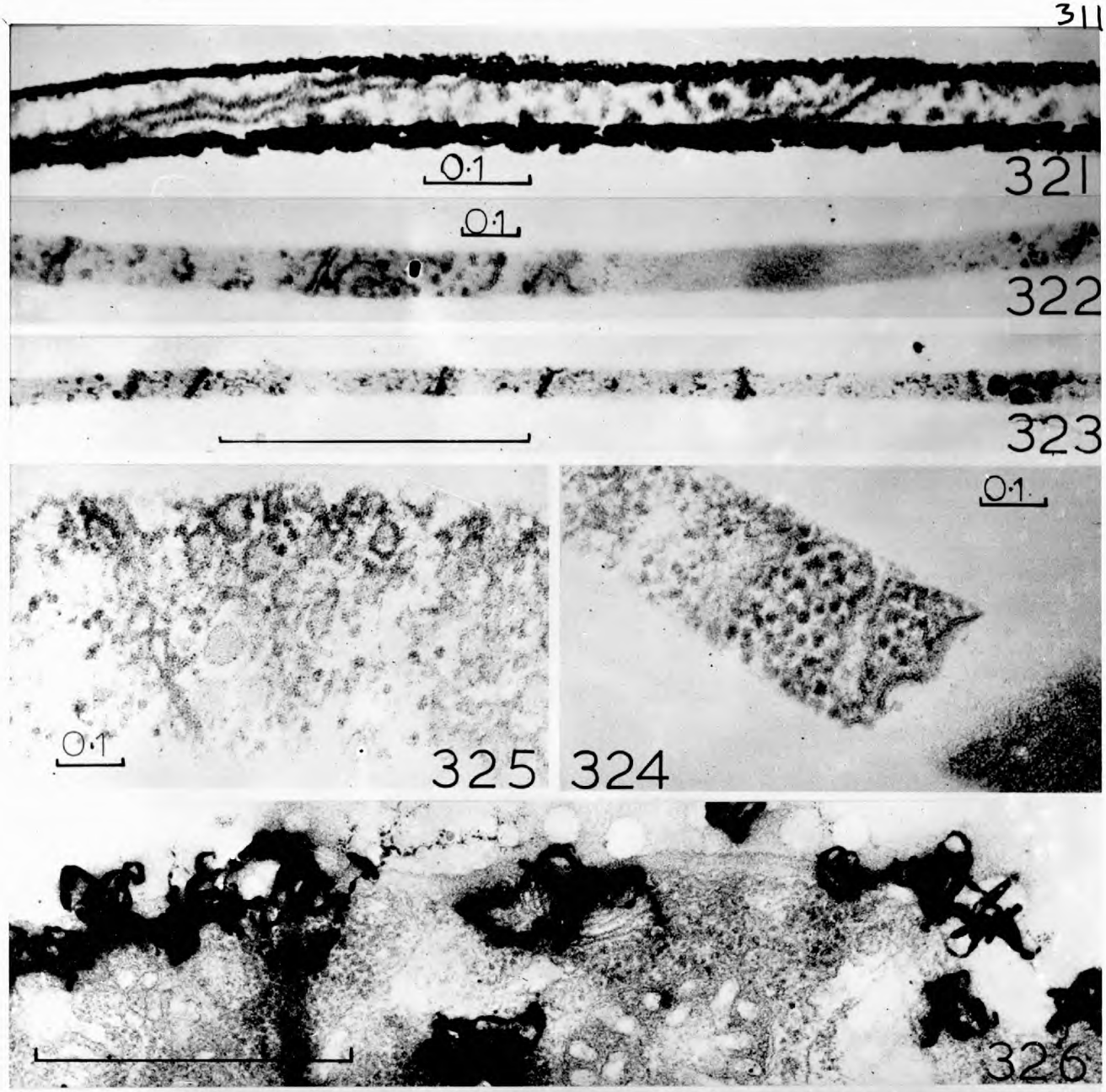

Fig.321. Resectioned silver section of epon embdded pea tissue vacuum coated with a gold/palladium alloy before embdding. Note irregular inner edges of metal. 800A/7/2. 6621.

Fig.322. Silver section of pea tissue irradiated with a focussed electron beam for c 15sec before embedding and resectioning. Note removal of lightly stained wall material. Retention of material is correlated with a high concentration of heavy metal stain. 800A/11/2. 12074.

Fig.323. Similar treatment to 322. Note spherical undistorted lipid droplets. 800A/11/1. 6685.

Fig.324. Thick section stained on one side with UAc followed by 2min Pb. Note even penetration of stain. 800AII/42/1. 6984.

Fig.325. Thick section stained on one side with UAc followed by 4min Pb. staining asymetry due to slow penetration. 800AII/43/1. 6987.

Fig.326. Hyphal apex fed with tritiated glucose for 15min followed by a 15min chase of OM. Note peripheral grains of silver which obscure details of structure. Centre grain is probably on a plasmalemmasome. 1504/1. 8091

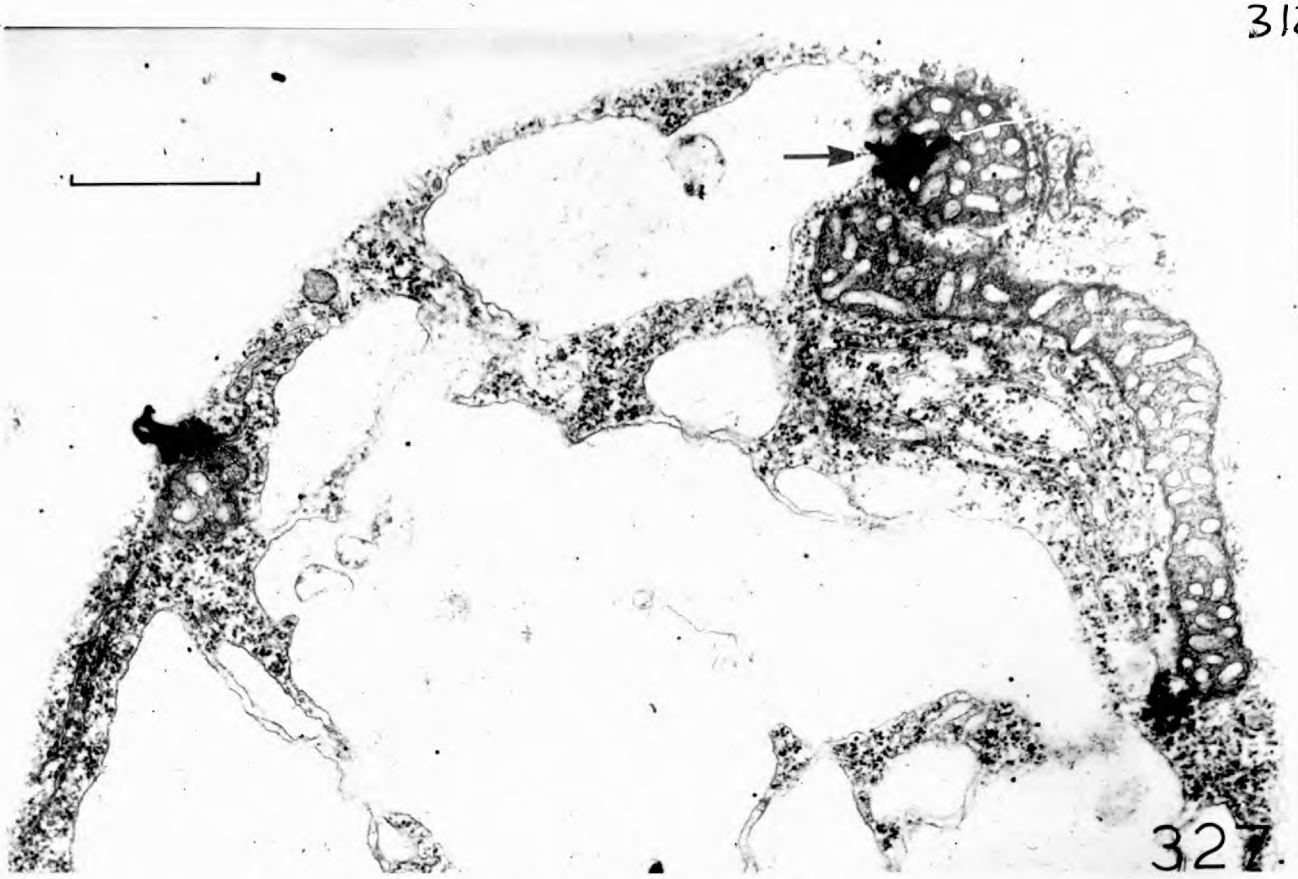

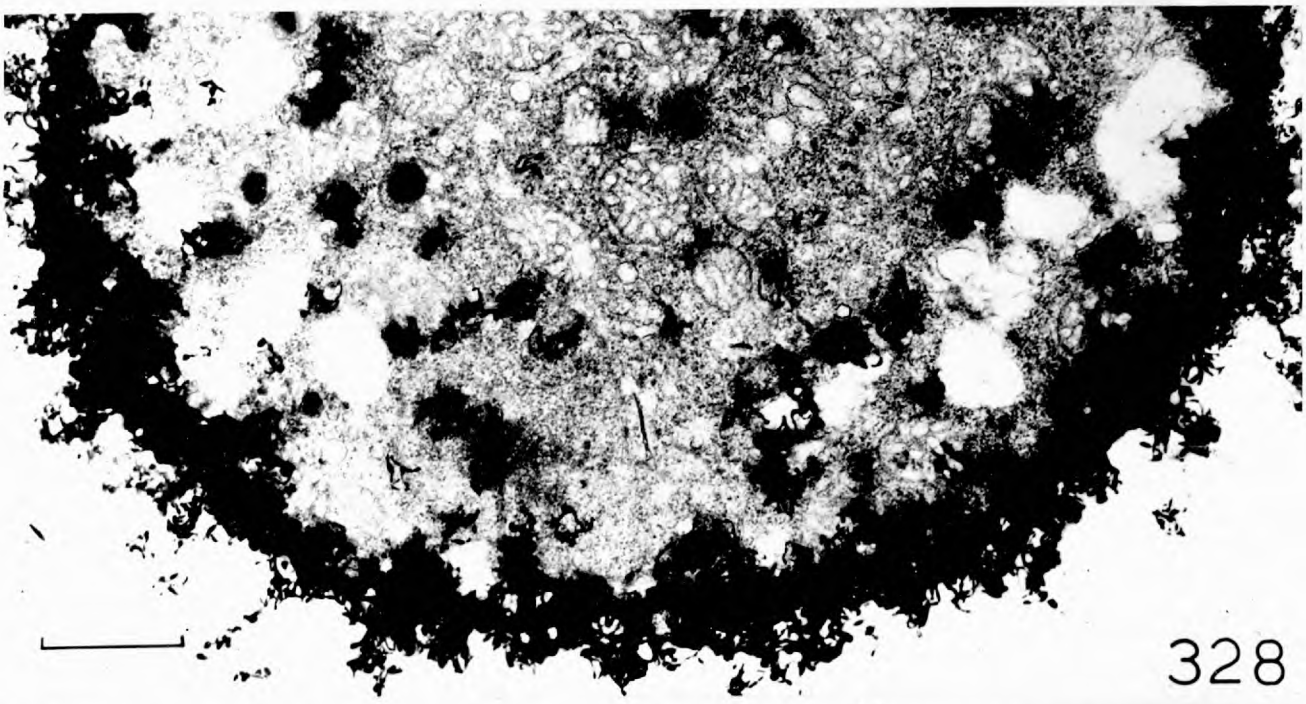

Fig.327. Subapical region of a hypha incubated in C^{14} glucose for 10 min followed by a chase of OM for 30min. Note typical low number of silver grains on wall and mitochondria. 1479/7. 14466.

Fig.328. Hyphal apex incubated in tritiated glucose for 15min followed directly by fixation. Note high concentration of grains around walls and a few internal grains. 1498/2. 8086.

REFERENCES

AFZELIUS, B. 1959. J. biophys. biochem. Cytol. 5, 269.

AIST, J.R. 1969. J. Cell Biol. 40, 120.

ALDRICH, H.C. 1967. Mycologia 59, 127.

ALEXOPOULOS, C.J. 1962. Introductory Mycology. 2nd.Edit. Wiley. New York and London.

ALLEN, R.D. 1969. J. Cell Biol. 40, 716.

ARONSON, J.M. & PRESTON, R.D. 1960a. J. biophys. biochem. Cytol. 8,247.

ARONSON, J.M. & PRESTON, R.D. 1960b. Proc. R. Soc. B 152, 346.

BAJER,A. 1968. Symp. Soc. exp. Biol. 22, 285.

BAKERSPIGEL, A. 1960. Am. J. Bot. 47, 94.

BARBER, G.A., ELBEIN, A.D. & HASSID, W.Z. 1964. J. biol. Chem. 239, 4056.

BARTNICKI-GARCIA,S. 1966. J. gen.Microbiol. 42, 57.

BARTON, R. 1965a. Nature Lond. 205, 200.

BARTON, R. 1965b. Planta 66, 95.

BARTON, R. 1967. J. Ultrastruct. Res. 20,6.

BARTON, R. 1968. Planta 82, 302.

BECKING, J.H., De BOER, W.E. & HOUWINK, A.L. 1964. Antonie van Leeuwenhoek 30, 343.

BERLIN, J.D. & BOWEN, C.C. 1964. Am. J. Bot. 51, 650.

BESSIS, M., BRETON-GORIUS, J. & THIÉRY, J.P. 1958. Rev. Hematol.13, 363.

BIKLE, D., TILNEY, L.G. & PORTER, K.R. 1966. Protoplasma 61. 322.

BOUCH, G.B. 1969. J. Cell Biol. 40, 446.

BOWERS, B. & KORN, E.D. 1968. J. Cell Biol. 39, 95.

BRACKER, C.E. 1967. A. Rev. Phytopathology 5, 343.

BRACKER, C.E. & BUTLER, E.E. 1963. Mycologia 55, 35.

BRENNER, D.M. & CARROLL, G.C. 1968. J. Bact. 95, 658.

BRIGHTMAN, M.W. & PALAY, S.L. 1963. J. Cell Biol. 19, 415.

BRINKLEY, B.R. & NICKLAS, B. 1968. J. Cell Biol. 39, 16a.

BRINKLEY, B.R. & STUBBLEFIELD, E. 1966. Chromosoma 19, 28.

BRINKLEY, B.R., STUBBLEFIELD, E. & HSU, T.C. 1967. J. Ultrastruct. Res. 19, 1.

BROWN, R.M. & BOLD, H.C. 1964. Phycological Studies V. University of Texas Publication No. 6417.

BRYAN, J.H.D. & BRINKLEY, B.R. 1964. Q. Jl microsc. Sci. 105, 367.

BÜSGEN, M. 1882. Jb. wiss. Bot. 13, 253. (in ROTHERT, 1895).

CALONGE, F.D., FIELDING, A.H. & BYRDE, R. 1969. J. gen Microbiol. 55, 177.

CARASSO, N. & FAVARD, P. 1965. J. Microscopie. 4, 395.

CARO, L.G. 1961. J. biophys. biochem. Cytol. 10, 37.

CARO, L.G. 1962. J. Cell Biol. 15, 189.

CARO, L.G. & van TUBERGEN, R.P. 1962. J. Cell Biol. 15, 173.

CARROLL, G.C. 1967. J. Cell Biol. 33, 218.

CASTLE, E.S. 1937. J. cell. comp. Physiol. 9, 477.

CHAPMAN, J.A. & VUJIČIĆ, R. 1965. J. gen Microbiol. 41, 275.

CLAUDE, A. 1968. J. Cell Biol. 39, 25a.

CLOWES, F.A.L. & JUNIPER, B.E. 1968. Botanical Monographs vol.8. "Plant Cells". Ed.. BURNETT, J.H. Blackwells. Oxford & Edinburgh.

COLHOUN, J. 1966. In The Fungus Spore, Proc. Symp. Colston Res. Soc. 18th, Bristol, England. 85. Ed. MADELIN, M.F. Butterworths, London.

COOPER, G.O. 1929. Trans. Wis. Acad. Sci. Arts. Lett. 24, 303.

COSSLETT, A. 1967. Jl R. microsc. Soc. 86, 315.

COTNER, F.B. 1930. Am. J. Bot. 17, 511.

COUCH, J.N. 1941. Am. J. Bot. 28, 704.

CRAWLEY, J.C.W. 1965. Nature Lond. 205, 200.

CRUMP, E. 1966. Personal communication in FULLER, 1966.

CRUMP, E. & BRANTON, D. 1966. Can. J. Bot. 44, 1393.

CUTTER, V.M. 1951. A. Rev. Microbiol. 5, 17.

DASHEK, W.V. & ROSEN, W.G. 1966. Protoplasma 61, 192.

De HARVEN, E. 1968. In Ultrastructure in Biological Systems, vol.3, The Nucleus. Eds. DALTON, A.J. & HAGUENAU, F. Academic Press, New York & London.

De ZOETEN, G.A. 1969. Neth. J. Pl. Path. 75, 109.

DINGLE, A.D. & FULTON, C. 1966. J. Cell Biol. 31, 43.

DIPPELL, R.V. 1967. Science N.Y. 158, 527.

DRAWERT, H. & MIX, M. 1961/62. Sitzber. Ges. Befoerder Ges. Naturw. Marburg. 83/84, 361.

ECHLIN, P. 1968. Jl R. microsc. Soc. 88, 407.

EHRLICH, M.R., SCHAFER, J.F. & EHRLICH, H.G. 1968. Can. J. Bot. 46, 17.

ESAU, K., CHEADLE, V.I. & GILL, R.H. 1966. Am. J. Bot. 53, 765.

FIESER, L.F. & FIESER, M. 1961. Advanced Organic Chemistry. Chapman & Hall, London.

FISCHER, A. 1894. Jb. wiss. Bot. 26, 187 (in KOLE, 1965).

FLEMMING, W. 1879. Arch. mikrosk. Anat. EnterMech. 16 (in WILSON, 1925)

FLITNEY, E.A. 1966. Jl R. microsc. Soc. 85, 353.

FOL, H. 1877. Arch. de.Zool.Exp. et Gén. 6, 145.

FOSTER, R.C. 1962. Ph.D. Thsis. Leeds. (in PARKER, PRESTON & FOGG, 1963)

FRANZINI-ARMSTRONG, C. & PORTER, K.R. 1964. J. Cell Biol. 22, 675.

FREDERICK, S.E., NEWCOMBE, E.H., VIGIL, E.L. & WERGIN, W.P. 1968. Planta 81, 229.

FREED, J.J., BHISEY, S.N. & SEBOWITZ, M.M. 1968. J. Cell Biol. 39, 46a.

FREI, E. & PRESTON, R.D. 1961. Proc. R. Soc. B. 154, 70.

FREY-WYSSLING, A., LÓPEZ-SÁEZ, J.F. & MÜHLETHALER, K. 1964. J.Ultrastrut Res. 10, 422.

FREY-WYSSLING, A. & MÜHLETHALER, K. 1965. Ultrastructural Plant Cytology. Elsevier. London.

FULLER, M.S. 1966. In The Fungus Spore, Proc. Symp. Colston Res. Soc., 18th, Bristol, England. 67. Ed. MADELIN, M. F. Butterworths, London.

FULLER, M.S. & REICHLE, R.E. 1965. Mycologia 57, 946.

FULLER, M.S. & REICHLE, R.E. 1968. Can. J. Bot. 46, 279.

GALL, J.G. 1961. J. biophys. biochem. Cytol. 10, 163.

GALL, J.G. 1966. J. Cell Biol. 31, 639.

GAY, J.L. & GREENWOOD, A.D. 1966. In The Fungus Spore, Proc. Symp. Colston Res. Soc., 18th, Bristol, England. 95. Ed. MADELIN, M.F. Butterworths, London.

GIBBONS, I.R. & GRIMSTONE, A.V. 1960. J. biophys. biochem. Cytol.7, 699.

GIBBS, S.P. 1962a. J. Ultrastruct. Res. 7, 418.

GIBBS, S.P. 1962b. J. Cell Biol. 15, 343.

GIRBARD, M. 1968. Symp. Soc. exp. Biol. 22, 249.

GREENLEE, T.K., ROSS, R. & HARTMAN, T.L. 1966. J. Cell Biol. 30, 59.

GREENWOOD, A.D. 1959. J. exp. Bot. 10, 55.

GREENWOOD, A.D. 1966a. Film shown by GAY & GREENWOOD, 1966.

GREENWOOD, A.D. 1966b. Discussion following FULLER, 1966.

GRIMSTONE, A.V. & KLUG, A. 1966. J. Cell Sci. 1, 351.

GROVE, S.N., BRACKER, C.E. & MORRÉ, D.J. 1967. Am. J. Bot. 54, 638.

GROVE, S.N., MORRÉ, D.J. & BRACKER, C.E. 1966. Proc. Indiana Acad. Sci. 76, 210.

HALE, L.J. 1965. Biological Laboratory Data. Methuen. London.

HARRIS, P.J. 1961. J. biophys. biochem. Cytol. 11, 419.

HARTOG, M. 1895. Trans. R. Ir. Acad. 30, 649.

HASHIMOTO, T. & YOSHIDA, N. 1966. Electron Microscopy Proc. Intern. Congr. Electron Microscopy, 6th. Kyoto, Vol.2. 305. Maruzen, Tokyo.

HAWKER, L.E. & GOODAY, M.A. 1967. J. gen. Microbiol. 49, 371.

HAWKER, L.E. & GOODAY, M.A. 1969. New Phytol. 68, 133.

HAWKER, L.E., GOODAY, M.A. & BRACKER, C.E. 1966. Nature Lond. 212, 635.

HAWKER, L.E. & McABBOTT, V. 1963. J. gen.Microbiol. 30, 401.

HEATH, I.B. & GREENWOOD, A.D. 1968. J. gen. Microbiol. 53, 287.

HEMMES, D.E. & HOHL, H.R. 1968. J. Cell Biol. 39, 168a.

HEMMES, D.E. & HOHL, H.R. 1969. Am. J. Bot. 56, 300.

HEPLER, P.K. & NEWCOMBE, E.H. 1964. J. Cell Biol. 20, 529.

HO, H.H., ZACHARIAH, K. & HICKMAN, C.J. 1967. Can. J. Bot. 45, 1765.

HO, H.H., ZACHARIAH, K. & HICKMAN, C.J. 1968. Can. J. Bot. 46, 37.

HOFFMAN, L. & MANTON, I. 1963. Am. J. Bot. 50, 455.

HOHL, H.R. & HAMAMOTO, D.R. 1967. Am. J. Bot. 54, 1131.

HÖHNK, W. 1933. Am. J. Bot. 20, 45.

HÖHNK, W. 1935. Abhandl Naturwiss Ver. Bremen. 29, 308.

HOLMES, K.V. & CHOPPIN, P.W. 1968. J. Cell Biol. 39, 526.

HOLTZMAN, E., NOVIKOFF, A.B. & VILLAVERDE, H. 1967. J. Cell Biol. 33, 419.

HOTCHKISS, R.D. 1948. Archs. Biochem. 16, 131.

HUNSLEY, D. & BURNETT, J.H. 1968. Nature Lond. 218, 462.

HUXLEY, H.E. & ZUBAY, G. 1961. J. biophys. biochem. Cytol. 11, 273.

HYDE, B.B. 1967. J. Ultrastruct. Res. 18, 25.

ICHIDA, A.A. & FULLER, M.S. 1968. Mycologia 60, 141.

JENKINS, R.A. 1967. J. Cell Biol. 34, 463.

JENSEN, W.A. 1962. Botanical Histochemistry. Freeman. San Fransisco & London.

JOHNSON, H.G. & PORTER, K.R. 1968. J. Cell Biol. 38, 403.

JOKELAINEN, P.T. 1965. J. Cell Biol. 24, 433.

JOKELAINEN, P.T. 1967. J. Ultrastruct. Res. 19, 19.

JONES, R.F. & LEWIN, R.A. 1960. Expl. Cell Res. 19, 408.

KALNINS, V.I. 1968. J. Cell Biol. 39, 70a.

KELLENBERGER, E., RYTER, A. & SÉCHAUD, J. 1958. J. biophys. biochem. Cytol. 4, 671.

KING, J.E. & BUTLER, R.D. 1968. Trans. Br. mycol. Soc. 51, 689.

KING, J.E., COLHOUN, J. & BUTLER, R.D. 1968. Trans. Br. mycol. Soc. 51, 269.

KISLEV, N., SWIFT, H. & BOGORAD, L. 1965. J. Cell Biol. 25, 327.

KOCH, W. & SCHNEPF, E. 1967. Arch. Mikrobiol. 57, 196.

KOLE, A.P. 1965. In The Fungi. Vol.1. The Fungal Cell. Ed. AINSWORTH, G.C. & SUSSMAN, A.S. Acadmeic Press. New York & London.

KREGER, D.R. 1960. Proc. K. ned. Akad. Wet. C. 63, 613.(in FREY-WYSSLING & MÜHLETHALER , 1965).

KRISHAN, A. & BUCK, R.C. 1965. J. Cell Biol. 24, 433.

KUBAI, D.F. & RIS, H. 1969. J. Cell Biol. 40, 508.

LAFONTAINE, J-G. 1968. In Ultrastructure in Biological Systems.Vol.3. The Nucleus. Eds. DALTON, A.J. & HAGUENAU, F. Academic Press, New York & London.

LAMPORT, D.T.A. 1965. Advances in Botanical Research. 2. Ed.PRESTON, R.D. Academic Press. New York & London.

LANG, N.J. 1963. J. Cell Biol. 19, 631.

LAURENT, E. 1885. Bull. Acad. Roy. Belg.,3me série. T10, 57. (in CASTLE, 1937.

LEADBEATER, B.S.C. 1969. Br. phycol. J. 4, 3.

LEDBETTER, M.C. & PORTER, K:R. 1963. J. Cell Biol. 19, 239.

LESSIE, P.E. & LOVETT, J.S. 1968. Am. J. Bot. 55, 220.

LUFT, J.H. 1961. J. biophys. biochem. Cytol. 9, 409.

LYKX, P. 1965a. Expl. Cell Res. 39, 643.

LYKX, P. 1965b. Expl. Cell Res. 39, 658.

MÄCKEL, H.G. 1928. Jb. wiss. Bot. 69, 517.

MADDY, A.H. 1964. Biochim. biophys. Acta. 88, 390.

MANOCHA, M.S. & SHAW, M. 1964. Nature Lond. 203, 1402.

MANTON, I. 1964a. J. exp. Bot. 15, 399.

MANTON, I. 1964b. Jl R. microsc. Soc. 83, 317.

MANTON, I. 1964c. Jl R. microsc. Soc. 82, 279.

MANTON, I. 1965. Advances in Botanical Research. 2. Ed. PRESTON, R.D Acadmeic Press. New York & London.

MANTON, I. 1966. J. Cell Sci. 1, 375.

MANTON, I. 1968. Proc. Linn. Soc. Lond. 179, 147

MANTON, I., CLARKE, B. & GREENWOOD, A.D. 1951. J. exp. Bot. 2, 321.

MANTON, I., CLARKE, B. & GREENWOOD, A.D. 1955. J. exp. Bot. 6, 126.

MANTON, I., CLARKE, B., GREENWOOD, A.D. & FLINT, E.A. 1952. J. exp. Bot. 3, 204.

MANTON, I. & ETTL, H. 1965. J. Linn. Soc.(Bot). 59, 175.

MANTON,I. & HARRIS, K. 1966. J. Linn. Soc.(Bot.).59, 397.

MANTON, I. & von STOSCH, H.A. 1966. Jl R. microsc. Soc. 85, 119.

MARCHANT, R. 1966. Ann. Bot. N.S. 30, 821.

MARCHANT, R., PEAT, A. & BANBURY, G.H. 1967. New Phytol. 66, 623.

MARCHANT, R. & ROBARDS, A.W. 1968. Ann. Bot. N.S. 32, 457.

MARCHANT, R. & SMITH, D.G. 1968. Arch. Mikrobiol. 63, 85.

MARINOZZI, V. 1961. J. biophys. biochem. Cytol. 9, 121.

MARKHAM, R., FREY, S. & HILLS, G.J. 1963. Virology 20, 88.

MASSALSKI, A.K. 1969. Ph.D. Thesis. Leeds.

MAZIA, D. 1961. "The Cell" vol.3. Ed. BRACHET, J. & MIRSKY, A.E. Academic Press, New York & London.

MAZIA, D. 1967. Symp. Int. Soc. Cell Biol. 6, 39. Ed. WARREN, K.B. Academic Press, New York.

MAZIA, D., HARRIS, P.J. & BIBRING, T. 1960. J. biophys. biochem. Cytol. 7, 1.

McCLURE, W.K., PARK, D. & ROBINSON, P.M. 1968. J. gen. Microbiol. 50, 177.

McMANUS, M.A. & ROTH, L.E. 1968. Mycologia 60, 426.

MEIER, H. 1958. Biochim. biophys. Acta. 28, 229.

MEIER, H. & WEBSTER, J. 1954. J. exp. Bot. 5, 401.

MIZUKAMI, I. & GALL, J.G. 1966. J. Cell Biol. 29, 97.

MOLLENHAUER, H.H. & WHALEY, W.G. 1963. J. Cell Biol. 17, 222.

MOLLENHAUER, H.H., WHALEY, W.G. & LEECH, J.H. 1961. J. Ultrastruct. Res. 5, 193.

MOOR, H. 1966a. Balzers High Vacuum Report. 9. Balzers A G 9496 Balzers. Fürstentum, Lichtenstein.

MOOR, H. 1966b. J. Cell Biol. 29, 153.

MOOR, H. 1967. Protoplasma 64, 89.

MOOR, H. & MÜHLETHALER, K. 1963. J. Cell Biol. 17, 609.

MOORE, R.T. 1964. Z. Zellforsch. mikrosk. Anat. 63, 921.

MOORE, R.T. & McALEAR, J.H. 1961. Mycologia 53, 194.

MÜHLETHALER, K. 1967. A. Rev. Pl. Physiol. 18, 1.

NAGAI, M. & TAKAHASHI, T. 1962. Trans. Mycol. Soc. Japan. 3, 19.

NICKERSON, W.J., TABER, W.A. & FALCONE, G. 1956. Can. J. Microbiol. 2, 575.

NICKLAS, B.R. 1965. J. Cell Biol. 25, 119.

NIR, I., KLEIN, S. & POLJAKOFF-MAYBER, A. 1969. Aust. J. biol. Sci. 22, 17.

NORTHCOTE, D.H. 1969. Proc. R. Soc. B. 173, 21.

NORTHCOTE, D.H. & LEWIS, D.R. 1968. J. Cell Sci. 3, 199.

NORTHCOTE, D.H. & PICKETT-HEAPS, J.D. 1966. Biochem. J. 98, 159.

NOVIKOFF, A.B., QUINTANE, N., VILLAVERDE, H. & FORSCHIRM, R. 1964. J. Cell Biol. 23, 68a.

OLIVE, L.S. 1953. Bot. Rev. 19, 439.

OLIVE, L.S. 1965. In The Fungi, vol.1. The Fungal Cell. 143. Eds. AINSWORTH, G.C. & SUSSMAN, A.S. Academic Press, New York & London.

OLSON, L.W. & FULLER, M.S. 1968. Arch. Mikrobiol. 62, 237.

OSTER, G. 1955. In Physical Techniques in Biological Research, vol.1. Eds. OSTER, G. & POLLISTER, A.W. Academic Press, New York & London.

PALADE, G.E. & CARO, L.G. 1964. J. Cell Biol. 20, 473.

PARKER, B.C., PRESTON, R.D. & FOGG, G.E. 1963. Proc. R. Soc. B.158, 435.

PEACHY, L.D. 1958. J. biophys. biochem. Cytol. 4, 233.

PEARSE, A.G.E. 1961. Histochemistry, Theoretical and Applied. 2nd. Edit. Churchill, London.

PEASE, D.L. 1963. J. Cell Biol.18, 313.

PEAT, A. & BANBURY, G.H. 1967. New Phytol.66, 475.

PHILLIPS, D.M. 1966. J. Cell Biol. 31, 635.

PHILLIPS, R. & SHORTT, T. 1964. Jl R. microsc. Soc. 82, 263.

PICKETT-HEAPS, J.D. 1967a. J. Histochem. Cytochem. 15, 442.

PICKETT-HEAPS, J.D. 1967b. J. Ultrastruct. Res. 18, 287.

PITELKA, D.R. 1963. Electron Microscope Structure of Protozoa. Pergammon Press. New York.

POLLISTER, A.W. & POLLISTER, P.F. 1943. Ann. N.Y. Acad. Sci. 45, 1.

PORTER, K.A. 1966. In Principles of Biomolecular Organizations. Ed. WOLSTENHOLME, G.E.W. & O'CONNOR, M. Little, Brown & Co. Boston.

PORTER, K.A. & BLUM, J. 1953. Anat. Rec. 117, 685 (in ZELANDER & EKHOLM, 1960).

PORTER, K.R. & MACHADO, R.D. 1960. J. biophys. biochem. Cytol.7, 167.

PRESTON, R.D. 1964. In Formation of Wood in Forest Trees. Ed. ZIMMERMAN, M. Academic Press. New York & London.

PRESTON, R.D. & GOODMAN, R.N. 1968. Jl R. microsc. Soc. 88, 513.

RAPER, J.R. 1936. J. Elisha Mitchell scient. Soc. 52, 274.

RAY, P.M. 1967. J. Cell Biol. 35, 659.

REEVES, F. 1967. Mycologia 59, 1018.

REICHLE, R.E. 1969. Mycologia 61, 30.

REICHLE, R.E. & FULLER, M.S. 1967. Am. J. Bot. 54, 81.

REINHARDT, M.O. 1892. Jb. wiss. Bot. 23, 479.(in ZALOKAR, 1959).

RENAUD, F.L. & SWIFT, H. 1964. J. Cell Biol. 23, 339.

REYNOLDS, E.S. 1963. J. Cell Biol. 17, 208.

RINGO, D.L. 1967a. J. Ultrastruct. Res. 17, 266.

RINGO, D.L. 1967b. J. Cell Biol. 33, 543.

RIZVI, S.R.H. 1964. Ph.D. Thesis. Hull.(in ROBERTSON, 1965).

RIZVI, S.R.H. & ROBERTSON, N.F. 1965. Trans. Br. mycol. Soc. 46, 469.

ROBARDS, A.W. & KIDWAI, P. 1969. New Phytol. 68, 343.

ROBBINS, E. & GONATAS, N.K. 1964. J. Cell Biol. 21, 429.

ROBBINS, E. & JENTZSCH, G. 1969. J. Cell Biol. 40, 678.

ROBBINS, E., JENTZSCH, G. & MICALI, A. 1968. J. Cell Biol. 36, 329.

ROBERTSON, N.F. 1958. Ann. Bot. N.S. 22, 159.

ROBERTSON, N.F. 1965. In The Fungi, vol.1. The Fungal Cell. 613. Eds. AINSWORTH, G.C. & SUSSMAN, A.S. Academic Press, New York & London.

ROBERTSON, N.F. 1968. A. Rev. Phytopathology 6, 115.

ROBINOW, C.F. & BAKERSPIGEL, A. 1965. In The Fungi, vol.1. The Fungal Cell, 119. Eds. AINSWORTH, G.C. & SUSSMAN, A.S. Academic Press. New York & London.

ROBINOW, C.F. & MARAK, J. 1966. J. Cell Biol. 29, 129.

ROELOFSEN, P.A. 1965. In Advances in Botanical Research, 2. Ed. PRESTON, R.D. Academic Press. New York & London.

ROSEN, W.G. 1968. A. Rev. Pl. Physiol. 19, 435.

ROSENBAUM, J.L. & CARLSON, K. 1969. J. Cell Biol. 40, 415.

ROSENBAUM, J.L. & CHILD, F.M. 1967. J. Cell Biol. 34, 345.

ROSENBAUM, J.L., MOULDER, J.E. & RINGO, D.L. 1969. J. Cell Biol.41, 600.

ROSS, R. & BARNSTEIN, P. 1969. J. Cell Biol. 40, 366.

ROTHERT, L. 1888. Beitr. Biol. Pflanzen 5, 291 (in HARTOG, 1895).

ROTHERT, L. 1894. Ber. Deut. Botan. Ges. 12, 268 (in CRUMP & BRANTON, 1966.).

RUDZINSKA, M.A. 1965. J. Cell Biol. 25, 459.

SAGER, L. 1967. J. theoret. Biol. 14, 225.

SASSEN, M.M.A. 1964. Acta. bot. neerl. 13, 175.

SATIR, P. 1965. Protoplasmatologia III E, 1.

SCHRADER, E. 1938. Flora, Jena. 32, 125.

SCHUSTER, F. 1963. J. Protozool. 10, 297.

SCHUSTER, F. 1964. J. Protozool. 11, 202.

SHANOR, L. 1937. J. Elisha Mitchell scient. Soc. 53, 119.

SHELANSKI, M.L. & TAYLOR, E.W. 1968. J. Cell Biol. 38, 304.

SIEVERS, A. 1963. Protoplasma 56, 188.

SJÖSTRAND, F.S. 1953. Experientia 9, 114(in ZELANDER & EKHOLM, 1960).

SLIFKIN, M.K. 1967. Mycologia 59, 431.

SLIFKIN, M.K. 1968. J. Elisha Mitchell scient. Soc. 84, 184.

SMITH, F.E.V. 1923. Ann.Bot. N.S. 37, 63.

SMITH, J.H. 1923. Ann. Bot. N.S. 37, 341.

SPARROW, F.K. 1958. Mycologia 50, 797.

STAEHELIN. A. 1966. Z. Zellforsch. mikrosk. Anat. 74, 325.

STUBBLEFIELD, E. & BRINKLEY, B.R. 1967. Symp. Int. Soc. Cell Biol. 6, 175. Ed. WARREN, K.B. Academic Press, New York.

TERZAKIS, J.A., SPINZ, H. & WARD, R.A. 1967. J. Cell Biol. 34, 311.

THOMAS, P.L. & ISAAC, P.K. 1967. Can. J. Bot. 45, 1473.

TILNEY, L.G. & PORTER, K.R. 1967. J. Cell Biol. 34, 327.

TOLBERT, N.E., OESER, A., KISAKI, T., HAGEMAN, R.H. & YAMAZAKA, R.K. 1968. J. biol Chem. 243, 5179.

TORMEY, J. McD. 1964. J. Cell Biol. 23, 658.

TROW, A.H. 1895. Ann. Bot. N.S. 9, 609.

TUCKER, J.B. 1967. J. Cell Sci. 2, 481

TURIAN, G. & OULEVEY, N. 1968. Experientia 24, 733.

VAN ITERSON, W. 1964. J. Cell Biol. 20, 361.

VILLEMEZ, C.L., McNAB, J.B. & ALBERSHEIM, P. 1968. Nature Lond. 218,878.

VLK, W. 1939. Arch. Protistenk. 92, 157. (in KOLE, 1965).

VUJIČIĆ, R., CHAPMAN, J.A. & COLHOUN, J. 1965. Trans. Br. mycol. Soc. 48, 153.

WALDEYER, W. 1888. Arch. mikrosk. Anat. EnterMech. 32.(in WILSON, 1925).

WARD, H.M. 1883. Q. Jl microsc. Sci. 23, 273.

WEINTRAUB, M. & RAGETLI, H.W.J. 1968. J. Cell Biol. 38, 316.

WHALEY, W.G., KEPHART, J.E. & MOLLENHAUER, H.H. 1959. Am. J. Bot. 46, 743.

WILLIAMS, M.A. & MEEK, G.A. 1966. Jl R. microsc. Soc. 85, 337.

WILSENACH, R. & KESSEL, M. 1965. J. gen. Microbiol. 40, 401.

WILSON, E.B. 1925. The Cell in Development and Heredity. 3rd. Edit. Macmillan. New York.

WOLFE, J. 1968. J. Cell Biol. 39, 143a.

ZALOKAR, M. 1953. Archs. Biochem. Biophys. 44, 330.

ZALOKAR, M. 1959. Am. J. Bot. 46, 602.

ZELANDER, T. & EKHOLM, R. 1960. J. Ultrastruct. Res. 4, 413.

NAMES AND ADDRESSES OF SUPPLIERS

A.E.I., G.E.C.-A.E.I.(Electronics) Ltd., Harlow, Essex.

BALZERS HIGH VACUUM LTD., Northbridge Rd., Berkhamsted, Herts.

B.D.H. CHEMICALS LTD., Poole, Dorset.

CAMBRIDGE INSTRUMENT CO. LTD., 13 Grosvenor Place, London, S.W.1.

DAVIS GELATINE LTD., Warwick, England.

GE-FE-RI, Via Maritima, Frosinone, Italy.

GURR, GEORGE T., LTD., Carlisle Rd., The Hyde, London, N.W.9.

HOPKINS & WILLIAMS LTD., Chadwell Heath, Essex.

ILFORD LTD., Professional Products Division, 53-54 Berwick St., London, W.1.

I.V.I.C., Instituto Venezolano De Investigaciones Cientificas, Caracas, Venezuela.

JOHNSON MATTHEY LTD., 72-73 Hatton Garden, London, E.C.1.

KODAK LTD., Kodak House, Kingsway, London, W.C.2.

L.K.B. INSTRUMENTS LTD., L.K.B. House, 137 Anerley Rd., London, S.E.20.

MASON & MORTON LTD., Fir Tree House, Headstone Drive, Wealdstone, Harrow, Middx.

MAY & BAKER LTD., Dagenham, Essex.

OXOID LTD., London, S.E.1.

POLARON EQUIPMENT LTD., Delviljem House, Shakespeare Rd., Finchley, London, N.3.

RADIOCHEMICAL CENTRE, Amersham, Bucks.

REICHERT. SHANDON SCIENTIFIC CO. LTD., 65 Pound Lane, Willesden, London, N.W.10. (British agents)

SIGMA LONDON CHEMICAL CO. LTD., 12 Lettice St., London, S.W.6.

SMETHURST HIGHLIGHT, Sidcot Heaton, Bolton, Lancs.

SORVALL. V.A. HOWE & CO. LTD., 46 Pembridge Rd., London, W.11. (British agents)

TAAB LABORATORIES, 52 Kidmore End Rd., Emmer Green, Reading, Berks.

VICKERS LTD., Purley Way, Croydon, CR94HN.

ZEISS (OBERKOCHEN). DEGENHARDT & CO. LTD., 20-22 Mortimer St., Carl Zeiss House, London, W.1. (British agents)

ACKNOWLEDGEMENTS

I would like to express my sincere appreciation of my supervisor, M. A.D. Greenwood, whose skill, patience, encouragement and support have contributed so much to this work. I would also like to thank Dr. J.L. Gay for his numerous helpful and encouraging discussions, the members of Imperial College Botany Department who have helped in various ways during the course of this work and the staff of the Applied Optics Division of the Imperial College Physics Department for the use of the microdensitometer. I have also profited considerably from the unpublished micrographs sent to me by Dr. C.F. Robinow and from several discussions with Professor I. Manton.

Finally, I shall record my gratitude to my wife, Mrs. M.C. Heath, who has helped in so many ways during the course of the work and in the production of this thesis, and to Mrs. W.I.L. Roy who expertly typed the manuscript.

This work was carried out during the tenure of a Studentship from the Science Research Council.